

**CENOZOIC SURFACE UPLIFT AND BASIN FORMATION IN THE PERUVIAN
CENTRAL ANDES**

A Dissertation Presented to

the Faculty of the Department of Earth and Atmospheric Sciences

University of Houston

In Partial Fulfillment

of the Requirements for the Degree

Doctor of Philosophy

By

Kurt Eric Sundell

December 2017

**CENOZOIC SURFACE UPLIFT AND BASIN FORMATION IN THE PERUVIAN
CENTRAL ANDES**

Kurt Eric Sundell

APPROVED:

Dr. Joel E. Saylor, Chairman

Dr. Thomas J. Lapen

Dr. Peter Copeland

Dr. Alexander C. Robinson

Dr. John Bershaw, Portland State University

**Dean, College of Natural Sciences and
Mathematics**

ACKNOWLEDGMENTS

I am indebted to the hard work and infinite patience of my advisor, Joel Saylor, as well as Ph.D. committee members, Peter Copeland, Tom Lapen, Alex Robinson, and external committee member, John Bershaw. I gratefully acknowledge assistance in southern Peru from Erick Gil and the Gil family. This work benefitted from discussions with Nick Bartschi, Brian Horton, Margarete Jadamec, Clay Painter, Nick Perez, Tyson Smith, Eugene Szymanski. I thank Richard Styron, Paola Usnayo, and Dustin Villarreal for assisting in the field and great discussions along the way. I also thank Lily Schaffer for random 5 a.m. talks in the hallways about research and life. George Gehrels and Noah McLean provided thoughtful reviews for Chapter 2. Yongjun Gao and Minako Righter provided invaluable laboratory assistance. Toti Larson produced the majority of stable isotope data at UT Austin presented in Chapter 4. Fieldwork and analytical costs were supported by grants from the National Science Foundation (EAR- 1550097), the National Geographic Society Committee for Research and Exploration, Geological Society of America Grants-in-Aid, International Association of Sedimentologists, Sigma Xi, and scholarships from the Joe and Lucy Steward Memorial Endowment, the Sam Penn Memorial Endowment, Houston Alumni Association, British Petroleum, and Marathon Oil Corporation. Finally, I am grateful my wife is kind and patient enough to go through this academic experience with me.

DEDICATION

To my parents.

**CENOZOIC SURFACE UPLIFT AND BASIN FORMATION IN THE PERUVIAN
CENTRAL ANDES**

An Abstract of a Dissertation

Presented to

the Faculty of the Department of Earth and Atmospheric Sciences

University of Houston

In Partial Fulfillment

of the Requirements for the Degree

Doctor of Philosophy

By

Kurt Eric Sundell

December 2017

ABSTRACT

Surface uplift and basin subsidence are central to the debate regarding geodynamic processes involved in the development and maintenance of high topography in the central Andes, yet these issues remain largely unaddressed in the high-elevation hinterland of southern Peru. This dissertation presents a combination of stratigraphy, sediment provenance, and stable isotopic geochemistry which bear on the geodynamic controls of orogen evolution in southern Peru. Basin analysis and modeling of the Altiplano region provides updated characterization, chronology, and quantitative provenance information. Results show that the Western Cordillera was a progressively more proximal source for the Altiplano basin sediments and that sediment accumulation rates increased from ~ 36 m/Myr to >150 m/Myr between 58 and 23 Ma, consistent with deposition in a northeastward-migrating flexural foreland basin system. Transition to hinterland basin deposition in the northernmost Altiplano is marked by a 23–9 Ma angular unconformity, after which localized sedimentation began again with increased accumulation rates >800 m/Myr, likely due to strike-slip subsidence. Late Oligocene to modern surface uplift patterns were determined from regional stable isotopic trends of water preserved in hydrated volcanic glasses benchmarked against isotopic signatures of modern waters. Results show the northern cordilleras of southern Peru were at modern elevation by ~ 22 Ma. To the south, elevation increased rapidly by ~ 2.5 km between 22 and 17 Ma in the Western Cordillera, and between 17 and 12 Ma in the Altiplano, pointing to isostatic uplift interpreted to be from foundering of mantle lithosphere via Rayleigh-Taylor instability. The Eastern Cordillera was uplifted much slower, with ~ 2

km of elevation gain between 25 and 10 Ma, consistent with crustal shortening in the absence of significant lithospheric thickening. Collectively, results highlight along- and across-strike variability in geodynamic processes consistent with models of orogenic cyclicity. Cenozoic foreland basin variability along orogenic strike between southern Peru and northwest Argentina was controlled by Paleozoic–Mesozoic stratigraphic and structural fabric that resulted in thicker deposits, earlier onset of rapid sediment accumulation, and earlier higher-frequency high-flux magmatism in the north. New U-Pb data visualization/reduction and mixture modeling software packages (UPbToolbox and DZmix) were developed for, and provided with this work.

TABLE OF CONTENTS

CHAPTER 1: Introduction	1
CHAPTER 2: Unmixing Detrital Geochronology Age Distributions	3
CHAPTER 3: Peruvian Altiplano Stratigraphy Highlights Along-strike Variability in Foreland Basin Evolution of the Cenozoic Central Andes	33
CHAPTER 4: Variable Late Cenozoic Surface Uplift across Southern Peru	89
REFERENCES	108
APPENDIX 1: Random Sampling-weighting of Fifty Sources	122
APPENDIX 2: Supplementary Material for Chapter 3	123
APPENDIX 3: Detrital Zircon U-Pb Methods	128
APPENDIX 4: Detrital Zircon U-Pb Integrated Data	130
APPENDIX 5: Modern Water Data and Elevation Modeling	212
APPENDIX 6: Volcanic Glass Stable Isotope Data and Modeling	220
APPENDIX 7: Volcanic Zircon U-Pb Geochronology Results	224
APPENDIX 8: Lapse Rate Calculation	244
APPENDIX 9: Volcanic Zircon U-Pb Geochronology Methods	247

CHAPTER 1

Introduction

The Andean plateau is the broad region of high (>3 km) topography in the center of the Andes. It stretches approximately 1800 km from southern Peru to northern Argentina and is widest (350 – 400 km) in Bolivia (Isacks, 1988). The Pacific margin of the South American continent has undergone subduction since at least the late Paleozoic, with evidence of arc magmatism throughout the Mesozoic (Allmendinger et al., 1983). There is general consensus that the development of the Andean plateau began in the early Cenozoic as a result of continued east-directed subduction of the Nazca plate (Allmendinger et al., 1997); however, disagreements abound regarding when the Andean plateau attained significantly high (>2 km) topography (e.g., Garzzone et al., 2008; Insel et al., 2010), and what geodynamic mechanism(s) controlled topographic development (e.g., Isacks, 1988; Pope and Willet, 1998; Garzzone et al., 2008).

The Andean plateau is Earth's largest modern plateau to develop as a result of ocean-continent convergence in the absence of continental collision, and its origins have been the focus of ongoing geological and geophysical research, as well as analogue and numerical models (e.g., DeCelles et al., 2015). The latter present testable hypotheses for the location, timing, rate, and magnitude of four key observables: basin subsidence, surface uplift, and by inference, rock exhumation, and crustal shortening.

Most research on basin formation and uplift history of this region has focused on the central and southern Andean plateau of Bolivia, Chile, and Argentina (e.g., Gregory-Wodzicki, 1998; Garzzone et al., 2008). However, the northern Andean plateau stretches

well into southern Peru where there are multiple temporally overlapping but spatially separate Paleogene (Kayra and Soncco basins) and Neogene (Ayacucho, Crucero, Descanso, Huacochullo, Tincopalca, Macusani, Paruro, Punacancha) foreland and intermontane hinterland basins that have had little to no investigation involving basin analysis or paleoaltimetry (Carlotto, 2013). These Peruvian sedimentary basins contain a record of the formation and deformation history associated with Cenozoic construction of the Andean plateau, and hence an opportunity to compare field-based observations to model-based predictions.

In the following chapters, I investigate geodynamic mechanisms for the Cenozoic development of the Peruvian central Andes. Chapter 2 outlines a detrital age distribution mixture model that is applied to provenance modeling. Chapter 3 is a detailed account of Cenozoic stratigraphy in the northernmost Altiplano. Chapter 4 presents new proxy estimates of paleoelevation from stable isotopic analysis of hydrated volcanic glass data benchmarked against modern water data. New U-Pb data visualization/reduction and mixture modeling software packages (UPbToolbox and DZmix) are provided with this work in the Texas Digital Library.

CHAPTER 2

Unmixing Detrital Geochronology Age Distributions

Published September 20, 2017, Geochemistry, Geophysics, Geosystems

Authors:

Kurt E. Sundell

Joel E. Saylor¹

¹**Department of Earth and Atmospheric Sciences, University of Houston, Houston, Texas, USA**

Introduction

Since the advent of laser ablation inductively coupled plasma mass spectrometry, there has been a dramatic increase in both number of samples (N) and sample size (n) of detrital zircon U-Pb geochronological data sets (e.g., Pullen et al., 2014; Vermeesch and Garzanti, 2015). This technique has become a method of choice for geoscientists interested in source-to-sink questions requiring detailed sediment provenance analysis including sediment budgeting, sediment routing, paleogeography, and determining maximum depositional age (e.g., Gehrels et al., 2011; Laskowski et al., 2013; Perez and Horton, 2014). Early interpretations of detrital age distributions relied on qualitative comparison based on the presence or absence of characteristic source populations for a given geologic setting, often highlighted by vertical bars on vertically stacked finite mixture distributions (probability density plots (PDPs) or kernel density estimates (KDEs)). This approach suffers from many problems, two of which are interpreter bias, and potential broad-brush provenance interpretations exacerbated by oversmoothing old and young ages in PDPs and KDEs, respectively. Furthermore, as N and n continue to

grow larger, data management becomes a more pressing issue, and this type of visual comparison tends to break down completely.

More recently, quantitative techniques have been adapted to aid comparison of detrital data sets (e.g., Gehrels, 2000; Amidon et al., 2005; Saylor et al., 2013; Vermeesch, 2013; Satkoski et al., 2013; Kimbrough et al., 2015; Licht et al., 2016; Saylor and Sundell, 2016; Vermeesch, 2016; Wissink et al., 2016). Application of these methods has typically focused on the forward mixing problem of comparing source signatures mixed based on observations (e.g., relative outcrop area) to a mixed sample age distribution; few have considered the inverse problem of determining the mixing proportions of potential source samples through model-based comparison to a mixed sample (e.g., Saylor et al., 2013; Kimbrough et al., 2015; Licht et al., 2016). Extracting mixing proportions of source samples is particularly important in geologic settings with a significant amount of sediment recycling where detrital samples are largely sourced from other clastic sedimentary rocks (e.g., Campbell et al., 2005; Perez and Horton, 2014).

We present a new method of quantifying source mixing proportions through a combination of inverse Monte Carlo modeling and optimized forward modeling. We first demonstrate the model's ability to reproduce source contributions using simple and complex synthetic data sets, and empirical detrital zircon U-Pb data from North America (Laskowski et al., 2013). Testing of these data sets mixed in known proportions shows the model is capable of perfectly determining mixing proportions of source contributions from mixed samples without any *a priori* information of source sample contribution. We then test the model on two published detrital zircon U-Pb empirical data sets. The first empirical data set consists of relatively low- n (mean $n = 95$) age distributions

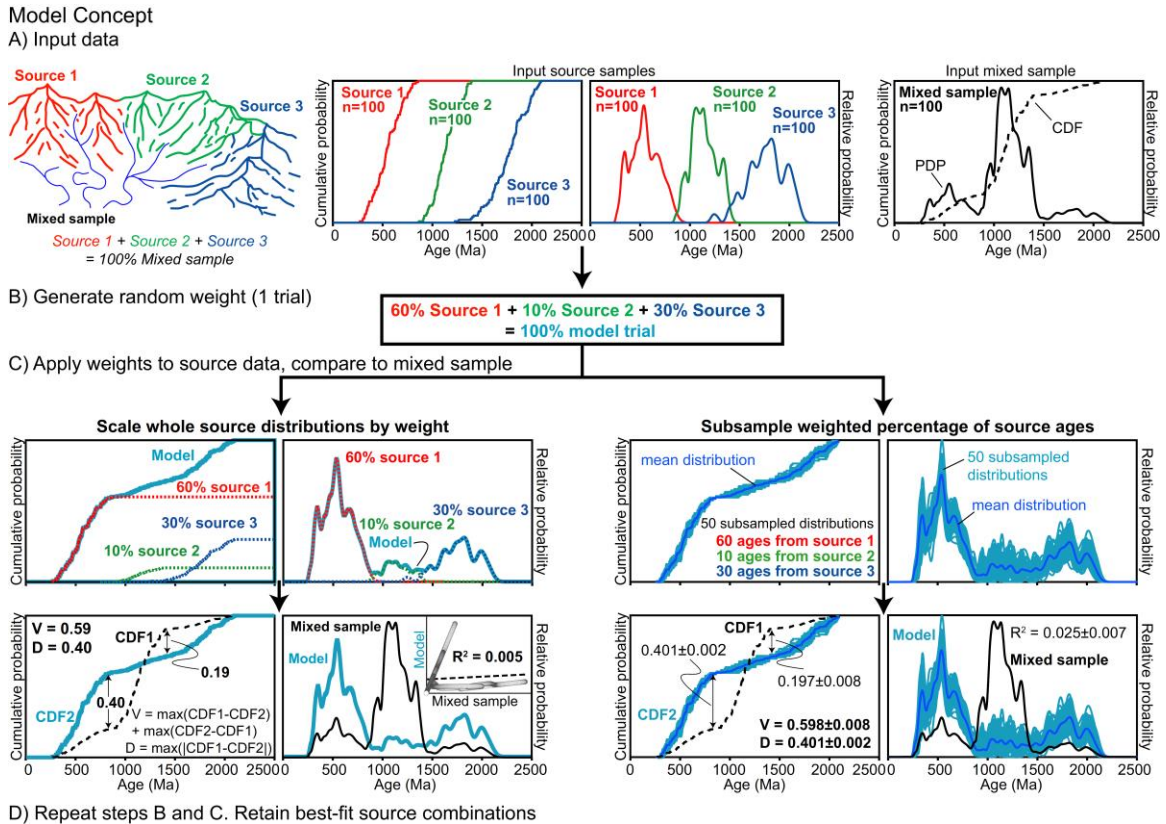


Figure 2.1. Inverse Monte Carlo model concept showing the steps taken to run one trial. (A) Synthetic detrital age distribution representing three potential source signatures shown as cumulative distribution plots (CDFs, left) and probability density plots (PDPs, center). Synthetic data is comprised of three source samples each with 100 ages and 2 – 5% uncertainty at the 1σ level. A mixed sample with actual distribution of 20% of source 1, 70% of source 2, and 10% of source 3 is shown on the right. (B) Example random weighting to be applied to the three source samples. (C) Randomly generated weights from B applied to source CDFs and PDPs (left) or converted to percent of ages randomly subsampled from source age distributions ($s = 100$ and $S = 50$). Quantitative comparison of model trial (in blue) to mixed sample (in black) using the KS test D statistic, Kuiper test V statistic, and Cross-correlation coefficient R^2 . Results yield a single value when random weighting is applied to CDFs or PDPs (left), but give a range (shown as mean and standard deviation) when based on the subsampled source ages (right). (D) Steps B and C are repeated a user specified number of times (number of trials) and a user-specified percent of best model fits are retained.

characterizing modern river sand mixed samples that are sourced from sedimentary units in their respective catchments (Saylor et al., 2013). The second empirical data set consists

of relatively high- n ($n \geq 800$), mixed loess and paleosol samples from central China (Licht et al., 2016).

The model described here has been implemented as a MATLAB-based graphical user interface (GUI) stand-alone executable (.exe file), DZmix. As an executable, DZmix does not require installation of MATLAB. Both the GUI and source code are provided in the Texas Digital Library, along with a step-by-step user manual and all data sets discussed below.

Model Concept

Inverse Monte Carlo mixture modeling

The inverse Monte Carlo model implements two different methods of constructing model source age distributions for comparison to mixed sample distributions (Figure 2.1). In both methods model source distributions based on randomly generated weights are quantitatively compared to a mixed sample a user-specified number of times (number of trials) using the Kolmogorov-Smirnov (KS) test D statistic and the Kuiper test V statistic calculated from CDFs, and cross-correlation of finite mixture distributions (PDPs or KDEs). The first method of constructing model source distributions simply scales each source's CDF and finite mixture distributions by the randomly generated weights, and sums them together to produce a single CDF and PDP/KDE model source distribution (e.g., Amidon et al., 2005; Saylor et al., 2013). The second method converts each randomly generated weight into an integer number of ages to be subsampled from each source, totaling a user-specified sample size (s), and repeated a user-specified number of times for each model trial (S). This latter approach was developed by Licht et al. (2016) as a modification of methods outlined in Amidon et al. (2005). In the Licht et

al. (2016) study, s and S are set at 800 and 200, respectively (Licht et al. use n and N). We adopt the convention of s and S to avoid confusion with number of input source samples, N , and individual sample size, n .

Both methods of constructing model source distributions are demonstrated on a synthetic data set in Figure 2.1. Here, one example model trial with randomly generated weights of 60%, 10%, and 30% is applied to both methods. The first method applies these random weights to scale whole distributions that sum to a single age distribution for comparison to the mixed sample (Figure 2.1B-C, left). The second method randomly subsamples 60 ages from source 1, 10 ages from source 2, and 30 ages from source 3 ($s = 100$ ages), which is repeated $S = 50$ times to produce 50 different CDFs and PDPs for comparison to the mixed sample (Figure 2.1B-C, right). The second method is much more computationally intensive than the first because it requires multiple rounds of subsampling source ages and constructing model CDFs and finite mixture distributions for each trial.

Monte Carlo model random weighting

A critical part of the mixing model is the method of randomly weighting each source sample age distribution. The ideal random weighting scheme is one that is capable of testing the entire sample-weighting space ranging from equal weighting for all samples to extremely asymmetric weighting (i.e., high and/or low weights for one or more samples). The latter critically effects the model's ability to exclude non-contributing samples from the final, best-fit weighting.

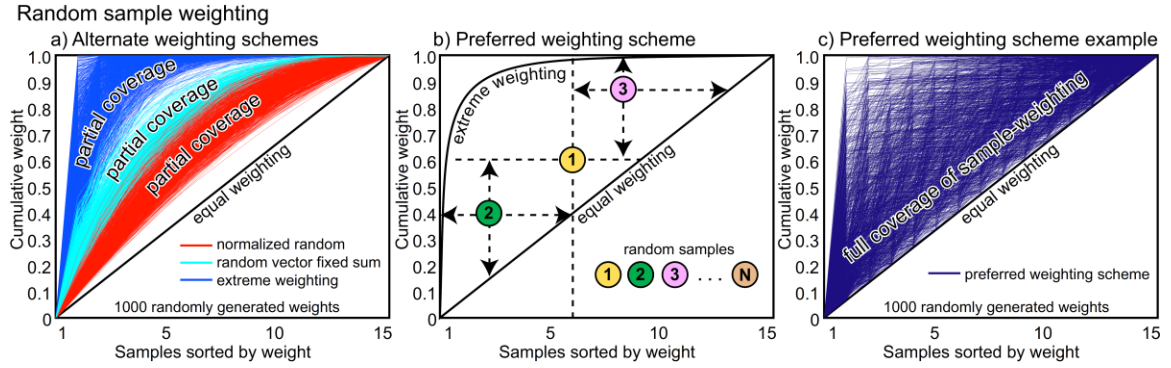


Figure 2.2. Random weighting schemes shown as cumulative distribution functions (CDFs). (A) One-thousand randomly generated CDFs using the three different weighting schemes tested in this study. All three prove to be inadequate because none of them cover the full range of potential weighting combinations (area above the equal weight line). (B) Preferred weighting scheme implemented in the Monte Carlo mixing model. (C) One-thousand randomly generated CDF weights following preferred random weighting method shown in (B). This method of random weighting ensures testing both equal weighting (equal contribution of all source samples) and extreme weighting (contribution from only one or a few source samples).

To test different random weighting schemes, randomly generated sample weights are plotted as CDF curves with samples sorted by weight on the x axis and cumulative probability on the y axis (Figure 2.2). This allows visualization of the range of weights generated from each method before they are to be randomly assigned to a group of source samples. We initially tested three different random weighting schemes, all of which failed to meet the requirements mentioned above. In the first weighting scheme, N samples are each given a random number that is normalized by the sum of those random numbers (“normalized random”, Figure 2.2A). Although this method of generating random weights is simple and intuitive, it fails to test even a third of the possible weighting combinations, is heavily bias toward the median (0.5 before normalization), and tends toward equal weighting with increased N (red lines in Figure 2.2A). The second

weighting scheme uses a conditional distribution of uniform random variables distributed over 0 and 1 that guarantees uniform random weighting (“random vector fixed sum”, Figure 2.2A). Although it yields a higher distribution of weights than the previous method, and resolves the issue of bias toward the median, it still cannot cover the random weighting space (light blue lines in Figure 2.2A). The third weighting scheme first randomly selects a weight between 0 and 1, which is then subtracted from the sum of the total sample remaining (beginning with a total of 1). Subsequent random weights may only be selected within the remainder $(1 - \sum \text{weights})$. The final weight assignment is simply the sum total weights subtracted from 1. This scheme tends to give very high weights to one or a few samples, and low weights (usually close to 0) to the rest, resulting in ‘extreme’ weighting of samples (blue lines in Figure 2.2A). Even if all three of these weighting schemes are implemented, there is still an obvious gap in the generated weights (Figure 2.2A) that is exacerbated with increasing numbers of potential source samples (Appendix 1), which would result in significant bias in the Monte Carlo mixing model.

An alternative, preferred weighting scheme is schematically shown in Figure 2.2B. Here, sample weights are determined by first choosing a random sample number between 0 and N (x axis) and assigning it a random number between 0 and 1 (y axis) above the equal weight line (Figure 2.2B). All subsequent random samples in both dimensions are restricted in where they can be placed as to result in a monotonically increasing function. Following construction of the CDF, the weights are randomized by sample number and applied to the source samples. This weighting scheme ensures full

coverage of possible weighting assignments when plotted as a CDF (Figure 2.2C), regardless of how many source samples are weighted (Appendix 2).

Quantitative comparison of age distributions

Three comparison methods are used to compare source sample age distributions to mixed samples: the two-sample KS test D statistic, the two-sample Kuiper test V statistic, and the cross-correlation coefficient (coefficient of determination, R^2) (Figure 2.1C). The KS D statistic is the maximum absolute distance between two CDFs: $D = \max(|CDF_1 - CDF_2|)$ (Stephens, 1970). The Kuiper test is a common variant of the KS test, and is the sum of the maximum distance between two CDFs subtracted from one another: $V = \max(CDF_1 - CDF_2) + \max(CDF_2 - CDF_1)$ (Kuiper, 1960; Press et al., 2007). The cross-correlation coefficient is calculated as the coefficient of determination (R^2) of cross plots of finite mixture distribution quantiles (PDPs or KDEs) (Saylor et al., 2012, 2013; Saylor and Sundell, 2016).

Each of these methods of comparing age distributions has its strengths and weaknesses. The KS D and Kuiper test V statistics are the basis for well-established statistical methods (Kuiper, 1960; Stephens, 1970; Press et al., 2007); using the difference between two CDFs, as opposed to p-values generated from those differences, has recently been established as a useful tool for comparison of detrital age distributions (e.g., Satkoski et al., 2013; Vermeesch, 2013; Saylor and Sundell, 2016). The cross-correlation coefficient has also recently been adapted for use in detrital geochronology quantitative comparison (Saylor et al., 2012, 2013), and has been shown to have more discriminatory power than the KS and Kuiper test D and V statistics, with more sensitivity to the number and proportion of age modes in finite mixture distributions

(Saylor and Sundell, 2016). The cross-correlation coefficient of PDPs also takes into account sample uncertainty by using the analytical uncertainty of each age as the kernel for individual Gaussian curves that are summed and normalized to construct the finite mixture distribution. Neither the KS test D statistic nor the Kuiper test V statistic takes into account sample uncertainty, as the empirical CDFs are constructed solely based on mean ages of an age distribution. In some cases, this may be considered a strength, for example if comparing detrital age distributions with wildly varying uncertainties which could potentially bias PDPs toward individual ages of high and low kurtosis for young and old ages, respectively. This could be resolved by using KDEs, as they too do not incorporate age uncertainty, but only if a proper bandwidth can be determined (e.g., Andersen et al., 2016). Finally, the KS test is more sensitive about the median of the age distribution, whereas the Kuiper test guarantees equal sensitivity across the entire range of ages in the samples (Kuiper, 1960; Press et al., 2007).

None of these comparison methods are statistical hypothesis tests. The KS D statistic and Kuiper V statistic are required to generate p-values, but are in themselves only measures of similarity when interpreted in the absence of associated p-values. Although p-values can give statistical measures of confidence, they are not well-suited for comparison of detrital geochronology data because they reject the null hypothesis at a higher rate than predicted for the selected p-value (Vermeesch, 2013; Saylor and Sundell, 2016). The cross-correlation coefficient is a statistical measure of 2-dimensional scatter plots, but in its implementation here is merely a relative measure of similarity between finite mixture distributions. Thus, results for all three tests are always relative, and no hard cutoff or absolute confidence levels can be used when interpreting model results.

Forward modeling

Although unmixing detrital age distributions can be approached using a forward model, it is computationally intensive to do so. In a deterministic forward model, all possible combinations of sources summing to 100% are calculated, and the best-fit model result, or range of top model results, are interpreted as the most probable source contributions for a given mixed sample. Unfortunately, this method is highly computationally intensive, even for a relatively small number of source samples, because the number of possible permutations that sum to 100% for source contributions at the integer percent level is given by

$$\frac{(N + d - 2)!}{(N - 1)!} \times \frac{1}{(d - 1)!}$$

where N is the number of source samples and d is the number of possible source weights for an individual source sample ($d = 101$ for 0 to 100% in increments of 1%). For low- N ($N \leq 4$) data sets, it is reasonable to take a forward modeling approach (e.g., Licht et al., 2016), as 3 and 4 samples only have 5,151 and 176,851 possible combinations that sum to 100%. However, as N becomes larger, there are simply too many combinations of sources to be computationally efficient: 5 sources results in 4,598,126 potential source combinations; 10 sources results in 4,263,421,511,271. In contrast, the inverse Monte Carlo approach is capable of handling any number of input source samples.

A forward modeling approach is feasible if it is first constrained by the inverse Monte Carlo modeling results, and highly efficient if implemented as a forward optimization routine. We implemented two different optimization methods, both initially constrained by results from the inverse Monte Carlo model. The first method is an

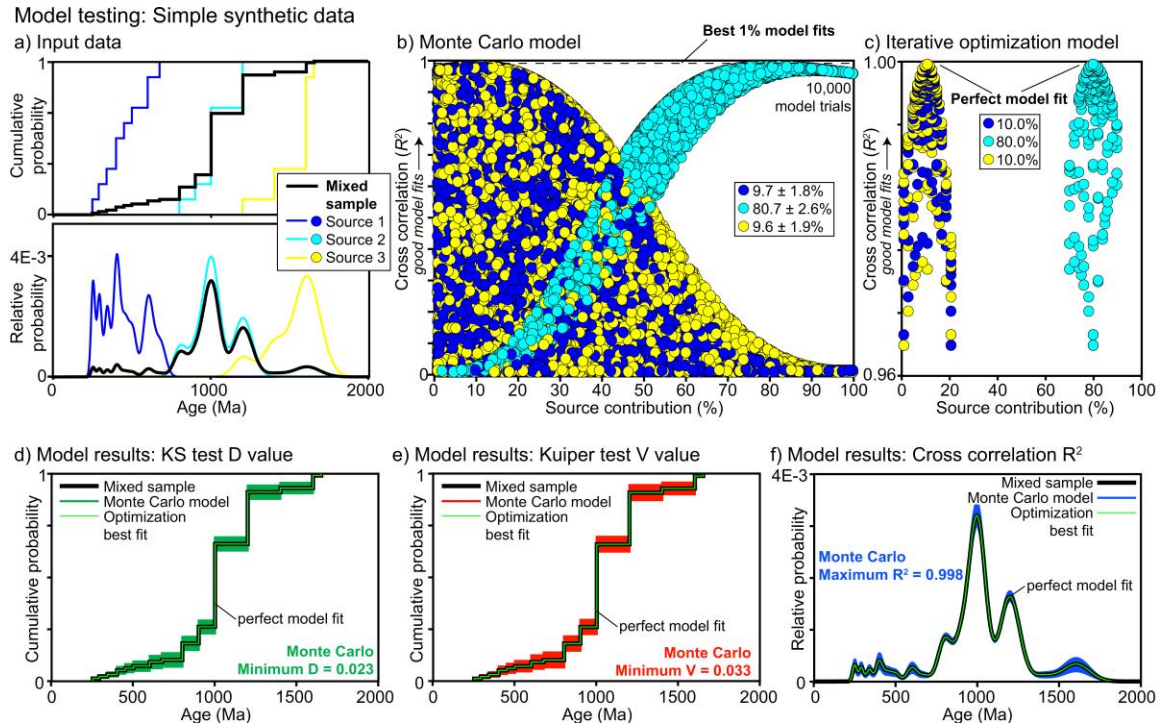


Figure 2.3. Simple synthetic data and model results. (A) Input synthetic source and mixed samples shown as cumulative distribution functions (upper) and probability density plots (lower). The mixed sample comprises 10% of source 1, 80% of source 2, and 10% of source 3. (B) Results of all 10,000 model trials, showing the percent contribution of each combination of sources and the Cross-correlation coefficient model result for each combination. (C) Results of the iterative optimization model, showing source combinations tested, and Cross-correlation coefficient for each combination. (D – F) Model results using the KS test D statistic (green) and Kuiper test V statistic (red) plotted as cumulative distribution functions (CDFs), and Cross-correlation coefficient R^2 (blue) as probability density plots. Black lines represent the mixed age distribution.

iterative forward model that takes the range of source contributions based on the mean and standard deviation of Monte Carlo results, and expands this range to be multiple of 10%. For example, a Monte Carlo-modeled individual source contribution of $25 \pm 7\%$, would have a range of 18 – 32%, which would be used to constrain the forward model at 10 – 40%. The forward model then tests all possible combination of sources at a 10% ‘grid spacing’. A user-specified number of best fits is then used to constrain

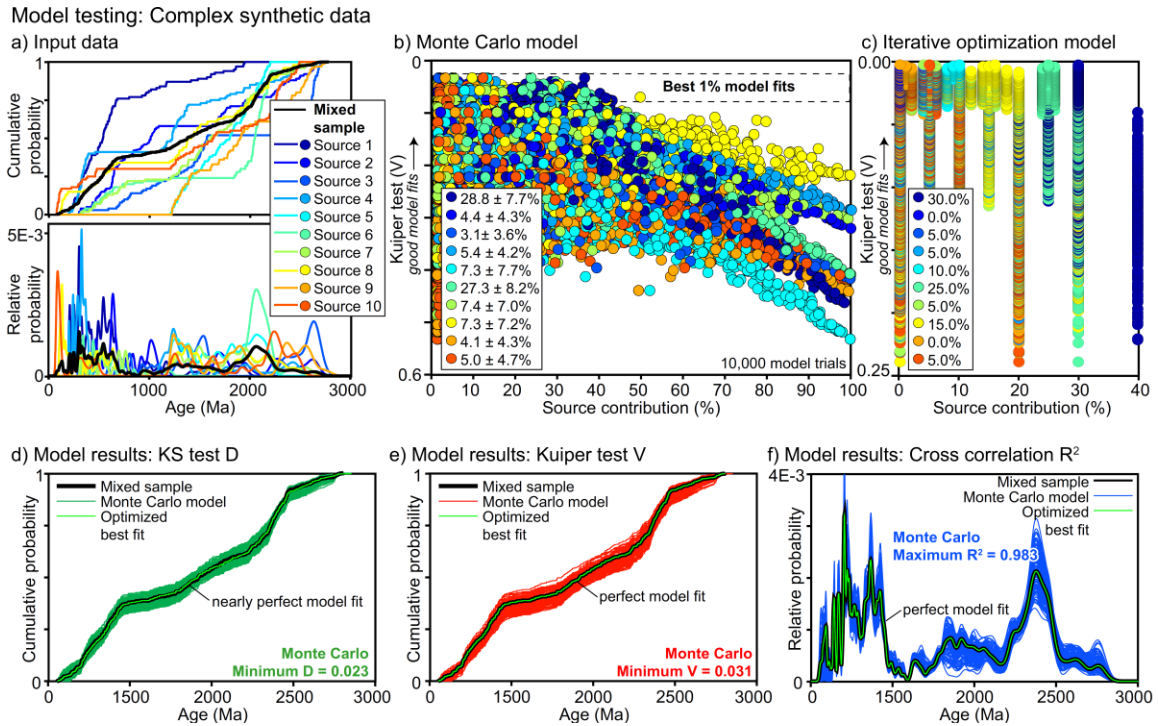


Figure 2.4. Complex synthetic data and model results. (A) Input synthetic source and mixed samples shown as cumulative distribution functions (upper) and probability density plots (lower). The mixed sample comprises 30, 0, 5, 5, 10, 25, 5, 15, 0, and 5% of sources 1 through 10, respectively. (B) Results of all 10,000 model trials, showing the percent contribution of each combination of sources and the Kuiper test V statistic model result for each combination. (C) Results of the iterative optimization model, showing source combinations tested, and Kuiper test V statistic for each combination. (D – F) Model results using the KS test D statistic (green) and Kuiper test V statistic (red) plotted as cumulative distribution functions (CDFs), and Cross-correlation coefficient (blue) as probability density plots. Black lines represent the mixed age distribution.

subsequent iterations at smaller increments (grid spacing) of 5%, 2%, and finally 1%. The best model fit is reported at the 1% level. The second optimization routine utilizes the interior-point constrained nonlinear optimization algorithm (fmincon) from the MATLAB Optimization Toolbox™. In this approach, the function minimization algorithm attempts to minimize the KS test D and Kuiper test V values calculated from CDFs, and $1 - R^2$ from cross-correlation of finite mixture distributions. A user-specified

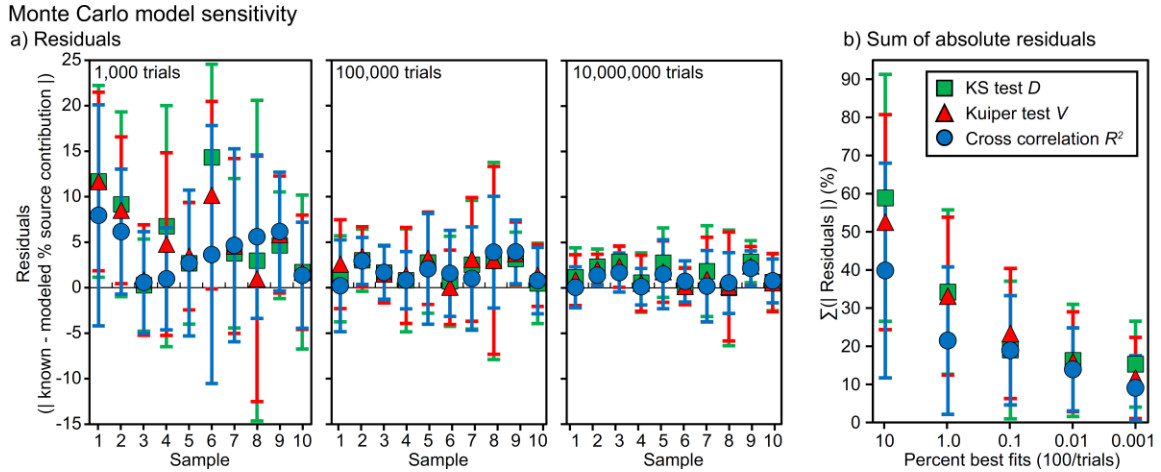


Figure 2.5. Monte Carlo sensitivity testing results based on the number of model trials of the complex synthetic data set shown in Figure 2.4 shows (A) an increasingly good fit between models and known source contributions with increasing numbers of trials run (corresponding to a lower percentage retained). (B) Summed absolute residuals show that the Cross-correlation coefficient achieves approximately the same accuracy as the Kuiper V or KS D statistic with an order of magnitude fewer model trials.

number of best fits (mean values of source contributions) from the Monte Carlo model results are used as initial guesses that the interior-point algorithm then iterates on to find a minimum function value. The lowest of these values is reported as the best model fit.

Model Testing

Mixtures of synthetic data sets in known proportions

The first test of the Monte Carlo mixing model is a proof-of-concept style test on a simple synthetic data set consisting of three, nearly unimodal source samples with minimal overlap in age populations (Figure 2.3A). Each of the 3 source data sets has 10 ages with 5% uncertainty at the 1σ level. A mixed sample was generated with a known contribution from each source sample of 10% from source 1, 80% from source 2, and 10% from source 3.

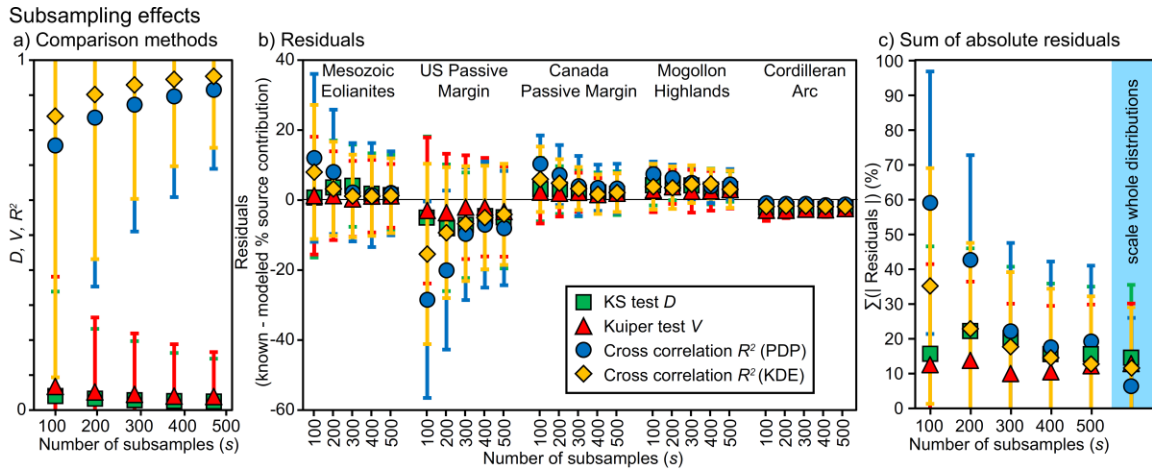


Figure 2.6. Inverse Monte Carlo model sensitivity based on subsample size (s) with the empirical North America data set from Laskowski et al. (2013) mixed in known proportions of 40, 30, 20, 10, and 0%. (A) While all comparison methods show a better fit between model and known distributions with increasing subsample size s , the Kuiper V and KS D statistics show the least improvement. (B) Residuals decrease for each of the potential source areas with increasing sample size. (C) Summed absolute residuals for the Cross-correlation coefficient decrease with increasing sample size, while those for the D and V value do not change within uncertainty. Residuals are generally higher and show more variability compared to scaling whole source distributions (highlighted in blue).

A second test of the Monte Carlo mixing model is on a more complex synthetic data set consisting of 10 source samples with multimodal, overlapping age populations (Figure 2.4A). Each of the 10 samples has 100 ages with uncertainty between 2 and 12% at the 1σ level. For comparison, a mixed sample was generated with known contributions from each source sample of 30, 0, 5, 5, 10, 25, 5, 15, 0, and 5% from sources 1 through 10, respectively.

Monte Carlo model sensitivity testing

We conducted two sensitivity tests of the Monte Carlo mixing model. The first is a test of the accuracy and efficiency of the model when scaling whole source distributions that uses the complex synthetic data set. The motivation for this test is to see how many

trials are required to perfectly match complex data mixed in known proportions; if the known mixtures cannot be matched by the model then perhaps the complex data are too complicated for it. In this test the number of trials is varied, and the top percentage is reported as the best 100 model fits. Hence, percentages vary by changing the number of model trials ranging from 10^3 (10% best fits) to 10^7 (0.001% best fits) (Figure 2.5).

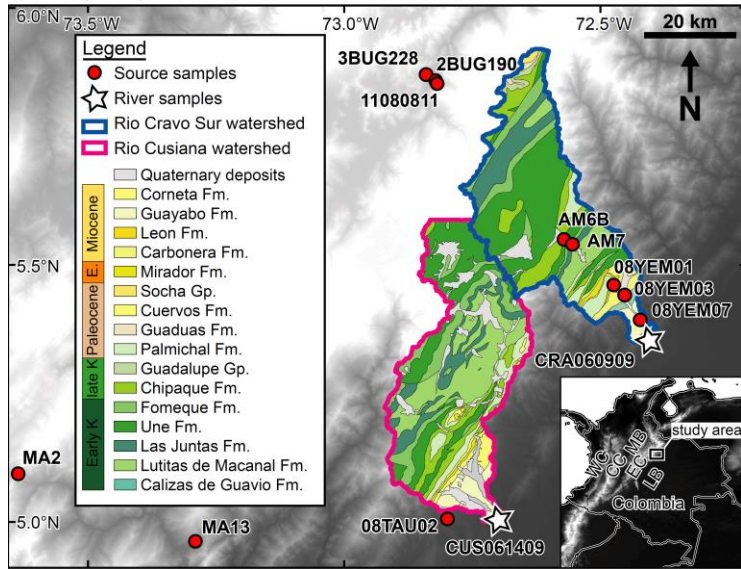
The second sensitivity test of the model uses a compilation of detrital zircon U-Pb data from North America (Laskowski et al., 2013). We constructed a data set of 5 source samples consisting of 500 randomly subsampled ages from five of the characteristic North American source groups: Mesozoic Eolianites, US Passive Margin, Canada Passive Margin, Mogollon Highlands, and Cordilleran Arc (Laskowski et al., 2013). We then mixed these source samples in known proportions to construct a synthetically mixed sample of empirical data in proportions of 40, 30, 20, 10, and 0%, respectively. The Monte Carlo model then randomly subsamples a total of 100 – 500 ages from these sources with tests in increments of 100 ($s = 100, 200, 300, 400, \text{ and } 500$) 50 times for each model trial ($S = 50$). The purpose of this is to test the effects of the two different source scaling methods (Figure 2.1B and C), to compare sample size effects when subsampling ages to construct source distributions (Licht et al., 2016) (Figure 2.1 B-D), right), and to compare results from cross-correlation of PDPs versus KDEs (using a 20 Myr kernel bandwidth) (Figure 2.6).

Mixtures of empirical data sets in unknown proportions

The first empirical data set is published detrital zircon U-Pb geochronology data from north-central Colombia (Saylor et al., 2013). This data set consists of mixed sample age distributions from two modern river sand samples collected from the trunk streams of

Empirical data set: Colombia

a) Geologic map



b) Detrital zircon U-Pb data

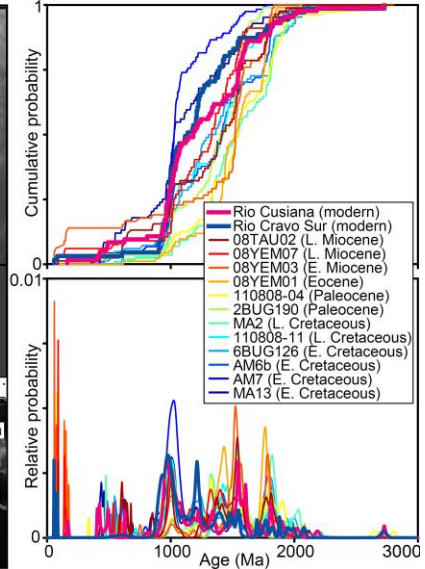


Figure 2.7. (A) Map of study area and sample locations in Colombia modified from Saylor et al. (2013). (B) Source and mixed sample data as cumulative distribution functions (upper) and probability density plots (lower) of detrital zircon U-Pb data considered in this study.

Rio Cravo Sur and Rio Cusiana, with source age distributions from sedimentary rocks in their respective drainage basins (Saylor et al., 2013) (Figure 2.7 and 2.8A). Sedimentary rocks in these catchments include Cretaceous shallow and transitional marine mudstones and sandstones, Paleocene coastal-deltaic shales, coals, sandstones, and fluvial mudstones and sandstones, early Eocene alluvial fan and fluvial sandstones with subordinate conglomerates, late Eocene coastal and marine mudstones and sandstones, and Miocene non-marine alluvial deposits (Cooper et al., 1995; Horton et al., 2010; Saylor et al., 2013, and references therein). Detrital zircon U-Pb age distribution for each source sample was characterized either directly within the catchments (e.g., samples AM6B), or by proxy from equivalent strata outside of the catchment area (e.g., sample MA2). We chose this study area for a number of reasons. First, it is a modern system with

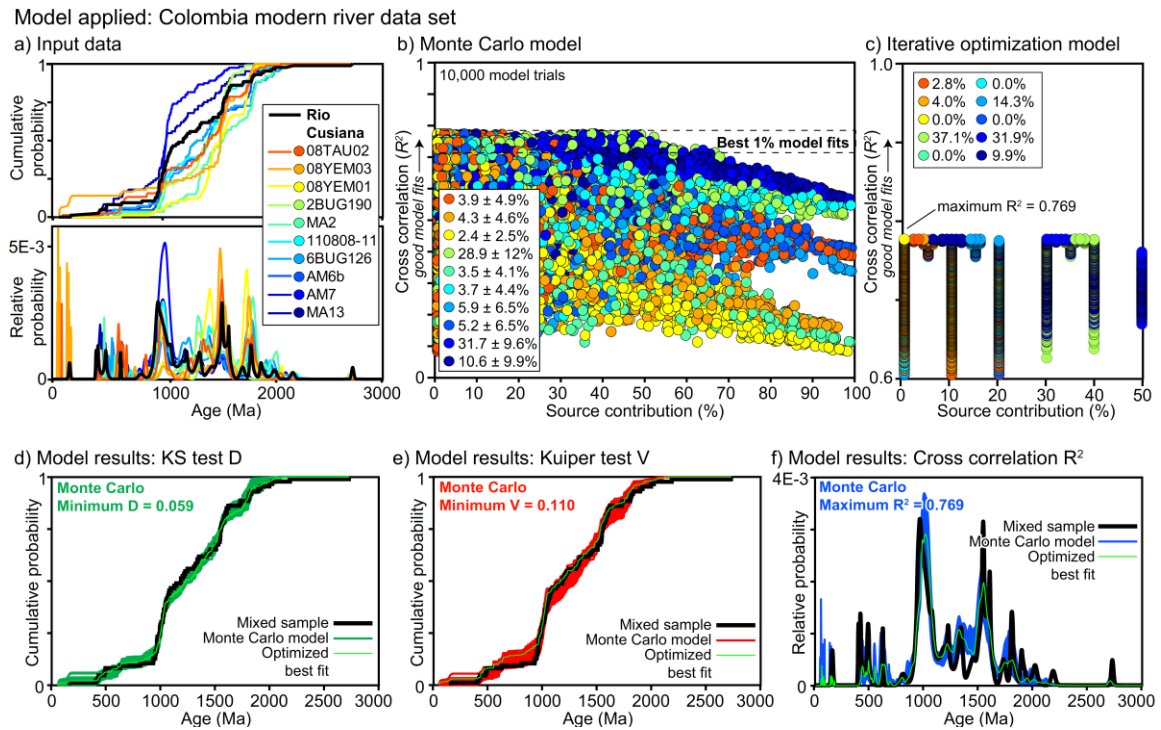
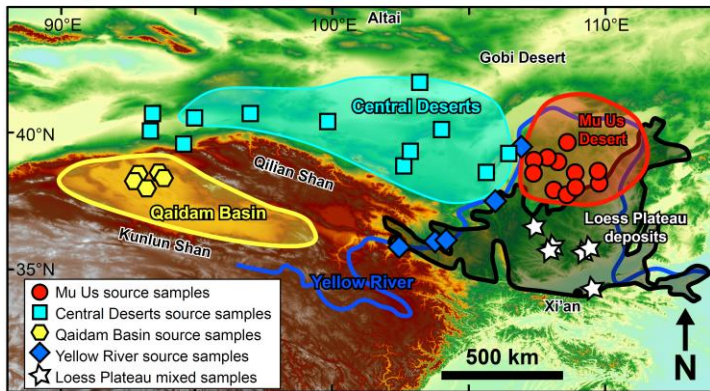


Figure 2.8. Data and model results from the Rio Cusiana data set (Saylor et al., 2013). (A) Input source sample data from the river catchment (or by proxy outside the catchment) and mixed sample data from river sand shown as cumulative distribution functions (upper) and probability density plots (lower). (B) Results of all 10,000 model trials, showing the percent contribution of each combination of sources and the Cross-correlation coefficient model result for each combination. (C) Results of the iterative optimization model, showing source combinations tested, and Cross-correlation coefficient for each combination. (D – F) Model results using the KS test D statistic (green) and Kuiper test V statistic (red) plotted as cumulative distribution functions (CDFs), and Cross-correlation coefficient (blue) as probability density plots. Black lines represent the mixed age distribution.

a simple geologic setting of two drainage basins comprised of simple drainage networks, so we know what units are currently being sourced. Second, the catchments are relatively small, and hence should be easily characterized. Third, the units have well-defined detrital zircon U-Pb age distributions from sedimentary rocks (Horton et al., 2010; Saylor et al., 2013), each with a characteristic age distribution presumably combined into a single mixture at the trunk streams of the drainage networks where modern sands were sampled (Figure 2.7A).

Empirical data set: Central China

a) Geologic map



b) Input data

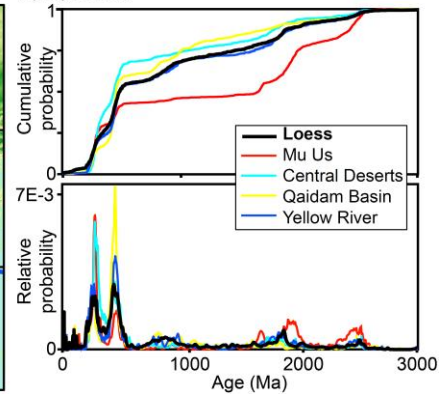


Figure 2.9. (A) Map of study area and sample locations in central China modified from Licht et al. (2016). (B) Source and mixed sample data as cumulative distribution functions (upper) and probability density plots (lower) of detrital zircon U-Pb data considered in this study.

Finally, because only sedimentary rocks are sourced, igneous zircon fertility (e.g., Moecher and Samson, 2006; Dickinson, 2008) is a nonissue; however, differential zircon contribution based on source grain size or hydrodynamic sorting (e.g., Garzanti et al., 2009; Lawrence et al., 2011) could be problematic, as units comprised of dominantly mudrocks likely contribute little to the river sand detrital age distribution.

The second empirical data set is a compilation of detrital zircon U-Pb data from the Loess Plateau in central China consisting of a large compilation of source samples for comparison to eolian loess and paleosol mixed samples (Licht et al., 2016, and references therein). In total, 37 source samples are combined regionally into 4 large-*n* source samples, and 8 loess samples and 9 paleosol samples are combined into 2 mixed samples (Licht et al., 2016) (Figures 2.9 and 2.10A). The four potential provenience zones are the Mu Us desert, the Central deserts, The Qaidam Basin, and the Yellow River (Figure 2.9A), which consist of eolian dune, yarding, lacustrine, and fluvial sandstone deposits

(Licht et al., 2016). The first reason for testing this data set is to compare results of our mixing model directly to results in Licht et al. (2016), who implement construction of model source age distributions by random subsampling of source ages (Figure 2.1B-D, right). We also chose this data set compilation because it affords a test of large- n samples, which are predicted to provide a better characterization of age distributions (e.g., Pullen et al., 2014; Saylor and Sundell, 2016). Finally, we chose this data set because of the scale of the geologic setting: eolian transport distances would have to be > 1000 km in some cases in this study area, which is in stark contrast to the short (< 100 km) fluvial transport distances of the Colombia geologic setting.

Results

For unmixing synthetic and empirical data, model results generated using the KS D statistic, Kuiper V statistic, and cross-correlation coefficient (R^2) are reported as the mean and one standard deviation of the best 100 model fits (lowest D and V, highest R^2) of 10,000 model trials, which represents the top 1% of model trials. Results are shown compared to mixed sample CDFs and finite mixture distributions. Reporting of model sensitivity testing results differs slightly as described below.

Mixtures of synthetic sources in known proportions

Results from the first proof-of-concept test of simple synthetic data demonstrate that the top 1% of the Monte Carlo mixing model trials reproduce known source sample percent contributions within 1σ uncertainty (Figure 2.3). Figure 2.3B shows the range of randomly generated weight combinations of input source samples versus the resulting PDP cross-correlation coefficient for all 10,000 trials of this model run. The top 1% of the model age distributions compared with the mixed age distributions shows that

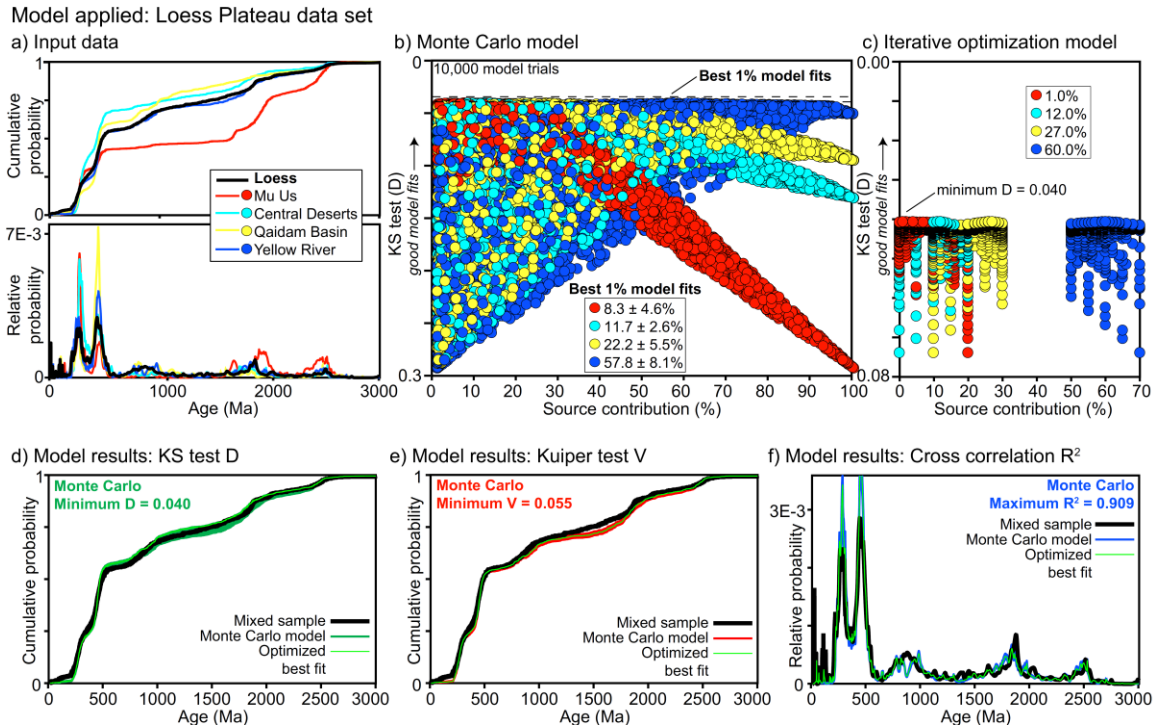


Figure 2.10. Data and model results from the Loess Plateau data set (Licht et al., 2016). (A) Input source sample data shown as cumulative distribution functions (upper) and probability density plots (lower). (B) Results of all 10,000 model trials, showing the percent contribution of each combination of sources and the KS test D value model result for each combination. (C) Results of the iterative optimization model, showing source combinations tested, and KS test D value for each combination. (D–F) Model results using the KS test D statistic (green) and Kuiper test V statistic (red) plotted as cumulative distribution functions (CDFs), and Cross-correlation coefficient (blue) as probability density plots. Black lines represent the mixed sample age distribution.

although there is a slight range about the mixed sample, each quantitative method accurately predicts the known source contribution without any a priori knowledge of it. Low minimum D and V values of 0.02 and 0.03, and a high maximum R^2 of 0.998, also demonstrates a nearly perfect match between the known and modeled sample weights for the single best-fit trial of the Monte Carlo model. Furthermore, both optimization routines yield exact matches to known source sample contributions with minimum D and V values of 0, and a maximum R^2 of 1 (Figure 2.3D – F).

Results of the second proof-of-concept test of complex synthetic data are generally similar to those of the simple synthetic data, but show higher variability (Figure 2.4). There is a considerably larger range in the best 1% model fits, as shown by plotting weight combinations against resulting Kuiper test V value (Figure 2.4B), as well as a larger swath of results about the CDFs and PDP in Figures 2.4D – F. Nevertheless, the top 1% of Monte Carlo model results reproduce the known source contributions within 1σ uncertainty (with one exception where a non-contributing source is 0.1% beyond the 1σ uncertainty range). Despite the increased variability, iterative optimization models constrained by inverse Monte Carlo results yield a nearly perfect model fit for the KS test D of 0.007, and perfect model fits for Kuiper V of 0, and cross-correlation R^2 of 1; minimum search optimization yields perfect model fits for all comparison methods with $D = 0$, $V = 0$, and $R^2 = 1$, respectively.

Monte Carlo model sensitivity testing

Residuals (modeled contributions subtracted from known contributions) from scaling whole age distributions of the complex synthetic data set systematically decrease with increasing trials (Figure 2.5). Results show relatively high residuals with large standard deviations based on the top 10% of 1,000 model trials (Figure 2.5A). Residuals at this 10% level are on average slightly higher with larger standard deviation for the KS D statistic at $6 \pm 10\%$, compared to the Kuiper V and cross-correlation coefficient which give mean and standard deviations of $5 \pm 9\%$ and $4 \pm 8\%$, respectively. Model results show a dramatic improvement when attempting more model trials and retaining a lower percent of best fits for all comparison methods (Figures 2.5B and C). For this complex data set, the sum of residuals for all ten samples is as low as 0.15 ± 0.11 for the KS D

statistic, 0.12 ± 0.11 for the Kuiper V statistic, and 0.09 ± 0.08 for the cross-correlation (0.001% best model fits), requiring 10^7 model trials (Figure 2.5 D). The cross-correlation reaches this minima with an order of magnitude fewer model runs, and with lower uncertainty for 10^6 trials (0.01% model fits, Figure 2.5D). In nearly all sensitivity tests, the cross-correlation yields both lower absolute residuals with lower associated standard deviations than the other two comparison methods (Figure 2.5).

Inverse Monte Carlo modeling by randomly subsampling raw ages from source distributions of empirical data from Laskowski et al. (2013) mixed in known proportions shows drastically different results compared to scaling whole distributions. In all cases the model gives better results when subsampling more ages (larger s), but are highly variable for all comparison methods, D, V, and R^2 (Figure 2.6A). cross-correlation of finite mixture distributions shows higher variability in resulting R^2 values, and with higher residuals (modeled contributions subtracted from known contributions) than corresponding D and V model results (Figure 2.6A). In all subsampling cases ($s = 100$ to 500) the Kuiper test V comparison method gives the lowest residuals and cross-correlation of PDPs gives the highest (Figures 2.6B and C); however, none give lower residuals than when scaling whole source distributions (Figure 2.6C).

Mixtures of empirical sources in unknown proportions

A key difference between testing synthetic data and testing empirical data is we do not know the true contribution from each source sample. For brevity, and because model results are generally similar among empirical data sets, we only present and discuss results of Rio Cusiana from the Colombia data set (Saylor et al., 2013), and the loess sample from the Loess Plateau data set (Licht et al., 2016).

Inverse Monte Carlo model results for Rio Cusiana yield an imperfect match (Figure 2.8). As with the synthetic data set, plotting sample weight combinations against cross-correlation coefficient shows that the best-fit scenario is indeed a mixture of the sources, but in the case of the empirical data yields an imperfect fit with a maximum $R^2 = 0.769$ (Figure 2.8B). Although these model results are indeed an improvement over those reported by Saylor et al. (2013) based on comparison of source samples weighted equally ($R^2 = 0.64$) and by percent area in the catchment ($R^2 = 0.73$), they are still far from a perfect fit, and apparently cannot match the mixed river sample age distribution based on the input source data; this is also the case for the minimum D and V values of 0.059 and 0.110, respectively. Results based on optimization routines are similar to each other, and to best fit inverse Monte Carlo results, with minimum D of 0.053 – 0.055, minimum V of 0.098, and a maximum R^2 value of 0.778 (Figures 2.8D – F).

Inverse Monte Carlo model results for the Loess plateau data set are generally similar to those presented in Licht et al. (2016) (Figure 2.10), regardless the source scaling method employed (scaling whole source distributions or randomly sampling ages from within those distributions, Figure 2.1). Figure 2.10B shows Monte Carlo model source combinations plotted against KS test D values, with sample source contributions of $7.7 \pm 4.7\%$ for Mu Us, $11.3 \pm 2.5\%$ for the Central Deserts, $21.8 \pm 4.6\%$ for Qaidam, and $59.2 \pm 7.4\%$ for the Yellow River. These results are generally similar to those of Licht et al. (2016), who report source contributions of 6 – 8% from the Mu Us, 12 – 14% for the Central Deserts, 14 – 20% for the Qaidam basin, and 58 – 68% for the Yellow river. The Monte Carlo model yields minimum D and V values of 0.040 and 0.055, and a maximum R^2 value of 0.909 (Figures 2.10D – F). Optimization routines yield no

improvement in D, V, or R² values, but give slightly different best-fit model weights compared with those determined through inverse Monte Carlo modeling: 1% for Mu Us, 12% for the Central Deserts, 27% for Qaidam, and 60% for the Yellow River.

Discussion

Differences among comparison methods

Quantitative comparison methods employed in the mixing model (KS D, Kuiper V, and cross-correlation) give broadly similar results based on tests involving synthetic and empirical data. Each method is capable of reproducing mixing proportions of source age distributions with a high degree of confidence from both simple and complex synthetic data (Figures 2.3 and 2.4) and empirical data (Figures 2.8 and 2.10). Sensitivity testing of complex synthetic data demonstrates each methods' ability to accurately quantify source contribution of detrital age distributions if the source and mixed samples are adequately characterized. The mixture model is also capable of covering the entire range of combinations of a given set of source samples, as demonstrated in the visualized Monte Carlo plots in Figures 3B, 4B, 8B, and 10B. Complete coverage of each potential source sample along both the x and y axes in these plots is indicative of three things: 1) the mixture model successfully samples the full range of source combinations, including extreme weights, 2) the model disregards source samples that do not contribute to the mixed sample age distribution, and 3) a mixture of source samples, rather than any single sample, yields the closest approximation to the mixed sample for data sets tested here. This gives credibility to the random weighting method implemented in the mixing model (Figures 2.2B and C), and would likely not be possible had alternative weighting schemes been implemented (Figure 2.2A).

Comparison methods yield similar results when scaling whole source age distributions for comparison to mixed samples, but differ when subsampling raw source ages. Cross correlation of PDPs has a clear advantage over the other methods when scaling whole source distributions (Figure 2.1B-D, left), as demonstrated by sensitivity test results showing lower absolute residuals and associated standard deviations with fewer model trials (Figure 2.5). However, when randomly subsampling ages to build source distributions (Figure 2.1B – D, right) the cross correlation of PDPs and KDEs appear to perform poorly compared to the KS and Kuiper D and V methods (Figure 2.6). We attribute these highly variable results of cross-correlation to finite mixture distributions being inherently more complex, with the chance of higher variability in distribution shape. Further, cross-correlation of PDPs yields highly variable results even compared to cross-correlation of KDEs (Figure 2.6). This latter point is likely a result of highly differing sample uncertainties in the North America empirical data compilation (Laskowski et al., 2013), and potentially exacerbated by selection of small numbers of ages from some samples (e.g., 5% of 100 ages would require that only 5 ages would be drawn from that source).

On consideration of the empirical river and catchment samples, all of the comparison methods yield imperfect model fits. Because we know the model is capable of reproducing known mixture proportions when there is indeed a viable solution (e.g., Figures 2.3 and 2.4), we interpret this poor fit as an indication the source samples cannot reproduce the mixed river sample in any mixture, and that perhaps the sediment sources in the drainage basin, the mixed sample, or both, have been inadequately characterized.

Our preferred comparison methods differ depending on type of source scaling (Figure 2.1B and C). Cross-correlation of mixture distributions is our preferred comparison method when scaling whole source distributions for several reasons which can be summarized as follows: 1) it appears to be the most sensitive with more discriminatory power than the KS test D statistic and the Kuiper test V statistic based on tests of complex synthetic data, 2) it requires fewer trials to produce model results with lower residuals than the KS D and Kuiper V statistics, and 3) it hones in more quickly to reasonable estimates for source weights when there is a viable solution from the input data (Figure 2.5C). Our preferred comparison method when subsampling raw source ages is the Kuiper test V statistic primarily based on consistently low residuals when varying the number of subsampled ages (s) (Figure 2.6C). That said, results are variable among comparison methods when subsampling source ages, and never produce model fits as good as when scaling whole source distributions (Figure 2.6C), which warrants further testing of this technique. However, a test of this would require very large input data sets subsampled to large model comparisons ($s > 1000$). Unfortunately, it is extremely computationally intensive to perform such a test. Users are encouraged to interpret results with caution for all comparison methods when subsampling raw source age distributions, especially given the amount of relatively low- n legacy data sets in the literature.

Implications for applied studies

Although our preferred method for quantitative comparison is the cross-correlation coefficient of PDPs with scaling whole source distributions, we recommend the use of at least both the cross-correlation coefficient and Kuiper test V statistic, as each has particular strengths and weaknesses. This is particularly important for applied studies

of ancient sample data where the true mixture of sources is always a nonunique solution, and it is more difficult to determine source contribution than, for example, the Saylor et al. (2013) modern river data set presented above. This latter point raises an important question of what does it mean if the mixing model is not capable of reproducing a mixture of input sources with a high degree of confidence (high KS D and Kuiper V, and/or low cross-correlation R^2 values)? For the modern river study, the mixing model can only produce a maximum cross-correlation of PDPs of 0.77 for Rio Cusiana. For comparison, this is higher than equally weighted source samples and source samples scaled by catchment outcrop area (0.64 and 0.73, respectively) (Saylor et al., 2013). Although higher values means the Monte Carlo mixing model does a better job of matching the river sample age distributions, there is clearly something missing. It is not that the sample data are too complex to match because when there is a solution, as in the sensitivity test example (Figure 2.5) and forward optimization results of synthetic data (Figures 2.3C and 2.4C), the mixing model can clearly find it. We interpret such situations of poor model fits as an inadequate characterization of the source and/or mixed sample, possibly due to small sample sizes. It may also reflect failure to identify some age component(s) in the source area.

The Loess Plateau model results provide a nice comparison to the Colombia modern river results because it is a study in the ancient rather than the modern, it is on a much larger scale (1000s of km), and it incorporates much larger- n data sets for comparison. The Loess Plateau model results, although not perfect, give much better model results compared to the Colombia data set. It appears sample size is a dominant

control on model results, and low- n source and/or mixed samples should be treated with caution as they may lead to misinterpretation of sediment provenance.

For the Saylor et al. (2013) study, as well as other studies in both the modern and ancient, uncertainty can be mitigated in a number of ways: 1) by increasing the sample size (n) for all samples, both for source and mixed samples, 2) by eliminating proxy source samples and only sampling within the drainage basins (specific only to modern river studies), 3) by considering differences in zircon abundance within different source units to avoid bias based on zircon size due to hydrodynamic sorting (Morton and Hallsworth, 1994; Gehrels, 2000; Garzanti et al., 2009; Lawrence et al., 2011), or differential igneous zircon fertility (e.g., Moecher and Samson, 2006; Dickinson, 2008), and 4) by analyzing multiple samples from the same interval or broadening the number of source intervals considered to better characterize potential sources. This aspect of the research provides important feedbacks to experiment design and execution. Having demonstrated that the model can find a perfect solution when one exists will hopefully guide future provenance research to search for a mixture of sources that provides such a perfect fit.

Mixing model implementation

The Monte Carlo mixing model has been developed into a MATLAB-based graphical user interface (GUI). The GUI is available as a stand-alone executable (.exe file), along with the annotated source script in the Texas Digital Library. We also include a step-by-step user manual, with which the results presented in this manuscript are easily reproduced for both synthetic and empirical data sets.

All results produced by the mixing model are nonunique, as the mixing model will estimate mixing proportions regardless of the quality of the comparison fit. All results should be interpreted with a thorough understanding of geologic context, and in consideration of alternative comparison techniques such as multidimensional scaling (e.g., Vermeesch, 2013). Furthermore, although there is a significant improvement in model fits with an increased number of model trials (Figure 2.5), there is a tradeoff between compute time and desired goodness of fit. How many models trials required for the mixing model to predict accurate and robust results is highly dependent on sample complexity; the number of model trials is only limited by the computer's memory. Sensitivity testing of the Monte Carlo method is essential in order to develop a first-order sense of source and mixed sample complexity, and to determine what is required to produce a model fits within desired limits.

Conclusions

We present a MATLAB-based inverse Monte Carlo method of randomly constructing source age distributions for comparison to individual mixed samples to determine mixing proportions of source sample contributions. Inverse Monte Carlo results may be used to constrain forward optimization routines to find a single best model fit. This model is applied to synthetic data in a proof-of-concept style test of the model, and published detrital zircon U-Pb empirical data from North America (Laskowski et al., 2013), Colombia (Saylor et al., 2013) and central China (Licht et al., 2016). Sensitivity testing of complex synthetic data show the mixing model is capable of sampling the full range of source sample weightings, and can reproduce sample age distributions as CDFs and PDPs very similar to the known distribution; poor model fits are attributed to

inadequate characterization of source and/or mixed samples. Sensitivity testing of subsampling source distributions for comparison to mixed samples based on empirical data from North America (Laskowski et al., 2013) shows results are highly variable among comparison methods, and users are cautioned in this approach for low- n data sets. The mixing model presented here, source code, and user manual, are available in the Texas Digital Library.

CHAPTER 3

Peruvian Altiplano stratigraphy highlights along-strike variability in foreland basin evolution of the Cenozoic central Andes

Submitted for publication in Tectonics August 21, 2017

Authors:

Kurt E. Sundell

Joel E. Saylor¹

Thomas J. Lapen¹

Richard H. Styron²

Dustin Villarreal¹

Paola Usnayo³

José Cárdenas³

¹Department of Earth and Atmospheric Sciences, University of Houston, Houston, Texas, USA

¹Earth Analysis, Seattle, Washington, USA

²Departamento Académico de Geología, Universidad San Antonio Abad del Cusco, Cusco, Peru

Introduction

Cenozoic basins archive the ongoing development of the central Andes, and development of the Andean plateau, Earth's second largest modern orogenic plateau. Protracted subduction of the Nazca oceanic plate beneath the South American continent resulted in mountain building, and generation of the low relief, high-elevation topography of the Altiplano. Nearly continuous, non-marine sedimentation during the Cenozoic records the Andean deformational history in the Altiplano-Puna plateau, which is characterized by high (~3800 m average) elevation, dominantly internal drainage, and relatively subdued relief compared to the higher elevation, more rugged terrains of the

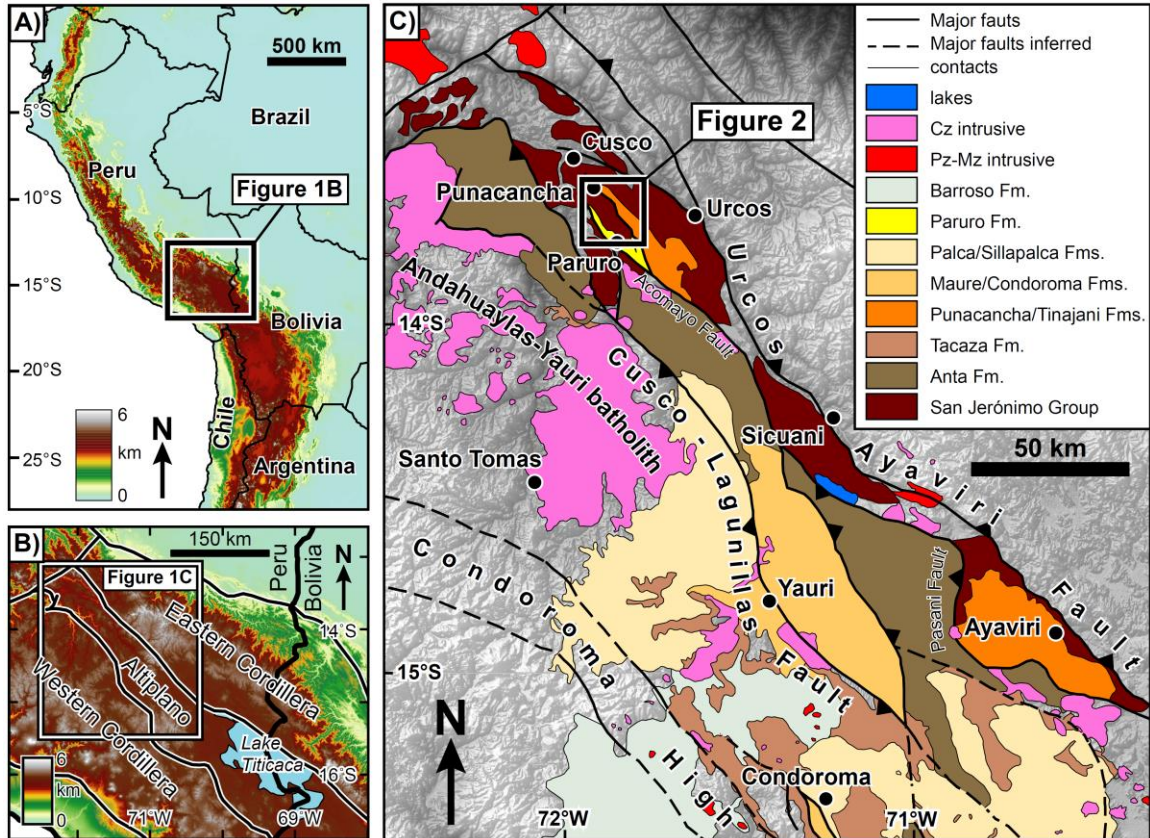


Figure 3.1. (A) Digital elevation model (DEM) of the Andean plateau from HYDRO1K data. (B) Physiographic regions of the northern extent of the Andean plateau. (C) Regional geologic map of southern Peru showing Cenozoic stratigraphy and Paleozoic–Cenozoic intrusive units redrafted from Carlotto (2013) overlain upon a hillshade DEM generated from Shuttle Radar Topography Mission 90 m data.

adjacent Western Cordilleran magmatic arc and Eastern Cordilleran fold-and-thrust belt (Figure 3.1B).

Early records of cross-cutting and stratigraphic relationships in this region set the foundation for, and continue to shape our current understanding of Andean plateau formation (e.g., Forbes, 1861; Berry, 1917; Newell, 1946, 1949). Although there is a general consensus that the Andean plateau formed in the Cenozoic (e.g., Jordan et al.,

1983; Isacks, 1988; Allmendinger et al., 1997), debates persist on the relative timing of different geodynamic processes controlling its formation (e.g., Barnes and Ehlers, 2009; Ehlers and Poulsen, 2009). For example, models calling solely on crustal shortening to explain regional elevation gain (e.g., Lamb, 2011) are typically at odds with views of plateau formation, suggesting a decoupling of surface uplift and crustal shortening (e.g., Garzzone et al., 2006, 2008; Saylor and Horton, 2014; Kar et al., 2016). Critical to addressing such questions are records of basin subsidence, surface uplift, and crustal deformation at different locations along orogenic strike. However, such records in the northern part of the Andean plateau of southern Peru have largely been obscured thick volcanic deposits (e.g., Mamani et al., 2008, 2010; Demouy et al., 2012), deformational overprinting during periods of oblique convergence (Carlotto, 2013), and contractional reactivation preexisting structures (e.g., Perez et al., 2016a). Cenozoic stratigraphy of the Peruvian Altiplano is a critical, yet relatively unexplored record of tectonic processes active during the Cenozoic construction of the Andean plateau.

Despite hosting a nearly complete record Cenozoic stratigraphy chronicling the mountain building history of the central Andes, the northernmost Altiplano of southern Peru has received less research focus compared to its central and southern counterparts in Bolivia, Chile, and Argentina (e.g., Coutand et al., 2001; Horton et al., 2001, 2002; Oncken et al., 2006; Strecker et al., 2007; DeCelles et al., 2015). While recent work in southern Peru has focused on the Eocene–Miocene sedimentary record by highlighting prolonged basin subsidence, episodes of punctuated deformation, and a broadly similar structural style of deformation and basin development to the Altiplano of Bolivia (Perez

and Horton, 2014; Horton et al., 2015), geodynamic implications of foreland basin system development in the northern reaches of the Peruvian Altiplano have not been thoroughly addressed.

We present new sediment provenance data in the context of ~6200 m of non-marine siliciclastic stratigraphy to address the Cenozoic tectonic history of this part of the central Andes. Provenance indicators from paleocurrent measurements, conglomerate clast counts, sandstone petrography, multidimensional scaling and mixture modeling of detrital zircon U-Pb data, and zircon roundness quantification, all suggest dominant sediment sourcing from the Peruvian Western Cordillera and/or western Altiplano throughout the Cenozoic, with little input from formations in the nearby (~50 km) modern Eastern Cordillera. Detrital zircon mixture modeling using DZmix (Sundell and Saylor, 2017) reveals brief pulses of Ordovician-age sediment input at ~36 and ~7 Ma, interpreted as timing of shortening-related exposure and sediment recycling. Mixture modeling further highlights the important role sediment recycling plays in this region. Development of an angular unconformity from 23–9 Ma is consistent with previously documented periods of deformation along strike to the south (Perez and Horton, 2014; Horton et al, 2015). When combined with sediment provenance indicators, results are consistent with the development and northeastward migration of a foreland basin system (*sensu* DeCelles and Giles, 1996). Details of this system provide predictive power for local and regional geodynamic processes, in particular the timing and location of hinterland loading due to crustal thickening and/or surface uplift in the Western Cordillera, and basin subsidence to the east. Further, results provide a comparison to

previously documented foreland systems in the modern Altiplano and Eastern Cordillera along strike to the south (e.g., Horton et al., 2001, 2002, 2015; DeCelles and Horton, 2003; DeCelles et al., 2011), and reveal an apparent southward younging in the onset of high sedimentation rates resulting in thicker stratigraphic packages later in the process of foreland basin system evolution. Finally, consideration of the results of this research in the context of published records of magmatism, igneous geochemistry, and limited records of crustal shortening and surface uplift, support models calling on cyclical orogenic processes (e.g., DeCelles et al., 2009; Ramos, 2009; Ramos et al., 2014; DeCelles et al., 2015), but highlight major temporal differences in the onset and tempo of cyclicity along orogenic strike.

Geologic Background

The Pacific margin of the South American continent has undergone continuous ocean-continent convergence since at least the late Paleozoic resulting in Earth's longest modern continuous mountain chain (Allmendinger et al., 1983), and development of the Andean plateau, the most prominent modern topographic feature associated with ocean-continent convergence. Despite long-lived subduction and the protracted magmatic and tectonic history of the region (e.g., Chew et al., 2007; Bahlburg et al., 2011), the Andean plateau developed in the Cenozoic (Jordan et al., 1983; Allmendinger et al., 1997). Isacks (1988) define the Andean plateau as the broad area of high (>3 km) topography in the central Andes that stretches north-south approximately 1800 km from southern Peru to northern Argentina, and east-west 350–400 km at its widest across Bolivia (Figure 3.1A). It can be divided into physiographic regions, which from west to east are

the modern interface between the subducting Nazca oceanic plate and the South American continent of the Precordillera (Figure 3.1A), the active volcanic arc of the Western Cordillera, the broad and relatively flat-lying region of internal drainage that defines the Altiplano Plateau, the rugged and high topography of the earlier Eastern Cordilleran/Inteandean retroarc orogenic front, the modern retroarc fold-and-thrust belt of the Subandean zone, and the modern flexural foreland basin to the east in Amazonia (Figure 3.1B).

Tectonic history and sediment recycling

Determining sediment sources for the Cenozoic Altiplano is complicated by a tectonic history with multiple episodes of sedimentary rock formation and subsequent exhumation and recycling. The oldest (>1200 Ma) potential sediment source areas in southern Peru are basement rocks of the Arequipa Massif along the Pacific coast of the Precordillera, and rocks of the Amazonian craton to the east (Chew et al., 2007, 2008; Bahlburg et al., 2009, 2011; Reimann et al., 2010). Sediments from these areas were widely dispersed across the region during the Mesoproterozoic Grenville-Sunsas orogeny (1200–900 Ma) (Bahlburg et al., 2011). Sediments of middle Neoproterozoic–early Paleozoic age (750–500 Ma) may originate from subduction at a Proto-Andean margin (Chew et al., 2008), or from the Brazillian shield farther east (Reimann et al., 2010).

Ordovician to modern stratigraphy incorporates sediments from the tectonic events mentioned above, as well as magmatic intrusions and volcanic deposits in the middle Mesozoic–Pleistocene. Deformation, reworking, and dispersal of sediments occurred throughout the Paleozoic during the Famatinian orogeny, which also produced

new source signatures from subduction-related magmatism that stretched continuously along the western edge of South America from modern Patagonia through Argentina to Venezuela (Chew et al., 2007). A Permian–Triassic back-arc extensional episode in southeastern Peru resulted in formation of the regionally-extensive, up to 3 km thick Mitu Group, as well as emplacement of multiple intrusive complexes of Triassic age (Kontak et al., 1990). Continued convergence between the Nazca and South American plates resulted in abundant arc magmatism in the early Jurassic (200–175 Ma), late Cretaceous–early Paleocene (90–60 Ma) (Demouy et al., 2012), and late Cenozoic (Mamani et al., 2010).

Study area

The most complete package of Cenozoic stratigraphy exposed in the northern Altiplano is located just south of Cusco, Peru (Figures 3.1C and 3.2). This area is structurally complex. Preserved Cenozoic sedimentary basins are bounded by northwest-trending contractional structures that parallel those of the regional physiographic boundaries, perpendicular to the modern subduction direction of the Nazca plate (Figures 3.1 and 3.2). Key regional structures are the northeast-vergent Cusco-Lagunillas Fault to the southwest and the southwest-vergent Urcos-Ayaviri fault system to the northeast (Figure 3.1C). The primary local structure in the area is the northeast-vergent San Juan de Quihuares Fault, which appears to be the northern continuation of the Pasani Fault near Ayaviri (Perez and Horton, 2014) via the Acomayo Fault (Figure 3.1C).

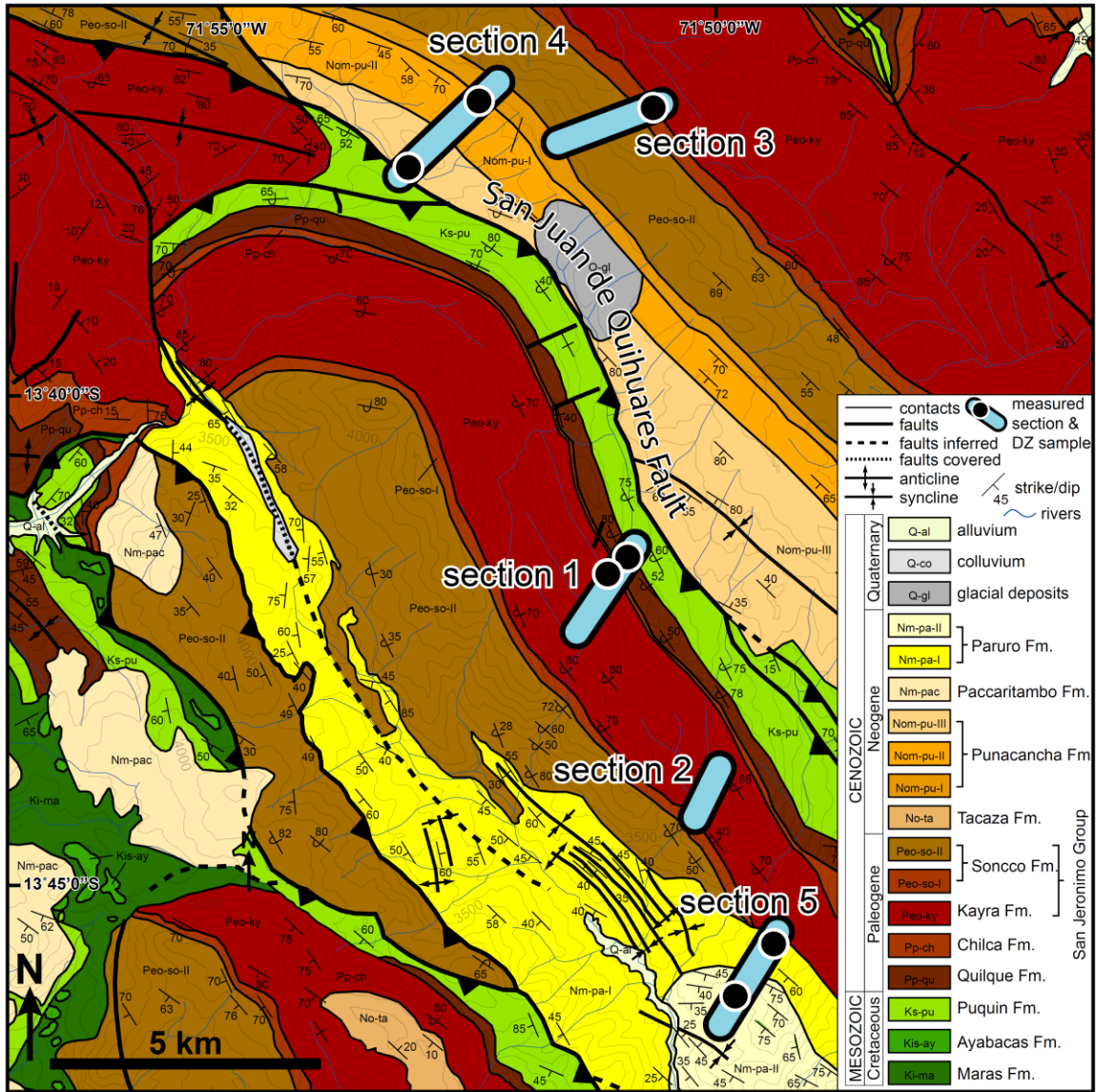


Figure 3.2. (A) Geologic map of the study area in the northernmost Altiplano near Cusco, Peru (modified from the Instituto Geológico Minero y Metalúrgico (INGEMMET) and Carlotto (2013)). DZ = Detrital zircon.

Despite such structural complexity, identification of formations in the field area, and logging a composite Cenozoic stratigraphic package was relatively straightforward

Figure 3.3 (next page). Composite Cenozoic stratigraphy of the northernmost Altiplano showing lithofacies codes to the right corresponding to observations and interpretations of depositional processes listed in Table A2.1. Paleocurrent data are shown as black arrows (north is up, arrow points toward sediment transport direction; N = stations, n = individual measurements). Conglomerate clast count results are shown as pie diagrams.

with the aid of previous mapping by the Instituto Geológico Minero y Metalúrgico (INGEMMET), and summary of previous basin research by Carlotto (2013). The oldest Cenozoic stratigraphy in the region is the Quilque Formation. Where measured, it sits atop late Cretaceous stratigraphy overturned $\sim 70^\circ$ likely due to deformation along the San Juan de Quihuas and Acomayo faults (section 1 of Figure 3.2). Structural dip of Paleogene stratigraphy (the Quilque, Chilca, Kayra, Soncco, and Punacancha formations) gradually changes up section from $\sim 70^\circ$ overturned to upright $\sim 50^\circ$, and continues to shallow in the Neogene Punacancha Formation to $\sim 40^\circ$ (sections 2–4 of Figure 3.2). The Punacancha Formation is truncated by the San Juan de Quihuas Fault (Figures 3.1C and 3.2). The regionally-limited and discontinuous Miocene Paruro Formation outcrops in the study area as a small syncline sitting in angular unconformity above the Kayra, Soncco, and Punacancha formations (section 5 of Figure 3.2), and bounded by the Acomayo Fault to the southwest (Figures 3.1C and 3.2).

Sedimentology and Stratigraphy

Methods

Lithofacies identification and associations

Stratigraphy was measured in the field at decimeter resolution with a standard 1.5 m Jacob's staff using a modified lithofacies classification scheme from Miall (2010)

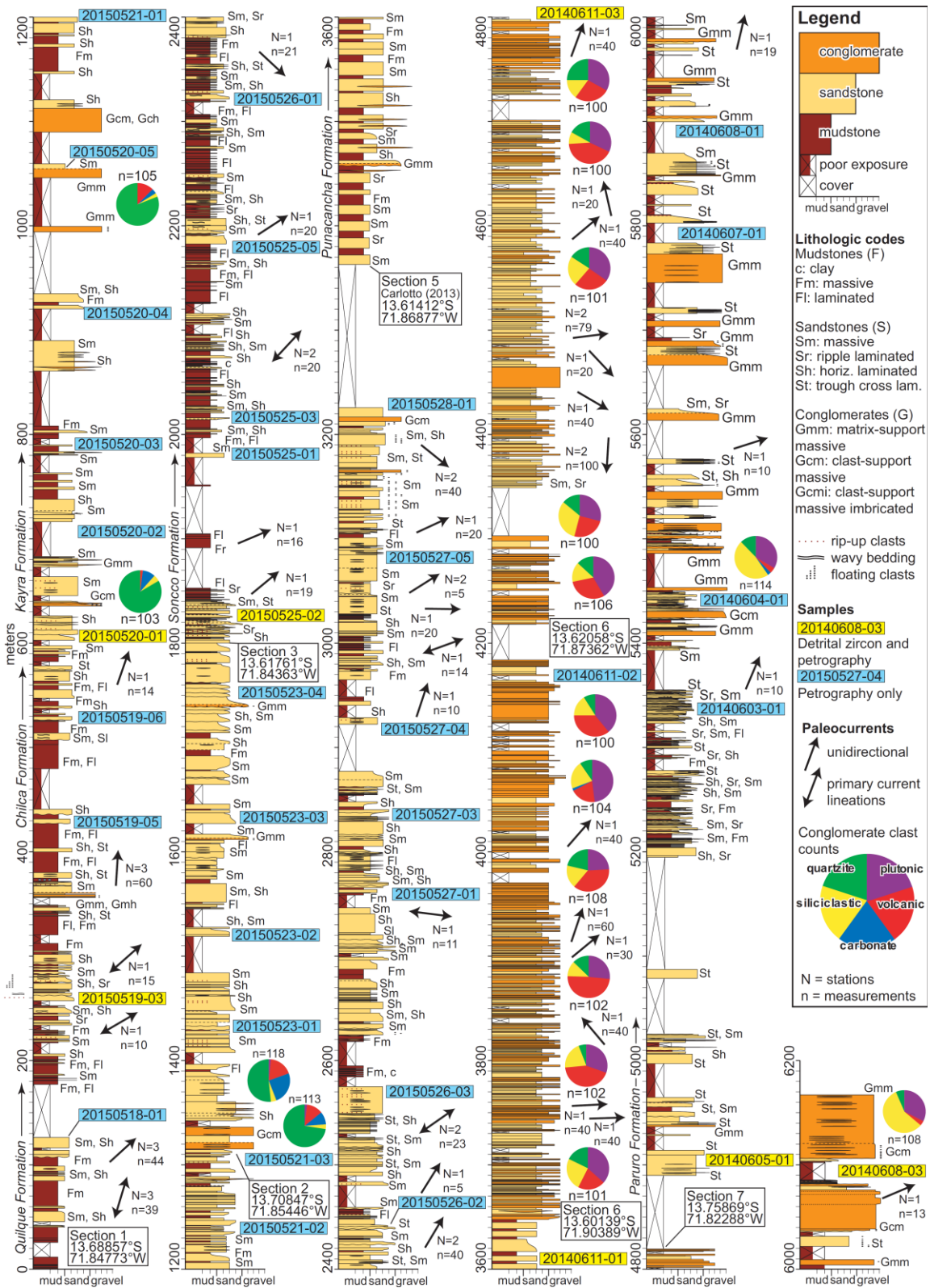




Figure 3.4. Photographs of key lithofacies. (A) Photo example of lithofacies and key sedimentary structures. (A) Fm/Fl: Alternating layers of massive and laminated siltstone. (B) Sm/Sr: Massive and ripple-cross-stratified sandstone. (C) Sh: Horizontally-laminated sandstone. (D) St: Trough-cross-stratified sandstone. (E) Gmm and Gcm: Matrix- and clast-supported conglomerate. (f) Gmm and Gcm: Mixture of structureless and clast-supported imbricated conglomerates.

modified from Miall (1977). This classification scheme aids interpretation of depositional process by characterizing beds based on primary depositional features: bedding thickness, grain size, texture, and sedimentary structures. Eleven different lithofacies were identified, and are labeled to the right of the detailed composite stratigraphic section in Figure 3.3.

Lithofacies codes are summarized in Table A2.1. Siltstones and limited claystones (Fm, Fl, and c) and are interpreted as deposition from suspension settling; massive mudstones may also result from post-depositional bioturbation (Figure 3.4A). Sandstones varied from massive (Sm), to ripple- or trough-cross-stratified, (Sr, St), and horizontally-laminated (Figures 3.4B-D). Sm is typical of rapid deposition with limited stable bedform development, or potentially massive due to post-depositional sediment reworking and redistribution from bioturbation. Ripple- and trough-cross-stratified sandstones (Sr and St) form from ripple and dune migration under unidirectional, lower-flow regime flow conditions, whereas horizontally-laminated sandstones (Sh) form in supercritical, upper-flow regime plane-bed flow conditions with relatively high velocity ≥ 100 cm/s and/or in shallow water (e.g., Bridge and Best, 1988). Four conglomeratic lithofacies were identified. Massive matrix- and clast-supported conglomerates (Gmm and Gcm) are indicative of hyperconcentrated, plastic (high strength) debris flows and pseudoplastic pressure- or buoyancy-modified deposition, respectively (Figure 3.4E). Clast-supported imbricated conglomerates (Gcmi) indicate traction transport of migrating subaqueous barforms under unidirectional flow conditions, whereas similar deposits with

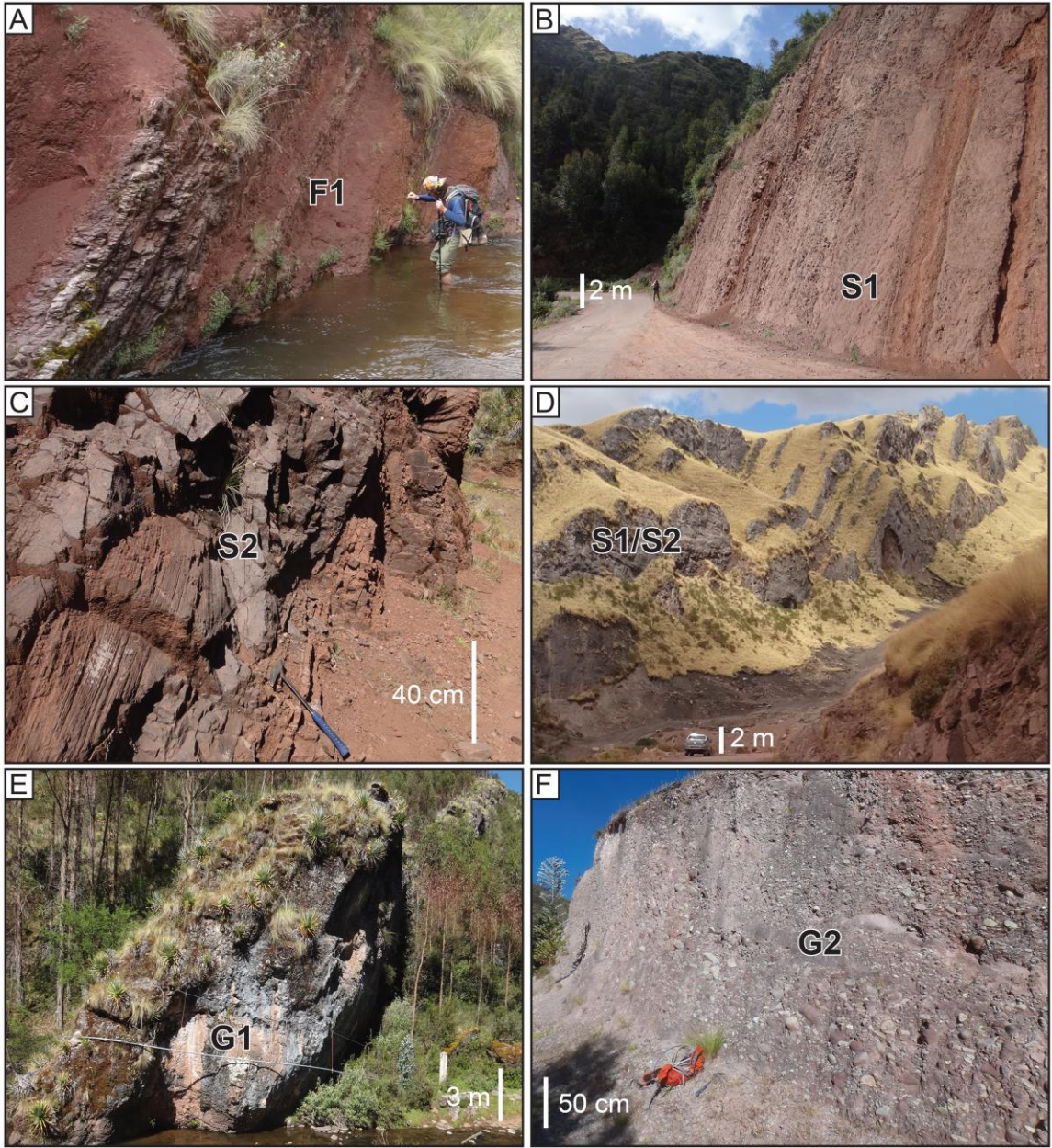
Figure 3.5 (next page). Photographs of key lithofacies associations. (A) Lithofacies association F1: thick packages of Fm and Fl mudstones with thinly interbedded very-fine–fine grained tabular Sm and Sh sandstones. (B) Lithofacies S1: thick, tabular sandstone sheets dominated by non-erosive Sm and Sh sandstones with limited St, with lesser interbedded mudstones; bedding bases typically show little basal scour. (C) Lithofacies association S2: Dominantly St, Sh, and Sm sandstones with limited Fm and Fl mudstones, typically with basal scour. (D) Laterally continuous sandstone units, characteristic of the Cusco, Peru area and other Altiplano basins (e.g., Hampton and Horton, 2007). (E) Lithofacies association G1: dominantly Gcm and lesser Gmm conglomerate with a sharp, non-erosive base (also see Figure 3.4E). (F) Lithofacies association G2: mixture of Gmm, Gcm, Gcmi, and Gchi, typically is less laterally-continuous with an erosive base.

crude horizontal bedding also suggest traction transport (Gch), but resulting from deposition of subaqueous bars, gravel sheets, or gravel lag deposits (Figure 3.4F).

Lithofacies codes were grouped into 5 lithofacies associations to aid interpretation of depositional environment. Associations are similar to those presented in Perez and Horton (2014) and Horton et al. (2015), as their study areas along strike to the south (Figure 3.1C) share many similar stratigraphic characteristics, and to Altiplano stratigraphy in general (e.g., Hampton and Horton, 2007).

Lithofacies association F1 consists of thick (1–10s of m) packages of mudstones (Fm and Fl) with thinly interbedded (1–10s of cm) very-fine to fine-grain, tabular, often fining-upward, solitary beds or stacked bed sets (Campbell, 1967) of Sm, Sr, and Sh sandstones. F1 packages are interpreted as overbank deposition in a fluvial floodplain depositional environment (Figure 3.5A).

Lithofacies association S1 comprises thick (1–10s of m), tabular sandstone sheets dominated by Sm and Sh bodies with limited St, as well as rare, thin (1–10s of cm) interbedded Fm and Fl beds. Beds included in lithofacies association S1 have limited



basal erosion or scour. We interpret lithofacies association S1 as the products of sand sheet deposition in a broad, potentially low-relief, unconfined fluvial system, similar to sand sheets documented elsewhere in the Bolivian Altiplano (Hampton and Horton, 2007) (Figure 3.5B).

Lithofacies association S2 contains St, Sh, and Sm bodies with limited mudstone interbeds. The key difference between S1 and S2 is the presence of significant basal scour and erosive channel forms (Figure 3.5C); these associations are similar in that they both form thick, laterally continuous, often amalgamated sandstone units that in many cases extend for multiple km, likely from deposition in a broad, braided fluvial depositional environment (Figure 3.5D).

Associations G1 and G2 both have Gmm and Gcm. The main difference is G1 shows little to no basal scour characteristic of hyperconcentrated debris flows in an alluvial fan setting (Figures 3.4E and 3.5E), whereas G2 has basal scour, is at times lenticular, and in some cases is imbricated (Gcmi) and/or crudely horizontally bedded (Gch), all of which are indicative of deposition of subaqueous gravelly bars, side bars, or channel fills in a braided fluvial or alluvial fan setting.

Paleocurrent analysis and conglomerate clast counting

Paleocurrent measurements were taken from preserved ripple bedforms, trough-cross-stratified sandstones, clast-supported imbricated conglomerates, primary-current lineations (parting lineations), and limited flute casts. Measurement of trough cross-bedding and calculation of paleoflow direction follows methods outlined in DeCelles et al. (1983). All measurements were corrected for deformational tilt using Rick Allmendinger's Stereonet 7 (Allmendinger, 2005).

Gravel clasts in conglomeratic units were counted in a roughly 100 x 100 cm area (minimum 100 clasts at each station). Clasts were divided into five different rock types: quartzite/metasedimentary, siliciclastic, volcanic, plutonic, and carbonate.

Sandstone petrography

Sandstone petrography involves statistical assessment of framework grains (quartz, feldspar, and lithic fragments) through identification of their modal abundances. Framework grain modal abundance is a function of provenance type, and governed by the tectonic setting during the timing of erosion (Dickinson and Suczek, 1979). Petrographic thin sections were made from fine- to coarse-grained sandstones, and stained for plagioclase and potassium feldspar to facilitate grain identification. Four-hundred sand-sized grains were counted in 37 sandstone samples following the Gazzi-Dickinson method of point counting (Table A2.2; Gazzi, 1966; Dickinson and Suczek, 1979).

Results

Six Cenozoic formations were identified in the field and measured: the Quilque, Chilca, Kayra, Soncco, Punacancha, and Paruro formations. Formation descriptions presented below are organized from oldest to youngest, and grouped where similar. Results are shown in Figure 3.3 and summarized in Figure 3.6.

Quilque and Chilca formations

The Quilque and Chilca formations represent the oldest Cenozoic rocks in the region. These formations are relatively thin compared to younger Cenozoic formations stratigraphically up section, composing only ~600 of the ~6200 m of measured

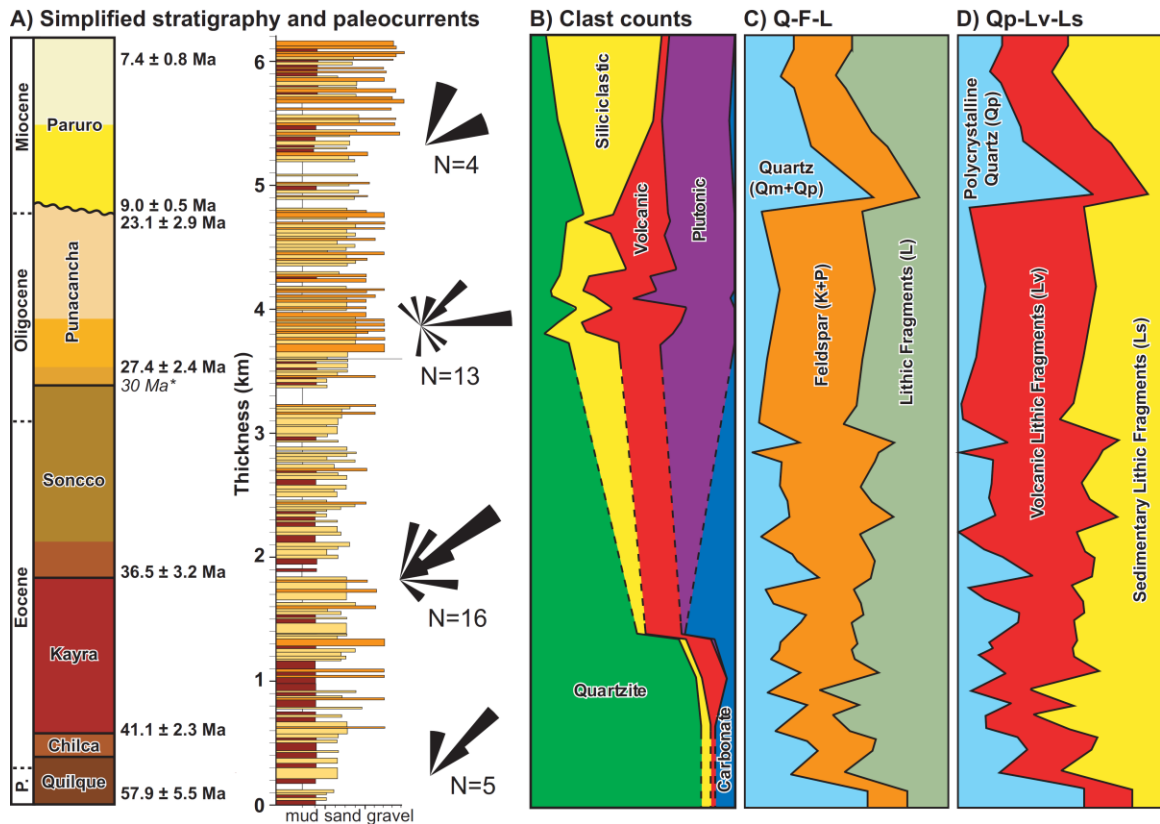


Figure 3.6. Stratigraphy results summary (A) Simplified stratigraphy and combined paleocurrent rose diagrams for Quilque-Chilca, Kayra-Soncco, Punacancha, and Paruro formations (N = number of stations). Maximum depositional ages from detrital zircon U-Pb geochronology are in bold to the right of the stratigraphy (* indicates fission-track ages reported in Carlotto (2013)). (B) Cumulative clast-count results showing up-section changes in conglomerate clast composition. (C) Sandstone petrography quartz-feldspar-lithic fragment (Q-F-L) results shown cumulatively. (D) Sandstone petrography polycrystalline quartz-volcanic lithics-sedimentary lithics (Qp-Lv-Ls) shown cumulatively.

stratigraphy presented here. These characteristically dark-red units represent an extensive period of low sediment accumulation with limited exposure in the Cusco area.

The Quilque Formation is a ~400 m thick coarsening-upward succession sitting disconformably above the latest Cretaceous siliciclastic and terrestrial carbonate Puquín Formation. Basal mudstones contain abundant 0.1–0.3 mm diameter charophyte fossils

(terrestrial algae), identified as *Nitellopsis supraplana sulcate* (based on visual comparison to Antoine et al. (2016), their Figures 4 F-H), which suggests a Paleocene–early Eocene stratigraphic age (Mourier et al., 1988). This is consistent with previous interpretations of Paleocene age also based on charophyte fossils (*Lamprothamnium*, Carlotto, 1998), and a new detrital zircon U-Pb maximum depositional age of 57.9 ± 5.5 Ma. The Quilque Formation comprises calcareous-cemented mudstones and rare black fissile shales, paleosols, and marls at its base, and abruptly transitions to thick packages of calcareous-cemented dark red mudstones (F1) and tabular beds of very-fine- to fine-grain, feldspar-rich, calcareous-cemented sandstones (dominantly S1 with minor S2). Rare preservation of trough cross-bedding and primary current lineations shows northeast-directed paleoflow. Conglomerate compositions are dominantly quartzite (Figure 3.6). The concentration of quartz decreases up section with roughly equal proportions of feldspar and lithic fragments, and a greater proportion of volcanic fragments than sedimentary fragments (Figures 3.6C-D).

The Chilca Formation is a ~200 m thick coarsening-upward package of dark-red mudstones and sandstones. The contact between the Quilque and Chilca formations has been previously documented as regionally disconformable (Carlotto, 2013); however, this relationship was not observed in the field due to poor exposure of these fine-grained units. Bedding geometry and sedimentary structures are similar to the upper Quilque with tabular S1 sandstones interbedded within thick packages of F1 mudstones. The Chilca overall has more F1 than S1 intervals compared to the underlying Quilque Formation.

Limited St shows northeast-directed paleoflow. Sandstone composition is similar to the Quilque Formation, but with a slight increase in quartz (Figure 3.6).

Kayra and Soncco formations (San Jerónimo Group)

The Kayra and Soncco formations compose the San Jerónimo Group, which is a ~2800 m thick package of stratigraphy with 500–1000 m thick coarsening-upward packages of S1 sandstones and F1 mudstones. Sandstone packages in this group are distinct and pervasive in the region as they make up thick (10s of m), laterally-continuous (many km), tabular sandstone sheets in and around Cusco, Peru (Figure 3.5D).

The Kayra formation is ~1200 thick and sits conformably above the Chilca Formation. The maximum depositional age of the base of the Kayra is 41.1 ± 2.3 Ma based on detrital zircon U-Pb data (Figure 3.6); this is slightly younger than a previously reported 53–46 Ma age (Carlotto, 1998; Carlotto et al., 2005, 2011). The lower Kayra Formation comprises thick packages of F1 mudstones with laterally continuous beds of non-erosive S1 sandstone and minor St that gives way to G2 and minor G1 conglomerates. The upper Kayra is dominated by S1 sandstones with minor F1 and S2 calcareous-cemented mudstones and sandstones. Sandstones in the upper Kayra contain an overall increase in S2, as well as abundant mud rip-up clasts, small bits of charcoal, and plant material. Paleocurrent indicators are lacking where the stratigraphy was measured; however, excellent, but stratigraphically discontinuous exposures of the Kayra Formation southwest of Cusco show predominantly north-northeast paleoflow (Carlotto, 1998; Carlotto, 2013). Conglomerate clasts in the lower Kayra are dominated by quartzite, with subordinate siliciclastic, carbonate, and volcanic clasts. The upper Kayra

conglomerates are also dominated by quartzites, but with an increase in carbonate and volcanic clasts (Figures 3.3 and 3.6B). Sandstone compositions show a slight decrease in quartz and concomitant increase in plagioclase and volcanic lithic fragments. Relative proportions of sedimentary lithics decrease up section compared to volcanic lithics (Figure 3.6D).

The Soncco Formation is ~1600 m thick with two distinct coarsening-upward successions (Figures 3.3 and 3.6A). The age of the basal Soncco was previously reported as 44–42 Ma (Carlotto, 1998; Carlotto et al., 2005); however, the maximum depositional age of the base of the Soncco slightly younger at 36.5 ± 3.2 Ma based on detrital zircon U-Pb data (Figure 3.6). The lower Soncco Formation marks an abrupt transition from the sandstone-dominated upper Kayra to ~800 m of dark red F1 mudstone deposition. This mudstone-dominated interval contains pervasive burrowing. As the formation coarsens up section, there is an increase in S1 sandstone deposition with abundant, large (up to 20 cm diameter) mud rip-up clasts. Volcaniclastic input and large (0.1–0.5 mm) plagioclase crystals increase toward the upper Soncco Formation. The uppermost Soncco Formation, just below the transition to the Punacancha Formation, contains large reworked pebble-size volcanic fragments in medium- to coarse-grain sandstones; however, no volcanic tuffs were found in either formation (cf., Carlotto, 2013). Paleocurrent indicators from preserved ripple bedforms, trough-cross-stratified sandstones, primary current lineations, and rare flute casts, show east- and northeast-directed paleoflow. Sandstone petrography reveals an increase in plagioclase compared to quartz and lithic fragments (Figures 3.6C-

D), and interestingly, an increase in accessory minerals such as amphiboles and pyroxenes.

Punacancha Formation

The Punacancha Formation is ~1400 m thick and comprises multiple coarsening-upward successions (Figures 3.3 and 3.6A). Detrital zircon U-Pb maximum depositional ages for the base and top of the section bracket deposition between 27.4 ± 2.4 Ma and 23.1 ± 2.9 Ma (Figure 3.6); the basal age is similar to that previously reported by Carlotto et al. (2011) of ~30 Ma. The lower Punacancha Formation primarily comprises thick F1 mudstone and S1 sandstone beds. The upper Punacancha Formation comprises S1 and S2 sandstones with thick discontinuous packages of G1 and lenticular G2 conglomerates. The majority of the sandstone beds are Sm, with limited Sh and St. Although variable, paleocurrent measurements from the Punacancha Formation generally show northeast-directed paleoflow, consistent with previous measurements by Chavez et al. (1994). Conglomerate clast counts show varying proportions of quartzite, siliciclastics, volcanic, and plutonic clasts with limited carbonate clasts. Despite the changes in lithofaces and stratigraphic architecture, sandstone compositions are remarkably similar to that of the upper Soncco Formation.

Paruro Formation

The Paruro Formation is ~1400 m thick and sits in angular unconformity above the Punacancha Formation. The Paruro Formation has a basal age previously documented at 10.1 ± 1.1 Ma based on biotite K/Ar dating of a basal tuff, as well as Miocene age charophyte fossils (*Chara* and *Rhabdochara*) (Carlotto, 1998). Detrital zircon U-Pb

geochronology maximum depositional ages place the base and top of the section at 9.0 ± 0.5 Ma and 7.4 ± 0.8 Ma (Figure 3.6). The formation is dominated by thick packages of S2 sandstone and G2 conglomerate beds. Covered intervals are typically a mix of F1 mudstones and very friable S2 coarse-grain sandstones. Paleocurrent measurements show northeast-directed paleoflow. Conglomerate clast compositions are similar to those of the underlying Punacancha Formation, but show a continued increase in siliciclastic clasts and decrease in quartzite and volcanic clasts (Figure 3.6B). Sandstone compositions show a dramatic increase in quartz at the base of the section, followed by a return to plagioclase- and lithic-fragment-dominated compositions (Figure 3.6C), and an increase in sedimentary fragments up section (Figure 3.6D).

Summary and interpretation

The Paleocene–early Eocene Quilque and Chilca formations reflect the end of Cretaceous carbonate deposition and the beginning of clastic infilling of the Altiplano basin in this region. This change in depositional environment is indicative of a larger regional transition from carbonate to siliciclastic deposition for the remainder of the Cenozoic. Basal Quilque deposition marks this change in depositional environment from low energy, fresh water (or brackish) lacustrine, as indicated by abundant charophyte fossils, to fluvial and floodplain depositional environments. Northeast-directed paleocurrent measurements and quartzite-dominated conglomerates indicate sediment sourcing from the Western Cordillera and/or western Altiplano to the southwest, as quartzite formations are pervasive in those regions. The Chilca formation is essentially a

continuation of upper Quilque stratigraphy with deposition in a predominantly fluvial floodplain environment, but with a slight decrease in fluvial energy.

The Eocene Kayra and Soncco formations (San Jerónimo Group) show a drastic increase in sediment input as broadly coarsening-upward packages, and an overall increase in sandstone-to-mudstone ratio. The depositional environment near the base of this group is interpreted as fluvial floodplain with brief episodes of fluvial braid plain deposition, which then gives way up section to extensive periods of unconfined sand-sheet deposition in a broad, wide fluvial system. These formations mark a transition point, as they reflect an increase in fluvial energy and a drastic increase in sediment input. Paleocurrent indicators are consistent with sediment sourced from the west and southwest; conglomerate clast counts support this interpretation (Figure 3.6), as quartzite-dominated formations abound in the Western Cordillera and Altiplano physiographic regions. Collectively, these interpretations point to an increasingly proximal Western Cordilleran and/or western Altiplano sediment source. Sandstone petrography supports this interpretation (Figure 3.6, Table A2.3), as the increased presence of accessory minerals such as euhedral hornblendes and clinopyroxenes is characteristic of primary volcanic input with short transport distances, indicative of increased proximity of the Western Cordilleran volcanic arc.

The Oligocene–late Miocene Punacancha and Paruro formations represent some of the final stages of siliciclastic infilling of this part of the greater Altiplano. They also represent a change from fluvial-dominated to alluvial fan-dominated depositional environment based primarily on grain size and lithofacies. The Punacancha Formation

represents a coalescing of alluvial fans (bajada) pouring sediment off the immediately-adjacent retroarc fold-and-thrust belt of the Western Cordillera. Variable paleocurrent measurements to the north and southeast support this interpretation, as the retroarc fold-and-thrust belt front would have likely had a northwest-southeast oriented strike. The increase in the proportion of plutonic clasts in conglomerates is consistent with exhumation and erosion of the proximal 48–32 Ma Andahuaylas-Yauri batholith consisting of earlier gabbro–diorite compositions later intruded by granodiorites and quartz monzodiorites (Perelló et al. 2003). Above the angular unconformity that separates these formations, sandstone compositions change from dominantly quartz at the base of the formation, then steadily return to dominantly plagioclase through the rest of the section; this is consistent with tapping of a new sediment source followed by renewed sediment sourcing of the Western Cordillera and western Altiplano during the transition from retroarc foreland basin deposition to proximal hinterland basin deposition between 23 and 9 Ma (Figure 3.6C).

Detrital Zircon

Methods

U-Pb geochronology

Detrital zircon U-Pb geochronology was conducted at the University of Houston. Zircon grains were extracted from fine- to coarse-grained sandstones following standard mineral separation procedures of crushing, disc milling, water tabling, density separation, and magnetic separation. Grains were washed in full strength nitric acid, dried, and

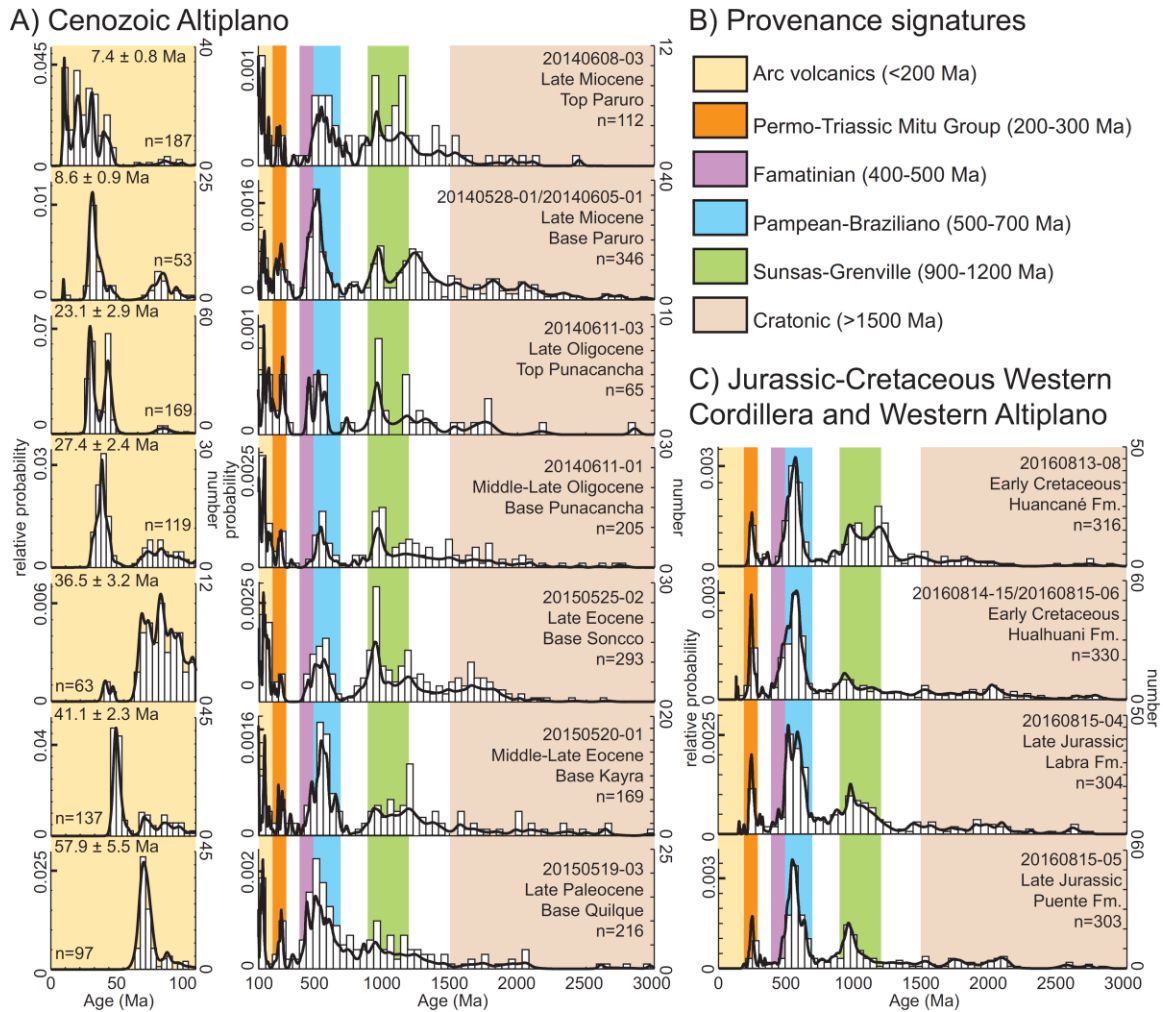


Figure 3.7. Detrital zircon U-Pb geochronology results shown as probability density plots (black lines) and histograms (white bars), and characteristic sediment source detrital zircon U-Pb age groups. (A) Detrital zircon U-Pb results for Cenozoic Altiplano basin stratigraphy. Note the change in scale between ages 0–100 Ma and 100–3000 Ma; the former are typically an order of magnitude higher due to ongoing late Cretaceous–Cenozoic volcanism. The youngest age is shown for each sample; n = total number of ages. (B) Characteristic sediment source groups (see Perez and Horton, 2014 and references therein). (C) Detrital zircon U-Pb results for Jurassic–Cretaceous potential source samples from the Western Cordillera and western Altiplano. Note the similarity in characteristic age populations from these samples and Cenozoic Altiplano stratigraphy.

poured onto two-sided tape for analysis by laser ablation using a Photon Machines Analyte 193 ArF excimer laser attached to a pulse-counting detector fitted to a Varian 810 quadrupole mass spectrometer (Shaulis et al., 2010). A $\sim 19.7 \mu\text{m}$ spot size was used for all analyses with a fluence of 2.99 J/cm^2 and 10 Hz repetition rate for 200 shots, resulting in approximately 20 s of ablate time, with ~ 8 s of background measurement and ~ 7 s of washout. All other machine parameters are outlined in Shaulis et al. (2010). All U-Pb data was reduced using a MATLAB-based program, U-Pb Toolbox, a data reduction and visualization program developed for the University of Houston (see Texas Digital Library for U-Pb Toolbox software, and Appendix 3 for further analytical and data reduction details).

Samples from the Cenozoic Altiplano basin were collected from the Quilque, Kayra, Soncco, Punacancha, and Paruro formations. A pumice-rich reworked tuff was also collected from the base of the Paruro Formation. Samples were collected from the Jurassic–Cretaceous Puente, Labra, Hualhuani, and Huancané formations, which have not been previously characterized in the region. These potential source samples were compiled with previously published Paleozoic–Mesozoic detrital zircon U-Pb data for comparison to Cenozoic basin samples (summarized in Table A2.4).

The youngest detrital zircon U-Pb age, or age population in a detrital sample represents the maximum possible depositional age of the strata, which can provide important age estimates in siliciclastic stratigraphy lacking alternative methods of age control. Recent work along strike to the south near Ayaviri (Figure 3.2C) has shown the youngest zircons from sandstones in this region closely approximate true depositional age

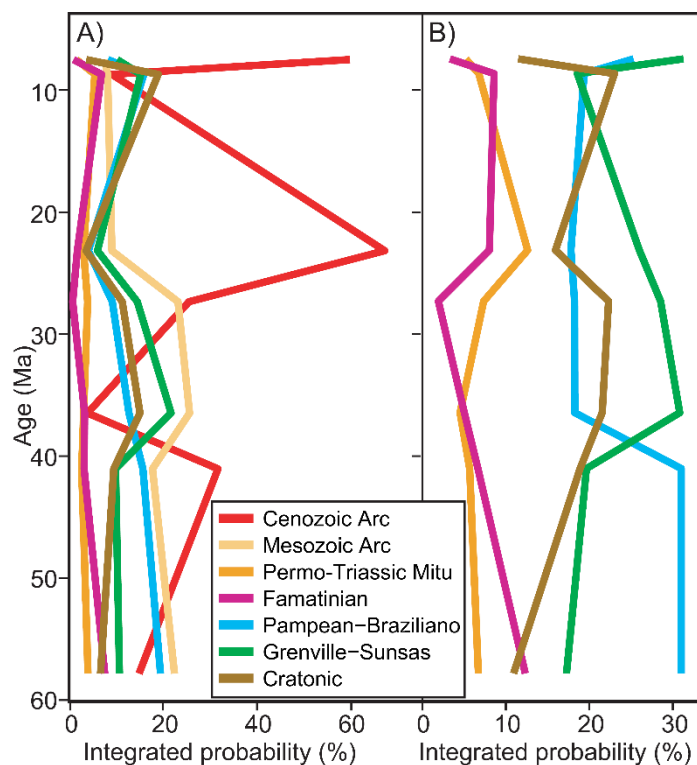


Figure 3.8. (A) Integrations of Cenozoic Altiplano detrital zircon probability density plots (Figure 3.7A) by characteristic age groups (Figure 3.8B) plotted against maximum depositional age. (B) Same as part A, but with ages <200 Ma removed to enhance the older provenance signal. Colored lines in legend represent characteristic age populations from Perez and Horton (2014).

due to ongoing volcanic input throughout the Cenozoic (Perez and Horton, 2014). Given the likelihood of approximating true age of the stratigraphy in this type of tectonic setting (Cawood et al., 2012), maximum possible depositional ages were used to calculate sediment accumulation rates for comparison to previously documented Andean plateau foreland basin stratigraphy to the south.

Multidimensional scaling (MDS)

Multidimensional scaling (MDS) is a superset of principal component analysis that has recently been adapted for comparison of detrital data sets (Vermeesch, 2013),

and shown to facilitate comparison of multiple detrital data sets (e.g., Che and Li, 2013). Metric MDS (cf., non-metric MDS) produces Cartesian plots in N dimensions through conversion of sample dissimilarity to disparity via linear transformation and iterative rearrangement of data in Cartesian space, seeking to minimize the misfit between intersample distance and disparity (termed “stress”). A low stress level indicates a reasonable transformation, and a correlation between sample dissimilarity and distance, resulting in similar samples clustering closer together in Cartesian space. Metric MDS is applied by first constructing a pairwise dissimilarity matrix of detrital age distributions. One such metric used to calculate dissimilarity between detrital samples is the two-sample Kolmogorov-Smirnov (KS) statistic D value (the maximum distance between two empirical cumulative distribution functions, CDFs) (Stephens, 1970). Because the KS test is more sensitive about the median, and does not take into account sample uncertainty, we constructed a dissimilarity matrix using the coefficient of non-determination ($1-R^2$), where R^2 is the cross-correlation coefficient of probability density plots. This quantitative measure of similarity is more sensitive than the KS test D value both for the number of age modes in a detrital age distribution, as well as the relative proportions of those modes (Saylor et al., 2013; Saylor and Sundell, 2016).

Mixture modeling

Mixture modeling of detrital zircon U-Pb data was used to determine the contributions of individual sediment sources by randomly mixing together potential source age distribution probability density plots for comparison to basin samples. The mixing model employed here, DZmix (Sundell and Saylor, 2017), takes an inverse Monte

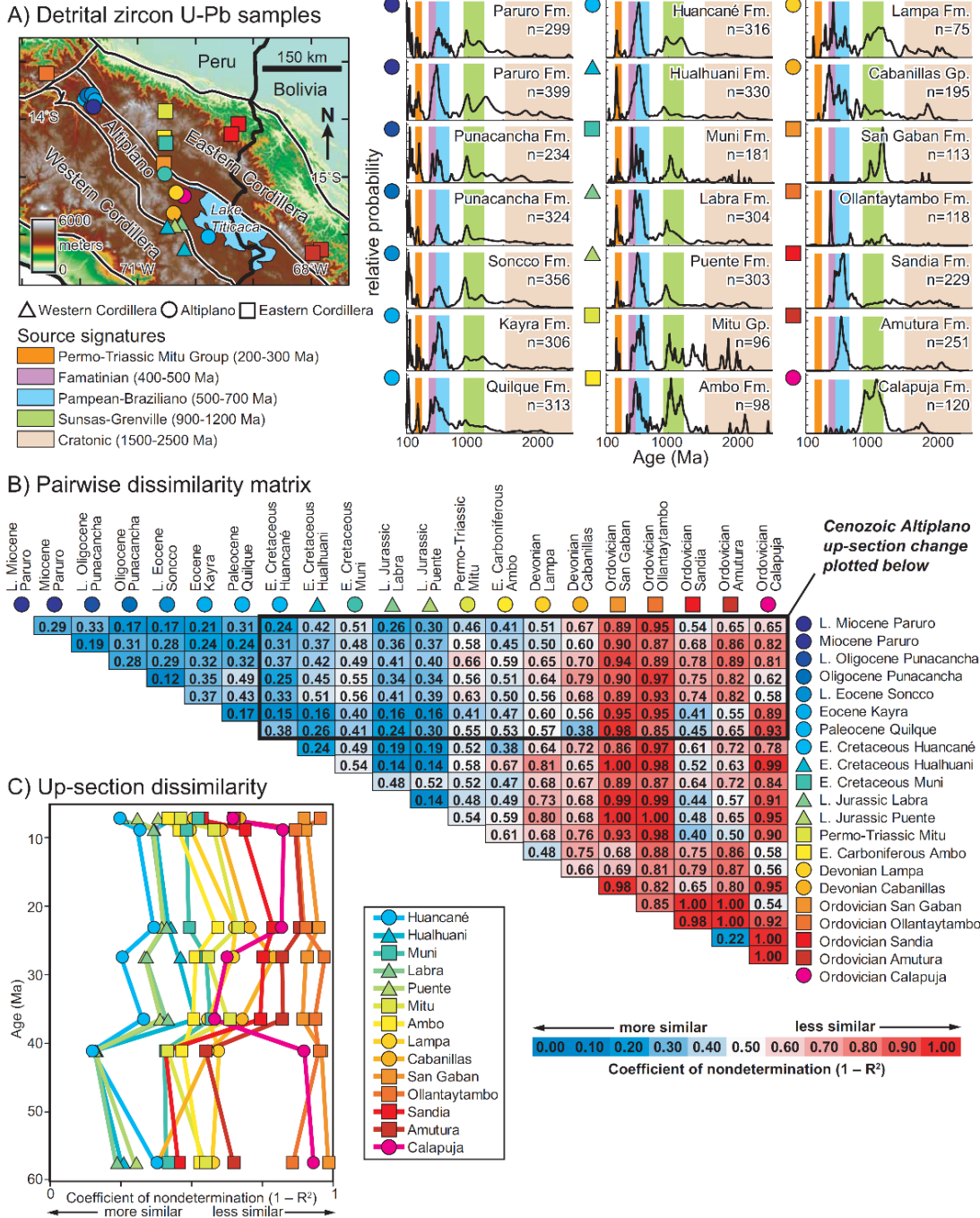


Figure 3.9. (A) Regional compilation of detrital zircon U-Pb data. (B) Pairwise dissimilarity matrix used to construct multidimensional scaling plots in Figure 3.10. (C) Dissimilarity values from Figure 3.9B (thick black box) for each potential source plotted against Cenozoic Altiplano samples' detrital zircon U-Pb maximum depositional age. Note the greater similarity in younger Mesozoic sources and at times the Paleozoic Calapuja Formation, compared to other potential sources.

Carlo approach of randomly scaling each source age distribution by a random set of percent contributions that sum to 100%, sums those scaled distributions to give a single model distribution, and quantitatively compares that model distribution to a basin sample distribution through Cross-correlation. This process is repeated 100,000 times for each basin sample, and the best 100 model fits (0.1%) are used to calculate the mean and standard deviation (1σ) contribution from each potential source. Source distributions have few ages younger than 200 Ma (8 out of 2,693), and therefore only ages older than 200 Ma were considered in the mixture modeling.

Roundness

Zircon roundness has been previously used as a proxy for sediment transport distance (Decou et al., 2013; cf., Muhlbauer et al., 2017). Roundness was calculated for zircon grains with concordant U-Pb age dates. To quantify zircon roundness, we developed a MATLAB-based code to employ the roundness quantification method outlined in Diepenbroek et al. (1992). This method uses the relationship between the centroid of a grain and the distance from the centroid to its perimeter based on two-dimensional images of individual zircon grains. The MATLAB code calculates roundness in the following steps: 1) Each image is converted into a binary matrix of ones and zeros, 2) the perimeter and centroid of the grain are determined and converted from Cartesian to polar coordinates to measure the magnitude of the ray (ρ) from the reference point (origin/centroid) to perimeter for θ angles of 0 to 359°, 3) harmonics are calculated using a fast Fourier transform of a θ - ρ x-y plot, 4) harmonics are normalized to the 0th Fourier coefficient (which removes any grain-size effects) and the first harmonic is removed

(which removes the aspect-ratio effect), and finally 5) the 2nd–24th harmonics are summed and scaled to maximize the sensitivity between 0 and 1. We benchmarked our code to results in Diepenbroek et al. (1992) using the Krumbein (1941) roundness table, as was done in the original Diepenbroek et al. study. Because detrital zircons vary considerably in size and shape, especially in aspect ratio, we tested the code on synthetic data (drafted zircon images of different sizes and shapes) to verify its utility for zircon. We found the method of Diepenbroek et al. (1992) gave the more consistent results for zircons compared to alternative roundness quantification methods (e.g., Takashimizu and Iiyoshi, 2016).

Results

U-Pb geochronology

Nine samples from seven stratigraphic levels of Cenozoic Altiplano stratigraphy and five samples from four Jurassic–Cretaceous potential sediment source formations were analyzed (Figure 3.7). Results are reported with characteristic age groups shown as colored vertical bars to highlight potential sediment sources. These age groups include arc volcanic rocks (<200 Ma), the Permo-Triassic Mitu Group (200–300 Ma), the Famatinian orogeny (400–500 Ma), the Pampean-Braziliano orogeny (500–700 Ma), Sunsas-Grenville (900–1200 Ma), and cratonic rocks (>1500 Ma) (Figure 3.7B). All Cenozoic Altiplano basin and Jurassic–Cretaceous potential source samples show similar proportions of each of these characteristic groups. Potential sediment source samples are combined with previously characterized potential source formations (see Table A2.4

and references therein). Potential source formations also show many of the same characteristic age groups (Figure 3.7).

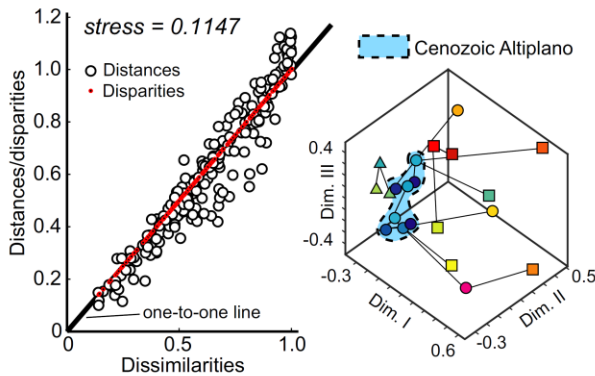
Results for maximum depositional ages for all but one sample are within 2σ uncertainty of the mean and 1σ propagated uncertainty of the youngest three grain ages, as recommended by Dickinson and Gehrels (2009). The exception is the base of the Paruro Formation: the youngest single-grain maximum possible depositional age is 8.6 ± 0.9 Ma, but the mean and 2σ uncertainty of the youngest three grains is 19.9 ± 3.7 Ma, which is clearly too old. Fortunately, we also sampled a pumice-rich reworked tuff (sample 20140605-02) that gave a basal age of 9.0 ± 0.5 Ma. This is within uncertainty of a previously reported biotite K/Ar age from a basal tuff of 10.1 ± 1.1 Ma reported by Carlotto (2013). For all other samples the single youngest age was used to infer maximum depositional age.

Detrital zircon U-Pb maximum possible depositional ages bracket the timing of deposition for the ~6200 m of stratigraphy between ~58 and ~7 Ma. (Figures 3.6A and 3.7A). Sediment accumulation rates based on stratigraphic thickness and single-grain maximum possible depositional ages gives 36 m/Myr during Quilque and Chilca deposition, 261 m/Myr during Kayra deposition, 175 m/Myr during Soncco deposition, 333 m/Myr during Punacancha deposition, and 875 m/Myr during Paruro deposition. A basal age of 10.1 Ma for the Paruro Formation from Carlotto (2013) gives a rate of ~520 m/Myr.

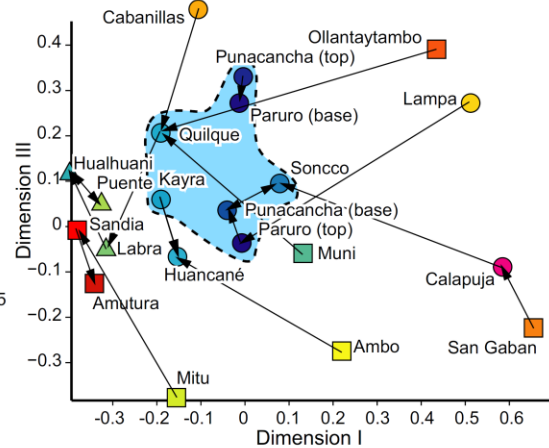
Visual comparison of Cenozoic Altiplano probability density plots is difficult because they show very similar proportions of the characteristic age groups typically

Multidimensional scaling (MDS)

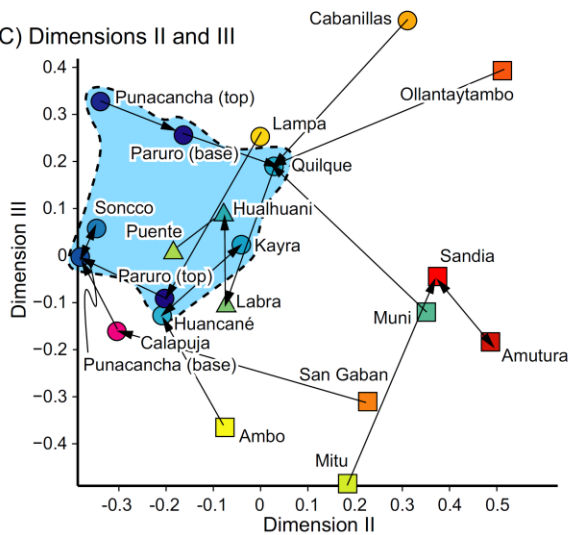
A) Shepard plot and 3D MDS



B) Dimensions I and III



C) Dimensions II and III



D) Dimensions I and II

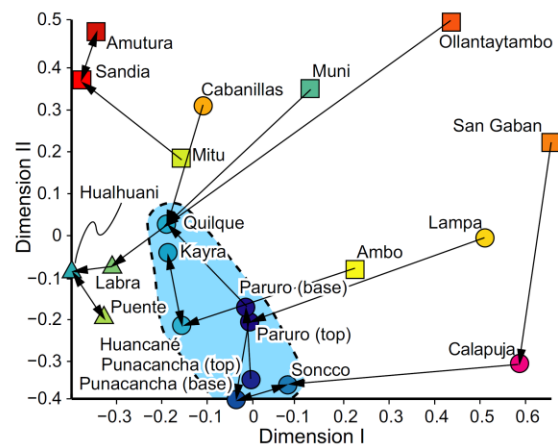


Figure 3.10. Three-dimensional (3D) multidimensional scaling (MDS) results using the pairwise dissimilarity matrix in Figure 3.10B. (A) Shepard plot and 3D MDS showing transformation from dissimilarity to distances and disparities. A low stress level of 0.1147 indicates a reasonable transformation. Light blue polygon corresponds to rough outlines of Cenozoic Altiplano samples in parts B–D. (B) Dimensions I and III from 3D MDS results. (C) Dimensions II and III from 3D MDS results. (D) Dimensions I and II from 3D MDS results. Black arrows indicate samples' nearest neighbor. Note the similarity in Cenozoic Altiplano samples to one another indicating minimal change in sediment source through time, as well as their similarity to Jurassic–Mesozoic formations indicating potentially large sediment contributions from these sources, and relatively limited sourcing from most of the Paleozoic formations. Also note the Calapuja Formation's nearest neighbor is the Soncco Formation, indicating it may have been significant sediment to the northern Altiplano at ~36 Ma.

found in detrital zircon U-Pb age distributions from southern Peru (e.g., Bahlburg et al., 2009, 2011; Reimann et al., 2010; Perez and Horton, 2014). Integration of probability density plots based on characteristic source age ranges plotted against maximum depositional age aids first-order up-section comparison of these data (Figure 3.8A). Results show Cenozoic arc volcanic ages occur in high percentages (30–70%) in the lower Kayra (~41 Ma), upper Punacancha (~23 Ma), and upper Paruro (~7 Ma) formations, and are relatively low (10–25%) in the Quilque, Soncco, and lower Paruro Formations. Mesozoic arc volcanics show a steady decrease from 20–30% in the lower sections to <10% at the top (Figure 3.8A). A second set of integrations shown in Figure 3.8B with ages <200 Ma removed helps to identify potential provenance signatures potentially obscured by pervasive volcanism throughout the middle Cretaceous–Cenozoic. Even with the younger ages removed, Permo-Triassic Mitu and Famatinian source ages represent only 10–15%, and typically <10% throughout the section. Pampean-Braziliano ages consistently make up 20–30% with higher percentages in the Quilque and Kayra formations. Grenville-Sunsas ages make up 15–30%, with the highest proportions in the Soncco and upper Paruro formations. Cratonic signatures compose roughly 10–20% of Altiplano age distributions, with the lowest proportions at the bottom and top of the measured stratigraphy.

Multidimensional scaling (MDS)

Detrital zircon samples from Cenozoic Altiplano stratigraphy were compared to each other and to fourteen potential source samples (Figure 3.9A) using three-dimensional (3D) MDS (Figure 3.10). The pairwise dissimilarity matrix used to construct

MDS plots shown in Figure 3.9B is color-coded to distinguish more and less similar age distributions. A complementary assessment to MDS is plotting the dissimilarity values themselves with stratigraphic age (maximum depositional age). This reveals the most similar source age distributions to Cenozoic Altiplano basin age distributions are Jurassic–Cretaceous formations (Figure 3.9C). Among the input sediment source distributions, the least-similar distributions are older Paleozoic sources, except for the Calapuja Formation in the Soncco and upper Paruro formations (Figure 3.9B).

Transformation from dissimilarity to distance and disparity in 3D gives a good correlation as shown by a low stress (0.1147, Figure 3.10A). 3D MDS plots show Altiplano basin samples are most similar to each other and to Jurassic–Cretaceous source samples (Figures 3.10B–D). Among the input sediment source distributions, Paleozoic source samples are the most dissimilar, as shown by greater distances from the cluster of Altiplano samples (Figure 3.9B). Although the Calapuja Formation is far from the cluster of Altiplano basin samples, its nearest neighbor (black arrows in Figures 3.10B–D) is the Soncco Formation, implying high similarity and a good candidate as a sediment source at ~36 Ma (Figure 3.11B–D).

Mixture modeling

Detrital zircon U–Pb mixture modeling shows late Jurassic–early Cretaceous formations make up 55–65% of the sediment input to Cenozoic Altiplano sediments (Figure 3.11A). The remainder is a mixture of Permo–Triassic and older formations, with relatively large (25–30%) contributions from the Ordovician Calapuja Formation at ~36 and ~7 Ma. Up-section changes in sediment sourcing among formations in the Western

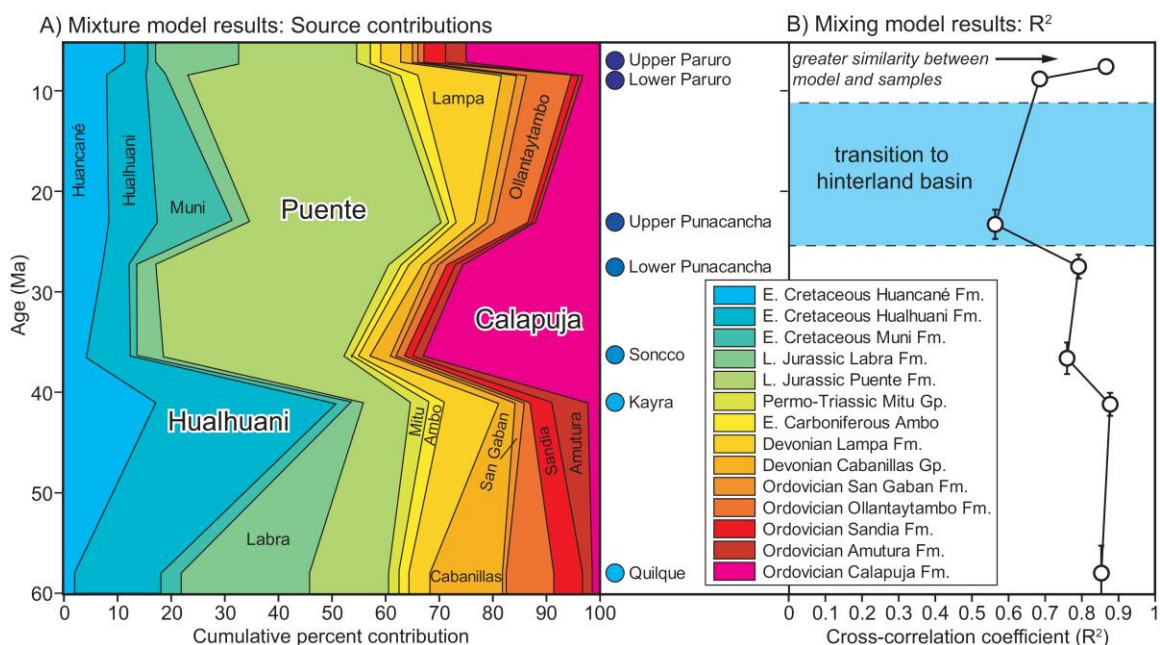


Figure 3.11. Detrital zircon U-Pb age distribution mixture modeling results using methods outlined in Chapter 2. See Figure 3.9A for sediment source formations and data. (A) Up-section changes in source contribution shown cumulatively with younger formations on the left and older on the right. Note the predominance of sediment sourcing from the Hualhuani, Puente, and Calapuja formations. Jurassic and younger sources account for nearly 60% of sediment sourced in the Altiplano throughout the Cenozoic. Note that up-section changes do not imply continuity, but rather are interpolations of results between sample unmixing results. (B) Maximum depositional age plotted against cross-correlation R^2 for the top 100 of 100,000 model fits for each sample (0.1%). The model is able to reproduce Cenozoic Altiplano age distributions reasonably well (as indicated by a high R^2 value), except for the upper Punacancha and lower Paruro formations. The former may be due to low sample size of ages > 200 Ma ($n = 56$); both model misfits may be due to a missing sediment source not included in the data compilation.

Cordillera show that sediment was sourced dominantly from the Hualhuani and Puente formations from 50–42 Ma, after which the contribution from the Puente Formation increased to 22–43% from 36–7 Ma (Figure 3.11A).

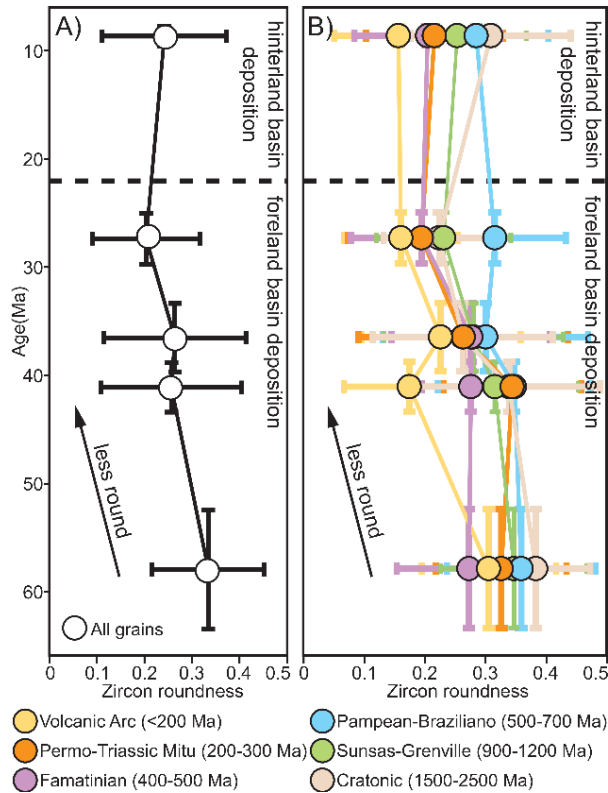


Figure 3.12. Zircon roundness results. (A) Maximum deposition age versus mean and 1σ standard deviation zircon roundness. (B) Maximum depositional age versus mean roundness of grains divided into characteristic age groups. The Paleogene up-section decrease in roundness is consistent with a decrease in sediment transport distance as cratonward migration of the retroarc fold-and-thrust belt and magmatic arc brings sediment sources closer to the study location.

Mean Cross-correlation coefficients of the top 0.1% model fits indicate that the model can reproduce detrital age distributions for all Paleogene samples except the late Oligocene (upper Punacancha). Mean Cross-correlation coefficients of >0.7 for this interval approach that for a perfect mixture model fit of $R^2 = 1$. This indicates that the sources are well-characterized, and that the selected source samples may indeed represent the true sources from which Paleogene strata were derived. However, the upper

Punacancha and lower Paruro formations show poorer model fits (Figure 3.11B). This is consistent with interpretations of sedimentology and stratigraphy above that point to a time of changing geodynamic setting and mode of subsidence from flexural foreland to hinterland basin subsidence.

Roundness

Zircon roundness results plotted against U-Pb maximum possible depositional age show a decrease in roundness from ~58 to ~27 Ma for combined samples (Figure 3.12A), and for samples divided into characteristic sediment source age groups based on their U-Pb ages (Figure 3.12B). In both cases, zircons become more round in the late Miocene, but not to the level of roundness shown in the Paleocene.

Application of the Student's t-test to zircon roundness versus age confirms that the observed roundness trends are statistically robust. The t-test tests the null hypothesis that two independent samples come from distributions with equal mean values based on their standard deviations (Hazewinkel, 2001). For roundness results using all grains from each sample (Figure 3.12A), 80% of mean values up section are statistically different from one another at the 95% confidence level; all samples are different at the 90% confidence level. The base of the Quilque, Punacancha, and Paruro samples (i.e., comparison of the oldest and youngest of our interpreted foreland basin samples, and an interpreted hinterland basin sample) are statistically different from one another at the 95% confidence level. Roundness results subdivided into characteristic source populations (Figure 3.12B) are less statistically robust: 52% of results have statistically different means from one another at the 95% confidence level; 72% are different at the

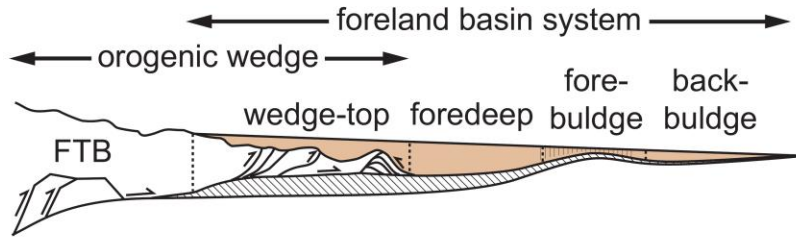
70% confidence level. The base of the Quilque is statistically different from the Paruro for all subpopulations of ages at the 95% confidence level except for Famatinian age zircons where it is different at the 90% confidence level. Punacancha zircons are not statistically different from Paruro zircons when divided into individual subpopulations.

Summary and interpretation

Results from detrital zircon U-Pb geochronology and quantitative provenance methods are consistent among themselves and to sedimentology and stratigraphy results presented above, indicating sediment mostly derived from the Western Cordillera and western Altiplano throughout the Cenozoic. Mixing-model results are consistent with a conceptual unroofing sequence, whereby initial unroofing of the Lower Cretaceous Hualhuani Formation in the Paleocene–early Eocene is followed by erosion of the Jurassic Puente and Ordovician Calapuja formations from 36–7 Ma (Figure 3.11A). Assuming introduction of new sediment sources can be linked to crustal deformation, pulses of Calapuja sediment sourcing are interpreted as times of increased contractional deformation where hanging wall thrust blocks expose and recycle underlying Ordovician stratigraphy at ~36 and ~7 Ma (Figure 3.11A). A decrease in zircon roundness is interpreted as a decrease in fluvial transport distance, which is consistent with thrust-belt advance and encroachment of Western Cordilleran sediment sources toward the study area between ~58 and ~27 Ma. Interestingly, this decrease in roundness is seen in recycled zircons from sediment sources that make up the majority of ages >200 Ma, as

well as ages <200 Ma that are most likely derived from Mesozoic–Cenozoic arc

A) Foreland basin system



B) Foreland basin system migration and sediment accumulation

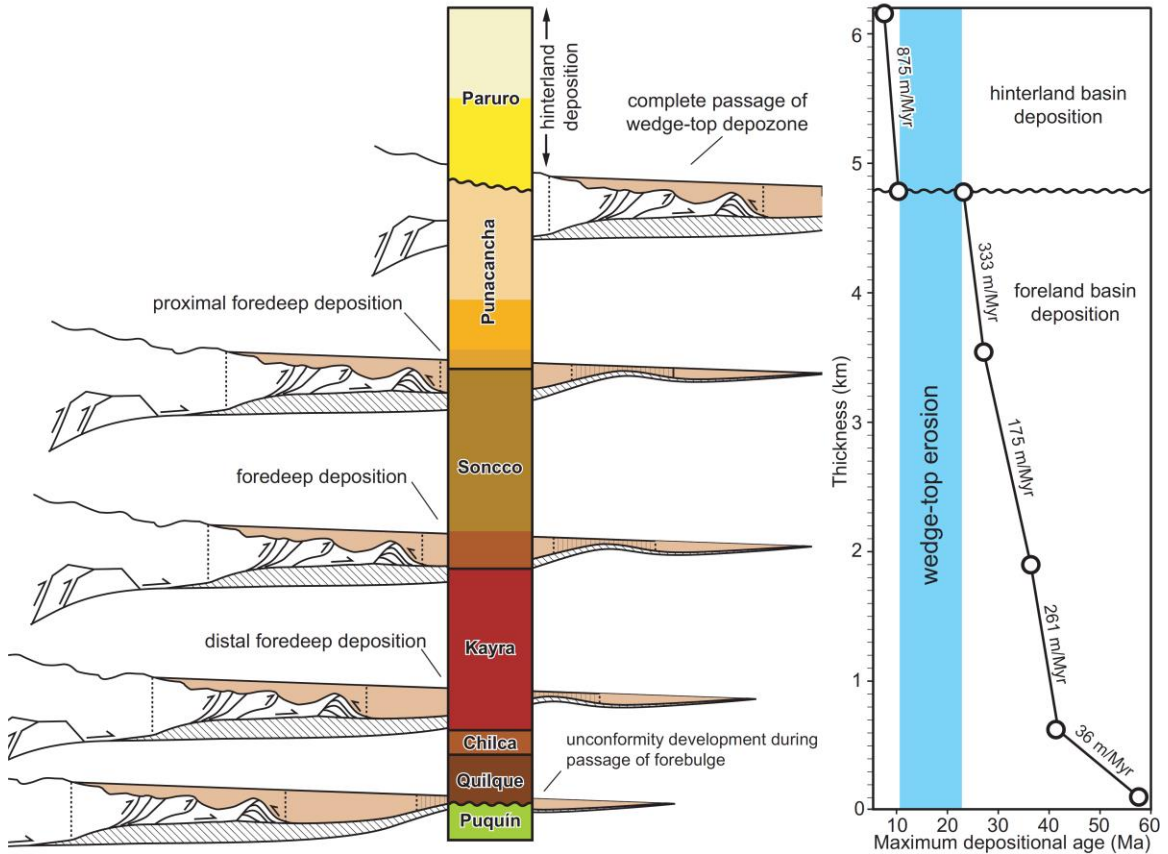


Figure 3.13. A) Foreland basin system (sensu DeCelles and Giles, 1996). B) Foreland to hinterland basin transition in the context of a migrating foreland basin system, and sediment accumulation rates calculated from measured sediment thicknesses and detrital zircon U-Pb maximum depositional ages.

volcanism. The trend toward less-round grains ends at the base of the latest Oligocene Punacancha Formation, consistent with transition to hinterland basin deformation and increased sediment recycling.

Discussion

Paleogene foreland basin development

Stratigraphy and sediment provenance results interpreted in the context of age control provided by detrital zircon U-Pb maximum depositional ages points to Paleogene development of a flexural foreland basin system in the northernmost Peruvian Altiplano. Thick (100–500 m) coarsening-upward packages of siliciclastic stratigraphy in an overall coarsening-upward succession typifies this geodynamic setting (DeCelles, 2012). Low sediment-accumulation rates (<50 m/Myr) from 58–41 Ma, followed by rates >150 m/Myr from 41–23 Ma are consistent with initial deposition of distal foredeep mudstones and fine-grained sandstones transitioning to more proximal foredeep deposition of thick packages of sandstones and conglomerates (DeCelles and Giles, 1996; Xie and Heller, 2009; DeCelles, 2012; Allen and Allen, 2013) (Figure 3.13). Paleocurrent measurements from Paleogene stratigraphy consistently show northeast-directed paleoflow from highlands to the west (i.e., the Western Cordillera). Conglomerate clast counts show a decrease in quartzite and increase in plutonic and sedimentary clasts which may be interpreted as initial sourcing of ubiquitous Mesozoic quartzites in the Western Cordillera followed by tapping of the deeper, locally-intruded Eocene–Oligocene plutonic rocks of the Andahuaylas-Yauri batholith along the northeastern boundary of the Western Cordillera (Figure 3.1C). Sandstone compositions consistently contain abundant volcanic

fragments and plagioclase feldspar with an overall decrease in monocrystalline and polycrystalline quartz throughout the Paleogene, further suggesting consistent sediment sourcing from the Western Cordilleran volcanic arc. Sediment provenance information from detrital zircon quantitative methods (MDS and mixture modeling) supports this interpretation, as Cenozoic Altiplano age distributions are more similar to Mesozoic source formations prevalent in the Western Cordillera and western Altiplano than to Paleozoic strata to the east (Figures 3.10 and 3.11). Detrital zircons decrease in roundness through the Paleogene for all characteristic sediment source age groups, including those interpreted to be sourced from arc volcanics (Figure 3.12). Decreased roundness, interpreted as shorter sediment transport distance, is consistent with increasing proximity of the Western Cordillera from 58 to 23 Ma as it migrated toward the modern study area (Figure 3.13).

Increased sediment input and accommodation along with continued sediment sourcing from formations from the west and southwest is consistent with flexural subsidence induced by increasing proximity and loading by the Western Cordillera in the Paleogene (Figure 3.13). Alternative Paleogene subsidence mechanisms such as strike-slip, extensional, thermal, and dynamic subsidence processes are not supported by observations in the region (see discussion in Horton et al., 2015). Modern crustal thickness variations in the Andean plateau are consistent with Airy isostatic support (Beck et al., 1996), and thus much of the Paleogene Western Cordillera was likely Airy-isostatically supported as well.

Modern departure from Airy isostasy along the eastern edge of the Andean plateau is interpreted from a breakdown in the expected inverse correlation between topography and Bouguer gravity anomalies (Horton and DeCelles, 1997). This was likely also the case in the Paleogene, with a change from Airy isostatic to flexural support from the topographic high of the orogenic wedge to the leading eastern edge, similar to the modern Subandes.

Neogene transition to hinterland basin deposition

The angular unconformity between the Punacancha and Paruro formations from 23 to 9 Ma marks the change from foreland to hinterland basin deposition following passage of the northeastward-migrating wedge-top depozone (Figure 3.13). Neogene stratigraphy of the Paruro Formation represents renewed deposition following deformation, uplift, and denudation as propagation of the retroarc thrust front deformed and consumed earlier foreland basin deposits before ultimately merging with the developing Eastern Cordillera (Figure 3.13); remnant wedge-top deposits are preserved as the Anta Formation to the west and southwest along the northeastern boundary of the modern Western Cordillera (Carlotto, 2013) (Figure 3.1C). Conglomerate clast counts show an increase in sedimentary clasts interpreted as recycling of previously deposited foreland basin stratigraphy in a hinterland basin setting (Figure 3.6). Sandstone petrography reveals a major increase in mono- and polycrystalline quartz at the base of the Paruro Formation before returning to compositions similar to those in the Paleogene (Figures 3.6C-D), which when combined with mixing model results may be interpreted as increased sediment input from shortening-related exposure of Ordovician–Devonian

stratigraphy (Figure 3.11). Zircons from the base of the Paruro Formation show an increase in roundness, marking the end of a trend toward decreased roundness during the Paleogene, consistent with recycling of previous deposits in the hinterland following the final passage of the foredeep and wedge-top depozones. The timing of foreland-hinterland basin transition in the Cusco region is slightly younger than documented along strike to the south in the Ayaviri Basin between 29 and 26 Ma based on well-dated growth strata in the footwall of the Eastern Cordillera backthrust belt (Perez and Horton, 2014; Horton et al., 2015).

Results from sediment composition and detrital zircon U-Pb mixture modeling, when combined with consistently north-northeast-directed paleocurrents, points to shortening-related deformation to the west and southwest of the study area. Candidate structures along the boundary of, and within the modern western Altiplano are the east-vergent Cusco-Lagunillas and/or Pasani-Acomayo regional fault systems (Figures 3.1C and 3.2). The 23–9 Ma angular unconformity brackets local Neogene deformation. Candidate structures based on cross-cutting relationships are the east-vergent Acomayo and/or San Juan de Quihuares thrust faults. This timing of shortening is consistent with the Pasani fault to the southeast which currently bounds the Ayaviri basin, interpreted to be most recently active from 18–16 Ma (Perez and Horton, 2014). The Acomayo fault and/or San Juan de Quihuares faults may represent a northern continuation of the Pasani fault system in the Peruvian Altiplano, as it shares a similar vergence direction and crosscuts many of the same rock units (Figure 3.1C). If accurate, these structures may

point to a regionally-connected system of deformation during the late stages of Andean plateau development.

Sediment accumulation rates of the Miocene Paruro Formation are very high (>800 m/Myr), and cover a short (< 3 Myr) time interval (Figure 3.13). Such high rates and short deposition durations are characteristic of strike-slip subsidence (Xie and Heller, 2009; Allen and Allen, 2013). The Paruro Formation has been interpreted as a strike-slip basin (Carlotto, 2013), as have other structures in the Peruvian Andean plateau based on magmatism and inferred plate dynamics (e.g., Soler and Bonhomme, 1990). Where preserved, the basin has a high length-to-width ratio of ~9:1, which is on the upper end of typical elongate strike-slip basins (Nilsen and Sylvester, 1999). Invoking strike-slip faulting also implies vertical-axis rotations, which has been suggested to explain development of the Bolivian orocline from 25–12 Ma, with continued transpressional deformation post 12 Ma throughout the Peruvian Altiplano (Rousse et al., 2005). Despite stratigraphic and provenance records pointing to a strike-slip subsidence mechanism, there is little supporting structural evidence (i.e. there are few mapped strike-slip faults in the area). This may be explained by overprinting of left-lateral transpressional structures by more dip-slip contraction, which is consistent with the changing plate convergence geometry in the middle to late Miocene from oblique to more orthogonal convergence (Pilger, 1984; Pardo-Casas and Molnar, 1987).

We envision the transition from foreland to hinterland basin deposition should be accompanied by a change from regional flexurally supported crust to locally isostatically supported crust. As in the modern, there was likely interplay of both flexural and isostatic

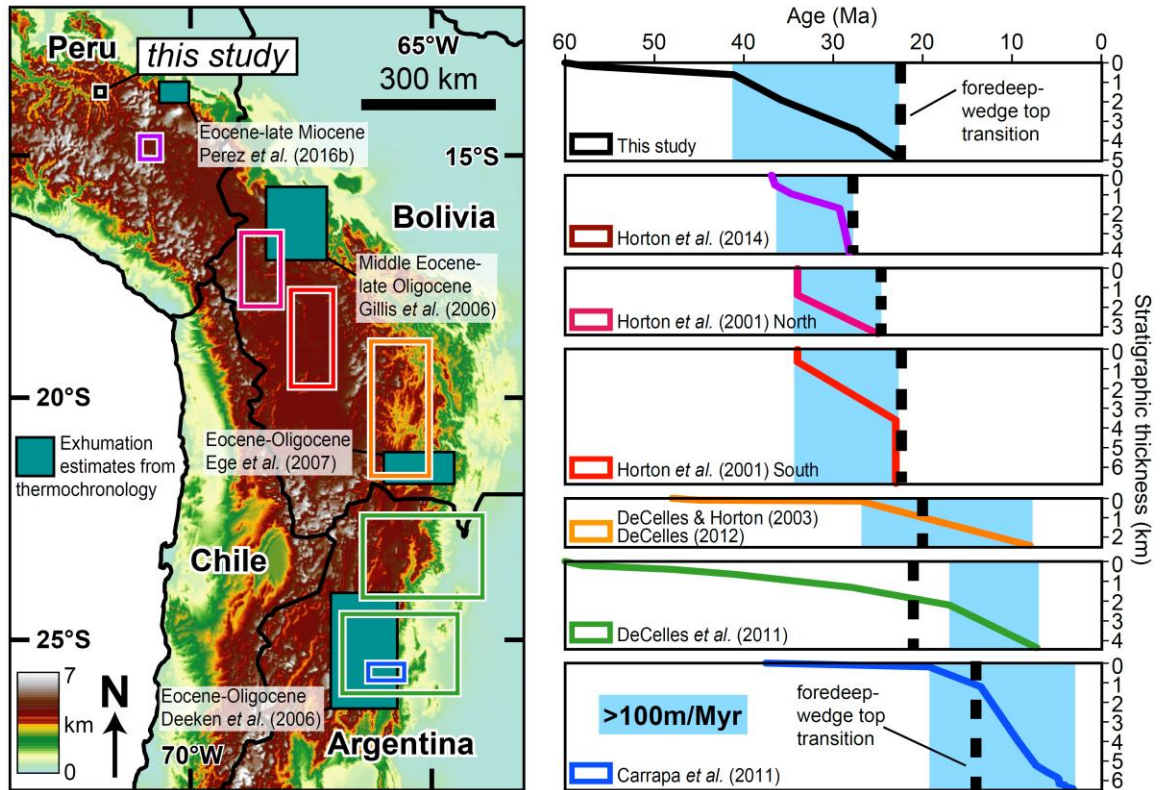


Figure 3.14. Locations of foreland basin records (colored boxes) and estimates of timing of shortening-related exhumation based on thermochronology (blue boxes). Sediment accumulation curves of foreland basin stratigraphy documented in the modern Altiplano and Eastern Cordillera for the Andean plateau. Note the systematically younger onset of rapid subsidence to the south and thicker foredeep deposits in the north.

support for the growing load of the nascent Andean plateau in the Paleogene. The crustal thickness in the modern Altiplano and adjacent Cordilleras is up to 60–70 km (Beck and Zandt, 2002), which cannot be supported by lithospheric flexure alone (Molnar and Lyon-Caen, 1988). The location of the modern forebulge east of the Andean plateau (Horton and DeCelles, 1997) further precludes complete flexural support in the modern Peruvian Altiplano.

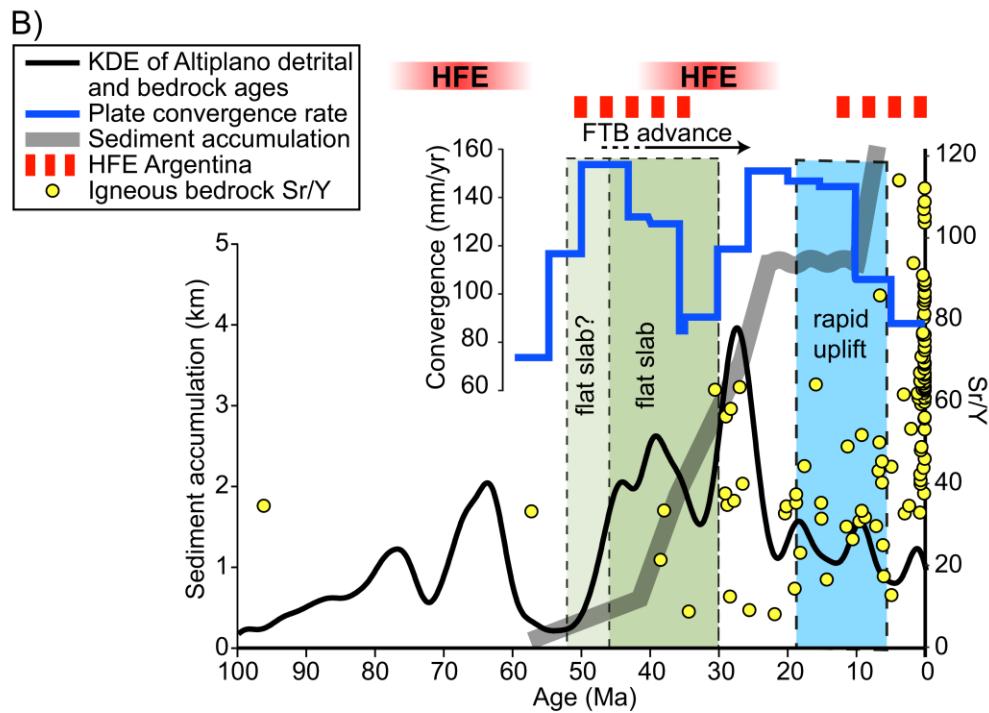
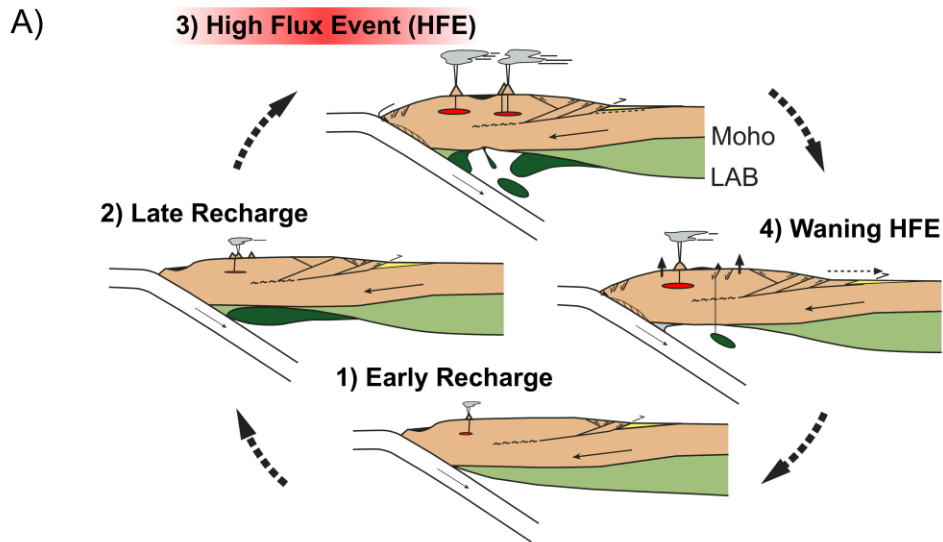
Geodynamic implications: basin subsidence and surface uplift

Peruvian Altiplano foreland basin stratigraphy highlights significant along-strike variability in the timing and location of foreland deposition of a regionally-contiguous Cenozoic foreland basin system that extended for hundreds of km along strike of the eastern Andean margin from southern Peru, through Bolivia, and into northwest Argentina (Horton et al., 2001, 2002, 2015; DeCelles and Horton, 2003; DeCelles et al., 2011; Carrapa et al., 2012) (Figure 3.14). The onset of high (>100 m/Myr) sediment accumulation rates occur earlier in the northern Andean plateau of southern Peru and northern Bolivia (40 – 35 Ma), and later in southern Bolivia and Argentina (30 – 20 Ma) (Figure 3.14) (Horton et al., 2001, 2002, 2015; DeCelles and Horton, 2003; DeCelles et al., 2011; Carrapa et al., 2012). Assuming coeval structural evolution, this results in the thickest sections of foreland basin stratigraphy deposited during foredeep deposition in the north, and during wedge-top deposition in the south. In fact, most wedge-top deposits in the north are not preserved in the same locations as the foredeep deposits, or not preserved at all.

The trend of high sediment-accumulation rates occurring later temporally, and later in terms of typical foreland basin system development (DeCelles and Giles, 1996) could be the result of bias in the location of preserved and documented foreland deposits relative to the propagating orogenic wedge. To determine whether there is a difference in the onset of rapid sediment accumulation from north to south, the predicted migration of the Andean flexural wave may be compared to relative locations following the methods of DeCelles and DeCelles (2001). Here, flexural wave migration rate = shortening rate +

rate of orogenic wedge widening. There is a nearly 20 Myr difference in the onset of rapid (>100 m/Myr) sediment accumulation between the northern and southern locations. Long-term shortening rates in the Cenozoic Andes are ~ 10 mm/yr (Oncken et al., 2006). The DeCelles and DeCelles (2001) method gives a long-term wedge widening rate of ~ 8 mm/yr, yielding a flexural wave migration rate of ~ 18 mm/yr. Thus, a 20 Myr difference in the timing of onset of rapid sediment accumulation rate would require a ~ 360 km difference in their locations for the flexural wave to pass between the sites. In this context, the relative location of these studies cannot account for the difference in the onset of rapid sediment accumulation, and there must be an explanation for the apparent trend involving the complex convergence history of the central Andes. A likely scenario involves inheritance of orogen-scale, antecedent structural and stratigraphic differences of the central Andes (McGroder et al., 2015), which may have caused Cenozoic foreland development to respond differently along orogenic strike (discussed further below).

Development of a foreland basin system in the northern Peruvian Altiplano requires lithospheric loading of the Western Cordilleran hinterland and relative subsidence to the east in the location of the modern Eastern Cordillera. The former can be explained through increased topography and proximity of the Paleogene Western Cordilleran magmatic arc and orogenic front to the study area (Mamani et al., 2008, 2010), as elevations were likely moderately high (1–2 km) before the middle Miocene (Saylor and Horton, 2014). However, the latter is in contrast to thermochronometric data from the Eastern Cordillera, which suggest pulses of exhumation and building of topography in the middle Eocene–late Oligocene (Gillis et al., 2006), and Eocene to late



Miocene (Perez et al., 2016b), overlapping in time when foreland basin records predict relative subsidence.

There are similar conflicting lines of evidence between flexural-foreland-related basin subsidence interpreted from stratigraphic records and shortening-related

Figure 3.15 (previous page). A) Orogenic cyclicity model modified from DeCelles et al. (2015). This model predicts A-1) partial melting of underthrust continental lower crust and mantle lithosphere drives high-flux magmatism and emplacement of a high-density restitic and eclogitic crustal root; A-2) development of a dense restite or eclogite keel resulting in decreased elevation and subcritical orogenic wedge taper that drives internal deformation; A-3) foundering of gravitationally-unstable crustal root via Rayleigh-Taylor instabilities; and A-4) supercritical wedge taper that drives rapid foreland basin system migration and propagation of the retroarc fold-and-thrust belt (Figure 15A-4). B) Compilation of data from southern Peru in the context of the orogenic cyclicity model. Kernel density estimate of combined ages from Cenozoic Altiplano detrital zircon U-Pb samples and igneous bedrock ages (from 13–18° S). Plate convergence rates (in blue) from Pardo-Casas and Molnar (1987) do not correlate with apparent cyclicity. Sr/Y data (yellow circles) were filtered to exclude samples containing SiO₂ >65 wt.% to avoid differentiation effects on trace elements.

exhumation interpreted from thermochronology in other parts of the central Andes. For example, foreland basin records in southern Bolivia reveal Oligocene (to possibly earliest Miocene) foredeep deposition (DeCelles and Horton, 2003) the same time and general location as Ege et al. (2007) interpret late Eocene–Oligocene exhumation and cooling (Figure 3.14). Further, foreland basin records in northwest Argentina require flexural subsidence and Eocene–Oligocene foredeep deposition (DeCelles et al., 2011) at the same time as Eocene–Oligocene shortening-related deformation interpreted from thermochronology (e.g., Deeken et al., 2006). Reconciling these conflicting lines of evidence between basin subsidence and thermochronometric records in the Andean Eastern Cordillera requires one of the following: 1) that the preserved stratigraphy discussed above does not represent a classically defined foreland basin system, 2) reinterpretation of existing thermochronology data, or 3) revision of our understanding of the geodynamics of foreland basins, perhaps with an alternative flexural model for foreland basin development capable of incorporating an Eastern Cordilleran load within

the flexed lithospheric plate. DeCelles and Horton (2003) invoke a similar model for the latter in the Bolivian Andes, but do not explain in detail the geodynamics for such a system. Reconciling these conflicting lines of evidence provides an avenue for future investigation.

Foreland basin development and cyclical orogenic processes

Models of orogenic cyclicity for Cordilleran-type mountain belts have been used to explain records of mountain building in the context of predictable, cyclical geodynamic processes manifested as periods of high-flux magmatism, crustal thickening, and surface uplift (Haschke et al., 2002, 2006; DeCelles et al., 2009, 2015; Ramos, 2009; Ramos et al., 2014; DeCelles and Graham, 2015) (Figure 3.15A). The model of DeCelles et al. (2015) predicts that partial melting of underthrust continental lower crust and mantle lithosphere drives periodicity in high-flux magmatism and emplacement of a high-density restitic and eclogitic crustal root during magma generation and lower crustal thickening (Figure 3.15A-1). Development of a dense restite or eclogite keel results in decreased regional elevation and a subcritical state of orogenic wedge taper that drives internal deformation and regional elevation gain in order to build wedge taper (Figure 3.15A-2) (*sensu* Davis et al., 1983). This takes place until a critical mass of the gravitationally-unstable crustal root founders via Rayleigh-Taylor instabilities (Göğüş and Pysklywec, 2008; Currie et al., 2015) or mantle-lithosphere delamination (Kay and Kay, 1993; Krystopowicz and Currie, 2013) into the underlying asthenosphere, ultimately resulting in a net elevation gain through isostatic adjustment (Figure 3.15A-3), and accompanied by ignimbrite eruptions. Increased elevation places the orogen into a state

of supercritical wedge taper that drives rapid foreland-directed propagation of the retroarc fold-and-thrust belt and concomitant migration of the foreland basin system (Figure 3.15A-4). The cycle then begins anew, repeating in a 25–50 Myr time scale, with the rate of repetition of the cycle is dependent on, among other factors, the rate of simple-shear underthrusting of lower crust and lithospheric material.

Some observations in support of the orogenic cyclicity model in the southeastern Andean plateau of northwest Argentina have not been observed in southern Peru. For example, evidence for lithospheric foundering through Rayleigh-Taylor instability and/or lithospheric delamination, as expressed by periods of mantle-derived magmatic input with decreased $^{143}\text{Nd}/^{144}\text{Nd}$ and elevated La/Yb and/or Sm/Y values (e.g., Kay et al., 1994; Haschke et al., 2002, 2006; Chapman et al., 2015; Profeta et al., 2015), have yet to be documented in southern Peru. Similarly, there are no records of Cenozoic hinterland extension in southern Peru, as have been observed in the Puna plateau (e.g., Schoenbohm and Strecker, 2009). There are no Paleogene surface elevation estimates; proxy records only address the middle Miocene and younger, suggesting rapid surface uplift from 18–16 Ma in the Western Cordillera (Saylor and Horton, 2014) and 10–6 Ma in the Altiplano (Kar et al., 2016).

The majority of observations in support of the orogenic cyclicity model in the central Andes come from southern Bolivia and northwest Argentina (e.g., Carrapa and DeCelles, 2015; DeCelles et al., 2015; Ducea et al., 2015), leaving southern Peru largely undiscussed in terms of cyclical processes. Despite this, many similar cyclical processes are indeed observed in this region. There are apparent pulses of magmatism from bedrock

ages compiled from the Central Andes Geochemical and Geochronology Database (<http://andes.gzg.geo.uni-goettingen.de/>) and Cenozoic detrital zircon U-Pb samples (Figure 3.15B). Sediment accumulation rate dramatically increases during the high-flux event between 50 and 30 Ma, which coincides with an inboard step of widespread magmatism in southern Peru (Mamani et al., 2010), which may have increased flexural loading due to magmatic emplacement. Magmatic loading has been previously invoked to explain flexural subsidence of the lithosphere for other orogenic systems (e.g., Peterman and Sims, 1988). While this specific aspect of orogenesis has not been discussed in terms of cyclical orogenic processes, it is an interesting and testable corollary to the original model.

Timing of crustal deformation is a critical part of the cyclicity model. Records of crustal deformation in southern Peru are rare due to pervasive and ongoing Cenozoic arc volcanism (Oncken et al., 2006; Perez and Horton, 2014). However, assuming the position of the magmatic arc interpreted by Mamani et al. (2010) tracks orogenic wedge propagation, the retroarc fold-and-thrust belt is predicted to rapidly advance northeastward in southern Peru from 45–30 Ma (Figure 3.15B). Further, detrital zircon U-Pb mixture modeling presented here points to shortening-related deformation at ~36 Ma and post ~7 Ma (Figure 3.11). In the context of the cyclicity model, this is predicted to occur after intense magmatism and regional elevation gain in the hinterland. Although there is evidence of the former, there are no Paleogene surface uplift estimates to support the latter. Isotopic data predicted to track crustal thickening (e.g., Sr/Y; Chapman et al., 2015; Profeta et al., 2015), shows an increase at 30 Ma (yellow circles in Figure 3.15B),

particularly in the ‘Paracas domain’ (14–15° S) of southern Peru (Mamani et al., 2010). (Sr/Y data were filtered to exclude samples containing SiO₂ >65 wt. % to avoid differentiation effects on trace elements.) This latter observation is predicted by the cyclicity model to occur during building of orogenic wedge taper preceding rapid surface uplift, and consistent with timing of Oligocene retroarc deformation and Miocene surface uplift records in the Peruvian Western Cordillera (Saylor and Horton, 2014).

Cyclical observations in southern Peru and northwest Argentina are slightly out of phase. This is highlighted by the timing of high-flux events and intense magmatic activity in northwest Argentina at 50–45 and 15–5 (DeCelles et al., 2015), which is slightly younger than observed in southern Peru (Figure 3.15B). This southward offset in predicted phases of the model also tracks the apparent southward-younging onset of rapid sedimentation (Figure 3.14). A key difference in the orogenic cyclicity model of DeCelles et al. (2015) and DeCelles et al. (2009) from other cyclicity models (e.g., Ramos, 2009; Ramos et al., 2014), is the role underthrust continental material plays in driving cyclicity. Specifically, underthrust continental lower crust and mantle lithosphere is more prone to melting and producing abnormally high fluxes of magma production and emplacement of dense restite and eclogite (Ducea and Barton, 2007), thus producing gravitational instability leading to foundering of the mantle lithosphere. The rate of upper plate lithospheric underthrusting is controlled by the geometry and basement involvement of the fold-and-thrust belt. Cenozoic contractional deformation on the eastern edge of the central Andes is at least in part controlled by preexisting Paleozoic and Mesozoic structural domains (McGroder et al., 2015). There is a distinct difference in

inherited structures south of the Bolivia-Argentina border where a transition from the Bolivian salient and in situ South American basement, to where lithosphere dominated by accreted terranes and antecedent Paleozoic structural fabrics are located (McGroder et al., 2015). This may control the north-to-south transition from dominantly thin-skinned fold-and-thrust belt contractional deformation in southern Peru through southern Bolivia to more basement-involved deformation in northwest Argentina during the Cenozoic, and the rate of lithospheric underthrusting. If the rate at which continental material is underthrust directly controls when and where high-flux events occur, then the preexisting structural fabric of the Paleozoic–Mesozoic central Andes may explain the apparent out-of-phase cycles observed between southern Peru and northwest Argentina. This hypothesis provides testable predictions of the orogenic cyclicity model along orogenic strike from southern Peru to northwest Argentina.

Conclusions

The ~6200 m of Cenozoic non-marine siliciclastic stratigraphy and new depositional chronology based on detrital zircon U-Pb maximum depositional ages in the northern Altiplano of southern Peru records the development and passage of a foreland basin system. Foredeep deposition occurs from 41–23 Ma, as evidenced by high (>150 m/Myr) sediment accumulation rates, and is followed by a transition to hinterland basin deposition in the latest Paleogene. Rapid (>800 m/Myr) Miocene deposition of the Paruro Formation may reflect strike-slip subsidence related to regional transpression. Sediment provenance indicators consistently point to western-sourced sediments from the Cenozoic Western Cordillera and western Altiplano throughout the Paleogene.

Our results suggest there was a regionally-contiguous Paleogene foreland basin system on the eastern edge of the Andes for hundreds of km along strike. Development of a foreland basin system requires Paleogene lithospheric loading of the Western Cordilleran hinterland and relative flexural subsidence to the east in the location of the modern Eastern Cordillera. Comparison of basin subsidence with thermochronometric evidence of coeval shortening-induced exhumation and foreland basin deposition, which suggests an incomplete understanding of the evolution of this archetypal retroarc foreland basin system.

Our results also highlight significant along-strike differences in foreland basin evolution: foredeep deposits are thinner, and the timing of high sediment accumulation rate is systematically later from north to south. Peruvian Altiplano stratigraphy, considered in the context of magmatism, igneous geochemistry, and surface uplift records supports models of orogenic cyclicity. However, high-flux magmatic events occur earlier and with shorter cycles in southern Peru compared to northwest Argentina. Along-strike variability controlled by structural Paleozoic–Mesozoic tectonic fabric preceding development of the Cenozoic Andean plateau may control the rate of simple shear underthrusting of continental lithospheric material and hence modulate the tempo of orogenic cycles.

CHAPTER 4

Variable Late Cenozoic Surface Uplift across Southern Peru

To be submitted for publication in Proceedings of the National Academy of Sciences of the United States of America, November, 2017

Authors:

Kurt E. Sundell

Joel E. Saylor¹

Thomas J. Lapen¹

¹**Department of Earth and Atmospheric Sciences, University of Houston, Houston, Texas, USA**

Introduction

The central Andean orogen is the archetypal ocean-continent convergent boundary, and Earth's second largest modern orogenic plateau (Allmendinger et al., 1997). Development of ~4 km-high topography in the central Andes took place largely in the Cenozoic during east-directed subduction of oceanic lithosphere (Allmendinger et al., 1997). However, details of how and when this high topography was attained have been the subject of considerable debate (Garzione et al., 2008; Barnes and Ehlers, 2009; Ehlers and Poulsen, 2009; Saylor and Horton, 2014). All geodynamic models explaining surface uplift of the Andes, irrespective the controlling mechanism ultimately driving the development of elevated topography, require removal of mantle lithosphere in order to generate isostatic adjustment and surface uplift. Geodynamic models make specific spatial and temporal predictions for surface uplift and crustal shortening. For example, removal of lower crust or mantle lithosphere via large-scale mantle convection, or foundering of Rayleigh-Taylor instabilities has been proposed as a viable mechanism for

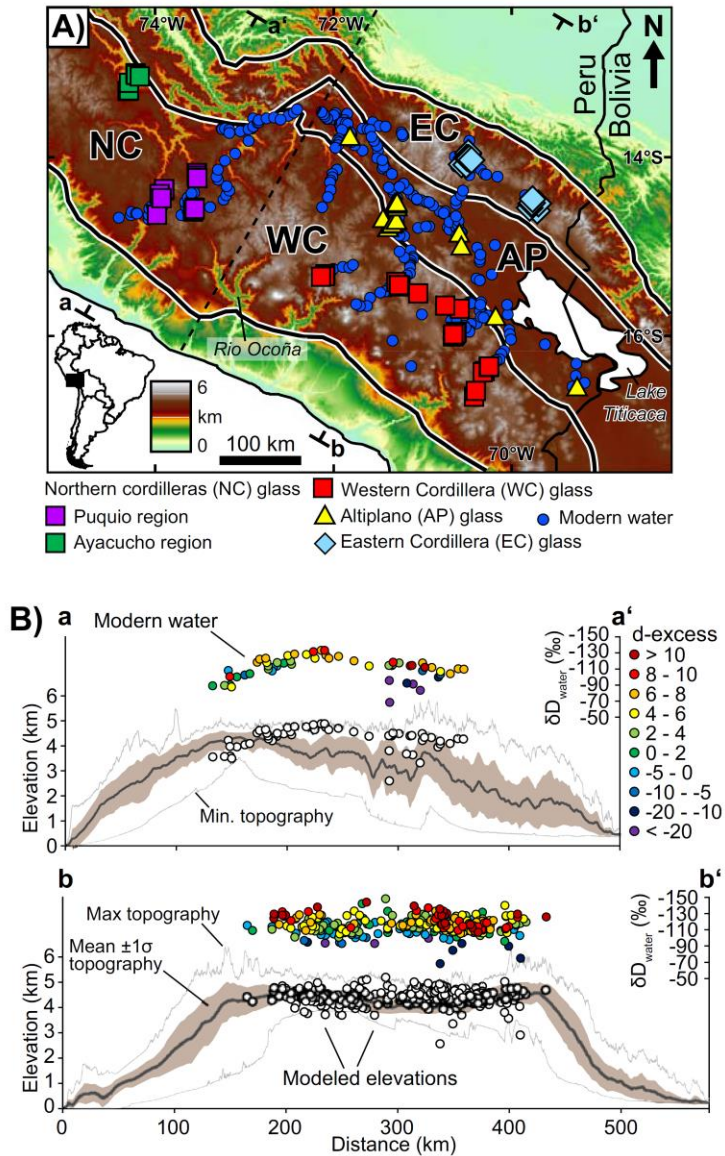


Figure 4.1. (A) Digital elevation model showing the extent of the Andean plateau generated from Shuttle Radar Topography Mission 90m elevation data. Physiographic regions characterizing the central Andes: NC = northern cordilleras, WC = Western Cordillera, AP = Altiplano, EC = Eastern Cordillera. Topographic swaths a-a' and b-b' are 140 and 340 km wide, respectively. (B) Topographic swaths shown in part A with mean, minimum, maximum, and one standard deviation (brown shading) elevations. Modern water measurements are color-coded to d-excess values. White circles are elevation values modeled using a modified non-linear isotopic lapse rate of Rowley (2007) (see text for details).

wholesale (e.g., England and Houseman, 1989), or localized (e.g., Göğüş and Pysklywec, 2008) rapid (e.g., > 0.5 km/Myr) surface uplift decoupled from crustal shortening.

Alternatively, incremental removal by ablative subduction (e.g., Pope and Willet, 1998), thermal weakening (e.g., Isacks, 1988), or underthrusting of detached mantle lithosphere (e.g., Ducea, 2001), predicts slower (e.g., < 0.5 km/Myr) surface uplift in concert with crustal shortening.

The tectonic evolution of the greater Andean orogen, Earth's longest continuous modern mountain chain, in part controls climate patterns of the region. The central Andes receive the overwhelming majority of their moisture from Atlantic-sourced equatorial easterlies that traverse the Amazon basin (Lenters and Cook, 1997). Progressive rainout of heavier D and ^{18}O isotopes over the Amazon is balanced by re-evaporated (recycled) moisture and forest transpiration within the Amazon basin resulting in an inland isotopic gradient considerably lower than the global average (Salati et al., 1979; Moreira et al., 1997). Moisture is deflected southward by the topography of the northern Andes and transported by the South American low-level jet, eventually penetrating the central Andes from the northeast and east, resulting in heavy precipitation along the Eastern Cordillera, the majority of which falls in austral summer. This results in increasingly arid conditions to the west, culminating in the Atacama Desert, one of the driest deserts on Earth. The timing of establishment of hyperarid conditions is debated to have occurred sometime between the late Oligocene and latest Miocene; this timing is critical for understanding climate-orogenic interactions in the central Andes (Rech et al., 2010; Mulch et al., 2010; Schlunegger et al., 2010).

Surface uplift is central to questions of climate and tectonics. The horizontal forces that drive tectonic plate motion are proportional to the forces required to uplift and support mountain ranges (England and Molnar, 1990); topography in turn drives critical climate feedbacks of local (Schlunegger et al., 2010), regional (e.g., Insel et al., 2012), and global (Raymo and Ruddiman, 1992) significance. Despite such interest and importance in the study of vertical motion of the Earth's surface, it remains difficult to measure in the geologic past because only proxy methods may be used. Methods applied to the central Andes have been based on timing of crustal shortening (Isacks, 1988), or on geomorphic features such as regional tilt resulting from monocline development (Jordan et al., 2010), paleosurface peneplain mapping (Kennan et al., 1997), or river incision (Jeffery et al., 2013). Alternatively, biological proxies have been used to infer surface uplift of the central Andes including phylogenetics of high-elevation biotaxa (Picard et al., 2008), palynology and paleobotany (Muñoz and Charrier, 1996), and leaf physiognomy (Gregory-Wodzicki, 1998). Limitations of these techniques include preservation potential, recording rock uplift rather than surface uplift (sensu England and Molnar, 1990), or in many cases non-unique interpretation. More recently developed paleoelevation proxies exploit the light stable isotopic record by measuring soil carbonate $\delta^{18}\text{O}$ (e.g., Garzzone et al., 2008), mean annual air temperatures inferred from carbonate clumped isotope Δ_{47} variations (e.g., Huntington and Lechler, 2015), or paleoenvironmental waters preserved in hydrated volcanic glass (Cassel and Breecker, 2016). These stable isotopic proxies may be subject to diagenetic alteration and/or isotopic overprinting; however, when preserved pristinely, these proxies can be coupled

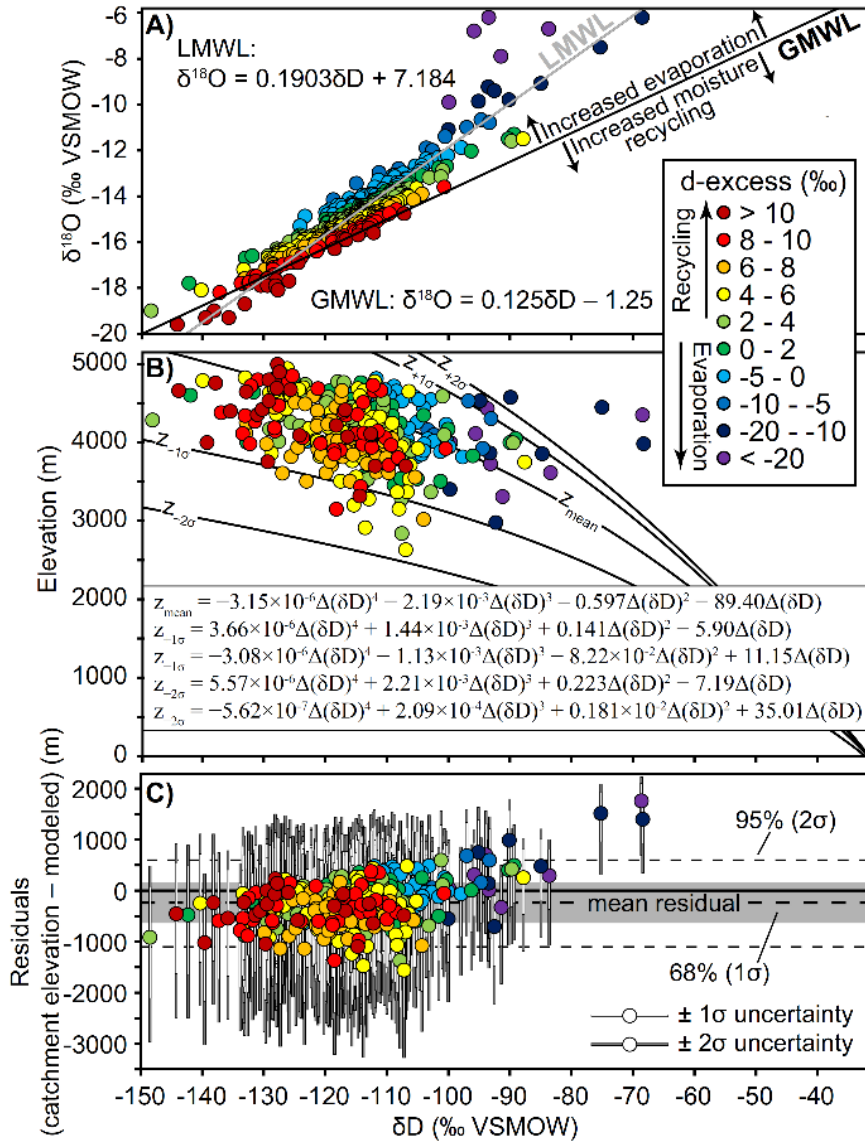


Figure 4.2. Modern water stable isotopic values from samples shown in Figure 4.1A (δD and $\delta^{18}\text{O}$ relative to VSMOW) compared to GMWL color-coded to d-excess values (complete sample details are in Appendix 5). Two highly evaporated points not shown at -2.9 and $+5.6$ ‰ $\delta^{18}\text{O}$ (B) Modern water δD values converted to elevation based on lapse rate modified from Rowley (2007). (C) Residuals (mean catchment elevations – modeled elevations). The majority of water values yield overestimates in catchment mean elevation resulting in a negative mean residual (-246 ± 427 m at 1σ).

with isotopic or temperature lapse rates to infer paleoelevation. Lapse rates based on modern samples must account for lapse rate changes as surface elevations increase (Insel et al., 2012).

Application of D/H isotopic analyses of hydrated volcanic glass to paleoaltimetry is a particularly powerful stable isotopic technique because water-glass isotopic fractionation is independent of temperature, and glass is a durable closed system once fully hydrated (Friedman et al., 1993; Casey, 2008). There has long been definitive evidence for the existence of molecular water in silicate glasses (e.g., Stöckhert, 1982) incorporated post-depositionally at low temperatures rather than from the original magmatic source (Friedman et al., 1993). Although the primary mechanism of low-temperature water absorption is debated (e.g., Valle et al., 2010), many agree that incorporation of water into glass involves the selective removal of susceptible alkali ion reaction sites on the glass surface (Charles, 1958), and continues with subsequent diffusion into glass through replacement of large-radius alkali metal cations (e.g., Na, K) with H⁺ and D⁺ ions (e.g., Calliteau et al., 2008; Casey, 2008). Following hydration, glasses form alteration products in the form of gels, phyllosilicates, or phosphates (Valle et al., 2010), a process recognized as early as the 1840s (Von Waltershausen, 1845). Formation of gel layers in glasses rich in SiO₂ and depleted in alkali metal oxides (e.g., Na₂O, K₂O) acts to impede further corrosion on the surfaces of glass shards (Casey, 2008). Insofar as glass is not significantly altered, heated, or subjected to extreme pH conditions (Nolan and Bindeman, 2013), there is sufficient water content to dominate over potential magmatic water signal (Seligman et al., 2016), and exterior clays have been sufficiently removed (Cassel and Breecker, 2016), glass D/H compositions are representative of preserved ancient environmental water (Friedman et al., 1993), and thus useful in determining past elevations of orogens with extensive volcanism.

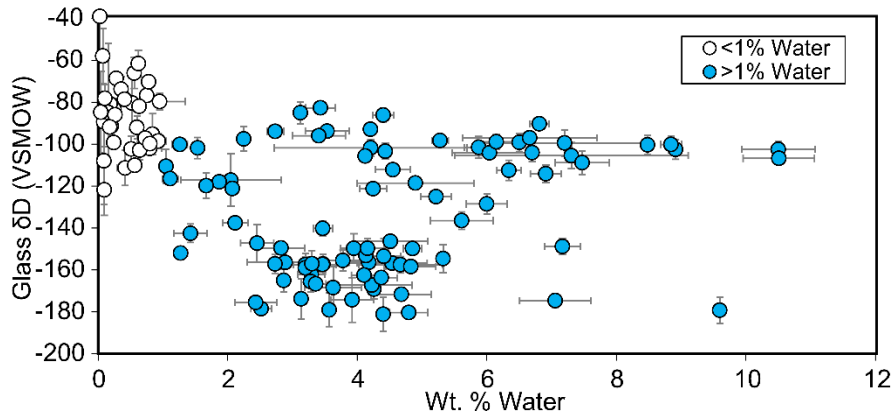


Figure 4.3. Volcanic glass weight % water plotted against raw δD measurements (samples shown in Figure 4.1A and details tabulated in Appendix 5). Glasses with low hydration (<1 weight %) are biased toward positive values due to instrumentation sensitivity, and are not considered in paleoelevation calculations.

We present stable isotopic data from 376 modern stream water samples (179 new) and 136 volcanic glass samples (117 new samples, 488 individual aliquots) spanning the central Andes of southern Peru (Figure 4.1A and Appendix 5). Water samples were collected during five field seasons in the austral winters of 2010, 2011, and 2014–2016. Results show that mean catchment elevations can be calculated by applying a nonlinear isotopic lapse rate (Rowley, 2007) to modern water D/H ratios. Further, successful reproduction of modern elevations from Pliocene–Pleistocene glass samples using this same lapse rate sets the foundation for interpreting paleoelevations from preserved waters deeper in the geologic past. Paleoelevation estimates from hydrated volcanic glasses, temporally controlled by new zircon U-Pb dates and published age dates, reveal spatially and temporally variable late Cenozoic surface uplift episodes and variable surface uplift rates across the Peruvian central Andes. The northern cordilleras of southern Peru attained modern elevation by ~ 22 Ma. The Western Cordillera and Altiplano rose to

modern elevation rapidly between 22 and 17 Ma and 17 and 12 Ma, respectively, whereas the Eastern Cordillera gained elevation more slowly between 25 and 10 Ma. Differing surface uplift rates and temporal coincidence with crustal shortening implicate multiple geodynamic processes active during the Cenozoic construction of the Peruvian central Andes (cf., Barnes and Ehlers, 2009). The timing of development of high topography, and spatial comparison to modern stable isotopic patterns, suggests the hyperarid Pacific coast of the central Andes was established by the early to middle Miocene.

Methods

All stable isotopic results for modern water and volcanic glass are reported using δ notation relative to Vienna standard mean ocean water (VSMOW) (detailed results are reported in Appendices 5 and 6). Modern water results were combined with results presented in Bershaw et al. (2016). New water samples were collected in austral winter months of May and June in 2015 and July and August in 2016, and analyzed at the University of Rochester Stable Isotope Ratios in the Environment Analytical Laboratory (SIREAL) using off-axis integrated cavity output spectroscopy on a Los Gatos Research liquid water isotope analyzer. For each analysis, ~900 nL of water were injected into a heated block of the water isotope analyzer. A single analysis is based on fourteen individual injections, ignoring the first three in order to avoid memory effects, with a minimum of five injections used to calculate the final isotopic value. Results are reported relative to VSMOW and normalized such that H and O are both 0‰ for VSMOW, and –428 and –55.5 for Vienna Standard Light Antarctic Precipitation (VSLAP). Volcanic samples were crushed and milled to < 500 μm and water tabled. Glass was prepared

following methods outlined in Cassel and Breecker (2016). The light water table fraction was wet sieved to 125 and 250 μm , soaked in 6N HCl for 24 h, sonic bathed for 1 to 4 h, dried, magnetically separated, density separated using lithium sodium metatungstate (LST) with a density between 2.40 and 2.45 g/mL, and bathed in $\sim 10\%$ HF for 8 to 10 s. Samples were examined with a petrographic microscope to check for purity. Samples of 1.5–2.5 mg were packed into Ag crucibles and analyzed on a thermal combustion element analyzer at the University of Texas at Austin and the University of Arizona. Results were combined with those presented in Saylor and Horton (2014). For the 45 samples lacking age control, zircons were extracted from the water table heavy fraction using standard heavy liquid separation with methylene iodide with a density between 3.30 and 3.32 g/mL and magnetic separation. Zircons were analyzed by laser-ablation inductively-coupled-plasma mass-spectrometry (LA-ICP-MS) at the University of Houston and the LaserChron center at the University of Arizona (see Appendices 7 and 9 for details of LA-ICP-MS, data reduction, and initial-Pb corrections).

Results

Modern water isotopic signatures are reported relative to Vienna Standard Mean Ocean Water (VSMOW) as δD and $\delta^{18}\text{O}$. Results from the Peruvian central Andes deviate from the global meteoric water line (GMWL) defined as $\delta\text{D} = 8 \times \delta^{18}\text{O} + 10$ (Craig, 1961) (Figure 4.2A). Comparison of the local meteoric water line (LMWL) to the GMWL allows for calculation of the δD in individual water samples resulting from non-equilibrium conditions ($d\text{-excess} = \delta\text{D} - 8 \times \delta^{18}\text{O}$), and can be used to understand evaporative processes and/or moisture sourcing (Dansgaard, 1964; Fröhlich et al., 2001).

The LMWL deviates from the GMWL primarily due to evaporative effects rather than moisture recycling, as results with very negative d-excess values largely control the regression producing the LMWL (Figure 4.2A). Water δD values show a general increase from east to west, which is especially pronounced across the northern cordilleras (Figure 4.1B).

The hypsometric mean (mean drainage basin elevation) was calculated for each modern water D/H ratios using a modified version of the atmospheric lapse rate model of Rowley (2007). This lapse rate was derived from a polynomial regression of modeled changes in the O isotopic composition of precipitation due to adiabatic expansion and condensation with changes in elevation (equation 5 in Rowley, 2007). The model uses modern temperature and relative humidity combinations that result in $\delta^{18}O$ values of precipitation between 0 and -25‰ (Rowley, 2007). The lapse rate and associated uncertainties were linearly converted from the O system to D/H (δD) using the GMWL (Figure 4.2B). The lapse rate is benchmarked to low-elevation isotopic compositions and applied to a specific region by calculating the hypsometric mean elevation for incremental changes ($\Delta\delta D$) from that low-elevation baseline (Figure 4.2B) (Rowley, 2007). Here we normalize to $\delta D = -31.6\text{‰}$, converted using the GMWL from the average isotopic composition of precipitation reported for Trinidad, Bolivia of $\delta^{18}O = -5.2\text{‰}$ (Gonfiantini et al., 2001; Rowley, 2007). The non-linear lapse of Rowley (2007) is similar to changes in O isotopic compositions induced by elevation gain from isotope-tracking general circulation modeling (Insel et al., 2012). Results show 96% of absolute residuals (catchment mean elevation – modeled elevation) are less than 1000 m; 71% are

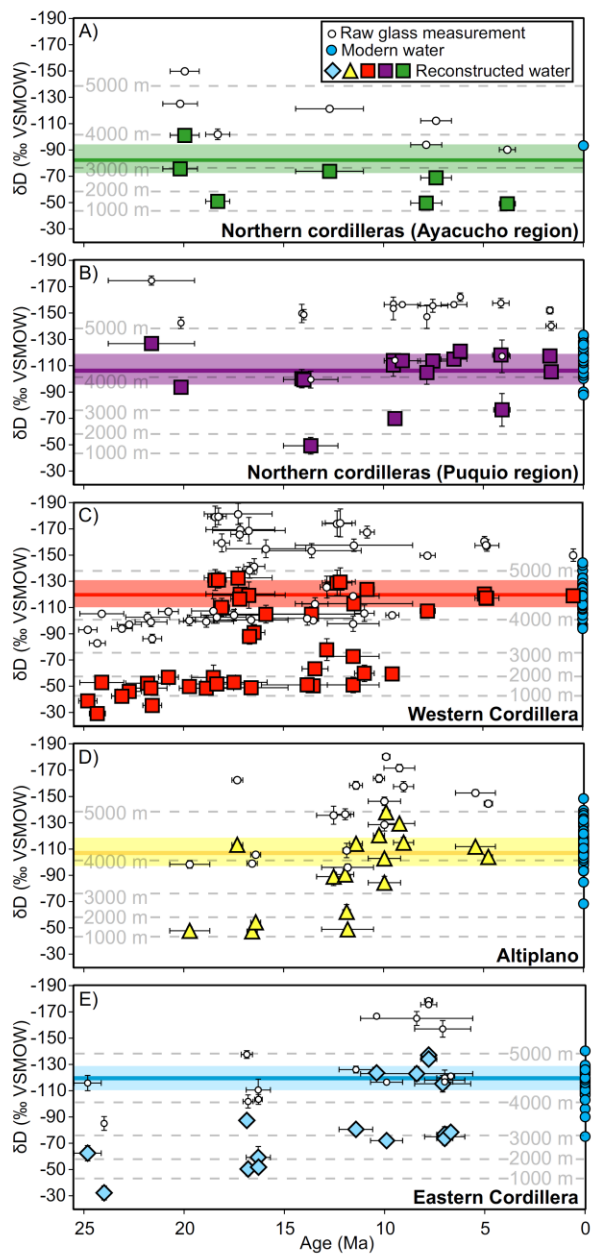


Figure 4.4. Volcanic glass stable isotopic raw measurements (white circles) and corresponding reconstructed and climate-change-corrected water values. Age dates and sources are tabulated in Appendix 6. Blue circles represent modern waters for each physiographic region: northern cordilleras (A) Ayacucho and (B) Puquio regions. (C) Western Cordillera. (D) Altiplano. (E) Eastern Cordillera. Symbol shapes and colors are keyed to Figure 4.1. Colored bars are the mean and 1σ range of topography for where samples were collected. Note relatively positive values may result from evaporative enrichment. Gray dashed lines are paleoelevation estimates based on a modified lapse rate from Rowley (2007). All uncertainties are 1σ .

less than 500 m (Figure 4.2C). The lapse rate performs better in the southern Western Cordillera, Altiplano, and Eastern Cordillera to the south (b-b', Figure 4.1) with 98% and 72% of absolute residuals less than 1000 m and 500 m, compared to 86% and 66% in the north, respectively. Modeled elevations show a spatial trend in overestimation in the east and underestimation in the west, which is also more pronounced in the north (Figure 4.1B). Reconstructed elevations give minor overestimates compared to true elevations, resulting in a mean residual of -246 ± 427 m (1σ). Waters with low d-excess typically yield underestimates in mean catchment elevation, whereas waters with high d-excess combined with low δD , as in solid precipitation at high elevations (i.e., snow) (e.g., Bershaw et al., 2012), are more likely to yield overestimates (Figure 4.1B).

Volcanic glass stable isotopic results (δD_{glass}) are considered in four groups based on physiographic region: the northern cordilleras, Western Cordillera, Altiplano, and Eastern Cordillera (Figure 1A). In all study areas, glasses that are incompletely hydrated with < 1 weight % water (Friedman et al., 1993) are biased toward relatively positive isotopic signatures ($\delta D = -100$ to -40‰) (Figure 4.3). These spurious results are likely due to sensitivity limitations during isotopic measurement, and potentially representative of a magmatic water source (Seligman et al., 2016; Martin et al., 2017), and so were excluded from further consideration. Hydrated glasses with > 1 weight % water yielded a range of δD values from -181 to -83‰ (Figure 4.3). Ancient water δD values were determined from the measured δD of glass by correcting for water-glass isotopic fractionation of $\delta D_{\text{paleowater}} = 1.034(1000 + \delta D_{\text{glass}}) - 1000$ (Friedman et al., 1993), and for global changes in ocean water chemistry since the late Oligocene (Zachos et al., 2001).

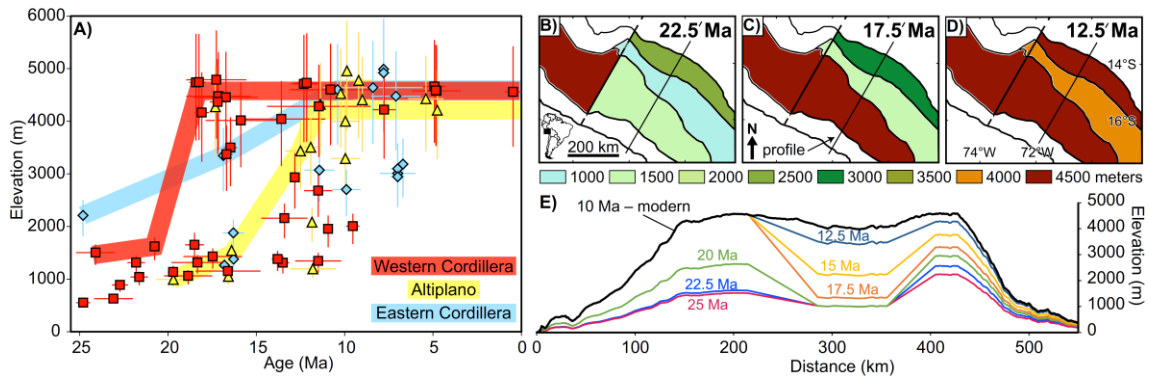


Figure 4.5. (A) Paleoelevation interpretation for the Western Cordillera (red line), Altiplano (yellow line), and Eastern Cordillera (blue line) based on the most negative reconstructed water values presented in Figure 4.5. Note the late Oligocene Eastern Cordillera is only constrained by one data point. (B–D) Surface uplift history of the Peruvian central Andes at resolution of typical general circulation models. (E) Topographic profile (topographic swath b–b’ in Figure 4.1A and parts B–D) calculated by multiplying the modern mean topography by percentage elevation. Boundaries are linearly interpolated (between 215 – 285 km and 355 – 405 km distance along profile x axis) between physiographic regions.

This adjustment results in more positive δD values than raw hydrated volcanic glass values, with even more positive values in older glasses (Figure 4.4). Because environmental waters of the geologic past were subject to the same evaporative enrichment effects as the modern, typically resulting in increased δD values and underestimates in paleoelevation, interpretation of isotopic changes in moisture is based on the most negative isotopic values for each physiographic region (Bershaw et al., 2016).

The northern cordilleras show near modern reconstructed paleoenvironmental waters values by ~22 Ma. Reconstructed waters for the Western Cordillera, Altiplano, and Eastern Cordillera that are older than 10 Ma are in disequilibrium with modern waters, and decrease to modern values by 10 Ma (Figure 4.4). The Western Cordillera yields $\delta D_{\text{paleowater}}$ values of -50 to -30‰ between 25 and 22 Ma, followed by an abrupt

decrease to modern $\delta D_{\text{paleowater}}$ values between 22 and 17 Ma that persists until present (Figure 4.4C). The Altiplano shows $\delta D_{\text{paleowater}}$ of -40‰ at ~ 20 Ma and two potential isotopic changes toward modern water values, one at ~ 17 Ma and one later between 17 and 12 Ma (Figure 4.4D). We interpret the latter as the actual shift in paleoenvironmental waters based on a variety of independent geologic observations and previous paleoelevation work (see below). The Eastern Cordillera yields late Oligocene $\delta D_{\text{paleowater}}$ values of -60‰ that steadily decrease to modern values between 25 and 10 Ma (Figure 4.4E).

Paleoelevation calculations based on reconstructed paleoenvironmental waters and the modified isotopic lapse rate of Rowley (2007) reveal spatial and temporal variability in surface uplift patterns across the Peruvian central Andes. Specifically, the northern cordilleras were at or above modern elevation as early as 22 Ma (Figure 4.4A). The Western Cordillera increased from ~ 1500 m elevation to modern (~ 4500 m) between 22 and 17 Ma (Figure 4.5A). The Altiplano was uplifted slightly slower and later, increasing from 1000 – 1500 m to modern elevation (4000 m) between 17 and 12 Ma (Figure 4.5A). The Eastern Cordillera shows extremely protracted surface uplift from ~ 2500 m at ~ 25 Ma to modern elevations at 10 Ma (Figure 4.5A).

Discussion

Modern water isotopic compositions faithfully reproduce elevations using a non-linear isotopic lapse rate, providing a benchmark for interpreting paleoelevation from ancient environmental waters. Rainout during orographic ascent of moisture along the Eastern Cordillera of southern Peru produces a strong isotopic gradient resulting in the

relative depletion of heavier D over H isotopes that inversely correlates with elevation, as observed globally across the windward sides of mountains (Poage and Chamberlain, 2001). However, leeward moisture patterns are more complicated than typical orographic barriers because following orographic ascent and rainout of heavier isotopes, the moisture traverses over a high orogenic plateau rather than returning to relatively low elevations (e.g., the Sierra Nevada Mountains). During the traverse across high topography, moisture undergoes subcloud evaporation and moisture recycling effects resulting in an inland gradient to heavier isotopic compositions (Bershaw et al., 2016). Despite significant moisture recycling, variably arid conditions, and evaporative effects resulting in divergence of the LMWL from the GMWL (Figure 4.2A), modern waters successfully reproduce modern elevations. Minor elevation overestimation (300 – 400 m) along the Eastern Cordillera in southern Peru results from a higher isotopic gradient than that of the non-linear isotopic lapse rate. This effect is balanced by increased moisture recycling and a shift to more positive isotopic values to the west (Bershaw et al., 2016), resulting in the lowest residuals ($|\text{catchment mean elevation} - \text{modeled elevation}|$) in the central part of the plateau. Aridity and moisture recycling increase to the west, resulting in minor elevation underestimates in the Western Cordillera (10 – 50 m) and northern cordilleras (100 – 200 m). Surprisingly, there is little to no correlation between d-excess and residual values, except for highly evaporated waters ($\text{d-excess} < -10\text{‰}$). Thus, barring extreme evaporative effects, elevation estimates based on δD values appear to be applicable even in arid regions assuming selection of an appropriate lapse rate.

Calculating paleoelevation from volcanic glass δD isotopic compositions relies on proper correction for water-glass isotopic fractionation, late Cenozoic climate change, and level of glass hydration. In the absence a correction for global climate change, reconstructed waters could be misinterpreted as a decrease in elevation or increase in aridity. Correcting for the late Oligocene – Pleistocene increase in stable isotopic values of oceanic water flattens observed trends toward more positive δD_{glass} values, most notably in the Puquio region of the northern cordilleras (Figure 4.4B) and the Western Cordillera (Figure 4.4C). Consideration of volcanic glass δD_{glass} signatures from non-hydrated glasses (< 1 weight % water) could potentially lead to geologic misinterpretation, as these data tend to yield very positive (-100 to -40%) δD_{glass} values resulting in surface uplift underestimates and/or larger shifts in isotopic records than may have taken place.

Spatial and temporal variability in surface uplift rate requires differing geodynamic processes to generate and maintain high topography. Because no change is recorded in the northern cordilleras of southern Peru, and it may have been at high elevation earlier than ~ 22 Ma, we cannot discern the geodynamic process that controlled the development of high topography. The modern lithospheric structure of this region is considerably different than farther south where the mantle lithosphere is thinner and subduction angle is steeper, as it is very close to the transition between steep and flat slab subduction (Phillips and Clayton, 2014), as well as the Nazca ridge (Hampel, 2002), both of which may have played a role in the early attainment of elevated topography.

High rates of surface uplift of the Western Cordillera and Altiplano are consistent with foundering of mantle lithosphere via Rayleigh-Taylor instabilities. The timing of lithospheric removal beneath the Western Cordillera precedes that of the Altiplano by at least 5 Myr, consistent with the densest material in a magmatic arc being located directly under the thickened arc itself, where restite emplacement and eclogitization dominate (Ducea, 2001). The slow surface uplift of the Eastern Cordillera and higher initial elevations compared to areas in the west are consistent with limited lithospheric shortening due to ablative subduction (e.g., Pope and Willet, 1998), thermal weakening (e.g., Isacks, 1988), or underthrusting of detached mantle lithosphere (Ducea, 2001), in concert with crustal shortening.

Variable surface uplift across the Peruvian central Andes is consistent with independent geologic observations and previous paleoelevation estimates. Early, high topography of the northern cordilleras is consistent with river incision modeling of middle Miocene to present of Rio Ocoña (Figure 4.1A) that indicates 1 to 3 km of elevation by at least 16 Ma (Jeffery et al., 2013). Results presented here bolster previous paleoelevation estimates for the Western Cordillera suggesting rapid early Miocene surface uplift (Saylor and Horton, 2014). Results also suggest surface uplift and attainment of modern elevations in the Altiplano by 12 Ma, ~6 Myr earlier than previous estimates (Kar et al., 2016). Attainment of modern elevation in the Altiplano between 17 and 12 Ma is consistent with molecular phylogenetics and phylochronologic analysis that requires at least 2 km elevation in the early Miocene in southernmost Peru in order to sustain high-elevation-dwelling *Globodera pallida* potato parasite nematodes (Picard et

al., 2008). Middle to late Miocene unconformity development followed by deposition of isolated intermontane basins in the Altiplano (Carlotto, 2013) also supports the timing of rapid surface uplift between 17 and 12 Ma (Figure 4.5). The relative elevations of these physiographic regions are consistent with independent geologic observations as well. Sediment delivery to the northernmost Altiplano near Cusco, Peru was consistently sourced from the Western Cordillera throughout the Cenozoic (Carlotto, 2013). Moreover, detrital zircon data from the Subandes and modern rivers east of the Eastern Cordillera contain very few Cenozoic ages (Pepper et al., 2016; Perez et al., 2016), suggesting sediment capturing within the orogenic hinterland due to blocking by a high Eastern Cordillera and sediment accumulation in a relatively low Altiplano. The timing and mechanism for uplift inferred for the Eastern Cordillera are both consistent with a late Paleogene onset of shortening which peaked at ~25 Ma and then steadily decreased until cessation at 10 Ma (Oncken et al., 2006).

The paleoelevation model presented here has implications for regional climate trends and climate modeling research. Extreme arid conditions along the Pacific coast are due to a combination of subtropical latitudes, the Humboldt oceanic current fetching cold waters from the southeast Pacific, and constant high atmospheric pressure conditions, all of which act to drive away atmospheric moisture (Takahashi and Battisti, 2007). The mere presence of the Andes is enough to lower sea surface temperature and promote evaporation in the region (Takahashi and Battisti, 2007). Paleoelevation estimates presented here all suggest moderately high topography (at least 2 km) of the central Andean orogen between 13°S and 17°S by 15 Ma, which in turn indicates the

establishment of an arid central Andean Pacific coast. This is consistent with work suggesting the onset of hyperaridity in the Atacama Desert region and southern Peruvian Pacific coast took place in the middle Miocene (Alpers and Brimhall, 1988), as well as previous work suggesting near modern elevations in northern Chile by the early to middle Miocene based on palynology and paleobotany of lacustrine deposits (Muñoz and Charrier, 1996), regional tilting and monocline development (e.g., Jordan et al., 2010), and orography-induced preservation of hyperarid salic gypsisols in the Atacama Desert (Schlunegger et al., 2010). The Eastern Cordillera was high enough to block moisture-laden air masses as early as 25 Ma (Figure 4.5). If the Altiplano was as low as predicted before 12 Ma, and so too was the Abancay region to the north (Picard et al., 2008), then moisture would have penetrated far into the orogenic hinterland resulting in reduced aridity along the Pacific coast. In this latter case, the onset of hyperarid conditions would have occurred after ~17 Ma, subsequent to rapid surface uplift of the Western Cordillera. Whether initial moisture blockage took place along the emerging Eastern Cordillera, or directly adjacent to the Western Cordillera is uncertain, but both cases would result in establishment of arid conditions along the Pacific coast of South America by early to middle Miocene. Implications for climate-topography interactions such as these are testable with estimates of paleoelevation as inputs to climate models (Figure 4.5B–D). Such model inputs are critical to testing topography-climate feedbacks, and are at the resolution of many general circulation models (e.g., Insel et al., 2012).

REFERENCES

- Allen, P. A., and J. R. Allen (2013), Basin analysis: Principles and application to petroleum play assessment, John Wiley & Sons.
- Allmendinger, R. (2005), Stereonet, Program for stereographic projection.
- Allmendinger, R. W., T. E. Jordan, S. M. Kay, and B. L. Isacks (1997), The evolution of the Altiplano-Puna plateau of the Central Andes, *Annual Review of Earth and Planetary Sciences*, 25(1), 139-174.
- Allmendinger, R. W., V. A. Ramos, T. E. Jordan, M. Palma, and B. L. Isacks (1983), Paleogeography and Andean structural geometry, northwest Argentina, *Tectonics*, 2(1), 1-16.
- Alpers, C. N., and G. H. Brimhall (1988), Middle Miocene climatic change in the Atacama Desert, northern Chile: Evidence from supergene mineralization at La Escondida, *Geological Society of America Bulletin*, 100(10), 1640-1656.
- Amidon, W. H., D. W. Burbank, and G. E. Gehrels (2005), Construction of detrital mineral populations: insights from mixing of U–Pb zircon ages in Himalayan rivers, *Basin Research*, 17(4), 463-485.
- Andersen, T., M. Elburg, and A. Cawthorn-Blazeby (2016a), U–Pb and Lu–Hf zircon data in young sediments reflect sedimentary recycling in eastern South Africa, *Journal of the Geological Society*, 173(2), 337-351.
- Andersen, T., M. Kristoffersen, and M. A. Elburg (2016b), How far can we trust provenance and crustal evolution information from detrital zircons? A South African case study, *Gondwana Research*, 34, 129-148.
- Antoine, P.-O., M. A. Abello, S. Adnet, A. J. A. Sierra, P. Baby, G. Billet, M. Boivin, Y. Calderon, A. Candela, and J. Chabain (2016), A 60-million-year Cenozoic history of western Amazonian ecosystems in Contamana, eastern Peru, *Gondwana Research*, 31, 30-59.
- Bahlburg, H., J. D. Vervoort, S. A. Du Frane, B. Bock, C. Augustsson, and C. Reimann (2009), Timing of crust formation and recycling in accretionary orogens: Insights learned from the western margin of South America, *Earth-Science Reviews*, 97(1), 215-241.
- Bahlburg, H., J. D. Vervoort, S. A. DuFrane, V. Carlotto, C. Reimann, and J. Cárdenas (2011), The U–Pb and Hf isotope evidence of detrital zircons of the Ordovician Ollantaytambo Formation, southern Peru, and the Ordovician provenance and paleogeography of southern Peru and northern Bolivia, *Journal of South American Earth Sciences*, 32(3), 196-209.
- Barnes, J., and T. Ehlers (2009), End member models for Andean Plateau uplift, *Earth-Science Reviews*, 97(1), 105-132.
- Beck, S. L., and G. Zandt (2002), The nature of orogenic crust in the central Andes, *Journal of Geophysical Research: Solid Earth*, 107(B10).

- Beck, S. L., G. Zandt, S. C. Myers, T. C. Wallace, P. G. Silver, and L. Drake (1996), Crustal-thickness variations in the central Andes, *Geology*, 24(5), 407-410.
- Berry, E. W. (1917), The Age of the Bolivian Andes, *Proceedings of the National Academy of Sciences*, 3(4), 283-285.
- Bershaw, J., Penny, S. M., & Garziona, C. N. (2012). Stable isotopes of modern water across the Himalaya and eastern Tibetan Plateau: Implications for estimates of paleoelevation and paleoclimate. *Journal of Geophysical Research: Atmospheres*, 117(D2).
- Bershaw, J., J. E. Saylor, C. N. Garziona, A. Leier, and K. E. Sundell (2016), Stable isotope variations ($\delta^{18}\text{O}$ and δD) in modern waters across the Andean Plateau, *Geochimica et Cosmochimica Acta*, 194, 310-324.
- Bridge, J. S., and J. L. Best (1988), Flow, sediment transport and bedform dynamics over the transition from dunes to upper-stage plane beds: implications for the formation of planar laminae, *Sedimentology*, 35(5), 753-763.
- Cailleteau, C., F. Angeli, F. Devreux, S. Gin, J. Jestin, P. Jollivet, and O. Spalla (2008), Insight into silicate-glass corrosion mechanisms, *Nature Materials*, 7(12), 978-983.
- Campbell, C. V. (1967), Lamina, laminaset, bed and bedset, *Sedimentology*, 8(1), 7-26.
- Campbell, I. H., P. W. Reiners, C. M. Allen, S. Nicolescu, and R. Upadhyay (2005), He–Pb double dating of detrital zircons from the Ganges and Indus Rivers: implication for quantifying sediment recycling and provenance studies, *Earth and Planetary Science Letters*, 237(3), 402-432.
- Carlotto, V. (1998), Evolution andine et raccourcissement au niveau de Cusco (13°-16° S), Pérou: Enregistrement sédimentaire, chronologie, contrôles paléogéographiques, évolution cinématique, Université Joseph-Fourier-Grenoble I.
- Carlotto, V. (2013), Paleogeographic and tectonic controls on the evolution of Cenozoic basins in the Altiplano and Western Cordillera of southern Peru, *Tectonophysics*, 589, 195-219.
- Carlotto, V., J. Cardénas, and G. Carlier (2011), Geología del Cuadrángulo de Cusco 28-s-1: 50 000. INGEMMET, Boletín, Serie A: Carta Geológica Nacional, 138, 255.
- Carlotto, V., G. Carlier, E. Jaillard, J. Cardenas, L. Cerpa, T. Flores, and O. Latorre (2005), Las cuencas terciarias sinorogénicas en el Altiplano y en la Cordillera Occidental, *Boletín de la Sociedad geologica del Perú*, 6(spécial), 103 à126.
- Carrapa, B., and P. G. DeCelles (2015), Regional exhumation and kinematic history of the central Andes in response to cyclical orogenic processes, *Geological Society of America Memoirs*, 212, 201-213.
- Carrapa, B., S. Bywater-Reyes, P. G. DeCelles, E. Mortimer, and G. E. Gehrels (2011), Late Eocene–Pliocene basin evolution in the Eastern Cordillera of northwestern

Argentina (25–26 S): regional implications for Andean orogenic wedge development, *Basin Research*, 24(3), 249-268.

Casey, W. H. (2008), Glass and mineral corrosion: Dynamics and durability, *Nature Materials*, 7(12), 930-932.

Cassel, E. J., and D. O. Breecker (2017), Long-term stability of hydrogen isotope ratios in hydrated volcanic glass, *Geochimica et Cosmochimica Acta*, 200, 67-86.

Cawood, P. A., C. Hawkesworth, and B. Dhuime (2012), Detrital zircon record and tectonic setting, *Geology*, 40(10), 875-878.

Chapman, J. B., M. N. Ducea, P. G. DeCelles, and L. Profeta (2015), Tracking changes in crustal thickness during orogenic evolution with Sr/Y: An example from the North American Cordillera, *Geology*, 43(10), 919-922.

Charles, R. (1958), Static fatigue of glass. I, *Journal of Applied Physics*, 29(11), 1549-1553.

Chavez, R., W. Gil, S. Mamani, M. Sotomayor, J. Cardenas, and V. Carlotto (1994), *Sedimentología y estratigrafía de la formación Punacancha (Eoceno?) en la región de Cusco*, paper presented at VIII Congreso Peruano de Geología.

Che, X., and G. Li (2013), Binary sources of loess on the Chinese Loess Plateau revealed by U–Pb ages of zircon, *Quaternary Research*, 80(3), 545-551.

Chew, D. M., U. Schaltegger, J. Košler, M. J. Whitehouse, M. Gutjahr, R. A. Spikings, and A. Mišković (2007), U-Pb geochronologic evidence for the evolution of the Gondwanan margin of the north-central Andes, *Geological Society of America Bulletin*, 119(5-6), 697-711.

Chew, D. M., T. Magna, C. L. Kirkland, A. Mišković, A. Cardona, R. Spikings, and U. Schaltegger (2008), Detrital zircon fingerprint of the Proto-Andes: Evidence for a Neoproterozoic active margin?, *Precambrian Research*, 167(1), 186-200.

Cooper, M., F. Addison, R. Alvarez, M. Coral, R. H. Graham, A. Hayward, S. Howe, J. Martinez, J. Naar, and R. Peñas (1995), Basin development and tectonic history of the Llanos Basin, Eastern Cordillera, and middle Magdalena Valley, Colombia, *AAPG bulletin*, 79(10), 1421-1442.

Coutand, I., P. R. Cobbold, M. Urreiztieta, P. Gautier, A. Chauvin, D. Gapais, E. A. Rossello, and O. López-Gamundí (2001), Style and history of Andean deformation, Puna plateau, northwestern Argentina, *Tectonics*, 20(2), 210-234.

Craig, H. (1961), Standard for reporting concentrations of deuterium and oxygen-18 in natural waters, *Science*, 133(3467), 1833-1834.

Currie, C. A., M. N. Ducea, P. G. DeCelles, and C. Beaumont (2015), Geodynamic models of Cordilleran orogens: Gravitational instability of magmatic arc roots, *Geological Society of America Memoirs*, 212, 1-22.

- Dansgaard, W. (1964), Stable isotopes in precipitation, *Tellus*, 16(4), 436-468.
- Davis, D., J. Suppe, and F. Dahlen (1983), Mechanics of fold-and-thrust belts and accretionary wedges, *Journal of Geophysical Research: Solid Earth*, 88(B2), 1153-1172.
- DeCelles, P., and P. DeCelles (2001), Rates of shortening, propagation, underthrusting, and flexural wave migration in continental orogenic systems, *Geology*, 29(2), 135-138.
- Decelles, P. G. (2012), Foreland Basin Systems Revisited, in *Tectonics of Sedimentary Basins: Recent Advances*, edited, John Wiley and Sons, 405-426.
- DeCelles, P. G., and K. A. Giles (1996), Foreland basin systems, *Basin research*, 8(2), 105-123.
- DeCelles, P. G., and B. K. Horton (2003), Early to middle Tertiary foreland basin development and the history of Andean crustal shortening in Bolivia, *Geological Society of America Bulletin*, 115(1), 58-77.
- DeCelles, P. G., and S. Graham (2015), Cyclical processes in the North American Cordilleran orogenic system, *Geology*, 43(6), 499-502.
- DeCelles, P. G., R. P. Langford, and R. K. Schwartz (1983), Two new methods of paleocurrent determination from trough cross-stratification, *Journal of Sedimentary Research*, 53(2).
- DeCelles, P. G., M. N. Ducea, P. Kapp, and G. Zandt (2009), Cyclicity in Cordilleran orogenic systems, *Nature Geoscience*, 2(4), 251-257.
- DeCelles, P. G., B. Carrapa, B. Horton, and G. E. Gehrels (2011), Cenozoic foreland basin system in the central Andes of northwestern Argentina: Implications for Andean geodynamics and modes of deformation, *Tectonics*, 30(6).
- DeCelles, P. G., G. Zandt, S. Beck, C. Currie, M. N. Ducea, P. Kapp, G. E. Gehrels, B. Carrapa, J. Quade, and L. Schoenbohm (2015), Cyclical orogenic processes in the Cenozoic central Andes, *Geological Society of America Memoirs*, 212, MWR212-222.
- Decou, A., H. Von Eynatten, I. Dunkl, D. Frei, and G. Wörner (2013), Late Eocene to Early Miocene Andean uplift inferred from detrital zircon fission track and U–Pb dating of Cenozoic forearc sediments (15–18 S), *Journal of South American Earth Sciences*, 45, 6-23.
- Deeken, A., E. R. Sobel, I. Coutand, M. Haschke, U. Riller, and M. R. Strecker (2006), Development of the southern Eastern Cordillera, NW Argentina, constrained by apatite fission track thermochronology: From early Cretaceous extension to middle Miocene shortening, *Tectonics*, 25(6), 1-21.
- Demouy, S., J.-L. Paquette, M. de Saint Blanquat, M. Benoit, E. A. Belousova, S. Y. O'Reilly, F. García, L. C. Tejada, R. Gallegos, and T. Sempere (2012), Spatial and temporal evolution of Liassic to Paleocene arc activity in southern Peru unraveled by zircon U–Pb and Hf in-situ data on plutonic rocks, *Lithos*, 155, 183-200.

- Dickinson, W. R. (2008), Impact of differential zircon fertility of granitoid basement rocks in North America on age populations of detrital zircons and implications for granite petrogenesis, *Earth and Planetary Science Letters*, 275(1), 80-92.
- Dickinson, W. R., and C. A. Suzek (1979), Plate tectonics and sandstone compositions, *Aapg Bulletin*, 63(12), 2164-2182.
- Dickinson, W. R., and G. E. Gehrels (2009), Use of U–Pb ages of detrital zircons to infer maximum depositional ages of strata: a test against a Colorado Plateau Mesozoic database, *Earth and Planetary Science Letters*, 288(1), 115-125.
- Diepenbroek, M., A. Bartholomä, and H. Ibbeken (1992), How round is round? A new approach to the topic ‘roundness’ by Fourier grain shape analysis, *Sedimentology*, 39(3), 411-422.
- Ducea, M. (2001), The California arc: Thick granitic batholiths, eclogitic residues, lithospheric-scale thrusting, and magmatic flare-ups, *GSA today*, 11(11), 4-10.
- Ducea, M. N., and M. D. Barton (2007), Igniting flare-up events in Cordilleran arcs, *Geology*, 35(11), 1047-1050.
- Ducea, M. N., S. R. Paterson, and P. G. DeCelles (2015), High-volume magmatic events in subduction systems, *Elements*, 11(2), 99-104.
- Ehlers, T. A., and C. J. Poulsen (2009), Influence of Andean uplift on climate and paleoaltimetry estimates, *Earth and Planetary Science Letters*, 281(3), 238-248.
- England, P., and G. Houseman (1989), Extension during continental convergence, with application to the Tibetan Plateau, *Journal of Geophysical Research: Solid Earth*, 94(B12), 17561-17579.
- England, P., and P. Molnar (1990), Surface uplift, uplift of rocks, and exhumation of rocks, *Geology*, 18(12), 1173-1177.
- Forbes, D. (1861), On the geology of Bolivia and southern Peru, *Quarterly Journal of the Geological Society*, 17(1-2), 7-62.
- Friedman, I., J. Gleason, and A. Warden (1993), Ancient climate from deuterium content of water in volcanic glass, *Climate change in continental isotopic records*, 309-319.
- Froehlich, K., J. Gibson, and P. Aggarwal (2001), Deuterium excess in precipitation and its climatological significance, *International Atomic Energy Agency, C&S Papers Series*, 13, 54-66.
- Garzanti, E., S. Andò, and G. Vezzoli (2009a), Grain-size dependence of sediment composition and environmental bias in provenance studies, *Earth and Planetary Science Letters*, 277(3), 422-432.
- Garzanti, E., S. Andò, and G. Vezzoli (2009b), Grain-size dependence of sediment composition and environmental bias in provenance studies, *Earth and Planetary Science Letters*, 277(3), 422-432.

- Garzione, C. N., P. Molnar, J. C. Libarkin, and B. J. MacFadden (2006), Rapid late Miocene rise of the Bolivian Altiplano: Evidence for removal of mantle lithosphere, *Earth and Planetary Science Letters*, 241(3), 543-556.
- Garzione, C. N., G. D. Hoke, J. C. Libarkin, S. Withers, B. MacFadden, J. Eiler, P. Ghosh, and A. Mulch (2008), Rise of the Andes, *Science*, 320(5881), 1304-1307.
- Garzione, C. N., N. McQuarrie, N. D. Perez, T. A. Ehlers, S. L. Beck, N. Kar, N. Eichelberger, A. D. Chapman, K. M. Ward, and M. N. Ducea (2017), Tectonic Evolution of the Central Andean Plateau and Implications for the Growth of Plateaus, *Annual Review of Earth and Planetary Sciences*, 45.
- Gazzi, P. (1966), The upper Cretaceous Flysch sandstones (Modena Apennine); comparison with the Monghidoro Flysch, *Mineralogica et Petrographica Acta*, 12, 69-97.
- Gehrels, G. E. (2000), Introduction to detrital zircon studies of Paleozoic and Triassic strata in western Nevada and northern California, *Special Paper of the Geological Society of America*, 347, 1-17.
- Gehrels, G. E., R. Blakey, K. E. Karlstrom, J. M. Timmons, B. Dickinson, and M. Pecha (2011), Detrital zircon U-Pb geochronology of Paleozoic strata in the Grand Canyon, Arizona, *Lithosphere*, 3(3), 183-200.
- Gillis, R. J., B. K. Horton, and M. Grove (2006), Thermochronology, geochronology, and upper crustal structure of the Cordillera Real: Implications for Cenozoic exhumation of the central Andean plateau, *Tectonics*, 25(6).
- Gonfiantini, R., M.-A. Roche, J.-C. Olivry, J.-C. Fontes, and G. M. Zuppi (2001), The altitude effect on the isotopic composition of tropical rains, *Chemical Geology*, 181(1), 147-167.
- Gregory-Wodzicki, K. M., W. McIntosh, and K. Velasquez (1998), Climatic and tectonic implications of the late Miocene Jakokkota flora, Bolivian Altiplano, *Journal of South American Earth Sciences*, 11(6), 533-560.
- Göğüş, O. H., and R. N. Pysklywec (2008a), Near-surface diagnostics of dripping or delaminating lithosphere, *Journal of Geophysical Research: Solid Earth*, 113(B11).
- Göğüş, O. H., and R. N. Pysklywec (2008b), Mantle lithosphere delamination driving plateau uplift and synconvergent extension in eastern Anatolia, *Geology*, 36(9), 723-726.
- Hampel, A. (2002), The migration history of the Nazca Ridge along the Peruvian active margin: a re-evaluation, *Earth and Planetary Science Letters*, 203(2), 665-679.
- Hampton, B. A., and B. K. Horton (2007), Sheetflow fluvial processes in a rapidly subsiding basin, Altiplano plateau, Bolivia, *Sedimentology*, 54(5), 1121-1148.
- Haschke, M., W. Siebel, A. Günther, and E. Scheuber (2002), Repeated crustal thickening and recycling during the Andean orogeny in north Chile (21–26 S), *Journal of Geophysical Research: Solid Earth*, 107(B1).

- Haschke, M., A. Günther, D. Melnick, H. Echtler, K.-J. Reutter, E. Scheuber, and O. Oncken (2006), Central and southern Andean tectonic evolution inferred from arc magmatism, in *The Andes*, edited, pp. 337-353, Springer.
- Hazewinkel, M. (2001), Student t-test, *Encyclopedia of Mathematics*, Springer, Berlin, Germany, ISBN, 978-971.
- Horton, B., B. Hampton, and G. Waanders (2001), Paleogene synorogenic sedimentation in the Altiplano plateau and implications for initial mountain building in the central Andes, *Geological Society of America Bulletin*, 113(11), 1387-1400.
- Horton, B., B. Hampton, B. LaReau, and E. Baldellon (2002), Tertiary provenance history of the northern and central Altiplano (central Andes, Bolivia): A detrital record of plateau-margin tectonics, *Journal of Sedimentary Research*, 72(5), 711-726.
- Horton, B. K., and P. G. DeCelles (1997), The modern foreland basin system adjacent to the Central Andes, *Geology*, 25(10), 895-898.
- Horton, B. K., N. D. Perez, J. D. Fitch, and J. E. Saylor (2014), Punctuated shortening and subsidence in the Altiplano Plateau of southern Peru: Implications for early Andean mountain building, *Lithosphere*, 7(2), 117-137.
- Horton, B. K., M. Parra, J. E. Saylor, J. Nie, A. Mora, V. Torres, D. F. Stockli, and M. R. Strecker (2010), Resolving uplift of the northern Andes using detrital zircon age signatures, *GSA Today*, 20(7), 4-10.
- Huntington, K. W., and A. R. Lechler (2015), Carbonate clumped isotope thermometry in continental tectonics, *Tectonophysics*, 647, 1-20.
- Insel, N., C. J. Poulsen, T. A. Ehlers, and C. Sturm (2012), Response of meteoric $\delta^{18}\text{O}$ to surface uplift—Implications for Cenozoic Andean Plateau growth, *Earth and Planetary Science Letters*, 317, 262-272.
- Isacks, B. L. (1988), Uplift of the central Andean plateau and bending of the Bolivian orocline, *Journal of Geophysical Research: Solid Earth*, 93(B4), 3211-3231.
- Jaimes, F., and D. Romero (1996), *Las cuencas sin-orogénicas de la región del Cusco: La cuenca Paruro (Mioceno superior)*, Tesis Ingeniero Geólogo, Universidad Nacional San Antonio Abad, Cusco.
- Jeffery, M. L., T. A. Ehlers, B. J. Yanites, and C. J. Poulsen (2013), Quantifying the role of paleoclimate and Andean Plateau uplift on river incision, *Journal of Geophysical Research: Earth Surface*, 118(2), 852-871.
- Jordan, T., P. Nester, N. Blanco, G. Hoke, F. Dávila, and A. Tomlinson (2010), Uplift of the Altiplano-Puna plateau: A view from the west, *Tectonics*, 29(5), 1-31.
- Kar, N., C. N. Garzzone, C. Jaramillo, T. Shanahan, V. Carlotto, A. Pullen, F. Moreno, V. Anderson, E. Moreno, and J. Eiler (2016), Rapid regional surface uplift of the northern Altiplano plateau revealed by multiproxy paleoclimate reconstruction, *Earth and Planetary Science Letters*, 447, 33-47.

- Kay, R. W., and S. M. Kay (1993), Delamination and delamination magmatism, *Tectonophysics*, 219(1), 177-189.
- Kay, S. M., B. Coira, and J. Viramonte (1994), Young mafic back arc volcanic rocks as indicators of continental lithospheric delamination beneath the Argentine Puna plateau, central Andes, *Journal of Geophysical Research: Solid Earth*, 99(B12), 24323-24339.
- Kennan, L., S. Lamb, and L. Hoke (1997), High-altitude palaeosurfaces in the Bolivian Andes: evidence for late Cenozoic surface uplift, Geological Society, London, Special Publications, 120(1), 307-323.
- Kimbrough, D. L., M. Grove, G. E. Gehrels, R. J. Dorsey, K. A. Howard, O. Lovera, A. Aslan, P. K. House, and P. A. Pearthree (2015), Detrital zircon U-Pb provenance of the Colorado River: A 5 my record of incision into cover strata overlying the Colorado Plateau and adjacent regions, *Geosphere*, 11(6), 1719-1748.
- Košler, J., H. P. Longerich, and M. N. Tubrett (2002), Effect of oxygen on laser-induced elemental fractionation in LA-ICP-MS analysis, *Analytical and Bioanalytical Chemistry*, 374(2), 251-254.
- Krumbein, W. C. (1941), Measurement and geological significance of shape and roundness of sedimentary particles, *Journal of Sedimentary Research*, 11(2).
- Krystopowicz, N. J., and C. A. Currie (2013), Crustal eclogitization and lithosphere delamination in orogens, *Earth and Planetary Science Letters*, 361, 195-207.
- Kuiper, N. H. (1960), Tests concerning random points on a circle, paper presented at *Indagationes Mathematicae (Proceedings)*, Elsevier.
- Lamb, S. (2011), Did shortening in thick crust cause rapid Late Cenozoic uplift in the northern Bolivian Andes?, *Journal of the Geological Society*, 168(5), 1079-1092.
- Laskowski, A. K., P. G. DeCelles, and G. E. Gehrels (2013), Detrital zircon geochronology of Cordilleran retroarc foreland basin strata, western North America, *Tectonics*, 32(5), 1027-1048.
- Lawrence, R. L., R. Cox, R. W. Mapes, and D. S. Coleman (2011), Hydrodynamic fractionation of zircon age populations, *Geological Society of America Bulletin*, 123(1-2), 295-305.
- Lenters, J., and K. Cook (1997), On the origin of the Bolivian high and related circulation features of the South American climate, *Journal of the Atmospheric Sciences*, 54(5), 656-678.
- Licht, A., A. Pullen, P. Kapp, J. Abell, and N. Giesler (2016), Eolian cannibalism: Reworked loess and fluvial sediment as the main sources of the Chinese Loess Plateau, *Geological Society of America Bulletin*, 128(5-6), 944-956.
- Mamani, M., A. Tassara, and G. Wörner (2008), Composition and structural control of crustal domains in the central Andes, *Geochemistry, Geophysics, Geosystems*, 9(3), 1-13.

- Mamani, M., G. Wörner, and T. Sempere (2010), Geochemical variations in igneous rocks of the Central Andean orocline (13 S to 18 S): Tracing crustal thickening and magma generation through time and space, *Geological Society of America Bulletin*, 122(1-2), 162-182.
- Martin, E., Bindeman, I., Balan, E., Palandri, J., Seligman, A., & Villemant, B. (2017). Hydrogen isotope determination by TC/EA technique in application to volcanic glass as a window into secondary hydration. *Journal of Volcanology and Geothermal Research*, 346, 1-13.
- McGroder, M. F., R. O. Lease, and D. M. Pearson (2015), Along-strike variation in structural styles and hydrocarbon occurrences, Subandean fold-and-thrust belt and inner foreland, Colombia to Argentina, *Geological Society of America Memoirs*, 212, 79-113.
- Miall, A. (2010), *The geology of stratigraphic sequences*, Springer Science & Business Media.
- Miall, A. D. (1977), Lithofacies types and vertical profile models in braided river deposits: a summary.
- Moecher, D. P., and S. D. Samson (2006), Differential zircon fertility of source terranes and natural bias in the detrital zircon record: Implications for sedimentary provenance analysis, *Earth and Planetary Science Letters*, 247(3), 252-266.
- Molnar, P., and H. Lyon-Caen (1988), Some simple physical aspects of the support, structure, and evolution of mountain belts, *Geological Society of America Special Papers*, 218, 179-208.
- Moreira, M., L. Sternberg, L. Martinelli, R. Victoria, E. Barbosa, L. Bonates, and D. Nepstad (1997), Contribution of transpiration to forest ambient vapour based on isotopic measurements, *Global Change Biology*, 3(5), 439-450.
- Morton, A. C., and C. Hallsworth (1994), Identifying provenance-specific features of detrital heavy mineral assemblages in sandstones, *Sedimentary Geology*, 90(3), 241-256.
- Mourier, T., P. Bengtson, M. Bonhomme, E. Buge, H. Cappetta, J. Crochet, M. Feist, K. Hirsch, E. Jaillard, and G. Laubacher (1988), The Upper Cretaceous-Lower Tertiary marine to continental transition in the Bagua basin, northern Perú, *Newsletters on Stratigraphy*, 19, 143-177.
- Muhlbauer, J. G., C. M. Fedo, and G. L. Farmer (2017), Influence of textural parameters on detrital-zircon age spectra with application to provenance and paleogeography during the Ediacaran– Terreneuvian of southwestern Laurentia, *Geological Society of America Bulletin*, B31611. 31611.
- Mulch, A., C. E. Uba, M. R. Strecker, R. Schoenberg, and C. P. Chamberlain (2010), Late Miocene climate variability and surface elevation in the central Andes, *Earth and Planetary Science Letters*, 290(1), 173-182.

- Muñoz, N., and R. Charrier (1996), Uplift of the western border of the Altiplano on a west-vergent thrust system, northern Chile, *Journal of South American Earth Sciences*, 9(3-4), 171-181.
- Newell, N. D. (1946), Geological investigations around Lake Titicaca, *American Journal of Science*, 244(5), 357-366.
- Newell, N. D. (1949), Geology of the lake Titicaca region, Peru and Bolivia, *Geological Society of America Memoirs*, 36, 1-124.
- Nilsen, T. H., and A. G. Sylvester (1999), Strike-slip basins: Part 1, The Leading Edge, 18(10), 1146-1152.
- Nolan, G. S., and I. N. Bindeman (2013), Experimental investigation of rates and mechanisms of isotope exchange (O, H) between volcanic ash and isotopically-labeled water, *Geochimica et Cosmochimica Acta*, 111, 5-27.
- Oncken, O., D. Hindle, J. Kley, K. Elger, P. Victor, and K. Schemmann (2006), Deformation of the central Andean upper plate system—Facts, fiction, and constraints for plateau models, in *The Andes*, edited, pp. 3-27, Springer.
- Paces, J. B., and J. D. Miller (1993), Precise U-Pb ages of Duluth complex and related mafic intrusions, northeastern Minnesota: Geochronological insights to physical, petrogenetic, paleomagnetic, and tectonomagmatic processes associated with the 1.1 Ga midcontinent rift system, *Journal of Geophysical Research: Solid Earth*, 98(B8), 13997-14013.
- Pardo-Casas, F., and P. Molnar (1987), Relative motion of the Nazca (Farallon) and South American plates since Late Cretaceous time, *Tectonics*, 6(3), 233-248.
- Pepper, M., G. Gehrels, A. Pullen, M. Ibanez-Mejia, K. M. Ward, and P. Kapp (2016), Magmatic history and crustal genesis of western South America: Constraints from U-Pb ages and Hf isotopes of detrital zircons in modern rivers, *Geosphere*, 12(5), 1532-1555.
- Perelló, J., V. Carlotto, A. Zárate, P. Ramos, H. Posso, C. Neyra, A. Caballero, N. Fuster, and R. Muhr (2003), Porphyry-style alteration and mineralization of the middle Eocene to early Oligocene Andahuaylas-Yauri Belt, Cuzco region, Peru, *Economic Geology*, 98(8), 1575-1605.
- Perez, N. D., and B. K. Horton (2014), Oligocene-Miocene deformational and depositional history of the Andean hinterland basin in the northern Altiplano plateau, southern Peru, *Tectonics*, 33(9), 1819-1847.
- Perez, N. D., B. K. Horton, and V. Carlotto (2016a), Structural inheritance and selective reactivation in the central Andes: Cenozoic deformation guided by pre-Andean structures in southern Peru, *Tectonophysics*, 671, 264-280.
- Perez, N. D., B. K. Horton, N. McQuarrie, K. Stuebner, and T. A. Ehlers (2016b), Andean shortening, inversion and exhumation associated with thin-and thick-skinned deformation in southern Peru, *Geological Magazine*, 153(5-6), 1013-1041.

- Peterman, Z. E., and P. Sims (1988), The Goodman Swell: A lithospheric flexure caused by crustal loading along the Midcontinent Rift System, *Tectonics*, 7(5), 1077-1090.
- Phillips, K., and R. W. Clayton (2014), Structure of the subduction transition region from seismic array data in southern Peru, *Geophysical Journal International*, 196(3), 1889-1905.
- Picard, D., T. Sempere, and O. Plantard (2008), Direction and timing of uplift propagation in the Peruvian Andes deduced from molecular phylogenetics of highland biotaxa, *Earth and Planetary Science Letters*, 271(1), 326-336.
- Pilger, R. H. (1984), Cenozoic plate kinematics, subduction and magmatism: South American Andes, *Journal of the Geological Society*, 141(5), 793-802.
- Poage, M. A., and C. P. Chamberlain (2001), Empirical relationships between elevation and the stable isotope composition of precipitation and surface waters: considerations for studies of paleoelevation change, *American Journal of Science*, 301(1), 1-15.
- Pope, D. C., and S. D. Willett (1998), Thermal-mechanical model for crustal thickening in the central Andes driven by ablative subduction, *Geology*, 26(6), 511-514.
- Press, W. H. (2007), *Numerical recipes 3rd edition: The art of scientific computing*, Cambridge university press.
- Profeta, L., M. N. Ducea, J. B. Chapman, S. R. Paterson, S. M. H. Gonzales, M. Kirsch, L. Petrescu, and P. G. DeCelles (2015), Quantifying crustal thickness over time in magmatic arcs, *Scientific reports*, 5.
- Pullen, A., M. Ibáñez-Mejía, G. E. Gehrels, J. C. Ibáñez-Mejía, and M. Pecha (2014), What happens when n= 1000? Creating large-n geochronological datasets with LA-ICP-MS for geologic investigations, *Journal of Analytical Atomic Spectrometry*, 29(6), 971-980.
- Ramos, V. A. (2009), Anatomy and global context of the Andes: Main geologic features and the Andean orogenic cycle, *Geological Society of America Memoirs*, 204, 31-65.
- Ramos, V. A., V. D. Litvak, A. Folguera, and M. Spagnuolo (2014), An Andean tectonic cycle: From crustal thickening to extension in a thin crust (34–37 SL), *Geoscience Frontiers*, 5(3), 351-367.
- Raymo, M. E., and W. F. Ruddiman (1992), Tectonic forcing of late Cenozoic climate, *Nature*, 359(6391), 117-122.
- Rech, J. A., B. S. Currie, E. D. Shullenberger, S. P. Dunagan, T. E. Jordan, N. Blanco, A. J. Tomlinson, H. D. Rowe, and J. Houston (2010), Evidence for the development of the Andean rain shadow from a Neogene isotopic record in the Atacama Desert, Chile, *Earth and Planetary Science Letters*, 292(3), 371-382.
- Reimann, C., H. Bahlburg, E. Kooijman, J. Berndt, A. Gerdes, V. Carlotto, and S. López (2010), Geodynamic evolution of the early Paleozoic Western Gondwana margin 14–17

S reflected by the detritus of the Devonian and Ordovician basins of southern Peru and northern Bolivia, *Gondwana Research*, 18(2), 370-384.

Rousse, S., S. Gilder, M. Fornari, and T. Sempere (2005), Insight into the Neogene tectonic history of the northern Bolivian Orocline from new paleomagnetic and geochronologic data, *Tectonics*, 24(6), 1-23.

Rowley, D. B., and C. N. Garzione (2007), Stable isotope-based paleoaltimetry, *Annual Review of Earth and Planetary Sciences*, 35, 463-508.

Salati, E., A. Dall'Olio, E. Matsui, and J. R. Gat (1979), Recycling of water in the Amazon basin: an isotopic study, *Water Resources Research*, 15(5), 1250-1258.

Satkoski, A. M., B. H. Wilkinson, J. Hietpas, and S. D. Samson (2013), Likeness among detrital zircon populations—An approach to the comparison of age frequency data in time and space, *Geological Society of America Bulletin*, 125(11-12), 1783-1799.

Saylor, J. E., and B. K. Horton (2014), Nonuniform surface uplift of the Andean plateau revealed by deuterium isotopes in Miocene volcanic glass from southern Peru, *Earth and Planetary Science Letters*, 387, 120-131.

Saylor, J. E., and K. E. Sundell (2016), Quantifying comparison of large detrital geochronology data sets, *Geosphere*, GES01237. 01231.

Saylor, J. E., B. K. Horton, D. F. Stockli, A. Mora, and J. Corredor (2012), Structural and thermochronological evidence for Paleogene basement-involved shortening in the axial Eastern Cordillera, Colombia, *Journal of South American Earth Sciences*, 39, 202-215.

Saylor, J. E., J. N. Knowles, B. K. Horton, J. Nie, and A. Mora (2013a), Mixing of source populations recorded in detrital zircon U-Pb age spectra of modern river sands, *The Journal of Geology*, 121(1), 17-33.

Saylor, J. E., J. N. Knowles, B. K. Horton, J. Nie, and A. Mora (2013b), Mixing of source populations recorded in detrital zircon U-Pb age spectra of modern river sands, *The Journal of Geology*, 121(1), 17-33.

Schlunegger, F., F. Kober, G. Zeilinger, and R. von Rotz (2010), Sedimentology-based reconstructions of paleoclimate changes in the Central Andes in response to the uplift of the Andes, Arica region between 19 and 21 S latitude, northern Chile, *International Journal of Earth Sciences*, 99(1), 123-137.

Schoenbohm, L. M., and M. R. Strecker (2009), Normal faulting along the southern margin of the Puna Plateau, northwest Argentina, *Tectonics*, 28(5), 1-21.

Seligman, A. N., Bindeman, I. N., Watkins, J. M., & Ross, A. M. (2016). Water in volcanic glass: From volcanic degassing to secondary hydration. *Geochimica et Cosmochimica Acta*, 191, 216-238.

Shaulis, B., Lapen, T. J., & Toms, A. (2010). Signal linearity of an extended range pulse counting detector: Applications to accurate and precise U-Pb dating of zircon by laser ablation quadrupole ICP-MS. *Geochemistry, Geophysics, Geosystems*, 11(11), 1-12.

- Sláma, J., J. Košler, D. J. Condon, J. L. Crowley, A. Gerdes, J. M. Hanchar, M. S. Horstwood, G. A. Morris, L. Nasdala, and N. Norberg (2008), Plešovice zircon—a new natural reference material for U–Pb and Hf isotopic microanalysis, *Chemical Geology*, 249(1), 1-35.
- Soler, P., and M. G. Bonhomme (1990), Relation of magmatic activity to plate dynamics in central Peru from Late Cretaceous to present, *Geological Society of America Special Papers*, 241, 173-192.
- Stacey, J. t., and J. Kramers (1975), Approximation of terrestrial lead isotope evolution by a two-stage model, *Earth and Planetary Science Letters*, 26(2), 207-221.
- Stephens, M. A. (1970a), Use of the Kolmogorov-Smirnov, Cramér-Von Mises and related statistics without extensive tables, *Journal of the Royal Statistical Society. Series B (Methodological)*, 115-122.
- Stephens, M. A. (1970b), Use of the Kolmogorov-Smirnov, Cramér-Von Mises and related statistics without extensive tables, *Journal of the Royal Statistical Society. Series B (Methodological)*, 115-122.
- Stolper, E. (1982), Water in silicate glasses: an infrared spectroscopic study, *Contributions to Mineralogy and Petrology*, 81(1), 1-17.
- Strecker, M., R. Alonso, B. Bookhagen, B. Carrapa, G. Hilley, E. Sobel, and M. Trauth (2007), Tectonics and climate of the southern central Andes, *Annual Review of Earth and Planetary Sciences*, 35, 747-787.
- Sundell, K. E., and J. E. Saylor (2017), Unmixing detrital geochronology age distributions, edited, *Geochemistry, Geophysics, Geosystems*, 18(8), 2872–2886.
- Takahashi, K., and D. S. Battisti (2007), Processes controlling the mean tropical Pacific precipitation pattern. Part I: The Andes and the eastern Pacific ITCZ, *Journal of Climate*, 20(14), 3434-3451.
- Takashimizu, Y., and M. Iiyoshi (2016), New parameter of roundness R: circularity corrected by aspect ratio, *Progress in Earth and Planetary Science*, 3(1), 2.
- Valle, N., A. Verney-Carron, J. Sterpenich, G. Libourel, E. Deloule, and P. Jollivet (2010), Elemental and isotopic (29 Si and 18 O) tracing of glass alteration mechanisms, *Geochimica et Cosmochimica Acta*, 74(12), 3412-3431.
- Vermeesch, P. (2013), Multi-sample comparison of detrital age distributions, *Chemical Geology*, 341, 140-146.
- Vermeesch, P., and E. Garzanti (2015), Making geological sense of ‘Big Data’ in sedimentary provenance analysis, *Chemical Geology*, 409, 20-27.
- Vermeesch, P., A. Resentini, and E. Garzanti (2016), An R package for statistical provenance analysis, *Sedimentary Geology*, 336, 14-25.

Von Waltershausen, W. S. (1845), Über die submarinen Ausbrüche in der tertiären Formation des Val di Noto im Vergleich mit verwandten Erscheinungen am Ätna, Gött Stud, 1(37), 1-431.

Wissink, G. K., and G. D. Hoke (2016), Eastern margin of Tibet supplies most sediment to the Yangtze River, Lithosphere, 8(6), 601-614.

Xie, X., and P. L. Heller (2009), Plate tectonics and basin subsidence history, Geological Society of America Bulletin, 121(1-2), 55-64.

Zachos, J., M. Pagani, L. Sloan, E. Thomas, and K. Billups (2001), Trends, rhythms, and aberrations in global climate 65 Ma to present, Science, 292(5517), 686-693.

APPENDIX 1

Random Sampling-weighting of Fifty Sources

Supplemental Material for Chapter 2

Random sample-weighting schemes

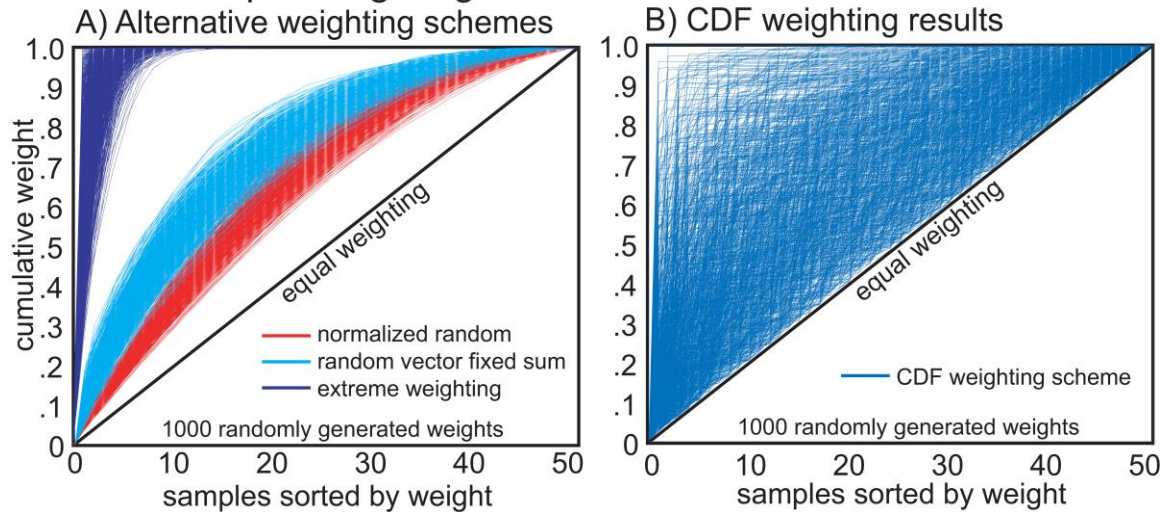


Figure A1.1. Random weighting schemes shown as cumulative distribution functions (CDFs). (A) One-thousand randomly generated CDFs using the three different weighting schemes tested in this study. All three prove to be inadequate because none of them cover the full range of potential weighting combinations (area above the equal weight line). (B) One-thousand randomly generated CDF weights following preferred random weighting method. This method of random weighting ensures testing both equal weighting (equal contribution of all source samples) and extreme weighting (contribution from only one or a few source samples).

APPENDIX 2

Table A2.1: Lithofacies Classifications

Lithofacies Code	Observation	Interpretation
c	Thinly laminated or structureless claystone	Suspension settling, swam deposits
Fm(c)	Structureless mudstone (c indicates carbonaceous)	Overbank deposits and suspension settling, often redistributed by post-depositional bioturbation
Fl	Laminated mudstone	Overbank, waning flood, or abandoned channel deposits
Sm	Structureless sandstone	Rapid sand deposition without stable bedform development, or post depositional redistribution via bioturbation
Sr	Assymetric ripple cross-stratified sandstone	Migrating 2-D or 3-D ripple bedforms in lower flow regime
St	Trough cross-stratified sandstone	unidirectional flow in shallow channels
Sh	Horizontally laminated sandstone	Migration of sinuous-crested and lingoid dunes in subaqueous unidirectional flow
Gmm	Matrix-supported structureless poorly sorted disorganized conglomerate	Supercritical upper flow regime plane bed flow of high velocity ≥ 100 cm/s or in very shallow water
Gcm	Clast-supported structureless poorly sorted disorganized conglomerate	Plastic or cohesive (high strength) debris flow, buoyancy modified sand sheet and hyperconcentrated flow
Gcmi	Clast-supported conglomerate, structureless and imbricated	Pseudoplastic debris flow, clast rich, pressure or buoyancy modified sheet flood deposition
Gchi	Clast-supported conglomerate, crudely horizontally bedded, imbricated (i)	Traction transport of migrating subaqueous barforms in unsteady flow
		Deposition by shallow traction currents, longitudinal barforms and gravel sheets or lag deposits

Table A2.2: Sandstone petrography modal point-counting parameters

Qm	Monocrystalline quartz
Qp	Polycrystalline quartz
Qpt	Polycrystalline foliated quartz
P	Plagioclase feldspar
K	Alkali feldspar (perthitic, orthoclase and sanidine)
Km	Alkali feldspar (microcline)
Lsc	Lithic siliciclastic claystone
Lss	Lithic siliciclastic siltstone
Lcl	Lithic carbonate limestone
Lch	Lithic chert
Lv	Lithic volcanics
Lpb	Lithic plutonic gabbroic
Lpg	Lithic plutonic granitic
Lms	Lithic metamorphic slate
Lmp	Lithic metamorphic
Lmg	Lithic metamorphic gneiss
Apx	Accessory mineral (pyroxene group)
Aam	Accessory mineral (amphibole group)
Amu	Accessory mineral (muscovite)
Azn	Accessory mineral (zircon)
Amg	Accessory mineral (magnetite)

Q Total quartz ($Qm + Qp + Qms + Lch$)

F Total feldspar ($K + P$)

Lv Total volcanic lithic fragments ($Lvf + Lvi + Lvm + Lvl$)

Lm Total metamorphic lithic fragments ($Lmg + Lmf + Lmn$)

Ls Total sedimentary lithic fragments ($Lsc + Lss + Lsm$)

L Total lithic fragments ($Lv + Lm + Ls$)

Lt Total lithic fragments with chert ($Lv + Lm + Ls + Lch$)

Table A2.3: Sandstone petrography results

Stratigraphic

Sample Name	Level (m)	Q	F	L	Qm	F	L	Qm	P	K	Qp	Lv	Ls
20150518-01	125	66	21	13	61	24	14	72	28	0	48	44	7
20150519-03	260	25	29	46	20	31	49	39	60	1	12	57	32
20150519-05	430	39	30	31	34	32	34	51	49	0	21	48	31
20150519-06	530	34	37	29	29	40	31	42	58	0	18	58	23
20150520-01	610	16	40	43	13	42	45	24	72	4	8	80	12
20150520-02	720	27	21	53	13	24	62	35	57	7	23	69	8
20150520-03	800	34	28	39	26	31	43	45	54	1	21	57	21
20150520-04	920	12	28	60	6	30	64	17	76	7	10	75	16
20150520-05	1060	30	42	28	23	46	31	33	64	3	24	64	12
20150521-01	1190	14	45	41	10	47	43	17	80	2	10	78	12
20150521-02	1250	19	39	42	17	40	43	29	67	4	6	83	11
20150521-03	1310	19	41	39	15	44	41	26	73	1	12	65	23
20150523-01	1470	30	28	42	29	28	43	51	45	4	3	74	22
20150523-02	1530	33	31	36	30	32	38	48	52	0	12	72	16
20150523-03	1640	15	47	37	13	49	38	21	75	3	7	74	19
20150523-04	1750	11	47	41	5	51	44	9	88	3	14	72	14
20150525-02	1830	40	28	32	36	30	34	55	44	1	15	71	15
20150525-01	1980	28	42	30	22	46	33	32	68	0	22	67	11
20150525-03	2040	26	43	32	13	50	37	20	79	0	32	58	10
20150525-05	2180	9	53	38	0	58	42	0	83	17	19	69	12
20150526-01	2320	24	56	20	18	60	22	23	76	1	27	64	9
20150526-02	2460	23	45	32	15	50	35	23	77	0	24	69	7
20150526-03	2580	19	43	38	16	45	39	26	74	0	9	84	7
20150527-01	2770	20	50	30	17	52	31	24	75	1	12	85	3
20150527-03	2840	4	68	28	1	70	29	1	91	8	10	84	6
20150527-04	2920	29	51	20	24	55	21	31	69	0	26	45	30
20150527-05	3090	8	45	47	2	48	50	4	93	3	11	80	10
20150528-01	3220	9	51	40	1	56	43	2	97	1	16	78	6
20140611-01	3600	12	51	36	8	54	38	14	86	0	10	73	17
20140611-02	4170	19	51	30	13	55	32	19	81	0	20	62	17
20140611-03	4800	9	54	37	5	57	38	8	92	0	11	78	11
20140605-01	4900	69	25	6	66	27	7	71	29	0	63	9	29
20140603-01	5330	36	41	23	32	44	25	42	57	1	23	46	31
20140604-01	5450	34	35	32	30	37	33	45	54	0	15	65	20
20140607-01	5800	27	28	46	21	30	49	41	59	0	15	52	33
20140608-01	5890	20	29	51	15	31	54	33	67	0	9	45	46
20140608-03	6100	27	31	43	21	33	46	39	60	0	14	55	31

Table A2.4: Detrital Zircon U-Pb Sample Data

Data Source	Sample Name	Physiographic Region	Fm. or Gp. Name	Geologic Age	Latitude	Longitude	n
<i>this study</i>	20140608-03	Altiplano	Top Paruro Fm.	L. Miocene	-13.76799	-71.82979	299
<i>this study</i>	20140528-01				-13.75312	-71.83511	258
<i>this study</i>	20140605-01	Altiplano	Base Paruro Fm.	Miocene	-13.75913	-71.82329	141
<i>this study</i>	20140605-02				-13.75969	-71.82277	19
<i>this study</i>	20140611-03	Altiplano	Top Punacancha Fm.	L. Oligocene	-13.62829	-71.88537	234
<i>this study</i>	20140611-01	Altiplano	Base Punacancha Fm.	Oligocene	-13.61641	-71.87318	324
<i>this study</i>	20150525-02	Altiplano	Soncco Fm.	L. Eocene	-13.61761	-71.84363	356
<i>this study</i>	20150520-01	Altiplano	Kayra Fm.	Eocene	-13.69650	-71.85138	306
<i>this study</i>	20150519-03	Altiplano	Quilque Fm.	L. Paleocene	-13.69364	-71.84798	313
<i>this study</i>	20160813-08	Altiplano	Huancané Fm.	E. Cretaceous	-16.05183	-69.77223	316
Reimann et al. (2010)	La1	Altiplano	Lampa Fm.	Devonian	-15.29212	-70.33677	75
Reimann et al. (2010)	Cab6	Altiplano	Cabanillas Gp.	Devonian	-15.62735	-70.38471	107
	Cab18				-15.63089	-70.38242	88
Reimann et al. (2010)	Ja7	Altiplano	Calapuja Fm.	Ordovician	-15.31527	-70.24419	120
<i>this study</i>	20160814-15	Western Cordillera	Hualhuani Fm.	E. Cretaceous	-16.27508	-70.19324	209
	20160815-06				-15.86207	-70.44615	121
<i>this study</i>	20160815-04	Western Cordillera	Labra Fm.	L. Jurassic	-15.85268	-70.30539	304
<i>this study</i>	20160815-05	Western Cordillera	Puente Fm.	L. Jurassic	-15.86480	-70.42625	303
Perez and Horton (2014)	NPPR12-25 NPDZP003	Eastern Cordillera	Muni Fm.	E. Cretaceous	-14.37551	-70.54854	92
					-14.89772	-70.53311	89
Perez and Horton (2014)	NPDZP006	Eastern Cordillera	Mitu Gp.	Permo-Triassic	-13.85975	-70.51526	96
Perez and Horton (2014)	NPDZP004	Eastern Cordillera	Ambo Fm.	E. Carboniferous	-14.35608	-70.55628	98
Perez and Horton (2014)	TC054	Eastern Cordillera	San Gaban Fm.	Ordovician	-14.84825	-70.56136	113
Bahlburg et al. (2011)	Oy13	Eastern Cordillera	Ollantaytambo Fm.	Ordovician	-13.21600	-72.58700	118
Reimann et al. (2010)	San 12	Eastern Cordillera	Sandia Fm.	Ordovician	-14.14366	-69.28065	118
	San 17				-14.25353	-69.40898	111
Reimann et al. (2010)	Coro 18	Eastern Cordillera	Amutura Fm.	Ordovician	-16.26904	-67.82120	124
	Am 20				-16.32674	-67.97069	127

APPENDIX 3

Detrital Zircon U-Pb Geochronology Methods

Supplemental Material for Chapter 3

Zircon grains were separated from fine- to coarse-grained sandstones following standard mineral separation procedures of crushing, disc milling, water tabling, heavy liquids and magnetic separation. Grains were washed in full strength nitric acid, dried, and poured onto two-sided tape for analysis. Grains were chosen at random and ablated using a Photon Machines Analyte 193 ArF excimer laser attached to a pulse counting detector fitted to a Varian 810 quadrupole mass spectrometer (Shaulis et al., 2010). For all analyses a $\sim 19.7 \mu\text{m}$ spot size was used with a fluence of 2.99 J/cm^2 and 10 Hz repetition rate for 200 shots, resulting in approximately 20 seconds of ablate time, with ~ 8 seconds of background measurement and ~ 7 seconds of washout following each analysis. All other machine parameters are similar to those outlined in Shaulis et al. (2010).

ICP-MS data was recorded and exported using Quantum. Raw data was baseline corrected and integrated using Igor Iolite, and filtered using an in-house MATLAB-based graphical user interface (GUI) at the University of Houston. Individual analyses were background corrected by taking the mean counts per second for each isotope for the first ~ 7 seconds and subtracting that value from each spectrum for the total analysis time. A constant integration window was chosen for each sample run (between 12 – 27 seconds analysis time) in order to calculate mean isotopic ratios and 2 standard error for each integration. Integration windows were held constant for all analyses and standards for individual runs because no downhole fractionation correction was conducted (c.f., Košler

et al., 2002). This ‘averaging’ approach was used to calculate raw standard ratios for fractionation and drift corrections.

Analyses were filtered based on percent sample uncertainty and concordance. In lieu of making a common Pb correction (Stacey & Kramers, 1975), we added 15% uncertainty to analyses age dates < 600Ma (for $^{206}\text{Pb}/^{238}\text{U}$) because the typical correction standard common Pb correction of Stacey & Kramers (1975) drastically increases $^{207}\text{Pb}/^{235}\text{U}$ concordia error ellipse for ‘young’ ages, resulting in acceptance of highly discordant ages. The $^{206}\text{Pb}/^{238}\text{U} - ^{207}\text{Pb}/^{206}\text{Pb}$ transition for reported ages (best ages) was set at 1000 Ma. Analyses with >15% uncertainty, >10% reverse discordance were rejected. Ages >600 Ma with >20% uncertainty were also rejected. All ages (both filtered and rejected), as well as standard analyses for each analytical session are reported in Supplementary Material S2.

For mineral standards we used well-characterized standards: Plešovice zircon, originating from potassic granulite in the southern Bohemian Massif, Czech Republic, with an ID-TIMS age of 337.13 ± 0.37 Ma (Sláma et al., 2008), as our primary standard to correct raw mass spectrometer ratios. We also used FC5z zircon from the Duluth Complex in Minnesota, USA, with an accepted age similar to samples AS3 and FC1 from Paces & Miller, (1993) that have an accepted age of 1099.1 ± 0.5 Ma, as our external standard to ensure machine run stability and for comparison to primary standards.

APPENDIX 4

Table A4.1: Detrital Zircon U-Pb Integrated Data for the Puente Formation

Spot	Ratios						Ages (Ma)						Best Age	Disc. (%)		
	207Pb/206Pb		207Pb/235U		206Pb/238U		206Pb/238U		207Pb/235U		207Pb/206Pb					
	±2σ	±2σ	±2σ	±2σ	±2σ	±2σ	±2σ	±2σ	±2σ	±2σ	±2σ					
<i>Puente Formation (20160815-05) Accepted Data</i>																
164	0.0569	11.2	0.2429	14.0	0.0309	8.7	0.60	196.5	16.7	220.8	27.8	489.0	246.3	196.5	16.7	11.0
163	0.0483	10.1	0.2418	10.8	0.0363	3.9	0.34	229.8	8.7	219.9	21.3	114.8	239.4	229.8	8.7	-4.5
106	0.0514	8.5	0.2683	14.2	0.0378	11.1	0.80	239.4	26.2	241.4	30.6	260.5	195.2	239.4	26.2	0.8
253	0.0529	6.5	0.2788	8.7	0.0382	5.9	0.67	241.6	13.9	249.7	19.3	326.4	147.0	241.6	13.9	3.2
322	0.0522	10.0	0.2756	11.3	0.0383	6.3	0.48	242.2	14.9	247.1	24.8	294.7	227.5	242.2	14.9	2.0
36	0.0567	12.7	0.3024	16.5	0.0387	11.1	0.64	244.8	26.6	268.3	38.8	478.6	280.9	244.8	26.6	8.8
51	0.0609	12.0	0.3257	12.6	0.0388	5.2	0.32	245.4	12.6	286.3	31.3	634.4	257.5	245.4	12.6	14.3
176	0.0660	8.2	0.3558	9.6	0.0391	5.4	0.52	247.4	13.1	309.1	25.6	805.1	171.6	247.4	13.1	20.0
184	0.0529	4.5	0.2858	5.6	0.0392	3.7	0.60	247.8	9.0	255.3	12.6	324.8	101.6	247.8	9.0	2.9
129	0.0573	10.9	0.3169	11.7	0.0401	4.2	0.37	253.7	10.6	279.5	28.6	501.7	239.6	253.7	10.6	9.2
338	0.0525	4.3	0.2959	4.0	0.0408	4.2	0.45	258.1	10.7	263.2	9.4	309.3	98.8	258.1	10.7	2.0
326	0.0523	6.7	0.2945	9.2	0.0408	7.0	0.68	258.1	17.8	262.1	21.1	297.9	153.4	258.1	17.8	1.5
212	0.0517	4.8	0.2922	6.5	0.0410	4.3	0.66	258.8	11.0	260.3	14.8	273.9	111.0	258.8	11.0	0.6
53	0.0515	4.9	0.2923	5.4	0.0412	4.3	0.51	260.2	10.9	260.3	12.5	261.6	112.8	260.2	10.9	0.1
152	0.0521	8.6	0.2962	11.7	0.0412	8.0	0.68	260.5	20.5	263.4	27.1	289.3	195.4	260.5	20.5	1.1
182	0.0600	8.9	0.3444	10.2	0.0416	5.2	0.48	262.8	13.3	300.5	26.5	604.4	193.2	262.8	13.3	12.5
345	0.0514	9.8	0.2985	11.2	0.0421	8.0	0.51	265.9	21.0	265.2	26.1	259.1	226.1	265.9	21.0	-0.3
165	0.0554	8.6	0.3262	11.7	0.0427	8.1	0.68	269.7	21.5	286.7	29.3	427.8	192.6	269.7	21.5	5.9
317	0.0613	10.7	0.3702	12.0	0.0438	7.1	0.47	276.3	19.2	319.8	32.9	650.5	229.0	276.3	19.2	13.6
336	0.0533	8.6	0.3588	10.3	0.0488	7.3	0.58	307.2	22.0	311.3	27.7	342.2	193.6	307.2	22.0	1.3
132	0.0558	3.5	0.3812	5.0	0.0495	3.5	0.72	311.7	10.8	327.9	14.1	444.5	78.1	311.7	10.8	4.9
320	0.0528	4.4	0.3723	5.7	0.0511	5.0	0.67	321.3	15.6	321.3	15.8	321.7	99.7	321.3	15.6	0.0
30	0.0556	10.9	0.4257	16.1	0.0555	12.2	0.74	348.3	41.4	360.1	48.9	437.0	242.7	348.3	41.4	3.3
213	0.0545	4.9	0.4171	5.8	0.0556	3.0	0.51	348.6	10.3	354.0	17.2	389.7	111.1	348.6	10.3	1.5
90	0.0544	4.4	0.4487	9.3	0.0598	8.1	0.88	374.3	29.3	376.4	29.1	388.9	99.4	374.3	29.3	0.5
180	0.0669	9.2	0.5984	13.7	0.0648	10.3	0.74	405.0	40.3	476.2	52.0	835.7	191.5	405.0	40.3	15.0
107	0.0593	8.1	0.5342	14.0	0.0653	11.2	0.82	407.9	44.1	434.6	49.7	578.7	176.7	407.9	44.1	6.1
16	0.0696	6.5	0.6549	8.1	0.0682	6.3	0.63	425.6	25.9	511.5	32.7	916.4	132.8	425.6	25.9	16.8
206	0.0574	8.0	0.5952	11.3	0.0752	8.1	0.71	467.4	36.4	474.2	42.9	507.0	175.0	467.4	36.4	1.4
73	0.0573	3.4	0.5950	4.6	0.0753	3.4	0.68	468.2	15.3	474.0	17.3	502.5	74.0	468.2	15.3	1.2
324	0.0625	7.2	0.6586	7.7	0.0764	4.3	0.40	474.5	19.8	513.7	31.1	692.2	153.2	474.5	19.8	7.6
54	0.0569	3.4	0.6047	4.1	0.0771	3.3	0.60	478.8	15.2	480.2	15.7	486.9	74.9	478.8	15.2	0.3
219	0.0580	4.8	0.6182	6.4	0.0773	4.3	0.66	479.7	20.1	488.7	24.7	531.2	104.5	479.7	20.1	1.8
304	0.0581	7.8	0.6262	12.1	0.0782	9.1	0.77	485.6	42.5	493.7	47.4	531.7	170.6	485.6	42.5	1.7
134	0.0585	11.3	0.6315	16.2	0.0784	11.6	0.72	486.3	54.4	497.0	63.6	546.7	245.9	486.3	54.4	2.2
299	0.0598	2.7	0.6520	6.2	0.0790	5.5	0.90	490.4	26.2	509.7	24.8	597.2	59.5	490.4	26.2	3.8
349	0.0592	8.4	0.6488	8.4	0.0795	6.1	0.36	493.2	28.8	507.7	33.6	573.9	183.2	493.2	28.8	2.9
75	0.0627	8.4	0.6924	11.7	0.0801	8.5	0.69	496.6	40.5	534.2	48.6	698.5	179.9	496.6	40.5	7.1
189	0.0572	6.8	0.6336	9.2	0.0803	6.3	0.68	497.8	30.2	498.4	36.4	500.8	150.0	497.8	30.2	0.1
98	0.0658	12.6	0.7338	16.4	0.0808	10.6	0.64	501.1	51.3	558.8	70.7	801.3	264.8	501.1	51.3	10.3
230	0.0557	6.3	0.6297	8.6	0.0819	6.1	0.69	507.6	29.7	495.9	33.9	442.2	139.4	507.6	29.7	-2.4
77	0.0605	11.4	0.6841	16.1	0.0820	11.7	0.71	507.9	57.1	529.2	66.6	622.3	245.7	507.9	57.1	4.0
1	0.0569	4.1	0.6441	4.9	0.0821	3.2	0.56	508.6	15.6	504.9	19.5	487.8	89.8	508.6	15.6	-0.7
247	0.0574	2.9	0.6534	4.9	0.0825	4.1	0.80	511.0	19.9	510.6	19.5	508.6	64.1	511.0	19.9	-0.1
92	0.0671	7.9	0.7648	11.3	0.0827	8.0	0.71	512.3	39.5	576.8	49.9	839.6	165.0	512.3	39.5	11.2
191	0.0585	2.6	0.6693	3.7	0.0830	2.7	0.70	513.9	13.3	520.3	15.0	548.4	57.5	513.9	13.3	1.2
26	0.0588	4.6	0.6726	4.6	0.0830	4.1	0.44	514.1	20.2	522.3	18.8	558.0	100.5	514.1	20.2	1.6
210	0.0589	6.3	0.6787	9.2	0.0836	6.8	0.73	517.3	34.0	526.0	38.0	563.7	136.7	517.3	34.0	1.6
135	0.0808	7.1	0.9312	10.4	0.0836	7.7	0.73	517.4	38.2	668.2	51.1	1217.0	139.4	517.4	38.2	22.6
181	0.0597	4.1	0.6881	5.5	0.0836	4.1	0.68	517.4	20.5	531.7	22.9	593.6	87.9	517.4	20.5	2.7
80	0.0593	4.1	0.6873	8.8	0.0840	8.2	0.89	520.1	40.9	531.1	36.3	579.0	88.8	520.1	40.9	2.1
96	0.0639	4.7	0.7417	9.8	0.0842	8.8	0.88	521.3	43.9	563.4	42.3	737.3	98.9	521.3	43.9	7.5
342	0.0584	13.4	0.6833	18.8	0.0848	14.0	0.70	524.8	70.3	528.8	77.8	546.2	293.5	524.8	70.3	0.8
150	0.0606	2.9	0.7093	3.9	0.0849	2.9	0.68	525.1	14.8	544.3	16.5	625.4	61.8	525.1	14.8	3.5
100	0.0585	4.7	0.6854	8.8	0.0850	7.5	0.84	526.0	38.0	530.0	36.3	547.6	103.3	526.0	38.0	0.8
269	0.0578	3.3	0.6812	5.0	0.0855	5.0	0.78	528.7	25.6	527.5	20.4	522.3	73.0	528.7	25.6	-0.2
307	0.0581	7.0	0.6854	11.0	0.0855	8.4	0.77	528.8	42.8	530.1	45.4	535.3	153.6	528.8	42.8	0.2
237	0.0553	7.5	0.6522	10.9	0.0856	8.0	0.73	529.2	40.7	509.8	43.9	423.8	167.2	529.2	40.7	-3.8
161	0.0593	5.1	0.7008	7.3	0.0857	5.5	0.72	529.8	27.7	539.3	30.7	579.7	110.4	529.8	27.7	1.8
327	0.0584	4.5	0.6918	5.1	0.0859	4.1	0.54	531.5	20.9	533.9	21.2	544.2	98.3	531.5	20.9	0.5
34	0.0604	7.0	0.7210	9.0	0.0866	6.3	0.63	535.3	32.6	551.2	38.2	617.8	151.2	535.3	32.6	2.9
195	0.0583	3.5	0.6974	5.0	0.0868	3.7	0.72	536.6	18.9	537.2	21.0	540.0	76.8	536.6	18.9	0.1
259	0.0595	7.7	0.7126	11.4	0.0869	8.8	0.74	537.2	45.2	546.3	48.3	584.5	167.5	537.2	45.2	1.7

Table A4.1 (continued): Detrital Zircon U-Pb Integrated Data for the Puente Formation

Spot	Ratios						Ages (Ma)						Best Age	Disc. (%)		
	207Pb/206Pb		207Pb/235U		206Pb/238U		206Pb/238U		207Pb/235U		207Pb/206Pb					
	±2σ	±2σ	±2σ	±2σ	Rho	±2σ	±2σ	±2σ	±2σ	±2σ	±2σ					
<i>Puente Formation (20160815-05) Accepted Data</i>																
151	0.0596	7.4	0.7157	10.0	0.0870	6.9	0.68	538.0	35.5	548.1	42.4	590.6	159.8	538.0	35.5	1.9
86	0.0572	11.5	0.6872	18.4	0.0872	14.3	0.78	538.7	73.9	531.1	76.3	498.9	253.3	538.7	73.9	-1.4
248	0.0614	9.1	0.7390	13.3	0.0872	9.8	0.73	539.2	50.6	561.8	57.6	654.4	195.9	539.2	50.6	4.0
315	0.0599	5.5	0.7211	7.4	0.0873	6.8	0.71	539.8	35.1	551.3	31.6	599.3	118.6	539.8	35.1	2.1
103	0.0606	10.2	0.7307	15.7	0.0874	12.0	0.76	540.3	62.1	557.0	67.3	625.8	219.7	540.3	62.1	3.0
58	0.0601	4.2	0.7247	5.0	0.0874	3.6	0.56	540.3	18.5	553.5	21.4	608.1	91.8	540.3	18.5	2.4
198	0.0606	6.1	0.7310	8.6	0.0875	6.1	0.71	540.8	31.8	557.1	36.9	624.4	130.9	540.8	31.8	2.9
102	0.0592	6.9	0.7189	10.9	0.0880	8.5	0.77	543.8	44.4	550.0	46.2	576.1	149.8	543.8	44.4	1.1
9	0.0590	3.8	0.7166	4.5	0.0881	3.3	0.54	544.5	17.0	548.6	19.0	565.7	83.8	544.5	17.0	0.7
156	0.0596	2.7	0.7240	4.0	0.0882	3.5	0.74	544.6	18.3	553.0	17.1	587.9	59.3	544.6	18.3	1.5
57	0.0606	4.5	0.7363	5.7	0.0882	4.3	0.63	544.7	22.3	560.2	24.5	623.8	96.0	544.7	22.3	2.8
71	0.0623	4.7	0.7576	6.0	0.0882	4.1	0.64	544.8	21.4	572.7	26.5	684.8	99.3	544.8	21.4	4.9
138	0.0592	4.2	0.7197	5.3	0.0882	3.3	0.62	545.0	17.4	550.5	22.6	573.2	91.1	545.0	17.4	1.0
242	0.0584	4.2	0.7125	6.6	0.0885	5.1	0.77	546.5	26.7	546.2	28.0	545.0	91.7	546.5	26.7	-0.1
330	0.0579	4.9	0.7080	6.0	0.0888	4.7	0.60	548.2	24.9	543.6	25.2	524.3	108.3	548.2	24.9	-0.8
231	0.0586	12.3	0.7198	18.2	0.0890	13.5	0.74	549.8	71.3	550.5	77.6	553.6	268.4	549.8	71.3	0.1
251	0.0566	5.3	0.6949	8.0	0.0891	6.0	0.75	550.0	31.8	535.7	33.3	475.3	117.3	550.0	31.8	-2.7
149	0.0613	3.9	0.7557	5.0	0.0895	3.4	0.64	552.3	18.0	571.5	21.8	648.7	82.7	552.3	18.0	3.4
155	0.0644	5.6	0.7984	7.3	0.0899	5.1	0.65	554.8	27.2	595.9	32.9	755.8	117.4	554.8	27.2	6.9
122	0.0627	6.9	0.7771	9.6	0.0900	6.5	0.70	555.3	34.5	583.8	42.8	696.5	147.4	555.3	34.5	4.9
296	0.0595	6.0	0.7379	9.2	0.0900	7.0	0.76	555.6	37.1	561.2	39.6	583.7	129.6	555.6	37.1	1.0
241	0.0684	6.5	0.8539	8.4	0.0905	5.3	0.64	558.7	28.6	626.8	39.5	880.7	134.5	558.7	28.6	10.9
56	0.0601	4.5	0.7500	6.1	0.0906	4.8	0.68	558.9	25.6	568.2	26.7	605.6	97.8	558.9	25.6	1.6
23	0.0594	4.7	0.7429	5.5	0.0907	4.3	0.56	559.4	23.0	564.1	23.7	583.0	101.6	559.4	23.0	0.8
292	0.0586	4.0	0.7335	6.5	0.0908	5.2	0.79	560.0	28.1	558.6	27.8	552.7	86.8	560.0	28.1	-0.3
295	0.0614	4.5	0.7680	7.5	0.0908	6.0	0.80	560.1	32.1	578.6	33.1	651.8	97.4	560.1	32.1	3.2
6	0.0590	6.0	0.7388	7.8	0.0908	5.2	0.64	560.2	27.9	561.7	33.6	567.9	130.7	560.2	27.9	0.3
331	0.0627	5.4	0.7862	6.2	0.0910	4.6	0.54	561.2	24.6	589.0	27.9	697.6	114.7	561.2	24.6	4.7
167	0.0626	4.7	0.7860	6.6	0.0911	5.0	0.70	562.2	27.0	588.9	29.5	693.4	100.5	562.2	27.0	4.5
46	0.0618	6.4	0.7776	7.1	0.0912	5.5	0.51	562.7	29.7	584.1	31.3	668.4	136.1	562.7	29.7	3.7
321	0.0605	5.1	0.7611	6.9	0.0913	5.7	0.69	563.0	30.9	574.6	30.2	621.1	109.4	563.0	30.9	2.0
223	0.0605	6.2	0.7617	9.1	0.0913	6.8	0.73	563.4	36.6	575.0	40.0	621.3	133.7	563.4	36.6	2.0
300	0.0592	5.2	0.7458	8.0	0.0914	5.8	0.76	563.6	31.2	565.8	34.8	574.7	113.1	563.6	31.2	0.4
287	0.0589	6.5	0.7434	9.2	0.0915	6.2	0.70	564.3	33.3	564.4	39.8	564.9	142.5	564.3	33.3	0.0
39	0.0597	4.9	0.7590	5.9	0.0922	5.0	0.61	568.3	27.0	573.4	26.0	593.9	106.1	568.3	27.0	0.9
48	0.0602	5.5	0.7657	6.5	0.0922	5.7	0.60	568.7	31.2	577.3	28.5	610.9	118.7	568.7	31.2	1.5
22	0.0589	5.4	0.7491	6.6	0.0923	4.8	0.58	568.9	26.4	567.7	28.5	563.2	118.7	568.9	26.4	-0.2
105	0.0595	6.3	0.7570	12.0	0.0923	9.9	0.85	569.3	53.7	572.3	52.4	584.2	137.1	569.3	53.7	0.5
291	0.0615	4.5	0.7849	6.9	0.0926	5.3	0.75	571.1	29.1	588.3	30.8	655.2	97.3	571.1	29.1	2.9
18	0.0643	4.9	0.8220	4.6	0.0928	3.5	0.30	571.9	19.2	609.1	21.2	750.3	103.3	571.9	19.2	6.1
63	0.0604	9.6	0.7725	13.7	0.0928	9.9	0.71	571.9	54.0	581.2	60.9	617.7	208.0	571.9	54.0	1.6
239	0.0579	3.8	0.7424	5.9	0.0930	4.5	0.76	573.0	24.8	563.8	25.4	526.7	83.7	573.0	24.8	-1.6
224	0.0593	6.1	0.7613	9.0	0.0931	6.8	0.74	573.6	37.2	574.7	39.7	579.1	133.1	573.6	37.2	0.2
190	0.0607	2.9	0.7794	3.5	0.0931	2.1	0.57	573.7	11.8	585.1	15.5	629.7	61.5	573.7	11.8	2.0
201	0.0610	6.7	0.7825	9.7	0.0931	7.2	0.73	573.7	39.4	586.9	43.5	638.4	143.1	573.7	39.4	2.3
264	0.0589	6.5	0.7581	9.5	0.0933	7.5	0.73	574.9	41.1	572.9	41.8	564.9	142.2	574.9	41.1	-0.4
64	0.0584	6.8	0.7515	7.8	0.0933	3.8	0.47	575.0	21.1	569.1	33.8	545.4	149.2	575.0	21.1	-1.0
81	0.0577	11.5	0.7430	17.8	0.0933	13.8	0.76	575.3	76.0	564.2	77.2	519.6	253.1	575.3	76.0	-2.0
339	0.0621	6.3	0.8018	6.9	0.0936	5.3	0.49	577.1	29.2	597.8	31.3	677.4	135.6	577.1	29.2	3.5
196	0.0648	6.9	0.8454	9.5	0.0947	6.6	0.69	583.2	36.6	622.1	44.0	766.5	144.4	583.2	36.6	6.3
276	0.0623	4.1	0.8135	5.4	0.0948	4.8	0.68	583.7	26.6	604.4	24.6	683.1	87.4	583.7	26.6	3.4
37	0.0720	7.2	0.9444	8.7	0.0952	6.0	0.57	585.9	33.8	675.2	42.7	985.4	146.6	585.9	33.8	13.2
83	0.0622	4.9	0.8184	9.2	0.0954	8.2	0.84	587.3	45.8	607.2	41.9	682.0	105.2	587.3	45.8	3.3
280	0.0605	3.1	0.7955	4.9	0.0954	4.3	0.78	587.6	24.1	594.3	22.0	619.9	67.0	587.6	24.1	1.1
33	0.0593	4.2	0.7814	5.1	0.0955	4.1	0.59	588.2	22.9	586.3	22.6	578.7	91.6	588.2	22.9	-0.3
285	0.0591	4.5	0.7788	6.6	0.0956	4.4	0.73	588.4	25.0	584.8	29.4	570.6	97.9	588.4	25.0	-0.6
168	0.0615	14.7	0.8107	20.6	0.0956	14.6	0.70	588.6	81.9	602.8	94.1	656.9	315.5	588.6	81.9	2.4
207	0.0608	2.6	0.8020	3.7	0.0956	2.8	0.71	588.8	15.7	597.9	16.9	632.6	56.7	588.8	15.7	1.5
123	0.0683	9.3	0.9037	10.9	0.0960	5.4	0.52	591.1	30.6	653.7	52.6	876.2	192.7	591.1	30.6	9.6
97	0.0597	4.8	0.7911	9.9	0.0961	8.9	0.88	591.3	50.3	591.8	44.6	593.8	103.1	591.3	50.3	0.1
186	0.0616	4.7	0.8191	6.6	0.0965	4.8	0.71	593.7	26.9	607.5	30.3	659.6	100.3	593.7	26.9	2.3
293	0.0595	10.3	0.7961	15.0	0.0971	11.0	0.73	597.2	62.6	594.6	67.6	584.9	223.1	597.2	62.6	-0.4
267	0.0592	4.6	0.7942	6.8	0.0972	6.1	0.75	598.2	34.6	593.5	30.5	575.8	99.8	598.2	34.6	-0.8

Table A4.1 (continued): Detrital Zircon U-Pb Integrated Data for the Puente Formation

Spot	Ratios						Rho	Ages (Ma)						Best Age	Disc. (%)	
	207Pb/206Pb		207Pb/235U		206Pb/238U			206Pb/238U		207Pb/235U		207Pb/206Pb				
	±2σ	±2σ	±2σ	±2σ	±2σ	±2σ		±2σ	±2σ	±2σ	±2σ	±2σ				
<i>Puente Formation (20160815-05) Accepted Data</i>																
3	0.0632	6.9	0.8504	8.9	0.0975	5.8	0.63	600.0	33.3	624.9	41.6	715.8	147.5	600.0	33.3	16.2
174	0.0627	8.5	0.8495	12.3	0.0983	9.2	0.73	604.6	53.0	624.4	57.5	696.6	180.2	604.6	53.0	13.2
278	0.0631	4.4	0.8573	5.8	0.0986	4.9	0.67	605.9	28.4	628.7	27.1	711.3	94.2	605.9	28.4	14.8
266	0.0596	4.7	0.8112	6.9	0.0986	6.2	0.75	606.4	35.6	603.1	31.4	590.6	100.9	606.4	35.6	-2.7
91	0.0615	4.9	0.8375	9.8	0.0988	8.4	0.86	607.6	48.6	617.8	45.3	655.2	105.7	607.6	48.6	7.3
281	0.0609	4.1	0.8403	5.6	0.1001	4.3	0.68	614.8	25.2	619.3	25.8	636.0	87.8	614.8	25.2	3.3
159	0.0611	6.1	0.8451	8.4	0.1003	6.1	0.69	616.2	35.9	622.0	39.1	643.1	130.8	616.2	35.9	4.2
84	0.0619	6.1	0.8607	12.1	0.1008	10.3	0.86	619.0	60.7	630.5	56.7	672.0	131.0	619.0	60.7	7.9
341	0.0606	4.9	0.8449	5.4	0.1011	5.1	0.57	620.6	30.0	621.9	25.0	626.4	104.6	620.6	30.0	0.9
254	0.0610	6.1	0.8510	9.0	0.1011	7.0	0.73	620.9	41.7	625.2	42.1	640.7	132.0	620.9	41.7	3.1
66	0.0610	10.3	0.8503	15.8	0.1011	12.1	0.76	621.0	71.9	624.8	74.1	638.5	220.7	621.0	71.9	2.7
232	0.0623	6.4	0.8709	8.6	0.1014	6.0	0.68	622.6	35.6	636.1	40.8	684.2	135.7	622.6	35.6	9.0
12	0.0623	4.1	0.8789	5.2	0.1023	4.0	0.63	628.0	23.7	640.4	24.9	684.1	88.6	628.0	23.7	8.2
250	0.0619	7.5	0.8814	11.0	0.1032	8.1	0.73	633.3	48.9	641.7	52.6	671.5	161.2	633.3	48.9	5.7
101	0.0616	3.3	0.8770	7.6	0.1033	7.0	0.90	633.9	42.1	639.4	36.1	658.6	71.7	633.9	42.1	3.8
178	0.0622	4.5	0.8903	5.4	0.1038	3.7	0.57	636.4	22.2	646.5	26.0	682.0	95.7	636.4	22.2	6.7
288	0.0645	4.8	0.9229	6.1	0.1038	3.3	0.63	636.6	20.0	663.9	29.9	757.5	101.5	636.6	20.0	16.0
28	0.0613	4.7	0.8804	4.8	0.1042	4.1	0.44	638.7	25.2	641.2	22.7	649.9	101.5	638.7	25.2	1.7
13	0.0638	5.7	0.9204	7.2	0.1047	5.1	0.61	641.9	31.2	662.6	35.1	733.6	121.6	641.9	31.2	12.5
177	0.0621	3.5	0.8978	5.4	0.1049	4.5	0.76	642.8	27.6	650.6	25.8	677.5	75.3	642.8	27.6	5.1
193	0.0619	4.9	0.8957	6.9	0.1049	4.8	0.69	643.2	29.6	649.4	33.0	671.1	105.9	643.2	29.6	4.2
187	0.0623	3.8	0.9037	5.1	0.1052	3.5	0.66	644.9	21.4	653.7	24.7	684.3	81.9	644.9	21.4	5.8
127	0.0605	4.7	0.8786	6.0	0.1053	3.6	0.63	645.3	22.3	640.2	28.4	622.6	100.5	645.3	22.3	-3.6
252	0.0621	9.2	0.9029	13.4	0.1055	9.7	0.72	646.6	59.8	653.3	64.5	676.4	197.1	646.6	59.8	4.4
116	0.0606	5.8	0.8856	9.0	0.1059	6.6	0.76	649.0	40.6	644.0	43.0	626.4	125.5	649.0	40.6	-3.6
271	0.0610	4.2	0.8980	5.9	0.1068	5.4	0.73	654.3	33.4	650.6	28.6	637.9	90.3	654.3	33.4	-2.6
124	0.0611	3.7	0.9047	5.5	0.1074	3.9	0.73	657.6	24.3	654.2	26.5	642.5	80.6	657.6	24.3	-2.4
229	0.0661	4.5	0.9958	6.4	0.1092	5.0	0.72	668.1	31.5	701.7	32.5	810.7	94.0	668.1	31.5	17.6
220	0.0629	4.8	0.9700	7.2	0.1118	5.5	0.74	683.1	36.0	688.5	36.2	706.1	102.9	683.1	36.0	3.3
117	0.0618	7.0	0.9595	10.5	0.1126	7.5	0.74	687.9	48.7	683.0	52.0	666.8	150.7	687.9	48.7	-3.2
333	0.0628	4.6	0.9804	5.3	0.1132	4.2	0.55	691.5	27.7	693.8	26.5	701.1	97.4	691.5	27.7	1.4
141	0.0659	3.2	1.0427	4.0	0.1147	2.5	0.59	699.9	16.9	725.3	20.6	804.6	67.2	699.9	16.9	13.0
274	0.0640	11.7	1.0346	16.6	0.1173	12.2	0.71	715.0	82.3	721.2	85.7	740.7	247.7	715.0	82.3	3.5
272	0.0653	3.6	1.0894	4.8	0.1210	4.6	0.71	736.1	32.0	748.2	25.4	784.4	75.1	736.1	32.0	6.2
328	0.0693	6.5	1.2021	7.5	0.1258	5.0	0.53	763.8	36.2	801.6	41.4	908.1	132.9	763.8	36.2	15.9
263	0.0662	3.4	1.1518	5.0	0.1263	4.5	0.75	766.5	32.9	778.1	27.0	811.5	70.6	766.5	32.9	5.5
115	0.0650	4.1	1.1350	7.9	0.1267	6.4	0.85	769.1	46.3	770.1	42.5	773.1	87.1	769.1	46.3	0.5
337	0.0631	10.3	1.1132	13.7	0.1279	10.1	0.66	776.2	74.0	759.7	73.5	711.6	218.8	776.2	74.0	-9.1
332	0.0688	5.0	1.2559	6.2	0.1324	5.0	0.63	801.8	37.5	826.1	35.0	892.1	102.3	801.8	37.5	10.1
38	0.0651	10.9	1.1916	15.1	0.1328	11.1	0.69	803.8	83.8	796.7	83.6	776.9	229.2	803.8	83.8	-3.5
347	0.0682	10.7	1.2876	12.8	0.1368	9.2	0.56	826.7	71.4	840.2	73.1	876.0	222.2	826.7	71.4	5.6
139	0.0721	6.6	1.3765	7.4	0.1384	3.5	0.46	835.6	27.3	878.9	43.8	989.6	134.3	835.6	27.3	15.6
21	0.0683	9.6	1.3185	12.9	0.1399	9.2	0.67	844.3	72.6	853.9	74.6	878.8	198.6	844.3	72.6	3.9
47	0.0743	5.7	1.4366	7.0	0.1402	6.2	0.64	845.9	48.9	904.3	41.9	1049.9	114.1	845.9	48.9	19.4
205	0.0734	5.7	1.4418	7.4	0.1425	4.7	0.63	858.9	37.6	906.5	44.2	1024.3	116.3	858.9	37.6	16.1
308	0.0702	4.4	1.3975	7.9	0.1444	6.5	0.83	869.4	52.7	887.9	46.6	934.2	89.9	869.4	52.7	6.9
344	0.0705	4.7	1.4092	4.7	0.1449	4.5	0.47	872.2	36.5	892.8	27.7	944.2	96.1	872.2	36.5	7.6
268	0.0692	7.0	1.3957	9.8	0.1463	7.6	0.70	880.0	62.7	887.1	57.9	904.9	145.2	880.0	62.7	2.7
8	0.0686	3.6	1.3842	4.3	0.1463	2.9	0.56	880.4	23.8	882.2	25.3	886.9	73.8	880.4	23.8	0.7
143	0.0704	2.8	1.4841	3.7	0.1528	2.5	0.64	916.7	21.7	923.9	22.2	941.1	58.0	916.7	21.7	2.6
61	0.0705	3.9	1.4862	5.6	0.1529	4.2	0.72	917.5	36.0	924.8	34.3	942.3	80.4	917.5	36.0	2.6
228	0.0708	2.8	1.4966	5.2	0.1533	4.9	0.85	919.5	41.7	929.0	31.9	951.6	56.3	919.5	41.7	3.4
104	0.0758	6.3	1.6029	9.7	0.1535	7.5	0.76	920.3	64.7	971.4	60.9	1088.8	125.9	920.3	64.7	15.5
302	0.0715	4.7	1.5180	7.5	0.1540	5.6	0.78	923.3	47.9	937.7	46.2	971.5	96.0	923.3	47.9	5.0
87	0.0749	4.4	1.6064	10.0	0.1555	8.9	0.90	931.6	77.1	972.7	62.9	1066.7	88.9	931.6	77.1	12.7
343	0.0684	7.3	1.4703	7.5	0.1559	5.0	0.39	934.0	43.2	918.2	45.6	880.7	150.2	934.0	43.2	-6.1
171	0.0684	10.9	1.4698	15.5	0.1560	11.1	0.71	934.3	96.5	918.1	93.8	879.2	225.4	934.3	96.5	-6.3
309	0.0746	4.2	1.6131	7.2	0.1568	5.8	0.82	938.9	50.9	975.3	45.3	1058.4	84.3	938.9	50.9	11.3
197	0.0754	5.4	1.6292	7.9	0.1568	5.7	0.72	939.0	50.0	981.5	49.5	1078.0	109.2	939.0	50.0	12.9
348	0.0761	8.3	1.6524	8.4	0.1576	6.2	0.38	943.2	54.4	990.5	53.0	1096.7	165.7	943.2	54.4	14.0
283	0.0721	6.2	1.5667	9.3	0.1577	7.2	0.74	943.9	63.1	957.1	57.5	987.5	126.2	943.9	63.1	4.4
194	0.0728	9.4	1.5833	13.5	0.1578	9.7	0.72	944.3	85.6	963.7	84.4	1008.2	191.2	944.3	85.6	6.3
130	0.0732	3.6	1.6086	5.2	0.1594	3.6	0.72	953.5	32.3	973.6	32.3	1019.2	72.1	953.5	32.3	6.4

Table A4.1 (continued): Detrital Zircon U-Pb Integrated Data for the Puente Formation

Spot	Ratios						Ages (Ma)						Best Age	Disc. (%)		
	207Pb/206Pb		207Pb/235U		206Pb/238U		206Pb/238U		207Pb/235U		207Pb/206Pb					
	±2σ	±2σ	±2σ	±2σ	Rho	±2σ	±2σ	±2σ	±2σ	±2σ	±2σ					
<i>Puente Formation (20160815-05) Rejected Data</i>																
144	0.0648	3.7	0.8799	5.3	0.0985	3.9	0.71	605.7	22.6	640.9	25.1	767.3	77.9	605.7	22.6	21.1
68	0.0680	3.9	0.9272	5.4	0.0990	3.9	0.69	608.3	22.7	666.2	26.3	867.3	81.0	608.3	22.7	29.9
260	0.0669	10.2	0.9132	12.3	0.0990	7.3	0.56	608.4	42.6	658.7	59.7	835.2	213.4	608.4	42.6	27.2
209	0.0615	15.3	0.8401	22.0	0.0990	15.8	0.72	608.7	91.7	619.2	102.4	658.0	328.9	608.7	91.7	7.5
211	0.0599	18.8	0.8443	27.1	0.1023	19.5	0.72	627.7	116.4	621.5	126.5	599.2	407.6	627.7	116.4	-4.7
140	0.1094	5.4	1.6016	7.0	0.1062	4.5	0.63	650.7	28.1	970.8	43.8	1788.9	99.1	650.7	28.1	63.6
245	0.0784	5.4	1.3670	7.4	0.1265	5.2	0.69	767.8	37.8	874.9	43.4	1156.6	106.3	767.8	37.8	33.6
257	0.1714	6.0	3.1153	8.4	0.1318	6.4	0.71	798.2	48.4	1436.5	64.7	2571.3	99.5	798.2	48.4	69.0
256	0.0862	3.4	1.5756	9.9	0.1325	9.6	0.94	802.3	72.4	960.6	61.4	1343.0	65.2	802.3	72.4	40.3
29	0.0958	6.6	1.7837	8.8	0.1350	7.1	0.68	816.2	54.7	1039.5	57.3	1544.8	123.6	816.2	54.7	47.2
67	0.0737	3.7	1.3759	5.6	0.1354	4.4	0.75	818.5	33.9	878.7	33.1	1033.4	75.3	818.5	33.9	20.8
52	0.0744	5.0	1.3961	6.8	0.1360	5.9	0.70	822.2	45.4	887.3	40.3	1053.4	99.8	822.2	45.4	22.0
279	0.0761	4.0	1.4448	8.1	0.1378	7.8	0.87	832.1	60.6	907.7	48.8	1096.5	80.4	832.1	60.6	24.1
137	0.0802	6.5	1.6062	7.8	0.1452	4.4	0.56	874.1	35.9	972.6	49.1	1202.4	128.5	874.1	35.9	27.3
173	0.0815	4.4	1.6345	6.1	0.1455	4.4	0.69	875.7	36.3	983.6	38.3	1232.9	86.6	875.7	36.3	29.0
301	0.1003	11.0	2.0861	13.5	0.1509	7.6	0.58	905.9	64.6	1144.3	93.1	1629.2	204.3	905.9	64.6	44.4
43	0.0726	15.1	1.5900	21.4	0.1588	15.5	0.71	950.2	137.4	966.3	134.1	1003.1	307.0	950.2	137.4	5.3
20	0.0708	4.8	1.7336	5.5	0.1777	4.2	0.54	1054.2	40.9	1021.1	35.4	950.7	97.6	950.7	97.6	-10.9
17	0.0840	4.8	1.8410	5.0	0.1590	4.1	0.45	951.3	36.1	1060.2	32.9	1291.9	93.8	951.3	36.1	26.4
154	0.3891	16.3	8.6196	17.8	0.1607	7.2	0.40	960.6	64.3	2298.6	163.4	3867.3	246.2	960.6	64.3	75.2
108	0.0759	15.0	2.0999	23.5	0.2007	17.9	0.77	1179.1	192.6	1148.8	163.0	1092.0	301.4	1092.0	301.4	-8.0
95	0.0889	3.2	2.0877	9.5	0.1703	9.1	0.94	1013.5	85.3	1144.8	65.0	1402.8	60.8	1402.8	60.8	27.8
72	0.0903	4.9	2.3793	7.4	0.1911	5.7	0.75	1127.2	59.0	1236.4	52.8	1432.1	93.2	1432.1	93.2	21.3
55	0.0935	10.3	2.2165	15.5	0.1720	11.8	0.75	1023.2	111.4	1186.3	108.7	1497.2	195.4	1497.2	195.4	31.7
113	0.0975	9.1	2.3434	15.3	0.1744	12.1	0.80	1036.3	115.6	1225.6	109.1	1576.1	170.0	1576.1	170.0	34.2
249	0.1012	8.6	3.1605	14.6	0.2266	11.8	0.81	1316.5	140.4	1447.6	112.7	1645.8	158.9	1645.8	158.9	20.0
14	0.1134	6.5	3.9016	8.6	0.2495	6.4	0.65	1435.7	81.9	1614.0	69.4	1855.2	117.8	1855.2	117.8	22.6
340	0.1138	26.8	4.6908	38.9	0.2990	28.6	0.73	1686.3	425.2	1765.6	337.7	1860.7	483.3	1860.7	483.3	9.4
185	0.1146	2.4	3.1558	4.6	0.1998	4.0	0.85	1174.0	42.9	1446.4	35.4	1873.3	43.4	1873.3	43.4	37.3
27	0.1247	5.0	4.5396	6.9	0.2640	6.3	0.72	1510.3	84.3	1738.3	57.2	2024.7	88.2	2024.7	88.2	25.4
319	0.1269	3.9	7.4507	5.4	0.4259	5.8	0.76	2287.1	112.6	2167.1	48.0	2055.2	68.9	2055.2	68.9	-11.3
5	0.1656	10.7	5.0285	13.0	0.2202	7.4	0.56	1283.1	86.6	1824.1	110.1	2513.6	180.3	2513.6	180.3	49.0
175	0.1730	3.1	8.9874	5.6	0.3767	5.1	0.84	2060.8	90.7	2336.7	51.6	2587.3	51.1	2587.3	51.1	20.4
133	0.2016	10.5	4.8072	11.8	0.1730	5.2	0.45	1028.4	49.3	1786.2	99.2	2839.1	171.7	2839.1	171.7	63.8
244	0.7179	5.9	62.2586	9.0	0.6290	6.9	0.76	3145.6	172.4	4211.0	90.2	4766.9	84.4	4766.9	84.4	34.0

Table A4.2 (continued): Detrital Zircon U-Pb Integrated Data for the Labra Formation

Table with columns: Spot, Ratios (207Pb/206Pb, 207Pb/235U, 206Pb/238U, Rho), Ages (Ma) (206Pb/238U, 207Pb/235U, 207Pb/206Pb, Best Age), Disc. (%). The table contains 39 data rows, each representing a zircon spot analysis with multiple isotope ratios and ages.

Table A4.2 (continued): Detrital Zircon U-Pb Integrated Data for the Labra Formation

Spot	Ratios						Rho	Ages (Ma)						Best Age	Disc. (%)	
	207Pb/206Pb		207Pb/235U		206Pb/238U			206Pb/238U		207Pb/235U		207Pb/206Pb				
	±2σ	±2σ	±2σ	±2σ	±2σ	±2σ		±2σ	±2σ	±2σ	±2σ	±2σ				
<i>Labra Formation (20160815-04) Rejected Data</i>																
241	0.0673	5.7	0.9500	9.8	0.1023	7.9	0.81	628.2	47.2	678.1	48.6	847.8	119.2	628.2	47.2	25.9
143	0.0741	5.4	1.0484	7.7	0.1026	5.4	0.71	629.7	32.5	728.1	39.9	1044.1	108.4	629.7	32.5	39.7
87	0.0855	13.2	1.2109	20.7	0.1027	16.0	0.77	630.4	95.9	805.6	115.8	1326.8	256.4	630.4	95.9	52.5
19	0.0699	5.9	0.9928	6.2	0.1030	3.5	0.37	632.2	20.8	700.2	31.4	925.0	121.2	632.2	20.8	31.7
52	0.0590	3.9	0.8433	5.0	0.1037	2.8	0.62	636.1	17.1	621.0	23.1	566.2	85.3	636.1	17.1	-12.3
301	0.0594	2.5	0.8671	3.7	0.1059	3.0	0.74	648.9	18.8	634.0	17.4	581.4	53.8	648.9	18.8	-11.6
209	0.1018	6.7	1.5004	7.8	0.1069	4.1	0.52	654.7	25.7	930.6	47.6	1657.3	123.5	654.7	25.7	60.5
92	0.0707	3.5	1.0827	4.6	0.1110	3.0	0.64	678.7	19.6	745.0	24.2	949.6	72.6	678.7	19.6	28.5
27	0.0713	5.9	1.1084	10.3	0.1128	9.0	0.82	688.9	59.0	757.4	54.9	965.3	120.4	688.9	59.0	28.6
199	0.1319	6.1	2.0870	8.8	0.1148	6.3	0.72	700.4	41.6	1144.5	60.8	2123.2	107.0	700.4	41.6	67.0
220	0.0765	6.3	1.2159	10.7	0.1153	8.8	0.81	703.3	58.4	807.9	59.9	1108.4	125.6	703.3	58.4	36.5
33	0.0591	9.3	0.9457	12.3	0.1161	8.6	0.65	707.9	57.4	675.9	60.7	570.7	203.2	707.9	57.4	-24.0
343	0.0716	6.4	1.1593	10.6	0.1175	8.7	0.80	716.2	59.3	781.6	57.9	973.3	130.7	716.2	59.3	26.4
232	0.1457	9.3	2.3681	18.0	0.1179	15.4	0.86	718.4	104.8	1233.0	129.1	2296.0	159.5	718.4	104.8	68.7
218	0.0717	2.9	1.1846	3.7	0.1198	2.5	0.64	729.7	17.6	793.4	20.5	977.0	58.6	729.7	17.6	25.3
91	0.1000	9.4	1.7037	12.6	0.1236	8.4	0.66	751.0	59.5	1009.9	80.7	1624.1	175.4	751.0	59.5	53.8
236	0.0726	3.3	1.2400	5.0	0.1238	3.6	0.75	752.5	25.4	818.9	28.2	1003.7	67.0	752.5	25.4	25.0
310	0.0737	3.7	1.3034	8.9	0.1282	8.2	0.91	777.8	60.2	847.2	51.1	1033.7	75.7	777.8	60.2	24.8
341	0.0787	3.5	1.5080	5.1	0.1390	4.4	0.75	838.8	34.6	933.6	31.4	1164.8	68.7	838.8	34.6	28.0
288	0.0765	3.7	1.4685	5.0	0.1393	3.8	0.66	840.6	29.8	917.5	30.0	1107.4	74.9	840.6	29.8	24.1
322	0.0921	3.8	1.7957	5.2	0.1413	3.9	0.68	852.2	31.2	1043.9	34.2	1470.5	72.8	852.2	31.2	42.0
82	0.0700	3.5	1.6879	4.6	0.1748	3.0	0.65	1038.4	29.0	1004.0	29.6	929.6	72.5	929.6	72.5	-11.7
133	0.0706	15.8	1.8774	22.6	0.1928	16.2	0.72	1136.5	168.8	1073.1	150.9	946.6	323.6	946.6	323.6	-20.1
314	0.0945	6.1	2.0683	9.4	0.1588	7.3	0.76	950.0	64.4	1138.4	64.2	1517.6	114.6	950.0	64.4	37.4
157	0.0652	20.8	1.4392	29.9	0.1601	21.5	0.72	957.5	191.4	905.4	181.3	780.3	437.8	957.5	191.4	-22.7
350	0.0734	15.3	1.6496	21.0	0.1631	14.7	0.68	973.9	133.0	989.4	133.5	1023.9	309.8	973.9	133.0	4.9
8	0.0716	6.0	1.7988	7.7	0.1821	5.1	0.63	1078.5	50.9	1045.0	50.4	975.6	123.0	975.6	123.0	-10.5
37	0.0717	6.7	1.9237	7.7	0.1945	5.5	0.53	1145.9	57.2	1089.3	51.4	978.0	135.9	978.0	135.9	-17.2
212	0.0735	15.5	1.8739	22.2	0.1849	15.9	0.71	1093.9	159.7	1071.9	148.0	1027.6	314.3	1027.6	314.3	-6.5
317	0.0879	18.0	2.2395	22.9	0.1848	14.3	0.62	1093.2	143.9	1193.5	161.9	1380.1	345.2	1380.1	345.2	20.8
234	0.0965	4.3	2.2348	6.5	0.1679	4.9	0.75	1000.6	45.2	1192.0	45.5	1558.1	80.3	1558.1	80.3	35.8
192	0.1029	3.9	3.0840	7.1	0.2173	5.8	0.84	1267.6	66.7	1428.7	54.2	1677.7	71.6	1677.7	71.6	24.4
20	0.1105	5.8	2.9209	6.8	0.1918	4.1	0.51	1131.1	42.1	1387.3	51.2	1806.9	106.2	1806.9	106.2	37.4
184	0.1106	4.2	2.7513	6.2	0.1804	4.5	0.74	1069.4	43.9	1342.4	46.2	1809.0	76.3	1809.0	76.3	40.9
285	0.1144	3.1	3.5876	6.3	0.2274	5.8	0.87	1321.1	69.4	1546.8	50.1	1870.4	56.6	1870.4	56.6	29.4
197	0.1190	5.2	4.0586	8.6	0.2474	6.7	0.80	1424.9	85.7	1646.0	70.0	1941.2	93.1	1941.2	93.1	26.6
101	0.1233	7.0	3.8498	9.3	0.2264	6.2	0.66	1315.5	74.4	1603.2	75.4	2005.0	124.1	2005.0	124.1	34.4
146	0.1239	8.3	4.0507	12.2	0.2371	9.0	0.74	1371.4	110.9	1644.4	99.9	2013.6	146.4	2013.6	146.4	31.9
193	0.1275	8.0	4.1495	13.2	0.2361	10.4	0.79	1366.3	128.6	1664.1	108.5	2063.4	141.5	2063.4	141.5	33.8
302	0.1291	16.7	6.6562	21.0	0.3738	12.7	0.60	2047.3	223.5	2066.8	187.1	2086.4	293.7	2086.4	293.7	1.9
233	0.1350	3.1	3.4542	4.8	0.1856	3.7	0.77	1097.5	37.2	1516.8	37.7	2163.8	53.3	2163.8	53.3	49.3
173	0.1377	7.5	5.0569	10.4	0.2663	7.2	0.69	1522.1	98.0	1828.9	88.5	2198.7	130.7	2198.7	130.7	30.8
127	0.1612	13.3	6.2149	15.7	0.2797	8.5	0.54	1589.7	119.9	2006.6	138.5	2468.0	224.0	2468.0	224.0	35.6
167	0.1895	6.0	9.1497	9.4	0.3502	7.3	0.77	1935.4	122.7	2353.1	86.6	2737.9	98.4	2737.9	98.4	29.3
347	0.2206	15.7	10.0949	17.3	0.3319	7.7	0.41	1847.7	123.8	2443.5	160.8	2984.9	253.4	2984.9	253.4	38.1
129	0.5151	9.5	16.4998	11.4	0.2323	6.4	0.55	1346.5	77.4	2906.2	109.6	4285.1	139.8	4285.1	139.8	68.6

Table A4.3 (continued): Detrital Zircon U-Pb Integrated Data for the Hualhuani Formation

Spot	Ratios						Ages (Ma)						Best Age	Disc. (%)		
	207Pb/206Pb		207Pb/235U		206Pb/238U		206Pb/238U		207Pb/235U		207Pb/206Pb					
	±2σ	±2σ	±2σ	±2σ	Rho	±2σ	±2σ	±2σ	±2σ	±2σ	±2σ					
<i>Hualhuani Formation 2 (20160815-06) Rejected Data</i>																
49	0.0954	8.2	1.9675	13.0	0.1495	10.1	0.77	898.1	85.0	1104.4	87.6	1536.9	154.8	898.1	85.0	41.6
96	0.0787	31.3	1.9503	42.0	0.1797	28.0	0.67	1065.1	275.1	1098.5	289.4	1165.4	621.1	1165.4	621.1	8.6
92	0.0823	18.5	2.2743	29.1	0.2004	22.5	0.77	1177.7	242.3	1204.3	208.0	1252.4	361.8	1252.4	361.8	6.0
33	0.0964	10.6	2.7080	16.3	0.2037	12.5	0.76	1195.3	136.1	1330.7	121.4	1555.8	198.2	1555.8	198.2	23.2
72	0.1003	19.6	3.2910	27.4	0.2380	19.2	0.70	1376.2	238.6	1478.9	217.0	1629.6	364.9	1629.6	364.9	15.5
20	0.1174	2.5	3.5777	4.1	0.2210	3.4	0.79	1287.2	40.0	1544.6	32.6	1917.2	45.6	1917.2	45.6	32.9
110	0.1208	3.7	4.2103	5.2	0.2527	4.1	0.71	1452.6	53.2	1676.0	42.9	1968.3	66.2	1968.3	66.2	26.2
74	0.1458	3.7	5.3723	6.1	0.2673	5.1	0.80	1527.1	69.3	1880.5	52.5	2296.9	63.9	2296.9	63.9	33.5
85	0.1752	21.0	9.2883	28.5	0.3844	19.3	0.68	2097.0	346.5	2366.9	267.0	2608.3	349.0	2608.3	349.0	19.6
7	0.1800	4.5	8.4949	8.9	0.3422	7.4	0.86	1897.3	122.2	2285.4	81.0	2653.2	74.9	2653.2	74.9	28.5
129	0.2070	5.0	11.7513	9.0	0.4117	7.9	0.83	2222.7	148.9	2584.8	84.0	2882.3	81.2	2882.3	81.2	22.9
11	0.6137	5.7	24.7832	9.9	0.2929	8.0	0.82	1655.9	116.7	3299.7	97.4	4540.8	82.9	4540.8	82.9	63.5
12	0.6371	5.3	36.0910	9.2	0.4108	7.2	0.82	2218.7	135.1	3669.0	91.6	4595.1	76.4	4595.1	76.4	51.7
108	0.8265	15.3	1185.0509	20.5	10.3993	13.8	0.67	15687.7	815.1	7187.3	210.5	4968.1	218.5	4968.1	218.5	-215.8

Table A4.4 (continued): Detrital Zircon U-Pb Integrated Data for the Huancané Formation

Spot	Ratios						Ages (Ma)						Best Age	Disc. (%)		
	207Pb/206Pb		207Pb/235U		206Pb/238U		206Pb/238U		207Pb/235U		207Pb/206Pb					
	±2σ	±2σ	±2σ	±2σ	Rho	±2σ	±2σ	±2σ	±2σ	±2σ	±2σ					
<i>Huancané Formation (20160813-08) Accepted Data</i>																
237	0.2098	3.7	14.4126	6.3	0.4982	4.5	0.81	2605.9	96.4	2777.3	59.9	2904.2	60.7	2904.2	60.7	10.3
<i>Huancané Formation (20160813-08) Rejected Data</i>																
9	0.1746	13.6	0.9240	17.3	0.0384	10.9	0.62	242.8	26.0	664.5	84.6	2602.1	225.8	242.8	26.0	63.5
173	0.0881	6.7	0.5433	10.0	0.0447	7.6	0.74	282.1	20.9	440.6	35.7	1384.1	128.1	282.1	20.9	36.0
299	0.0579	19.8	0.7440	28.5	0.0931	20.5	0.72	573.9	112.4	564.7	123.9	527.8	433.4	573.9	112.4	-1.6
264	0.0680	7.8	0.9315	10.1	0.0994	6.4	0.64	610.8	37.1	668.4	49.7	868.0	161.8	610.8	37.1	29.6
161	0.0580	8.2	0.7995	12.0	0.1000	9.1	0.73	614.7	53.5	596.5	54.0	528.1	180.3	614.7	53.5	-16.4
235	0.0668	7.0	0.9262	10.1	0.1006	6.9	0.72	617.7	40.5	665.6	49.4	831.4	146.9	617.7	40.5	25.7
46	0.0618	16.4	0.8585	22.6	0.1007	15.4	0.69	618.6	90.8	629.3	106.5	667.9	350.4	618.6	90.8	7.4
191	0.0583	3.9	0.8168	6.2	0.1015	4.8	0.77	623.4	28.3	606.2	28.1	542.7	86.2	623.4	28.3	-14.9
286	0.0578	5.9	0.8114	8.6	0.1018	6.4	0.72	624.8	38.2	603.2	39.1	522.8	129.8	624.8	38.2	-19.5
229	0.0667	14.5	0.9420	21.6	0.1025	16.1	0.74	628.9	96.3	674.0	106.9	827.6	302.4	628.9	96.3	24.0
200	0.0592	4.5	0.8448	6.7	0.1035	5.3	0.74	634.9	32.0	621.8	31.2	574.4	97.9	634.9	32.0	-10.5
166	0.0790	9.3	1.1688	16.2	0.1073	13.7	0.82	657.1	85.8	786.1	89.1	1171.8	183.3	657.1	85.8	43.9
209	0.0634	17.0	0.9713	25.0	0.1111	18.5	0.73	678.9	119.5	689.2	125.6	722.8	361.3	678.9	119.5	6.1
277	0.0922	4.6	1.4446	11.5	0.1136	10.6	0.92	693.8	69.6	907.6	69.3	1471.5	88.2	693.8	69.6	52.9
249	0.0869	11.6	1.4068	15.7	0.1174	10.5	0.68	715.4	71.2	891.8	93.6	1359.1	222.7	715.4	71.2	47.4
356	0.1233	15.3	2.0614	20.0	0.1213	13.0	0.65	738.0	90.6	1136.1	137.9	2004.0	271.9	738.0	90.6	63.2
97	0.0775	13.3	1.3196	23.3	0.1235	19.0	0.82	750.8	134.8	854.3	135.2	1133.7	264.7	750.8	134.8	33.8
316	0.0727	7.4	1.2686	9.4	0.1265	5.6	0.61	767.7	40.7	831.8	53.2	1007.0	151.0	767.7	40.7	23.8
276	0.1389	40.3	2.5389	46.1	0.1325	22.3	0.48	802.3	168.6	1283.2	349.1	2214.0	699.5	802.3	168.6	63.8
300	0.0619	4.4	1.1513	6.3	0.1348	4.6	0.71	815.2	34.9	777.9	34.3	672.3	95.0	815.2	34.9	-21.3
263	0.1588	23.2	3.0633	25.2	0.1399	9.7	0.39	844.3	76.8	1423.6	195.0	2442.6	392.5	844.3	76.8	65.4
256	0.0803	11.3	1.6677	16.4	0.1507	11.8	0.73	904.7	99.9	996.3	104.5	1203.8	221.7	904.7	99.9	24.8
204	0.1606	4.1	3.3869	5.1	0.1530	4.4	0.64	917.7	37.6	1501.4	39.9	2461.5	68.5	917.7	37.6	62.7
68	0.0697	13.9	1.6857	19.7	0.1754	14.1	0.71	1041.7	135.2	1003.1	126.3	919.8	286.4	919.8	286.4	-13.2
93	0.0703	33.5	1.7251	48.6	0.1779	35.2	0.72	1055.7	342.8	1017.9	322.8	937.6	686.9	937.6	686.9	-12.6
358	0.0820	7.2	1.8208	8.7	0.1610	5.1	0.56	962.5	45.6	1053.0	57.3	1245.6	141.1	962.5	45.6	22.7
34	0.0714	5.1	1.8248	7.7	0.1853	5.5	0.75	1095.8	55.5	1054.4	50.4	969.7	104.5	969.7	104.5	-13.0
186	0.0821	5.3	1.8582	9.1	0.1641	7.1	0.81	979.5	64.9	1066.3	60.2	1248.5	103.6	979.5	64.9	21.5
23	0.0722	16.9	1.8325	25.4	0.1841	18.8	0.74	1089.3	188.6	1057.2	168.3	991.5	344.4	991.5	344.4	-9.9
262	0.0755	16.7	1.7453	24.0	0.1677	17.2	0.72	999.2	159.0	1025.4	156.3	1081.9	335.8	999.2	159.0	7.6
354	0.0746	17.9	1.8758	25.8	0.1824	18.7	0.72	1080.1	185.7	1072.6	172.7	1057.3	359.8	1057.3	359.8	-2.2
117	0.0755	5.7	2.1637	7.7	0.2080	5.8	0.67	1218.1	64.1	1169.5	53.4	1080.6	114.8	1080.6	114.8	-12.7
349	0.0779	22.1	1.8303	31.3	0.1704	22.1	0.71	1014.3	207.9	1056.4	208.4	1144.4	439.8	1144.4	439.8	11.4
202	0.0810	15.4	2.5848	22.3	0.2314	16.2	0.72	1341.7	196.8	1296.3	164.6	1221.9	301.9	1221.9	301.9	-9.8
272	0.0828	17.4	2.3591	25.0	0.2067	17.9	0.72	1211.2	197.9	1230.3	180.0	1264.0	340.0	1264.0	340.0	4.2
224	0.0906	6.4	3.8329	8.5	0.3069	6.0	0.66	1725.2	91.2	1599.7	68.5	1438.0	121.3	1438.0	121.3	-20.0
240	0.0946	8.6	2.6649	12.0	0.2044	8.2	0.70	1198.9	89.3	1318.8	88.9	1519.4	162.9	1519.4	162.9	21.1
194	0.1102	14.3	3.7578	15.2	0.2474	5.2	0.34	1425.2	66.4	1583.8	122.4	1801.9	260.0	1801.9	260.0	20.9
2	0.1184	7.6	4.0451	12.4	0.2477	10.0	0.79	1426.7	128.0	1643.3	101.4	1932.7	136.8	1932.7	136.8	26.2
271	0.1190	4.5	3.9676	7.2	0.2418	5.7	0.78	1396.3	71.3	1627.6	58.6	1941.0	80.1	1941.0	80.1	28.1
267	0.1431	3.8	3.4865	7.1	0.1767	5.9	0.85	1049.1	57.4	1524.2	55.9	2264.9	65.0	2264.9	65.0	53.7
52	0.1766	18.5	7.9127	24.4	0.3250	15.8	0.65	1814.0	249.8	2221.1	223.3	2621.1	307.4	2621.1	307.4	30.8
295	0.1908	5.2	10.5407	9.7	0.4007	8.1	0.84	2172.4	149.6	2483.5	89.7	2748.8	86.1	2748.8	86.1	21.0

Table A4.5: Detrital Zircon U-Pb Integrated Data for the Quilque Formation

Spot	Ratios						Ages (Ma)						Best Age	Disc. (%)		
	207Pb/206Pb		207Pb/235U		206Pb/238U		206Pb/238U		207Pb/235U		207Pb/206Pb				±2σ	
	±2σ		±2σ		±2σ		±2σ		±2σ		±2σ					
<i>Quilque Formation (20150519-03) Accepted Data</i>																
354	0.0530	9.3	0.0660	13.4	0.0090	9.5	0.72	57.9	5.5	64.9	8.4	329.3	211.5	57.9	5.5	10.7
359	0.0533	8.1	0.0686	11.6	0.0093	8.2	0.72	59.9	4.9	67.4	7.5	343.2	182.7	59.9	4.9	11.2
187	0.0538	7.7	0.0696	12.7	0.0094	11.3	0.80	60.2	6.8	68.3	8.4	363.1	174.0	60.2	6.8	11.9
142	0.0449	8.6	0.0590	9.6	0.0095	3.8	0.44	61.1	2.3	58.2	5.4	-60.2	210.2	61.1	2.3	-5.0
194	0.0580	9.4	0.0763	14.6	0.0096	11.1	0.77	61.3	6.7	74.7	10.5	528.4	205.5	61.3	6.7	18.0
158	0.0471	8.9	0.0623	12.0	0.0096	7.7	0.68	61.5	4.7	61.3	7.2	56.5	211.4	61.5	4.7	-0.2
145	0.0460	9.0	0.0608	11.0	0.0096	6.2	0.58	61.6	3.8	59.9	6.4	-4.7	217.3	61.6	3.8	-2.7
384	0.0509	11.3	0.0675	16.4	0.0096	12.8	0.73	61.6	7.8	66.3	10.5	238.4	259.4	61.6	7.8	7.0
104	0.0508	9.0	0.0675	11.3	0.0096	7.0	0.61	61.8	4.3	66.3	7.3	231.6	207.1	61.8	4.3	6.8
369	0.0514	7.6	0.0683	14.3	0.0096	11.5	0.85	61.8	7.1	67.1	9.3	259.2	174.2	61.8	7.1	7.8
167	0.0675	13.0	0.0901	18.0	0.0097	12.7	0.69	62.1	7.9	87.6	15.1	852.3	271.1	62.1	7.9	29.1
287	0.0569	12.3	0.0760	14.3	0.0097	7.3	0.51	62.2	4.5	74.4	10.3	488.3	272.3	62.2	4.5	16.5
360	0.0548	10.1	0.0733	14.3	0.0097	10.2	0.71	62.3	6.3	71.8	9.9	402.8	226.2	62.3	6.3	13.3
177	0.0482	7.4	0.0646	11.7	0.0097	10.3	0.78	62.4	6.4	63.6	7.2	107.5	173.7	62.4	6.4	1.8
175	0.0578	10.9	0.0776	14.4	0.0097	10.6	0.66	62.5	6.6	75.9	10.6	520.8	239.9	62.5	6.6	17.6
164	0.0515	10.7	0.0693	13.1	0.0098	8.1	0.58	62.6	5.0	68.0	8.6	264.0	244.9	62.6	5.0	8.0
373	0.0521	7.9	0.0701	13.9	0.0098	11.5	0.83	62.7	7.2	68.8	9.3	288.5	179.8	62.7	7.2	8.9
103	0.0536	10.1	0.0725	11.4	0.0098	5.3	0.46	62.9	3.3	71.1	7.8	354.9	228.1	62.9	3.3	11.5
18	0.0492	5.9	0.0666	7.1	0.0098	4.2	0.55	62.9	2.6	65.4	4.5	157.9	138.2	62.9	2.6	3.8
262	0.0469	11.7	0.0635	14.0	0.0098	7.3	0.56	63.0	4.6	62.5	8.5	43.1	278.6	63.0	4.6	-0.8
179	0.0478	7.0	0.0648	10.2	0.0098	8.9	0.74	63.1	5.6	63.8	6.3	91.5	165.4	63.1	5.6	1.2
217	0.0544	7.5	0.0740	10.7	0.0099	7.9	0.71	63.3	5.0	72.5	7.5	387.0	169.4	63.3	5.0	12.7
253	0.0521	5.6	0.0710	8.9	0.0099	7.0	0.78	63.3	4.4	69.6	6.0	291.0	126.8	63.3	4.4	9.0
310	0.0532	11.2	0.0725	16.6	0.0099	12.1	0.74	63.4	7.6	71.0	11.4	338.0	253.8	63.4	7.6	10.8
184	0.0478	9.3	0.0652	14.2	0.0099	12.0	0.76	63.4	7.6	64.1	8.8	91.5	220.7	63.4	7.6	1.1
180	0.0490	8.8	0.0667	12.2	0.0099	10.0	0.70	63.4	6.3	65.6	7.7	146.7	207.1	63.4	6.3	3.4
229	0.0520	9.5	0.0709	11.8	0.0099	7.2	0.59	63.4	4.5	69.5	7.9	285.9	218.0	63.4	4.5	8.8
140	0.0460	8.0	0.0628	9.6	0.0099	4.9	0.55	63.4	3.1	61.8	5.8	0.0	193.4	63.4	3.1	-2.6
315	0.0509	8.8	0.0696	13.8	0.0099	10.2	0.77	63.6	6.4	68.3	9.1	237.2	203.1	63.6	6.4	6.9
101	0.0575	14.8	0.0787	16.8	0.0099	7.9	0.47	63.7	5.0	76.9	12.4	510.6	326.1	63.7	5.0	17.2
297	0.0570	11.2	0.0781	15.1	0.0099	10.1	0.67	63.7	6.4	76.4	11.1	493.4	246.6	63.7	6.4	16.6
282	0.0572	13.3	0.0784	15.1	0.0099	7.0	0.47	63.8	4.5	76.6	11.1	499.0	293.1	63.8	4.5	16.8
119	0.0547	9.3	0.0750	10.9	0.0099	5.8	0.52	63.8	3.7	73.4	7.8	399.6	209.2	63.8	3.7	13.1
245	0.0535	6.9	0.0734	9.2	0.0100	6.1	0.66	63.9	3.9	72.0	6.4	349.3	156.6	63.9	3.9	11.2
243	0.0518	8.9	0.0712	10.6	0.0100	5.8	0.55	64.0	3.7	69.8	7.2	275.1	203.1	64.0	3.7	8.4
106	0.0496	9.7	0.0683	12.2	0.0100	7.5	0.60	64.0	4.8	67.1	7.9	177.5	227.0	64.0	4.8	4.6
237	0.0542	8.9	0.0748	11.0	0.0100	6.5	0.59	64.2	4.1	73.2	7.8	380.8	199.6	64.2	4.1	12.4
256	0.0470	5.1	0.0649	9.1	0.0100	7.4	0.83	64.2	4.7	63.8	5.6	50.9	121.4	64.2	4.7	-0.5
161	0.0499	6.6	0.0688	7.9	0.0100	4.5	0.54	64.2	2.9	67.6	5.1	190.6	154.2	64.2	2.9	5.1
230	0.0523	8.1	0.0722	10.8	0.0100	7.1	0.65	64.2	4.5	70.8	7.4	299.3	185.5	64.2	4.5	9.3
291	0.0473	14.1	0.0653	18.2	0.0100	11.4	0.63	64.2	7.3	64.2	11.3	64.6	335.7	64.2	7.3	0.0
143	0.0484	13.6	0.0669	19.1	0.0100	13.2	0.70	64.3	8.5	65.8	12.1	120.9	319.7	64.3	8.5	2.3
387	0.0455	10.3	0.0629	16.1	0.0100	13.3	0.77	64.3	8.5	61.9	9.7	-30.1	248.6	64.3	8.5	-3.9
46	0.0572	13.0	0.0791	14.1	0.0100	5.3	0.38	64.3	3.4	77.3	10.5	498.1	287.0	64.3	3.4	16.7
176	0.0612	12.3	0.0848	17.0	0.0100	12.7	0.69	64.4	8.2	82.6	13.5	647.1	263.8	64.4	8.2	22.0
99	0.0538	10.6	0.0745	13.2	0.0100	7.9	0.60	64.4	5.1	73.0	9.3	363.0	238.9	64.4	5.1	11.7
212	0.0656	9.2	0.0912	12.1	0.0101	8.3	0.65	64.7	5.4	88.6	10.2	794.4	192.6	64.7	5.4	27.0
258	0.0554	10.8	0.0773	13.7	0.0101	8.3	0.62	64.8	5.3	75.6	10.0	430.0	239.9	64.8	5.3	14.2
182	0.0475	12.8	0.0663	18.5	0.0101	14.3	0.72	64.8	9.2	65.1	11.7	76.5	305.2	64.8	9.2	0.5
214	0.0532	6.9	0.0743	10.1	0.0101	7.9	0.73	64.9	5.1	72.8	7.1	338.0	157.3	64.9	5.1	10.8
91	0.0483	11.5	0.0678	13.1	0.0102	6.8	0.48	65.3	4.4	66.7	8.4	114.5	271.3	65.3	4.4	2.0
36	0.0488	13.2	0.0689	14.0	0.0102	4.7	0.34	65.7	3.1	67.7	9.2	137.3	309.0	65.7	3.1	2.9
83	0.0459	13.4	0.0649	16.7	0.0103	10.2	0.60	65.8	6.7	63.9	10.3	-8.1	323.1	65.8	6.7	-3.0
323	0.0461	7.5	0.0653	16.2	0.0103	13.8	0.89	65.8	9.0	64.2	10.1	4.2	181.2	65.8	9.0	-2.5
13	0.0517	14.2	0.0734	15.8	0.0103	7.0	0.44	66.1	4.6	72.0	11.0	271.5	325.3	66.1	4.6	8.2
246	0.0471	10.9	0.0670	12.7	0.0103	6.4	0.50	66.1	4.2	65.8	8.1	55.1	260.9	66.1	4.2	-0.5
112	0.0475	13.0	0.0677	17.9	0.0103	12.3	0.68	66.2	8.1	66.5	11.5	76.5	309.4	66.2	8.1	0.4
264	0.0498	12.0	0.0711	15.2	0.0104	8.9	0.61	66.4	5.9	69.8	10.2	187.4	280.1	66.4	5.9	4.9
267	0.0488	13.9	0.0698	15.9	0.0104	7.4	0.49	66.5	4.9	68.5	10.5	138.8	325.4	66.5	4.9	2.9
279	0.0492	12.8	0.0704	15.3	0.0104	8.3	0.55	66.6	5.5	69.1	10.2	155.9	299.0	66.6	5.5	3.6
14	0.0504	6.4	0.0722	7.2	0.0104	3.5	0.45	66.7	2.3	70.8	4.9	212.3	149.1	66.7	2.3	5.8
38	0.0502	9.9	0.0720	13.1	0.0104	8.6	0.66	66.7	5.7	70.5	8.9	202.8	229.1	66.7	5.7	5.4
286	0.0507	9.8	0.0729	11.5	0.0104	6.2	0.53	66.9	4.1	71.4	8.0	226.5	225.5	66.9	4.1	6.4

Table A4.5 (continued): Detrital Zircon U-Pb Integrated Data for the Quilque Formation

Spot	Ratios							Ages (Ma)						Disc. (%)		
	207Pb/ 206Pb		207Pb/ 235U		206Pb/ 238U		Rho	206Pb/ 238U		207Pb/ 235U		207Pb/ 206Pb			Best Age	
	$\pm 2\sigma$	$\pm 2\sigma$	$\pm 2\sigma$	$\pm 2\sigma$	$\pm 2\sigma$	$\pm 2\sigma$	$\pm 2\sigma$	$\pm 2\sigma$	$\pm 2\sigma$	$\pm 2\sigma$	$\pm 2\sigma$	$\pm 2\sigma$	$\pm 2\sigma$			
<i>Quilque Formation (20150519-03) Accepted Data</i>																
269	0.0524	6.5	0.3124	11.1	0.0433	8.7	0.81	273.0	23.4	276.0	26.9	301.9	147.6	273.0	23.4	1.1
93	0.0520	14.8	0.3120	19.6	0.0435	13.4	0.66	274.5	36.0	275.7	47.4	286.5	337.4	274.5	36.0	0.5
120	0.0550	5.4	0.3321	5.8	0.0438	2.6	0.39	276.2	7.0	291.2	14.7	413.4	120.3	276.2	7.0	5.2
166	0.0516	3.8	0.3165	5.5	0.0445	4.8	0.73	280.8	13.1	279.2	13.4	266.4	87.3	280.8	13.1	-0.5
162	0.0565	8.9	0.4291	11.0	0.0551	6.6	0.58	345.8	22.3	362.5	33.6	471.0	198.0	345.8	22.3	4.6
1	0.0523	5.9	0.4007	10.7	0.0555	8.7	0.84	348.3	29.5	342.2	31.1	300.5	133.4	348.3	29.5	-1.8
355	0.0543	7.3	0.4322	12.3	0.0577	9.9	0.81	361.8	34.7	364.8	37.6	383.8	163.3	361.8	34.7	0.8
153	0.0544	6.3	0.4402	10.4	0.0587	8.2	0.80	367.8	29.4	370.4	32.2	386.7	141.0	367.8	29.4	0.7
131	0.0604	6.9	0.5553	9.7	0.0667	6.8	0.70	416.3	27.5	448.5	35.0	616.8	148.4	416.3	27.5	7.2
379	0.0566	4.5	0.5357	12.6	0.0686	11.8	0.93	427.7	48.8	435.6	44.7	477.2	99.6	427.7	48.8	1.8
124	0.0630	12.6	0.6060	19.0	0.0698	14.3	0.75	434.7	60.0	481.0	72.9	708.6	268.0	434.7	60.0	9.6
205	0.0554	8.4	0.5330	13.6	0.0698	11.0	0.79	434.9	46.3	433.8	48.0	428.0	186.4	434.9	46.3	-0.3
178	0.0559	7.7	0.5423	12.6	0.0703	11.1	0.80	438.1	47.1	439.9	45.0	449.7	170.9	438.1	47.1	0.4
233	0.0591	5.0	0.5836	7.4	0.0716	5.5	0.73	445.8	23.6	466.8	27.5	571.7	108.6	445.8	23.6	4.5
151	0.0547	8.3	0.5459	11.9	0.0724	8.5	0.72	450.5	37.0	442.3	42.8	400.2	186.5	450.5	37.0	-1.8
53	0.0567	3.9	0.5682	4.9	0.0727	3.1	0.61	452.3	13.4	456.8	17.9	479.5	85.4	452.3	13.4	1.0
285	0.0562	6.3	0.5641	9.2	0.0728	6.7	0.73	453.0	29.5	454.2	33.8	460.4	140.5	453.0	29.5	0.3
115	0.0560	4.4	0.5632	5.2	0.0729	2.9	0.53	453.7	12.5	453.6	19.0	453.0	98.1	453.7	12.5	0.0
305	0.0578	3.7	0.5817	7.6	0.0730	6.1	0.87	454.4	27.0	465.6	28.2	520.9	81.5	454.4	27.0	2.4
281	0.0594	4.0	0.6025	6.0	0.0736	4.4	0.75	457.6	19.4	478.8	22.9	581.7	86.5	457.6	19.4	4.4
377	0.0594	5.1	0.6129	13.2	0.0748	12.2	0.92	465.3	54.9	485.4	51.1	581.8	110.1	465.3	54.9	4.2
232	0.0572	4.1	0.5899	6.1	0.0748	4.7	0.74	465.3	20.9	470.8	23.1	497.8	90.4	465.3	20.9	1.2
67	0.0549	5.8	0.5701	7.3	0.0753	4.0	0.62	467.7	18.2	458.1	27.0	410.0	129.2	467.7	18.2	-2.1
220	0.0585	8.3	0.6090	12.6	0.0755	9.7	0.76	469.1	43.7	482.9	48.5	549.2	180.4	469.1	43.7	2.9
240	0.0582	3.8	0.6087	6.7	0.0759	5.5	0.82	471.6	25.0	482.7	25.6	535.7	82.5	471.6	25.0	2.3
16	0.0555	5.8	0.5818	7.9	0.0761	5.6	0.68	472.6	25.4	465.6	29.6	431.4	129.2	472.6	25.4	-1.5
356	0.0610	8.6	0.6518	14.0	0.0775	11.1	0.79	481.0	51.3	509.6	56.3	639.9	185.0	481.0	51.3	5.6
2	0.0546	6.4	0.5955	11.4	0.0791	9.1	0.83	490.5	43.2	474.4	43.2	397.3	143.6	490.5	43.2	-3.4
216	0.0577	11.9	0.6340	17.7	0.0797	13.2	0.74	494.5	63.0	498.6	69.7	517.6	261.9	494.5	63.0	0.8
215	0.0585	5.0	0.6459	8.6	0.0800	7.3	0.81	496.4	34.9	506.0	34.1	549.6	109.8	496.4	34.9	1.9
144	0.0617	5.4	0.6851	6.9	0.0805	4.1	0.62	499.0	19.5	529.8	28.6	665.0	116.0	499.0	19.5	5.8
251	0.0599	10.6	0.6711	16.6	0.0812	12.8	0.77	503.4	62.1	521.4	68.0	601.0	230.0	503.4	62.1	3.5
283	0.0580	6.3	0.6533	9.6	0.0817	7.2	0.75	506.4	35.0	510.5	38.6	529.0	138.6	506.4	35.0	0.8
7	0.0600	6.3	0.6784	11.2	0.0820	8.9	0.83	508.3	43.4	525.8	46.0	602.6	136.0	508.3	43.4	3.3
321	0.0587	5.0	0.6642	15.5	0.0821	14.1	0.95	508.9	69.0	517.2	62.7	554.3	108.3	508.9	69.0	1.6
157	0.0631	6.1	0.7154	7.8	0.0823	4.3	0.64	509.6	21.2	548.0	33.2	710.7	128.8	509.6	21.2	7.0
59	0.0596	4.4	0.6789	5.6	0.0826	2.8	0.64	511.8	13.9	526.1	23.0	588.7	95.2	511.8	13.9	2.7
50	0.0589	6.5	0.6774	8.9	0.0834	6.1	0.68	516.4	30.5	525.2	36.7	563.8	142.0	516.4	30.5	1.7
210	0.0617	4.5	0.7117	9.7	0.0837	9.1	0.89	518.3	45.1	545.7	40.9	662.1	95.9	518.3	45.1	5.0
137	0.0573	8.7	0.6624	12.2	0.0839	8.5	0.70	519.3	42.7	516.1	49.3	501.8	191.0	519.3	42.7	-0.6
27	0.0610	4.3	0.7101	5.4	0.0844	3.5	0.62	522.6	17.8	544.8	22.8	638.8	91.6	522.6	17.8	4.1
376	0.0598	5.7	0.6962	12.9	0.0845	11.6	0.90	522.6	58.3	536.5	53.8	596.0	122.5	522.6	58.3	2.6
135	0.0572	5.6	0.6721	7.3	0.0852	4.6	0.64	527.2	23.5	522.0	29.8	499.4	123.8	527.2	23.5	-1.0
20	0.0554	5.5	0.6536	7.0	0.0855	4.5	0.62	529.0	22.9	510.7	27.9	429.8	121.9	529.0	22.9	-3.6
62	0.0665	8.4	0.7844	12.9	0.0855	9.5	0.76	529.0	48.3	588.0	57.6	822.7	175.1	529.0	48.3	10.0
271	0.0588	10.0	0.6946	15.0	0.0856	11.2	0.75	529.5	56.9	535.6	62.5	561.3	216.9	529.5	56.9	1.1
79	0.0562	8.9	0.6673	12.6	0.0861	9.1	0.71	532.2	46.5	519.0	51.1	461.5	197.2	532.2	46.5	-2.5
12	0.0592	10.8	0.7102	13.9	0.0870	8.9	0.63	537.9	46.1	544.8	58.8	574.1	234.4	537.9	46.1	1.3
105	0.0623	5.9	0.7492	9.2	0.0872	7.1	0.77	538.8	36.7	567.8	39.8	685.6	125.5	538.8	36.7	5.1
252	0.0586	5.9	0.7078	10.5	0.0876	8.7	0.83	541.5	45.3	543.4	44.4	551.5	129.7	541.5	45.3	0.4
30	0.0580	14.6	0.7023	20.9	0.0879	15.0	0.72	542.9	78.1	540.2	87.7	528.6	319.4	542.9	78.1	-0.5
84	0.0599	12.2	0.7257	17.0	0.0879	12.0	0.69	542.9	62.6	554.0	72.8	599.8	265.0	542.9	62.6	2.0
235	0.0617	5.3	0.7529	9.2	0.0885	7.5	0.81	546.5	39.1	569.9	40.1	664.5	114.2	546.5	39.1	4.1
274	0.0579	3.8	0.7106	7.2	0.0890	6.0	0.85	549.6	31.8	545.1	30.2	526.3	82.8	549.6	31.8	-0.8
174	0.0569	8.0	0.7012	12.4	0.0893	10.6	0.77	551.5	56.2	539.5	51.9	489.4	177.3	551.5	56.2	-2.2
307	0.0602	3.0	0.7440	7.1	0.0896	5.9	0.91	553.1	31.4	564.7	30.6	611.6	65.6	553.1	31.4	2.1
150	0.0574	8.3	0.7148	11.8	0.0903	8.3	0.71	557.4	44.2	547.6	49.8	506.8	183.2	557.4	44.2	-1.8
231	0.0598	4.8	0.7458	7.2	0.0905	5.5	0.74	558.3	29.2	565.8	31.4	596.1	104.8	558.3	29.2	1.3
272	0.0597	6.4	0.7447	10.3	0.0905	8.0	0.78	558.7	43.0	565.1	44.8	591.0	139.8	558.7	43.0	1.1
358	0.0643	4.1	0.8058	8.2	0.0908	7.0	0.86	560.6	37.8	600.1	37.2	752.4	87.2	560.6	37.8	6.6
32	0.0597	5.8	0.7491	7.5	0.0910	4.7	0.63	561.3	25.3	567.7	32.6	593.2	126.8	561.3	25.3	1.1
353	0.0710	9.1	0.8923	16.8	0.0912	14.4	0.84	562.5	77.7	647.6	80.7	956.8	186.8	562.5	77.7	13.1
65	0.0565	6.3	0.7199	8.5	0.0924	5.5	0.68	569.6	30.0	550.6	36.3	472.8	139.1	569.6	30.0	-3.4

Table A4.5 (continued): Detrital Zircon U-Pb Integrated Data for the Quilque Formation

Spot	Ratios							Ages (Ma)						Disc. (%)		
	207Pb/206Pb		207Pb/235U		206Pb/238U		Rho	206Pb/238U		207Pb/235U		207Pb/206Pb			Best Age	
	±2σ	±2σ	±2σ	±2σ	±2σ	±2σ		±2σ	±2σ	±2σ	±2σ					
<i>Quilque Formation (20150519-03) Rejected Data</i>																
156	0.0821	7.4	1.5513	10.6	0.1370	7.2	0.72	827.8	56.2	951.0	65.7	1248.0	144.4	827.8	56.2	33.7
293	0.0779	5.6	1.5909	8.5	0.1482	6.3	0.75	890.8	52.1	966.7	52.8	1143.4	110.6	890.8	52.1	22.1
80	0.0694	18.0	1.6821	25.8	0.1759	18.6	0.72	1044.4	179.3	1001.8	165.5	909.6	370.0	909.6	370.0	-14.8
261	0.0812	3.8	1.7208	8.8	0.1537	7.4	0.91	921.6	63.5	1016.3	56.6	1226.5	73.8	921.6	63.5	24.9
89	0.0689	5.1	1.5862	5.5	0.1670	3.6	0.44	995.4	32.8	964.8	34.5	895.7	105.0	995.4	32.8	-11.1
391	0.0724	12.4	1.9294	19.1	0.1933	15.2	0.76	1139.2	158.9	1091.3	128.1	997.0	251.2	997.0	251.2	-14.3
11	0.0776	15.5	2.3507	21.7	0.2198	15.1	0.70	1281.1	175.8	1227.8	155.4	1135.4	307.9	1135.4	307.9	-12.8
381	0.0781	3.6	2.3374	12.2	0.2170	11.6	0.95	1266.1	133.5	1223.7	86.7	1149.8	72.5	1149.8	72.5	-10.1
234	0.0810	16.8	1.8804	25.0	0.1684	18.5	0.74	1003.0	172.0	1074.2	167.2	1221.7	330.1	1221.7	330.1	17.9
44	0.0838	16.1	1.9836	22.7	0.1716	16.0	0.71	1020.9	151.1	1109.9	154.2	1288.9	312.5	1288.9	312.5	20.8
6	0.0905	13.0	2.3256	21.2	0.1863	16.5	0.79	1101.2	167.1	1220.1	151.6	1437.0	248.1	1437.0	248.1	23.4
132	0.1029	4.0	3.1159	8.9	0.2197	8.0	0.89	1280.0	93.1	1436.6	68.6	1676.8	73.7	1676.8	73.7	23.7
75	0.1029	5.4	2.8435	12.3	0.2003	11.2	0.90	1177.2	120.5	1367.1	92.8	1677.7	100.1	1677.7	100.1	29.8
56	0.1038	15.4	4.3430	21.9	0.3035	15.7	0.71	1708.4	235.1	1701.6	182.8	1693.2	283.2	1693.2	283.2	-0.9
148	0.1046	9.8	2.8719	13.9	0.1991	9.7	0.70	1170.3	103.4	1374.6	104.7	1707.9	181.1	1707.9	181.1	31.5
303	0.1058	3.8	2.6684	8.5	0.1830	7.2	0.90	1083.2	72.2	1319.7	62.7	1727.8	69.6	1727.8	69.6	37.3
71	0.1084	17.0	4.6496	25.0	0.3112	18.3	0.73	1746.6	280.7	1758.2	211.7	1772.1	310.3	1772.1	310.3	1.4
34	0.1085	11.8	3.0003	23.1	0.2005	19.9	0.86	1177.9	214.5	1407.7	177.9	1775.1	214.7	1775.1	214.7	33.6
390	0.1094	24.9	4.4060	34.5	0.2922	24.3	0.69	1652.4	353.9	1713.5	293.0	1788.9	453.6	1788.9	453.6	7.6
127	0.1167	5.6	3.8825	8.9	0.2413	7.0	0.78	1393.3	87.5	1610.1	71.8	1906.4	100.2	1906.4	100.2	26.9
55	0.1264	5.0	4.8286	10.9	0.2771	9.7	0.89	1576.5	136.1	1789.9	91.9	2048.5	88.4	2048.5	88.4	23.0
347	0.1822	8.2	9.1822	20.4	0.3654	19.4	0.92	2007.8	334.1	2356.3	188.8	2673.4	135.2	2673.4	135.2	24.9
357	0.2598	7.2	17.5638	11.9	0.4902	9.4	0.79	2571.6	199.8	2966.1	114.8	3245.8	113.9	3245.8	113.9	20.8

Table A4.6: Detrital Zircon U-Pb Integrated Data for the Kayra Formation

Spot	Ratios						Rho	Ages (Ma)						Disc. (%)		
	207Pb/ 206Pb	±2σ	207Pb/ 235U	±2σ	206Pb/ 238U	±2σ		206Pb/ 238U	±2σ	207Pb/ 235U	±2σ	207Pb/ 206Pb	±2σ		Best Age	±2σ
<i>Kayra Formation (20150520-01) Accepted Data</i>																
25	0.0488	16.4	0.0430	17.3	0.0064	5.6	0.32	41.1	2.3	42.8	7.3	136.1	386.3	41.1	2.3	3.8
8	0.0671	15.1	0.0609	18.4	0.0066	10.5	0.57	42.3	4.4	60.0	10.7	840.9	315.2	42.3	4.4	29.5
100	0.0501	16.9	0.0456	17.8	0.0066	5.4	0.31	42.5	2.3	45.3	7.9	198.0	393.7	42.5	2.3	6.3
10	0.0574	19.1	0.0527	19.8	0.0067	5.3	0.27	42.8	2.2	52.1	10.0	506.8	419.3	42.8	2.2	18.0
174	0.0752	27.3	0.0690	28.7	0.0067	8.9	0.31	42.8	3.8	67.8	18.8	1073.6	547.4	42.8	3.8	36.9
6	0.0430	17.2	0.0396	18.6	0.0067	6.9	0.37	42.9	3.0	39.4	7.2	-169.9	429.2	42.9	3.0	-8.9
56	0.0503	22.5	0.0465	23.3	0.0067	6.2	0.26	43.1	2.7	46.1	10.5	207.9	521.7	43.1	2.7	6.6
15	0.0540	16.9	0.0499	18.1	0.0067	6.6	0.36	43.1	2.8	49.5	8.7	369.1	380.1	43.1	2.8	12.8
309	0.0582	13.1	0.0540	14.5	0.0067	6.7	0.43	43.2	2.9	53.4	7.5	537.2	286.0	43.2	2.9	19.0
11	0.0510	26.7	0.0474	27.7	0.0067	7.3	0.26	43.3	3.2	47.0	12.7	240.3	615.3	43.3	3.2	7.9
69	0.0598	36.2	0.0557	36.9	0.0067	7.4	0.20	43.3	3.2	55.0	19.8	597.7	784.2	43.3	3.2	21.2
107	0.0505	12.0	0.0471	13.0	0.0068	4.8	0.38	43.5	2.1	46.8	5.9	216.9	278.8	43.5	2.1	7.0
201	0.0525	14.5	0.0491	17.3	0.0068	9.4	0.54	43.5	4.1	48.7	8.2	308.9	331.2	43.5	4.1	10.5
94	0.0500	25.9	0.0468	27.0	0.0068	7.6	0.29	43.6	3.3	46.4	12.2	194.5	601.1	43.6	3.3	6.1
21	0.0519	13.5	0.0486	14.0	0.0068	4.0	0.27	43.6	1.8	48.2	6.6	281.1	308.5	43.6	1.8	9.5
282	0.0754	21.8	0.0708	23.4	0.0068	8.5	0.36	43.8	3.7	69.5	15.7	1078.6	437.5	43.8	3.7	37.0
29	0.0627	18.4	0.0590	19.4	0.0068	6.1	0.31	43.9	2.7	58.2	11.0	697.0	391.7	43.9	2.7	24.6
381	0.0527	14.2	0.0499	15.4	0.0069	6.1	0.40	44.1	2.7	49.4	7.5	315.3	322.5	44.1	2.7	10.7
226	0.0536	21.4	0.0508	22.2	0.0069	5.8	0.26	44.1	2.5	50.3	10.9	353.1	484.2	44.1	2.5	12.2
31	0.0602	25.0	0.0571	27.4	0.0069	11.2	0.41	44.2	4.9	56.4	15.0	611.0	540.6	44.2	4.9	21.6
38	0.0441	22.2	0.0418	22.8	0.0069	5.6	0.23	44.2	2.4	41.6	9.3	-107.3	545.6	44.2	2.4	-6.3
314	0.0622	9.9	0.0590	11.9	0.0069	7.2	0.55	44.2	3.2	58.2	6.7	680.5	211.9	44.2	3.2	24.1
136	0.0552	19.7	0.0524	22.4	0.0069	10.5	0.48	44.2	4.6	51.9	11.3	421.4	440.3	44.2	4.6	14.8
303	0.0612	11.6	0.0582	12.5	0.0069	5.0	0.38	44.3	2.2	57.4	7.0	647.9	249.1	44.3	2.2	22.9
383	0.0544	13.8	0.0517	15.1	0.0069	5.9	0.39	44.3	2.6	51.2	7.5	389.1	310.6	44.3	2.6	13.5
225	0.0673	14.5	0.0640	15.4	0.0069	5.5	0.35	44.3	2.4	63.0	9.4	847.8	301.2	44.3	2.4	29.7
58	0.0566	12.1	0.0538	13.1	0.0069	5.2	0.38	44.3	2.3	53.2	6.8	474.3	267.7	44.3	2.3	16.7
121	0.0529	11.9	0.0503	13.1	0.0069	5.3	0.42	44.3	2.3	49.8	6.4	323.6	269.4	44.3	2.3	11.1
254	0.0627	16.2	0.0533	17.3	0.0069	6.2	0.36	44.3	2.7	52.8	8.9	455.9	358.7	44.3	2.7	16.0
235	0.0514	13.4	0.0490	14.5	0.0069	5.8	0.39	44.4	2.6	48.5	6.9	257.0	307.3	44.4	2.6	8.5
71	0.0568	20.1	0.0542	21.3	0.0069	7.1	0.33	44.4	3.2	53.6	11.1	484.6	444.1	44.4	3.2	17.1
358	0.0508	8.2	0.0485	9.7	0.0069	6.0	0.54	44.5	2.7	48.1	4.6	231.5	188.8	44.5	2.7	7.5
19	0.0565	13.9	0.0539	14.9	0.0069	5.5	0.36	44.5	2.4	53.4	7.7	470.5	307.2	44.5	2.4	16.6
376	0.0522	12.5	0.0499	13.5	0.0069	5.2	0.39	44.5	2.3	49.4	6.5	294.1	284.6	44.5	2.3	9.9
171	0.0622	14.1	0.0595	15.2	0.0069	5.6	0.38	44.6	2.5	58.7	8.7	682.1	300.9	44.6	2.5	24.1
114	0.0489	12.2	0.0469	13.1	0.0069	4.7	0.36	44.6	2.1	46.5	6.0	144.6	287.0	44.6	2.1	4.0
103	0.0533	15.2	0.0510	16.5	0.0070	6.5	0.40	44.7	2.9	50.6	8.2	339.5	344.0	44.7	2.9	11.6
316	0.0511	18.5	0.0491	19.3	0.0070	6.3	0.29	44.8	2.8	48.7	9.2	247.1	426.6	44.8	2.8	8.1
93	0.0647	20.1	0.0622	21.4	0.0070	7.3	0.34	44.8	3.2	61.2	12.7	763.8	424.4	44.8	3.2	26.9
41	0.0630	15.6	0.0606	16.6	0.0070	5.8	0.34	44.8	2.6	59.7	9.6	708.7	332.3	44.8	2.6	25.0
30	0.0507	8.4	0.0489	9.2	0.0070	4.0	0.43	44.9	1.8	48.4	4.4	225.0	193.1	44.9	1.8	7.2
261	0.0647	15.7	0.0626	16.8	0.0070	6.2	0.36	45.1	2.8	61.7	10.1	765.2	331.0	45.1	2.8	26.9
258	0.0473	5.1	0.0459	7.1	0.0070	5.0	0.70	45.2	2.2	45.6	3.2	66.3	121.2	45.2	2.2	0.9
98	0.0481	23.3	0.0469	24.3	0.0071	6.9	0.29	45.4	3.1	46.5	11.1	103.2	550.5	45.4	3.1	2.3
164	0.0655	20.5	0.0639	21.7	0.0071	6.8	0.32	45.5	3.1	62.9	13.2	789.0	431.2	45.5	3.1	27.7
361	0.0460	20.4	0.0450	21.3	0.0071	6.8	0.29	45.6	3.1	44.7	9.3	0.0	491.9	45.6	3.1	-2.0
120	0.0555	18.0	0.0543	20.2	0.0071	9.0	0.45	45.6	4.1	53.7	10.6	431.4	401.1	45.6	4.1	15.1
336	0.0537	13.1	0.0527	14.1	0.0071	5.3	0.38	45.7	2.4	52.1	7.2	360.6	294.7	45.7	2.4	12.4
145	0.0609	11.1	0.0597	14.9	0.0071	9.7	0.67	45.7	4.4	58.9	8.5	634.0	239.7	45.7	4.4	22.4
138	0.0582	16.7	0.0572	17.7	0.0071	5.8	0.34	45.7	2.6	56.4	9.7	538.3	365.3	45.7	2.6	19.0
232	0.0404	21.0	0.0397	21.8	0.0071	5.7	0.26	45.8	2.6	39.6	8.4	0.0	506.8	45.8	2.6	-15.7
176	0.0580	17.3	0.0571	21.2	0.0071	12.2	0.58	45.9	5.6	56.4	11.7	530.1	378.9	45.9	5.6	18.7
263	0.0496	15.4	0.0489	16.6	0.0071	6.2	0.36	45.9	2.8	48.4	7.8	175.3	360.2	45.9	2.8	5.2
178	0.0542	9.2	0.0535	11.0	0.0072	5.8	0.54	46.0	2.6	52.9	5.7	380.0	207.0	46.0	2.6	13.1
139	0.0609	14.5	0.0602	15.5	0.0072	5.2	0.35	46.1	2.4	59.4	8.9	636.1	312.4	46.1	2.4	22.4
307	0.0496	10.7	0.0491	11.6	0.0072	5.0	0.39	46.1	2.3	48.6	5.5	177.3	248.7	46.1	2.3	5.3
116	0.0581	13.1	0.0575	14.0	0.0072	5.0	0.35	46.1	2.3	56.8	7.7	534.5	286.4	46.1	2.3	18.8
393	0.0591	10.9	0.0586	13.8	0.0072	8.5	0.62	46.2	3.9	57.8	7.8	570.2	236.7	46.2	3.9	20.1
134	0.0681	16.0	0.0676	17.2	0.0072	6.0	0.36	46.2	2.8	66.4	11.0	873.0	331.8	46.2	2.8	30.4
341	0.0513	17.2	0.0511	19.2	0.0072	8.5	0.45	46.4	3.9	50.6	9.5	253.6	395.6	46.4	3.9	8.3
177	0.0547	16.5	0.0546	19.9	0.0072	11.1	0.56	46.5	5.1	54.0	10.5	400.2	369.1	46.5	5.1	13.9
101	0.0544	20.5	0.0546	21.7	0.0073	7.2	0.33	46.7	3.3	54.0	11.4	389.3	459.7	46.7	3.3	13.4
262	0.0509	15.6	0.0512	16.5	0.0073	5.4	0.32	46.8	2.5	50.7	8.1	236.6	360.7	46.8	2.5	7.6

Table A4.6 (continued): Detrital Zircon U-Pb Integrated Data for the Kayra Formation

Spot	Ratios						Ages (Ma)						Best Age	Disc. (%)		
	207Pb/206Pb		207Pb/235U		206Pb/238U		206Pb/238U		207Pb/235U		207Pb/206Pb					
		$\pm 2\sigma$		$\pm 2\sigma$		$\pm 2\sigma$		$\pm 2\sigma$		$\pm 2\sigma$		$\pm 2\sigma$				
<i>Kayra Formation (20150520-01) Accepted Data</i>																
152	0.0488	18.1	0.0491	18.9	0.0073	5.3	0.29	46.8	2.5	48.7	9.0	140.0	424.0	46.8	2.5	3.8
265	0.0646	14.5	0.0649	16.4	0.0073	8.0	0.47	46.9	3.7	63.9	10.2	760.3	305.0	46.9	3.7	26.7
382	0.0522	11.9	0.0526	12.8	0.0073	4.7	0.37	46.9	2.2	52.0	6.5	294.2	272.2	46.9	2.2	9.8
365	0.0467	14.9	0.0471	16.0	0.0073	6.2	0.36	47.0	2.9	46.7	7.3	33.0	356.5	47.0	2.9	-0.6
266	0.0658	14.1	0.0664	15.0	0.0073	5.2	0.33	47.0	2.4	65.2	9.5	799.3	296.4	47.0	2.4	28.0
372	0.0593	19.0	0.0600	20.8	0.0073	8.4	0.40	47.2	4.0	59.2	11.9	577.6	413.0	47.2	4.0	20.3
142	0.0567	15.1	0.0576	16.5	0.0074	6.6	0.41	47.3	3.1	56.9	9.1	480.6	333.1	47.3	3.1	16.8
397	0.0536	12.1	0.0549	14.1	0.0074	7.2	0.51	47.7	3.4	54.3	7.5	354.6	273.5	47.7	3.4	12.1
250	0.0587	30.9	0.0601	31.9	0.0074	8.0	0.25	47.8	3.8	59.3	18.4	554.5	674.7	47.8	3.8	19.5
389	0.0597	12.0	0.0612	13.5	0.0074	6.1	0.46	47.8	2.9	60.3	7.9	592.8	259.7	47.8	2.9	20.8
217	0.0546	11.1	0.0562	12.3	0.0075	5.5	0.43	47.9	2.6	55.5	6.7	397.9	249.6	47.9	2.6	13.7
299	0.0438	21.3	0.0455	25.8	0.0075	14.7	0.57	48.4	7.1	45.2	11.4	0.0	512.2	48.4	7.1	-7.1
243	0.0658	21.7	0.0687	23.6	0.0076	9.2	0.39	48.7	4.5	67.5	15.4	800.4	455.4	48.7	4.5	27.9
14	0.0734	21.9	0.0768	22.9	0.0076	6.7	0.29	48.7	3.3	75.1	16.6	1024.5	443.6	48.7	3.3	35.1
141	0.0438	16.1	0.0458	18.6	0.0076	9.1	0.49	48.8	4.4	45.5	8.3	0.0	389.3	48.8	4.4	-7.2
196	0.0931	32.2	0.0978	33.7	0.0076	10.0	0.29	48.9	4.9	94.7	30.5	1489.5	609.9	48.9	4.9	48.3
127	0.0531	20.9	0.0561	22.0	0.0077	6.7	0.32	49.2	3.3	55.4	11.9	333.3	474.2	49.2	3.3	11.2
75	0.0500	14.8	0.0532	15.8	0.0077	5.6	0.35	49.5	2.8	52.6	8.1	195.3	344.7	49.5	2.8	5.9
135	0.0700	18.3	0.0747	20.0	0.0077	7.9	0.41	49.7	3.9	73.1	14.1	928.9	374.8	49.7	3.9	32.1
264	0.0601	13.3	0.0645	14.9	0.0078	6.9	0.45	49.9	3.4	63.4	9.1	608.1	287.0	49.9	3.4	21.3
387	0.0571	13.8	0.0622	17.0	0.0079	9.8	0.58	50.8	5.0	61.3	10.1	494.1	304.3	50.8	5.0	17.2
260	0.0606	20.9	0.0676	24.8	0.0081	13.4	0.54	52.0	6.9	66.5	16.0	625.7	451.0	52.0	6.9	21.8
368	0.0526	14.7	0.0599	15.6	0.0083	5.6	0.33	53.1	2.9	59.1	9.0	309.6	335.2	53.1	2.9	10.2
166	0.0651	12.2	0.0747	12.9	0.0083	4.4	0.33	53.5	2.3	73.1	9.1	776.0	255.7	53.5	2.3	26.9
26	0.0479	11.2	0.0630	14.9	0.0095	10.0	0.66	61.2	6.1	62.0	9.0	93.7	264.4	61.2	6.1	1.3
249	0.0481	21.7	0.0640	23.7	0.0097	9.5	0.40	62.0	5.9	63.0	14.5	103.2	513.0	62.0	5.9	1.7
59	0.0485	6.0	0.0659	7.9	0.0098	5.3	0.65	63.2	3.3	64.8	5.0	124.7	142.1	63.2	3.3	2.5
118	0.0592	8.4	0.0808	9.2	0.0099	3.9	0.41	63.5	2.5	78.9	7.0	574.3	181.9	63.5	2.5	19.5
308	0.0609	7.4	0.0837	8.8	0.0100	5.4	0.55	64.0	3.4	81.7	6.9	634.1	159.3	64.0	3.4	21.6
224	0.0476	7.4	0.0655	8.5	0.0100	4.4	0.51	64.1	2.8	64.4	5.3	77.8	175.1	64.1	2.8	0.6
335	0.0513	11.4	0.0708	12.3	0.0100	4.3	0.37	64.2	2.8	69.5	8.2	256.4	262.4	64.2	2.8	7.6
302	0.0508	6.0	0.0703	7.5	0.0100	4.9	0.61	64.4	3.1	69.0	5.0	231.0	138.0	64.4	3.1	6.6
72	0.0509	13.6	0.0705	14.5	0.0100	5.0	0.34	64.4	3.2	69.1	9.7	236.3	313.5	64.4	3.2	6.9
371	0.0582	14.3	0.0823	16.9	0.0103	9.2	0.54	65.8	6.0	80.3	13.1	537.8	311.9	65.8	6.0	18.1
99	0.0527	15.0	0.0753	18.2	0.0104	10.3	0.57	66.4	6.8	73.7	12.9	315.7	340.5	66.4	6.8	9.8
399	0.0614	15.4	0.0883	18.3	0.0104	9.9	0.54	66.9	6.6	85.9	15.1	654.1	330.5	66.9	6.6	22.2
221	0.0476	8.4	0.0686	10.0	0.0104	5.5	0.54	67.0	3.6	67.4	6.5	81.7	199.9	67.0	3.6	0.6
170	0.0487	8.1	0.0704	10.4	0.0105	6.4	0.63	67.2	4.3	69.1	6.9	135.3	189.5	67.2	4.3	2.7
155	0.0511	13.6	0.0739	16.4	0.0105	8.9	0.55	67.2	6.0	72.4	11.4	246.5	314.3	67.2	6.0	7.1
52	0.0525	5.3	0.0760	6.3	0.0105	3.4	0.53	67.3	2.3	74.4	4.5	307.9	121.3	67.3	2.3	9.5
346	0.0519	13.8	0.0758	14.8	0.0106	5.7	0.37	67.9	3.8	74.2	10.6	279.6	314.7	67.9	3.8	8.4
153	0.0580	12.9	0.0857	15.8	0.0107	9.0	0.58	68.7	6.1	83.5	12.7	529.7	283.1	68.7	6.1	17.7
119	0.0491	11.1	0.0726	13.2	0.0107	7.2	0.54	68.8	4.9	71.2	9.1	153.5	258.9	68.8	4.9	3.4
162	0.0514	17.7	0.0771	18.7	0.0109	5.8	0.32	69.7	4.0	75.4	13.6	258.4	407.2	69.7	4.0	7.5
369	0.0510	11.6	0.0783	12.4	0.0111	4.9	0.35	71.3	3.5	76.5	9.2	242.0	268.4	71.3	3.5	6.8
293	0.0653	15.7	0.1046	16.9	0.0116	6.4	0.37	74.5	4.7	101.1	16.3	783.2	329.7	74.5	4.7	26.3
349	0.0641	10.3	0.1041	11.4	0.0118	5.3	0.44	75.5	3.9	100.5	10.9	744.7	216.7	75.5	3.9	24.9
189	0.0708	14.3	0.1158	19.6	0.0119	13.4	0.68	76.1	10.1	111.3	20.6	951.3	293.3	76.1	10.1	31.7
45	0.0502	7.5	0.0829	9.2	0.0120	5.6	0.58	76.7	4.2	80.8	7.2	204.2	174.1	76.7	4.2	5.1
374	0.0492	5.4	0.0815	6.5	0.0120	3.8	0.56	77.0	2.9	79.6	5.0	156.1	125.7	77.0	2.9	3.2
305	0.0493	7.5	0.0819	9.7	0.0120	6.6	0.63	77.2	5.0	79.9	7.5	162.1	176.3	77.2	5.0	3.4
70	0.0516	6.7	0.0863	8.3	0.0121	4.9	0.59	77.8	3.8	84.1	6.7	266.8	154.5	77.8	3.8	7.5
228	0.0598	15.1	0.1014	17.6	0.0123	9.1	0.51	78.7	7.1	98.1	16.5	598.0	328.0	78.7	7.1	19.7
317	0.0586	11.6	0.0996	12.7	0.0123	5.9	0.41	78.9	4.6	96.4	11.6	552.5	252.6	78.9	4.6	18.1
54	0.0489	12.1	0.0839	17.4	0.0124	12.6	0.72	79.7	10.0	81.8	13.7	145.4	283.8	79.7	10.0	2.6
57	0.0534	7.7	0.0919	8.9	0.0125	4.7	0.50	80.0	3.7	89.3	7.6	345.3	174.1	80.0	3.7	10.4
329	0.0595	7.2	0.1031	7.9	0.0126	4.2	0.42	80.5	3.3	99.6	7.5	585.0	155.9	80.5	3.3	19.2
357	0.0466	9.9	0.0816	13.6	0.0127	9.9	0.69	81.3	8.0	79.6	10.4	31.2	236.3	81.3	8.0	-2.0
33	0.0590	10.1	0.1033	11.1	0.0127	4.6	0.41	81.4	3.7	99.8	10.5	566.4	219.9	81.4	3.7	18.5
187	0.0585	10.0	0.1034	13.3	0.0128	8.5	0.66	82.1	6.9	99.9	12.6	549.9	218.3	82.1	6.9	17.9
96	0.0474	12.3	0.0842	14.7	0.0129	8.1	0.55	82.5	6.6	82.1	11.6	71.2	291.6	82.5	6.6	-0.5
133	0.0492	11.3	0.0898	15.8	0.0132	11.0	0.70	84.8	9.3	87.3	13.3	156.6	264.1	84.8	9.3	2.9
65	0.0514	9.0	0.0950	12.0	0.0134	7.9	0.66	85.8	6.8	92.1	10.6	259.0	207.4	85.8	6.8	6.9

Table A4.6 (continued): Detrital Zircon U-Pb Integrated Data for the Kayra Formation

Spot	Ratios						Rho	Ages (Ma)						Disc. (%)		
	207Pb/206Pb		207Pb/235U		206Pb/238U			206Pb/238U		207Pb/235U		207Pb/206Pb			Best Age	
	±2σ		±2σ		±2σ			±2σ		±2σ		±2σ			±2σ	
<i>Kayra Formation (20150520-01) Accepted Data</i>																
129	0.0504	12.2	0.0933	15.2	0.0134	8.9	0.60	85.9	7.6	90.6	13.2	215.6	281.8	85.9	7.6	5.2
280	0.0559	15.0	0.1037	15.8	0.0135	5.1	0.31	86.2	4.4	100.2	15.1	447.4	333.9	86.2	4.4	14.0
359	0.0483	10.0	0.0916	13.7	0.0137	9.8	0.68	88.0	8.6	89.0	11.7	115.2	236.9	88.0	8.6	1.1
394	0.0475	5.5	0.0909	6.6	0.0139	3.5	0.55	88.8	3.1	88.4	5.6	76.5	130.6	88.8	3.1	-0.5
66	0.0538	11.3	0.1032	12.8	0.0139	6.0	0.46	89.0	5.3	99.7	12.1	364.8	254.9	89.0	5.3	10.8
175	0.0577	6.5	0.1112	9.1	0.0140	6.2	0.70	89.5	5.5	107.1	9.3	517.1	142.6	89.5	5.5	16.4
380	0.0493	7.9	0.0960	10.9	0.0141	7.4	0.69	90.4	6.7	93.1	9.7	161.1	184.3	90.4	6.7	2.8
378	0.0466	8.4	0.0923	9.7	0.0144	4.9	0.51	91.9	4.5	89.6	8.3	29.9	200.3	91.9	4.5	-2.5
91	0.0472	11.6	0.0942	16.6	0.0145	11.9	0.72	92.8	11.0	91.4	14.5	57.3	276.0	92.8	11.0	-1.4
148	0.0529	6.8	0.1097	8.1	0.0150	3.9	0.55	96.1	3.7	105.7	8.1	325.9	154.1	96.1	3.7	9.0
340	0.0543	6.7	0.1169	8.3	0.0156	4.8	0.58	99.8	4.7	112.3	8.8	385.5	151.6	99.8	4.7	11.1
179	0.0607	8.7	0.1323	11.6	0.0158	7.5	0.66	101.1	7.6	126.1	13.8	627.6	188.3	101.1	7.6	19.8
289	0.0501	4.3	0.1101	5.5	0.0160	3.9	0.64	102.0	3.9	106.1	5.6	198.3	99.1	102.0	3.9	3.8
9	0.0595	9.5	0.1364	11.8	0.0166	7.0	0.59	106.3	7.4	129.9	14.4	585.5	205.8	106.3	7.4	18.1
188	0.0582	9.6	0.1547	12.1	0.0193	7.2	0.62	123.1	8.8	146.1	16.5	537.2	209.0	123.1	8.8	15.7
32	0.0497	6.9	0.1464	9.4	0.0214	6.4	0.68	136.2	8.6	138.7	12.2	181.8	161.0	136.2	8.6	1.8
64	0.0534	9.0	0.1619	10.3	0.0220	5.0	0.48	140.3	7.0	152.4	14.5	344.3	203.4	140.3	7.0	7.9
168	0.0513	7.4	0.1583	10.0	0.0224	6.8	0.67	142.7	9.6	149.2	13.9	254.0	169.5	142.7	9.6	4.4
7	0.0573	9.3	0.1800	10.9	0.0228	5.7	0.52	145.2	8.2	168.1	16.9	504.2	205.5	145.2	8.2	13.6
370	0.0539	5.9	0.1708	7.2	0.0230	4.5	0.57	146.5	6.5	160.1	10.6	366.3	132.7	146.5	6.5	8.5
337	0.0484	6.2	0.1549	7.7	0.0232	4.5	0.60	148.0	6.5	146.3	10.5	118.0	145.4	148.0	6.5	-1.2
163	0.0540	6.3	0.1783	9.2	0.0239	6.5	0.72	152.4	9.8	166.6	14.1	372.8	142.3	152.4	9.8	8.5
345	0.0633	8.3	0.2153	10.0	0.0247	5.9	0.57	157.1	9.2	198.0	18.0	717.8	175.4	157.1	9.2	20.6
181	0.0579	9.1	0.2212	13.0	0.0277	9.2	0.72	176.3	16.1	202.9	23.9	524.7	198.8	176.3	16.1	13.1
104	0.0483	7.7	0.1863	9.6	0.0280	5.7	0.60	177.8	10.0	173.5	15.3	115.6	180.9	177.8	10.0	-2.5
79	0.0504	13.5	0.2207	18.8	0.0317	13.1	0.69	201.4	26.0	202.5	34.5	214.6	313.3	201.4	26.0	0.5
332	0.0537	4.7	0.2830	6.2	0.0382	4.3	0.65	241.6	10.2	253.0	13.9	360.6	105.9	241.6	10.2	4.5
61	0.0521	4.7	0.2796	5.3	0.0390	2.8	0.46	246.4	6.7	250.3	11.8	287.8	108.2	246.4	6.7	1.6
108	0.0522	3.9	0.2852	5.1	0.0396	3.1	0.64	250.3	7.5	254.8	11.5	295.7	89.8	250.3	7.5	1.7
83	0.0565	8.6	0.3369	10.0	0.0432	5.3	0.51	272.9	14.2	294.8	25.7	472.1	190.1	272.9	14.2	7.4
53	0.0526	5.4	0.3153	7.4	0.0435	5.1	0.68	274.5	13.7	278.3	17.9	310.4	122.6	274.5	13.7	1.4
396	0.0548	6.2	0.3291	8.2	0.0436	5.3	0.66	275.0	14.3	288.9	20.5	403.0	138.1	275.0	14.3	4.8
319	0.0536	7.6	0.3280	9.9	0.0443	7.0	0.64	279.7	19.1	288.1	24.7	356.3	171.2	279.7	19.1	2.9
60	0.0587	4.9	0.3746	5.6	0.0463	3.0	0.49	291.5	8.7	323.1	15.6	557.4	107.2	291.5	8.7	9.8
230	0.0530	5.5	0.3866	7.6	0.0529	5.3	0.69	332.4	17.3	331.9	21.6	328.4	124.6	332.4	17.3	-0.2
190	0.0539	5.1	0.4009	8.2	0.0539	6.5	0.78	338.6	21.4	342.3	23.7	367.4	114.6	338.6	21.4	1.1
191	0.0537	9.3	0.4037	14.0	0.0545	10.5	0.75	342.0	35.1	344.3	40.8	360.0	209.1	342.0	35.1	0.7
151	0.0543	4.2	0.4717	6.0	0.0630	4.0	0.71	393.7	15.2	392.4	19.5	384.6	94.8	393.7	15.2	-0.3
97	0.0571	5.3	0.5450	6.9	0.0692	4.3	0.64	431.4	17.8	441.7	24.7	495.7	116.9	431.4	17.8	2.3
216	0.0572	4.1	0.5781	5.5	0.0734	3.9	0.66	456.3	17.0	463.2	20.4	497.5	91.1	456.3	17.0	1.5
204	0.0563	6.6	0.5925	9.9	0.0763	7.4	0.74	474.2	34.0	472.4	37.4	463.8	146.7	474.2	34.0	-0.4
34	0.0596	7.1	0.6278	8.5	0.0764	4.8	0.55	474.4	21.9	494.7	33.2	590.1	153.8	474.4	21.9	4.1
385	0.0561	9.7	0.5926	13.8	0.0766	9.9	0.72	475.8	45.3	472.5	52.3	456.9	214.1	475.8	45.3	-0.7
87	0.0574	4.0	0.6166	5.4	0.0779	3.8	0.68	483.6	17.9	487.7	20.8	507.3	87.3	483.6	17.9	0.9
273	0.0839	9.3	0.9072	12.7	0.0784	8.7	0.68	486.6	40.9	655.6	61.2	1290.8	180.8	486.6	40.9	25.8
50	0.0688	9.7	0.7494	10.5	0.0790	4.3	0.39	490.4	20.5	567.9	45.9	891.8	200.5	490.4	20.5	13.6
325	0.0598	4.3	0.6546	5.8	0.0794	4.7	0.67	492.7	22.2	511.3	23.2	595.4	94.1	492.7	22.2	3.6
143	0.0575	4.4	0.6356	5.7	0.0802	3.3	0.62	497.2	15.6	499.6	22.3	510.3	97.2	497.2	15.6	0.5
185	0.0595	3.2	0.6593	6.7	0.0804	5.5	0.88	498.6	26.2	514.2	27.0	584.1	70.4	498.6	26.2	3.0
213	0.0579	6.4	0.6702	8.9	0.0840	6.3	0.70	520.0	31.7	520.8	36.4	524.4	139.7	520.0	31.7	0.2
259	0.0681	9.2	0.7980	12.4	0.0850	8.2	0.66	525.8	41.4	595.7	55.8	871.7	191.4	525.8	41.4	11.7
43	0.0601	7.9	0.7074	11.3	0.0853	8.3	0.72	527.7	41.8	543.2	47.6	608.8	170.7	527.7	41.8	2.9
28	0.0579	3.6	0.6814	4.9	0.0854	3.5	0.68	528.2	17.6	527.6	20.3	525.1	79.9	528.2	17.6	-0.1
46	0.0606	4.9	0.7196	5.9	0.0861	3.5	0.56	532.5	18.0	550.5	24.9	625.3	105.3	532.5	18.0	3.3
286	0.0585	6.4	0.7004	9.3	0.0868	7.0	0.73	536.6	36.0	539.0	38.9	549.2	138.9	536.6	36.0	0.4
330	0.0605	10.1	0.7273	14.0	0.0872	9.9	0.70	539.0	51.1	555.0	60.0	621.1	216.9	539.0	51.1	2.9
3	0.0594	5.5	0.7229	8.1	0.0882	5.9	0.73	544.9	30.8	552.4	34.4	583.2	119.7	544.9	30.8	1.3
350	0.0568	8.9	0.6920	12.6	0.0884	9.1	0.71	545.9	47.5	534.0	52.4	483.4	196.4	545.9	47.5	-2.2
237	0.0593	4.2	0.7287	6.5	0.0891	5.1	0.76	550.3	26.7	555.8	27.8	578.4	91.1	550.3	26.7	1.0
296	0.0633	3.8	0.7834	4.7	0.0898	2.8	0.60	554.4	15.1	587.4	21.1	717.2	80.0	554.4	15.1	5.6
40	0.0591	5.3	0.7325	5.8	0.0899	2.8	0.43	555.2	15.1	558.0	25.1	569.5	115.0	555.2	15.1	0.5
327	0.0758	6.6	0.9449	7.6	0.0905	4.6	0.50	558.2	24.6	675.4	37.3	1088.7	131.9	558.2	24.6	17.4
267	0.0582	5.2	0.7302	7.3	0.0910	5.4	0.70	561.3	28.8	556.7	31.5	538.0	114.5	561.3	28.8	-0.8

Table A4.6 (continued): Detrital Zircon U-Pb Integrated Data for the Kayra Formation

Spot	Ratios						Rho	Ages (Ma)						Best Age	Disc. (%)	
	207Pb/206Pb	±2σ	207Pb/235U	±2σ	206Pb/238U	±2σ		206Pb/238U	±2σ	207Pb/235U	±2σ	207Pb/206Pb	±2σ			
	<i>Kayra Formation (20150520-01) Accepted Data</i>															
86	0.0778	14.2	1.8231	19.6	0.1699	13.6	0.69	1011.6	127.2	1053.8	129.2	1142.4	281.9	1142.4	281.9	11.5
209	0.0784	9.2	2.2556	13.2	0.2087	9.5	0.72	1222.1	106.2	1198.5	93.3	1156.3	183.3	1156.3	183.3	-5.7
125	0.0796	6.1	2.3785	8.7	0.2169	5.9	0.72	1265.2	67.6	1236.2	62.1	1185.9	119.9	1185.9	119.9	-6.7
160	0.0798	5.5	1.9542	8.3	0.1776	6.2	0.75	1054.0	59.9	1099.9	56.1	1191.8	108.4	1191.8	108.4	11.6
270	0.0801	4.8	2.1193	6.7	0.1919	4.8	0.69	1131.9	50.2	1155.1	46.2	1198.9	95.5	1198.9	95.5	5.6
13	0.0801	3.5	2.1642	4.9	0.1959	3.6	0.70	1153.4	37.8	1169.6	34.2	1199.8	69.4	1199.8	69.4	3.9
117	0.0802	5.7	2.0060	8.0	0.1814	5.7	0.71	1074.6	56.9	1117.5	54.3	1202.1	111.6	1202.1	111.6	10.6
76	0.0804	5.3	2.1763	7.2	0.1963	5.0	0.68	1153.3	52.9	1173.5	50.2	1207.2	103.9	1207.2	103.9	4.3
395	0.0806	7.8	2.0412	11.2	0.1838	8.0	0.72	1087.5	80.1	1129.4	76.5	1210.7	153.9	1210.7	153.9	10.2
364	0.0806	3.9	2.3627	8.0	0.2125	7.5	0.88	1242.0	85.0	1231.4	57.2	1212.8	76.0	1212.8	76.0	-2.4
292	0.0808	4.4	2.3145	6.2	0.2077	4.5	0.71	1216.3	49.7	1216.7	43.7	1217.5	85.9	1217.5	85.9	0.1
55	0.0809	4.1	2.2830	6.1	0.2046	4.7	0.73	1199.9	51.2	1207.1	43.2	1219.9	81.5	1219.9	81.5	1.6
268	0.0813	10.6	1.9059	15.1	0.1700	10.8	0.71	1012.2	101.3	1083.2	100.7	1228.8	208.3	1228.8	208.3	17.6
252	0.0813	6.7	2.3626	9.8	0.2107	7.2	0.73	1232.7	80.6	1231.4	70.2	1228.9	131.8	1228.9	131.8	-0.3
172	0.0836	4.6	2.3741	7.5	0.2059	5.9	0.79	1206.7	64.6	1234.8	53.8	1284.3	89.2	1284.3	89.2	6.0
49	0.0837	3.8	2.3703	5.6	0.2054	4.4	0.73	1204.5	47.8	1233.7	40.2	1285.1	74.7	1285.1	74.7	6.3
42	0.0843	4.3	2.3201	6.1	0.1997	4.6	0.71	1173.6	49.4	1218.5	43.5	1298.7	84.1	1298.7	84.1	9.6
173	0.0868	8.5	2.7418	15.1	0.2292	12.4	0.83	1330.2	149.5	1339.9	112.8	1355.3	164.1	1355.3	164.1	1.8
203	0.0870	3.0	2.8164	5.4	0.2348	4.6	0.83	1359.5	56.6	1359.9	40.7	1360.5	58.2	1360.5	58.2	0.1
81	0.0882	5.2	2.9798	7.8	0.2451	5.9	0.75	1413.2	74.8	1402.5	59.2	1386.2	99.4	1386.2	99.4	-1.9
4	0.0884	2.9	2.6499	4.5	0.2174	3.4	0.76	1268.3	39.4	1314.6	33.1	1390.9	56.1	1390.9	56.1	8.8
233	0.0889	10.9	2.8340	15.3	0.2311	10.8	0.71	1340.3	131.2	1364.6	115.5	1402.7	208.1	1402.7	208.1	4.4
240	0.0895	5.5	3.0407	8.0	0.2464	5.9	0.73	1419.9	75.3	1417.9	61.5	1414.8	105.4	1414.8	105.4	-0.4
111	0.0904	9.3	3.1303	13.5	0.2510	9.8	0.73	1443.7	126.9	1440.2	104.5	1435.0	177.3	1435.0	177.3	-0.6
218	0.0906	3.9	2.8118	5.6	0.2251	4.3	0.73	1308.6	51.0	1358.7	42.1	1438.4	73.9	1438.4	73.9	9.0
238	0.0973	3.0	2.9523	4.4	0.2200	3.3	0.72	1281.7	38.7	1395.4	33.2	1573.8	57.1	1573.8	57.1	18.6
274	0.0974	3.0	3.5227	4.6	0.2624	3.8	0.75	1502.1	50.6	1532.3	36.2	1574.3	56.9	1574.3	56.9	4.6
140	0.0974	8.8	3.1578	17.3	0.2351	14.8	0.86	1361.1	182.1	1446.9	134.3	1575.3	165.5	1575.3	165.5	13.6
18	0.0989	4.8	3.0789	6.8	0.2258	4.9	0.71	1312.5	58.3	1427.4	52.1	1603.3	89.7	1603.3	89.7	18.1
333	0.0994	7.0	3.4238	10.0	0.2499	7.4	0.72	1437.9	95.3	1509.9	79.1	1612.4	129.9	1612.4	129.9	10.8
132	0.1027	12.5	4.2161	17.6	0.2978	12.3	0.70	1680.3	181.3	1677.2	145.0	1673.3	230.7	1673.3	230.7	-0.4
343	0.1030	3.6	4.2426	5.6	0.2986	4.2	0.76	1684.6	62.3	1682.3	46.1	1679.4	67.0	1679.4	67.0	-0.3
180	0.1058	7.4	4.4843	11.3	0.3074	8.4	0.76	1727.7	127.6	1728.1	93.8	1728.5	135.0	1728.5	135.0	0.0
377	0.1072	6.9	4.7389	9.9	0.3206	7.0	0.72	1792.5	110.3	1774.1	82.9	1752.6	125.4	1752.6	125.4	-2.3
351	0.1129	4.0	5.1694	6.2	0.3320	5.0	0.77	1848.2	80.3	1847.6	52.8	1846.9	72.1	1846.9	72.1	-0.1
342	0.1221	3.0	4.7605	4.9	0.2828	3.8	0.79	1605.6	54.1	1778.0	41.2	1986.7	53.2	1986.7	53.2	19.2
227	0.1234	10.4	5.6834	14.9	0.3339	10.7	0.71	1857.4	172.8	1928.9	129.4	2006.6	185.2	2006.6	185.2	7.4
242	0.1235	12.2	6.0307	18.6	0.3543	14.1	0.76	1955.0	237.6	1980.3	163.4	2006.8	216.3	2006.8	216.3	2.6
373	0.1246	10.0	6.9789	14.2	0.4061	10.2	0.71	2197.3	189.3	2108.7	126.8	2023.4	177.2	2023.4	177.2	-8.6
306	0.1296	4.0	6.7254	5.7	0.3765	4.6	0.71	2059.9	81.3	2076.0	50.2	2091.9	71.0	2091.9	71.0	1.5
291	0.1316	5.4	6.4168	8.2	0.3536	6.2	0.74	1951.6	103.8	2034.6	71.7	2119.7	95.4	2119.7	95.4	7.9
300	0.1366	3.9	7.3759	5.7	0.3917	4.5	0.73	2130.7	82.5	2158.1	51.1	2184.2	67.7	2184.2	67.7	2.4
17	0.1475	6.4	8.6863	9.3	0.4272	6.8	0.73	2293.2	132.0	2305.6	85.2	2316.7	110.2	2316.7	110.2	1.0
156	0.1480	7.7	8.7514	12.0	0.4288	9.1	0.77	2300.5	177.0	2312.4	110.0	2323.0	131.4	2323.0	131.4	1.0
391	0.1539	4.5	9.1047	6.6	0.4291	4.8	0.74	2301.9	93.5	2348.6	60.8	2389.4	76.3	2389.4	76.3	3.7
344	0.1643	3.6	8.4128	5.8	0.3714	4.9	0.78	2035.8	85.3	2276.6	52.9	2500.4	61.1	2500.4	61.1	18.6
229	0.1770	5.7	10.0823	7.9	0.4132	5.5	0.69	2229.5	104.5	2442.4	73.4	2624.7	95.3	2624.7	95.3	15.1
44	0.1790	2.6	10.9260	3.3	0.4427	2.5	0.62	2362.9	48.7	2516.9	31.0	2643.5	43.7	2643.5	43.7	10.6
67	0.1806	10.4	10.9535	14.8	0.4398	10.5	0.71	2349.9	206.6	2519.2	138.4	2658.5	172.8	2658.5	172.8	11.6
331	0.2199	5.1	17.7732	7.3	0.5861	5.4	0.71	2973.6	128.7	2977.5	70.2	2980.2	82.7	2980.2	82.7	0.2
158	0.2391	4.9	16.4453	8.0	0.4989	6.2	0.79	2609.1	132.2	2903.1	76.6	3113.8	77.3	3113.8	77.3	16.2
247	0.2463	5.0	17.3361	9.7	0.5104	8.4	0.86	2658.5	183.3	2953.6	93.6	3161.3	78.8	3161.3	78.8	15.9
290	0.2551	4.9	21.0036	7.8	0.5971	6.2	0.78	3018.0	148.4	3138.8	75.4	3216.9	76.7	3216.9	76.7	6.2
354	0.2859	3.1	23.9298	4.5	0.6071	4.5	0.77	3058.5	109.3	3265.5	44.0	3395.2	47.6	3395.2	47.6	9.9
<i>Kayra Formation (20150520-01) Rejected Data</i>																
222	0.0819	23.1	0.0731	25.1	0.0065	9.9	0.39	41.6	4.1	71.7	17.4	1243.1	453.2	41.6	4.1	41.9
220	0.0665	9.0	0.0601	9.8	0.0066	4.0	0.39	42.1	1.7	59.3	5.6	821.3	187.7	42.1	1.7	28.9
298	0.1038	18.8	0.0946	20.0	0.0066	6.9	0.34	42.4	2.9	91.7	17.5	1693.9	345.7	42.4	2.9	53.7
219	0.0801	13.2	0.0737	14.2	0.0067	5.4	0.37	42.9	2.3	72.2	9.9	1198.3	260.3	42.9	2.3	40.6
326	0.0856	13.7	0.0816	14.9	0.0069	6.3	0.38	44.4	2.8	79.6	11.4	1330.0	266.0	44.4	2.8	44.3
184	0.0544	25.9	0.0523	31.6	0.0070	17.9	0.57	44.8	8.0	51.8	15.9	389.7	581.5	44.8	8.0	13.5
390	0.0713	13.3	0.0686	14.3	0.0070	5.1	0.36	44.8	2.3	67.3	9.3	964.8	272.5	44.8	2.3	33.4
51	0.0700	14.7	0.0674	15.7	0.0070	5.7	0.35	44.9	2.6	66.2	10.1	927.5	302.4	44.9	2.6	32.2

Table A4.6 (continued): Detrital Zircon U-Pb Integrated Data for the Kayra Formation

Spot	Ratios						Ages (Ma)						Best Age	Disc. (%)		
	207Pb/206Pb		207Pb/235U		206Pb/238U		206Pb/238U		207Pb/235U		207Pb/206Pb				±2σ	
	±2σ	±2σ	±2σ	±2σ	±2σ	±2σ	±2σ	±2σ	±2σ	±2σ						
<i>Kayra Formation (20150520-01) Rejected Data</i>																
12	0.1201	14.7	0.1158	16.3	0.0070	7.3	0.44	44.9	3.3	111.3	17.2	1958.3	261.6	44.9	3.3	59.6
144	0.0756	20.2	0.0731	21.9	0.0070	8.2	0.39	45.0	3.7	71.6	15.1	1083.7	405.1	45.0	3.7	37.1
74	0.0780	9.9	0.0768	11.0	0.0071	4.7	0.43	45.9	2.2	75.1	7.9	1147.1	197.0	45.9	2.2	39.0
202	0.0748	16.3	0.0737	17.6	0.0071	6.6	0.37	45.9	3.0	72.2	12.2	1063.0	327.6	45.9	3.0	36.4
276	0.0652	16.6	0.0643	22.8	0.0072	15.7	0.69	45.9	7.2	63.3	14.0	782.3	348.0	45.9	7.2	27.4
312	0.0587	20.3	0.0580	26.6	0.0072	17.4	0.65	46.0	8.0	57.3	14.8	556.6	442.4	46.0	8.0	19.6
334	0.0769	13.8	0.0767	14.9	0.0072	5.8	0.38	46.5	2.7	75.0	10.8	1118.2	274.5	46.5	2.7	38.1
392	0.0545	15.3	0.0543	22.0	0.0072	15.8	0.72	46.5	7.3	53.7	11.5	389.9	342.9	46.5	7.3	13.5
313	0.0876	14.7	0.0877	15.7	0.0073	6.1	0.36	46.6	2.8	85.4	12.9	1374.1	282.4	46.6	2.8	45.4
323	0.0876	10.7	0.0878	11.6	0.0073	4.9	0.39	46.7	2.3	85.5	9.5	1374.3	206.4	46.7	2.3	45.4
321	0.0736	14.7	0.0742	15.8	0.0073	6.0	0.36	47.0	2.8	72.7	11.1	1030.3	297.7	47.0	2.8	35.4
379	0.0961	16.9	0.0971	18.1	0.0073	6.4	0.36	47.1	3.0	94.1	16.2	1548.9	316.6	47.1	3.0	50.0
206	0.0714	10.0	0.0726	11.0	0.0074	4.6	0.41	47.4	2.2	71.2	7.5	968.4	204.0	47.4	2.2	33.4
322	0.0930	16.1	0.0963	17.1	0.0075	6.1	0.34	48.2	2.9	93.3	15.3	1488.6	305.3	48.2	2.9	48.4
27	0.0739	19.8	0.0768	20.6	0.0075	5.8	0.28	48.4	2.8	75.1	14.9	1039.2	398.8	48.4	2.8	35.6
123	0.1097	10.1	0.1147	11.5	0.0076	5.2	0.47	48.7	2.5	110.2	12.0	1794.1	183.9	48.7	2.5	55.8
35	0.1083	25.2	0.1138	26.9	0.0076	9.7	0.36	49.0	4.7	109.5	28.0	1770.6	459.4	49.0	4.7	55.3
131	0.1156	10.0	0.1227	12.2	0.0077	6.9	0.58	49.4	3.4	117.5	13.6	1889.8	179.7	49.4	3.4	57.9
212	0.0894	17.1	0.0956	17.8	0.0078	5.0	0.27	49.8	2.5	92.7	15.8	1413.5	327.5	49.8	2.5	46.3
147	0.0919	16.8	0.0983	18.1	0.0078	6.4	0.37	49.8	3.2	95.2	16.4	1466.2	318.8	49.8	3.2	47.7
182	0.0825	16.9	0.0904	19.5	0.0079	9.6	0.50	51.0	4.9	87.8	16.4	1257.5	330.5	51.0	4.9	41.9
375	0.0778	19.5	0.0857	21.0	0.0080	7.9	0.38	51.3	4.1	83.5	16.9	1142.1	387.0	51.3	4.1	38.6
1	0.0891	21.6	0.0991	23.8	0.0081	9.9	0.41	51.8	5.1	96.0	21.8	1405.9	414.5	51.8	5.1	46.0
150	0.0808	23.7	0.0903	25.2	0.0081	8.6	0.35	52.0	4.5	87.8	21.2	1216.1	465.4	52.0	4.5	40.7
102	0.0808	22.2	0.0915	22.9	0.0082	5.3	0.24	52.7	2.8	88.9	19.5	1216.1	437.1	52.7	2.8	40.7
315	0.1700	13.1	0.1945	14.6	0.0083	7.1	0.44	53.3	3.8	180.4	24.2	2557.6	220.0	53.3	3.8	70.5
126	0.1489	14.3	0.1705	16.0	0.0083	6.9	0.45	53.3	3.7	159.9	23.7	2333.2	245.6	53.3	3.7	66.6
231	0.1064	27.2	0.1224	28.2	0.0083	7.3	0.26	53.6	3.9	117.3	31.2	1738.6	499.3	53.6	3.9	54.3
355	0.0843	16.0	0.0983	18.4	0.0085	9.5	0.49	54.3	5.2	95.2	16.7	1299.3	311.5	54.3	5.2	43.0
320	0.2203	11.7	0.2610	12.5	0.0086	4.7	0.35	55.2	2.6	235.5	26.2	2982.6	188.5	55.2	2.6	76.6
23	0.1849	10.9	0.2199	12.6	0.0086	6.5	0.51	55.4	3.6	201.9	23.2	2697.7	179.8	55.4	3.6	72.6
362	0.2218	14.6	0.2648	16.9	0.0087	8.9	0.50	55.6	4.9	238.5	35.9	2993.5	234.8	55.6	4.9	76.7
324	0.2922	10.9	0.3528	12.5	0.0088	6.3	0.48	56.2	3.5	306.8	33.0	3429.2	169.9	56.2	3.5	81.7
279	0.1768	19.6	0.2302	21.3	0.0094	8.4	0.39	60.6	5.1	210.4	40.4	2623.1	326.0	60.6	5.1	71.2
130	0.0767	17.2	0.1023	19.0	0.0097	8.0	0.43	62.1	4.9	98.9	17.9	1113.4	342.5	62.1	4.9	37.2
20	0.0825	15.8	0.1115	17.3	0.0098	7.2	0.41	62.9	4.5	107.3	17.6	1256.8	308.8	62.9	4.5	41.4
195	0.1072	16.3	0.1548	17.2	0.0105	5.8	0.32	67.2	3.9	146.1	23.4	1752.1	298.1	67.2	3.9	54.0
311	0.0831	20.9	0.1237	25.3	0.0108	14.4	0.56	69.2	9.9	118.4	28.2	1272.4	407.1	69.2	9.9	41.6
248	0.0554	29.0	0.0827	40.8	0.0108	28.8	0.70	69.4	19.8	80.7	31.7	429.9	645.9	69.4	19.8	14.0
236	0.0741	12.8	0.1231	13.5	0.0121	4.6	0.33	77.3	3.5	117.9	15.1	1043.4	257.8	77.3	3.5	34.5
159	0.3694	27.0	0.6491	29.8	0.0127	12.5	0.42	81.6	10.2	507.9	119.7	3788.9	409.3	81.6	10.2	83.9
105	0.0478	17.9	0.0844	24.3	0.0128	16.4	0.68	82.0	13.4	82.3	19.2	88.6	424.3	82.0	13.4	0.3
239	0.3355	31.5	0.5938	39.6	0.0128	24.0	0.61	82.2	19.6	473.3	150.8	3642.3	481.9	82.2	19.6	82.6
198	0.0693	6.3	0.1249	8.2	0.0131	5.5	0.64	83.7	4.6	119.5	9.2	909.1	129.3	83.7	4.6	30.0
214	0.0733	7.5	0.1366	8.3	0.0135	3.7	0.42	86.5	3.2	130.0	10.2	1022.6	152.6	86.5	3.2	33.4
384	0.0759	20.2	0.1416	27.1	0.0135	18.1	0.67	86.7	15.6	134.5	34.2	1091.1	404.7	86.7	15.6	35.5
246	0.1147	11.2	0.2317	12.8	0.0146	6.4	0.49	93.7	6.0	211.6	24.5	1875.7	201.4	93.7	6.0	55.7
2	0.0793	13.9	0.1684	14.6	0.0154	4.5	0.30	98.5	4.4	158.0	21.4	1179.7	275.0	98.5	4.4	37.7
110	0.2320	17.6	0.4930	19.9	0.0154	9.2	0.46	98.6	9.0	406.9	66.8	3066.0	281.9	98.6	9.0	75.8
271	0.0596	24.0	0.1282	29.6	0.0156	17.2	0.58	99.8	17.1	122.5	34.1	588.5	521.5	99.8	17.1	18.5
211	0.0752	17.7	0.1743	23.8	0.0168	15.9	0.67	107.5	16.9	163.2	35.8	1073.4	356.2	107.5	16.9	34.1
284	0.0949	21.6	0.2276	22.8	0.0174	7.4	0.32	111.1	8.1	208.2	43.0	1527.0	407.8	111.1	8.1	46.6
301	0.0977	10.6	0.2423	12.0	0.0180	5.9	0.47	114.9	6.8	220.3	23.8	1581.2	198.7	114.9	6.8	47.8
186	0.0922	10.9	0.2659	13.3	0.0209	7.3	0.57	133.4	9.6	239.4	28.3	1472.0	206.9	133.4	9.6	44.3
278	0.0708	9.2	0.2071	12.0	0.0212	7.9	0.64	135.3	10.6	191.1	20.9	951.2	187.6	135.3	10.6	29.2
304	0.0494	24.7	0.1715	33.7	0.0252	23.1	0.68	160.3	36.6	160.8	50.2	167.5	576.5	160.3	36.6	0.3
124	0.0498	21.5	0.1732	30.5	0.0252	21.5	0.71	160.6	34.1	162.2	45.7	186.5	501.0	160.6	34.1	1.0
62	0.0823	9.9	0.2995	15.3	0.0264	11.7	0.76	168.0	19.5	266.0	35.9	1252.3	194.1	168.0	19.5	36.9
193	0.0575	17.5	0.2232	24.2	0.0282	16.7	0.69	179.0	29.5	204.6	44.8	510.5	385.0	179.0	29.5	12.5
257	0.1136	6.5	0.4685	7.6	0.0299	4.0	0.53	189.9	7.4	390.2	24.7	1858.5	116.9	189.9	7.4	51.3
161	0.2038	28.1	0.8518	29.2	0.0303	7.8	0.27	192.5	14.9	625.6	137.1	2856.7	457.0	192.5	14.9	69.2
194	0.6332	24.5	3.1938	28.9	0.0366	15.4	0.53	231.6	34.9	1455.7	227.0	4586.0	355.3	231.6	34.9	84.1
157	0.5944	37.7	4.3350	44.1	0.0529	22.9	0.52	332.3	74.0	1700.0	381.0	4494.4	548.7	332.3	74.0	80.5

Table A4.6 (continued): Detrital Zircon U-Pb Integrated Data for the Kayra Formation

Spot	Ratios							Ages (Ma)						Disc. (%)		
	207Pb/206Pb		207Pb/235U		206Pb/238U		Rho	206Pb/238U		207Pb/235U		207Pb/206Pb			Best Age	
	±2σ	±2σ	±2σ	±2σ	±2σ	±2σ		±2σ	±2σ	±2σ	±2σ	±2σ	±2σ			
<i>Kayra Formation (20150520-01) Rejected Data</i>																
128	0.0679	4.9	0.9162	6.9	0.0979	4.4	0.70	602.2	25.5	660.4	33.6	864.6	102.6	602.2	25.5	30.3
294	0.0663	3.2	0.9124	4.3	0.0999	3.0	0.67	613.7	17.8	658.3	20.7	814.6	66.4	613.7	17.8	24.7
73	0.0652	4.5	0.9043	6.2	0.1007	4.4	0.68	618.2	25.7	654.0	30.0	779.5	95.4	618.2	25.7	20.7
386	0.0674	7.5	0.9475	11.2	0.1020	8.3	0.75	626.3	49.5	676.8	55.3	848.7	155.0	626.3	49.5	26.2
400	0.0661	4.1	0.9446	5.1	0.1037	2.9	0.59	636.0	17.7	675.3	25.2	808.7	86.5	636.0	17.7	21.4
348	0.0648	21.6	1.0330	30.7	0.1157	21.9	0.71	705.6	146.1	720.4	159.7	767.0	455.5	705.6	146.1	8.0
82	0.0599	8.3	0.9644	12.0	0.1169	8.7	0.72	712.5	58.8	685.6	59.9	598.3	180.0	712.5	58.8	-19.1
199	0.2088	60.5	3.6814	63.2	0.1279	18.6	0.29	775.7	136.0	1567.3	554.1	2896.3	980.8	775.7	136.0	73.2
113	0.0670	14.5	1.6116	21.0	0.1743	15.2	0.73	1035.9	145.8	974.7	132.4	839.3	300.9	839.3	300.9	-23.4
255	0.0988	11.7	1.8943	13.5	0.1391	6.8	0.50	839.7	53.5	1079.1	90.2	1600.7	218.2	839.7	53.5	47.5
318	0.0977	7.7	2.0989	14.3	0.1557	12.4	0.84	933.0	108.1	1148.4	99.0	1581.6	144.6	933.0	108.1	41.0
92	0.0835	19.7	1.8395	30.7	0.1598	23.6	0.77	955.5	209.4	1059.7	204.4	1281.0	383.0	955.5	209.4	25.4
39	0.1004	10.5	2.2231	10.8	0.1606	3.0	0.25	960.1	27.0	1188.3	76.0	1631.4	195.1	960.1	27.0	41.1
244	0.0861	3.6	1.9207	6.3	0.1618	5.2	0.81	966.8	46.6	1088.3	42.0	1340.1	70.5	966.8	46.6	27.9
122	0.0861	14.5	1.9524	19.4	0.1645	12.9	0.67	981.8	117.4	1099.3	131.2	1339.8	279.3	981.8	117.4	26.7
167	0.0873	11.1	2.0867	12.4	0.1733	5.5	0.44	1030.3	52.8	1144.4	85.4	1367.8	214.1	1367.8	214.1	24.7
115	0.1043	7.5	3.0321	9.3	0.2108	5.6	0.59	1233.1	63.2	1415.7	71.5	1702.3	138.7	1702.3	138.7	27.6
149	0.1065	16.8	4.2549	22.4	0.2897	14.8	0.67	1640.2	215.1	1684.7	186.5	1740.5	307.1	1740.5	307.1	5.8
328	0.1102	4.6	3.0796	5.7	0.2027	4.3	0.61	1189.5	47.1	1427.6	43.6	1803.0	83.3	1803.0	83.3	34.0
207	0.1306	4.6	5.2924	7.0	0.2938	5.4	0.76	1660.7	79.7	1867.6	60.1	2106.4	80.4	2106.4	80.4	21.2
287	0.1428	20.6	3.7479	21.6	0.1904	6.6	0.29	1123.3	67.7	1581.7	174.8	2261.4	356.2	2261.4	356.2	50.3
275	0.1471	27.9	5.3155	33.8	0.2621	19.2	0.57	1500.4	257.2	1871.4	297.4	2312.6	478.9	2312.6	478.9	35.1
200	0.1581	4.3	4.3130	6.5	0.1978	5.0	0.75	1163.4	53.0	1695.8	53.7	2436.0	72.9	2436.0	72.9	52.2

Table A4.7: Detrital Zircon U-Pb Integrated Data for the Soncco Formation

Spot	Ratios						Rho	Ages (Ma)						Best Age	Disc. (%)	
	207Pb/206Pb	±2σ	207Pb/235U	±2σ	206Pb/238U	±2σ		206Pb/238U	±2σ	207Pb/235U	±2σ	207Pb/206Pb	±2σ			
<i>Soncco Formation (20150525-02) Accepted Data</i>																
145	0.0588	12.6	0.0460	15.1	0.0057	8.7	0.56	36.5	3.2	45.7	6.8	558.5	273.6	36.5	3.2	20.1
140	0.0734	21.9	0.0599	23.4	0.0059	8.3	0.35	38.0	3.2	59.1	13.4	1026.2	443.7	38.0	3.2	35.6
28	0.0554	13.4	0.0506	14.4	0.0066	5.8	0.37	42.6	2.5	50.1	7.0	427.9	297.7	42.6	2.5	15.1
178	0.0594	8.6	0.0758	10.6	0.0092	7.1	0.59	59.3	4.2	74.2	7.6	583.3	185.9	59.3	4.2	20.0
100	0.0507	11.0	0.0652	12.8	0.0093	6.5	0.50	59.8	3.8	64.1	7.9	229.0	254.7	59.8	3.8	6.8
350	0.0526	10.9	0.0694	12.1	0.0096	5.4	0.43	61.4	3.3	68.2	7.9	311.7	247.7	61.4	3.3	9.9
209	0.0538	12.2	0.0716	12.8	0.0097	4.3	0.31	61.9	2.7	70.2	8.7	361.3	274.4	61.9	2.7	11.8
191	0.0480	10.5	0.0646	12.4	0.0098	6.8	0.54	62.6	4.3	63.5	7.6	97.2	247.7	62.6	4.3	1.4
139	0.0535	8.8	0.0721	10.6	0.0098	6.4	0.56	62.8	4.0	70.7	7.3	348.6	199.4	62.8	4.0	11.2
65	0.0563	9.1	0.0761	10.2	0.0098	4.7	0.45	62.9	2.9	74.5	7.3	462.6	200.9	62.9	2.9	15.5
285	0.0558	14.8	0.0760	16.8	0.0099	7.6	0.48	63.3	4.8	74.3	12.1	445.7	328.9	63.3	4.8	14.9
346	0.0577	9.7	0.0785	11.2	0.0099	6.1	0.50	63.3	3.8	76.8	8.3	518.9	213.7	63.3	3.8	17.5
103	0.0675	13.8	0.0947	19.6	0.0102	13.9	0.71	65.3	9.0	91.8	17.2	852.6	286.3	65.3	9.0	28.9
61	0.0605	12.5	0.0860	16.0	0.0103	10.0	0.62	66.1	6.6	83.8	12.9	622.8	269.7	66.1	6.6	21.1
277	0.0565	8.8	0.0806	11.5	0.0103	7.0	0.64	66.4	4.6	78.7	8.7	472.9	194.5	66.4	4.6	15.7
240	0.0559	10.4	0.0800	12.1	0.0104	6.0	0.51	66.6	4.0	78.2	9.1	447.8	231.0	66.6	4.0	14.8
370	0.0531	12.1	0.0764	14.8	0.0104	8.2	0.57	67.0	5.4	74.8	10.7	331.9	274.8	67.0	5.4	10.4
297	0.0553	11.9	0.0798	13.2	0.0105	5.4	0.43	67.0	3.6	77.9	9.9	426.0	266.0	67.0	3.6	14.0
43	0.0583	37.6	0.0845	38.2	0.0105	6.9	0.18	67.4	4.7	82.4	30.2	542.6	821.6	67.4	4.7	18.2
147	0.0489	6.9	0.0710	9.5	0.0105	6.8	0.69	67.6	4.5	69.6	6.4	141.5	161.2	67.6	4.5	3.0
136	0.0475	24.9	0.0698	25.7	0.0107	7.0	0.25	68.4	4.7	68.5	17.1	73.3	592.1	68.4	4.7	0.2
231	0.0549	19.5	0.0828	20.7	0.0109	7.0	0.33	70.1	4.9	80.8	16.1	409.7	436.5	70.1	4.9	13.2
134	0.0507	16.1	0.0767	19.2	0.0110	10.7	0.54	70.4	7.5	75.0	13.9	226.1	371.6	70.4	7.5	6.2
76	0.0551	13.8	0.0858	16.3	0.0113	8.9	0.53	72.5	6.4	83.6	13.1	415.5	309.0	72.5	6.4	13.4
379	0.0571	12.8	0.0909	18.1	0.0116	12.6	0.71	74.0	9.3	88.3	15.3	493.9	281.2	74.0	9.3	16.2
9	0.0656	17.5	0.1045	18.5	0.0116	6.3	0.34	74.1	4.6	100.9	17.8	793.8	366.3	74.1	4.6	26.6
372	0.0527	9.2	0.0840	11.6	0.0116	6.9	0.61	74.1	5.1	81.9	9.1	315.9	208.6	74.1	5.1	9.5
183	0.0494	6.3	0.0790	8.0	0.0116	5.7	0.62	74.4	4.2	77.2	6.0	164.9	147.5	74.4	4.2	3.6
359	0.0552	9.7	0.0883	12.7	0.0116	8.2	0.65	74.4	6.1	86.0	10.5	421.4	217.0	74.4	6.1	13.5
383	0.0577	11.1	0.0929	12.4	0.0117	5.3	0.45	74.9	3.9	90.2	10.7	517.1	243.6	74.9	3.9	17.0
13	0.0494	11.1	0.0801	12.9	0.0118	6.8	0.51	75.4	5.1	78.2	9.7	164.8	260.4	75.4	5.1	3.6
321	0.0633	9.4	0.1030	10.7	0.0118	5.4	0.48	75.6	4.0	99.5	10.2	718.0	199.4	75.6	4.0	24.0
333	0.0515	13.2	0.0839	14.2	0.0118	5.7	0.37	75.8	4.3	81.8	11.2	261.3	303.0	75.8	4.3	7.4
306	0.0565	13.2	0.0927	15.1	0.0119	7.5	0.49	76.3	5.7	90.0	13.0	470.7	291.9	76.3	5.7	15.2
101	0.0528	10.7	0.0870	11.9	0.0119	5.2	0.44	76.5	4.0	84.7	9.7	321.2	242.3	76.5	4.0	9.6
351	0.0495	8.0	0.0826	11.2	0.0121	8.1	0.70	77.6	6.2	80.6	8.7	169.6	186.2	77.6	6.2	3.7
75	0.0588	12.8	0.0987	14.1	0.0122	6.4	0.43	78.1	5.0	95.6	12.9	558.8	278.0	78.1	5.0	18.3
327	0.0493	8.6	0.0834	11.4	0.0123	7.6	0.65	78.6	6.0	81.3	8.9	163.5	202.1	78.6	6.0	3.4
31	0.0564	8.7	0.0954	11.1	0.0123	7.0	0.61	78.6	5.4	92.5	9.8	467.7	193.5	78.6	5.4	15.0
93	0.0624	12.0	0.1059	14.2	0.0123	7.7	0.53	78.8	6.0	102.2	13.8	688.4	256.5	78.8	6.0	22.9
182	0.0551	11.0	0.0945	13.0	0.0124	7.4	0.53	79.7	5.8	91.7	11.4	415.4	246.7	79.7	5.8	13.0
90	0.0575	12.5	0.1019	13.3	0.0128	4.8	0.35	82.3	3.9	98.5	12.5	510.7	274.3	82.3	3.9	16.4
110	0.0496	8.9	0.0887	10.1	0.0130	4.7	0.48	83.1	3.9	86.3	8.4	175.4	208.0	83.1	3.9	3.7
267	0.0615	6.4	0.1101	8.4	0.0130	5.3	0.65	83.2	4.4	106.1	8.5	656.3	136.6	83.2	4.4	21.6
369	0.0497	5.3	0.0891	7.1	0.0130	4.3	0.68	83.3	3.6	86.7	5.9	180.4	122.7	83.3	3.6	3.9
164	0.0499	5.6	0.0896	8.5	0.0130	6.4	0.76	83.4	5.3	87.1	7.1	190.3	130.1	83.4	5.3	4.3
395	0.0682	16.3	0.1245	21.9	0.0132	14.6	0.67	84.8	12.3	119.1	24.6	874.9	337.1	84.8	12.3	28.8
42	0.0473	6.8	0.0869	9.1	0.0133	6.2	0.66	85.4	5.3	84.6	7.4	64.6	161.6	85.4	5.3	-0.8
394	0.0495	5.8	0.0924	6.8	0.0135	3.6	0.51	86.6	3.1	89.7	5.8	172.4	135.9	86.6	3.1	3.4
137	0.0464	6.9	0.0871	8.4	0.0136	5.4	0.58	87.1	4.7	84.8	6.8	19.9	164.7	87.1	4.7	-2.7
83	0.0571	11.6	0.1071	14.3	0.0136	8.5	0.59	87.1	7.4	103.3	14.1	495.3	256.3	87.1	7.4	15.7
400	0.0707	21.3	0.1334	24.1	0.0137	11.4	0.47	87.6	9.9	127.1	28.9	949.4	435.9	87.6	9.9	31.1
7	0.0491	4.6	0.0938	5.8	0.0139	3.5	0.59	88.7	3.1	91.0	5.0	152.2	108.8	88.7	3.1	2.5
263	0.0579	8.1	0.1111	9.4	0.0139	4.8	0.51	89.1	4.2	107.0	9.6	527.3	177.7	89.1	4.2	16.8
32	0.0490	5.0	0.0941	6.1	0.0139	3.7	0.56	89.2	3.3	91.3	5.3	147.9	117.4	89.2	3.3	2.4
150	0.0470	7.5	0.0919	9.9	0.0142	6.7	0.65	90.8	6.0	89.3	8.4	49.1	180.0	90.8	6.0	-1.7
324	0.0517	6.6	0.1036	9.5	0.0145	7.0	0.72	93.0	6.4	100.1	9.1	271.3	151.0	93.0	6.4	7.0
96	0.0542	5.8	0.1092	7.4	0.0146	4.6	0.62	93.4	4.3	105.2	7.4	381.3	129.6	93.4	4.3	11.2
193	0.0516	5.0	0.1043	6.7	0.0147	4.7	0.66	93.8	4.4	100.7	6.4	267.8	115.5	93.8	4.4	6.9
132	0.0478	5.6	0.0995	7.4	0.0151	5.2	0.65	96.7	5.0	96.4	6.8	87.0	133.8	96.7	5.0	-0.4
47	0.0494	4.4	0.1040	5.0	0.0153	3.0	0.50	97.7	2.9	100.5	4.8	166.3	101.9	97.7	2.9	2.7
278	0.0541	5.0	0.1154	7.5	0.0155	5.1	0.75	99.0	5.0	110.9	7.9	374.7	112.5	99.0	5.0	10.7
107	0.0513	5.7	0.1097	7.3	0.0155	4.3	0.62	99.3	4.2	105.7	7.3	252.3	131.3	99.3	4.2	6.0

Table A4.7 (continued): Detrital Zircon U-Pb Integrated Data for the Soncco Formation

Spot	Ratios						Rho	Ages (Ma)						Best Age	Disc. (%)	
	207Pb/ 206Pb	$\pm 2\sigma$	207Pb/ 235U	$\pm 2\sigma$	206Pb/ 238U	$\pm 2\sigma$		206Pb/ 238U	$\pm 2\sigma$	207Pb/ 235U	$\pm 2\sigma$	207Pb/ 206Pb	$\pm 2\sigma$			
<i>Soncco Formation (20150525-02) Accepted Data</i>																
304	0.0467	10.8	0.1031	15.7	0.0160	11.4	0.72	102.4	11.6	99.7	14.9	36.0	259.4	102.4	11.6	-2.7
340	0.0514	9.7	0.1141	14.2	0.0161	10.5	0.73	102.9	10.7	109.7	14.7	260.1	223.2	102.9	10.7	6.2
63	0.0475	14.8	0.1087	20.4	0.0166	14.1	0.69	106.1	14.8	104.7	20.3	73.0	352.3	106.1	14.8	-1.3
36	0.0483	5.8	0.1151	7.3	0.0173	4.7	0.61	110.5	5.1	110.6	7.6	112.9	136.4	110.5	5.1	0.1
123	0.0693	12.6	0.1683	14.0	0.0176	6.4	0.44	112.5	7.1	157.9	20.5	909.1	259.9	112.5	7.1	28.8
62	0.0459	5.9	0.1173	7.1	0.0185	4.0	0.55	118.3	4.7	112.6	7.6	-6.2	142.9	118.3	4.7	-5.1
343	0.0514	12.7	0.1359	17.3	0.0192	11.8	0.68	122.4	14.4	129.4	21.0	258.7	292.7	122.4	14.4	5.4
24	0.0498	4.7	0.1395	6.0	0.0203	4.2	0.62	129.7	5.4	132.6	7.5	185.4	109.9	129.7	5.4	2.2
128	0.0486	5.7	0.1377	6.7	0.0205	4.2	0.54	131.1	5.5	131.0	8.2	128.8	133.2	131.1	5.5	-0.1
361	0.0505	5.3	0.1439	7.8	0.0207	5.6	0.74	131.9	7.3	136.5	10.0	216.8	122.2	131.9	7.3	3.4
11	0.0483	8.9	0.1377	12.8	0.0207	9.3	0.72	132.1	12.1	131.0	15.7	112.2	209.8	132.1	12.1	-0.8
16	0.0508	5.5	0.1456	6.3	0.0208	4.0	0.51	132.5	5.2	138.0	8.2	233.6	126.8	132.5	5.2	4.0
237	0.0554	8.8	0.1587	11.2	0.0208	6.9	0.62	132.6	9.0	149.6	15.6	427.1	196.0	132.6	9.0	11.3
135	0.0520	12.5	0.1498	14.6	0.0209	7.9	0.52	133.3	10.5	141.7	19.4	284.6	286.8	133.3	10.5	5.9
310	0.0520	7.8	0.1533	9.5	0.0214	5.5	0.57	136.4	7.5	144.8	12.8	285.3	177.9	136.4	7.5	5.8
211	0.0488	3.5	0.1442	4.2	0.0214	3.1	0.59	136.6	4.2	136.8	5.4	139.6	81.8	136.6	4.2	0.1
127	0.0483	7.7	0.1428	10.0	0.0214	6.7	0.63	136.6	9.1	135.5	12.7	115.9	182.3	136.6	9.1	-0.8
188	0.0506	11.2	0.1504	14.6	0.0216	9.7	0.64	137.5	13.2	142.3	19.4	223.2	259.3	137.5	13.2	3.4
317	0.0516	10.3	0.1541	14.6	0.0216	10.4	0.71	138.0	14.2	145.5	19.7	269.9	235.6	138.0	14.2	5.2
82	0.0478	6.4	0.1467	8.7	0.0222	6.2	0.68	141.8	8.7	139.0	11.4	90.5	151.0	141.8	8.7	-2.1
133	0.0649	6.7	0.2026	8.7	0.0227	5.9	0.64	144.5	8.4	187.4	14.9	769.5	140.8	144.5	8.4	22.9
30	0.0521	6.1	0.1632	6.8	0.0227	3.3	0.44	144.9	4.8	153.5	9.6	288.4	139.1	144.9	4.8	5.6
189	0.0564	5.4	0.1828	7.7	0.0235	6.0	0.72	149.7	9.0	170.4	12.1	468.5	118.8	149.7	9.0	12.1
161	0.0478	8.0	0.1557	10.6	0.0236	6.7	0.65	150.4	10.0	146.9	14.5	90.8	190.6	150.4	10.0	-2.4
221	0.0513	10.5	0.1669	11.8	0.0236	5.6	0.45	150.5	8.4	156.7	17.1	252.6	242.4	150.5	8.4	4.0
25	0.0498	10.2	0.1625	13.9	0.0237	9.7	0.68	150.8	14.4	152.9	19.7	186.0	238.3	150.8	14.4	1.4
329	0.0524	11.0	0.1722	15.0	0.0238	10.3	0.68	151.8	15.5	161.3	22.3	302.9	251.6	151.8	15.5	5.9
176	0.0477	13.3	0.1577	18.3	0.0240	13.0	0.69	152.8	19.7	148.7	25.3	83.4	316.2	152.8	19.7	-2.8
389	0.0555	7.5	0.1874	10.0	0.0245	6.6	0.66	156.0	10.1	174.4	16.0	431.0	167.7	156.0	10.1	10.5
44	0.0528	8.7	0.1797	10.0	0.0247	5.2	0.49	157.3	8.0	167.8	15.4	318.1	198.6	157.3	8.0	6.2
283	0.0535	5.6	0.1850	7.1	0.0251	3.9	0.62	159.6	6.2	172.4	11.3	351.4	127.4	159.6	6.2	7.4
170	0.0506	7.5	0.1754	10.4	0.0251	7.6	0.69	159.9	12.0	164.1	15.7	224.5	174.4	159.9	12.0	2.5
326	0.0515	5.9	0.1821	7.7	0.0257	5.3	0.64	163.3	8.5	169.9	12.1	261.7	136.2	163.3	8.5	3.8
220	0.0520	6.7	0.1887	7.6	0.0263	4.1	0.47	167.4	6.7	175.5	12.3	286.6	154.1	167.4	6.7	4.6
210	0.0514	10.7	0.1890	15.3	0.0267	11.1	0.71	169.7	18.6	175.8	24.7	258.8	246.2	169.7	18.6	3.5
260	0.0545	4.7	0.2014	6.4	0.0268	4.4	0.69	170.4	7.3	186.3	10.9	393.3	104.9	170.4	7.3	8.5
117	0.0556	7.1	0.2073	8.6	0.0270	4.7	0.56	172.0	8.0	191.3	15.0	437.2	159.1	172.0	8.0	10.1
146	0.0521	10.1	0.1951	14.5	0.0272	10.6	0.72	172.9	18.0	181.0	24.0	288.4	229.7	172.9	18.0	4.5
109	0.0559	7.5	0.2117	9.2	0.0275	5.3	0.59	174.6	9.1	195.0	16.4	449.7	165.8	174.6	9.1	10.5
38	0.0519	5.5	0.1973	6.4	0.0276	3.6	0.50	175.4	6.2	182.8	10.7	279.2	126.9	175.4	6.2	4.0
302	0.0616	10.4	0.2394	12.2	0.0282	6.2	0.52	179.1	11.0	218.0	23.9	661.4	223.2	179.1	11.0	17.8
311	0.0519	15.5	0.2034	21.1	0.0284	14.4	0.68	180.5	25.6	188.0	36.2	282.8	353.7	180.5	25.6	4.0
352	0.0629	12.6	0.2733	14.9	0.0315	8.1	0.53	200.0	15.9	245.3	32.5	705.3	268.2	200.0	15.9	18.5
299	0.0550	7.4	0.2490	10.1	0.0329	6.6	0.67	208.5	13.5	225.8	20.4	410.2	166.4	208.5	13.5	7.7
201	0.0525	4.7	0.2441	5.6	0.0337	3.8	0.56	213.8	7.9	221.8	11.2	307.3	106.3	213.8	7.9	3.6
70	0.0552	5.2	0.2736	6.3	0.0359	3.8	0.57	227.7	8.4	245.6	13.7	420.5	115.3	227.7	8.4	7.3
334	0.0561	9.1	0.2931	13.1	0.0379	9.6	0.72	239.8	22.5	261.0	30.2	456.3	202.5	239.8	22.5	8.1
49	0.0510	5.4	0.2789	6.4	0.0396	3.8	0.52	250.5	9.3	249.7	14.1	242.6	125.4	250.5	9.3	-0.3
60	0.0560	6.4	0.3157	8.2	0.0409	5.2	0.63	258.5	13.2	278.6	20.0	450.7	141.8	258.5	13.2	7.2
98	0.0508	3.4	0.2873	5.6	0.0411	4.5	0.79	259.4	11.4	256.4	12.8	229.6	79.6	259.4	11.4	-1.1
15	0.0492	8.5	0.2849	12.3	0.0420	9.1	0.72	265.4	23.8	254.5	27.6	155.1	199.4	265.4	23.8	-4.3
250	0.0590	6.5	0.3459	9.9	0.0426	7.4	0.75	268.6	19.5	301.6	25.9	565.6	141.9	268.6	19.5	10.9
118	0.0579	8.5	0.3398	9.7	0.0426	4.6	0.48	268.6	12.0	297.0	25.0	526.5	186.7	268.6	12.0	9.6
380	0.0537	10.8	0.3296	15.7	0.0445	11.3	0.73	280.9	30.9	289.2	39.5	357.5	242.8	280.9	30.9	2.9
187	0.0573	4.4	0.5521	6.4	0.0699	5.3	0.73	435.5	22.1	446.4	23.1	502.6	96.9	435.5	22.1	2.4
356	0.0559	9.4	0.5446	14.1	0.0707	10.5	0.74	440.4	44.7	441.5	50.6	447.0	209.8	440.4	44.7	0.2
177	0.0564	4.0	0.5624	6.6	0.0723	6.3	0.81	450.2	27.4	453.1	24.2	467.9	89.4	450.2	27.4	0.6
266	0.0588	9.3	0.5928	13.6	0.0731	9.8	0.73	454.7	43.2	472.7	51.3	560.9	201.8	454.7	43.2	3.8
153	0.0554	3.5	0.5634	5.9	0.0737	5.1	0.81	458.6	22.6	453.7	21.5	429.4	77.2	458.6	22.6	-1.1
206	0.0567	3.3	0.5822	4.2	0.0744	3.1	0.62	462.7	14.0	465.8	15.6	481.5	73.3	462.7	14.0	0.7
256	0.0583	7.5	0.6043	11.2	0.0752	8.3	0.74	467.3	37.6	480.0	42.9	540.9	163.8	467.3	37.6	2.6
151	0.0578	4.4	0.6092	6.3	0.0764	5.0	0.72	474.8	22.7	483.1	24.4	522.7	96.5	474.8	22.7	1.7
243	0.0617	7.7	0.6502	11.8	0.0764	8.9	0.76	474.9	40.8	508.6	47.3	663.3	164.2	474.9	40.8	6.6

Table A4.7 (continued): Detrital Zircon U-Pb Integrated Data for the Soncco Formation

Spot	Ratios						Rho	Ages (Ma)						Best Age	Disc. (%)	
	207Pb/ 206Pb	±2σ	207Pb/ 235U	±2σ	206Pb/ 238U	±2σ		206Pb/ 238U	±2σ	207Pb/ 235U	±2σ	207Pb/ 206Pb	±2σ			
	<i>Soncco Formation</i>							<i>(20150525-02) Accepted Data</i>								
223	0.0596	4.4	0.6544	5.5	0.0796	3.9	0.61	494.0	18.5	511.2	22.2	588.5	95.6	494.0	18.5	3.4
55	0.0581	5.5	0.6437	7.9	0.0803	5.7	0.72	498.2	27.3	504.6	31.5	533.7	120.9	498.2	27.3	1.3
199	0.0603	4.8	0.6782	6.3	0.0815	4.7	0.65	505.3	22.8	525.7	26.0	615.3	104.3	505.3	22.8	3.9
190	0.0603	3.6	0.6776	5.7	0.0816	4.7	0.77	505.4	22.8	525.3	23.2	612.8	77.7	505.4	22.8	3.8
335	0.0585	3.6	0.6603	5.4	0.0818	4.4	0.75	506.8	21.4	514.8	21.8	550.3	77.9	506.8	21.4	1.5
112	0.0578	4.5	0.6602	6.6	0.0829	4.8	0.73	513.2	23.4	514.7	26.9	521.3	99.6	513.2	23.4	0.3
264	0.0650	4.3	0.7429	7.6	0.0829	6.2	0.82	513.4	30.6	564.1	32.8	774.3	90.6	513.4	30.6	9.0
154	0.0577	4.9	0.6608	7.8	0.0830	6.1	0.78	514.0	29.9	515.1	31.7	520.1	107.6	514.0	29.9	0.2
192	0.0601	5.5	0.6908	7.9	0.0834	5.8	0.71	516.3	28.8	533.3	32.6	606.8	119.9	516.3	28.8	3.2
289	0.0595	6.0	0.6844	9.5	0.0834	6.8	0.78	516.5	34.0	529.4	39.0	585.5	129.6	516.5	34.0	2.4
378	0.0595	4.8	0.6888	6.9	0.0839	4.5	0.71	519.5	22.6	532.1	28.4	586.2	104.6	519.5	22.6	2.4
73	0.0589	6.8	0.6932	9.5	0.0854	6.7	0.70	528.1	34.2	534.7	39.4	563.2	147.5	528.1	34.2	1.2
8	0.0654	3.8	0.7770	5.6	0.0861	4.1	0.73	532.5	21.1	583.8	24.9	788.5	80.5	532.5	21.1	8.8
37	0.0663	5.6	0.7877	8.1	0.0862	6.0	0.72	533.1	31.0	589.8	36.2	814.8	117.2	533.1	31.0	9.6
316	0.0599	4.6	0.7145	6.1	0.0865	4.2	0.66	534.7	21.8	547.4	26.0	600.5	99.5	534.7	21.8	2.3
393	0.0577	4.3	0.6926	6.0	0.0870	4.2	0.70	537.8	21.4	534.4	25.1	519.6	94.6	537.8	21.4	-0.6
318	0.0572	8.5	0.6894	12.3	0.0875	8.9	0.72	540.6	46.4	532.5	51.0	497.7	188.0	540.6	46.4	-1.5
286	0.0599	4.7	0.7280	7.7	0.0881	5.5	0.80	544.4	28.7	555.4	32.9	600.4	101.4	544.4	28.7	2.0
141	0.0586	4.4	0.7167	6.7	0.0887	5.3	0.75	547.7	27.6	548.7	28.2	552.9	96.0	547.7	27.6	0.2
131	0.0596	4.0	0.7325	5.8	0.0891	4.6	0.73	550.4	24.4	558.0	25.0	589.0	86.6	550.4	24.4	1.4
398	0.0651	6.2	0.8062	7.5	0.0898	4.3	0.56	554.3	22.8	600.3	34.0	778.2	130.5	554.3	22.8	7.7
124	0.0617	3.9	0.7728	4.8	0.0908	3.6	0.61	560.3	19.5	581.4	21.3	664.6	83.1	560.3	19.5	3.6
45	0.0577	8.1	0.7252	11.3	0.0911	8.1	0.70	562.3	43.6	553.7	48.3	518.7	177.8	562.3	43.6	-1.5
309	0.0573	3.3	0.7235	4.5	0.0915	3.3	0.67	564.4	17.8	552.7	19.0	504.9	73.5	564.4	17.8	-2.1
323	0.0596	7.4	0.7536	10.7	0.0917	7.8	0.72	565.6	42.3	570.3	46.7	589.2	160.9	565.6	42.3	0.8
113	0.0600	3.8	0.7684	5.5	0.0929	3.9	0.73	572.6	21.4	578.8	24.4	603.3	81.6	572.6	21.4	1.1
386	0.0607	5.9	0.7808	8.2	0.0933	5.7	0.70	574.8	31.3	585.9	36.7	629.3	127.0	574.8	31.3	1.9
290	0.0601	2.8	0.7723	5.3	0.0933	3.7	0.85	574.8	20.5	581.1	23.2	605.6	61.6	574.8	20.5	1.1
218	0.0622	5.7	0.8032	7.6	0.0937	5.7	0.68	577.5	31.4	598.7	34.6	679.7	120.7	577.5	31.4	3.5
115	0.0600	3.5	0.7762	4.9	0.0938	3.4	0.70	578.1	18.6	583.3	21.8	603.7	76.3	578.1	18.6	0.9
355	0.0586	4.1	0.7639	6.4	0.0946	4.9	0.77	582.7	27.3	576.2	28.1	550.8	89.5	582.7	27.3	-1.1
53	0.0601	3.9	0.7855	4.8	0.0947	3.1	0.58	583.3	17.5	588.6	21.4	608.9	84.5	583.3	17.5	0.9
34	0.0636	5.6	0.8465	7.4	0.0965	5.1	0.65	594.0	28.9	622.7	34.6	728.5	119.7	594.0	28.9	4.6
247	0.0647	4.2	0.8633	7.0	0.0967	5.4	0.80	595.2	31.0	631.9	32.9	765.7	88.7	595.2	31.0	5.8
91	0.0612	3.4	0.8204	5.2	0.0972	4.1	0.76	597.7	23.6	608.2	23.6	647.7	72.7	597.7	23.6	1.7
80	0.0590	8.5	0.7910	12.2	0.0972	8.9	0.72	598.3	50.9	591.7	55.0	566.8	185.7	598.3	50.9	-1.1
196	0.0594	9.6	0.7981	13.3	0.0974	9.5	0.69	599.3	54.2	595.8	59.8	582.2	207.6	599.3	54.2	-0.6
84	0.0609	3.0	0.8205	4.0	0.0978	3.1	0.67	601.2	17.7	608.3	18.5	634.8	64.7	601.2	17.7	5.3
99	0.0623	5.9	0.8461	8.5	0.0984	6.2	0.72	605.3	35.6	622.5	39.7	685.6	126.1	605.3	35.6	11.7
64	0.0620	4.9	0.8438	7.3	0.0988	5.5	0.74	607.2	32.2	621.2	34.1	672.9	104.8	607.2	32.2	9.8
315	0.0609	5.9	0.8401	7.8	0.1001	5.2	0.65	615.0	30.8	619.2	36.3	634.3	127.6	615.0	30.8	3.0
180	0.0595	4.9	0.8289	7.8	0.1010	6.6	0.78	620.0	39.3	613.0	36.0	587.2	106.6	620.0	39.3	-5.6
215	0.0627	8.4	0.8742	10.0	0.1011	6.0	0.55	620.6	35.5	637.9	47.5	699.4	178.2	620.6	35.5	11.3
152	0.0617	11.2	0.8593	16.4	0.1011	12.2	0.73	620.6	72.1	629.8	77.2	662.6	239.5	620.6	72.1	6.3
212	0.0628	6.7	0.8886	9.3	0.1027	6.8	0.70	629.9	41.0	645.6	44.6	700.9	141.8	629.9	41.0	10.1
272	0.0630	3.3	0.8926	6.3	0.1027	4.8	0.86	630.2	28.7	647.7	30.2	709.4	70.4	630.2	28.7	11.2
322	0.0607	3.2	0.8943	4.9	0.1068	3.9	0.75	654.2	24.0	648.7	23.3	629.4	69.8	654.2	24.0	-3.9
291	0.0652	5.9	0.9714	10.3	0.1081	8.2	0.82	661.6	51.5	689.2	51.8	780.3	123.2	661.6	51.5	15.2
399	0.0643	14.3	0.9661	23.7	0.1090	18.9	0.80	666.9	120.0	686.5	118.7	751.2	301.1	666.9	120.0	11.2
172	0.0685	5.1	1.1573	8.4	0.1225	7.2	0.80	744.9	50.6	780.7	45.6	884.3	104.8	744.9	50.6	15.8
245	0.0703	4.4	1.2145	7.4	0.1253	5.7	0.80	760.7	41.2	807.3	41.0	937.9	90.6	760.7	41.2	18.9
287	0.0697	7.7	1.2665	10.7	0.1317	7.0	0.70	797.7	52.2	830.8	60.8	920.4	158.3	797.7	52.2	13.3
387	0.0649	6.8	1.1958	9.8	0.1336	6.9	0.72	808.5	52.7	798.6	54.1	771.3	143.6	808.5	52.7	-4.8
279	0.0724	6.9	1.3650	10.4	0.1368	7.5	0.75	826.5	57.8	874.0	61.1	996.4	139.9	826.5	57.8	17.0
226	0.0734	5.8	1.3913	7.6	0.1374	5.1	0.65	829.9	40.1	885.3	45.0	1026.3	117.8	829.9	40.1	19.1
325	0.0693	4.7	1.3363	6.6	0.1399	5.0	0.71	844.2	39.9	861.6	38.5	906.6	97.1	844.2	39.9	6.9
313	0.0717	2.7	1.3886	5.0	0.1404	4.3	0.83	847.0	33.9	884.1	29.3	978.3	55.9	847.0	33.9	13.4
2	0.0708	5.3	1.4192	7.6	0.1454	5.5	0.72	875.1	44.7	897.0	45.2	951.4	108.5	875.1	44.7	8.0
205	0.0729	4.7	1.4723	6.3	0.1465	4.6	0.67	881.5	37.6	919.1	37.8	1010.3	94.4	881.5	37.6	12.7
78	0.0733	6.2	1.4840	9.3	0.1469	7.2	0.75	883.5	59.7	923.9	56.7	1021.6	124.7	883.5	59.7	13.5
19	0.0690	7.0	1.4070	9.2	0.1479	6.4	0.65	888.9	53.2	891.9	54.4	899.2	144.2	888.9	53.2	1.1
174	0.0705	5.3	1.4410	9.4	0.1482	8.2	0.83	891.0	68.6	906.1	56.6	943.2	109.4	891.0	68.6	5.5
255	0.0730	4.0	1.5090	6.9	0.1500	5.5	0.81	900.9	46.6	934.1	42.0	1013.1	82.1	900.9	46.6	11.1

Table A4.7 (continued): Detrital Zircon U-Pb Integrated Data for the Soncco Formation

Spot	Ratios							Ages (Ma)					Best Age	Disc. (%)		
	207Pb/ 206Pb		207Pb/ 235U		206Pb/ 238U		Rho	207Pb/ 235U		206Pb/ 238U						
	$\pm 2\sigma$	$\pm 2\sigma$	$\pm 2\sigma$	$\pm 2\sigma$	$\pm 2\sigma$	$\pm 2\sigma$		$\pm 2\sigma$	$\pm 2\sigma$	$\pm 2\sigma$						
<i>Soncco Formation (20150525-02) Accepted Data</i>																
10	0.0736	4.8	1.5271	6.5	0.1505	4.6	0.68	904.0	39.2	941.4	40.0	1029.8	96.8	904.0	39.2	12.2
362	0.0751	4.8	1.5644	7.0	0.1511	4.9	0.73	907.4	41.4	956.2	43.5	1070.3	96.2	907.4	41.4	15.2
3	0.0713	7.2	1.4985	10.0	0.1524	7.1	0.70	914.4	60.3	929.8	61.2	966.5	146.2	914.4	60.3	5.4
233	0.0723	7.4	1.5259	10.2	0.1532	7.1	0.69	918.6	61.0	940.9	62.8	993.3	151.4	918.6	61.0	7.5
373	0.0749	4.2	1.5815	6.1	0.1532	4.0	0.73	919.0	34.0	963.0	37.7	1064.7	84.2	919.0	34.0	13.7
97	0.0730	6.4	1.5429	9.6	0.1533	7.2	0.75	919.7	61.6	947.6	59.4	1013.2	130.2	919.7	61.6	9.2
208	0.0722	6.0	1.5431	8.7	0.1549	6.6	0.73	928.6	56.9	947.8	53.8	992.6	122.1	928.6	56.9	6.4
227	0.0748	3.3	1.6003	5.0	0.1551	4.0	0.74	929.4	34.5	970.3	31.0	1064.3	66.7	929.4	34.5	12.7
365	0.0743	4.6	1.5900	7.2	0.1552	5.1	0.77	930.3	44.5	966.3	45.1	1049.2	93.3	930.3	44.5	11.3
111	0.0750	12.9	1.6057	19.2	0.1553	14.2	0.74	930.5	123.4	972.4	120.9	1068.5	258.9	930.5	123.4	12.9
358	0.0737	3.4	1.5858	5.3	0.1561	4.1	0.77	935.3	35.8	964.6	33.0	1032.0	67.9	935.3	35.8	9.4
342	0.0777	4.1	1.6757	5.7	0.1565	4.4	0.70	937.1	38.4	999.3	36.2	1138.5	81.2	937.1	38.4	17.7
391	0.0736	5.7	1.5898	7.3	0.1566	4.5	0.63	937.9	39.1	966.2	45.3	1031.2	114.2	937.9	39.1	9.0
200	0.0740	7.5	1.6000	10.6	0.1568	7.7	0.70	938.7	67.7	970.2	66.2	1042.2	151.6	938.7	67.7	9.9
207	0.0756	3.4	1.6376	4.8	0.1571	3.9	0.72	940.5	33.8	984.8	30.2	1085.0	67.5	940.5	33.8	13.3
156	0.0705	4.2	1.6571	7.3	0.1704	5.9	0.82	1014.4	55.2	992.3	46.3	943.7	86.5	943.7	86.5	-7.5
275	0.0743	3.6	1.6147	6.3	0.1577	4.6	0.82	943.9	40.2	975.9	39.5	1048.7	73.4	943.9	40.2	10.0
72	0.0710	5.1	1.5460	7.6	0.1579	5.8	0.74	945.0	51.1	948.9	47.1	958.0	104.4	945.0	51.1	1.4
331	0.0781	4.9	1.7024	6.3	0.1581	4.5	0.63	946.4	39.4	1009.4	40.0	1148.8	97.0	946.4	39.4	17.6
336	0.0731	3.5	1.5997	5.9	0.1587	5.0	0.80	949.5	44.3	970.1	37.0	1017.1	71.8	949.5	44.3	6.7
364	0.0742	4.2	1.6274	6.3	0.1591	4.2	0.75	951.7	37.1	980.8	39.5	1046.7	84.0	951.7	37.1	9.1
58	0.0783	4.8	1.7259	8.3	0.1598	6.7	0.82	955.7	59.9	1018.2	53.1	1155.1	94.7	955.7	59.9	17.3
292	0.0751	3.4	1.6557	5.7	0.1598	3.8	0.80	955.9	34.1	991.7	35.9	1071.9	69.1	955.9	34.1	10.8
69	0.0745	3.1	1.6466	4.8	0.1602	3.7	0.75	958.0	32.9	988.3	30.1	1056.0	63.4	958.0	32.9	9.3
276	0.0754	4.4	1.6682	7.1	0.1605	5.1	0.79	959.5	45.2	996.5	45.0	1079.0	87.8	959.5	45.2	11.1
241	0.0784	10.8	1.7345	14.5	0.1605	9.6	0.67	959.6	85.3	1021.4	93.4	1156.4	214.3	959.6	85.3	17.0
330	0.0724	4.6	1.6121	7.1	0.1614	5.9	0.77	964.5	52.7	974.9	44.8	998.5	93.5	964.5	52.7	3.4
341	0.0719	3.3	1.6016	5.1	0.1615	4.4	0.77	965.1	39.2	970.8	32.1	983.9	67.6	965.1	39.2	1.9
85	0.0733	5.5	1.6361	8.2	0.1619	6.4	0.74	967.1	57.2	984.2	51.9	1022.7	112.1	967.1	57.2	5.4
181	0.0730	3.9	1.6295	6.7	0.1619	6.1	0.82	967.5	55.0	981.7	42.3	1013.4	78.7	967.5	55.0	4.5
308	0.0698	3.9	1.5589	5.4	0.1619	4.0	0.69	967.6	36.0	954.0	33.5	922.8	80.5	967.6	36.0	-4.8
102	0.0724	8.8	1.6174	13.2	0.1621	9.8	0.74	968.6	88.2	977.0	82.9	996.0	179.3	968.6	88.2	2.8
21	0.0723	12.2	1.6193	16.8	0.1625	11.7	0.69	970.7	105.6	977.7	105.8	993.5	247.4	970.7	105.6	2.3
374	0.0749	3.9	1.6808	6.0	0.1628	4.1	0.76	972.2	37.4	1001.3	38.3	1065.6	79.3	972.2	37.4	8.8
20	0.0719	3.7	1.6152	4.9	0.1628	3.8	0.67	972.5	34.1	976.1	30.8	984.4	74.7	972.5	34.1	1.2
382	0.0717	3.5	1.6089	5.5	0.1628	3.8	0.77	972.5	34.0	973.7	34.1	976.2	71.1	972.5	34.0	0.4
179	0.0730	6.1	1.6393	8.2	0.1629	6.5	0.68	973.0	58.6	985.4	51.7	1013.3	124.0	973.0	58.6	4.0
79	0.0732	13.7	1.6473	19.7	0.1632	14.2	0.72	974.4	128.9	988.5	125.1	1020.0	278.0	974.4	128.9	4.5
381	0.0725	9.9	1.6329	14.9	0.1632	11.0	0.75	974.8	99.7	983.0	94.3	1001.3	201.0	974.8	99.7	2.6
216	0.0752	4.4	1.6932	5.7	0.1633	4.3	0.64	975.2	39.3	1006.0	36.5	1073.8	88.9	975.2	39.3	9.2
254	0.0757	3.0	1.7181	5.5	0.1646	4.5	0.83	982.1	41.3	1015.3	35.0	1087.7	60.5	982.1	41.3	9.7
57	0.0719	10.0	1.6691	14.4	0.1683	10.3	0.72	1002.7	95.5	996.8	91.4	983.9	204.0	983.9	204.0	-1.9
116	0.0721	7.2	1.6504	10.7	0.1660	7.9	0.74	990.1	72.2	989.7	67.5	988.9	145.6	990.1	72.2	-0.1
157	0.0755	11.0	1.7312	15.4	0.1663	10.8	0.70	991.5	99.6	1020.2	99.7	1082.3	220.0	991.5	99.6	8.4
130	0.0743	14.1	1.7122	19.6	0.1672	13.8	0.70	996.8	127.4	1013.1	126.3	1048.5	283.4	996.8	127.4	4.9
26	0.0724	3.8	1.6829	5.0	0.1686	4.0	0.66	1004.3	37.6	1002.1	31.8	997.2	77.5	997.2	77.5	-0.7
22	0.0726	9.4	1.6905	13.5	0.1690	9.9	0.72	1006.5	92.1	1005.0	86.4	1001.7	191.0	1001.7	191.0	-0.5
59	0.0732	11.7	1.7342	17.2	0.1717	12.6	0.73	1021.7	118.6	1021.3	110.9	1020.5	236.9	1020.5	236.9	-0.1
173	0.0733	7.4	1.7107	12.1	0.1692	9.9	0.79	1007.8	92.6	1012.5	77.5	1022.7	150.0	1022.7	150.0	1.5
314	0.0738	3.2	1.8350	4.6	0.1804	3.5	0.72	1069.2	34.6	1058.1	30.2	1035.3	64.6	1035.3	64.6	-3.3
94	0.0741	5.4	1.8014	8.2	0.1762	6.2	0.75	1046.4	59.6	1046.0	53.6	1045.2	109.1	1045.2	109.1	-0.1
319	0.0742	2.1	1.7339	2.9	0.1694	2.3	0.69	1008.8	21.4	1021.2	18.6	1048.0	42.9	1048.0	42.9	3.7
121	0.0744	2.1	1.7847	3.1	0.1740	2.9	0.74	1034.3	27.5	1039.9	20.2	1051.8	43.3	1051.8	43.3	1.7
390	0.0745	3.4	1.8043	5.1	0.1757	3.6	0.74	1043.4	35.1	1047.0	33.0	1054.7	68.5	1054.7	68.5	1.1
280	0.0745	8.5	1.7354	13.0	0.1689	9.6	0.76	1006.1	89.5	1021.8	83.6	1055.4	170.6	1055.4	170.6	4.7
345	0.0751	3.7	1.8514	5.8	0.1788	5.0	0.77	1060.5	48.5	1063.9	38.0	1070.9	74.4	1070.9	74.4	1.0
232	0.0751	4.7	1.8491	6.2	0.1785	4.3	0.66	1058.6	41.7	1063.1	41.0	1072.3	94.4	1072.3	94.4	1.3
349	0.0754	5.9	1.8287	8.7	0.1758	6.9	0.74	1044.0	66.4	1055.8	57.5	1080.3	117.4	1080.3	117.4	3.4
89	0.0765	4.1	1.8484	5.7	0.1753	4.3	0.69	1041.4	41.7	1062.9	37.3	1107.3	81.8	1107.3	81.8	6.0
27	0.0767	5.7	2.1406	8.0	0.2024	6.1	0.71	1188.1	66.5	1162.0	55.2	1113.8	113.0	1113.8	113.0	-6.7
397	0.0769	5.4	1.9315	8.0	0.1822	6.0	0.74	1079.2	59.4	1092.1	53.8	1117.8	108.5	1117.8	108.5	3.5
238	0.0770	9.7	1.9400	15.0	0.1828	11.4	0.76	1082.4	113.4	1095.0	100.8	1120.3	193.7	1120.3	193.7	3.4
41	0.0770	12.6	1.9556	16.4	0.1841	10.6	0.64	1089.3	106.2	1100.4	110.4	1122.5	250.3	1122.5	250.3	3.0

Table A4.7 (continued): Detrital Zircon U-Pb Integrated Data for the Soncco Formation

Spot	Ratios						Rho	Ages (Ma)						Best Age	Disc. (%)	
	207Pb/206Pb		207Pb/235U		206Pb/238U			206Pb/238U		207Pb/235U		207Pb/206Pb				
	±2σ	±2σ	±2σ	±2σ	±2σ	±2σ		±2σ	±2σ	±2σ	±2σ	±2σ				
<i>Soncco Formation (20150525-02) Accepted Data</i>																
347	0.0772	7.6	2.0016	11.1	0.1880	8.5	0.73	1110.7	86.5	1116.0	75.5	1126.4	150.9	1126.4	150.9	1.4
1	0.0778	10.2	1.9498	14.0	0.1817	9.6	0.69	1076.3	95.1	1098.4	94.0	1142.5	202.3	1142.5	202.3	5.8
48	0.0781	5.5	2.2210	7.6	0.2063	5.6	0.69	1209.2	61.6	1187.7	53.5	1148.7	109.5	1148.7	109.5	-5.3
155	0.0781	4.5	2.0130	7.7	0.1869	6.2	0.82	1104.4	63.3	1119.9	52.6	1150.1	89.0	1150.1	89.0	4.0
40	0.0782	5.0	2.1256	7.1	0.1971	5.1	0.70	1159.7	54.6	1157.2	48.7	1152.3	100.0	1152.3	100.0	-0.6
296	0.0783	3.1	1.9169	5.4	0.1776	4.1	0.82	1054.0	39.5	1087.0	35.9	1153.8	61.7	1153.8	61.7	8.6
258	0.0784	4.5	1.8843	7.3	0.1742	5.7	0.78	1035.3	54.7	1075.6	48.5	1158.1	89.8	1158.1	89.8	10.6
363	0.0785	5.1	1.9632	7.6	0.1813	5.4	0.74	1107.3	53.2	1103.0	50.9	1160.0	100.7	1160.0	100.7	7.4
312	0.0790	8.1	1.8999	10.9	0.1743	7.4	0.67	1036.0	70.6	1081.0	72.9	1172.9	161.1	1172.9	161.1	11.7
298	0.0793	10.8	1.8979	16.5	0.1737	12.4	0.76	1032.3	117.9	1080.4	109.9	1178.5	212.7	1178.5	212.7	12.4
244	0.0794	12.9	1.8809	18.6	0.1718	13.3	0.72	1022.2	126.0	1074.4	123.8	1181.8	254.8	1181.8	254.8	13.5
253	0.0794	3.8	1.9936	6.3	0.1821	4.9	0.80	1078.5	49.0	1113.3	42.4	1182.0	74.4	1182.0	74.4	8.8
217	0.0796	3.5	2.0463	5.1	0.1865	4.4	0.74	1102.6	44.9	1131.1	34.7	1186.2	68.6	1186.2	68.6	7.1
284	0.0797	7.4	1.9540	11.5	0.1779	8.4	0.77	1055.2	82.2	1099.8	77.5	1189.1	145.6	1189.1	145.6	11.3
219	0.0797	6.8	2.0120	9.5	0.1831	7.0	0.70	1083.8	69.9	1119.6	64.4	1189.7	134.6	1189.7	134.6	8.9
354	0.0800	3.2	2.0431	5.3	0.1853	4.6	0.80	1095.9	46.2	1130.0	36.4	1196.2	62.9	1196.2	62.9	8.4
126	0.0801	4.8	2.2327	7.0	0.2022	5.5	0.72	1187.3	59.8	1191.4	49.0	1198.7	95.5	1198.7	95.5	0.9
252	0.0801	4.1	1.9682	6.5	0.1781	5.0	0.78	1056.6	48.6	1104.7	43.8	1200.5	80.2	1200.5	80.2	12.0
303	0.0801	5.1	1.9901	7.2	0.1801	5.0	0.71	1067.5	49.2	1112.2	49.0	1200.6	100.7	1200.6	100.7	11.1
108	0.0802	3.3	1.9641	6.3	0.1776	5.2	0.85	1054.0	50.2	1103.3	42.2	1201.8	64.8	1201.8	64.8	12.3
230	0.0802	2.3	2.1133	3.9	0.1911	3.3	0.80	1127.1	34.3	1153.1	26.6	1202.4	46.0	1202.4	46.0	6.3
377	0.0808	9.7	2.2144	14.4	0.1988	10.5	0.74	1168.7	112.6	1185.6	101.1	1216.5	190.1	1216.5	190.1	3.9
344	0.0808	2.9	2.2074	4.1	0.1981	3.7	0.73	1164.8	39.5	1183.4	28.7	1217.4	57.0	1217.4	57.0	4.3
114	0.0810	3.9	2.2065	6.0	0.1975	4.4	0.75	1162.0	46.8	1183.1	41.9	1221.9	77.4	1221.9	77.4	4.9
33	0.0810	11.2	2.2395	16.0	0.2005	11.5	0.72	1177.7	124.3	1193.5	112.7	1222.1	219.4	1222.1	219.4	3.6
337	0.0817	14.0	2.1808	20.4	0.1937	14.9	0.73	1141.3	155.5	1174.9	142.6	1237.4	274.5	1237.4	274.5	7.8
265	0.0823	6.9	2.0519	11.4	0.1808	8.9	0.80	1071.3	88.3	1132.9	77.7	1252.9	134.6	1252.9	134.6	14.5
56	0.0826	11.7	2.2987	16.1	0.2018	11.1	0.69	1185.1	120.6	1211.9	114.5	1259.9	228.0	1259.9	228.0	5.9
4	0.0827	5.4	2.1281	6.6	0.1866	3.8	0.58	1103.1	39.0	1158.0	45.5	1262.1	105.0	1262.1	105.0	12.6
357	0.0828	3.4	2.1472	5.2	0.1881	3.9	0.75	1111.3	39.4	1164.1	35.8	1263.8	67.1	1263.8	67.1	12.1
368	0.0828	9.9	2.1711	12.9	0.1902	8.1	0.65	1122.3	83.2	1171.8	90.1	1264.5	192.7	1264.5	192.7	11.2
295	0.0830	4.7	2.1317	7.3	0.1862	5.4	0.77	1100.6	54.3	1159.1	50.7	1270.3	91.7	1270.3	91.7	13.4
328	0.0836	12.0	2.3316	18.0	0.2023	13.6	0.75	1187.7	147.1	1222.0	128.8	1283.0	234.2	1283.0	234.2	7.4
281	0.0844	6.1	2.2695	9.6	0.1951	7.1	0.77	1149.1	74.8	1202.9	67.5	1300.7	118.6	1300.7	118.6	11.7
165	0.0846	8.9	2.1357	13.5	0.1831	10.1	0.75	1083.8	100.5	1160.4	93.5	1306.4	173.3	1306.4	173.3	17.0
269	0.0860	11.6	2.2382	17.3	0.1886	12.8	0.74	1114.0	131.1	1193.1	122.2	1339.3	224.2	1339.3	224.2	16.8
224	0.0864	5.2	2.5040	7.2	0.2101	5.2	0.69	1229.4	58.1	1273.2	52.3	1347.9	100.8	1347.9	100.8	8.8
186	0.0864	10.5	2.6694	15.1	0.2240	11.1	0.72	1302.8	131.5	1320.0	112.3	1348.2	203.5	1348.2	203.5	3.4
376	0.0865	4.0	2.4591	5.9	0.2062	4.0	0.75	1208.7	43.9	1260.1	42.7	1349.1	76.3	1349.1	76.3	10.4
236	0.0868	5.1	2.4402	7.2	0.2040	5.0	0.71	1196.8	54.6	1254.5	51.8	1355.0	97.5	1355.0	97.5	11.7
392	0.0879	4.7	2.6721	7.4	0.2204	5.7	0.78	1284.0	66.3	1320.8	54.7	1380.9	89.4	1380.9	89.4	7.0
17	0.0892	11.0	2.8165	15.8	0.2289	11.6	0.72	1329.0	138.9	1359.9	118.9	1408.9	211.5	1408.9	211.5	5.7
195	0.0905	7.9	2.7835	13.6	0.2231	11.3	0.81	1298.3	132.7	1351.1	102.0	1435.7	151.5	1435.7	151.5	9.6
119	0.0905	3.1	2.7129	4.7	0.2175	3.5	0.76	1268.4	40.0	1332.0	34.8	1435.7	58.5	1435.7	58.5	11.7
5	0.0908	5.9	2.7251	8.6	0.2177	6.4	0.73	1269.9	73.6	1335.3	64.3	1441.9	111.6	1441.9	111.6	11.9
274	0.0925	4.6	2.8430	7.1	0.2228	5.0	0.77	1296.8	58.2	1367.0	53.7	1478.4	86.9	1478.4	86.9	12.3
92	0.0929	2.3	3.0407	4.4	0.2375	4.0	0.85	1373.5	49.7	1417.9	33.8	1485.2	44.2	1485.2	44.2	7.5
234	0.0931	11.9	2.6807	18.9	0.2087	14.8	0.78	1222.0	164.4	1323.2	140.7	1490.9	224.7	1490.9	224.7	18.0
248	0.0932	3.3	2.8111	6.3	0.2188	5.2	0.85	1275.6	60.7	1358.5	47.6	1491.5	63.3	1491.5	63.3	14.5
305	0.0938	5.4	3.0611	7.0	0.2366	4.8	0.65	1368.9	58.8	1423.0	54.0	1505.0	101.6	1505.0	101.6	9.0
339	0.0947	11.8	2.8256	16.9	0.2165	12.2	0.72	1263.1	140.5	1362.4	127.3	1521.7	221.7	1521.7	221.7	17.0
74	0.0950	9.0	3.0265	11.4	0.2311	7.2	0.62	1340.4	87.5	1414.3	87.0	1527.6	168.7	1527.6	168.7	12.3
29	0.0955	7.5	3.3252	9.8	0.2525	6.8	0.64	1451.5	87.8	1487.0	76.6	1538.0	141.3	1538.0	141.3	5.6
307	0.0957	7.5	2.8876	10.7	0.2188	7.8	0.72	1275.5	90.3	1378.7	80.9	1542.3	140.4	1542.3	140.4	17.3
87	0.0962	5.7	3.4675	8.9	0.2615	7.1	0.77	1497.7	94.6	1519.9	70.0	1550.9	106.6	1550.9	106.6	3.4
229	0.0962	14.6	3.0305	18.2	0.2284	11.0	0.60	1326.1	132.4	1415.3	140.1	1552.2	273.9	1552.2	273.9	14.6
282	0.0965	13.6	3.3385	23.1	0.2508	18.5	0.81	1442.8	239.6	1490.1	182.1	1558.0	255.1	1558.0	255.1	7.4
159	0.0972	6.5	3.3828	11.4	0.2525	9.3	0.82	1451.5	121.0	1500.4	89.6	1570.2	122.0	1570.2	122.0	7.6
143	0.0981	3.8	3.7138	5.9	0.2744	4.8	0.77	1563.3	66.4	1574.3	47.0	1589.2	70.1	1589.2	70.1	1.6
367	0.0983	8.7	3.1967	11.9	0.2358	7.8	0.68	1364.8	96.5	1456.4	92.3	1592.7	162.6	1592.7	162.6	14.3
77	0.0987	8.3	3.4149	11.9	0.2509	8.7	0.72	1443.1	112.7	1507.8	93.9	1600.0	155.5	1600.0	155.5	9.8
129	0.1002	7.5	3.8319	12.7	0.2773	10.6	0.81	1577.8	147.7	1599.5	102.9	1628.2	139.0	1628.2	139.0	3.1
68	0.1005	6.6	3.8170	11.9	0.2756	10.0	0.83	1569.0	138.9	1596.3	96.1	1632.6	122.4	1632.6	122.4	3.9

Table A4.7 (continued): Detrital Zircon U-Pb Integrated Data for the Soncco Formation

Spot	Ratios						Ages (Ma)						Best Age	Disc. (%)		
	207Pb/206Pb		207Pb/235U		206Pb/238U		206Pb/238U		207Pb/235U		207Pb/206Pb					
	±2σ		±2σ		±2σ		±2σ		±2σ		±2σ					
<i>Soncco Formation (20150525-02) Accepted Data</i>																
50	0.1009	8.1	3.5314	10.4	0.2538	6.7	0.63	1457.8	87.3	1534.3	82.4	1641.3	150.3	1641.3	150.3	11.2
104	0.1015	2.1	3.4349	4.2	0.2455	3.4	0.87	1415.1	43.0	1512.4	33.2	1651.4	39.5	1651.4	39.5	14.3
261	0.1015	13.8	3.7402	22.5	0.2672	17.7	0.79	1526.7	240.3	1580.0	181.8	1652.0	256.4	1652.0	256.4	7.6
168	0.1018	13.1	3.6848	19.5	0.2626	14.4	0.74	1503.2	193.5	1568.1	157.1	1656.6	242.9	1656.6	242.9	9.3
71	0.1022	3.9	3.6283	6.1	0.2576	4.8	0.76	1477.4	62.9	1555.8	48.3	1663.8	72.9	1663.8	72.9	11.2
320	0.1023	6.4	3.9017	10.7	0.2767	8.6	0.80	1574.9	120.8	1614.0	86.6	1665.4	119.0	1665.4	119.0	5.4
268	0.1024	8.9	3.5501	13.6	0.2515	10.2	0.76	1446.4	132.6	1538.4	108.3	1667.3	164.7	1667.3	164.7	13.3
18	0.1025	6.5	3.6076	9.3	0.2553	7.1	0.72	1465.6	92.4	1551.2	73.7	1669.9	119.7	1669.9	119.7	12.2
197	0.1028	7.4	3.5799	9.2	0.2526	5.9	0.59	1451.7	76.3	1545.1	72.9	1675.3	136.7	1675.3	136.7	13.3
332	0.1031	9.7	3.7047	14.2	0.2607	10.7	0.73	1493.3	142.1	1572.4	114.4	1680.2	179.1	1680.2	179.1	11.1
262	0.1031	4.0	3.6009	6.5	0.2532	5.0	0.79	1454.9	65.4	1549.7	51.3	1681.6	73.7	1681.6	73.7	13.5
294	0.1039	5.4	4.1232	8.9	0.2877	6.6	0.79	1630.2	94.7	1658.9	72.5	1695.5	100.3	1695.5	100.3	3.9
125	0.1043	9.1	4.1574	14.5	0.2892	11.5	0.78	1637.4	165.8	1665.7	118.9	1701.5	167.6	1701.5	167.6	3.8
6	0.1045	4.5	3.8914	6.2	0.2700	4.3	0.69	1540.6	59.0	1611.9	50.0	1706.3	82.7	1706.3	82.7	9.7
14	0.1050	5.6	4.1747	8.3	0.2884	6.5	0.73	1633.5	94.4	1669.1	67.9	1714.1	103.9	1714.1	103.9	4.7
144	0.1060	7.5	4.4575	10.9	0.3050	8.1	0.73	1716.3	121.7	1723.1	90.7	1731.4	137.5	1731.4	137.5	0.9
106	0.1065	11.2	3.8186	14.8	0.2600	9.6	0.65	1490.0	127.5	1596.7	119.4	1740.5	204.7	1740.5	204.7	14.4
375	0.1070	7.1	3.9716	11.7	0.2693	9.1	0.80	1537.1	124.6	1628.4	95.0	1748.4	129.3	1748.4	129.3	12.1
88	0.1073	5.2	4.1394	10.5	0.2799	9.3	0.87	1590.7	131.7	1662.1	86.4	1753.6	95.8	1753.6	95.8	9.3
348	0.1073	6.3	3.8519	9.2	0.2604	7.1	0.73	1491.9	95.1	1603.7	74.5	1753.8	114.8	1753.8	114.8	14.9
396	0.1080	3.1	4.4800	5.2	0.3009	4.3	0.80	1695.8	64.1	1727.3	43.6	1765.6	57.3	1765.6	57.3	4.0
228	0.1085	14.2	3.7744	18.1	0.2523	11.3	0.62	1450.4	147.2	1587.3	146.5	1774.2	259.7	1774.2	259.7	18.3
384	0.1098	7.4	3.7908	11.7	0.2505	8.9	0.78	1441.0	114.8	1590.8	94.2	1795.4	134.4	1795.4	134.4	19.7
162	0.1102	4.7	4.5374	8.5	0.2987	6.8	0.83	1684.8	101.3	1737.9	70.8	1802.3	86.4	1802.3	86.4	6.5
213	0.1102	3.1	4.4217	4.3	0.2909	3.5	0.70	1646.0	51.5	1716.4	35.5	1803.4	56.4	1803.4	56.4	8.7
246	0.1106	4.9	4.4579	8.3	0.2923	6.5	0.81	1652.9	95.5	1723.2	68.6	1809.7	88.5	1809.7	88.5	8.7
371	0.1115	3.6	4.5515	5.8	0.2961	4.1	0.78	1672.2	60.8	1740.4	48.4	1823.5	66.0	1823.5	66.0	8.3
23	0.1123	3.4	5.1413	4.4	0.3320	3.3	0.63	1848.2	53.4	1843.0	37.2	1837.0	62.1	1837.0	62.1	-0.6
175	0.1124	2.7	4.5280	5.3	0.2922	5.8	0.89	1652.4	84.6	1736.1	44.5	1838.6	48.7	1838.6	48.7	10.1
249	0.1143	8.5	5.1584	13.2	0.3273	10.0	0.76	1825.2	158.7	1845.8	112.5	1869.0	153.4	1869.0	153.4	2.3
242	0.1144	6.1	4.3487	9.6	0.2757	7.3	0.77	1569.7	101.9	1702.6	79.4	1870.4	110.5	1870.4	110.5	16.1
138	0.1148	4.2	5.1244	6.5	0.3238	5.6	0.77	1808.0	87.7	1840.2	55.5	1876.7	75.7	1876.7	75.7	3.7
54	0.1169	4.1	5.3946	5.7	0.3348	4.3	0.70	1861.6	69.0	1884.0	49.1	1908.7	73.5	1908.7	73.5	2.5
366	0.1176	3.9	4.4262	6.5	0.2730	4.8	0.81	1556.1	66.3	1717.3	54.1	1919.8	69.7	1919.8	69.7	18.9
142	0.1236	2.7	6.0973	4.8	0.3577	4.2	0.82	1971.3	71.6	1989.9	41.6	2009.2	48.5	2009.2	48.5	1.9
169	0.1238	3.8	5.0224	7.2	0.2941	6.1	0.85	1662.1	88.8	1823.1	61.0	2012.4	67.6	2012.4	67.6	17.4
148	0.1302	3.2	6.5964	5.3	0.3676	4.6	0.80	2018.0	80.4	2058.9	47.0	2100.0	56.6	2100.0	56.6	3.9
259	0.1331	3.5	5.9736	6.2	0.3254	5.1	0.83	1816.1	80.8	1972.0	53.8	2139.8	60.6	2139.8	60.6	15.1
203	0.1372	5.5	6.7097	8.1	0.3547	6.3	0.74	1957.0	106.6	2073.9	71.8	2192.1	95.7	2192.1	95.7	10.7
46	0.1557	6.2	9.2458	8.9	0.4306	6.7	0.72	2308.2	129.5	2362.7	82.1	2410.0	105.7	2410.0	105.7	4.2
35	0.1795	5.3	10.1438	6.7	0.4099	4.4	0.62	2214.5	83.3	2448.0	62.0	2648.0	87.3	2648.0	87.3	16.4
<i>Soncco Formation (20150525-02) Rejected Data</i>																
51	0.0960	28.3	0.0721	29.6	0.0055	8.9	0.30	35.0	3.1	70.7	20.2	1547.0	531.3	35.0	3.1	50.4
81	0.1311	10.9	0.1154	11.8	0.0064	4.8	0.38	41.0	1.9	110.9	12.4	2112.5	190.8	41.0	1.9	63.0
222	0.0473	19.5	0.0627	27.7	0.0096	19.8	0.71	61.7	12.2	61.7	16.6	62.6	463.7	61.7	12.2	0.0
86	0.1142	10.6	0.1591	11.2	0.0101	4.0	0.32	64.8	2.6	149.9	15.6	1866.7	191.8	64.8	2.6	56.8
158	0.0701	8.2	0.1262	10.7	0.0131	6.7	0.64	83.6	5.6	120.7	12.1	930.7	168.9	83.6	5.6	30.7
95	0.3643	7.0	0.9066	8.2	0.0181	4.3	0.52	115.3	4.9	655.3	39.5	3767.7	105.9	115.3	4.9	82.4
225	0.0858	9.5	0.2617	13.7	0.0221	10.0	0.72	141.0	14.0	236.0	28.9	1334.4	183.7	141.0	14.0	40.3
293	0.1277	7.1	0.4110	8.5	0.0233	4.1	0.56	148.7	6.0	349.6	25.1	2067.2	124.3	148.7	6.0	57.5
300	0.0500	15.5	0.2048	22.7	0.0297	16.6	0.73	188.7	30.8	189.2	39.2	195.6	360.4	188.7	30.8	0.3
122	0.0551	19.5	0.2947	28.3	0.0388	20.5	0.72	245.2	49.4	262.2	65.4	417.4	435.0	245.2	49.4	6.5
39	0.0911	11.7	0.5217	12.8	0.0415	5.4	0.40	262.4	13.9	426.3	44.5	1448.0	222.9	262.4	13.9	38.4
198	0.0670	21.5	0.6001	26.4	0.0650	15.6	0.58	405.9	61.4	477.3	101.0	836.8	447.1	405.9	61.4	15.0
52	0.0585	16.0	0.5627	22.3	0.0698	15.5	0.69	434.8	65.2	453.3	81.6	548.1	350.4	434.8	65.2	4.1
353	0.0657	7.7	0.9368	12.0	0.1034	9.3	0.77	634.4	56.5	671.2	58.9	796.9	161.1	634.4	56.5	20.4
202	0.0746	6.1	1.2576	8.2	0.1222	5.8	0.67	743.4	41.0	826.8	46.3	1058.3	122.8	743.4	41.0	29.8
388	0.0787	13.7	1.3656	17.4	0.1258	10.8	0.62	764.0	77.5	874.3	102.4	1164.9	270.5	764.0	77.5	34.4
301	0.0869	5.7	1.5083	9.1	0.1259	7.0	0.78	764.3	50.4	933.7	55.5	1358.3	109.2	764.3	50.4	43.7
184	0.0741	6.1	1.3826	8.9	0.1354	7.0	0.73	818.7	53.8	881.6	52.8	1043.0	122.8	818.7	53.8	21.5
194	0.0784	16.0	1.4720	21.9	0.1362	15.1	0.68	823.1	117.0	918.9	133.4	1156.7	318.2	823.1	117.0	28.8
270	0.0822	5.2	1.6592	11.7	0.1464	10.2	0.90	880.6	84.3	993.1	74.4	1250.4	100.8	880.6	84.3	29.6
12	0.0722	22.1	1.4798	33.1	0.1486	24.7	0.75	893.2	206.5	922.1	203.3	992.1	448.4	893.2	206.5	10.0

Table A4.7 (continued): Detrital Zircon U-Pb Integrated Data for the Soncco Formation

Spot	Ratios						Rho	Ages (Ma)						Best Age	Disc. (%)	
	207Pb/206Pb		207Pb/235U		206Pb/238U			206Pb/238U		207Pb/235U		207Pb/206Pb				
	±2σ	±2σ	±2σ	±2σ	±2σ	±2σ		±2σ	±2σ	±2σ	±2σ	±2σ				
<i>Soncco Formation (20150525-02) Rejected Data</i>																
166	0.0748	18.4	1.5863	25.7	0.1539	18.0	0.70	922.7	154.8	964.8	161.5	1062.0	369.4	922.7	154.8	13.1
185	0.0796	8.4	1.7343	11.6	0.1580	8.4	0.69	945.8	73.6	1021.3	74.7	1186.9	165.4	945.8	73.6	20.3
360	0.0825	6.7	1.8152	8.9	0.1596	5.7	0.66	954.6	50.2	1051.0	58.3	1257.0	130.8	954.6	50.2	24.1
105	0.0761	17.1	1.6950	23.8	0.1615	16.4	0.69	965.0	147.4	1006.6	152.9	1098.4	342.3	965.0	147.4	12.1
338	0.0783	18.2	1.7499	25.8	0.1622	18.5	0.71	968.8	166.0	1027.1	168.5	1153.5	360.3	968.8	166.0	16.0
239	0.0773	19.3	1.7335	26.9	0.1627	18.8	0.70	972.0	169.3	1021.1	175.1	1127.7	384.2	972.0	169.3	13.8
120	0.0829	7.7	1.8771	9.4	0.1642	5.8	0.58	980.0	52.3	1073.0	62.5	1267.3	149.9	980.0	52.3	22.7
149	0.0728	19.7	1.7538	27.5	0.1746	19.2	0.70	1037.6	184.5	1028.6	179.7	1009.5	400.3	1009.5	400.3	-2.8
67	0.0772	15.6	1.8696	22.0	0.1757	15.6	0.71	1043.6	150.1	1070.4	146.6	1125.3	310.2	1125.3	310.2	7.3
171	0.0775	24.8	1.7963	37.3	0.1680	28.0	0.75	1001.1	260.1	1044.1	248.3	1135.4	493.3	1135.4	493.3	11.8
257	0.0807	17.5	1.8819	23.4	0.1691	15.6	0.66	1007.0	145.3	1074.7	156.7	1214.8	344.5	1214.8	344.5	17.1
235	0.0810	15.1	1.9608	21.5	0.1756	15.3	0.71	1042.8	147.0	1102.2	145.6	1221.4	297.1	1221.4	297.1	14.6
214	0.0838	16.7	2.6815	24.1	0.2321	17.5	0.72	1345.4	212.4	1323.4	179.8	1287.9	325.0	1287.9	325.0	-4.5
160	0.0845	15.3	2.3426	21.3	0.2011	14.7	0.70	1181.0	159.0	1225.3	152.7	1304.2	297.0	1304.2	297.0	9.4
167	0.0849	8.7	2.0468	12.3	0.1749	8.6	0.70	1039.2	82.7	1131.2	84.0	1312.5	169.4	1312.5	169.4	20.8
271	0.0868	13.9	2.0880	19.0	0.1745	12.7	0.68	1037.1	121.8	1144.9	130.9	1355.3	267.4	1355.3	267.4	23.5
204	0.0874	13.4	2.2025	20.0	0.1828	15.0	0.74	1082.0	149.5	1181.9	140.4	1369.5	257.2	1369.5	257.2	21.0
385	0.0889	19.8	2.6044	31.6	0.2124	24.5	0.78	1241.4	277.1	1301.9	235.7	1403.1	380.2	1403.1	380.2	11.5
163	0.0998	31.2	2.4498	40.2	0.1780	25.3	0.63	1055.9	246.9	1257.4	298.4	1620.9	580.6	1620.9	580.6	34.9
251	0.1029	3.5	2.8135	5.7	0.1983	4.4	0.79	1166.3	46.9	1359.1	42.7	1676.9	64.7	1676.9	64.7	30.4
273	0.1030	12.9	3.2046	18.2	0.2257	12.6	0.71	1312.1	150.0	1458.3	142.1	1678.2	238.9	1678.2	238.9	21.8
288	0.1252	12.1	4.9473	17.0	0.2866	11.7	0.71	1624.7	168.4	1810.4	144.7	2031.3	213.3	2031.3	213.3	20.0
66	0.2638	21.1	23.9470	30.8	0.6584	22.5	0.73	3260.8	577.0	3266.2	309.4	3269.6	331.1	3269.6	331.1	0.3

Table A4.8: Detrital Zircon U-Pb Integrated Data for the Punacancha Formation Base

Spot	Ratios						Rho	Ages (Ma)					Best Age	Disc. (%)		
	207Pb/206Pb	$\pm 2\sigma$	207Pb/235U	$\pm 2\sigma$	206Pb/238U	$\pm 2\sigma$		206Pb/238U	$\pm 2\sigma$	207Pb/235U	$\pm 2\sigma$	207Pb/206Pb			$\pm 2\sigma$	
<i>Punacancha Formation Base (20140611-01) Accepted Data</i>																
9	0.0496	20.2	0.0291	22.0	0.0043	8.6	0.39	27.4	2.4	29.1	6.3	175.0	472.2	27.4	2.4	6.0
361	0.0599	16.0	0.0360	16.9	0.0044	5.8	0.32	28.0	1.6	35.9	5.9	599.3	345.7	28.0	1.6	21.9
355	0.0509	11.1	0.0312	12.2	0.0045	5.5	0.42	28.6	1.6	31.2	3.8	236.1	256.5	28.6	1.6	8.3
215	0.0773	26.6	0.0480	28.1	0.0045	9.1	0.32	28.9	2.6	47.6	13.1	1130.2	529.6	28.9	2.6	39.2
345	0.0503	19.9	0.0314	22.7	0.0045	11.1	0.48	29.1	3.2	31.4	7.0	210.8	460.3	29.1	3.2	7.3
75	0.0714	26.2	0.0446	27.4	0.0045	8.2	0.29	29.2	2.4	44.3	11.9	968.4	534.2	29.2	2.4	34.2
309	0.0738	26.6	0.0465	27.6	0.0046	7.4	0.27	29.4	2.2	46.1	12.4	1036.5	536.6	29.4	2.2	36.3
256	0.0638	34.2	0.0413	35.2	0.0047	8.4	0.24	30.2	2.5	41.1	14.2	735.1	724.2	30.2	2.5	26.5
211	0.0664	16.7	0.0437	17.9	0.0048	6.6	0.36	30.7	2.0	43.5	7.6	817.6	348.0	30.7	2.0	29.3
333	0.0570	15.8	0.0378	17.7	0.0048	8.1	0.45	31.0	2.5	37.7	6.6	492.1	349.2	31.0	2.5	17.9
64	0.0655	24.2	0.0436	25.7	0.0048	8.7	0.33	31.1	2.7	43.3	10.9	790.2	508.4	31.1	2.7	28.3
141	0.0484	23.3	0.0324	24.4	0.0048	7.0	0.30	31.2	2.2	32.4	7.8	121.2	548.9	31.2	2.2	3.7
5	0.0504	10.7	0.0338	13.4	0.0049	8.0	0.60	31.2	2.5	33.7	4.5	215.1	248.4	31.2	2.5	7.4
217	0.0621	19.7	0.0416	20.8	0.0049	6.7	0.32	31.3	2.1	41.4	8.4	676.8	421.6	31.3	2.1	24.5
326	0.0635	16.5	0.0427	19.7	0.0049	10.8	0.54	31.4	3.4	42.5	8.2	724.3	349.5	31.4	3.4	26.1
25	0.0670	18.8	0.0458	19.8	0.0050	6.2	0.32	31.9	2.0	45.5	8.8	838.2	390.6	31.9	2.0	29.9
233	0.0692	20.3	0.0478	22.0	0.0050	8.2	0.38	32.2	2.6	47.4	10.2	904.4	419.0	32.2	2.6	32.0
283	0.0681	17.6	0.0471	20.9	0.0050	11.3	0.54	32.3	3.6	46.8	9.6	870.1	365.1	32.3	3.6	30.9
284	0.0521	13.8	0.0362	14.6	0.0050	4.7	0.32	32.4	1.5	36.1	5.2	291.4	315.2	32.4	1.5	10.3
80	0.0683	20.0	0.0490	21.4	0.0052	7.5	0.35	33.4	2.5	48.6	10.1	877.6	414.5	33.4	2.5	31.1
224	0.0662	24.9	0.0475	25.8	0.0052	6.6	0.25	33.5	2.2	47.1	11.9	813.2	521.3	33.5	2.2	29.0
306	0.0598	17.0	0.0429	18.4	0.0052	7.3	0.39	33.5	2.4	42.7	7.7	596.0	367.7	33.5	2.4	21.6
179	0.0517	18.5	0.0372	19.4	0.0052	5.8	0.30	33.5	1.9	37.0	7.0	273.5	422.9	33.5	1.9	9.6
301	0.0637	22.4	0.0460	23.7	0.0052	7.9	0.33	33.7	2.7	45.7	10.6	732.0	473.5	33.7	2.7	26.3
312	0.0471	12.7	0.0342	17.8	0.0053	12.5	0.70	33.9	4.2	34.1	6.0	51.9	304.3	33.9	4.2	0.7
111	0.0711	15.9	0.0518	20.6	0.0053	13.0	0.63	34.0	4.4	51.3	10.3	960.6	325.2	34.0	4.4	33.8
399	0.0512	15.5	0.0375	17.0	0.0053	7.0	0.41	34.1	2.4	37.4	6.2	249.5	356.7	34.1	2.4	8.6
247	0.0526	11.4	0.0387	13.9	0.0053	8.0	0.58	34.3	2.7	38.6	5.3	312.1	258.8	34.3	2.7	11.0
110	0.0565	13.3	0.0418	15.3	0.0054	7.5	0.49	34.4	2.6	41.5	6.2	473.5	294.5	34.4	2.6	17.1
171	0.0634	14.6	0.0468	15.4	0.0054	4.6	0.32	34.4	1.6	46.5	7.0	721.3	310.2	34.4	1.6	25.9
122	0.0583	15.8	0.0432	19.1	0.0054	10.6	0.56	34.5	3.7	42.9	8.0	542.1	345.8	34.5	3.7	19.6
143	0.0599	15.5	0.0445	16.7	0.0054	5.9	0.37	34.6	2.0	44.2	7.2	601.7	336.0	34.6	2.0	21.7
45	0.0526	13.8	0.0392	14.8	0.0054	5.4	0.36	34.8	1.9	39.1	5.7	311.3	314.1	34.8	1.9	11.0
172	0.0512	8.9	0.0384	9.9	0.0054	4.1	0.44	35.0	1.4	38.3	3.7	250.8	205.8	35.0	1.4	8.6
288	0.0558	16.3	0.0419	17.4	0.0054	6.3	0.36	35.0	2.2	41.7	7.1	445.3	361.7	35.0	2.2	16.0
120	0.0570	12.0	0.0428	13.1	0.0055	5.4	0.41	35.1	1.9	42.6	5.5	490.2	263.7	35.1	1.9	17.7
56	0.0585	13.8	0.0440	14.4	0.0055	4.4	0.30	35.1	1.5	43.7	6.2	549.0	300.4	35.1	1.5	19.8
337	0.0577	12.2	0.0434	13.4	0.0055	5.7	0.40	35.1	2.0	43.2	5.7	518.8	268.8	35.1	2.0	18.7
135	0.0566	16.5	0.0428	20.6	0.0055	12.4	0.60	35.3	4.4	42.5	8.6	474.6	364.3	35.3	4.4	17.1
272	0.0566	14.2	0.0428	15.6	0.0055	6.4	0.41	35.3	2.2	42.6	6.5	474.9	314.9	35.3	2.2	17.1
59	0.0524	16.9	0.0398	17.8	0.0055	5.7	0.32	35.4	2.0	39.6	6.9	302.4	385.7	35.4	2.0	10.6
113	0.0533	16.4	0.0405	17.1	0.0055	4.6	0.27	35.5	1.6	40.4	6.7	342.4	371.5	35.5	1.6	12.1
86	0.0677	19.0	0.0515	19.9	0.0055	6.1	0.30	35.5	2.2	51.0	9.9	860.6	393.4	35.5	2.2	30.5
81	0.0531	9.8	0.0404	11.2	0.0055	5.5	0.49	35.5	2.0	40.2	4.4	332.2	221.9	35.5	2.0	11.8
241	0.0561	19.1	0.0429	19.9	0.0055	5.4	0.28	35.6	1.9	42.6	8.3	456.7	423.2	35.6	1.9	16.4
366	0.0656	22.8	0.0501	23.6	0.0055	6.0	0.25	35.7	2.1	49.7	11.4	792.7	478.5	35.7	2.1	28.2
103	0.0583	13.8	0.0449	15.2	0.0056	6.4	0.42	35.9	2.3	44.6	6.6	539.6	301.9	35.9	2.3	19.4
74	0.0640	25.2	0.0494	26.6	0.0056	8.4	0.31	36.0	3.0	49.0	12.7	740.7	533.8	36.0	3.0	26.5
133	0.0536	15.0	0.0415	18.9	0.0056	11.5	0.61	36.1	4.1	41.3	7.6	352.8	338.4	36.1	4.1	12.5
26	0.0651	12.1	0.0505	13.4	0.0056	5.8	0.43	36.2	2.1	50.0	6.5	778.4	253.7	36.2	2.1	27.7
149	0.0568	19.1	0.0442	20.3	0.0056	6.2	0.34	36.3	2.3	43.9	8.7	485.2	422.7	36.3	2.3	17.4
290	0.0584	19.0	0.0455	21.0	0.0056	9.1	0.43	36.3	3.3	45.1	9.3	545.5	414.1	36.3	3.3	19.6
353	0.0534	9.9	0.0419	10.7	0.0057	4.3	0.37	36.5	1.6	41.6	4.4	346.5	224.1	36.5	1.6	12.3
47	0.0537	18.2	0.0421	19.0	0.0057	5.6	0.29	36.6	2.1	41.9	7.8	357.3	410.1	36.6	2.1	12.7
221	0.0533	12.7	0.0425	16.1	0.0058	10.0	0.62	37.2	3.7	42.2	6.7	340.4	287.0	37.2	3.7	12.0
40	0.0617	13.9	0.0492	15.2	0.0058	6.1	0.40	37.2	2.3	48.7	7.2	662.2	298.6	37.2	2.3	23.7
95	0.0482	28.5	0.0385	29.8	0.0058	8.5	0.29	37.2	3.1	38.3	11.2	109.9	673.2	37.2	3.1	3.0
89	0.0661	14.7	0.0536	16.4	0.0059	7.4	0.45	37.8	2.8	53.0	8.5	809.4	308.0	37.8	2.8	28.7
176	0.0554	10.4	0.0451	11.4	0.0059	4.6	0.41	38.0	1.7	44.8	5.0	428.9	232.3	38.0	1.7	15.3
126	0.0658	24.4	0.0539	27.5	0.0059	12.7	0.46	38.1	4.8	53.3	14.3	800.5	511.6	38.1	4.8	28.4
91	0.0503	14.9	0.0412	15.5	0.0059	4.3	0.28	38.2	1.6	41.0	6.2	208.6	345.6	38.2	1.6	6.9
207	0.0513	11.2	0.0428	12.2	0.0061	5.0	0.39	38.9	1.9	42.6	5.1	254.3	257.1	38.9	1.9	8.6
152	0.0513	12.0	0.0429	15.0	0.0061	8.7	0.60	39.0	3.4	42.7	6.3	252.5	276.3	39.0	3.4	8.5

Table A4.8 (continued): Detrital Zircon U-Pb Integrated Data for the Punacancha Formation Base

Spot	Ratios						Ages (Ma)						Best Age	Disc. (%)		
	207Pb/ 206Pb	±2σ	207Pb/ 235U	±2σ	206Pb/ 238U	±2σ	206Pb/ 238U	±2σ	207Pb/ 235U	±2σ	207Pb/ 206Pb	±2σ				
<i>Punacancha Formation Base (20140611-01) Accepted Data</i>																
155	0.0575	21.9	0.0485	23.0	0.0061	6.7	0.31	39.3	2.6	48.1	10.8	511.8	481.9	39.3	2.6	18.3
35	0.0584	16.7	0.0494	19.5	0.0061	10.0	0.52	39.4	3.9	49.0	9.3	545.5	365.4	39.4	3.9	19.5
121	0.0521	12.8	0.0441	14.1	0.0061	5.9	0.42	39.4	2.3	43.8	6.0	290.7	291.9	39.4	2.3	10.0
346	0.0669	22.7	0.0574	23.6	0.0062	6.7	0.27	39.9	2.7	56.6	13.0	836.1	472.9	39.9	2.7	29.5
11	0.0664	22.3	0.0569	24.1	0.0062	9.1	0.38	40.0	3.6	56.2	13.2	818.3	466.2	40.0	3.6	28.9
318	0.0563	14.5	0.0483	16.1	0.0062	7.0	0.43	40.0	2.8	47.9	7.5	463.5	320.7	40.0	2.8	16.5
372	0.0499	17.4	0.0432	19.4	0.0063	8.5	0.44	40.4	3.4	42.9	8.1	189.6	404.5	40.4	3.4	6.0
354	0.0547	16.5	0.0478	17.3	0.0063	5.6	0.31	40.8	2.3	47.4	8.0	398.0	368.8	40.8	2.3	14.0
219	0.0521	9.4	0.0458	10.4	0.0064	4.3	0.41	40.9	1.8	45.4	4.6	290.7	215.7	40.9	1.8	9.9
371	0.0770	20.4	0.0711	24.9	0.0067	14.4	0.58	43.0	6.2	69.8	16.8	1121.7	406.2	43.0	6.2	38.3
96	0.0482	14.4	0.0461	17.9	0.0069	10.5	0.59	44.6	4.7	45.8	8.0	108.7	340.4	44.6	4.7	2.6
99	0.0498	14.1	0.0482	20.2	0.0070	14.5	0.72	45.1	6.5	47.8	9.5	183.6	328.5	45.1	6.5	5.6
295	0.0663	18.6	0.0681	22.3	0.0074	12.4	0.55	47.8	5.9	66.9	14.4	816.9	388.4	47.8	5.9	28.5
187	0.0583	12.5	0.0728	16.7	0.0091	11.1	0.66	58.1	6.4	71.3	11.5	540.3	273.1	58.1	6.4	18.5
130	0.0592	12.9	0.0776	15.2	0.0095	8.0	0.52	61.0	4.8	75.9	11.1	574.4	281.4	61.0	4.8	19.6
227	0.0508	8.5	0.0677	9.3	0.0097	4.0	0.41	62.0	2.4	66.5	6.0	231.5	196.1	62.0	2.4	6.8
286	0.0571	15.6	0.0775	17.1	0.0098	7.1	0.41	63.1	4.5	75.8	12.5	496.0	343.6	63.1	4.5	16.7
21	0.0649	9.6	0.0896	12.4	0.0100	7.8	0.63	64.3	5.0	87.2	10.4	770.1	202.7	64.3	5.0	26.2
327	0.0475	11.6	0.0669	15.8	0.0102	10.9	0.68	65.4	7.1	65.7	10.1	75.8	274.9	65.4	7.1	0.4
285	0.0549	14.7	0.0773	15.3	0.0102	4.2	0.27	65.5	2.7	75.6	11.1	408.8	329.0	65.5	2.7	13.4
329	0.0570	10.6	0.0812	11.7	0.0103	5.2	0.43	66.3	3.4	79.3	8.9	490.9	233.5	66.3	3.4	16.4
53	0.0580	11.8	0.0844	14.7	0.0105	8.8	0.60	67.6	5.9	82.3	11.6	530.3	258.3	67.6	5.9	17.8
201	0.0515	7.8	0.0750	9.2	0.0106	5.1	0.54	67.7	3.4	73.4	6.5	263.4	179.0	67.7	3.4	7.8
100	0.0469	7.1	0.0690	10.2	0.0107	7.3	0.72	68.4	4.9	67.8	6.7	45.2	169.5	68.4	4.9	-0.9
28	0.0524	14.0	0.0775	18.5	0.0107	12.1	0.65	68.8	8.2	75.8	13.5	304.1	319.6	68.8	8.2	9.3
154	0.0520	9.2	0.0769	12.4	0.0107	8.1	0.67	68.9	5.5	75.3	9.0	283.7	210.1	68.9	5.5	8.5
7	0.0528	10.8	0.0790	12.5	0.0109	6.1	0.50	69.6	4.3	77.2	9.3	318.9	246.2	69.6	4.3	9.8
268	0.0546	18.2	0.0819	19.6	0.0109	7.0	0.36	69.8	4.9	79.9	15.0	395.3	408.9	69.8	4.9	12.7
267	0.0575	11.0	0.0883	12.4	0.0111	5.7	0.46	71.3	4.0	85.9	10.2	512.3	242.6	71.3	4.0	17.0
97	0.0510	17.1	0.0792	18.8	0.0113	7.7	0.41	72.2	5.5	77.4	14.0	242.7	395.0	72.2	5.5	6.8
70	0.0419	7.9	0.0665	9.0	0.0115	4.4	0.48	73.8	3.2	65.4	5.7	-231.2	198.4	73.8	3.2	-12.8
281	0.0573	11.4	0.0926	12.4	0.0117	5.0	0.40	75.2	3.7	89.9	10.6	502.0	249.8	75.2	3.7	16.4
310	0.0578	12.5	0.0937	15.0	0.0118	8.4	0.55	75.4	6.3	91.0	13.1	521.4	274.0	75.4	6.3	17.1
209	0.0556	8.6	0.0908	9.6	0.0118	4.6	0.46	75.9	3.5	88.2	8.1	436.8	190.8	75.9	3.5	14.0
170	0.0474	7.9	0.0776	10.8	0.0119	7.3	0.69	76.0	5.6	75.9	7.9	71.1	186.8	76.0	5.6	-0.2
381	0.0619	12.3	0.1014	13.1	0.0119	4.6	0.35	76.1	3.5	98.0	12.2	671.2	262.3	76.1	3.5	22.4
78	0.0500	9.3	0.0823	11.9	0.0119	7.5	0.62	76.5	5.7	80.3	9.2	196.1	215.7	76.5	5.7	4.8
3	0.0682	15.8	0.1136	17.1	0.0121	6.5	0.38	77.4	5.0	109.3	17.7	875.9	326.8	77.4	5.0	29.2
232	0.0590	9.2	0.0990	10.1	0.0122	3.9	0.41	78.0	3.0	95.9	9.2	567.8	200.2	78.0	3.0	18.7
374	0.0597	8.8	0.1005	11.9	0.0122	8.0	0.67	78.3	6.2	97.3	11.0	592.1	190.6	78.3	6.2	19.5
202	0.0489	11.2	0.0830	13.2	0.0123	7.2	0.54	78.8	5.6	80.9	10.3	143.5	261.8	78.8	5.6	2.6
246	0.0546	17.8	0.0931	18.8	0.0124	5.9	0.32	79.2	4.6	90.4	16.3	397.5	399.6	79.2	4.6	12.4
218	0.0479	8.2	0.0843	10.3	0.0128	6.2	0.60	81.7	5.0	82.1	8.1	95.6	194.4	81.7	5.0	0.6
148	0.0522	7.5	0.0925	8.9	0.0129	4.0	0.54	82.4	3.2	89.9	7.7	293.9	172.1	82.4	3.2	8.3
258	0.0487	6.9	0.0879	9.7	0.0131	6.6	0.70	83.8	5.5	85.5	7.9	134.1	161.9	83.8	5.5	2.0
156	0.0523	8.2	0.0953	9.7	0.0132	4.6	0.53	84.6	3.9	92.5	8.5	299.1	187.6	84.6	3.9	8.5
287	0.0482	6.6	0.0881	8.7	0.0133	5.8	0.66	84.9	4.9	85.7	7.2	109.4	155.1	84.9	4.9	1.0
373	0.0527	6.9	0.0982	8.9	0.0135	5.7	0.64	86.5	4.9	95.1	8.1	317.4	155.9	86.5	4.9	9.1
299	0.0555	9.4	0.1038	11.7	0.0136	7.1	0.59	86.8	6.1	100.3	11.1	433.9	209.1	86.8	6.1	13.4
242	0.0500	4.4	0.0951	5.3	0.0138	2.7	0.56	88.4	2.4	92.3	4.6	193.5	101.4	88.4	2.4	4.2
311	0.0494	11.0	0.0958	15.6	0.0141	11.2	0.71	90.0	10.0	92.9	13.9	167.2	255.9	90.0	10.0	3.1
15	0.0516	7.7	0.1010	10.6	0.0142	7.2	0.69	90.9	6.5	97.7	9.9	266.8	176.9	90.9	6.5	7.0
167	0.0498	5.8	0.0981	7.4	0.0143	4.2	0.63	91.5	3.8	95.1	6.7	184.3	134.1	91.5	3.8	3.7
297	0.0506	6.4	0.1005	8.4	0.0144	5.7	0.65	92.2	5.2	97.2	7.8	221.1	148.4	92.2	5.2	5.1
280	0.0512	9.0	0.1041	11.3	0.0148	6.8	0.60	94.5	6.4	100.6	10.8	247.7	206.5	94.5	6.4	6.1
313	0.0486	9.6	0.1037	13.5	0.0155	9.5	0.70	98.9	9.3	100.2	12.9	130.8	226.6	98.9	9.3	1.3
19	0.0568	6.4	0.1237	7.3	0.0158	3.5	0.49	101.0	3.5	118.4	8.2	484.6	141.0	101.0	3.5	14.7
334	0.0579	11.6	0.1269	14.3	0.0159	8.5	0.58	101.7	8.5	121.3	16.3	525.6	254.3	101.7	8.5	16.2
151	0.0504	7.1	0.1123	10.7	0.0162	7.7	0.75	103.4	7.9	108.1	10.9	212.2	163.4	103.4	7.9	4.3
186	0.0658	11.7	0.1470	12.6	0.0162	4.8	0.38	103.6	5.0	139.3	16.4	800.8	244.2	103.6	5.0	25.6
196	0.0562	13.7	0.1271	18.4	0.0164	12.3	0.66	104.9	12.8	121.5	21.0	459.4	304.5	104.9	12.8	13.6
142	0.0532	8.4	0.1219	10.2	0.0166	5.3	0.56	106.2	5.6	116.8	11.2	338.1	190.5	106.2	5.6	9.1
266	0.0540	11.1	0.1238	15.4	0.0166	10.7	0.69	106.3	11.2	118.5	17.2	371.2	249.1	106.3	11.2	10.3

Table A4.8 (continued): Detrital Zircon U-Pb Integrated Data for the Punacancha Formation Base

Spot	Ratios						Ages (Ma)						Best Age	Disc. (%)		
	207Pb/206Pb	±2σ	207Pb/235U	±2σ	206Pb/238U	±2σ	Rho	206Pb/238U	±2σ	207Pb/235U	±2σ	207Pb/206Pb			±2σ	
<i>Punacancha Formation Base (20140611-01) Accepted Data</i>																
52	0.0531	11.8	0.1318	15.5	0.0180	10.2	0.65	114.9	11.6	125.7	18.4	334.7	266.4	114.9	11.6	8.6
317	0.0519	10.3	0.1289	12.2	0.0180	6.6	0.54	115.0	7.6	123.1	14.2	281.9	234.9	115.0	7.6	6.6
400	0.0486	8.7	0.1250	12.1	0.0186	8.5	0.69	119.1	10.0	119.6	13.7	129.9	205.3	119.1	10.0	0.4
63	0.0553	18.6	0.1464	23.7	0.0192	14.7	0.62	122.6	17.8	138.7	30.7	423.1	414.1	122.6	17.8	11.6
384	0.0517	6.4	0.1428	8.4	0.0200	5.4	0.64	127.8	6.8	135.5	10.6	272.4	147.4	127.8	6.8	5.7
146	0.0504	4.5	0.1417	6.2	0.0204	3.4	0.72	130.1	4.4	134.6	7.9	214.8	103.4	130.1	4.4	3.3
394	0.0505	6.4	0.1425	8.3	0.0205	5.5	0.65	130.6	7.1	135.3	10.6	217.8	147.0	130.6	7.1	3.4
204	0.0627	10.1	0.1823	11.1	0.0211	4.8	0.42	134.5	6.4	170.1	17.4	699.4	214.3	134.5	6.4	20.9
364	0.0511	9.6	0.1495	13.9	0.0212	10.0	0.72	135.3	13.5	141.5	18.3	247.1	220.7	135.3	13.5	4.4
386	0.0510	6.9	0.1501	8.5	0.0213	5.0	0.58	136.2	6.7	142.0	11.2	240.8	158.5	136.2	6.7	4.1
127	0.0521	4.9	0.1554	6.4	0.0216	4.0	0.64	137.8	5.4	146.7	8.7	291.9	112.6	137.8	5.4	6.0
276	0.0501	11.4	0.1492	15.9	0.0216	11.1	0.70	137.9	15.1	141.2	21.0	197.4	264.6	137.9	15.1	2.4
157	0.0511	9.0	0.1529	12.1	0.0217	7.8	0.67	138.4	10.7	144.4	16.3	244.8	208.1	138.4	10.7	4.2
331	0.0513	6.5	0.1567	7.4	0.0221	3.9	0.48	141.1	5.4	147.8	10.2	256.2	150.1	141.1	5.4	4.5
71	0.0522	5.2	0.1609	5.9	0.0224	2.8	0.45	142.5	4.0	151.5	8.3	294.3	119.6	142.5	4.0	5.9
41	0.0472	8.7	0.1458	10.1	0.0224	5.2	0.50	142.7	7.3	138.2	13.0	61.2	207.2	142.7	7.3	-3.3
16	0.0545	5.4	0.1703	10.4	0.0227	8.8	0.85	144.5	12.6	159.7	15.3	390.8	121.6	144.5	12.6	9.5
193	0.0502	9.2	0.1572	12.8	0.0227	8.9	0.69	144.7	12.8	148.3	17.7	204.9	214.5	144.7	12.8	2.4
39	0.0543	13.7	0.1712	16.8	0.0229	9.6	0.58	145.7	13.9	160.4	24.9	383.7	307.2	145.7	13.9	9.2
230	0.0489	12.7	0.1572	17.9	0.0233	12.6	0.71	148.5	18.6	148.3	24.7	144.3	297.2	148.5	18.6	-0.2
164	0.0610	6.9	0.1960	9.6	0.0233	6.5	0.70	148.6	9.5	181.8	16.0	638.1	147.5	148.6	9.5	18.2
199	0.0509	12.5	0.1681	17.4	0.0240	12.1	0.69	152.8	18.2	157.8	25.4	234.4	289.3	152.8	18.2	3.2
181	0.0537	9.2	0.1808	10.5	0.0244	5.2	0.49	155.4	7.9	168.7	16.4	359.3	207.5	155.4	7.9	7.9
48	0.0492	6.4	0.1786	8.3	0.0263	5.4	0.64	167.4	8.9	166.9	12.8	159.7	148.7	167.4	8.9	-0.3
104	0.0510	7.9	0.1909	9.0	0.0271	4.2	0.47	172.6	7.2	177.4	14.6	240.8	182.8	172.6	7.2	2.7
69	0.0508	9.3	0.1952	11.7	0.0279	7.3	0.61	177.2	12.7	181.1	19.4	232.2	214.5	177.2	12.7	2.2
363	0.0568	9.4	0.2183	12.8	0.0279	9.0	0.68	177.4	15.7	200.5	23.3	482.2	207.8	177.4	15.7	11.5
245	0.0488	16.7	0.1963	20.9	0.0292	12.6	0.61	185.5	23.1	182.0	34.9	137.4	391.5	185.5	23.1	-1.9
88	0.0607	12.8	0.2476	13.5	0.0296	4.3	0.32	187.9	8.0	224.6	27.1	630.0	274.8	187.9	8.0	16.4
158	0.0540	12.6	0.2203	15.9	0.0296	9.4	0.61	187.9	17.5	202.2	29.1	372.2	284.3	187.9	17.5	7.1
1	0.0545	13.4	0.2260	18.3	0.0300	12.5	0.68	190.8	23.5	206.9	34.3	393.7	299.8	190.8	23.5	7.8
300	0.0679	14.6	0.2885	20.8	0.0308	14.9	0.71	195.6	28.6	257.4	47.4	866.3	303.6	195.6	28.6	24.0
105	0.0511	7.5	0.2219	9.9	0.0315	6.5	0.66	199.8	12.9	203.5	18.3	247.0	172.1	199.8	12.9	1.8
398	0.0575	13.0	0.2608	14.7	0.0329	7.0	0.47	208.7	14.5	235.3	31.0	509.9	285.2	208.7	14.5	11.3
58	0.0617	10.4	0.3180	11.8	0.0374	5.7	0.48	236.7	13.2	280.4	29.0	663.0	222.7	236.7	13.2	15.6
101	0.0520	4.8	0.2725	6.5	0.0380	4.4	0.68	240.6	10.4	244.7	14.2	283.9	110.2	240.6	10.4	1.7
382	0.0626	7.2	0.3383	8.2	0.0392	3.9	0.47	247.8	9.4	295.9	20.9	694.8	153.6	247.8	9.4	16.2
106	0.0532	6.1	0.2906	7.3	0.0396	4.0	0.55	250.3	9.8	259.0	16.6	338.5	137.6	250.3	9.8	3.4
239	0.0521	5.3	0.2880	8.1	0.0401	5.9	0.76	253.2	14.7	257.0	18.5	291.8	121.9	253.2	14.7	1.5
169	0.0504	3.7	0.2846	5.0	0.0409	2.8	0.68	258.5	7.1	254.3	11.2	215.5	85.7	258.5	7.1	-1.7
188	0.0521	3.0	0.3004	4.1	0.0418	2.8	0.68	264.1	7.4	266.7	9.6	290.4	68.6	264.1	7.4	1.0
294	0.0534	7.2	0.3117	10.0	0.0423	7.1	0.69	267.2	18.6	275.5	24.2	346.1	163.8	267.2	18.6	3.0
136	0.0525	5.3	0.3071	6.7	0.0424	4.2	0.62	267.9	10.9	271.9	16.0	306.7	120.6	267.9	10.9	1.5
83	0.0512	5.4	0.3014	6.7	0.0427	4.2	0.60	269.3	11.0	267.5	15.8	251.6	123.9	269.3	11.0	-0.7
292	0.0536	5.1	0.3273	7.7	0.0443	5.9	0.74	279.3	16.1	287.5	19.2	354.3	115.8	279.3	16.1	2.8
117	0.0546	4.9	0.4055	6.7	0.0538	4.5	0.68	338.1	14.8	345.6	19.7	396.4	110.7	338.1	14.8	2.2
118	0.0564	5.1	0.4405	9.2	0.0567	7.6	0.83	355.4	26.1	370.6	28.5	467.0	113.5	355.4	26.1	4.1
336	0.0555	7.9	0.5637	10.7	0.0736	7.4	0.68	458.0	32.8	453.9	39.1	433.3	175.3	458.0	32.8	-0.9
191	0.0575	4.8	0.6080	6.7	0.0768	4.8	0.70	476.7	22.2	482.3	25.9	508.9	106.1	476.7	22.2	1.2
240	0.0573	5.1	0.6366	7.0	0.0805	4.7	0.69	499.2	22.7	500.2	27.7	504.6	111.3	499.2	22.7	0.2
79	0.0581	3.8	0.6693	5.1	0.0835	3.6	0.67	517.2	18.1	520.3	20.7	533.9	82.4	517.2	18.1	0.6
236	0.0608	5.9	0.7143	8.7	0.0852	6.2	0.74	526.9	31.5	547.3	36.9	633.1	126.2	526.9	31.5	3.7
323	0.0566	3.4	0.6674	4.2	0.0856	2.7	0.59	529.2	13.6	519.2	17.1	475.1	75.2	529.2	13.6	-1.9
208	0.0581	7.3	0.6861	10.6	0.0857	7.7	0.72	530.1	39.3	530.4	43.7	532.1	160.4	530.1	39.3	0.1
390	0.0600	3.0	0.7136	4.4	0.0862	3.2	0.72	533.0	16.4	546.9	18.4	605.1	65.0	533.0	16.4	2.5
61	0.0653	14.6	0.7784	17.7	0.0865	10.0	0.56	534.8	51.1	584.6	78.7	783.0	306.8	534.8	51.1	8.5
214	0.0601	4.4	0.7248	5.9	0.0874	4.0	0.67	540.3	20.9	553.5	25.2	608.4	94.5	540.3	20.9	2.4
90	0.0619	5.7	0.7555	7.6	0.0885	5.0	0.66	546.5	26.1	571.4	33.2	671.8	121.9	546.5	26.1	4.4
255	0.0595	5.1	0.7286	6.9	0.0888	4.5	0.68	548.6	23.8	555.7	29.7	585.2	110.8	548.6	23.8	1.3
192	0.0589	9.7	0.7273	13.9	0.0895	9.9	0.71	552.5	52.6	554.9	59.3	564.9	211.9	552.5	52.6	0.4
93	0.0610	5.1	0.7532	6.6	0.0895	4.1	0.64	552.7	21.9	570.1	28.7	639.7	109.3	552.7	21.9	3.0
216	0.0588	2.8	0.7274	4.2	0.0897	3.2	0.74	553.5	16.7	555.1	17.8	561.4	61.2	553.5	16.7	0.3
261	0.0586	5.6	0.7342	8.6	0.0909	6.4	0.76	560.7	34.4	559.0	36.9	552.0	122.7	560.7	34.4	-0.3

Table A4.8 (continued): Detrital Zircon U-Pb Integrated Data for the Punacancha Formation Base

Spot	Ratios						Ages (Ma)						Disc. (%)			
	207Pb/ 206Pb		207Pb/ 235U		206Pb/ 238U		206Pb/ 238U		207Pb/ 235U		207Pb/ 206Pb			Best Age		
	±2σ	±2σ	±2σ	±2σ	±2σ	±2σ	±2σ	±2σ	±2σ	±2σ	±2σ	±2σ	±2σ			
<i>Punacancha Formation Base (20140611-01) Accepted Data</i>																
359	0.0589	9.0	0.7391	12.7	0.0910	9.3	0.71	561.2	49.8	561.9	55.0	564.7	196.6	561.2	49.8	0.1
54	0.0690	6.1	0.8665	9.2	0.0910	6.9	0.75	561.7	37.2	633.7	43.4	899.4	126.0	561.7	37.2	11.4
92	0.0594	5.5	0.7484	8.1	0.0913	6.0	0.74	563.5	32.3	567.3	35.4	582.8	118.7	563.5	32.3	0.7
213	0.0607	4.3	0.7646	5.5	0.0914	3.6	0.63	563.7	19.4	576.7	24.3	628.2	92.5	563.7	19.4	2.3
307	0.0628	3.6	0.7945	4.8	0.0917	3.4	0.67	565.5	18.3	593.7	21.4	703.1	75.7	565.5	18.3	4.8
340	0.0717	6.6	0.9128	7.6	0.0923	4.1	0.51	569.1	22.4	658.5	36.9	978.2	133.6	569.1	22.4	13.6
174	0.0595	3.9	0.7777	6.5	0.0948	5.0	0.80	583.7	28.1	584.2	29.0	586.2	84.8	583.7	28.1	0.1
226	0.0615	3.3	0.8109	4.6	0.0957	3.3	0.69	589.1	18.8	603.0	21.0	655.4	71.7	589.1	18.8	2.3
165	0.0634	4.0	0.8374	5.2	0.0959	2.8	0.65	590.1	15.9	617.7	24.1	720.5	84.8	590.1	15.9	4.5
132	0.0605	3.2	0.8135	4.5	0.0975	3.2	0.69	599.8	18.2	604.4	20.3	622.0	69.2	599.8	18.2	0.8
197	0.0598	2.8	0.8106	3.8	0.0983	3.0	0.70	604.2	17.2	602.8	17.4	597.4	59.6	604.2	17.2	-1.1
344	0.0597	4.4	0.8295	5.7	0.1007	4.0	0.64	618.6	23.7	613.4	26.4	594.2	96.1	618.6	23.7	-4.1
180	0.0613	7.1	0.8542	8.8	0.1011	5.2	0.59	620.9	31.0	626.9	41.4	648.8	153.0	620.9	31.0	4.3
12	0.0645	12.9	0.9236	18.7	0.1038	13.4	0.72	636.9	81.3	664.3	91.2	758.3	273.1	636.9	81.3	16.0
237	0.0612	3.4	0.8811	5.4	0.1044	3.9	0.78	640.2	23.6	641.6	25.9	646.6	73.9	640.2	23.6	1.0
139	0.0627	5.7	0.9427	7.0	0.1090	4.1	0.58	667.2	26.2	674.3	34.7	698.0	121.8	667.2	26.2	4.4
324	0.0657	5.9	1.0105	8.2	0.1115	5.8	0.70	681.5	37.4	709.1	41.8	797.5	123.3	681.5	37.4	14.5
358	0.0645	5.6	1.0670	7.8	0.1200	5.8	0.70	730.6	40.4	737.3	40.7	757.4	117.4	730.6	40.4	3.5
348	0.0690	4.8	1.2494	6.1	0.1314	4.1	0.62	795.7	30.9	823.1	34.2	898.0	98.1	795.7	30.9	11.4
128	0.0719	8.3	1.3160	9.1	0.1327	3.7	0.42	803.4	27.8	852.8	52.5	983.6	168.4	803.4	27.8	18.3
8	0.0702	7.9	1.2910	14.3	0.1333	12.0	0.84	806.7	90.7	841.7	82.2	935.2	161.3	806.7	90.7	13.7
265	0.0711	3.0	1.3920	4.4	0.1419	3.1	0.73	855.6	25.2	885.5	25.9	961.2	60.8	855.6	25.2	11.0
389	0.0699	3.0	1.3912	4.5	0.1443	3.3	0.74	868.8	27.2	885.2	26.4	926.4	62.0	868.8	27.2	6.2
18	0.0723	4.1	1.4555	6.0	0.1459	4.3	0.72	878.0	35.2	912.1	36.1	995.6	83.9	878.0	35.2	11.8
388	0.0767	8.2	1.6375	10.9	0.1548	7.2	0.66	927.7	61.9	984.8	68.7	1114.3	163.7	927.7	61.9	16.7
144	0.0749	5.0	1.6033	7.1	0.1552	4.6	0.71	930.0	39.6	971.5	44.6	1066.7	101.4	930.0	39.6	12.8
161	0.0701	7.1	1.6266	10.5	0.1682	7.6	0.74	1002.2	70.8	980.6	66.3	932.4	145.7	932.4	145.7	-7.5
150	0.0756	3.6	1.6304	5.7	0.1564	4.0	0.79	937.0	34.5	982.0	36.2	1084.0	71.4	937.0	34.5	13.6
77	0.0720	7.3	1.5646	11.0	0.1576	8.3	0.75	943.4	72.8	956.3	68.1	986.2	148.3	943.4	72.8	4.3
153	0.0734	3.8	1.6054	5.7	0.1587	3.6	0.75	949.6	31.9	972.3	35.5	1023.9	77.0	949.6	31.9	7.3
145	0.0731	4.7	1.6025	6.7	0.1589	4.1	0.73	950.7	35.8	971.2	42.1	1018.0	94.5	950.7	35.8	6.6
393	0.0731	7.6	1.6029	10.7	0.1590	7.5	0.70	951.0	66.6	971.3	67.1	1017.5	154.8	951.0	66.6	6.5
250	0.0763	7.9	1.6823	10.6	0.1599	6.9	0.66	956.2	61.7	1001.9	67.5	1103.1	158.8	956.2	61.7	13.3
335	0.0733	5.2	1.6209	7.6	0.1604	5.8	0.73	958.9	51.5	978.4	47.6	1022.3	104.7	958.9	51.5	6.2
315	0.0739	5.5	1.6343	7.2	0.1605	4.6	0.63	959.3	40.8	983.5	45.1	1038.0	111.9	959.3	40.8	7.6
24	0.0724	2.9	1.6186	4.7	0.1621	3.6	0.79	968.2	32.6	977.5	29.6	998.4	59.2	968.2	32.6	3.0
269	0.0735	3.7	1.6501	5.6	0.1628	4.1	0.74	972.2	37.2	989.6	35.5	1028.5	75.7	972.2	37.2	5.5
51	0.0732	3.6	1.6474	4.7	0.1633	3.2	0.65	975.3	28.7	988.6	29.9	1018.2	73.0	975.3	28.7	4.2
356	0.0717	5.5	1.7085	7.9	0.1729	6.1	0.72	1028.2	58.3	1011.7	50.9	976.1	112.2	976.1	112.2	-5.3
175	0.0734	3.5	1.6619	5.4	0.1642	4.0	0.75	980.0	36.2	994.1	34.1	1025.2	71.6	980.0	36.2	4.4
392	0.0747	6.7	1.6935	9.5	0.1644	6.7	0.70	981.0	61.0	1006.1	60.7	1061.0	135.7	981.0	61.0	7.5
13	0.0739	5.0	1.6747	7.3	0.1645	5.3	0.73	981.6	48.3	999.0	46.5	1037.4	101.2	981.6	48.3	5.4
391	0.0775	9.5	1.7626	12.9	0.1650	8.7	0.67	984.3	79.2	1031.8	83.6	1134.0	189.5	984.3	79.2	13.2
360	0.0743	7.0	1.6971	9.4	0.1657	6.6	0.67	988.6	60.8	1007.4	60.1	1048.6	140.8	988.6	60.8	5.7
273	0.0722	6.2	1.6514	8.9	0.1659	6.4	0.72	989.5	58.4	990.1	56.1	991.3	125.1	989.5	58.4	0.2
76	0.0808	7.2	1.8514	10.5	0.1663	7.7	0.73	991.5	70.9	1063.9	69.0	1215.7	141.0	991.5	70.9	18.4
350	0.0730	5.0	1.6757	7.1	0.1665	5.2	0.70	992.9	48.2	999.4	45.0	1013.5	102.0	992.9	48.2	2.0
212	0.0743	7.8	1.7066	11.6	0.1666	8.6	0.73	993.2	78.7	1011.0	74.2	1049.9	158.2	993.2	78.7	5.4
314	0.0745	4.0	1.7167	5.0	0.1672	3.2	0.62	996.8	29.2	1014.8	32.3	1053.9	79.7	996.8	29.2	5.4
289	0.0718	4.0	1.6577	5.9	0.1674	4.4	0.73	997.7	40.7	992.5	37.2	981.0	81.8	997.7	40.7	-1.7
303	0.0774	5.0	1.7873	7.6	0.1675	5.8	0.75	998.2	53.8	1040.8	49.7	1131.5	100.2	998.2	53.8	11.8
293	0.0728	11.2	1.6834	16.5	0.1677	12.2	0.74	999.5	113.1	1002.3	105.3	1008.3	226.3	999.5	113.1	0.9
225	0.0728	9.9	1.8142	14.3	0.1808	10.3	0.72	1017.6	101.8	1050.6	93.7	1007.2	201.1	1007.2	201.1	-6.4
254	0.0734	2.8	1.6978	4.4	0.1678	3.2	0.77	1000.1	29.4	1007.7	28.3	1024.2	57.1	1024.2	57.1	2.4
203	0.0734	5.4	1.7319	7.7	0.1710	5.6	0.71	1017.8	52.9	1020.4	49.7	1026.0	109.2	1026.0	109.2	0.8
262	0.0742	2.2	1.8256	3.6	0.1785	2.6	0.78	1058.9	25.3	1054.7	23.3	1046.0	45.3	1046.0	45.3	-1.2
46	0.0749	3.9	1.9388	4.9	0.1878	3.2	0.63	1109.5	32.8	1094.6	33.2	1064.9	77.7	1064.9	77.7	-4.2
37	0.0753	5.4	1.7603	7.9	0.1696	5.7	0.73	1009.7	53.5	1031.0	51.5	1076.4	108.2	1076.4	108.2	6.2
50	0.0760	3.5	1.7673	4.5	0.1687	3.0	0.64	1005.1	28.0	1033.5	29.4	1094.1	69.6	1094.1	69.6	8.1
369	0.0760	3.8	1.7936	5.8	0.1711	4.4	0.75	1017.9	41.4	1043.1	37.6	1096.3	76.1	1096.3	76.1	7.1
33	0.0764	7.2	1.8927	9.3	0.1798	5.9	0.64	1065.8	57.8	1078.5	61.6	1104.4	143.0	1104.4	143.0	3.5
66	0.0769	5.7	2.0992	7.6	0.1979	5.3	0.67	1164.2	56.6	1148.5	52.3	1119.0	112.8	1119.0	112.8	-4.0
243	0.0771	7.7	2.1371	11.4	0.2010	8.3	0.73	1180.8	89.5	1160.9	78.9	1123.9	153.8	1123.9	153.8	-5.1

Table A4.8 (continued): Detrital Zircon U-Pb Integrated Data for the Punacancha Formation Base

Spot	Ratios							Ages (Ma)							Best Age	Disc. (%)
	207Pb/ 206Pb		207Pb/ 235U		206Pb/ 238U		Rho	206Pb/ 238U		207Pb/ 235U		207Pb/ 206Pb		±2σ		
	±2σ	±2σ	±2σ	±2σ	±2σ	±2σ	±2σ	±2σ	±2σ	±2σ	±2σ	±2σ	±2σ			
<i>Punacancha Formation Base (20140611-01) Accepted Data</i>																
223	0.0780	5.1	2.0309	7.6	0.1888	5.6	0.74	1114.9	57.8	1125.9	51.7	1147.2	101.1	1147.2	101.1	2.8
73	0.0781	7.2	2.0556	10.1	0.1910	7.1	0.70	1126.8	73.2	1134.2	68.8	1148.2	143.3	1148.2	143.3	1.9
228	0.0782	13.6	1.8710	19.6	0.1736	14.2	0.72	1032.1	135.7	1070.9	130.6	1150.8	269.3	1150.8	269.3	10.3
57	0.0787	4.3	2.0270	7.3	0.1868	6.0	0.81	1104.2	60.8	1124.6	49.8	1164.3	85.0	1164.3	85.0	5.2
17	0.0788	5.2	2.0269	7.7	0.1866	5.6	0.74	1102.9	57.2	1124.6	52.6	1166.8	103.8	1166.8	103.8	5.5
279	0.0788	3.2	2.0386	4.9	0.1876	3.7	0.75	1108.5	37.6	1128.5	33.6	1167.2	64.1	1167.2	64.1	5.0
177	0.0794	5.4	2.2131	7.8	0.2023	5.6	0.72	1187.5	60.4	1185.2	54.3	1181.0	105.8	1181.0	105.8	-0.5
29	0.0802	6.9	2.0791	10.0	0.1880	7.2	0.72	1110.5	73.3	1142.0	68.6	1202.3	136.0	1202.3	136.0	7.6
160	0.0804	12.0	2.2936	17.8	0.2070	13.0	0.74	1212.7	143.9	1210.3	126.2	1206.1	236.0	1206.1	236.0	-0.5
238	0.0807	6.7	2.2698	10.0	0.2039	7.3	0.75	1196.2	79.9	1203.0	70.9	1215.0	131.3	1215.0	131.3	1.5
60	0.0808	12.2	2.3419	17.9	0.2103	13.2	0.73	1230.3	147.7	1225.1	128.3	1215.9	239.1	1215.9	239.1	-1.2
380	0.0808	6.1	1.9943	9.4	0.1789	7.2	0.76	1061.2	70.3	1113.6	63.6	1217.3	119.3	1217.3	119.3	12.8
125	0.0811	3.3	2.1933	4.4	0.1962	2.8	0.66	1154.8	29.1	1178.9	30.8	1223.4	65.5	1223.4	65.5	5.6
365	0.0812	7.3	1.9713	10.8	0.1761	7.9	0.73	1045.6	76.3	1105.8	72.6	1226.1	144.1	1226.1	144.1	14.7
14	0.0814	10.1	1.9396	17.1	0.1728	13.8	0.81	1027.7	130.8	1094.9	115.0	1231.0	198.5	1231.0	198.5	16.5
291	0.0820	7.0	2.1384	12.8	0.1891	10.9	0.84	1116.5	111.6	1161.3	89.1	1245.9	136.4	1245.9	136.4	10.4
129	0.0821	7.8	2.3757	12.3	0.2100	9.4	0.77	1228.7	105.0	1235.3	87.8	1246.9	153.3	1246.9	153.3	1.5
189	0.0825	7.1	2.3845	11.7	0.2096	9.3	0.79	1226.7	103.9	1237.9	83.8	1257.5	138.8	1257.5	138.8	2.5
397	0.0831	3.8	2.2409	5.6	0.1957	4.2	0.74	1152.1	44.3	1193.9	39.2	1270.5	73.5	1270.5	73.5	9.3
302	0.0836	13.4	2.1856	18.5	0.1896	12.8	0.69	1119.0	131.4	1176.4	129.7	1283.7	261.7	1283.7	261.7	12.8
200	0.0839	4.2	2.4386	5.3	0.2109	3.4	0.62	1233.6	38.6	1254.1	38.1	1289.3	80.9	1289.3	80.9	4.3
49	0.0850	4.6	2.5193	7.1	0.2151	5.5	0.76	1255.8	62.7	1277.6	51.7	1314.6	89.2	1314.6	89.2	4.5
43	0.0856	6.6	2.4513	9.2	0.2077	6.5	0.70	1216.5	72.1	1257.8	66.6	1329.2	127.9	1329.2	127.9	8.5
184	0.0862	9.6	2.6084	14.1	0.2195	10.4	0.73	1279.4	120.8	1303.0	104.1	1342.1	185.3	1342.1	185.3	4.7
195	0.0867	6.2	2.6182	8.5	0.2191	5.9	0.68	1277.3	68.7	1305.8	62.5	1352.9	120.4	1352.9	120.4	5.6
183	0.0870	5.7	2.4588	7.7	0.2049	5.1	0.67	1201.5	56.4	1260.0	55.6	1361.4	109.9	1361.4	109.9	11.7
162	0.0874	4.0	2.6187	5.9	0.2174	4.0	0.74	1267.9	46.3	1305.9	43.1	1368.9	76.3	1368.9	76.3	7.4
42	0.0883	7.3	2.8557	10.6	0.2346	7.8	0.73	1358.7	95.8	1370.3	80.2	1388.4	139.7	1388.4	139.7	2.1
168	0.0887	4.7	2.8668	7.2	0.2344	5.1	0.76	1357.7	62.6	1373.2	54.1	1397.5	90.2	1397.5	90.2	2.9
278	0.0909	3.8	3.2070	5.7	0.2559	4.2	0.75	1469.1	55.6	1458.8	44.0	1444.0	71.7	1444.0	71.7	-1.7
119	0.0916	6.2	2.8124	9.2	0.2227	6.8	0.74	1296.3	79.6	1358.9	69.3	1458.6	118.4	1458.6	118.4	11.1
68	0.0923	12.3	3.4137	18.5	0.2682	13.9	0.75	1531.9	189.1	1507.6	146.3	1473.5	234.1	1473.5	234.1	-4.0
332	0.0934	3.5	3.0306	4.5	0.2353	3.3	0.65	1362.0	40.2	1415.4	34.7	1496.6	66.0	1496.6	66.0	9.0
322	0.0935	10.5	2.7382	15.7	0.2124	11.7	0.74	1241.3	131.8	1338.9	117.2	1498.4	199.3	1498.4	199.3	17.2
124	0.0935	7.0	2.8476	9.0	0.2208	5.6	0.63	1286.2	65.5	1368.2	68.0	1498.7	132.8	1498.7	132.8	14.2
362	0.0939	8.6	2.7692	13.9	0.2139	11.2	0.79	1249.6	126.8	1347.3	104.2	1505.9	162.0	1505.9	162.0	17.0
30	0.0939	3.6	3.3886	5.1	0.2617	3.7	0.72	1498.5	48.9	1501.8	40.1	1506.4	67.2	1506.4	67.2	0.5
22	0.0943	8.9	3.2081	13.9	0.2467	10.6	0.76	1421.2	134.7	1459.1	107.7	1514.7	168.8	1514.7	168.8	6.2
229	0.0945	4.8	3.4795	6.7	0.2670	4.7	0.70	1525.6	64.4	1522.6	52.6	1518.4	90.1	1518.4	90.1	-0.5
259	0.0946	9.0	3.4701	14.7	0.2660	11.6	0.79	1520.7	156.7	1520.4	116.4	1520.1	169.6	1520.1	169.6	0.0
260	0.0968	6.8	3.5016	11.7	0.2624	9.5	0.81	1502.3	127.3	1527.6	93.0	1562.8	128.2	1562.8	128.2	3.9
94	0.0985	7.1	3.4016	9.5	0.2504	6.2	0.66	1440.4	79.7	1504.8	74.6	1596.6	133.5	1596.6	133.5	9.8
321	0.1003	11.9	3.8149	19.4	0.2759	15.3	0.79	1570.8	213.9	1595.9	157.3	1629.1	221.7	1629.1	221.7	3.6
137	0.1011	8.2	3.9528	12.8	0.2837	9.8	0.77	1609.7	139.7	1624.6	104.0	1643.8	152.3	1643.8	152.3	2.1
347	0.1014	7.1	4.1173	10.3	0.2946	7.7	0.73	1664.5	113.3	1657.7	84.6	1649.2	131.2	1649.2	131.2	-0.9
257	0.1024	11.9	3.9266	15.9	0.2782	10.4	0.66	1582.4	146.1	1619.2	129.1	1667.3	220.2	1667.3	220.2	5.1
44	0.1025	5.3	3.7814	8.1	0.2676	6.1	0.75	1528.4	83.5	1588.8	64.8	1669.9	98.1	1669.9	98.1	8.5
23	0.1028	6.4	3.8449	8.7	0.2711	5.9	0.69	1546.6	81.8	1602.2	70.6	1676.2	117.7	1676.2	117.7	7.7
6	0.1031	5.8	3.4765	7.0	0.2446	3.9	0.57	1410.6	49.5	1521.9	55.2	1680.3	106.4	1680.3	106.4	16.1
116	0.1040	4.1	4.0582	6.1	0.2831	4.4	0.74	1607.0	63.1	1645.9	49.7	1696.0	75.8	1696.0	75.8	5.2
159	0.1058	6.9	4.2895	10.1	0.2942	7.1	0.73	1662.3	103.3	1691.4	83.4	1727.6	127.5	1727.6	127.5	3.8
305	0.1081	14.3	4.3167	19.8	0.2896	13.7	0.69	1639.5	198.2	1696.6	164.6	1767.8	261.9	1767.8	261.9	7.3
32	0.1085	4.5	4.6140	6.8	0.3085	5.0	0.74	1733.2	76.0	1751.8	56.5	1774.0	82.9	1774.0	82.9	2.3
274	0.1085	7.8	4.4312	11.1	0.2962	7.8	0.71	1672.5	115.5	1718.2	92.1	1774.3	142.8	1774.3	142.8	5.7
4	0.1093	3.7	4.2926	5.8	0.2848	4.5	0.78	1615.3	64.3	1692.0	48.1	1788.3	66.7	1788.3	66.7	9.7
357	0.1102	8.1	4.8439	11.4	0.3189	8.4	0.70	1784.3	130.2	1792.6	96.6	1802.2	147.8	1802.2	147.8	1.0
112	0.1104	3.1	4.6839	4.7	0.3078	3.5	0.74	1729.8	52.6	1764.4	39.2	1805.5	57.0	1805.5	57.0	4.2
343	0.1146	3.8	5.1469	5.2	0.3256	3.9	0.70	1817.2	61.4	1843.9	44.4	1874.1	67.6	1874.1	67.6	3.0
2	0.1161	3.0	4.9946	4.4	0.3119	3.1	0.72	1750.1	46.9	1818.4	37.0	1897.5	54.8	1897.5	54.8	7.8
375	0.1208	6.2	4.6181	9.1	0.2774	6.7	0.73	1578.1	93.6	1752.6	76.3	1967.4	110.9	1967.4	110.9	19.8
194	0.1221	9.5	5.9591	13.8	0.3539	10.1	0.72	1953.4	170.4	1969.9	120.8	1987.2	169.8	1987.2	169.8	1.7
31	0.1243	3.7	6.0200	5.6	0.3512	4.2	0.75	1940.4	69.8	1978.7	48.8	2019.1	65.9	2019.1	65.9	3.9
316	0.1254	7.2	6.4193	10.3	0.3712	7.4	0.71	2035.3	129.2	2034.9	90.9	2034.6	127.7	2034.6	127.7	0.0

Table A4.8 (continued): Detrital Zircon U-Pb Integrated Data for the Punacancha Formation Base

Spot	Ratios							Ages (Ma)							Best Age	Disc. (%)
	207Pb/206Pb		207Pb/235U		206Pb/238U		Rho	206Pb/238U		207Pb/235U		207Pb/206Pb				
	±2σ	±2σ	±2σ	±2σ	±2σ	±2σ		±2σ	±2σ	±2σ	±2σ	±2σ				
<i>Punacancha Formation Base (20140611-01) Accepted Data</i>																
206	0.1267	10.1	5.4069	17.5	0.3096	14.3	0.82	1738.5	218.1	1885.9	150.7	2052.4	178.3	2052.4	178.3	15.3
367	0.1295	2.8	6.3092	4.1	0.3533	3.0	0.72	1950.5	50.9	2019.7	35.7	2091.2	49.5	2091.2	49.5	6.7
320	0.1298	3.1	6.3887	4.6	0.3569	3.5	0.73	1967.7	58.9	2030.7	40.1	2095.4	55.0	2095.4	55.0	6.1
370	0.1379	2.9	6.9812	4.0	0.3672	2.9	0.71	2016.1	50.5	2109.0	35.9	2200.9	49.6	2200.9	49.6	8.4
38	0.1468	4.2	8.4731	6.1	0.4187	4.3	0.73	2254.6	82.5	2283.0	55.8	2308.6	72.1	2308.6	72.1	2.3
341	0.1591	3.0	9.4659	4.5	0.4316	3.6	0.74	2312.9	69.4	2384.2	41.2	2445.8	51.3	2445.8	51.3	5.4
319	0.1740	4.3	11.6351	6.5	0.4849	4.9	0.74	2548.5	102.2	2575.5	60.7	2596.8	72.3	2596.8	72.3	1.9
163	0.1891	3.0	12.9469	4.6	0.4964	3.1	0.77	2598.5	67.0	2675.8	43.3	2734.8	48.8	2734.8	48.8	5.0
328	0.1953	3.8	12.9596	5.5	0.4813	4.2	0.72	2532.8	88.4	2676.7	52.0	2787.3	62.9	2787.3	62.9	9.1
<i>Punacancha Formation Base (20140611-01) Rejected Data</i>																
308	0.0683	14.3	0.0416	15.2	0.0044	5.3	0.34	28.5	1.5	41.4	6.2	876.5	295.0	28.5	1.5	31.3
352	0.0783	21.9	0.0488	23.2	0.0045	7.7	0.33	29.1	2.2	48.4	10.9	1154.1	434.3	29.1	2.2	39.9
235	0.0750	20.1	0.0478	21.1	0.0046	6.3	0.31	29.8	1.9	47.5	9.8	1068.8	403.4	29.8	1.9	37.3
304	0.0772	15.9	0.0493	17.3	0.0046	7.0	0.40	29.8	2.1	48.9	8.3	1126.8	316.6	29.8	2.1	39.1
62	0.0681	14.6	0.0436	15.9	0.0046	6.3	0.40	29.9	1.9	43.3	6.7	870.2	302.7	29.9	1.9	31.0
270	0.0456	18.9	0.0301	24.8	0.0048	16.0	0.64	30.8	4.9	30.2	7.4	-22.3	458.3	30.8	4.9	-2.2
379	0.0788	14.7	0.0548	17.2	0.0050	9.0	0.52	32.4	2.9	54.2	9.1	1168.3	290.2	32.4	2.9	40.2
36	0.0688	11.9	0.0489	12.8	0.0052	4.6	0.37	33.2	1.5	48.5	6.1	892.7	245.8	33.2	1.5	31.6
387	0.0690	13.4	0.0492	15.3	0.0052	7.5	0.49	33.3	2.5	48.7	7.3	897.3	275.6	33.3	2.5	31.8
376	0.0668	12.2	0.0490	13.8	0.0053	6.5	0.47	34.2	2.2	48.6	6.6	830.9	255.2	34.2	2.2	29.6
395	0.0717	12.4	0.0529	14.9	0.0054	8.2	0.55	34.4	2.8	52.3	7.6	977.7	253.3	34.4	2.8	34.3
275	0.0800	19.4	0.0597	21.5	0.0054	9.4	0.44	34.8	3.3	58.9	12.3	1197.2	381.8	34.8	3.3	40.9
98	0.0758	18.5	0.0567	19.6	0.0054	6.5	0.33	34.9	2.3	56.0	10.7	1089.7	370.6	34.9	2.3	37.7
84	0.0747	20.6	0.0564	21.5	0.0055	6.3	0.29	35.2	2.2	55.7	11.7	1059.3	414.9	35.2	2.2	36.8
67	0.0779	15.7	0.0590	16.5	0.0055	5.4	0.31	35.2	1.9	58.2	9.3	1145.3	311.2	35.2	1.9	39.4
248	0.0758	14.3	0.0574	15.7	0.0055	6.5	0.42	35.3	2.3	56.7	8.7	1090.7	285.9	35.3	2.3	37.7
385	0.0858	17.1	0.0660	18.7	0.0056	7.6	0.41	35.9	2.7	64.9	11.8	1334.3	330.9	35.9	2.7	44.8
210	0.0855	13.7	0.0666	15.1	0.0056	6.4	0.42	36.3	2.3	65.4	9.6	1327.6	265.4	36.3	2.3	44.5
114	0.0724	14.7	0.0564	15.7	0.0057	5.8	0.37	36.4	2.1	55.8	8.5	996.8	297.7	36.4	2.1	34.8
234	0.0777	19.5	0.0609	21.3	0.0057	8.3	0.39	36.5	3.0	60.0	12.4	1138.2	388.6	36.5	3.0	39.1
251	0.0825	23.2	0.0658	25.3	0.0058	10.1	0.40	37.2	3.8	64.7	15.9	1258.4	452.9	37.2	3.8	42.6
140	0.0843	14.6	0.0694	16.0	0.0060	6.1	0.40	38.4	2.3	68.1	10.5	1298.3	283.8	38.4	2.3	43.6
220	0.0981	13.0	0.0816	14.5	0.0060	6.4	0.44	38.8	2.5	79.6	11.1	1588.6	243.4	38.8	2.5	51.3
34	0.1015	18.4	0.0859	20.4	0.0061	8.7	0.43	39.4	3.4	83.7	16.4	1651.9	341.4	39.4	3.4	52.9
173	0.0641	18.4	0.0557	27.1	0.0063	19.8	0.73	40.5	8.0	55.0	14.5	745.1	389.3	40.5	8.0	26.4
339	0.1349	26.2	0.1221	30.1	0.0066	14.9	0.49	42.2	6.3	117.0	33.3	2162.3	456.5	42.2	6.3	63.9
338	0.2469	30.0	0.2464	32.3	0.0072	12.1	0.37	46.5	5.6	223.7	65.0	3165.2	476.3	46.5	5.6	79.2
271	0.0659	24.6	0.0722	32.2	0.0079	20.9	0.65	51.0	10.6	70.8	22.0	803.6	514.5	51.0	10.6	27.9
138	0.1538	15.2	0.1746	19.8	0.0082	12.8	0.64	52.9	6.7	163.4	29.9	2388.3	258.2	52.9	6.7	67.6
10	0.2291	16.3	0.2760	17.8	0.0087	7.2	0.40	56.1	4.0	247.5	39.1	3046.0	260.8	56.1	4.0	77.3
82	0.0711	13.8	0.1012	15.0	0.0103	6.1	0.40	66.3	4.0	97.9	14.0	959.2	281.6	66.3	4.0	32.3
147	0.0847	15.2	0.1227	19.9	0.0105	12.5	0.64	67.4	8.4	117.5	22.1	1308.2	295.7	67.4	8.4	42.7
123	0.4111	8.7	0.5997	10.5	0.0106	5.9	0.56	67.9	4.0	477.1	40.0	3950.1	130.5	67.9	4.0	85.8
107	0.0602	17.0	0.0955	24.9	0.0115	18.2	0.73	73.7	13.4	92.6	22.1	611.2	367.1	73.7	13.4	20.4
85	0.0489	20.7	0.0811	31.1	0.0120	23.1	0.74	77.0	17.7	79.2	23.7	144.8	486.1	77.0	17.7	2.7
65	0.0728	15.2	0.1273	16.2	0.0127	5.9	0.35	81.2	4.8	121.7	18.6	1009.1	307.4	81.2	4.8	33.3
131	0.0567	23.1	0.1032	28.5	0.0132	16.6	0.58	84.5	14.0	99.7	27.1	481.3	511.0	84.5	14.0	15.3
298	0.0951	8.8	0.1731	15.4	0.0132	12.7	0.82	84.6	10.7	162.1	23.1	1529.4	165.8	84.6	10.7	47.8
231	0.0498	16.8	0.0949	24.1	0.0138	17.2	0.72	88.5	15.1	92.0	21.2	184.2	390.8	88.5	15.1	3.8
185	0.0504	15.5	0.0973	21.6	0.0140	15.1	0.70	89.6	13.4	94.3	19.4	212.5	358.4	89.6	13.4	4.9
396	0.0525	31.5	0.1044	39.2	0.0144	23.4	0.60	92.4	21.4	100.9	37.6	306.9	717.0	92.4	21.4	8.4
351	0.1108	25.0	0.2248	28.6	0.0147	13.9	0.48	94.2	13.0	205.9	53.3	1812.4	453.7	94.2	13.0	54.3
178	0.2815	21.3	0.6500	23.5	0.0167	9.8	0.42	107.1	10.4	508.5	94.1	3371.4	332.5	107.1	10.4	78.9
253	0.0829	17.4	0.2175	18.6	0.0190	6.5	0.35	121.5	7.8	199.8	33.7	1267.8	339.2	121.5	7.8	39.2
249	0.3552	28.0	1.0929	30.7	0.0223	12.6	0.41	142.3	17.7	749.9	164.3	3729.6	425.9	142.3	17.7	81.0
325	0.0931	7.6	0.2929	8.5	0.0228	4.0	0.44	145.4	5.7	260.9	19.5	1490.8	144.4	145.4	5.7	44.3
190	0.1228	9.2	0.4952	14.2	0.0293	10.9	0.76	185.9	20.0	408.4	47.9	1997.1	163.1	185.9	20.0	54.5
102	0.0513	27.8	0.2260	39.7	0.0319	28.4	0.71	202.6	56.7	206.9	74.5	255.6	638.8	202.6	56.7	2.1
349	0.0505	35.4	0.2286	50.3	0.0328	35.8	0.71	208.3	73.4	209.0	95.3	217.5	819.1	208.3	73.4	0.4
282	0.0516	22.0	0.2354	28.7	0.0331	18.4	0.64	209.9	38.0	214.6	55.5	266.6	503.8	209.9	38.0	2.2
222	0.0525	29.1	0.2592	42.1	0.0358	30.4	0.72	227.0	67.9	234.0	88.2	305.1	662.0	227.0	67.9	3.0
134	0.0787	11.2	0.5845	20.8	0.0539	17.5	0.84	338.3	57.6	467.3	77.9	1164.0	222.2	338.3	57.6	27.6
264	0.0705	21.0	0.6858	26.4	0.0706	16.0	0.61	439.7	67.9	530.3	109.4	941.8	429.4	439.7	67.9	17.1

Table A4.8 (continued): Detrital Zircon U-Pb Integrated Data for the Punacancha Formation Base

Spot	Ratios						Rho	Ages (Ma)						Best Age	Disc. (%)	
	207Pb/206Pb		207Pb/235U		206Pb/238U			206Pb/238U		207Pb/235U		207Pb/206Pb				
	±2σ	±2σ	±2σ	±2σ	±2σ	±2σ		±2σ	±2σ	±2σ	±2σ	±2σ				
<i>Punacancha Formation Base (20140611-01) Rejected Data</i>																
72	0.0937	8.2	1.1512	9.3	0.0891	4.6	0.48	550.3	24.1	777.8	50.7	1501.8	154.6	550.3	24.1	29.2
115	0.1194	8.5	1.6205	9.7	0.0984	4.6	0.48	605.2	26.6	978.2	60.8	1947.5	151.2	605.2	26.6	68.9
296	0.0588	5.9	0.8340	8.4	0.1029	6.2	0.71	631.3	37.3	615.8	38.9	559.5	128.9	631.3	37.3	-12.8
87	0.0592	4.8	0.8794	7.0	0.1078	5.1	0.72	659.8	32.0	640.7	33.2	573.5	104.7	659.8	32.0	-15.0
20	0.0710	14.6	1.0651	20.4	0.1089	14.1	0.69	666.1	89.4	736.3	107.0	956.3	299.4	666.1	89.4	30.4
383	0.0687	8.9	1.0870	11.1	0.1148	6.5	0.59	700.5	43.4	747.0	58.5	889.2	184.5	700.5	43.4	21.2
55	0.0878	9.8	1.3976	15.1	0.1154	11.5	0.76	704.2	76.4	887.9	89.5	1378.5	188.9	704.2	76.4	48.9
263	0.0734	4.6	1.3098	5.5	0.1294	2.8	0.55	784.4	20.9	850.1	31.5	1025.6	92.7	784.4	20.9	23.5
377	0.0737	5.0	1.3749	7.6	0.1353	5.7	0.75	817.8	43.5	878.3	44.5	1033.8	101.7	817.8	43.5	20.9
182	0.0771	18.0	1.5084	23.1	0.1419	14.5	0.63	855.2	116.1	933.8	142.1	1124.3	359.1	855.2	116.1	23.9
252	0.0872	5.5	1.7153	7.7	0.1427	5.3	0.70	860.0	42.6	1014.3	49.3	1364.4	105.9	860.0	42.6	37.0
378	0.0805	4.9	1.6882	6.6	0.1522	4.6	0.68	913.1	38.8	1004.1	42.4	1208.4	95.7	913.1	38.8	24.4
108	0.0715	17.8	1.5319	25.3	0.1553	18.0	0.71	930.7	156.0	943.3	156.6	972.8	362.2	930.7	156.0	4.3
109	0.0851	14.2	1.8909	23.0	0.1611	18.1	0.79	962.8	161.6	1077.9	154.0	1318.5	276.0	962.8	161.6	27.0
166	0.0717	24.0	1.8529	35.1	0.1874	25.5	0.73	1107.1	259.2	1064.5	235.3	978.2	489.6	978.2	489.6	-13.2
330	0.0713	16.9	1.6108	24.9	0.1639	18.3	0.73	978.5	166.4	974.4	157.2	965.1	345.5	978.5	166.4	-1.4
205	0.0736	27.4	1.7713	38.2	0.1746	26.6	0.70	1037.5	255.1	1035.0	252.7	1029.7	553.4	1029.7	553.4	-0.8
198	0.0848	29.8	1.9768	41.9	0.1691	29.5	0.70	1007.0	275.1	1107.6	290.0	1311.1	577.5	1311.1	577.5	23.2
368	0.0920	10.5	2.5306	14.5	0.1995	10.0	0.69	1172.7	107.5	1280.9	106.0	1467.1	199.6	1467.1	199.6	20.1
277	0.1013	15.1	4.0430	20.6	0.2895	14.1	0.68	1639.0	203.9	1642.9	169.6	1647.9	279.6	1647.9	279.6	0.5
342	0.1044	3.5	3.1708	5.6	0.2202	4.5	0.77	1283.1	52.5	1450.1	43.0	1704.2	65.1	1704.2	65.1	24.7
244	0.1062	18.0	5.0002	26.2	0.3413	19.0	0.73	1893.2	312.7	1819.4	225.6	1735.9	330.4	1735.9	330.4	-9.1
27	0.1154	23.0	5.8220	34.2	0.3660	25.3	0.74	2010.7	438.0	1949.7	305.6	1885.5	414.8	1885.5	414.8	-6.6

Table A4.9: Detrital Zircon U-Pb Integrated Data for the Punacancha Formation Top

Spot	Ratios						Ages (Ma)						Disc. (%)			
	207Pb/ 206Pb		207Pb/ 235U		206Pb/ 238U		Rho	206Pb/ 238U		207Pb/ 235U		207Pb/ 206Pb		Best Age		
	±2σ	±2σ	±2σ	±2σ	±2σ	±2σ		±2σ	±2σ	±2σ	±2σ	±2σ				
<i>Punacancha Formation Top (20140611-03) Accepted Data</i>																
269	0.0541	13.0	0.0268	18.1	0.0036	12.6	0.69	23.1	2.9	26.9	4.8	376.3	293.1	23.1	2.9	13.9
186	0.0621	18.6	0.0329	20.6	0.0038	8.9	0.42	24.7	2.2	32.8	6.6	677.9	397.9	24.7	2.2	24.8
101	0.0580	24.5	0.0308	25.6	0.0039	7.4	0.28	24.8	1.8	30.8	7.8	531.4	537.3	24.8	1.8	19.6
352	0.0548	27.6	0.0293	28.6	0.0039	7.5	0.26	24.9	1.9	29.3	8.2	402.7	617.8	24.9	1.9	14.9
306	0.0534	29.6	0.0288	30.7	0.0039	8.3	0.27	25.2	2.1	28.8	8.7	343.8	669.2	25.2	2.1	12.6
82	0.0663	19.7	0.0359	21.2	0.0039	7.9	0.37	25.3	2.0	35.8	7.5	817.0	412.6	25.3	2.0	29.5
311	0.0477	21.4	0.0258	22.5	0.0039	6.9	0.30	25.3	1.7	25.9	5.7	83.3	508.3	25.3	1.7	2.4
96	0.0689	20.1	0.0375	21.1	0.0039	6.4	0.30	25.4	1.6	37.4	7.7	896.5	415.4	25.4	1.6	32.1
141	0.0525	25.2	0.0286	26.0	0.0040	7.2	0.26	25.4	1.8	28.7	7.4	307.5	572.9	25.4	1.8	11.2
261	0.0693	19.7	0.0378	21.9	0.0040	9.7	0.44	25.5	2.5	37.7	8.1	906.8	405.8	25.5	2.5	32.4
258	0.0692	19.5	0.0378	20.3	0.0040	6.0	0.29	25.5	1.5	37.7	7.5	903.7	401.5	25.5	1.5	32.3
297	0.0693	23.1	0.0378	24.5	0.0040	8.1	0.33	25.5	2.1	37.7	9.1	906.7	475.8	25.5	2.1	32.4
239	0.0724	22.8	0.0398	24.4	0.0040	8.4	0.35	25.6	2.2	39.6	9.5	998.5	462.9	25.6	2.2	35.3
114	0.0511	11.8	0.0281	13.1	0.0040	6.2	0.45	25.6	1.6	28.1	3.6	244.7	270.9	25.6	1.6	8.8
74	0.0713	20.0	0.0391	21.1	0.0040	6.7	0.32	25.6	1.7	39.0	8.1	964.6	409.2	25.6	1.7	34.3
325	0.0697	25.8	0.0383	27.2	0.0040	8.8	0.32	25.6	2.2	38.2	10.2	920.3	529.5	25.6	2.2	32.8
320	0.0642	20.2	0.0355	21.1	0.0040	6.3	0.29	25.6	1.6	35.4	7.3	747.1	426.6	25.8	1.6	27.1
295	0.0626	18.7	0.0347	19.6	0.0040	5.8	0.29	25.9	1.5	34.7	6.7	693.9	399.5	25.9	1.5	25.3
98	0.0799	28.3	0.0445	29.4	0.0040	8.3	0.28	26.0	2.2	44.2	12.7	1194.5	557.8	26.0	2.2	41.2
283	0.0608	17.6	0.0340	18.6	0.0041	6.0	0.32	26.1	1.6	34.0	6.2	632.4	379.8	26.1	1.6	23.1
118	0.0702	19.6	0.0393	22.3	0.0041	10.9	0.48	26.1	2.8	39.2	8.6	933.5	401.9	26.1	2.8	33.2
380	0.0638	26.5	0.0360	27.9	0.0041	8.8	0.31	26.3	2.3	35.9	9.9	735.2	561.9	26.3	2.3	26.7
150	0.0542	13.5	0.0306	14.9	0.0041	6.6	0.42	26.4	1.7	30.6	4.5	378.7	304.1	26.4	1.7	13.9
27	0.0731	20.7	0.0413	22.1	0.0041	7.9	0.34	26.4	2.1	41.1	8.9	1016.9	419.8	26.4	2.1	35.9
163	0.0516	22.5	0.0293	23.8	0.0041	8.0	0.33	26.5	2.1	29.3	6.9	267.9	516.1	26.5	2.1	9.7
238	0.0638	21.2	0.0363	22.4	0.0041	6.8	0.31	26.5	1.8	36.2	8.0	736.1	449.5	26.5	1.8	26.7
147	0.0536	16.7	0.0305	17.4	0.0041	5.4	0.28	26.5	1.4	30.5	5.2	352.6	377.6	26.5	1.4	12.9
99	0.0694	19.9	0.0395	21.1	0.0041	7.0	0.32	26.6	1.9	39.4	8.1	909.7	410.4	26.6	1.9	32.5
376	0.0702	21.6	0.0403	23.4	0.0042	9.1	0.39	26.8	2.4	40.1	9.2	935.3	442.2	26.8	2.4	33.3
37	0.0435	27.3	0.0250	28.9	0.0042	10.1	0.33	26.8	2.7	25.1	7.1	-140.4	674.9	26.8	2.7	-7.0
210	0.0501	29.3	0.0288	30.4	0.0042	8.2	0.27	26.8	2.2	28.8	8.6	197.4	680.3	26.8	2.2	6.9
257	0.0513	24.1	0.0296	24.9	0.0042	6.2	0.25	26.9	1.7	29.6	7.3	255.6	553.6	26.9	1.7	9.2
307	0.0569	9.4	0.0329	10.5	0.0042	4.8	0.45	26.9	1.3	32.8	3.4	487.9	207.4	26.9	1.3	17.9
277	0.0642	19.2	0.0371	20.4	0.0042	6.7	0.33	27.0	1.8	37.0	7.4	746.6	406.5	27.0	1.8	27.1
169	0.0505	22.7	0.0292	23.4	0.0042	5.6	0.23	27.0	1.5	29.3	6.7	219.7	525.4	27.0	1.5	7.8
398	0.0690	32.6	0.0399	34.2	0.0042	10.4	0.31	27.0	2.8	39.8	13.3	897.8	671.9	27.0	2.8	32.1
153	0.0628	18.6	0.0364	19.8	0.0042	7.0	0.34	27.0	1.9	36.3	7.0	700.2	395.4	27.0	1.9	25.5
38	0.0547	14.8	0.0317	15.9	0.0042	6.6	0.37	27.1	1.8	31.7	5.0	398.0	331.9	27.1	1.8	14.6
203	0.0651	20.5	0.0379	22.2	0.0042	8.5	0.38	27.2	2.3	37.8	8.2	778.6	431.7	27.2	2.3	28.1
54	0.0693	19.5	0.0403	22.0	0.0042	10.4	0.47	27.2	2.8	40.2	8.7	907.8	401.5	27.2	2.8	32.4
400	0.0705	23.4	0.0411	24.2	0.0042	6.2	0.26	27.2	1.7	40.9	9.7	942.8	478.6	27.2	1.7	33.5
299	0.0713	21.2	0.0416	22.7	0.0042	8.2	0.36	27.2	2.2	41.4	9.2	965.7	433.4	27.2	2.2	34.2
271	0.0867	31.2	0.0507	32.6	0.0042	9.5	0.29	27.3	2.6	50.2	16.0	1353.4	602.5	27.3	2.6	45.7
15	0.0742	21.3	0.0435	22.8	0.0042	8.6	0.35	27.3	2.3	43.2	9.7	1048.0	430.3	27.3	2.3	36.8
111	0.0543	19.5	0.0318	20.9	0.0043	7.9	0.37	27.3	2.1	31.8	6.5	384.9	437.1	27.3	2.1	14.1
379	0.0566	27.7	0.0332	28.8	0.0043	7.8	0.27	27.4	2.1	33.2	9.4	477.9	613.2	27.4	2.1	17.6
102	0.0703	20.1	0.0414	21.1	0.0043	6.6	0.30	27.5	1.8	41.2	8.5	937.4	412.4	27.5	1.8	33.3
392	0.0697	18.1	0.0413	19.5	0.0043	7.3	0.37	27.6	2.0	41.1	7.8	918.1	371.3	27.6	2.0	32.7
304	0.0666	19.9	0.0395	22.4	0.0043	10.4	0.46	27.6	2.9	39.3	8.7	825.5	415.5	27.6	2.9	29.7
321	0.0495	17.1	0.0294	18.1	0.0043	6.2	0.34	27.7	1.7	29.4	5.3	173.3	398.3	27.7	1.7	5.9
394	0.0946	41.6	0.0562	44.0	0.0043	14.4	0.33	27.7	4.0	55.5	23.8	1520.4	784.1	27.7	4.0	50.1
222	0.0591	28.9	0.0352	29.8	0.0043	7.2	0.24	27.8	2.0	35.1	10.3	571.9	629.7	27.8	2.0	20.9
20	0.0640	17.8	0.0383	18.7	0.0043	6.2	0.30	28.0	1.7	38.2	7.0	740.6	377.6	28.0	1.7	26.8
360	0.0640	21.6	0.0385	23.1	0.0044	8.2	0.36	28.0	2.3	38.3	8.7	742.8	456.2	28.0	2.3	26.9
234	0.0541	23.4	0.0325	25.3	0.0044	9.5	0.38	28.0	2.6	32.5	8.1	373.9	527.1	28.0	2.6	13.7
285	0.0610	19.8	0.0367	21.0	0.0044	7.0	0.33	28.1	2.0	36.6	7.5	638.1	426.5	28.1	2.0	23.3
160	0.0536	15.3	0.0323	21.0	0.0044	14.4	0.68	28.1	4.0	32.3	6.7	354.1	345.7	28.1	4.0	12.9
267	0.0538	19.7	0.0325	20.8	0.0044	6.7	0.32	28.2	1.9	32.5	6.6	364.3	443.6	28.2	1.9	13.3
332	0.0574	19.9	0.0347	21.1	0.0044	7.2	0.33	28.2	2.0	34.7	7.2	508.0	437.1	28.2	2.0	18.6
135	0.0508	13.0	0.0308	14.7	0.0044	7.6	0.47	28.3	2.1	30.8	4.5	231.5	300.1	28.3	2.1	8.2
397	0.0738	20.4	0.0448	21.4	0.0044	6.3	0.29	28.3	1.8	44.5	9.3	1035.0	412.6	28.3	1.8	36.3
366	0.0712	46.1	0.0433	47.4	0.0044	11.0	0.23	28.4	3.1	43.0	20.0	964.2	940.8	28.4	3.1	34.1
248	0.0518	16.3	0.0315	17.4	0.0044	6.0	0.35	28.4	1.7	31.5	5.4	277.6	372.9	28.4	1.7	10.0

Table A4.9 (continued): Detrital Zircon U-Pb Integrated Data for the Punacancha Formation Top

Spot	Ratios						Ages (Ma)						Best Age	Disc. (%)		
	207Pb/206Pb		207Pb/235U		206Pb/238U		206Pb/238U		207Pb/235U		207Pb/206Pb					
	±2σ	±2σ	±2σ	±2σ	Rho	±2σ	±2σ	±2σ	±2σ	±2σ	±2σ					
<i>Punacancha Formation Top (20140611-03) Accepted Data</i>																
309	0.0534	15.2	0.0325	15.8	0.0044	4.3	0.27	28.4	1.2	32.5	5.1	347.0	344.8	28.4	1.2	12.6
259	0.0714	27.1	0.0437	30.5	0.0044	14.0	0.46	28.5	4.0	43.4	13.0	969.7	553.6	28.5	4.0	34.3
104	0.0453	25.5	0.0277	26.7	0.0044	8.1	0.30	28.6	2.3	27.8	7.3	-39.6	619.5	28.6	2.3	-2.8
336	0.0722	20.2	0.0445	20.9	0.0045	5.6	0.26	28.7	1.6	44.2	9.0	992.1	410.2	28.7	1.6	35.0
377	0.0656	14.4	0.0406	15.3	0.0045	5.3	0.34	28.9	1.5	40.4	6.1	794.2	301.9	28.9	1.5	28.6
381	0.0506	17.8	0.0314	19.2	0.0045	7.1	0.37	29.0	2.1	31.4	5.9	224.3	411.9	29.0	2.1	7.9
35	0.0565	23.6	0.0352	25.7	0.0045	10.6	0.40	29.1	3.1	35.2	8.9	471.7	522.2	29.1	3.1	17.2
106	0.0643	14.8	0.0409	17.0	0.0046	8.7	0.49	29.6	2.6	40.7	6.8	751.4	311.7	29.6	2.6	27.1
75	0.0654	19.4	0.0417	21.4	0.0046	9.1	0.43	29.8	2.7	41.5	8.7	785.7	406.6	29.8	2.7	28.2
355	0.0552	23.3	0.0354	24.4	0.0047	7.3	0.30	29.9	2.2	35.3	8.5	420.9	520.4	29.9	2.2	15.3
7	0.0503	20.1	0.0324	24.1	0.0047	13.1	0.55	30.0	3.9	32.3	7.7	207.1	467.0	30.0	3.9	7.1
358	0.0694	17.9	0.0452	18.8	0.0047	5.8	0.30	30.3	1.7	44.8	8.3	911.9	369.3	30.3	1.7	32.4
11	0.0659	35.0	0.0429	36.4	0.0047	9.7	0.27	30.4	2.9	42.7	15.2	803.2	733.7	30.4	2.9	28.8
359	0.0735	27.1	0.0480	29.2	0.0047	11.0	0.37	30.4	3.3	47.6	13.6	1028.5	548.3	30.4	3.3	36.0
229	0.0428	26.3	0.0280	27.1	0.0047	6.8	0.25	30.5	2.1	28.0	7.5	-179.3	655.2	30.5	2.1	-8.8
375	0.0685	44.5	0.0451	45.9	0.0048	11.5	0.25	30.7	3.5	44.8	20.1	883.3	919.5	30.7	3.5	31.4
86	0.0840	28.2	0.0554	30.0	0.0048	10.5	0.35	30.7	3.2	54.7	16.0	1292.7	547.9	30.7	3.2	43.8
373	0.0583	18.4	0.0385	22.2	0.0048	12.5	0.56	30.8	3.8	38.3	8.4	540.1	402.5	30.8	3.8	19.7
121	0.0757	25.1	0.0509	25.9	0.0049	6.6	0.24	31.4	2.1	50.4	12.7	1087.5	504.0	31.4	2.1	37.8
119	0.0915	37.2	0.0618	38.3	0.0049	9.5	0.24	31.5	3.0	60.9	22.7	1457.9	706.9	31.5	3.0	48.3
268	0.0550	18.5	0.0374	19.1	0.0049	5.0	0.26	31.7	1.6	37.3	7.0	410.7	412.6	31.7	1.6	14.9
199	0.0771	29.3	0.0548	32.0	0.0052	13.0	0.40	33.1	4.3	54.1	16.9	1123.1	583.6	33.1	4.3	38.8
247	0.0746	25.4	0.0532	27.0	0.0052	9.2	0.34	33.3	3.1	52.6	13.9	1058.0	510.4	33.3	3.1	36.8
148	0.0647	22.4	0.0467	25.7	0.0052	12.9	0.49	33.6	4.3	46.3	11.7	766.2	472.0	33.6	4.3	27.4
361	0.0700	19.2	0.0525	20.6	0.0054	7.7	0.37	35.0	2.7	52.0	10.5	929.7	393.3	35.0	2.7	32.7
396	0.0676	29.2	0.0518	31.0	0.0056	10.4	0.34	35.7	3.7	51.3	15.5	855.5	607.3	35.7	3.7	30.3
391	0.0700	28.8	0.0541	29.5	0.0056	6.4	0.22	36.0	2.3	53.5	15.4	928.2	590.6	36.0	2.3	32.6
196	0.0541	13.3	0.0422	15.5	0.0057	8.1	0.52	36.3	2.9	41.9	6.4	376.3	298.5	36.3	2.9	13.4
331	0.0664	17.9	0.0517	22.5	0.0057	13.6	0.60	36.3	4.9	51.2	11.2	817.9	374.7	36.3	4.9	29.0
23	0.0618	24.9	0.0484	26.2	0.0057	8.6	0.32	36.5	3.1	48.0	12.3	666.7	532.7	36.5	3.1	23.9
374	0.0559	33.0	0.0441	35.1	0.0057	12.1	0.34	36.8	4.4	43.8	15.1	450.3	732.5	36.8	4.4	16.1
317	0.0742	25.3	0.0592	26.3	0.0058	7.4	0.27	37.2	2.7	58.4	14.9	1046.6	510.4	37.2	2.7	36.3
319	0.0589	14.0	0.0472	15.6	0.0058	7.0	0.44	37.3	2.6	46.8	7.1	564.0	304.6	37.3	2.6	20.2
322	0.0635	15.7	0.0512	20.7	0.0058	13.5	0.65	37.6	5.1	50.7	10.2	724.9	333.4	37.6	5.1	25.9
296	0.0581	19.4	0.0468	20.4	0.0058	6.5	0.31	37.6	2.4	46.5	9.3	534.4	425.2	37.6	2.4	19.2
256	0.0653	24.4	0.0527	27.9	0.0059	13.6	0.49	37.6	5.1	52.1	14.2	784.6	512.8	37.6	5.1	27.9
116	0.0509	9.0	0.0415	10.0	0.0059	4.7	0.43	38.0	1.8	41.3	4.0	238.5	207.9	38.0	1.8	8.0
155	0.0899	31.7	0.0733	34.4	0.0059	13.4	0.38	38.0	5.1	71.9	23.8	1424.2	606.3	38.0	5.1	47.1
29	0.0416	38.7	0.0339	39.5	0.0059	8.4	0.21	38.0	3.2	33.9	13.2	-253.1	979.1	38.0	3.2	-12.3
156	0.0541	14.0	0.0442	18.2	0.0059	11.9	0.64	38.1	4.5	43.9	7.8	376.0	314.2	38.1	4.5	13.3
221	0.0488	10.3	0.0399	12.9	0.0059	8.0	0.60	38.1	3.0	39.7	5.0	138.0	242.9	38.1	3.0	4.0
146	0.0525	35.4	0.0433	36.3	0.0060	8.5	0.23	38.4	3.3	43.0	15.3	305.6	805.3	38.4	3.3	10.6
219	0.0648	20.4	0.0536	22.2	0.0060	8.8	0.39	38.5	3.4	53.0	11.5	769.2	430.3	38.5	3.4	27.3
122	0.0656	33.0	0.0544	33.9	0.0060	8.2	0.23	38.6	3.2	53.8	17.8	795.1	692.7	38.6	3.2	28.2
341	0.0548	10.1	0.0455	10.9	0.0060	4.6	0.40	38.8	1.8	45.2	4.8	402.2	225.2	38.8	1.8	14.3
63	0.0567	14.3	0.0472	19.0	0.0060	12.5	0.66	38.8	4.8	46.8	8.7	480.9	315.9	38.8	4.8	17.2
95	0.0469	9.9	0.0392	11.4	0.0061	5.8	0.49	39.0	2.2	39.1	4.3	42.7	236.8	39.0	2.2	0.2
335	0.0528	13.9	0.0442	15.4	0.0061	7.0	0.44	39.0	2.7	43.9	6.6	318.8	314.9	39.0	2.7	11.1
227	0.0505	6.2	0.0424	7.2	0.0061	3.6	0.49	39.1	1.4	42.2	3.0	218.5	144.6	39.1	1.4	7.2
275	0.0727	19.5	0.0611	20.3	0.0061	5.7	0.27	39.2	2.2	60.2	11.9	1005.7	396.2	39.2	2.2	34.9
198	0.0685	15.9	0.0578	18.5	0.0061	9.5	0.51	39.4	3.7	57.1	10.3	882.5	329.3	39.4	3.7	31.0
110	0.0554	8.9	0.0468	9.8	0.0061	4.5	0.42	39.4	1.8	46.4	4.5	429.6	199.3	39.4	1.8	15.3
52	0.0473	23.9	0.0400	26.4	0.0061	11.6	0.42	39.4	4.6	39.8	10.3	64.7	570.0	39.4	4.6	1.0
176	0.0724	19.1	0.0613	23.9	0.0061	14.4	0.60	39.4	5.7	60.4	14.0	997.0	387.4	39.4	5.7	34.7
36	0.0488	9.0	0.0414	10.3	0.0061	6.0	0.50	39.5	2.4	41.2	4.2	139.9	210.3	39.5	2.4	4.1
149	0.0559	14.3	0.0474	18.9	0.0062	12.6	0.66	39.6	5.0	47.1	8.7	446.9	317.5	39.6	5.0	15.9
313	0.0590	14.1	0.0502	18.1	0.0062	11.5	0.63	39.6	4.5	49.7	8.8	568.5	307.6	39.6	4.5	20.3
32	0.0635	12.7	0.0540	16.3	0.0062	10.5	0.62	39.7	4.1	53.4	8.5	724.0	270.4	39.7	4.1	25.7
51	0.0517	10.6	0.0441	13.9	0.0062	9.5	0.65	39.7	3.8	43.8	6.0	272.9	242.4	39.7	3.8	9.3
90	0.0638	11.0	0.0544	15.1	0.0062	10.3	0.68	39.7	4.1	53.7	7.9	735.1	233.7	39.7	4.1	26.1
181	0.0538	13.9	0.0459	17.1	0.0062	10.2	0.58	39.7	4.0	45.5	7.6	361.7	313.5	39.7	4.0	12.7
91	0.0495	14.8	0.0422	18.3	0.0062	10.8	0.59	39.7	4.3	42.0	7.5	170.4	345.2	39.7	4.3	5.3
264	0.0642	16.6	0.0548	19.9	0.0062	11.0	0.55	39.8	4.4	54.2	10.5	747.4	350.4	39.8	4.4	26.5

Table A4.9 (continued): Detrital Zircon U-Pb Integrated Data for the Punacancha Formation Top

Spot	Ratios							Ages (Ma)						Best Age	Disc. (%)	
	207Pb/206Pb		207Pb/235U		206Pb/238U		Rho	206Pb/238U		207Pb/235U		207Pb/206Pb				
	±2σ	±2σ	±2σ	±2σ	±2σ	±2σ		±2σ	±2σ	±2σ	±2σ	±2σ				
<i>Punacancha Formation Top (20140611-03) Accepted Data</i>																
260	0.0502	17.9	0.0429	20.2	0.0062	9.5	0.47	39.8	3.8	42.6	8.5	205.2	414.8	39.8	3.8	6.6
105	0.0532	13.7	0.0454	17.6	0.0062	11.3	0.63	39.8	4.5	45.1	7.8	336.6	310.2	39.8	4.5	11.7
369	0.0606	22.5	0.0518	25.2	0.0062	11.3	0.45	39.8	4.5	51.3	12.6	626.1	485.9	39.8	4.5	22.3
84	0.0841	26.9	0.0720	28.8	0.0062	10.6	0.36	39.9	4.2	70.6	19.7	1295.9	522.1	39.9	4.2	43.5
132	0.0557	8.7	0.0478	10.0	0.0062	5.4	0.49	39.9	2.1	47.4	4.6	441.6	193.7	39.9	2.1	15.7
197	0.0570	21.6	0.0489	23.5	0.0062	9.4	0.40	40.0	3.8	48.5	11.1	491.2	475.3	40.0	3.8	17.5
24	0.0682	20.3	0.0585	21.2	0.0062	6.8	0.30	40.0	2.7	57.7	11.9	874.2	420.0	40.0	2.7	30.7
8	0.0647	24.6	0.0556	25.9	0.0062	8.0	0.31	40.0	3.2	54.9	13.8	765.4	517.5	40.0	3.2	27.1
347	0.0602	15.1	0.0520	19.8	0.0063	12.9	0.65	40.2	5.2	51.4	9.9	611.2	325.4	40.2	5.2	21.8
131	0.0672	17.1	0.0581	20.4	0.0063	11.3	0.54	40.3	4.5	57.3	11.4	845.1	356.7	40.3	4.5	29.8
272	0.0449	10.8	0.0390	15.2	0.0063	10.7	0.71	40.4	4.3	38.8	5.8	-59.0	262.4	40.4	4.3	-4.1
390	0.1005	37.2	0.0871	38.6	0.0063	10.3	0.27	40.4	4.1	84.8	31.5	1632.6	692.1	40.4	4.1	52.3
14	0.0475	8.8	0.0412	10.1	0.0063	5.3	0.48	40.4	2.1	41.0	4.0	72.4	210.0	40.4	2.1	1.3
130	0.0540	15.8	0.0471	21.4	0.0063	14.7	0.68	40.7	6.0	46.7	9.8	369.4	354.9	40.7	6.0	13.0
154	0.0548	16.1	0.0479	20.0	0.0063	12.0	0.59	40.7	4.9	47.5	9.3	404.0	360.8	40.7	4.9	14.2
68	0.0591	13.1	0.0518	18.7	0.0064	13.4	0.71	40.8	5.4	51.3	9.4	572.5	285.5	40.8	5.4	20.4
31	0.0607	16.1	0.0533	18.8	0.0064	10.0	0.52	40.9	4.1	52.7	9.6	629.5	346.4	40.9	4.1	22.4
9	0.0542	17.7	0.0475	20.3	0.0064	9.8	0.49	40.9	4.0	47.1	9.3	378.2	398.5	40.9	4.0	13.3
318	0.0536	14.7	0.0471	17.6	0.0064	9.8	0.55	40.9	4.0	46.7	8.0	354.8	332.6	40.9	4.0	12.4
2	0.0479	8.3	0.0421	11.6	0.0064	8.0	0.70	41.0	3.3	41.9	4.8	96.0	197.2	41.0	3.3	2.2
94	0.0074	175.1	0.0065	175.2	0.0064	6.5	0.04	41.0	2.7	6.6	11.5	-26705	1E+05	41.0	2.7	-524.8
85	0.0501	22.6	0.0441	27.0	0.0064	15.0	0.55	41.0	6.1	43.8	11.6	198.9	523.8	41.0	6.1	6.4
56	0.0647	13.9	0.0571	14.5	0.0064	4.5	0.30	41.1	1.8	56.4	8.0	763.9	292.6	41.1	1.8	27.0
34	0.0512	24.0	0.0456	25.0	0.0064	7.6	0.29	41.4	3.2	45.2	11.1	251.6	551.2	41.4	3.2	8.4
157	0.0664	20.1	0.0597	23.1	0.0065	11.6	0.49	41.9	4.9	58.9	13.2	817.5	420.0	41.9	4.9	28.8
231	0.0634	22.9	0.0583	24.8	0.0067	9.5	0.38	42.9	4.0	57.6	13.9	722.5	485.6	42.9	4.0	25.6
382	0.0619	14.6	0.0570	16.1	0.0067	6.9	0.43	42.9	2.9	56.3	8.8	669.4	311.7	42.9	2.9	23.7
246	0.0612	16.6	0.0567	20.5	0.0067	12.1	0.59	43.2	5.2	56.0	11.2	644.7	355.8	43.2	5.2	22.9
13	0.0643	11.1	0.0597	14.3	0.0067	9.1	0.63	43.3	3.9	58.9	8.2	751.8	234.6	43.3	3.9	26.5
172	0.0581	27.5	0.0541	29.2	0.0068	9.9	0.34	43.4	4.3	53.5	15.2	532.3	602.4	43.4	4.3	18.9
218	0.0526	12.2	0.0520	16.0	0.0072	10.4	0.64	46.0	4.8	51.4	8.0	313.4	277.6	46.0	4.8	10.6
265	0.0668	27.7	0.1055	29.2	0.0114	9.1	0.31	73.4	6.7	101.8	28.3	832.7	577.5	73.4	6.7	27.9
389	0.0584	16.9	0.0927	18.1	0.0115	6.5	0.36	73.8	4.7	90.1	15.6	544.1	368.6	73.8	4.7	18.0
266	0.0744	19.5	0.1208	20.7	0.0118	7.0	0.34	75.5	5.2	115.8	22.7	1051.9	392.3	75.5	5.2	34.8
59	0.0539	17.8	0.0895	20.5	0.0120	10.3	0.50	77.2	7.9	87.1	17.1	367.4	400.9	77.2	7.9	11.4
378	0.0846	24.7	0.1407	28.2	0.0121	13.6	0.48	77.3	10.5	133.7	35.4	1307.0	479.8	77.3	10.5	42.2
206	0.0718	16.6	0.1203	19.5	0.0122	10.3	0.53	77.9	8.0	115.4	21.2	979.3	337.5	77.9	8.0	32.5
183	0.0578	17.1	0.0979	18.8	0.0123	7.9	0.41	78.7	6.2	94.8	17.0	523.3	375.6	78.7	6.2	17.0
226	0.0583	13.0	0.0993	15.1	0.0123	7.8	0.51	79.1	6.1	96.2	13.9	542.4	284.0	79.1	6.1	17.7
64	0.0601	10.7	0.1037	12.0	0.0125	5.6	0.46	80.2	4.4	100.2	11.5	607.1	231.2	80.2	4.4	20.0
4	0.0481	11.8	0.0868	13.7	0.0131	6.8	0.51	83.9	5.7	84.6	11.1	102.2	278.4	83.9	5.7	0.7
65	0.0595	17.9	0.1101	20.7	0.0134	10.4	0.50	85.9	8.9	106.0	20.9	586.1	389.0	85.9	8.9	19.0
127	0.0552	10.1	0.1134	12.5	0.0149	7.8	0.58	95.4	7.4	109.0	12.9	418.5	226.5	95.4	7.4	12.5
46	0.0574	11.3	0.1300	15.5	0.0164	11.0	0.68	105.0	11.4	124.1	18.1	507.8	248.6	105.0	11.4	15.4
340	0.0581	13.2	0.1659	19.1	0.0207	13.9	0.72	132.0	18.2	155.8	27.7	535.3	289.7	132.0	18.2	15.3
76	0.0526	10.1	0.1607	14.0	0.0222	9.7	0.69	141.3	13.6	151.3	19.7	311.2	230.4	141.3	13.6	6.6
254	0.0610	11.3	0.1866	12.3	0.0222	4.9	0.40	141.4	6.8	173.7	19.7	640.0	242.6	141.4	6.8	18.6
364	0.0506	10.8	0.1621	13.0	0.0232	7.2	0.55	148.1	10.5	152.5	18.4	221.1	250.2	148.1	10.5	2.9
69	0.0547	17.7	0.1942	19.3	0.0257	7.6	0.39	163.7	12.2	180.2	31.8	402.0	397.3	163.7	12.2	9.1
300	0.0556	12.0	0.2088	14.2	0.0272	7.7	0.54	173.3	13.1	192.5	24.9	435.7	266.3	173.3	13.1	10.0
60	0.0518	11.6	0.1966	15.8	0.0275	10.7	0.68	174.9	18.5	182.3	26.3	278.2	265.0	174.9	18.5	4.0
70	0.0570	15.0	0.2258	16.0	0.0287	5.7	0.35	182.7	10.2	206.8	29.9	491.1	329.9	182.7	10.2	11.7
237	0.0553	10.3	0.2413	12.6	0.0316	7.0	0.57	200.7	13.8	219.5	24.8	426.0	229.6	200.7	13.8	8.6
161	0.0566	6.1	0.2637	10.3	0.0338	8.5	0.80	214.3	17.8	237.6	21.8	475.0	135.6	214.3	17.8	9.8
253	0.0620	16.3	0.3134	19.8	0.0367	11.3	0.57	232.3	25.8	276.8	48.1	673.0	347.9	232.3	25.8	16.1
370	0.0542	13.9	0.3095	18.2	0.0414	11.7	0.65	261.7	30.1	273.8	43.7	378.9	312.6	261.7	30.1	4.4
209	0.0572	13.3	0.3453	17.5	0.0438	11.5	0.65	276.4	31.0	301.2	45.6	498.1	292.2	276.4	31.0	8.2
208	0.0576	7.4	0.3507	10.1	0.0441	7.1	0.68	278.3	19.2	305.2	26.8	516.5	163.0	278.3	19.2	8.8
291	0.0518	5.0	0.3160	6.8	0.0442	4.8	0.68	279.0	13.0	278.9	16.6	277.8	113.9	279.0	13.0	0.0
276	0.0536	11.9	0.3359	15.3	0.0455	9.6	0.63	286.7	27.0	294.1	39.0	353.0	269.4	286.7	27.0	2.5
202	0.0578	9.4	0.3958	12.6	0.0496	8.5	0.67	312.3	25.9	338.6	36.4	523.1	206.4	312.3	25.9	7.8
385	0.0639	9.3	0.6600	11.7	0.0749	7.1	0.61	465.4	31.9	514.6	47.4	739.5	197.0	465.4	31.9	9.6
124	0.0577	6.9	0.6003	8.7	0.0755	6.1	0.61	469.1	27.4	477.4	33.3	517.6	152.2	469.1	27.4	1.7

Table A4.9 (continued): Detrital Zircon U-Pb Integrated Data for the Punacancha Formation Top

Spot	Ratios						Ages (Ma)						Best Age	Disc. (%)		
	207Pb/206Pb		207Pb/235U		206Pb/238U		206Pb/238U		207Pb/235U		207Pb/206Pb					
	±2σ	±2σ	±2σ	±2σ	±2σ	±2σ	±2σ	±2σ	±2σ	±2σ	±2σ					
<i>Punacancha Formation Top (20140611-03) Accepted Data</i>																
12	0.0569	5.3	0.5944	7.7	0.0758	5.6	0.73	471.1	25.3	473.7	29.3	486.2	116.5	471.1	25.3	0.5
289	0.0615	5.4	0.6498	6.9	0.0767	4.4	0.63	476.2	20.4	508.4	27.8	655.6	116.2	476.2	20.4	6.3
330	0.0640	10.1	0.7235	12.9	0.0820	8.1	0.62	507.8	39.6	552.7	54.9	742.3	213.0	507.8	39.6	8.1
92	0.0590	4.7	0.7007	6.5	0.0862	4.7	0.69	532.9	23.9	539.2	27.4	566.2	102.6	532.9	23.9	1.2
81	0.0654	5.0	0.7809	6.4	0.0865	4.2	0.64	535.1	21.8	586.0	28.7	788.6	104.4	535.1	21.8	8.7
88	0.0639	5.1	0.7750	6.5	0.0880	4.2	0.63	543.9	22.0	582.6	28.9	736.8	107.6	543.9	22.0	6.7
211	0.0615	5.2	0.7561	6.6	0.0892	4.2	0.61	550.9	22.4	571.8	28.8	655.6	112.2	550.9	22.4	3.6
326	0.0882	12.8	1.1295	16.7	0.0929	10.9	0.65	572.7	59.9	767.5	90.4	1386.3	245.4	572.7	59.9	25.4
279	0.0633	7.5	0.8226	10.0	0.0942	6.7	0.67	580.6	37.4	609.5	45.9	718.3	158.3	580.6	37.4	4.7
164	0.0618	4.9	0.8043	6.4	0.0944	4.3	0.64	581.2	24.0	599.2	29.0	668.0	105.3	581.2	24.0	3.0
175	0.0625	13.4	0.8162	19.0	0.0948	13.5	0.71	583.6	75.2	605.9	86.8	690.4	285.8	583.6	75.2	3.7
126	0.0622	5.3	0.8347	6.0	0.0974	4.1	0.52	599.1	23.5	616.2	27.8	679.8	112.2	599.1	23.5	2.8
194	0.0684	4.9	1.1608	6.3	0.1231	4.1	0.63	748.6	29.2	782.3	34.6	879.7	101.7	748.6	29.2	14.9
50	0.0645	12.8	1.1065	18.0	0.1245	12.9	0.70	756.3	92.2	756.5	96.1	757.1	270.2	756.3	92.2	0.1
145	0.0700	6.7	1.6503	8.7	0.1711	6.0	0.64	1018.0	56.4	989.7	55.0	927.4	137.4	927.4	137.4	-9.8
107	0.0770	7.0	1.6616	8.7	0.1564	5.7	0.60	936.9	49.9	994.0	55.5	1122.0	140.5	936.9	49.9	16.5
140	0.0710	5.4	1.6678	6.0	0.1703	3.7	0.46	1013.9	34.4	996.3	37.9	957.8	110.3	957.8	110.3	-5.9
18	0.0724	6.0	1.6140	9.4	0.1616	7.7	0.77	965.7	69.5	975.7	58.9	998.1	122.5	965.7	69.5	3.2
97	0.0715	6.2	1.6026	8.7	0.1625	6.3	0.70	970.9	57.0	971.2	54.6	972.1	127.2	970.9	57.0	0.1
61	0.0745	3.9	1.6730	5.3	0.1629	3.7	0.68	973.1	33.3	998.3	33.5	1054.2	78.3	973.1	33.3	7.7
30	0.0715	3.6	1.6125	5.5	0.1636	4.8	0.76	976.7	43.7	975.1	34.7	971.5	74.3	976.7	43.7	-0.5
230	0.0748	8.9	1.7021	12.4	0.1651	8.5	0.70	984.8	78.0	1009.3	79.3	1062.9	178.4	984.8	78.0	7.3
125	0.0722	8.8	1.7304	12.3	0.1737	9.0	0.70	1032.6	86.0	1019.9	79.2	992.8	179.6	992.8	179.6	-4.0
17	0.0723	7.8	1.7627	11.5	0.1767	8.9	0.74	1049.1	86.6	1031.8	74.5	995.4	157.5	995.4	157.5	-5.4
45	0.0732	10.4	1.7190	15.2	0.1702	11.5	0.73	1013.2	107.6	1015.6	98.0	1020.9	210.5	1020.9	210.5	0.7
225	0.0744	12.3	1.7240	17.0	0.1680	11.7	0.69	1001.1	108.7	1017.5	109.6	1053.1	247.8	1053.1	247.8	4.9
78	0.0785	3.8	1.8504	5.5	0.1709	4.0	0.72	1017.0	38.0	1063.6	36.3	1160.5	75.7	1160.5	75.7	12.4
190	0.0787	12.6	2.0989	18.2	0.1934	13.2	0.72	1139.6	137.5	1148.5	125.8	1165.2	249.9	1165.2	249.9	2.2
79	0.0797	12.8	1.8591	17.5	0.1692	12.0	0.68	1007.8	111.7	1066.7	116.3	1189.2	253.4	1189.2	253.4	15.3
71	0.0801	3.0	2.0821	4.5	0.1885	3.4	0.74	1113.0	35.3	1142.9	30.7	1200.1	59.0	1200.1	59.0	7.3
21	0.0802	11.8	2.1902	18.2	0.1982	14.1	0.76	1165.4	150.6	1177.9	127.8	1201.0	232.8	1201.0	232.8	3.0
67	0.0815	14.8	1.9724	20.2	0.1754	13.9	0.68	1041.9	133.3	1106.1	137.1	1234.7	289.6	1234.7	289.6	15.6
49	0.0830	8.3	2.1252	11.2	0.1858	8.0	0.67	1098.6	80.7	1157.0	77.3	1268.2	162.5	1268.2	162.5	13.4
191	0.0845	6.4	2.2799	8.6	0.1956	5.9	0.67	1151.5	61.8	1206.1	60.8	1305.2	124.1	1305.2	124.1	11.8
393	0.0856	3.9	2.4478	5.8	0.2075	4.2	0.74	1215.5	46.7	1256.8	41.5	1328.2	74.8	1328.2	74.8	8.5
28	0.0874	4.6	2.7998	7.0	0.2324	5.7	0.75	1347.0	69.3	1355.5	52.1	1368.8	88.6	1368.8	88.6	1.6
249	0.0956	3.4	3.3899	4.8	0.2573	3.3	0.72	1475.8	43.9	1502.1	38.0	1539.3	63.1	1539.3	63.1	4.1
354	0.0976	10.6	3.0927	12.9	0.2299	7.5	0.58	1333.8	90.7	1430.9	99.4	1578.4	197.6	1578.4	197.6	15.5
117	0.1038	5.9	3.8634	7.7	0.2698	5.4	0.65	1539.9	74.4	1606.1	62.6	1694.0	108.7	1694.0	108.7	9.1
327	0.1055	7.1	3.9980	10.8	0.2749	8.4	0.76	1565.8	116.2	1633.8	88.0	1722.4	129.6	1722.4	129.6	9.1
212	0.1082	9.1	4.8362	12.9	0.3242	9.2	0.71	1810.0	145.4	1791.2	108.9	1769.4	166.9	1769.4	166.9	-2.3
189	0.1086	5.6	4.5516	7.6	0.3040	5.6	0.69	1711.2	83.5	1740.4	63.4	1775.8	101.3	1775.8	101.3	3.6
312	0.1102	5.2	4.2810	8.0	0.2818	6.3	0.77	1600.4	89.7	1689.7	66.1	1802.4	93.7	1802.4	93.7	11.2
5	0.1357	6.6	6.5390	10.2	0.3495	7.6	0.76	1932.1	126.2	2051.2	89.8	2173.0	115.7	2173.0	115.7	11.1
173	0.2040	3.7	14.6705	5.6	0.5216	4.3	0.75	2706.0	95.9	2794.1	53.4	2858.3	60.6	2858.3	60.6	5.3
<i>Punacancha Formation Top (20140611-03) Rejected Data</i>																
339	0.0814	21.0	0.0444	22.5	0.0040	8.3	0.36	25.5	2.1	44.1	9.7	1230.2	412.7	25.5	2.1	42.3
305	0.0831	16.0	0.0456	17.6	0.0040	7.5	0.42	25.6	1.9	45.3	7.8	1272.7	311.7	25.6	1.9	43.5
89	0.0732	15.9	0.0409	16.6	0.0041	5.0	0.29	26.1	1.3	40.7	6.6	1018.1	322.0	26.1	1.3	35.9
41	0.0719	12.5	0.0403	13.4	0.0041	5.5	0.36	26.1	1.4	40.1	5.3	984.3	254.6	26.1	1.4	34.8
372	0.0846	20.7	0.0474	21.9	0.0041	7.0	0.32	26.2	1.8	47.0	10.0	1305.8	402.0	26.2	1.8	44.4
1	0.0771	15.8	0.0434	17.2	0.0041	6.5	0.39	26.3	1.7	43.2	7.3	1124.1	315.2	26.3	1.7	39.1
205	0.0667	13.8	0.0376	14.8	0.0041	5.5	0.36	26.3	1.5	37.4	5.4	827.6	286.9	26.3	1.5	29.8
204	0.0743	19.2	0.0420	21.0	0.0041	8.7	0.41	26.3	2.3	41.7	8.6	1050.3	386.4	26.3	2.3	36.9
80	0.0817	23.5	0.0462	24.7	0.0041	7.6	0.31	26.4	2.0	45.9	11.1	1237.8	460.6	26.4	2.0	42.5
315	0.0840	20.7	0.0478	22.0	0.0041	7.8	0.34	26.6	2.1	47.4	10.2	1292.8	402.1	26.6	2.1	44.0
302	0.0949	24.3	0.0541	25.8	0.0041	8.9	0.34	26.6	2.4	53.5	13.5	1526.8	457.6	26.6	2.4	50.3
100	0.0878	21.8	0.0505	22.9	0.0042	7.1	0.30	26.9	1.9	50.1	11.2	1377.2	419.0	26.9	1.9	46.3
213	0.0710	15.5	0.0409	16.9	0.0042	6.7	0.39	26.9	1.8	40.7	6.7	957.2	317.5	26.9	1.8	34.0
236	0.1079	21.9	0.0623	23.8	0.0042	9.1	0.39	26.9	2.4	61.3	14.2	1764.7	401.0	26.9	2.4	56.1
342	0.0981	18.2	0.0568	21.2	0.0042	11.0	0.51	27.0	3.0	56.1	11.6	1588.3	340.9	27.0	3.0	51.8
39	0.0837	15.1	0.0486	16.4	0.0042	7.3	0.40	27.1	2.0	48.2	7.7	1285.3	293.5	27.1	2.0	43.8
201	0.0811	16.0	0.0475	17.7	0.0042	7.7	0.43	27.3	2.1	47.1	8.2	1223.8	314.2	27.3	2.1	42.0

Table A4.9 (continued): Detrital Zircon U-Pb Integrated Data for the Punacancha Formation Top

Spot	Ratios						Ages (Ma)						Best Age	Disc. (%)		
	207Pb/206Pb		207Pb/235U		206Pb/238U		206Pb/238U		207Pb/235U		207Pb/206Pb					
		$\pm 2\sigma$		$\pm 2\sigma$		$\pm 2\sigma$		$\pm 2\sigma$		$\pm 2\sigma$		$\pm 2\sigma$				
<i>Punacancha Formation Top (20140611-03) Rejected Data</i>																
16	0.1082	20.7	0.0634	22.0	0.0042	7.9	0.33	27.3	2.1	62.4	13.3	1768.6	378.2	27.3	2.1	56.2
329	0.0742	19.9	0.0435	21.3	0.0043	7.5	0.35	27.4	2.1	43.3	9.0	1047.4	402.2	27.4	2.1	36.8
6	0.0953	13.7	0.0559	15.5	0.0043	7.2	0.47	27.4	2.0	55.2	8.4	1533.3	257.7	27.4	2.0	50.4
174	0.1186	23.6	0.0698	25.7	0.0043	10.3	0.40	27.4	2.8	68.5	17.0	1935.5	421.9	27.4	2.8	59.9
250	0.1177	27.1	0.0696	28.4	0.0043	8.4	0.30	27.6	2.3	68.3	18.8	1921.1	486.0	27.6	2.3	59.6
350	0.1088	14.2	0.0644	15.9	0.0043	7.1	0.44	27.6	2.0	63.3	9.7	1779.8	259.8	27.6	2.0	56.4
33	0.0738	17.6	0.0438	18.8	0.0043	7.0	0.35	27.7	1.9	43.5	8.0	1035.6	355.7	27.7	1.9	36.4
262	0.0767	21.9	0.0456	23.0	0.0043	7.0	0.30	27.7	1.9	45.3	10.2	1112.3	437.7	27.7	1.9	38.7
399	0.0817	24.3	0.0486	25.6	0.0043	8.2	0.32	27.7	2.3	48.2	12.1	1239.5	476.0	27.7	2.3	42.4
287	0.0969	18.7	0.0579	20.2	0.0043	7.6	0.37	27.8	2.1	57.1	11.2	1566.2	350.5	27.8	2.1	51.2
388	0.0746	19.3	0.0447	20.3	0.0043	6.3	0.31	28.0	1.8	44.4	8.8	1057.2	387.7	28.0	1.8	37.0
351	0.0832	21.4	0.0499	22.8	0.0044	8.0	0.35	28.0	2.2	49.5	11.0	1273.4	417.6	28.0	2.2	43.4
170	0.1186	13.8	0.0720	16.1	0.0044	8.3	0.51	28.3	2.3	70.6	11.0	1935.9	246.9	28.3	2.3	59.9
187	0.1358	20.2	0.0824	21.8	0.0044	8.4	0.38	28.3	2.4	80.4	16.9	2173.7	352.3	28.3	2.4	64.8
193	0.1479	14.3	0.0910	15.7	0.0045	6.5	0.41	28.7	1.9	88.4	13.3	2321.7	245.7	28.7	1.9	67.5
308	0.0856	12.1	0.0529	15.7	0.0045	10.0	0.64	28.8	2.9	52.3	8.0	1329.3	234.5	28.8	2.9	44.9
383	0.0962	26.4	0.0594	28.0	0.0045	9.3	0.33	28.8	2.7	58.6	15.9	1551.1	495.6	28.8	2.7	50.8
292	0.0770	18.0	0.0475	21.4	0.0045	11.5	0.54	28.8	3.3	47.1	9.8	1120.1	359.5	28.8	3.3	38.9
53	0.0857	18.0	0.0530	18.8	0.0045	6.1	0.29	28.8	1.8	52.4	9.6	1331.2	347.5	28.8	1.8	45.0
281	0.1123	21.9	0.0697	23.8	0.0045	9.3	0.39	29.0	2.7	68.4	15.7	1836.5	397.0	29.0	2.7	57.7
338	0.0849	13.0	0.0532	15.3	0.0045	8.2	0.53	29.2	2.4	52.6	7.8	1313.2	251.7	29.2	2.4	44.5
263	0.0751	15.1	0.0471	17.2	0.0045	8.2	0.48	29.2	2.4	46.7	7.9	1070.0	304.1	29.2	2.4	37.4
371	0.0788	26.1	0.0494	30.5	0.0045	15.7	0.52	29.2	4.6	49.0	14.6	1167.1	516.7	29.2	4.6	40.3
363	0.1425	19.9	0.0896	21.3	0.0046	7.6	0.36	29.3	2.2	87.2	17.8	2257.7	344.3	29.3	2.2	66.3
357	0.0752	12.9	0.0476	13.6	0.0046	4.6	0.33	29.5	1.3	47.2	6.3	1074.1	258.1	29.5	1.3	37.5
137	0.1151	32.0	0.0748	34.1	0.0047	12.2	0.34	30.3	3.7	73.2	24.1	1882.2	577.1	30.3	3.7	58.6
232	0.0779	19.7	0.0510	22.2	0.0048	10.1	0.46	30.6	3.1	50.5	10.9	1143.4	391.0	30.6	3.1	39.5
235	0.1113	15.5	0.0730	18.1	0.0048	9.1	0.52	30.6	2.8	71.5	12.5	1820.4	281.2	30.6	2.8	57.2
284	0.1348	15.0	0.0886	16.6	0.0048	7.1	0.43	30.7	2.2	86.2	13.7	2161.0	261.8	30.7	2.2	64.4
316	0.1767	15.8	0.1180	17.6	0.0048	7.9	0.44	31.1	2.5	113.2	18.8	2622.0	262.4	31.1	2.5	72.5
58	0.1584	12.8	0.1064	15.0	0.0049	7.9	0.52	31.3	2.5	102.7	14.7	2439.1	217.2	31.3	2.5	69.5
288	0.1901	23.4	0.1277	25.7	0.0049	10.6	0.41	31.3	3.3	122.0	29.6	2742.7	385.4	31.3	3.3	74.3
348	0.1596	19.6	0.1077	20.9	0.0049	7.4	0.34	31.5	2.3	103.9	20.7	2451.0	332.1	31.5	2.3	69.7
224	0.1813	13.6	0.1232	15.2	0.0049	7.0	0.44	31.7	2.2	118.0	16.9	2664.7	226.0	31.7	2.2	73.1
188	0.0781	16.8	0.0531	18.0	0.0049	6.6	0.35	31.7	2.1	52.5	9.2	1148.9	334.6	31.7	2.1	39.6
180	0.1613	15.4	0.1104	16.6	0.0050	6.4	0.37	31.9	2.0	106.3	16.7	2469.7	259.9	31.9	2.0	70.0
48	0.1334	20.6	0.0927	22.8	0.0050	10.1	0.43	32.4	3.3	90.0	19.6	2143.3	360.5	32.4	3.3	64.0
57	0.1204	33.1	0.0844	36.1	0.0051	14.4	0.40	32.7	4.7	82.3	28.5	1961.9	590.9	32.7	4.7	60.3
365	0.1259	12.9	0.0884	14.2	0.0051	5.9	0.42	32.7	1.9	86.0	11.7	2042.0	227.8	32.7	1.9	61.9
139	0.1699	17.6	0.1195	20.5	0.0051	11.1	0.52	32.8	3.6	114.6	22.3	2556.4	294.1	32.8	3.6	71.4
192	0.0827	25.7	0.0588	31.6	0.0052	18.4	0.58	33.2	6.1	58.1	17.8	1263.1	502.5	33.2	6.1	42.9
215	0.1899	18.9	0.1362	19.8	0.0052	6.3	0.30	33.4	2.1	129.6	24.1	2741.2	310.5	33.4	2.1	74.2
356	0.1246	24.8	0.0894	27.7	0.0052	12.4	0.45	33.5	4.1	87.0	23.1	2023.4	439.9	33.5	4.1	61.5
240	0.1974	15.7	0.1482	17.1	0.0054	6.5	0.39	35.0	2.3	140.4	22.4	2804.9	256.5	35.0	2.3	75.1
241	0.0879	23.6	0.0662	25.4	0.0055	9.5	0.38	35.1	3.3	65.1	16.0	1381.1	452.6	35.1	3.3	46.1
129	0.1486	27.8	0.1119	29.9	0.0055	11.1	0.36	35.1	3.9	107.7	30.6	2329.6	476.8	35.1	3.9	67.4
138	0.0952	25.7	0.0728	29.2	0.0055	14.2	0.47	35.6	5.1	71.3	20.1	1531.8	484.6	35.6	5.1	50.0
171	0.2396	17.8	0.1858	19.0	0.0056	6.8	0.35	36.2	2.5	173.0	30.2	3117.5	282.8	36.2	2.5	79.1
22	0.1032	16.6	0.0812	18.5	0.0057	8.5	0.44	36.7	3.1	79.3	14.1	1683.1	306.9	36.7	3.1	53.7
324	0.1087	24.0	0.0870	28.6	0.0058	15.7	0.54	37.3	5.8	84.7	23.3	1777.4	438.0	37.3	5.8	55.9
128	0.1002	19.7	0.0811	21.1	0.0059	7.9	0.35	37.7	3.0	79.2	16.0	1627.3	367.2	37.7	3.0	52.3
184	0.0869	12.4	0.0710	13.5	0.0059	5.5	0.39	38.1	2.1	69.6	9.1	1357.8	239.6	38.1	2.1	45.3
362	0.1772	20.6	0.1449	23.4	0.0059	11.0	0.47	38.1	4.2	137.4	30.0	2626.7	341.9	38.1	4.2	72.3
177	0.0542	16.1	0.0445	22.2	0.0059	15.2	0.69	38.2	5.8	44.2	9.6	380.8	362.4	38.2	5.8	13.5
303	0.0942	30.9	0.0776	32.3	0.0060	9.3	0.29	38.4	3.6	75.9	23.6	1512.1	583.1	38.4	3.6	49.4
334	0.0641	24.9	0.0532	32.3	0.0060	20.7	0.64	38.7	8.0	52.6	16.6	746.1	525.2	38.7	8.0	26.5
182	0.0672	13.1	0.0564	14.7	0.0061	7.0	0.46	39.1	2.7	55.7	8.0	845.5	272.3	39.1	2.7	29.8
252	0.0930	26.4	0.0781	28.3	0.0061	10.0	0.36	39.1	3.9	76.3	20.8	1488.5	500.0	39.1	3.9	48.8
93	0.2641	20.3	0.2222	23.9	0.0061	12.6	0.53	39.2	4.9	203.7	44.1	3271.4	318.8	39.2	4.9	80.8
165	0.0490	17.7	0.0414	24.7	0.0061	17.3	0.70	39.4	6.8	41.2	10.0	146.3	415.5	39.4	6.8	4.3
395	0.0458	19.8	0.0388	27.0	0.0061	18.4	0.68	39.5	7.2	38.6	10.2	-14.4	479.6	39.5	7.2	-2.2
72	0.1061	19.3	0.0899	21.2	0.0061	8.8	0.41	39.5	3.4	87.4	17.7	1733.0	354.1	39.5	3.4	54.8
344	0.0876	27.4	0.0746	28.5	0.0062	8.0	0.28	39.7	3.2	73.0	20.1	1373.5	527.6	39.7	3.2	45.7

Table A4.9 (continued): Detrital Zircon U-Pb Integrated Data for the Punacancha Formation Top

Spot	Ratios						Rho	Ages (Ma)						Best Age	Disc. (%)	
	207Pb/206Pb		207Pb/235U		206Pb/238U			206Pb/238U		207Pb/235U		207Pb/206Pb				±2σ
	±2σ	±2σ	±2σ	±2σ	±2σ	±2σ		±2σ	±2σ	±2σ	±2σ	±2σ				
<i>Punacancha Formation Top (20140611-03) Rejected Data</i>																
113	0.0584	17.3	0.0498	23.4	0.0062	15.9	0.67	39.7	6.3	49.3	11.3	546.4	378.4	39.7	6.3	19.5
233	0.0852	23.4	0.0726	24.5	0.0062	7.1	0.29	39.7	2.8	71.2	16.8	1319.9	453.1	39.7	2.8	44.2
216	0.0720	13.0	0.0620	16.6	0.0062	10.5	0.62	40.1	4.2	61.0	9.8	984.9	264.2	40.1	4.2	34.3
310	0.1305	39.8	0.1132	42.0	0.0063	13.7	0.32	40.4	5.5	108.9	43.4	2105.2	698.1	40.4	5.5	62.9
386	0.0605	24.2	0.0526	29.3	0.0063	16.5	0.56	40.5	6.7	52.0	14.9	621.9	522.6	40.5	6.7	22.2
333	0.1129	23.2	0.0988	24.6	0.0063	8.2	0.33	40.8	3.3	95.7	22.4	1847.3	419.6	40.8	3.3	57.4
185	0.0608	20.9	0.0537	29.2	0.0064	20.5	0.70	41.2	8.4	53.1	15.1	630.6	450.1	41.2	8.4	22.4
280	0.0795	20.7	0.0707	23.1	0.0065	10.1	0.44	41.5	4.2	69.4	15.5	1184.7	409.9	41.5	4.2	40.3
43	0.1202	44.2	0.1072	49.7	0.0065	22.9	0.46	41.6	9.5	103.4	48.9	1959.1	789.4	41.6	9.5	59.8
103	0.0563	24.9	0.0503	36.1	0.0065	26.1	0.72	41.6	10.8	49.8	17.5	465.7	552.2	41.6	10.8	16.5
83	0.3423	14.4	0.3105	16.1	0.0066	7.3	0.45	42.3	3.1	274.5	38.7	3673.3	219.6	42.3	3.1	84.6
368	0.2885	14.6	0.2621	18.0	0.0066	10.4	0.58	42.3	4.4	236.4	37.9	3409.3	227.4	42.3	4.4	82.1
44	0.0600	17.7	0.0547	23.9	0.0066	16.2	0.67	42.4	6.9	54.0	12.6	604.0	383.6	42.4	6.9	21.5
10	0.2619	17.4	0.2392	20.9	0.0066	11.5	0.55	42.6	4.9	217.8	40.9	3258.2	273.9	42.6	4.9	80.5
167	0.0523	27.5	0.0479	39.1	0.0066	27.8	0.71	42.6	11.8	47.5	18.1	300.0	626.0	42.6	11.8	10.2
47	0.0854	15.7	0.0784	18.3	0.0067	9.9	0.52	42.8	4.2	76.7	13.5	1325.2	303.9	42.8	4.2	44.2
207	0.1004	20.6	0.0926	27.1	0.0067	17.7	0.65	43.0	7.6	90.0	23.4	1631.7	383.7	43.0	7.6	52.2
273	0.0939	20.4	0.0867	23.0	0.0067	10.7	0.47	43.0	4.6	84.4	18.7	1507.1	385.4	43.0	4.6	49.1
367	0.0972	21.3	0.0900	24.0	0.0067	10.9	0.46	43.2	4.7	87.5	20.1	1570.7	399.4	43.2	4.7	50.7
314	0.0786	18.4	0.0730	23.0	0.0067	13.8	0.60	43.3	6.0	71.6	15.9	1161.9	365.5	43.3	6.0	39.5
387	0.2341	19.4	0.2177	22.7	0.0067	11.8	0.52	43.3	5.1	200.0	41.3	3080.2	310.4	43.3	5.1	78.3
179	0.1031	13.9	0.0965	18.0	0.0068	11.5	0.64	43.6	5.0	93.5	16.1	1681.1	256.7	43.6	5.0	53.4
294	0.0319	34.4	0.0302	40.9	0.0069	22.1	0.54	44.1	9.7	30.2	12.1	-975.2	1008.6	44.1	9.7	-46.1
274	0.0994	17.9	0.0944	20.3	0.0069	9.4	0.46	44.2	4.1	91.6	17.7	1613.7	334.2	44.2	4.1	51.7
228	0.0567	28.3	0.0541	40.9	0.0069	29.5	0.72	44.5	13.1	53.5	21.3	479.7	626.2	44.5	13.1	16.9
77	0.0551	24.6	0.0526	33.4	0.0069	22.6	0.68	44.5	10.0	52.1	17.0	415.1	550.8	44.5	10.0	14.5
42	0.0844	19.0	0.0808	21.6	0.0069	10.7	0.48	44.6	4.8	78.9	16.4	1301.6	369.0	44.6	4.8	43.5
337	0.0939	11.6	0.0905	13.2	0.0070	6.5	0.48	44.9	2.9	88.0	11.2	1506.2	219.6	44.9	2.9	49.0
178	0.0983	15.2	0.0960	16.7	0.0071	7.0	0.42	45.5	3.2	93.1	14.9	1593.0	284.1	45.5	3.2	51.1
62	0.1297	17.8	0.1322	19.5	0.0074	7.9	0.40	47.5	3.8	126.1	23.1	2093.5	313.7	47.5	3.8	62.3
136	0.0882	26.4	0.0905	34.6	0.0074	22.6	0.65	47.8	10.7	88.0	29.1	1387.7	506.5	47.8	10.7	45.7
25	0.0595	23.4	0.0617	31.0	0.0075	20.6	0.66	48.3	9.9	60.8	18.3	585.0	506.9	48.3	9.9	20.5
349	0.1503	18.7	0.1571	24.1	0.0076	15.2	0.63	48.7	7.4	148.2	33.2	2349.2	320.2	48.7	7.4	67.1
144	0.2086	13.0	0.2230	14.5	0.0078	7.0	0.45	49.8	3.5	204.4	26.8	2894.7	210.2	49.8	3.5	75.6
168	0.0628	29.3	0.0675	39.1	0.0078	25.9	0.66	50.0	12.9	66.3	25.1	702.2	622.8	50.0	12.9	24.6
217	0.2510	21.0	0.2738	26.4	0.0079	16.1	0.60	50.8	8.1	245.7	57.6	3190.9	332.4	50.8	8.1	79.3
115	0.1535	22.7	0.1702	27.7	0.0080	15.9	0.57	51.6	8.2	159.6	40.9	2385.7	387.0	51.6	8.2	67.7
251	0.2263	15.8	0.2704	19.2	0.0087	10.9	0.57	55.6	6.0	243.0	41.5	3026.4	252.7	55.6	6.0	77.1
328	0.2781	13.8	0.3443	16.2	0.0090	8.8	0.53	57.6	5.0	300.4	42.3	3352.3	215.4	57.6	5.0	80.8
286	0.3134	19.7	0.3948	24.2	0.0091	14.0	0.58	58.6	8.2	337.9	69.5	3538.0	303.9	58.6	8.2	82.6
123	0.3113	15.6	0.4003	17.4	0.0093	8.1	0.44	59.8	4.8	341.9	50.5	3527.5	240.7	59.8	4.8	82.5
152	0.2295	13.3	0.3064	17.3	0.0097	11.3	0.64	62.1	7.0	271.4	41.3	3048.9	212.6	62.1	7.0	77.1
151	0.0773	14.7	0.1128	15.9	0.0106	6.2	0.38	67.9	4.2	108.6	16.4	1128.7	293.0	67.9	4.2	37.5
55	0.0711	13.6	0.1049	14.5	0.0107	5.2	0.35	68.6	3.6	101.3	14.0	959.8	277.1	68.6	3.6	32.2
40	0.0687	10.8	0.1020	12.2	0.0108	6.3	0.47	69.0	4.3	98.6	11.5	890.4	223.2	69.0	4.3	30.0
26	0.0948	21.0	0.1438	22.9	0.0110	9.5	0.40	70.6	6.6	136.4	29.3	1523.9	396.5	70.6	6.6	48.3
245	0.0781	13.5	0.1190	16.5	0.0110	9.3	0.57	70.8	6.6	114.2	17.8	1149.6	268.1	70.8	6.6	37.9
143	0.0668	11.2	0.1022	11.6	0.0111	4.0	0.27	71.2	2.8	98.8	10.9	830.1	233.2	71.2	2.8	28.0
108	0.1187	30.1	0.1911	31.8	0.0117	10.3	0.32	74.8	7.7	177.6	51.8	1937.2	539.2	74.8	7.7	57.9
109	0.0749	16.1	0.1308	18.0	0.0127	8.4	0.45	81.1	6.8	124.8	21.1	1066.6	323.1	81.1	6.8	35.0
158	0.5052	14.0	0.8860	16.6	0.0127	9.3	0.54	81.5	7.5	644.2	79.5	4256.4	206.1	81.5	7.5	87.4
200	0.0518	19.9	0.0909	25.6	0.0127	16.0	0.63	81.5	13.0	88.3	21.6	276.7	456.7	81.5	13.0	7.7
214	0.1429	16.1	0.2635	17.6	0.0134	7.3	0.40	85.6	6.2	237.5	37.2	2262.8	277.8	85.6	6.2	63.9
323	0.1857	19.2	0.3438	21.5	0.0134	9.7	0.45	86.0	8.3	300.0	55.9	2704.7	317.0	86.0	8.3	71.3
223	0.1422	15.7	0.3797	20.9	0.0194	13.9	0.66	123.7	17.0	326.8	58.5	2253.7	271.3	123.7	17.0	62.2
244	0.2225	17.2	0.6333	22.9	0.0206	15.0	0.66	131.7	19.6	498.2	90.3	2999.0	276.9	131.7	19.6	73.6
3	0.0858	7.3	0.2624	11.3	0.0222	8.6	0.77	141.5	12.0	236.6	23.9	1332.6	140.4	141.5	12.0	40.2
343	0.0552	24.5	0.1761	33.9	0.0231	23.4	0.69	147.5	34.1	164.7	51.6	419.8	547.5	147.5	34.1	10.4
195	0.0954	9.7	0.3148	12.1	0.0239	7.3	0.59	152.4	11.0	277.9	29.3	1536.9	182.8	152.4	11.0	45.2
66	0.0484	17.4	0.1677	24.8	0.0251	17.7	0.71	159.9	28.0	157.4	36.2	119.8	410.2	159.9	28.0	-1.6
120	0.0771	12.3	0.2883	14.7	0.0271	8.5	0.55	172.4	14.5	257.2	33.5	1125.0	244.5	172.4	14.5	33.0
290	0.1004	24.1	0.3887	31.9	0.0281	20.9	0.65	178.6	36.7	333.4	90.8	1630.7	448.0	178.6	36.7	46.4
159	0.2559	14.4	1.1324	15.7	0.0321	6.6	0.40	203.7	13.3	768.9	84.9	3221.4	227.6	203.7	13.3	73.5

Table A4.9 (continued): Detrital Zircon U-Pb Integrated Data for the Punacancha Formation Top

Spot	Ratios						Ages (Ma)						Best Age	Disc. (%)		
	207Pb/206Pb		207Pb/235U		206Pb/238U		206Pb/238U		207Pb/235U		207Pb/206Pb					
	±2σ	±2σ	±2σ	±2σ	Rho	±2σ	±2σ	±2σ	±2σ	±2σ	±2σ					
<i>Punacancha Formation Top (20140611-03) Rejected Data</i>																
73	0.1407	19.5	0.6258	22.8	0.0323	11.9	0.52	204.7	24.0	493.5	89.4	2235.7	336.9	204.7	24.0	58.5
384	0.0562	22.0	0.2860	28.7	0.0369	18.4	0.64	233.8	42.2	255.4	64.9	459.1	488.9	233.8	42.2	8.5
270	0.0821	46.2	0.7667	60.7	0.0677	39.3	0.65	422.3	160.6	577.9	273.7	1248.6	904.8	422.3	160.6	26.9
87	0.0684	7.7	0.9613	11.4	0.1019	8.5	0.74	625.5	50.8	684.0	57.0	881.3	159.7	625.5	50.8	29.0
133	0.0972	19.4	1.4779	24.5	0.1103	15.2	0.61	674.3	97.4	921.4	149.5	1571.1	362.7	674.3	97.4	57.1
220	0.0751	15.5	1.1834	19.9	0.1142	12.6	0.63	697.2	83.5	792.9	110.0	1072.4	311.3	697.2	83.5	35.0
142	0.0651	6.3	1.2981	8.2	0.1446	5.9	0.64	870.6	47.6	844.9	46.9	777.9	132.3	870.6	47.6	-11.9
112	0.0806	6.1	1.7879	7.4	0.1610	4.7	0.57	962.1	41.7	1041.1	48.4	1210.7	119.8	962.1	41.7	20.5
19	0.0730	15.8	1.6429	19.7	0.1632	12.0	0.59	974.3	108.7	986.8	124.8	1014.8	320.9	974.3	108.7	4.0
134	0.0725	16.1	1.7298	22.5	0.1731	16.0	0.70	1029.2	152.4	1019.7	145.7	999.3	327.4	999.3	327.4	-3.0
162	0.0755	21.3	1.9860	31.0	0.1908	22.7	0.73	1125.7	234.2	1110.8	212.7	1081.6	427.0	1081.6	427.0	-4.1
298	0.0846	15.2	2.2040	20.6	0.1889	14.0	0.68	1115.5	143.6	1182.3	145.0	1306.7	294.3	1306.7	294.3	14.6
346	0.0851	17.7	2.2179	26.5	0.1890	19.8	0.74	1116.0	202.8	1186.7	187.7	1318.0	343.7	1318.0	343.7	15.3
166	0.0854	25.5	3.0503	35.7	0.2590	25.1	0.70	1484.7	332.6	1420.3	279.9	1325.1	493.2	1325.1	493.2	-12.0
301	0.0991	17.1	2.3973	22.9	0.1755	15.3	0.67	1042.3	147.2	1241.8	165.5	1606.8	318.3	1606.8	318.3	35.1
353	0.2196	8.6	8.3684	11.3	0.2764	7.4	0.65	1573.3	103.6	2271.8	102.7	2977.6	138.1	2977.6	138.1	47.2
255	0.2693	12.3	7.6470	21.5	0.2060	17.6	0.82	1207.4	194.2	2190.4	195.6	3301.7	193.1	3301.7	193.1	63.4
242	0.7938	15.6	389.4475	23.2	3.5582	17.1	0.74	9778.8	865.1	6059.1	239.3	4910.7	223.8	4910.7	223.8	-99.1
345	0.8425	24.8	7914.6477	75.2	68.1294	71.0	0.94	27306.9	5583.8	9114.7	991.8	4995.4	355.1	4995.4	355.1	-446.6
242	0.9888	100.7	293.3519	133.9	2.1516	88.3	0.66	7400.0	4494.9	5772.2	1875	5221.6	1431.5	5221.6	1431.5	-41.7

Table A4.10: Detrital Zircon U-Pb Integrated Data for the Paruro Formation Base

Spot	Ratios							Ages (Ma)						Disc. (%)		
	207Pb/206Pb		207Pb/235U		206Pb/238U		Rho	206Pb/238U		207Pb/235U		207Pb/206Pb			Best Age	
	±2σ	±2σ	±2σ	±2σ	±2σ	±2σ		±2σ	±2σ	±2σ	±2σ	±2σ	±2σ			
<i>Paruro Formation Base 1 (20140605-01) Accepted Data</i>																
308	0.0642	9.3	0.0956	10.4	0.0108	5.9	0.46	69.3	4.1	92.7	9.2	746.6	196.4	69.3	4.1	25.2
186	0.0593	15.1	0.0955	20.9	0.0117	14.5	0.69	74.9	10.8	92.6	18.5	577.1	329.1	74.9	10.8	19.1
230	0.0595	12.5	0.0973	18.5	0.0119	13.4	0.73	76.0	10.1	94.3	16.6	584.1	272.3	76.0	10.1	19.3
193	0.0614	5.7	0.1144	7.1	0.0135	3.9	0.58	86.5	3.3	110.0	7.4	653.0	123.4	86.5	3.3	21.3
53	0.0588	6.5	0.1154	8.0	0.0142	5.2	0.60	91.1	4.7	110.9	8.4	558.9	140.8	91.1	4.7	17.8
334	0.0525	7.1	0.1119	9.1	0.0154	5.8	0.62	98.8	5.6	107.7	9.3	308.2	162.2	98.8	5.6	8.2
130	0.0661	11.8	0.1757	14.9	0.0193	9.2	0.62	123.1	11.2	164.4	22.7	809.5	246.1	123.1	11.2	25.1
330	0.0590	6.0	0.1632	7.1	0.0201	4.1	0.54	128.1	5.2	153.5	10.2	566.6	131.3	128.1	5.2	16.6
208	0.0661	9.8	0.2410	10.9	0.0265	4.6	0.45	168.3	7.6	219.2	21.6	808.3	204.8	168.3	7.6	23.2
3	0.0665	9.4	0.3306	12.1	0.0361	8.1	0.64	228.4	18.1	290.0	30.5	821.9	195.4	228.4	18.1	21.3
236	0.0642	5.5	0.3687	9.1	0.0416	6.4	0.81	263.0	16.5	318.7	25.0	748.8	116.2	263.0	16.5	17.5
332	0.0620	4.3	0.3628	5.5	0.0425	3.7	0.62	268.1	9.6	314.3	14.8	672.8	91.6	268.1	9.6	14.7
200	0.0580	7.4	0.3510	10.1	0.0439	6.9	0.68	277.0	18.6	305.5	26.6	529.0	162.0	277.0	18.6	9.3
139	0.0671	5.8	0.6474	6.9	0.0700	3.7	0.54	435.9	15.7	506.9	27.7	841.2	121.3	435.9	15.7	14.0
114	0.0685	10.8	0.6896	15.2	0.0730	10.7	0.70	454.1	47.0	532.6	63.2	884.7	223.4	454.1	47.0	14.7
190	0.0729	11.4	0.7637	13.4	0.0760	6.9	0.52	472.4	31.3	576.2	58.8	1010.0	230.9	472.4	31.3	18.0
25	0.0747	9.0	0.7854	11.9	0.0763	7.9	0.66	473.8	36.0	588.6	53.4	1060.2	180.3	473.8	36.0	19.5
147	0.0647	10.5	0.6934	15.0	0.0778	10.8	0.72	482.8	50.4	534.9	62.5	763.7	220.6	482.8	50.4	9.7
185	0.0742	6.2	0.8090	7.5	0.0791	4.4	0.57	490.7	20.9	601.9	34.1	1046.5	124.1	490.7	20.9	18.5
205	0.0599	4.4	0.6610	5.7	0.0800	3.8	0.65	496.2	18.1	515.2	23.1	600.5	94.3	496.2	18.1	3.7
12	0.0802	6.2	0.8906	7.8	0.0806	4.8	0.61	499.5	23.3	646.7	37.5	1201.4	122.1	499.5	23.3	22.8
269	0.0587	4.5	0.6635	7.0	0.0819	5.1	0.77	507.6	24.7	516.7	28.2	557.3	97.0	507.6	24.7	1.8
293	0.0660	13.8	0.7531	19.7	0.0828	14.2	0.71	512.5	70.1	570.0	86.2	806.4	288.6	512.5	70.1	10.1
352	0.0632	5.3	0.7296	7.0	0.0838	4.7	0.66	518.6	23.3	556.3	30.0	713.9	111.6	518.6	23.3	6.8
362	0.0847	9.1	0.9881	12.8	0.0846	9.0	0.70	523.6	45.5	697.8	64.7	1308.7	176.3	523.6	45.5	25.0
33	0.0671	5.2	0.7929	6.3	0.0857	3.6	0.57	529.9	18.4	592.8	28.3	841.4	107.8	529.9	18.4	10.6
119	0.0654	3.5	0.7738	4.5	0.0858	2.8	0.63	530.7	14.2	581.9	19.9	787.1	72.8	530.7	14.2	8.8
254	0.0771	6.8	0.9172	9.2	0.0863	5.5	0.68	533.6	28.4	660.9	44.8	1123.3	135.5	533.6	28.4	19.3
75	0.0564	3.7	0.6734	4.5	0.0866	4.2	0.65	535.4	21.4	522.7	18.5	467.8	81.4	535.4	21.4	-2.4
359	0.0805	5.4	0.9670	7.3	0.0871	5.0	0.67	538.6	25.8	686.9	36.7	1208.9	106.8	538.6	25.8	21.6
303	0.0677	6.0	0.8229	8.4	0.0881	6.5	0.71	544.4	34.1	609.6	38.6	860.4	123.5	544.4	34.1	10.7
373	0.0607	3.6	0.7482	4.9	0.0894	3.3	0.67	551.9	17.4	567.2	21.2	629.0	78.3	551.9	17.4	2.7
153	0.0805	6.2	0.9992	7.6	0.0900	4.6	0.58	555.7	24.5	703.4	38.7	1209.1	121.9	555.7	24.5	21.0
221	0.0611	3.9	0.7715	7.0	0.0916	5.4	0.84	565.1	29.3	580.6	31.0	641.8	83.2	565.1	29.3	2.7
94	0.0684	11.6	0.8783	15.5	0.0931	10.4	0.66	574.0	57.2	640.1	73.6	880.9	239.8	574.0	57.2	10.3
357	0.0623	5.3	0.8038	7.3	0.0936	5.0	0.68	577.1	27.6	599.0	32.8	682.7	113.7	577.1	27.6	3.7
30	0.0715	5.4	0.9525	7.0	0.0966	4.5	0.64	594.3	25.8	679.4	34.9	972.6	109.9	594.3	25.8	12.5
36	0.0647	4.6	0.8987	6.9	0.1007	5.2	0.74	618.3	30.6	651.0	33.1	766.1	97.1	618.3	30.6	19.3
294	0.0625	3.4	0.9081	5.3	0.1053	4.6	0.78	645.5	28.0	656.0	25.5	692.5	71.5	645.5	28.0	6.8
313	0.0650	4.1	0.9869	5.7	0.1102	5.0	0.71	673.8	32.1	697.1	28.6	773.1	87.2	673.8	32.1	12.8
364	0.0688	3.1	1.1917	4.5	0.1257	3.4	0.73	763.4	24.7	796.7	24.9	891.3	63.6	763.4	24.7	14.4
133	0.0682	6.3	1.2070	8.2	0.1283	5.2	0.64	778.0	38.1	803.8	45.4	876.0	130.2	778.0	38.1	11.2
333	0.0665	4.5	1.1841	6.4	0.1291	4.8	0.72	782.9	35.3	793.2	35.3	822.3	93.3	782.9	35.3	4.8
131	0.0693	11.4	1.2568	16.4	0.1314	11.8	0.72	796.1	88.1	826.5	92.8	908.9	234.2	796.1	88.1	12.4
231	0.0694	5.3	1.2649	8.3	0.1321	6.2	0.77	800.1	46.5	830.1	47.3	911.4	108.8	800.1	46.5	12.2
86	0.0764	5.8	1.5686	7.9	0.1488	5.7	0.69	894.3	47.6	957.9	49.2	1106.8	115.2	894.3	47.6	19.2
82	0.0717	4.0	1.5387	5.4	0.1557	4.3	0.68	932.9	37.7	946.0	33.2	976.6	81.3	932.9	37.7	4.5
267	0.0711	8.8	1.5514	13.0	0.1582	9.5	0.74	946.7	83.5	951.1	80.7	961.3	179.6	946.7	83.5	1.5
176	0.0737	4.5	1.6130	6.9	0.1588	5.0	0.76	949.9	43.9	975.3	43.3	1032.8	90.6	949.9	43.9	8.0
77	0.0774	5.3	1.7068	6.4	0.1599	4.9	0.59	955.9	43.1	1011.1	41.2	1132.5	105.5	955.9	43.1	15.6
97	0.0755	11.3	1.6963	16.3	0.1629	11.9	0.72	973.1	107.9	1007.2	104.8	1082.0	226.7	973.1	107.9	10.1
284	0.0808	5.9	1.8185	8.7	0.1632	6.8	0.74	974.7	61.9	1052.1	57.0	1216.5	115.7	974.7	61.9	19.9
112	0.0800	10.8	1.8117	15.3	0.1642	10.9	0.71	979.9	99.0	1049.7	100.5	1197.9	212.4	979.9	99.0	18.2
93	0.0710	4.9	1.6079	6.9	0.1643	5.1	0.71	980.9	46.6	973.3	43.5	956.2	99.7	980.9	46.6	-2.6
326	0.0774	4.2	1.7619	5.9	0.1650	4.4	0.69	984.6	40.5	1031.6	38.0	1132.5	84.3	984.6	40.5	13.1
84	0.0758	5.2	1.7278	7.0	0.1653	5.2	0.67	986.4	47.6	1018.9	45.0	1089.5	105.0	986.4	47.6	9.5
319	0.0752	5.3	1.7172	7.7	0.1656	5.8	0.72	987.8	53.2	1015.0	49.2	1074.1	106.2	987.8	53.2	8.0
32	0.0747	3.2	1.7097	4.6	0.1659	3.3	0.71	989.6	30.2	1012.2	29.6	1061.4	65.3	989.6	30.2	6.8
286	0.0786	3.5	1.8045	5.5	0.1665	4.8	0.77	992.5	44.3	1047.1	35.7	1162.7	69.9	992.5	44.3	14.6
385	0.0811	8.5	1.8762	12.8	0.1678	9.6	0.75	999.9	88.8	1072.7	85.1	1224.0	167.2	999.9	88.8	18.3
154	0.0743	12.9	1.7710	19.0	0.1730	14.1	0.74	1028.5	133.7	1034.9	124.2	1048.5	259.7	1048.5	259.7	1.9
312	0.0755	5.0	1.9283	7.2	0.1853	6.0	0.73	1095.7	60.9	1090.9	48.0	1081.4	100.3	1081.4	100.3	-1.3
302	0.0774	4.0	1.8676	5.5	0.1750	4.7	0.70	1039.9	44.7	1069.7	36.2	1131.0	79.0	1131.0	79.0	8.1

Table A4.10 (continued): Detrital Zircon U-Pb Integrated Data for the Paruro Formation Base

Spot	Ratios						Ages (Ma)						Disc. (%)			
	207Pb/206Pb		207Pb/235U		206Pb/238U		206Pb/238U		207Pb/235U		207Pb/206Pb			Best Age		
	±2σ	±2σ	±2σ	±2σ	Rho	±2σ	±2σ	±2σ	±2σ	±2σ	±2σ	±2σ		±2σ		
<i>Paruro Formation Base 1 (20140605-01) Accepted Data</i>																
295	0.0777	4.2	1.8483	6.2	0.1725	5.2	0.74	1026.1	49.0	1062.8	40.8	1139.0	83.3	1139.0	83.3	9.9
220	0.0779	4.7	2.0684	6.5	0.1925	3.9	0.70	1134.7	41.1	1138.4	44.8	1145.5	93.4	1145.5	93.4	0.9
132	0.0781	2.9	1.8393	4.4	0.1707	3.2	0.74	1016.2	30.1	1059.6	28.6	1150.2	57.9	1150.2	57.9	11.7
327	0.0793	10.9	2.0386	15.8	0.1865	11.6	0.72	1102.5	117.3	1128.5	108.1	1178.8	215.8	1178.8	215.8	6.5
14	0.0794	8.4	1.8789	12.6	0.1717	9.5	0.75	1021.5	89.9	1073.7	83.6	1181.3	165.3	1181.3	165.3	13.5
24	0.0795	13.6	1.9170	19.2	0.1749	13.5	0.70	1039.0	129.8	1087.0	128.7	1184.5	269.3	1184.5	269.3	12.3
345	0.0800	6.3	2.1615	8.8	0.1959	6.3	0.71	1153.4	66.5	1168.7	61.5	1197.3	123.5	1197.3	123.5	3.7
192	0.0803	4.0	2.1567	6.1	0.1947	4.5	0.76	1147.0	46.9	1167.2	42.4	1205.0	77.9	1205.0	77.9	4.8
400	0.0811	7.1	2.1226	10.9	0.1899	8.3	0.76	1120.6	85.2	1156.2	75.5	1223.5	140.2	1223.5	140.2	8.4
23	0.0811	4.5	1.8843	5.9	0.1685	3.9	0.65	1003.7	36.5	1075.6	39.3	1224.2	88.6	1224.2	88.6	18.0
95	0.0811	4.6	2.2283	6.2	0.1992	4.6	0.68	1171.0	48.8	1190.0	43.5	1224.5	89.9	1224.5	89.9	4.4
250	0.0812	6.3	2.1711	9.5	0.1938	6.8	0.75	1142.0	70.9	1171.8	66.3	1227.3	124.2	1227.3	124.2	7.0
127	0.0814	8.7	1.9151	12.2	0.1706	8.6	0.70	1015.4	80.5	1086.4	81.5	1231.5	169.8	1231.5	169.8	17.5
8	0.0818	10.1	1.9968	14.7	0.1771	10.9	0.72	1051.2	105.9	1114.4	99.6	1239.9	198.5	1239.9	198.5	15.2
55	0.0819	3.3	2.1951	4.1	0.1944	3.4	0.61	1145.3	35.8	1179.5	28.3	1242.6	65.5	1242.6	65.5	7.8
273	0.0825	7.5	2.2470	11.0	0.1976	7.9	0.73	1162.5	83.5	1195.9	77.3	1256.6	146.6	1256.6	146.6	7.5
57	0.0826	3.8	2.1926	5.2	0.1925	4.3	0.70	1134.8	45.2	1178.7	36.0	1260.2	73.7	1260.2	73.7	10.0
379	0.0827	3.7	2.1805	5.0	0.1912	3.3	0.67	1127.9	34.6	1174.8	34.6	1262.3	72.0	1262.3	72.0	10.7
235	0.0830	3.3	2.2686	7.4	0.1982	5.7	0.91	1165.4	60.9	1202.6	52.5	1269.9	63.9	1269.9	63.9	8.2
389	0.0831	8.0	2.0559	11.0	0.1795	7.5	0.68	1064.4	73.7	1134.3	75.3	1270.6	157.0	1270.6	157.0	16.2
383	0.0833	4.5	1.9856	6.2	0.1729	4.3	0.69	1028.3	40.7	1110.6	41.8	1275.6	87.3	1275.6	87.3	19.4
5	0.0833	5.8	2.3371	7.4	0.2035	5.2	0.62	1194.2	56.9	1223.6	52.7	1275.8	113.6	1275.8	113.6	6.4
274	0.0833	5.7	2.2589	7.4	0.1967	4.8	0.63	1157.3	50.5	1199.6	51.8	1276.5	111.5	1276.5	111.5	9.3
206	0.0834	4.4	2.1924	6.4	0.1907	4.3	0.72	1125.1	44.4	1178.6	44.6	1278.3	86.1	1278.3	86.1	12.0
87	0.0834	13.6	2.1252	19.5	0.1848	14.1	0.72	1093.3	142.0	1157.0	135.7	1278.3	265.2	1278.3	265.2	14.5
174	0.0836	5.1	2.3220	8.4	0.2015	6.5	0.79	1183.5	69.9	1219.0	59.6	1282.5	100.0	1282.5	100.0	7.7
341	0.0838	6.8	2.3741	10.0	0.2055	7.4	0.73	1204.6	80.9	1234.8	71.4	1287.9	131.9	1287.9	131.9	6.5
305	0.0844	5.0	2.4651	6.8	0.2119	5.8	0.69	1239.1	65.2	1261.9	49.1	1300.9	97.5	1300.9	97.5	4.8
104	0.0847	5.4	2.2300	7.3	0.1910	4.9	0.67	1126.6	50.6	1190.5	51.0	1308.6	104.9	1308.6	104.9	13.9
217	0.0847	4.2	2.1997	5.3	0.1883	2.4	0.64	1112.4	24.1	1181.0	37.3	1308.8	82.1	1308.8	82.1	15.0
347	0.0852	10.7	2.7158	17.5	0.2312	13.9	0.79	1341.0	168.6	1332.8	130.8	1319.6	206.9	1319.6	206.9	-1.6
65	0.0852	4.8	2.2841	5.9	0.1944	5.0	0.62	1144.9	52.6	1207.4	41.5	1320.9	93.2	1320.9	93.2	13.3
79	0.0858	7.7	2.5553	10.9	0.2161	8.3	0.70	1261.3	94.8	1288.0	79.4	1332.6	149.7	1332.6	149.7	5.4
160	0.0862	3.0	2.2151	5.3	0.1863	3.9	0.82	1101.2	39.7	1185.8	37.1	1343.6	58.8	1343.6	58.8	18.0
92	0.0866	4.6	2.4312	6.1	0.2036	4.2	0.66	1194.6	46.2	1251.9	44.2	1351.9	89.3	1351.9	89.3	11.6
62	0.0895	3.9	2.7121	5.2	0.2199	4.6	0.69	1281.1	53.4	1331.8	38.7	1414.2	74.8	1414.2	74.8	9.4
26	0.0897	4.3	2.5223	5.5	0.2040	3.4	0.62	1196.5	37.5	1278.5	40.0	1419.0	82.3	1419.0	82.3	15.7
81	0.0903	4.0	2.8266	5.2	0.2269	4.1	0.65	1318.3	48.5	1362.6	38.7	1432.8	75.8	1432.8	75.8	8.0
309	0.0933	6.9	2.6984	8.1	0.2098	5.6	0.55	1227.6	62.4	1328.0	60.3	1493.8	130.3	1493.8	130.3	17.8
255	0.0933	11.9	3.1247	16.8	0.2429	11.5	0.70	1401.6	145.0	1438.8	130.1	1494.3	226.0	1494.3	226.0	6.2
66	0.0934	5.6	3.0403	7.6	0.2360	6.3	0.69	1366.0	77.9	1417.8	58.1	1496.5	106.1	1496.5	106.1	8.7
98	0.0961	2.9	3.0025	3.4	0.2267	2.5	0.56	1317.0	30.1	1408.3	25.6	1549.1	53.6	1549.1	53.6	15.0
270	0.0967	4.9	3.1630	6.7	0.2372	4.3	0.68	1372.4	53.2	1448.2	51.9	1561.3	92.2	1561.3	92.2	12.1
277	0.0980	4.1	3.5175	5.6	0.2602	4.0	0.69	1490.9	53.6	1531.2	44.3	1587.3	76.2	1587.3	76.2	6.1
378	0.1024	9.9	3.4763	15.3	0.2461	11.7	0.77	1418.6	149.4	1521.9	121.5	1668.6	182.6	1668.6	182.6	15.0
287	0.1033	7.6	3.4109	10.2	0.2394	7.1	0.66	1383.7	88.7	1506.9	79.9	1684.7	140.9	1684.7	140.9	17.9
296	0.1069	8.9	4.4576	14.2	0.3024	11.4	0.78	1703.1	170.2	1723.1	118.5	1747.5	162.6	1747.5	162.6	2.5
135	0.1090	4.5	3.9127	5.8	0.2603	3.6	0.63	1491.4	48.4	1616.3	47.0	1783.0	82.2	1783.0	82.2	16.4
233	0.1092	7.1	4.3363	11.0	0.2879	8.0	0.77	1631.0	115.6	1700.3	91.4	1786.8	129.6	1786.8	129.6	8.7
340	0.1100	6.3	3.9266	8.3	0.2590	5.4	0.65	1484.5	71.9	1619.2	67.3	1799.0	114.9	1799.0	114.9	17.5
194	0.1100	5.7	4.6104	8.0	0.3039	5.6	0.70	1710.8	84.1	1751.2	66.5	1799.7	104.0	1799.7	104.0	4.9
52	0.1102	7.3	3.8327	10.2	0.2522	7.4	0.70	1450.1	95.9	1599.6	82.5	1802.7	133.5	1802.7	133.5	19.6
229	0.1126	4.8	4.6416	7.7	0.2990	5.7	0.79	1686.6	84.3	1756.8	64.6	1841.3	86.0	1841.3	86.0	8.4
189	0.1126	5.4	4.9332	8.4	0.3177	6.3	0.77	1778.5	98.3	1808.0	71.4	1842.1	98.4	1842.1	98.4	3.5
304	0.1129	7.3	4.9663	10.7	0.3191	8.6	0.73	1785.5	133.4	1813.6	90.5	1846.0	132.2	1846.0	132.2	3.3
375	0.1157	6.4	4.3297	9.0	0.2714	6.3	0.70	1547.8	87.4	1699.0	74.7	1891.0	115.9	1891.0	115.9	18.1
355	0.1168	5.4	5.3643	7.7	0.3331	5.6	0.72	1853.2	90.5	1879.2	66.2	1908.0	96.3	1908.0	96.3	2.9
18	0.1175	3.8	5.2405	5.8	0.3233	4.6	0.76	1806.0	72.4	1859.2	49.3	1919.3	67.7	1919.3	67.7	5.9
387	0.1220	5.4	5.3587	7.1	0.3185	4.6	0.65	1782.2	71.5	1878.3	60.6	1986.3	95.5	1986.3	95.5	10.3
399	0.1239	6.8	6.1585	11.7	0.3604	9.6	0.81	1984.0	163.6	1998.6	102.9	2013.6	120.7	2013.6	120.7	1.5
16	0.1249	3.9	5.4519	5.3	0.3167	3.9	0.68	1773.6	60.3	1893.0	45.6	2026.7	68.7	2026.7	68.7	12.5
337	0.1249	4.3	6.0241	6.0	0.3498	4.3	0.70	1933.7	72.3	1979.3	52.1	2027.4	75.9	2027.4	75.9	4.6
339	0.1251	2.6	5.6471	3.4	0.3273	2.5	0.65	1825.3	39.8	1923.3	29.7	2030.7	46.6	2030.7	46.6	10.1

Table A4.10 (continued): Detrital Zircon U-Pb Integrated Data for the Paruro Formation Base

Spot	Ratios							Ages (Ma)							Best Age	Disc. (%)
	207Pb/206Pb		207Pb/235U		206Pb/238U		Rho	206Pb/238U		207Pb/235U		207Pb/206Pb				
	±2σ		±2σ		±2σ			±2σ		±2σ		±2σ				
<i>Paruro Formation Base 1 (20140605-01) Accepted Data</i>																
212	0.1264	2.7	6.0729	4.2	0.3485	2.7	0.77	1927.6	44.8	1986.4	36.6	2048.1	48.5	2048.1	48.5	5.9
196	0.1314	3.4	6.4407	5.2	0.3555	4.0	0.75	1960.9	67.7	2037.8	45.7	2116.6	59.8	2116.6	59.8	7.4
42	0.1335	14.5	5.8461	15.1	0.3177	4.4	0.29	1778.6	69.0	1953.3	131.9	2143.9	253.1	2143.9	253.1	17.0
103	0.1335	4.2	6.6962	6.0	0.3637	4.5	0.72	1999.5	77.8	2072.1	53.3	2145.1	73.3	2145.1	73.3	6.8
390	0.1363	7.3	6.1942	9.5	0.3295	6.1	0.64	1836.0	97.4	2003.6	83.6	2181.2	127.6	2181.2	127.6	15.8
142	0.1425	8.2	7.1074	10.7	0.3618	6.9	0.64	1990.9	118.9	2125.0	95.8	2257.3	141.8	2257.3	141.8	11.8
353	0.1459	6.4	7.4537	8.7	0.3704	5.9	0.67	2031.3	102.7	2167.4	78.1	2298.9	110.8	2298.9	110.8	11.6
99	0.1474	5.5	7.4343	7.3	0.3658	5.1	0.66	2009.4	87.8	2165.1	65.1	2316.2	94.2	2316.2	94.2	13.2
226	0.1494	4.3	7.3198	6.9	0.3554	4.9	0.78	1960.2	83.4	2151.2	61.8	2338.9	73.9	2338.9	73.9	16.2
314	0.1508	3.9	8.9848	5.5	0.4321	4.2	0.70	2315.1	81.8	2336.5	50.3	2355.2	67.1	2355.2	67.1	1.7
88	0.1591	3.7	9.5115	5.1	0.4337	3.9	0.69	2322.2	75.8	2388.7	46.6	2445.9	62.2	2445.9	62.2	5.1
181	0.1798	3.5	11.2917	5.5	0.4555	4.2	0.77	2419.8	84.0	2547.5	51.2	2650.8	57.6	2650.8	57.6	8.7
348	0.1884	4.1	13.3824	5.6	0.5151	3.9	0.68	2678.4	84.5	2707.0	52.6	2728.5	67.4	2728.5	67.4	1.8
144	0.2142	4.5	16.2589	6.7	0.5504	5.0	0.74	2826.9	115.3	2892.1	64.3	2937.9	72.8	2937.9	72.8	3.8
4	0.2896	5.9	25.2511	7.0	0.6325	4.5	0.54	3159.3	112.6	3318.0	68.4	3415.3	92.1	3415.3	92.1	7.5
<i>Paruro Formation Base 1 (20140605-01) Rejected Data</i>																
109	0.1950	16.5	0.0467	18.1	0.0017	7.5	0.41	11.2	0.8	46.3	8.2	2784.7	269.8	11.2	0.8	75.9
237	0.3356	11.6	0.1037	14.7	0.0022	8.3	0.61	14.4	1.2	100.2	14.0	3643.0	177.2	14.4	1.2	85.6
172	0.0694	22.1	0.0380	29.8	0.0040	20.0	0.67	25.6	5.1	37.9	11.1	910.8	455.7	25.6	5.1	32.5
100	0.0808	11.2	0.0449	12.3	0.0040	5.4	0.42	25.9	1.4	44.6	5.4	1217.0	219.3	25.9	1.4	41.9
335	0.0835	15.0	0.0518	17.4	0.0045	8.9	0.51	28.9	2.6	51.3	8.7	1281.4	291.7	28.9	2.6	43.6
183	0.1096	17.6	0.0681	20.9	0.0045	11.3	0.54	29.0	3.3	66.8	13.5	1792.1	320.3	29.0	3.3	56.7
222	0.0708	9.5	0.0457	11.7	0.0047	6.5	0.59	30.1	2.0	45.4	5.2	950.6	194.0	30.1	2.0	33.6
219	0.0966	17.9	0.0635	19.9	0.0048	8.5	0.44	30.7	2.6	62.5	12.1	1559.5	335.4	30.7	2.6	51.0
256	0.1228	13.1	0.0824	15.8	0.0049	8.3	0.56	31.3	2.6	80.4	12.2	1997.0	232.6	31.3	2.6	61.1
124	0.1577	14.0	0.1068	16.7	0.0049	9.1	0.55	31.6	2.9	103.1	16.4	2430.9	236.9	31.6	2.9	69.3
46	0.1400	15.2	0.0955	17.7	0.0049	9.1	0.52	31.8	2.9	92.6	15.7	2226.9	262.5	31.8	2.9	65.6
291	0.1288	10.7	0.0886	15.0	0.0050	10.6	0.70	32.1	3.4	86.2	12.4	2081.9	188.7	32.1	3.4	62.8
90	0.1295	13.1	0.0907	15.2	0.0051	7.8	0.51	32.7	2.6	88.2	12.8	2091.3	230.1	32.7	2.6	63.0
281	0.1421	11.3	0.1000	12.6	0.0051	5.9	0.44	32.8	1.9	96.8	11.6	2253.1	194.7	32.8	1.9	66.1
166	0.1601	16.1	0.1177	18.4	0.0053	8.7	0.49	34.3	3.0	113.0	19.7	2456.7	272.1	34.3	3.0	69.7
381	0.1578	9.8	0.1174	11.9	0.0054	6.7	0.56	34.7	2.3	112.7	12.6	2431.8	165.9	34.7	2.3	69.2
184	0.1920	14.7	0.1433	16.2	0.0054	6.9	0.42	34.8	2.4	136.0	20.6	2759.0	241.0	34.8	2.4	74.4
179	0.2404	13.3	0.1839	16.5	0.0055	9.6	0.59	35.7	3.4	171.4	26.0	3122.9	212.3	35.7	3.4	79.2
41	0.1533	11.5	0.1173	13.5	0.0056	7.0	0.52	35.7	2.5	112.7	14.4	2383.0	196.2	35.7	2.5	68.3
11	0.1017	12.9	0.0788	14.8	0.0056	7.7	0.50	36.1	2.8	77.0	11.0	1654.8	238.3	36.1	2.8	53.1
350	0.2441	12.3	0.1964	14.2	0.0058	7.2	0.50	37.5	2.7	182.1	23.7	3146.7	195.4	37.5	2.7	79.4
247	0.1533	7.9	0.1248	10.4	0.0059	6.3	0.65	38.0	2.4	119.4	11.7	2383.5	134.7	38.0	2.4	68.2
221	0.1258	10.5	0.1039	12.0	0.0060	5.2	0.48	38.5	2.0	100.4	11.4	2040.2	186.2	38.5	2.0	61.6
34	0.1253	13.2	0.1036	14.4	0.0060	5.9	0.40	38.6	2.3	100.1	13.7	2032.5	232.9	38.6	2.3	61.5
158	0.0998	12.0	0.0830	14.9	0.0060	8.7	0.58	38.8	3.4	81.0	11.6	1621.2	224.3	38.8	3.4	52.1
285	0.2779	9.5	0.2362	15.0	0.0062	11.8	0.77	39.6	4.6	215.3	29.0	3351.4	149.1	39.6	4.6	81.6
111	0.2583	12.9	0.2201	14.7	0.0062	7.0	0.48	39.7	2.8	202.0	27.0	3236.1	203.9	39.7	2.8	80.3
234	0.2359	19.0	0.2027	21.8	0.0062	10.2	0.49	40.1	4.1	187.4	37.3	3092.4	302.9	40.1	4.1	78.6
276	0.0983	10.6	0.0847	14.9	0.0062	10.6	0.71	40.1	4.2	82.5	11.8	1593.0	197.5	40.1	4.2	51.4
167	0.2941	11.3	0.2533	13.4	0.0062	7.0	0.54	40.1	2.8	229.2	27.5	3439.4	175.6	40.1	2.8	82.5
145	0.3045	17.0	0.2645	21.3	0.0063	12.9	0.60	40.5	5.2	238.3	45.3	3493.4	263.6	40.5	5.2	83.0
169	0.0812	21.7	0.0714	23.7	0.0064	9.5	0.41	41.0	3.9	70.0	16.0	1225.3	425.5	41.0	3.9	41.5
386	0.1267	8.6	0.1127	9.7	0.0065	4.5	0.47	41.5	1.9	108.4	10.0	2052.1	151.6	41.5	1.9	61.8
162	0.1685	13.9	0.1507	19.9	0.0065	14.1	0.72	41.7	5.9	142.5	26.4	2542.5	232.2	41.7	5.9	70.8
201	0.1177	18.4	0.1061	20.0	0.0065	7.9	0.39	42.0	3.3	102.4	19.5	1921.2	330.5	42.0	3.3	59.0
380	0.3609	11.3	0.3340	14.1	0.0067	8.4	0.60	43.1	3.6	292.6	35.9	3753.5	172.4	43.1	3.6	85.3
113	0.3090	17.2	0.2870	18.7	0.0067	7.3	0.39	43.3	3.1	256.2	42.4	3516.0	266.3	43.3	3.1	83.1
331	0.2154	15.7	0.2004	17.1	0.0067	6.8	0.39	43.3	2.9	185.4	29.0	2946.7	254.2	43.3	2.9	76.6
180	0.1048	10.1	0.0978	12.4	0.0068	7.2	0.59	43.5	3.1	94.7	11.2	1710.7	185.3	43.5	3.1	54.1
170	0.2161	10.8	0.2052	13.6	0.0069	8.1	0.61	44.2	3.6	189.5	23.6	2951.8	175.1	44.2	3.6	76.7
47	0.3555	11.1	0.3435	12.6	0.0070	6.0	0.48	45.0	2.7	299.8	32.8	3730.9	168.7	45.0	2.7	85.0
70	0.3179	13.8	0.3105	15.9	0.0071	8.3	0.50	45.5	3.8	274.6	38.3	3559.6	212.6	45.5	3.8	83.4
349	0.3790	11.7	0.3715	14.5	0.0071	8.6	0.59	45.7	3.9	320.8	39.8	3827.7	176.4	45.7	3.9	85.8
318	0.0799	15.5	0.0786	21.9	0.0071	15.6	0.71	45.9	7.1	76.9	16.2	1193.4	305.1	45.9	7.1	40.3
367	0.1508	11.1	0.1506	12.3	0.0072	5.2	0.42	46.5	2.4	142.4	16.3	2355.6	190.3	46.5	2.4	67.3
307	0.2746	10.9	0.2769	12.9	0.0073	7.7	0.53	47.0	3.6	248.2	28.4	3332.8	171.2	47.0	3.6	81.1
159	0.3856	12.4	0.4023	15.0	0.0076	8.5	0.56	48.6	4.1	343.3	43.8	3853.7	187.8	48.6	4.1	85.8

Table A4.10 (continued): Detrital Zircon U-Pb Integrated Data for the Paruro Formation Base

Spot	Ratios						Rho	Ages (Ma)						Best Age	Disc. (%)	
	207Pb/ 206Pb	$\pm 2\sigma$	207Pb/ 235U	$\pm 2\sigma$	206Pb/ 238U	$\pm 2\sigma$		206Pb/ 238U	$\pm 2\sigma$	207Pb/ 235U	$\pm 2\sigma$	207Pb/ 206Pb	$\pm 2\sigma$			
271	0.3634	10.7	0.3804	12.4	0.0076	5.9	0.49	48.7	2.9	327.3	34.6	3764.2	163.1	48.7	2.9	85.1
278	0.1796	15.9	0.1881	21.6	0.0076	14.7	0.68	48.8	7.1	175.0	34.7	2649.4	263.0	48.8	7.1	72.1
115	0.2788	21.8	0.2998	24.0	0.0078	10.2	0.42	50.1	5.1	266.2	56.4	3356.3	340.1	50.1	5.1	81.2
266	0.3985	15.5	0.4352	18.4	0.0079	9.7	0.54	50.9	4.9	366.9	56.6	3903.5	232.5	50.9	4.9	86.1
310	0.1069	13.0	0.1193	17.0	0.0081	11.3	0.64	52.0	5.9	114.4	18.4	1747.1	238.9	52.0	5.9	54.6
338	0.4245	12.1	0.4836	14.2	0.0083	7.5	0.52	53.0	4.0	400.5	46.9	3998.2	180.3	53.0	4.0	86.8
240	0.2692	11.9	0.3109	16.8	0.0084	11.5	0.71	53.8	6.2	274.8	40.5	3301.5	186.5	53.8	6.2	80.4
195	0.1647	19.3	0.1912	25.7	0.0084	17.0	0.66	54.1	9.2	177.7	42.0	2504.2	324.8	54.1	9.2	69.6
38	0.6113	8.3	0.7425	10.4	0.0088	6.2	0.60	56.5	3.5	563.9	44.8	4535.0	120.5	56.5	3.5	90.0
214	0.4477	14.5	0.5516	17.1	0.0089	8.8	0.53	57.3	5.0	446.1	61.8	4077.7	216.2	57.3	5.0	87.1
165	0.4460	19.1	0.5611	22.2	0.0091	11.1	0.51	58.6	6.5	452.2	81.2	4072.0	284.6	58.6	6.5	87.1
101	0.3898	14.5	0.4976	17.9	0.0093	10.6	0.59	59.4	6.3	410.1	60.4	3870.2	218.4	59.4	6.3	85.5
157	0.0677	10.1	0.0876	14.1	0.0094	9.9	0.70	60.2	5.9	85.3	11.5	860.3	209.3	60.2	5.9	29.4
225	0.1662	9.6	0.2165	12.1	0.0094	7.0	0.61	60.6	4.2	199.0	21.9	2520.2	162.1	60.6	4.2	69.5
64	0.0819	7.6	0.1068	8.3	0.0095	5.0	0.44	60.7	3.0	103.0	8.1	1242.1	148.2	60.7	3.0	41.1
129	0.4977	10.5	0.6519	13.5	0.0095	8.5	0.63	60.9	5.1	509.6	54.1	4234.4	154.2	60.9	5.1	88.0
272	0.4760	12.6	0.6284	15.6	0.0096	9.1	0.59	61.4	5.6	495.1	61.2	4168.5	186.2	61.4	5.6	87.6
63	0.3972	15.2	0.5301	16.6	0.0097	7.3	0.40	62.1	4.5	431.9	58.4	3898.3	228.9	62.1	4.5	85.6
321	0.4762	12.6	0.6500	14.9	0.0099	8.1	0.53	63.5	5.1	508.5	59.8	4169.2	186.9	63.5	5.1	87.5
122	0.0687	10.0	0.0989	14.4	0.0104	10.4	0.72	66.9	6.9	95.7	13.1	891.1	205.8	66.9	6.9	30.1
203	0.0884	8.8	0.1282	10.8	0.0105	6.2	0.58	67.4	4.2	122.5	12.4	1392.0	168.7	67.4	4.2	45.0
121	0.0630	6.6	0.0944	7.9	0.0109	4.3	0.55	69.7	3.0	91.6	6.9	707.0	139.3	69.7	3.0	23.9
239	0.0816	8.6	0.1291	11.5	0.0115	6.8	0.67	73.5	5.0	123.2	13.4	1235.7	168.6	73.5	5.0	40.3
61	0.1896	15.5	0.3076	16.2	0.0118	5.8	0.31	75.4	4.4	272.4	38.8	2739.0	254.2	75.4	4.4	72.3
49	0.0692	9.6	0.1138	12.4	0.0119	7.9	0.63	76.4	6.0	109.4	12.9	905.6	197.7	76.4	6.0	30.2
9	0.1899	10.0	0.3225	13.6	0.0123	9.5	0.68	78.9	7.5	283.9	33.6	2741.6	164.2	78.9	7.5	72.2
323	0.0887	7.5	0.1511	8.1	0.0124	3.3	0.38	79.2	2.6	142.9	10.8	1397.6	143.3	79.2	2.6	44.6
123	0.0693	12.5	0.1212	14.7	0.0127	7.7	0.52	81.3	6.2	116.2	16.2	908.4	258.1	81.3	6.2	30.1
72	0.1670	17.8	0.2940	20.2	0.0128	10.0	0.47	81.8	8.1	261.7	46.7	2527.8	298.8	81.8	8.1	68.7
395	0.0823	13.8	0.1463	21.3	0.0129	16.3	0.76	82.6	13.4	138.6	27.7	1251.8	270.3	82.6	13.4	40.4
163	0.2518	7.9	0.4859	9.4	0.0140	4.8	0.55	89.6	4.3	402.1	31.3	3196.2	124.6	89.6	4.3	77.7
372	0.1951	15.1	0.3789	17.7	0.0141	9.3	0.52	90.2	8.3	326.2	49.5	2785.3	247.5	90.2	8.3	72.4
7	0.1391	9.5	0.2816	10.2	0.0147	4.4	0.36	93.9	4.1	251.9	22.7	2216.5	165.1	93.9	4.1	62.7
290	0.2176	12.6	0.4706	14.8	0.0157	7.9	0.52	100.3	7.9	391.6	48.0	2963.1	203.5	100.3	7.9	74.4
29	0.0840	9.0	0.1818	12.5	0.0157	8.6	0.69	100.4	8.6	169.6	19.5	1292.5	175.7	100.4	8.6	40.8
322	0.4218	51.7	0.9221	62.9	0.0159	35.8	0.57	101.4	36.1	663.5	316.3	3988.5	773.3	101.4	36.1	84.7
215	0.2451	15.9	0.5414	17.8	0.0160	7.8	0.46	102.5	7.9	439.4	63.6	3153.4	251.6	102.5	7.9	76.7
393	0.1506	11.0	0.3493	14.9	0.0168	10.1	0.68	107.6	10.8	304.2	39.2	2352.5	187.6	107.6	10.8	64.6
328	0.1501	8.5	0.3913	10.6	0.0189	6.5	0.59	120.8	7.8	335.3	30.2	2346.9	146.1	120.8	7.8	64.0
374	0.4035	32.8	1.0732	36.2	0.0193	15.3	0.42	123.2	18.7	740.3	192.4	3922.3	492.1	123.2	18.7	83.4
51	0.3881	23.2	1.0387	25.3	0.0194	10.4	0.40	123.9	12.7	723.3	131.7	3863.8	349.7	123.9	12.7	82.9
78	0.0703	9.2	0.1961	11.8	0.0202	8.0	0.62	129.2	10.3	181.8	19.7	936.6	189.6	129.2	10.3	29.0
354	0.1612	7.5	0.4504	8.7	0.0203	4.4	0.50	129.3	5.6	377.6	27.4	2468.6	126.9	129.3	5.6	65.8
125	0.0833	15.2	0.2564	18.0	0.0223	9.6	0.54	142.3	13.6	231.7	37.2	1276.2	295.5	142.3	13.6	38.6
346	0.3856	24.9	1.1972	27.7	0.0225	12.1	0.44	143.6	17.2	799.3	154.4	3853.7	376.0	143.6	17.2	82.0
264	0.3155	8.1	0.9810	12.6	0.0226	9.4	0.77	143.8	13.4	694.1	63.3	3547.8	124.2	143.8	13.4	79.3
343	0.0935	6.8	0.2952	8.1	0.0229	4.4	0.54	145.9	6.4	262.7	18.8	1498.4	129.4	145.9	6.4	44.4
106	0.1377	8.2	0.4363	9.9	0.0230	5.6	0.56	146.5	8.1	367.6	30.4	2198.0	141.8	146.5	8.1	60.2
351	0.4612	11.7	1.4909	14.3	0.0234	8.2	0.58	149.4	12.2	926.7	86.9	4121.8	173.0	149.4	12.2	83.9
394	0.0849	10.0	0.2959	13.8	0.0253	9.6	0.69	161.0	15.2	263.2	32.0	1312.5	193.4	161.0	15.2	38.8
118	0.1734	13.0	0.6564	13.7	0.0275	4.1	0.30	174.6	7.1	512.4	55.1	2590.8	217.3	174.6	7.1	65.9
150	0.0723	10.4	0.2852	13.2	0.0286	8.2	0.61	182.0	14.6	254.8	29.7	993.0	211.7	182.0	14.6	28.6
21	0.0846	10.2	0.3540	13.3	0.0303	8.6	0.64	192.7	16.3	307.7	35.4	1306.6	198.9	192.7	16.3	37.4
238	0.1834	9.5	0.8428	12.6	0.0333	7.5	0.66	211.4	15.5	620.7	58.6	2683.8	157.8	211.4	15.5	65.9
329	0.3119	9.0	1.4335	12.2	0.0333	8.4	0.68	211.4	17.6	903.0	73.0	3530.2	138.4	211.4	17.6	76.6
68	0.5243	27.4	2.4278	30.7	0.0336	14.3	0.45	212.9	30.0	1250.9	224.2	4311.0	401.9	212.9	30.0	83.0
202	0.0990	12.5	0.5295	13.2	0.0388	4.5	0.33	245.2	10.7	431.5	46.5	1606.0	232.8	245.2	10.7	43.2
366	0.6027	16.5	3.2945	20.5	0.0396	12.2	0.59	250.6	30.0	1479.8	161.1	4514.6	239.8	250.6	30.0	83.1
137	0.1657	6.2	0.9244	10.0	0.0405	7.9	0.78	255.7	19.7	664.7	49.0	2515.0	104.7	255.7	19.7	61.5
19	0.0818	6.4	0.4615	8.1	0.0409	5.1	0.61	258.4	13.0	385.3	25.9	1241.2	125.3	258.4	13.0	32.9
356	0.1220	12.8	0.7015	13.8	0.0417	5.2	0.37	263.4	13.4	539.7	57.8	1985.5	227.9	263.4	13.4	51.2
283	0.0744	5.3	0.4302	6.2	0.0419	3.9	0.53	264.9	10.0	363.3	18.9	1052.0	106.4	264.9	10.0	27.1
265	0.0727	7.4	0.4324	9.6	0.0431	5.8	0.64	272.3	15.5	364.9	29.3	1005.7	149.9	272.3	15.5	25.4

Table A4.10 (continued): Detrital Zircon U-Pb Integrated Data for the Paruro Formation Base

Spot	Ratios						Rho	Ages (Ma)						Best Age	Disc. (%)	
	207Pb/206Pb	$\pm 2\sigma$	207Pb/235U	$\pm 2\sigma$	206Pb/238U	$\pm 2\sigma$		206Pb/238U	$\pm 2\sigma$	207Pb/235U	$\pm 2\sigma$	207Pb/206Pb	$\pm 2\sigma$			
	<i>Paruro Formation Base 1 (20140605-01) Rejected Data</i>															
211	0.4720	7.5	2.8883	9.2	0.0444	4.9	0.57	279.9	13.4	1378.9	69.1	4156.1	111.6	279.9	13.4	79.7
300	0.1877	6.4	1.1596	8.6	0.0448	6.4	0.67	282.6	17.6	781.8	47.0	2722.1	105.2	282.6	17.6	63.9
199	0.7665	54.5	5.1417	66.1	0.0487	37.5	0.57	306.2	112.1	1843.0	632.9	4860.7	781.4	306.2	112.1	83.4
384	0.0954	7.5	0.6640	9.1	0.0505	5.2	0.57	317.3	16.0	517.1	36.8	1536.9	140.6	317.3	16.0	38.6
198	0.0869	10.7	0.6883	13.6	0.0575	8.4	0.61	360.2	29.4	531.8	56.3	1357.5	206.7	360.2	29.4	32.3
371	0.2449	10.2	2.0760	13.6	0.0615	9.0	0.66	384.7	33.6	1140.9	93.4	3151.9	161.9	384.7	33.6	66.3
398	0.2751	9.3	2.4294	10.8	0.0641	5.4	0.50	400.2	20.8	1251.3	77.5	3335.2	145.9	400.2	20.8	68.0
317	0.3353	34.4	3.1084	37.1	0.0672	14.0	0.38	419.4	57.0	1434.8	293.1	3641.6	526.5	419.4	57.0	70.8
10	0.1955	7.7	1.8952	8.6	0.0703	4.5	0.46	438.1	18.9	1079.4	57.3	2788.6	125.6	438.1	18.9	59.4
50	0.0778	5.5	0.7944	6.5	0.0740	3.9	0.53	460.3	17.4	593.6	29.0	1142.8	108.8	460.3	17.4	22.5
288	0.1003	9.2	1.0528	11.3	0.0761	6.9	0.58	472.9	31.7	730.3	58.9	1630.0	171.6	472.9	31.7	35.2
6	0.0833	8.3	0.9025	8.7	0.0786	3.6	0.31	487.8	16.8	653.1	41.8	1275.7	162.0	487.8	16.8	25.3
148	0.0923	13.2	1.0108	20.6	0.0794	15.8	0.76	492.6	74.9	709.3	105.3	1473.9	251.3	492.6	74.9	30.5
28	0.3373	18.3	3.7465	21.2	0.0806	10.8	0.51	499.4	51.7	1581.4	171.5	3650.7	279.4	499.4	51.7	68.4
39	0.1152	9.8	1.3185	10.5	0.0830	3.8	0.36	514.2	19.0	853.8	60.7	1882.6	176.7	514.2	19.0	39.8
246	0.1250	8.4	1.4545	9.7	0.0844	4.1	0.50	522.4	20.5	911.7	58.3	2028.4	148.9	522.4	20.5	42.7
40	0.0907	7.9	1.0592	9.1	0.0847	4.6	0.50	524.3	23.1	733.4	47.5	1439.5	150.4	524.3	23.1	28.5
73	0.1249	20.1	1.4639	25.6	0.0850	16.0	0.62	526.1	80.9	915.6	155.5	2026.9	356.6	526.1	80.9	42.5
292	0.0945	6.0	1.1184	7.0	0.0858	4.1	0.52	530.7	21.0	762.2	37.5	1518.6	113.3	530.7	21.0	30.4
110	0.0888	7.6	1.0726	8.0	0.0876	2.6	0.33	541.6	13.7	740.0	42.1	1398.9	145.0	541.6	13.7	26.8
397	0.1116	13.1	1.3579	16.0	0.0883	9.3	0.58	545.3	48.5	871.0	94.1	1825.2	237.5	545.3	48.5	37.4
15	0.0901	6.5	1.1100	7.6	0.0893	4.3	0.53	551.6	22.5	758.2	40.7	1427.9	123.4	551.6	22.5	27.2
263	0.0845	5.5	1.0411	7.9	0.0893	5.3	0.72	551.6	27.9	724.4	41.1	1304.4	107.5	551.6	27.9	23.9
108	0.0906	5.7	1.1232	6.5	0.0899	3.2	0.49	555.1	17.1	764.5	34.8	1438.0	108.0	555.1	17.1	27.4
242	0.0876	7.6	1.0976	9.8	0.0909	5.4	0.64	560.6	29.3	752.2	52.2	1374.1	146.5	560.6	29.3	25.5
282	0.1101	10.4	1.4037	13.4	0.0925	8.8	0.64	570.1	48.1	890.5	79.8	1801.1	188.5	570.1	48.1	36.0
324	0.1022	11.3	1.3210	12.7	0.0938	6.0	0.46	577.8	32.9	854.9	73.6	1664.1	209.3	577.8	32.9	32.4
241	0.1118	7.3	1.4491	9.3	0.0940	4.9	0.63	579.3	27.4	909.5	56.0	1828.4	132.7	579.3	27.4	36.3
102	0.1037	9.0	1.3629	10.1	0.0953	4.8	0.46	587.0	26.9	873.1	59.0	1691.3	165.1	587.0	26.9	32.8
117	0.1277	10.7	1.7357	11.7	0.0986	4.6	0.40	606.3	26.8	1021.9	75.4	2065.9	188.8	606.3	26.8	70.7
210	0.0759	5.5	1.0319	7.0	0.0986	3.9	0.61	606.4	22.3	719.9	35.9	1091.9	111.0	606.4	22.3	44.5
315	0.0957	7.0	1.3166	8.4	0.0998	5.0	0.56	613.1	29.3	853.0	48.5	1542.0	131.0	613.1	29.3	60.2
279	0.0694	8.0	0.9551	10.2	0.0999	6.4	0.62	613.6	37.7	680.7	50.5	909.7	164.0	613.6	37.7	32.6
138	0.2121	22.7	2.9401	25.3	0.1005	11.1	0.44	617.4	65.3	1392.3	193.7	2922.0	367.3	617.4	65.3	78.9
223	0.0826	8.9	1.1451	11.1	0.1006	6.3	0.60	617.8	36.9	774.9	60.3	1259.2	174.2	617.8	36.9	50.9
311	0.0725	9.4	1.0090	13.7	0.1009	10.4	0.73	619.8	61.6	708.4	69.9	1000.4	191.6	619.8	61.6	38.0
175	0.0673	2.9	0.9396	4.4	0.1012	2.8	0.76	621.6	16.8	672.7	21.7	847.8	60.8	621.6	16.8	26.7
248	0.0658	11.9	0.9201	18.4	0.1014	13.8	0.76	622.5	81.8	662.4	89.6	800.5	248.7	622.5	81.8	22.2
363	0.0724	10.2	1.0129	15.0	0.1014	11.0	0.73	622.8	65.1	710.3	76.5	998.1	207.0	622.8	65.1	37.6
368	0.0671	4.4	0.9396	5.7	0.1016	3.7	0.63	623.7	22.0	672.7	27.9	840.2	91.6	623.7	22.0	25.8
316	0.0845	4.5	1.1901	5.3	0.1022	3.3	0.53	627.0	19.5	796.0	29.3	1303.8	87.7	627.0	19.5	51.9
20	0.0799	6.7	1.1266	7.5	0.1022	3.4	0.44	627.5	20.3	766.1	40.4	1195.0	132.9	627.5	20.3	47.5
301	0.0668	7.7	0.9558	10.6	0.1037	7.8	0.69	636.3	47.0	681.1	52.5	832.2	159.7	636.3	47.0	23.5
71	0.0744	10.3	1.0696	14.2	0.1043	10.1	0.69	639.7	61.6	738.5	74.6	1051.2	208.4	639.7	61.6	39.1
67	0.0817	5.8	1.1795	6.8	0.1047	5.2	0.57	641.6	31.7	791.1	37.5	1239.3	113.3	641.6	31.7	48.2
156	0.1940	15.5	2.8440	18.2	0.1063	9.6	0.52	651.3	59.2	1367.2	137.2	2776.6	253.5	651.3	59.2	76.5
344	0.0736	11.0	1.0845	15.2	0.1068	10.5	0.69	654.2	65.2	745.8	80.2	1031.7	222.1	654.2	65.2	36.6
45	0.0720	9.7	1.0655	11.2	0.1073	5.7	0.50	657.2	35.3	736.5	58.8	985.9	197.6	657.2	35.3	33.3
262	0.3780	7.1	5.6033	8.7	0.1075	4.5	0.57	658.2	28.2	1916.6	75.0	3824.0	107.9	658.2	28.2	82.8
249	0.0838	4.8	1.2496	6.4	0.1082	3.4	0.68	662.4	21.2	823.2	36.0	1286.9	93.1	662.4	21.2	48.5
289	0.1869	2.9	2.7899	4.8	0.1082	4.5	0.81	662.6	28.5	1352.8	35.8	2715.3	47.5	662.6	28.5	75.6
224	0.0756	4.9	1.1470	7.3	0.1101	4.9	0.74	673.1	31.5	775.8	39.6	1084.1	98.1	673.1	31.5	37.9
136	0.0715	14.0	1.0879	20.1	0.1104	14.4	0.72	675.2	92.5	747.5	106.8	970.3	285.7	675.2	92.5	30.4
261	0.2243	11.5	3.4277	14.8	0.1108	9.1	0.63	677.4	58.4	1510.8	117.0	3012.2	185.0	677.4	58.4	77.5
252	0.1126	12.4	1.7402	16.2	0.1121	10.3	0.65	685.0	66.7	1023.5	105.1	1841.4	224.2	685.0	66.7	62.8
336	0.1879	12.5	2.9869	13.5	0.1153	5.2	0.37	703.3	34.3	1404.3	102.9	2724.1	206.1	703.3	34.3	74.2
376	0.1533	10.6	2.4412	11.1	0.1155	3.3	0.30	704.6	22.2	1254.8	80.3	2383.0	180.9	704.6	22.2	70.4
188	0.1164	13.7	1.8681	17.9	0.1164	11.5	0.64	709.8	77.0	1069.8	118.7	1901.6	247.0	709.8	77.0	62.7
152	0.0890	10.9	1.4402	18.2	0.1174	14.7	0.80	715.6	99.5	905.8	109.8	1403.6	208.4	715.6	99.5	49.0
187	0.0695	2.8	1.1275	4.3	0.1176	3.4	0.76	716.7	23.2	766.5	23.2	914.8	57.9	716.7	23.2	21.7
80	0.0760	3.9	1.2398	4.7	0.1183	3.5	0.58	720.5	24.0	818.8	26.3	1096.1	78.2	720.5	24.0	34.3
43	0.1792	17.1	2.9484	18.3	0.1193	6.8	0.37	726.8	46.8	1394.4	140.0	2645.2	283.0	726.8	46.8	72.5
151	0.0807	5.9	1.3404	7.6	0.1204	4.9	0.63	733.1	34.0	863.4	44.0	1214.4	115.1	733.1	34.0	39.6

Table A4.10 (continued): Detrital Zircon U-Pb Integrated Data for the Paruro Formation Base

Spot	Ratios						Ages (Ma)						Best Age	Disc. (%)		
	207Pb/206Pb		207Pb/235U		206Pb/238U		206Pb/238U		207Pb/235U		207Pb/206Pb					
	±2σ	±2σ	±2σ	±2σ	±2σ	±2σ	±2σ	±2σ	±2σ	±2σ	±2σ	±2σ				
	<i>Paruro Formation Base 1 (20140605-01) Rejected Data</i>															
74	0.0778	5.1	1.3308	6.3	0.1241	4.9	0.60	754.0	34.6	859.2	36.5	1141.4	101.9	754.0	34.6	33.9
27	0.0834	4.7	1.4408	5.6	0.1252	3.1	0.54	760.6	21.9	906.1	33.6	1279.6	92.0	760.6	21.9	40.6
96	0.1014	12.3	1.7507	13.2	0.1252	5.0	0.35	760.7	35.5	1027.4	85.4	1649.5	229.0	760.7	35.5	53.9
22	0.0804	5.6	1.4104	7.7	0.1273	5.3	0.68	772.5	38.7	893.3	45.6	1205.6	110.1	772.5	38.7	35.9
392	0.0760	4.7	1.3371	5.9	0.1276	3.6	0.62	774.2	26.4	862.0	34.3	1094.9	93.1	774.2	26.4	29.3
17	0.2300	5.8	4.1041	6.5	0.1294	3.4	0.47	784.5	25.0	1655.1	53.5	3052.1	92.3	784.5	25.0	74.3
396	0.0838	4.0	1.5019	5.2	0.1300	3.3	0.63	787.7	24.2	931.1	31.6	1288.0	78.4	787.7	24.2	38.8
149	0.0961	9.8	1.7509	12.4	0.1321	7.8	0.62	799.9	59.0	1027.5	80.5	1550.0	183.2	799.9	59.0	48.4
168	0.1354	11.3	2.5188	13.8	0.1349	7.7	0.57	815.9	59.1	1277.5	100.9	2169.1	197.5	815.9	59.1	62.4
388	0.0948	9.3	1.7772	11.1	0.1359	6.2	0.56	821.4	47.7	1037.1	72.5	1525.0	174.4	821.4	47.7	46.1
358	0.1125	7.4	2.1279	9.1	0.1372	5.3	0.58	828.7	41.5	1157.9	62.6	1840.1	133.3	828.7	41.5	55.0
306	0.1458	10.8	2.7751	12.4	0.1381	6.9	0.49	833.8	54.0	1348.9	92.5	2296.8	186.4	833.8	54.0	63.7
85	0.2968	22.4	5.7440	29.9	0.1404	19.9	0.66	846.8	157.9	1938.0	264.4	3453.4	347.1	846.8	157.9	75.5
365	0.1670	11.2	3.2937	13.0	0.1430	6.7	0.51	861.7	54.3	1479.6	101.6	2528.1	187.5	861.7	54.3	65.9
1	0.0775	4.9	1.5528	5.3	0.1454	3.3	0.44	874.9	27.0	951.6	32.7	1133.4	96.8	874.9	27.0	22.8
258	0.1526	4.4	3.0714	6.9	0.1459	4.4	0.78	878.2	36.5	1425.6	52.5	2375.6	74.9	878.2	36.5	63.0
59	0.3412	21.5	6.8680	23.3	0.1460	9.4	0.39	878.4	77.4	2094.5	209.7	3668.3	328.3	878.4	77.4	76.1
54	0.0869	5.5	1.7508	7.2	0.1462	5.0	0.64	879.4	41.0	1027.5	46.3	1357.8	105.8	879.4	41.0	35.2
161	0.0819	5.1	1.6602	6.7	0.1471	4.0	0.66	884.5	33.3	993.5	42.6	1242.4	99.1	884.5	33.3	28.8
37	0.0902	6.2	1.8893	8.5	0.1519	5.8	0.68	911.8	49.7	1077.3	56.3	1429.4	118.0	911.8	49.7	36.2
257	0.1163	8.6	2.4491	11.4	0.1527	7.0	0.66	916.3	59.7	1257.2	82.4	1900.0	153.9	916.3	59.7	51.8
369	0.0797	2.5	1.6900	3.6	0.1537	2.7	0.73	921.8	23.0	1004.8	22.9	1190.5	48.7	921.8	23.0	22.6
140	0.0791	4.0	1.6772	5.4	0.1538	3.7	0.67	922.3	31.8	999.9	34.3	1174.2	78.9	922.3	31.8	21.5
298	0.1113	4.7	2.3621	6.4	0.1539	5.0	0.69	923.0	43.2	1231.2	45.8	1820.5	84.9	923.0	43.2	49.3
13	0.0813	4.3	1.7307	6.9	0.1544	5.5	0.78	925.5	47.2	1020.0	44.4	1228.8	84.1	925.5	47.2	24.7
44	0.0802	6.4	1.7454	9.1	0.1578	6.5	0.71	944.3	57.1	1025.4	58.9	1202.8	126.4	944.3	57.1	21.5
91	0.0710	27.3	1.8607	41.4	0.1899	31.2	0.75	1121.1	321.2	1067.2	280.3	958.7	557.2	958.7	557.2	-16.9
228	0.0837	4.5	1.8530	7.3	0.1606	5.3	0.79	960.2	47.1	1064.5	48.0	1284.8	87.5	960.2	47.1	25.3
178	0.0819	4.1	1.8158	5.7	0.1607	3.6	0.70	960.8	32.4	1051.2	37.4	1243.9	79.9	960.8	32.4	22.8
297	0.1351	3.7	3.0356	5.9	0.1630	5.2	0.78	973.4	46.9	1416.6	45.2	2164.9	65.3	973.4	46.9	55.0
197	0.0996	5.8	2.2518	6.9	0.1640	3.8	0.54	978.8	34.5	1197.4	48.4	1616.7	108.0	978.8	34.5	39.5
177	0.1102	8.7	2.5054	12.4	0.1648	8.6	0.71	983.6	78.9	1273.6	90.2	1803.2	158.7	983.6	78.9	45.5
259	0.0887	6.8	2.0223	10.3	0.1653	7.1	0.75	986.1	65.4	1123.0	70.0	1398.5	131.0	986.1	65.4	29.5
120	0.0869	7.8	1.9846	10.8	0.1657	7.5	0.69	988.4	68.5	1110.3	73.0	1357.4	149.7	988.4	68.5	27.2
173	0.0899	2.9	2.0771	5.5	0.1675	4.5	0.85	998.6	41.2	1141.3	37.8	1423.7	55.1	998.6	41.2	29.9
213	0.0932	8.4	2.1538	11.2	0.1676	7.2	0.66	998.9	66.6	1166.3	77.6	1492.0	158.5	998.9	66.6	33.0
134	0.0852	4.4	1.9958	7.0	0.1700	5.4	0.77	1012.0	50.3	1114.1	47.2	1319.1	85.7	1319.1	85.7	23.3
171	0.0870	21.1	2.4768	29.9	0.2065	21.2	0.71	1210.3	233.7	1265.3	219.9	1360.0	406.7	1360.0	406.7	11.0
377	0.0893	8.1	2.1317	10.3	0.1732	6.4	0.62	1029.5	60.5	1159.1	71.1	1410.3	154.5	1410.3	154.5	27.0
360	0.0894	5.4	2.2438	7.5	0.1821	5.2	0.70	1078.4	52.1	1194.9	52.5	1412.0	102.5	1412.0	102.5	23.6
155	0.0904	11.1	2.1235	16.2	0.1704	11.9	0.73	1014.2	111.8	1156.5	112.5	1433.8	211.3	1433.8	211.3	29.3
280	0.0914	2.9	2.4255	4.9	0.1925	4.5	0.81	1135.1	46.5	1250.2	35.0	1454.2	55.6	1454.2	55.6	21.9
48	0.0920	4.1	2.1499	4.7	0.1694	2.5	0.51	1009.1	23.5	1165.0	32.9	1467.8	77.2	1467.8	77.2	31.3
89	0.0927	6.8	2.1848	9.7	0.1709	7.2	0.72	1016.9	67.5	1176.2	67.8	1482.6	128.4	1482.6	128.4	31.4
361	0.0930	5.8	2.4756	7.6	0.1930	5.0	0.65	1137.6	52.4	1264.9	55.3	1488.6	109.7	1488.6	109.7	23.6
146	0.0942	11.9	2.4788	13.1	0.1908	5.8	0.43	1125.6	59.6	1265.9	95.4	1512.9	224.4	1512.9	224.4	25.6
260	0.0957	7.5	2.6094	10.7	0.1977	7.4	0.72	1162.8	79.0	1303.3	79.0	1542.7	140.8	1542.7	140.8	24.6
35	0.0965	6.6	2.7550	8.8	0.2072	5.8	0.65	1213.7	63.9	1343.4	65.4	1556.6	124.7	1556.6	124.7	22.0
245	0.1006	5.5	2.8924	8.3	0.2086	5.8	0.76	1221.2	64.0	1379.9	62.9	1634.7	101.5	1634.7	101.5	25.3
116	0.1007	5.9	2.4643	7.4	0.1775	4.3	0.59	1053.0	42.1	1261.6	53.2	1637.3	110.0	1637.3	110.0	35.7
391	0.1016	7.1	2.3518	9.4	0.1680	6.2	0.66	1000.8	57.5	1228.1	67.1	1652.8	130.9	1652.8	130.9	39.4
320	0.1056	4.6	2.5069	5.5	0.1721	3.4	0.57	1023.8	32.0	1274.0	40.1	1725.3	83.6	1725.3	83.6	40.7
56	0.1058	5.4	3.2411	6.6	0.2222	4.5	0.58	1293.4	52.7	1467.0	50.9	1728.3	99.2	1728.3	99.2	25.2
253	0.1058	9.1	2.5725	10.5	0.1763	4.7	0.50	1046.9	45.7	1292.9	76.6	1728.5	166.5	1728.5	166.5	39.4
141	0.1066	9.3	2.8645	12.3	0.1948	8.0	0.65	1147.4	84.6	1372.6	92.8	1742.8	170.9	1742.8	170.9	34.2
126	0.1068	4.2	2.8426	5.2	0.1931	3.0	0.58	1138.0	31.0	1366.9	39.1	1745.2	77.4	1745.2	77.4	34.8
191	0.1074	3.1	3.5875	5.7	0.2423	4.6	0.83	1398.6	57.3	1546.8	45.2	1755.6	57.5	1755.6	57.5	20.3
325	0.1079	5.8	2.6619	6.9	0.1790	4.1	0.54	1061.3	40.3	1318.0	50.6	1764.0	105.3	1764.0	105.3	39.8
143	0.1094	6.9	2.6042	9.7	0.1726	6.9	0.70	1026.6	65.2	1301.8	71.3	1789.6	125.5	1789.6	125.5	42.6
182	0.1099	5.3	2.6871	6.6	0.1773	3.9	0.60	1052.2	37.8	1324.9	49.0	1798.0	96.0	1798.0	96.0	41.5
216	0.1155	5.3	3.3952	6.7	0.2132	3.5	0.63	1246.0	39.3	1503.3	52.7	1887.5	95.0	1887.5	95.0	34.0
275	0.1165	8.4	2.7810	9.5	0.1731	4.5	0.46	1029.2	42.9	1350.4	70.8	1903.5	151.2	1903.5	151.2	45.9
31	0.1169	10.7	2.9500	11.5	0.1829	4.2	0.37	1083.1	42.0	1394.8	87.3	1910.1	192.0	1910.1	192.0	43.3

Table A4.10 (continued): Detrital Zircon U-Pb Integrated Data for the Paruro Formation Base

Spot	Ratios							Ages (Ma)					Best Age	Disc. (%)		
	207Pb/ 206Pb		207Pb/ 235U		206Pb/ 238U		Rho	206Pb/ 238U		207Pb/ 235U		207Pb/ 206Pb				
	±2σ	±2σ	±2σ	±2σ	±2σ	±2σ		±2σ	±2σ	±2σ	±2σ	±2σ				
<i>Paruro Formation Base 1 (20140605-01) Rejected Data</i>																
342	0.1170	10.6	3.9447	14.9	0.2445	10.5	0.70	1410.3	132.5	1622.9	121.1	1910.8	190.5	1910.8	190.5	26.2
268	0.1241	10.9	2.9671	14.4	0.1734	9.3	0.65	1030.6	88.1	1399.2	109.8	2016.4	193.3	2016.4	193.3	48.9
251	0.1287	3.9	4.4952	6.5	0.2532	4.7	0.80	1455.2	61.4	1730.1	53.9	2080.9	68.5	2080.9	68.5	30.1
207	0.1314	11.7	3.8143	13.0	0.2106	5.2	0.43	1231.9	58.9	1595.8	104.6	2116.3	205.6	2116.3	205.6	41.8
69	0.1321	8.1	3.2720	9.1	0.1797	5.5	0.47	1065.2	54.0	1474.4	70.5	2125.8	141.9	2125.8	141.9	49.9
299	0.1346	3.6	5.0416	5.0	0.2716	4.2	0.71	1549.1	58.5	1826.3	42.5	2158.9	63.1	2158.9	63.1	28.2
209	0.1421	8.6	3.5179	10.4	0.1796	5.6	0.56	1064.5	54.7	1531.2	82.3	2253.0	148.6	2253.0	148.6	52.8
58	0.1429	6.3	4.4428	7.1	0.2255	4.2	0.48	1310.7	49.4	1720.3	59.2	2262.7	109.1	2262.7	109.1	42.1
60	0.1463	7.7	6.0725	9.8	0.3011	6.8	0.62	1696.6	100.8	1986.3	85.4	2302.9	132.3	2302.9	132.3	26.3
76	0.1495	16.1	3.6272	19.3	0.1760	11.2	0.55	1045.2	108.0	1555.5	155.2	2339.7	275.7	2339.7	275.7	55.3
244	0.1545	5.6	4.5012	8.0	0.2114	5.2	0.72	1236.1	58.6	1731.2	66.9	2395.8	95.0	2395.8	95.0	48.4
243	0.1596	15.7	4.9616	21.0	0.2255	13.6	0.66	1310.8	161.7	1812.8	179.6	2451.3	266.4	2451.3	266.4	46.5
128	0.1692	10.4	4.5393	15.6	0.1946	11.6	0.75	1146.1	121.8	1738.2	130.4	2549.8	174.1	2549.8	174.1	55.1
232	0.1702	16.1	6.2858	17.9	0.2679	7.4	0.43	1530.0	100.7	2016.5	157.9	2559.5	269.9	2559.5	269.9	40.2
218	0.1795	9.1	4.9435	13.5	0.1998	9.7	0.74	1174.1	104.5	1809.7	114.6	2647.9	150.8	2647.9	150.8	55.7
227	0.1918	5.9	7.2228	8.0	0.2731	4.9	0.68	1556.7	68.0	2139.3	71.5	2757.6	97.2	2757.6	97.2	43.6
164	0.1977	4.8	6.3676	7.6	0.2336	5.6	0.77	1353.5	68.0	2027.8	66.8	2807.1	79.0	2807.1	79.0	51.8
105	0.1978	8.3	5.2065	9.4	0.1909	4.4	0.47	1126.4	45.7	1853.7	79.9	2807.9	135.4	2807.9	135.4	59.9
107	0.1999	8.7	5.2236	9.5	0.1895	3.8	0.39	1118.6	38.6	1856.5	80.8	2825.7	142.0	2825.7	142.0	60.4
2	0.5734	21.7	14.7325	25.1	0.1863	13.0	0.51	1101.5	131.3	2798.1	243.4	4442.1	315.8	4442.1	315.8	75.2
83	0.6642	18.3	48.0154	22.5	0.5243	13.4	0.58	2717.4	296.2	3952.0	227.7	4655.2	264.4	4655.2	264.4	41.6
370	0.8494	18.3	9867.1330	27.5	84.2494	20.6	0.75	28658.1	1329.9	9338.5	286.8	5006.9	261.1	5006.9	261.1	-472.4
<i>Paruro Formation Base 2 (20140528-01) Accepted Data</i>																
227	0.0489	57.9	0.0090	58.9	0.0013	10.6	0.18	8.6	0.9	9.1	5.4	142.2	1359.7	8.6	0.9	5.4
12	0.0948	45.5	0.0516	47.1	0.0039	12.2	0.26	25.4	3.1	51.1	23.5	1524.1	857.3	25.4	3.1	50.3
212	0.0588	16.1	0.0322	17.6	0.0040	6.9	0.41	25.6	1.8	32.2	5.6	558.3	350.9	25.6	1.8	20.5
260	0.0416	24.6	0.0236	27.5	0.0041	12.5	0.45	26.5	3.3	23.7	6.5	-251.2	621.6	26.5	3.3	-11.8
138	0.0515	9.4	0.0297	11.1	0.0042	5.8	0.52	26.9	1.6	29.8	3.2	264.3	216.5	26.9	1.6	9.5
205	0.0616	26.9	0.0356	28.8	0.0042	10.2	0.36	26.9	2.7	35.5	10.0	661.9	575.8	26.9	2.7	24.1
335	0.0668	24.3	0.0390	26.1	0.0042	9.6	0.37	27.2	2.6	38.8	9.9	830.8	506.1	27.2	2.6	29.9
95	0.0557	18.3	0.0326	22.9	0.0042	14.0	0.60	27.3	3.8	32.6	7.3	439.7	407.8	27.3	3.8	16.1
252	0.0687	35.0	0.0404	36.2	0.0043	9.7	0.26	27.5	2.7	40.2	14.3	890.1	722.6	27.5	2.7	31.8
146	0.0834	31.3	0.0494	32.5	0.0043	8.6	0.27	27.7	2.4	49.0	15.6	1279.0	610.8	27.7	2.4	43.6
76	0.0608	19.1	0.0361	20.3	0.0043	7.4	0.34	27.7	2.0	36.1	7.2	632.4	411.7	27.7	2.0	23.1
111	0.0896	36.7	0.0545	38.1	0.0044	10.2	0.27	28.4	2.9	53.9	20.0	1417.0	701.6	28.4	2.9	47.3
262	0.0651	37.8	0.0398	39.3	0.0044	10.9	0.28	28.6	3.1	39.7	15.3	777.3	793.9	28.6	3.1	28.0
246	0.0601	13.1	0.0369	16.3	0.0045	9.9	0.60	28.7	2.8	36.8	5.9	605.7	283.0	28.7	2.8	22.1
400	0.0611	61.7	0.0376	62.7	0.0045	11.3	0.18	28.7	3.2	37.4	23.1	643.3	1325.8	28.7	3.2	23.4
376	0.0478	28.9	0.0296	30.0	0.0045	7.8	0.26	28.8	2.2	29.6	8.7	91.7	685.7	28.8	2.2	2.6
53	0.0671	15.8	0.0416	16.8	0.0045	5.9	0.34	28.9	1.7	41.4	6.8	841.2	328.4	28.9	1.7	30.1
29	0.0711	42.4	0.0452	44.2	0.0046	12.8	0.29	29.6	3.8	44.8	19.4	960.7	866.3	29.6	3.8	34.0
322	0.0722	23.1	0.0460	25.0	0.0046	10.0	0.39	29.7	3.0	45.7	11.2	991.3	468.8	29.7	3.0	34.9
201	0.0709	27.8	0.0452	28.9	0.0046	7.7	0.27	29.8	2.3	44.9	12.7	953.4	569.0	29.8	2.3	33.7
208	0.0665	23.2	0.0425	24.4	0.0046	7.3	0.31	29.8	2.2	42.3	10.1	822.6	484.0	29.8	2.2	29.5
388	0.0566	27.5	0.0366	28.9	0.0047	8.8	0.31	30.2	2.7	36.5	10.4	474.7	608.1	30.2	2.7	17.3
64	0.0641	21.0	0.0415	23.6	0.0047	10.5	0.45	30.2	3.2	41.3	9.5	745.5	443.8	30.2	3.2	26.9
383	0.0428	49.1	0.0284	50.3	0.0048	11.2	0.22	31.0	3.5	28.4	14.1	-180.2	1224.8	31.0	3.5	-8.9
223	0.0699	35.0	0.0478	36.4	0.0050	10.0	0.28	31.9	3.2	47.4	16.9	925.0	719.5	31.9	3.2	32.7
307	0.0615	20.3	0.0425	23.8	0.0050	12.3	0.52	32.2	3.9	42.2	9.8	657.9	436.3	32.2	3.9	23.8
77	0.0714	24.6	0.0497	26.4	0.0050	9.9	0.36	32.5	3.2	49.2	12.7	968.2	501.7	32.5	3.2	34.1
154	0.0528	13.1	0.0376	14.3	0.0052	5.6	0.40	33.2	1.9	37.5	5.3	322.3	298.0	33.2	1.9	11.5
371	0.0747	34.0	0.0533	36.0	0.0052	11.6	0.32	33.3	3.8	52.7	18.5	1059.5	685.2	33.3	3.8	36.9
236	0.0605	17.7	0.0448	19.0	0.0054	7.1	0.36	34.6	2.4	44.5	8.3	620.9	381.5	34.6	2.4	22.4
14	0.0647	15.5	0.0499	16.8	0.0056	6.8	0.39	35.9	2.4	49.4	8.1	763.7	327.0	35.9	2.4	27.2
159	0.0677	15.1	0.0523	17.4	0.0056	8.6	0.50	36.0	3.1	51.8	8.8	859.7	313.9	36.0	3.1	30.4
245	0.0557	18.8	0.0441	22.8	0.0057	13.2	0.57	36.9	4.8	43.8	9.8	438.4	417.7	36.9	4.8	15.7
66	0.0533	10.5	0.0468	12.3	0.0064	5.8	0.52	40.9	2.4	46.4	5.6	342.8	238.3	40.9	2.4	11.9
116	0.0735	19.3	0.0647	22.2	0.0064	10.9	0.49	41.1	4.5	63.7	13.7	1027.1	391.2	41.1	4.5	35.5
373	0.0525	50.6	0.0503	51.3	0.0069	8.3	0.16	44.6	3.7	49.8	24.9	308.3	1152.0	44.6	3.7	10.5
170	0.0524	15.1	0.0745	20.6	0.0103	13.9	0.68	66.2	9.2	72.9	14.5	300.9	343.9	66.2	9.2	9.3
377	0.0769	21.2	0.1167	22.1	0.0110	6.3	0.28	70.5	4.4	112.1	23.5	1119.7	423.5	70.5	4.4	37.1
238	0.0825	29.3	0.1343	31.7	0.0118	12.0	0.38	75.6	9.0	127.9	38.1	1258.2	573.7	75.6	9.0	40.9
386	0.0634	10.6	0.1033	12.4	0.0118	6.3	0.51	75.7	4.7	99.8	11.8	721.2	225.7	75.7	4.7	24.1

Table A4.10 (continued): Detrital Zircon U-Pb Integrated Data for the Paruro Formation Base

Spot	Ratios							Ages (Ma)						Best Age	Disc. (%)	
	207Pb/206Pb		207Pb/235U		206Pb/238U		206Pb/238U		207Pb/235U		207Pb/206Pb					
	$\pm 2\sigma$	$\pm 2\sigma$	$\pm 2\sigma$	$\pm 2\sigma$	$\pm 2\sigma$	$\pm 2\sigma$	$\pm 2\sigma$	$\pm 2\sigma$	$\pm 2\sigma$	$\pm 2\sigma$	$\pm 2\sigma$	$\pm 2\sigma$				
	<i>Paruro Formation Base 2 (20140528-01) Accepted Data</i>															
306	0.0593	12.7	0.0970	16.3	0.0119	10.3	0.63	76.0	7.8	94.0	14.7	579.0	275.5	76.0	7.8	19.2
209	0.0540	6.6	0.0886	8.5	0.0119	5.0	0.63	76.3	3.8	86.2	7.0	371.6	148.6	76.3	3.8	11.6
6	0.0481	36.1	0.0796	36.8	0.0120	7.4	0.20	76.9	5.6	77.8	27.6	105.9	852.9	76.9	5.6	1.2
147	0.0537	9.7	0.0904	11.3	0.0122	5.7	0.51	78.2	4.4	87.9	9.5	360.3	219.7	78.2	4.4	11.0
352	0.0516	7.4	0.0881	8.5	0.0124	3.8	0.48	79.4	3.0	85.7	7.0	267.6	170.6	79.4	3.0	7.5
61	0.0516	13.6	0.0896	16.8	0.0126	9.6	0.59	80.8	7.7	87.2	14.1	265.6	312.7	80.8	7.7	7.3
40	0.0602	7.7	0.1125	8.6	0.0136	4.2	0.45	86.8	3.6	108.2	8.8	609.3	166.1	86.8	3.6	19.8
37	0.0531	7.6	0.1403	10.7	0.0191	7.8	0.71	122.3	9.4	133.3	13.4	335.0	171.7	122.3	9.4	8.3
83	0.0495	7.2	0.1313	9.7	0.0192	7.0	0.67	122.9	8.5	125.2	11.4	169.9	167.4	122.9	8.5	1.9
286	0.0563	7.2	0.1601	9.4	0.0206	6.5	0.65	131.5	8.5	150.8	13.2	464.8	158.7	131.5	8.5	12.8
277	0.0607	11.3	0.1762	16.1	0.0211	11.7	0.71	134.4	15.6	164.8	24.5	627.7	243.3	134.4	15.6	18.5
190	0.0551	8.9	0.1691	10.2	0.0223	4.9	0.49	141.9	6.9	158.7	14.9	416.9	198.1	141.9	6.9	10.6
79	0.0505	7.3	0.1570	9.4	0.0226	6.4	0.63	143.8	9.2	148.1	13.0	217.3	169.8	143.8	9.2	2.9
353	0.0536	7.7	0.1667	8.9	0.0226	4.3	0.51	143.9	6.2	156.5	13.0	352.7	174.4	143.9	6.2	8.1
308	0.0663	14.8	0.2092	17.7	0.0229	9.7	0.55	145.9	14.0	192.8	31.1	814.4	309.6	145.9	14.0	24.3
191	0.0519	13.1	0.1660	14.0	0.0232	4.9	0.35	147.8	7.1	155.9	20.2	281.8	300.2	147.8	7.1	5.2
384	0.0616	10.4	0.2105	12.4	0.0248	6.8	0.55	157.8	10.6	193.9	22.0	660.2	223.6	157.8	10.6	18.6
354	0.0694	14.6	0.2513	15.9	0.0262	6.1	0.39	167.0	10.0	227.6	32.4	912.1	301.2	167.0	10.0	26.6
225	0.0492	4.8	0.1963	6.8	0.0289	5.0	0.70	183.9	9.0	182.0	11.4	157.5	113.4	183.9	9.0	-1.0
67	0.0529	7.5	0.2205	9.4	0.0302	5.0	0.60	191.8	9.4	202.3	17.2	326.4	171.3	191.8	9.4	5.2
135	0.0663	17.9	0.2879	23.1	0.0315	14.5	0.63	199.9	28.6	256.9	52.4	816.1	374.8	199.9	28.6	22.2
132	0.0590	5.5	0.2777	7.8	0.0341	5.6	0.71	216.4	11.9	248.9	17.1	566.8	119.5	216.4	11.9	13.0
340	0.0534	7.4	0.2529	9.6	0.0343	6.0	0.63	217.6	12.8	229.0	19.7	346.9	168.1	217.6	12.8	4.9
161	0.0541	7.0	0.2657	9.3	0.0356	6.0	0.66	225.7	13.3	239.2	19.8	374.6	158.1	225.7	13.3	5.7
196	0.0568	4.0	0.2877	5.8	0.0367	4.0	0.71	232.5	9.1	256.7	13.1	484.6	88.9	232.5	9.1	9.5
182	0.0535	6.3	0.2745	8.3	0.0372	5.3	0.66	235.4	12.1	246.3	18.3	351.0	142.0	235.4	12.1	4.4
2	0.0661	12.4	0.3455	18.7	0.0379	14.0	0.75	239.7	33.0	301.4	48.9	811.0	259.5	239.7	33.0	20.5
8	0.0535	13.0	0.2895	18.5	0.0393	13.1	0.71	248.3	31.8	258.1	42.1	348.4	294.6	248.3	31.8	3.8
217	0.0527	7.0	0.2874	9.5	0.0395	6.1	0.68	250.0	14.9	256.5	21.4	317.1	158.0	250.0	14.9	2.6
337	0.0525	5.4	0.2921	7.8	0.0403	5.5	0.72	255.0	13.6	260.2	17.9	308.1	122.9	255.0	13.6	2.0
297	0.0556	7.0	0.3190	9.0	0.0416	5.9	0.62	262.7	15.3	281.2	22.0	437.4	156.2	262.7	15.3	6.6
99	0.0545	8.5	0.3135	11.3	0.0417	8.0	0.66	263.5	20.6	276.9	27.4	391.3	191.3	263.5	20.6	4.8
369	0.0528	7.5	0.3055	10.9	0.0420	7.8	0.72	264.9	20.2	270.7	25.9	320.7	170.6	264.9	20.2	2.1
86	0.0666	9.4	0.3905	14.7	0.0425	11.9	0.77	268.4	31.3	334.7	42.0	825.6	195.5	268.4	31.3	19.8
221	0.0557	4.0	0.3372	6.5	0.0439	4.9	0.79	277.1	13.3	295.0	16.7	439.3	89.7	277.1	13.3	6.1
370	0.0535	8.8	0.3273	10.8	0.0444	6.2	0.58	280.1	16.9	287.5	27.1	348.4	198.7	280.1	16.9	2.6
18	0.0581	7.9	0.3601	10.4	0.0449	7.2	0.65	283.3	20.0	312.3	28.0	534.6	173.3	283.3	20.0	9.3
391	0.0655	6.7	0.4177	8.0	0.0463	4.5	0.56	291.7	12.9	354.4	24.1	789.0	139.7	291.7	12.9	17.7
85	0.0575	9.0	0.3826	10.3	0.0483	6.1	0.49	303.8	18.2	328.9	28.9	510.7	198.5	303.8	18.2	7.6
273	0.0539	11.6	0.3742	17.4	0.0504	13.4	0.75	316.7	41.3	322.8	48.2	366.8	261.9	316.7	41.3	1.9
130	0.0570	7.9	0.3964	11.6	0.0504	8.5	0.73	317.1	26.4	339.1	33.5	492.1	174.9	317.1	26.4	6.5
131	0.0627	7.5	0.4405	11.5	0.0510	8.8	0.76	320.4	27.4	370.6	35.7	698.1	159.9	320.4	27.4	13.6
73	0.0722	12.1	0.5247	17.1	0.0527	12.2	0.71	331.2	39.5	428.3	59.8	991.5	246.4	331.2	39.5	22.7
143	0.0606	7.1	0.4449	9.4	0.0533	6.1	0.66	334.7	20.0	373.7	29.4	623.5	152.6	334.7	20.0	10.4
141	0.0901	12.1	0.8382	19.0	0.0675	14.6	0.77	421.1	59.5	618.2	88.1	1426.7	231.3	421.1	59.5	31.9
69	0.0555	12.8	0.5331	19.1	0.0697	14.0	0.74	434.3	58.7	433.9	67.7	431.9	286.0	434.3	58.7	-0.1
178	0.0592	3.9	0.5878	7.1	0.0720	5.4	0.84	448.1	23.3	469.5	26.6	575.3	84.3	448.1	23.3	4.5
188	0.0585	6.5	0.5892	9.2	0.0731	6.6	0.70	454.6	29.1	470.4	34.7	548.0	142.9	454.6	29.1	3.3
239	0.0623	6.6	0.6331	9.5	0.0737	7.1	0.72	458.3	31.6	498.0	37.5	685.1	140.3	458.3	31.6	8.0
374	0.0640	8.1	0.6500	10.9	0.0737	7.4	0.67	458.5	32.6	508.5	43.8	740.0	170.9	458.5	32.6	9.8
313	0.0577	5.8	0.5905	8.3	0.0742	6.0	0.72	461.5	26.7	471.2	31.2	518.7	126.8	461.5	26.7	2.1
172	0.0576	5.0	0.5943	8.1	0.0748	6.1	0.79	465.1	27.2	473.6	30.6	514.9	109.2	465.1	27.2	1.8
105	0.0569	5.2	0.5873	8.0	0.0749	6.1	0.76	465.5	27.3	469.2	29.9	487.3	114.4	465.5	27.3	0.8
332	0.0592	3.4	0.6198	5.1	0.0759	3.6	0.75	471.4	16.5	489.7	20.0	576.1	74.0	471.4	16.5	3.7
42	0.0643	5.9	0.6735	8.5	0.0760	6.4	0.72	472.1	29.1	522.8	34.8	751.1	123.9	472.1	29.1	9.7
281	0.0590	7.6	0.6221	10.8	0.0764	7.8	0.71	474.9	35.7	491.2	42.1	567.9	166.4	474.9	35.7	3.3
33	0.0606	10.9	0.6400	15.0	0.0766	10.5	0.69	475.5	48.1	502.3	59.7	626.2	233.9	475.5	48.1	5.3
359	0.0591	7.3	0.6305	10.4	0.0774	7.3	0.72	480.7	34.0	496.4	41.0	569.6	158.5	480.7	34.0	3.2
360	0.0692	6.2	0.7457	8.6	0.0781	5.7	0.69	484.8	26.8	565.7	37.3	906.0	128.6	484.8	26.8	14.3
247	0.0575	4.6	0.6209	7.5	0.0783	6.3	0.79	485.8	29.3	490.4	29.1	511.9	101.5	485.8	29.3	0.9
7	0.0601	4.4	0.6629	5.8	0.0800	3.7	0.65	496.0	17.8	516.4	23.3	607.8	94.8	496.0	17.8	4.0
382	0.0587	8.9	0.6505	12.5	0.0804	8.8	0.70	498.3	42.1	508.8	50.1	556.1	194.4	498.3	42.1	2.1
39	0.0747	10.5	0.8316	12.1	0.0808	6.3	0.50	500.7	30.5	614.5	56.0	1059.6	212.1	500.7	30.5	18.5

Table A4.10 (continued): Detrital Zircon U-Pb Integrated Data for the Paruro Formation Base

Spot	Ratios							Ages (Ma)							Disc. (%)	
	207Pb/ 206Pb		207Pb/ 235U		206Pb/ 238U		Rho	206Pb/ 238U		207Pb/ 235U		207Pb/ 206Pb		Best		
	$\pm 2\sigma$	$\pm 2\sigma$	$\pm 2\sigma$	$\pm 2\sigma$	$\pm 2\sigma$	$\pm 2\sigma$		$\pm 2\sigma$	$\pm 2\sigma$	Age	$\pm 2\sigma$					
<i>Paruro Formation Base 2 (20140528-01) Accepted Data</i>																
346	0.0571	13.5	0.6426	19.3	0.0816	13.7	0.71	505.8	66.6	503.9	76.9	495.7	298.2	505.8	66.6	-0.4
123	0.0586	8.2	0.6594	12.5	0.0817	9.2	0.75	506.0	44.8	514.2	50.3	551.0	180.1	506.0	44.8	1.6
195	0.0660	4.1	0.7457	5.8	0.0819	4.1	0.72	507.4	19.8	565.7	25.2	807.8	84.9	507.4	19.8	10.3
137	0.0615	7.2	0.6959	8.9	0.0820	5.2	0.58	508.1	25.3	536.4	37.1	658.5	155.4	508.1	25.3	5.3
254	0.0583	4.2	0.6600	7.1	0.0821	6.1	0.81	508.5	29.7	514.6	28.6	541.7	91.3	508.5	29.7	1.2
257	0.0631	5.8	0.7190	8.9	0.0826	7.1	0.76	511.7	34.8	550.1	37.9	712.3	123.8	511.7	34.8	7.0
148	0.0652	12.0	0.7455	13.1	0.0829	5.2	0.40	513.7	25.6	565.6	56.8	780.5	251.4	513.7	25.6	9.2
356	0.0567	9.2	0.6496	13.1	0.0831	9.2	0.71	514.4	45.6	508.2	52.5	480.5	204.0	514.4	45.6	-1.2
298	0.0678	9.4	0.7775	12.6	0.0832	8.7	0.67	515.1	42.8	584.0	56.2	861.8	195.4	515.1	42.8	11.8
341	0.0628	9.0	0.7225	11.6	0.0834	7.2	0.63	516.4	35.5	552.2	49.3	702.7	191.9	516.4	35.5	6.5
59	0.0659	5.8	0.7605	7.5	0.0837	4.6	0.64	518.3	22.9	574.3	32.8	802.5	121.0	518.3	22.9	9.7
142	0.0624	6.9	0.7221	9.9	0.0840	6.9	0.71	519.9	34.7	551.9	42.0	686.6	148.2	519.9	34.7	5.8
90	0.0680	7.5	0.7897	10.4	0.0843	7.9	0.70	521.6	39.6	591.0	46.7	867.4	154.6	521.6	39.6	11.7
192	0.0604	9.8	0.7030	14.3	0.0844	10.4	0.73	522.4	52.1	540.6	60.1	617.8	212.5	522.4	52.1	3.4
333	0.0646	5.6	0.7521	7.7	0.0845	5.0	0.68	522.7	25.2	569.5	33.4	760.9	119.0	522.7	25.2	8.2
378	0.0625	6.2	0.7308	8.6	0.0847	5.9	0.69	524.4	29.9	557.0	36.8	692.6	131.9	524.4	29.9	5.9
202	0.0682	5.1	0.8116	6.9	0.0863	4.3	0.68	533.4	22.1	603.4	31.3	875.6	105.1	533.4	22.1	11.6
288	0.0728	11.1	0.8714	16.4	0.0868	12.2	0.73	536.7	62.8	636.3	77.5	1008.0	226.2	536.7	62.8	15.6
11	0.0657	7.8	0.7906	9.2	0.0872	5.2	0.54	539.1	26.7	591.5	41.3	798.1	162.9	539.1	26.7	8.9
97	0.0595	4.9	0.7168	5.6	0.0874	4.0	0.53	540.0	20.7	548.8	23.8	585.4	105.9	540.0	20.7	1.6
224	0.0598	5.9	0.7238	9.2	0.0878	6.8	0.77	542.3	35.6	552.9	39.1	596.6	127.9	542.3	35.6	1.9
63	0.0602	4.1	0.7309	6.8	0.0880	5.0	0.80	544.0	26.0	557.1	29.2	610.9	89.4	544.0	26.0	2.4
364	0.0657	6.8	0.7971	8.3	0.0881	4.4	0.57	544.0	22.9	595.2	37.3	795.4	142.6	544.0	22.9	8.6
164	0.0619	8.1	0.7511	12.6	0.0881	9.4	0.77	544.1	49.1	568.8	54.8	669.2	172.7	544.1	49.1	4.4
109	0.0678	6.4	0.8240	9.2	0.0881	6.7	0.72	544.3	34.8	610.3	42.3	863.2	133.1	544.3	34.8	10.8
316	0.0624	4.1	0.7686	5.9	0.0893	4.8	0.72	551.4	25.2	579.0	26.2	688.7	88.3	551.4	25.2	4.8
65	0.0574	4.3	0.7093	7.2	0.0897	5.2	0.81	553.5	27.6	544.3	30.4	506.0	94.5	553.5	27.6	-1.7
162	0.0620	4.7	0.7688	7.2	0.0899	5.3	0.75	554.8	28.2	579.1	31.7	675.4	101.0	554.8	28.2	4.2
367	0.0707	8.9	0.8808	11.0	0.0904	6.2	0.59	557.7	33.3	641.4	52.4	948.3	182.7	557.7	33.3	13.0
23	0.0596	4.9	0.7425	6.7	0.0904	5.0	0.68	558.1	26.5	563.9	29.1	587.4	106.8	558.1	26.5	1.0
112	0.0704	3.8	0.8907	5.4	0.0918	3.7	0.71	566.1	20.0	646.8	25.7	939.7	77.4	566.1	20.0	12.5
127	0.0587	6.7	0.7565	10.2	0.0935	7.5	0.75	576.1	41.4	572.0	44.8	555.5	146.6	576.1	41.4	-0.7
28	0.0576	5.7	0.7497	7.9	0.0944	5.8	0.70	581.6	32.4	568.0	34.4	514.1	124.2	581.6	32.4	-2.4
342	0.0630	4.5	0.8273	6.2	0.0952	4.1	0.69	586.1	23.2	612.1	28.4	709.7	94.9	586.1	23.2	4.3
140	0.0605	4.1	0.7973	6.3	0.0956	4.7	0.76	588.7	26.4	595.3	28.4	620.6	89.0	588.7	26.4	1.1
312	0.0579	7.8	0.7674	10.7	0.0961	7.3	0.68	591.7	41.5	578.3	47.0	526.0	170.7	591.7	41.5	-2.3
177	0.0640	10.8	0.8622	16.4	0.0978	12.1	0.75	601.2	69.2	631.3	77.0	740.6	227.7	601.2	69.2	18.8
291	0.0616	5.3	0.8367	8.0	0.0985	6.4	0.75	605.8	36.7	617.4	37.0	659.8	114.4	605.8	36.7	8.2
157	0.0625	5.9	0.8578	8.6	0.0996	6.1	0.73	612.1	35.6	628.9	40.5	689.8	125.8	612.1	35.6	11.3
275	0.0610	5.8	0.8422	8.7	0.1002	7.0	0.75	615.6	41.3	620.4	40.5	637.9	124.3	615.6	41.3	3.5
167	0.0645	3.4	0.8978	7.3	0.1010	6.2	0.89	620.1	36.6	650.6	35.3	757.9	72.1	620.1	36.6	18.2
41	0.0614	4.2	0.8679	6.0	0.1025	4.6	0.71	629.3	27.6	634.4	28.2	652.7	90.1	629.3	27.6	3.6
48	0.0621	8.7	0.8888	12.4	0.1039	9.2	0.71	637.0	55.6	645.7	59.1	676.3	185.2	637.0	55.6	5.8
261	0.0652	7.2	1.0009	12.3	0.1113	10.1	0.81	680.1	65.0	704.3	62.8	782.0	152.0	680.1	65.0	13.0
57	0.0614	5.7	0.9473	8.5	0.1120	6.1	0.74	684.1	39.8	676.7	42.0	652.0	123.3	684.1	39.8	-4.9
3	0.0644	3.7	0.9954	5.4	0.1121	3.9	0.72	684.7	25.2	701.5	27.3	755.6	78.6	684.7	25.2	9.4
126	0.0682	5.0	1.1018	12.2	0.1171	11.0	0.91	714.0	74.2	754.2	65.0	875.4	104.2	714.0	74.2	18.4
70	0.0690	10.4	1.1725	16.1	0.1233	12.5	0.76	749.6	88.4	787.8	88.6	897.7	215.0	749.6	88.4	16.5
268	0.0696	14.3	1.2156	19.1	0.1266	12.8	0.66	768.6	92.6	807.7	106.7	917.2	293.2	768.6	92.6	16.2
96	0.0677	3.1	1.2732	4.5	0.1364	4.3	0.76	824.5	33.5	833.8	25.4	858.9	63.8	824.5	33.5	4.0
351	0.0661	4.2	1.2434	6.0	0.1365	4.0	0.71	824.9	31.0	820.4	33.5	808.3	88.0	824.9	31.0	-2.1
106	0.0732	7.5	1.3796	10.4	0.1367	7.2	0.69	826.0	56.0	880.3	61.4	1019.3	152.6	826.0	56.0	19.0
295	0.0742	4.0	1.5133	5.4	0.1479	4.2	0.68	889.2	34.7	935.8	33.2	1047.1	80.6	889.2	34.7	15.1
4	0.0740	9.5	1.5536	13.4	0.1522	9.5	0.71	913.5	80.7	951.9	83.0	1041.9	191.5	913.5	80.7	12.3
175	0.0712	4.8	1.4991	8.6	0.1527	6.7	0.83	915.9	56.8	930.0	52.2	963.5	98.1	915.9	56.8	4.9
136	0.0713	7.0	1.5319	10.9	0.1557	8.4	0.77	933.0	72.7	943.3	67.0	967.3	142.7	933.0	72.7	3.5
398	0.0772	14.9	1.6755	21.2	0.1574	15.2	0.71	942.5	132.9	999.3	135.8	1126.2	296.3	942.5	132.9	16.3
176	0.0764	6.2	1.6612	10.3	0.1577	7.8	0.80	944.0	68.5	993.8	65.2	1105.5	123.7	944.0	68.5	14.6
233	0.0766	3.4	1.6679	8.6	0.1579	8.0	0.92	944.9	70.0	996.4	54.9	1111.5	68.9	944.9	70.0	15.0
174	0.0771	4.3	1.6777	7.6	0.1579	5.7	0.82	944.9	49.7	1000.1	48.1	1123.2	86.6	944.9	49.7	15.9
250	0.0725	5.0	1.5880	7.7	0.1590	6.2	0.76	951.0	54.4	965.5	48.2	998.7	102.3	951.0	54.4	4.8
80	0.0796	13.4	1.7656	18.3	0.1609	12.8	0.68	961.6	114.1	1032.9	119.4	1187.1	264.6	961.6	114.1	19.0
248	0.0726	6.8	1.6162	10.4	0.1614	8.1	0.75	964.5	72.4	976.5	65.1	1003.6	138.7	964.5	72.4	3.9

Table A4.10 (continued): Detrital Zircon U-Pb Integrated Data for the Paruro Formation Base

Spot	Ratios						Ages (Ma)						Best Age	Disc. (%)		
	207Pb/206Pb	$\pm 2\sigma$	207Pb/235U	$\pm 2\sigma$	206Pb/238U	$\pm 2\sigma$	Rho	206Pb/238U	$\pm 2\sigma$	207Pb/235U	$\pm 2\sigma$	207Pb/206Pb			$\pm 2\sigma$	
	<i>Paruro Formation Base 2 (20140528-01) Accepted Data</i>															
311	0.0763	7.6	1.7133	11.9	0.1629	9.2	0.77	973.0	83.5	1013.5	76.7	1102.2	152.3	973.0	83.5	11.7
155	0.0740	8.9	1.6739	12.2	0.1641	8.2	0.69	979.5	74.9	998.7	77.9	1041.0	179.7	979.5	74.9	5.9
210	0.0788	4.6	1.7880	6.9	0.1645	4.9	0.76	981.7	44.7	1041.1	45.2	1168.0	90.1	981.7	44.7	16.0
92	0.0774	3.9	1.7563	5.6	0.1646	5.0	0.73	982.1	45.8	1029.5	36.2	1131.7	78.5	982.1	45.8	13.2
350	0.0785	5.1	1.8052	7.5	0.1669	5.4	0.74	994.8	49.7	1047.4	49.3	1158.7	101.2	994.8	49.7	14.1
263	0.0719	12.2	1.6607	18.3	0.1674	13.7	0.75	998.0	126.7	993.6	116.5	984.1	248.1	998.0	126.7	-1.4
38	0.0725	4.4	1.7327	6.0	0.1733	4.6	0.69	1030.2	43.4	1020.8	38.9	1000.6	89.3	1000.6	89.3	-3.0
55	0.0729	6.2	1.7043	9.6	0.1696	7.2	0.76	1010.0	67.3	1010.2	61.4	1010.5	125.9	1010.5	125.9	0.1
215	0.0733	3.6	1.7444	6.5	0.1725	5.0	0.83	1026.0	47.5	1025.1	41.9	1023.0	73.5	1023.0	73.5	-0.3
206	0.0734	6.8	1.7761	9.7	0.1754	6.7	0.72	1041.9	64.9	1036.8	63.2	1025.9	137.2	1025.9	137.2	-1.6
259	0.0735	8.5	1.8268	13.3	0.1802	10.4	0.77	1068.0	102.8	1055.1	87.5	1028.5	172.0	1028.5	172.0	-3.8
119	0.0749	3.8	1.7472	6.1	0.1692	4.6	0.78	1008.0	43.2	1026.1	39.1	1065.1	76.2	1065.1	76.2	5.4
392	0.0757	7.8	1.8540	12.7	0.1777	10.0	0.79	1054.3	97.1	1064.8	83.8	1086.6	156.6	1086.6	156.6	3.0
349	0.0763	6.5	1.7753	10.1	0.1688	7.6	0.77	1005.2	70.4	1036.4	65.8	1102.9	129.9	1102.9	129.9	8.9
100	0.0767	7.7	1.8497	10.5	0.1749	7.6	0.68	1038.9	73.2	1063.3	69.6	1113.7	154.1	1113.7	154.1	6.7
82	0.0768	11.4	1.9174	18.3	0.1810	14.5	0.78	1072.6	143.7	1087.2	122.6	1116.5	226.9	1116.5	226.9	3.9
207	0.0770	3.0	1.8536	4.8	0.1745	3.3	0.79	1037.0	31.8	1064.7	31.4	1121.9	59.4	1121.9	59.4	7.6
114	0.0773	11.9	2.1347	19.1	0.2004	14.9	0.78	1177.5	160.6	1160.1	132.8	1127.8	236.8	1127.8	236.8	-4.4
300	0.0779	9.8	1.8836	14.3	0.1754	10.5	0.73	1041.6	101.1	1075.3	95.3	1144.4	195.5	1144.4	195.5	9.0
54	0.0785	8.3	1.9731	11.1	0.1822	7.2	0.66	1079.0	71.7	1106.4	74.8	1160.5	164.9	1160.5	164.9	7.0
285	0.0786	4.6	1.8656	6.9	0.1721	5.7	0.75	1023.8	53.7	1069.0	46.0	1162.4	92.1	1162.4	92.1	11.9
280	0.0789	9.4	1.9630	14.3	0.1804	10.8	0.75	1069.3	106.8	1102.9	96.3	1169.9	186.5	1169.9	186.5	8.6
124	0.0789	6.8	1.9119	10.5	0.1757	7.8	0.76	1043.2	75.0	1085.2	70.1	1170.7	135.2	1170.7	135.2	10.9
276	0.0795	7.1	1.8833	10.8	0.1718	8.6	0.76	1021.8	80.9	1075.2	71.6	1185.1	139.3	1185.1	139.3	13.8
348	0.0798	4.2	2.1835	6.6	0.1985	4.8	0.78	1167.2	51.4	1175.8	45.9	1191.6	82.2	1191.6	82.2	2.0
293	0.0799	4.6	2.1296	8.2	0.1933	7.2	0.83	1139.3	75.2	1158.5	57.0	1194.4	90.4	1194.4	90.4	4.6
226	0.0799	8.0	2.0759	11.9	0.1884	9.0	0.75	1112.7	92.1	1140.9	82.0	1194.8	156.9	1194.8	156.9	6.9
362	0.0799	4.2	2.2872	5.8	0.2076	3.8	0.70	1215.9	42.3	1208.3	41.3	1194.9	82.7	1194.9	82.7	-1.8
108	0.0804	8.5	2.1234	12.4	0.1916	9.1	0.73	1129.9	94.0	1156.4	85.7	1206.4	166.6	1206.4	166.6	6.3
89	0.0805	8.6	2.2136	12.5	0.1993	9.7	0.73	1171.8	103.5	1185.4	88.0	1210.2	169.1	1210.2	169.1	3.2
315	0.0807	8.1	2.1288	12.4	0.1912	9.7	0.76	1128.0	100.1	1158.2	86.1	1215.1	159.6	1215.1	159.6	7.2
325	0.0810	5.2	2.1239	7.2	0.1903	5.0	0.69	1122.9	51.5	1156.6	49.5	1220.3	102.2	1220.3	102.2	8.0
242	0.0810	2.9	2.2327	6.1	0.2000	6.0	0.88	1175.2	64.5	1191.4	43.0	1220.8	57.9	1220.8	57.9	3.7
200	0.0815	5.6	2.0577	8.4	0.1831	6.0	0.75	1083.8	60.3	1134.9	57.8	1233.8	110.6	1233.8	110.6	12.2
265	0.0815	4.6	2.0586	7.8	0.1831	6.5	0.80	1084.0	64.6	1135.1	53.5	1234.2	91.1	1234.2	91.1	12.2
243	0.0819	3.9	2.1556	6.8	0.1910	6.2	0.82	1126.6	63.8	1166.8	47.1	1242.3	76.3	1242.3	76.3	9.3
185	0.0820	3.6	2.1021	5.9	0.1860	4.9	0.79	1099.5	49.1	1149.5	40.6	1245.0	70.5	1245.0	70.5	11.7
343	0.0826	9.1	2.1181	13.8	0.1859	10.4	0.75	1099.3	104.9	1154.7	95.6	1260.3	177.0	1260.3	177.0	12.8
93	0.0831	5.9	2.4445	8.5	0.2134	6.8	0.73	1247.0	77.7	1255.8	61.1	1270.9	114.6	1270.9	114.6	1.9
235	0.0842	8.2	2.3999	12.2	0.2068	9.2	0.74	1211.8	101.5	1242.6	87.4	1296.3	158.9	1296.3	158.9	6.5
363	0.0842	6.2	2.0847	8.4	0.1795	5.5	0.68	1064.4	53.9	1143.8	57.6	1297.7	120.3	1297.7	120.3	18.0
84	0.0849	6.9	2.7519	10.3	0.2350	8.5	0.75	1360.4	103.7	1342.6	76.7	1314.3	133.5	1314.3	133.5	-3.5
107	0.0852	6.3	2.4706	10.1	0.2102	7.9	0.78	1230.0	88.5	1263.5	73.0	1320.9	122.0	1320.9	122.0	6.9
50	0.0865	8.5	2.7735	12.0	0.2326	8.7	0.71	1348.1	105.5	1348.4	90.1	1348.9	164.5	1348.9	164.5	0.1
46	0.0866	5.9	2.5539	7.3	0.2140	5.0	0.60	1250.0	57.1	1287.5	53.4	1350.8	113.4	1350.8	113.4	7.5
303	0.0869	5.5	2.3552	7.1	0.1965	4.7	0.64	1156.5	50.0	1229.1	50.6	1358.8	105.3	1358.8	105.3	14.9
194	0.0872	8.0	2.3879	11.0	0.1986	7.6	0.69	1167.7	81.1	1239.0	79.1	1365.1	153.5	1365.1	153.5	14.5
249	0.0881	5.8	2.6857	10.1	0.2211	8.4	0.82	1287.5	98.5	1324.5	74.5	1384.9	110.8	1384.9	110.8	7.0
385	0.0891	8.7	3.1667	12.5	0.2579	9.0	0.72	1479.0	118.4	1449.1	96.5	1405.4	165.9	1405.4	165.9	-5.2
56	0.0903	8.7	2.5707	10.8	0.2065	6.3	0.59	1210.3	69.3	1292.3	79.0	1431.4	165.6	1431.4	165.6	15.4
81	0.0906	6.4	3.0688	9.9	0.2456	8.0	0.76	1415.5	101.1	1424.9	76.0	1439.1	122.7	1439.1	122.7	1.6
305	0.0926	10.8	2.7754	17.5	0.2175	13.8	0.79	1268.5	158.9	1348.9	131.7	1478.9	205.2	1478.9	205.2	14.2
122	0.0930	8.2	2.8929	16.0	0.2257	13.7	0.86	1312.0	162.7	1380.1	121.5	1486.9	154.5	1486.9	154.5	11.8
271	0.0930	14.4	3.5194	21.5	0.2744	16.3	0.75	1563.3	227.0	1531.6	171.8	1488.1	271.8	1488.1	271.8	-5.1
78	0.0939	11.2	3.1898	16.7	0.2465	12.7	0.74	1420.2	161.5	1454.7	130.2	1505.4	212.4	1505.4	212.4	5.7
88	0.0950	5.8	2.9369	10.0	0.2243	8.9	0.82	1304.5	105.4	1391.5	75.7	1527.5	108.7	1527.5	108.7	14.6
328	0.0951	7.1	3.3463	10.6	0.2553	7.9	0.74	1465.8	103.9	1491.9	83.0	1529.3	133.4	1529.3	133.4	4.2
258	0.0959	6.1	3.6292	9.9	0.2746	8.1	0.79	1564.0	112.8	1556.0	79.3	1545.1	114.6	1545.1	114.6	-1.2
222	0.0962	11.7	3.2358	16.9	0.2439	12.2	0.73	1407.1	154.1	1465.8	132.1	1551.8	218.9	1551.8	218.9	9.3
339	0.0962	5.8	3.3687	8.6	0.2539	6.2	0.74	1458.4	81.5	1497.2	67.6	1552.4	108.5	1552.4	108.5	6.1
104	0.0970	11.8	3.1183	16.5	0.2333	11.8	0.70	1351.6	144.5	1437.2	127.6	1566.3	221.0	1566.3	221.0	13.7
214	0.0973	7.7	3.2881	10.2	0.2451	6.5	0.66	1413.4	81.9	1478.3	79.7	1572.7	143.5	1572.7	143.5	10.1
98	0.1007	14.5	3.3132	22.1	0.2387	16.8	0.75	1379.7	209.1	1484.2	173.7	1636.8	270.1	1636.8	270.1	15.7

Table A4.10 (continued): Detrital Zircon U-Pb Integrated Data for the Paruro Formation Base

Spot	Ratios						Ages (Ma)						Best Age	Disc. (%)		
	207Pb/ 206Pb	±2σ	207Pb/ 235U	±2σ	206Pb/ 238U	±2σ	Rho	206Pb/ 238U	±2σ	207Pb/ 235U	±2σ	207Pb/ 206Pb			±2σ	
	<i>Paruro Formation Base 2 (20140528-01) Accepted Data</i>															
49	0.1013	10.3	3.9497	16.6	0.2829	13.1	0.78	1605.8	185.8	1623.9	135.0	1647.5	191.5	1647.5	191.5	2.5
36	0.1014	4.3	3.6929	6.3	0.2643	4.9	0.72	1511.6	66.2	1569.8	50.0	1649.0	80.3	1649.0	80.3	8.3
399	0.1030	10.2	3.8314	14.7	0.2697	10.6	0.72	1539.1	145.2	1599.4	119.2	1679.7	189.1	1679.7	189.1	8.4
145	0.1033	8.3	3.7980	13.1	0.2667	10.2	0.78	1524.2	137.8	1592.3	106.0	1683.7	153.1	1683.7	153.1	9.5
153	0.1044	6.9	3.6066	10.3	0.2505	7.6	0.74	1441.0	97.9	1551.0	81.8	1704.2	126.9	1704.2	126.9	15.4
160	0.1048	10.0	4.4906	16.1	0.3107	12.5	0.78	1743.9	191.7	1729.2	134.4	1711.5	184.4	1711.5	184.4	-1.9
357	0.1065	5.2	4.6452	7.5	0.3162	5.2	0.72	1771.2	80.0	1757.4	62.8	1741.1	96.2	1741.1	96.2	-1.7
347	0.1084	7.8	4.5107	11.6	0.3018	8.5	0.74	1700.2	127.1	1732.9	97.1	1772.7	142.1	1772.7	142.1	4.1
16	0.1103	3.6	4.7372	4.5	0.3116	3.8	0.65	1748.6	57.7	1773.8	38.0	1803.7	64.7	1803.7	64.7	3.1
193	0.1116	3.2	4.8746	5.5	0.3167	4.5	0.82	1773.7	69.1	1797.9	46.5	1826.0	57.9	1826.0	57.9	2.9
71	0.1124	4.6	4.5279	10.0	0.2921	9.1	0.89	1651.8	132.2	1736.1	83.0	1839.3	83.5	1839.3	83.5	10.2
320	0.1133	4.7	4.7668	6.5	0.3051	4.9	0.69	1716.6	73.7	1779.1	54.8	1853.2	85.0	1853.2	85.0	7.4
396	0.1137	4.2	4.6416	5.8	0.2960	4.0	0.69	1671.6	58.8	1756.8	48.6	1859.7	76.3	1859.7	76.3	10.1
334	0.1153	12.2	5.1757	17.9	0.3255	13.1	0.73	1816.4	206.9	1848.6	153.8	1885.1	219.7	1885.1	219.7	3.6
204	0.1198	2.6	5.0144	4.5	0.3035	3.2	0.81	1708.6	47.5	1821.8	37.7	1953.7	47.3	1953.7	47.3	12.5
19	0.1225	4.1	5.5303	6.0	0.3275	5.0	0.73	1826.4	79.8	1905.3	51.7	1992.4	73.5	1992.4	73.5	8.3
87	0.1249	4.3	5.8762	5.5	0.3412	5.0	0.67	1892.5	82.2	1957.7	47.4	2027.4	75.3	2027.4	75.3	6.7
133	0.1276	3.3	5.1631	6.3	0.2934	5.5	0.86	1658.7	80.2	1846.6	53.6	2065.3	57.4	2065.3	57.4	19.7
317	0.1284	4.1	6.4692	6.5	0.3653	5.5	0.78	2007.2	94.1	2041.7	56.9	2076.8	72.0	2076.8	72.0	3.4
282	0.1292	6.4	6.6804	10.0	0.3750	7.9	0.77	2053.0	138.1	2070.0	88.8	2087.1	113.3	2087.1	113.3	1.6
279	0.1314	4.5	6.8764	7.5	0.3796	6.6	0.81	2074.2	116.7	2095.6	66.9	2116.7	78.8	2116.7	78.8	2.0
216	0.1317	12.3	6.2230	18.3	0.3428	13.4	0.74	1900.1	221.3	2007.7	161.7	2120.3	215.7	2120.3	215.7	10.4
219	0.1318	8.6	6.4929	13.0	0.3574	9.6	0.75	1970.0	162.8	2044.9	114.9	2121.4	149.8	2121.4	149.8	7.1
103	0.1355	9.0	6.5879	13.8	0.3527	10.8	0.76	1947.6	182.2	2057.7	122.6	2169.9	156.6	2169.9	156.6	10.2
186	0.1375	8.0	5.9641	10.5	0.3146	7.0	0.65	1763.2	107.3	1970.6	91.6	2195.9	138.7	2195.9	138.7	19.7
319	0.1556	5.3	8.0833	8.0	0.3767	6.4	0.75	2061.1	112.3	2240.4	72.6	2408.5	90.6	2408.5	90.6	14.4
375	0.1809	3.6	12.2889	5.6	0.4927	4.2	0.76	2582.5	89.6	2626.7	52.2	2661.0	59.9	2661.0	59.9	2.9
163	0.1818	9.9	10.5872	15.8	0.4225	12.2	0.78	2271.6	234.6	2487.6	147.3	2669.0	163.4	2669.0	163.4	14.9
151	0.1921	2.9	13.7096	4.7	0.5175	3.6	0.78	2688.6	78.5	2729.9	44.2	2760.5	48.4	2760.5	48.4	2.6
<i>Paruro Formation Base 2 (20140528-01) Rejected Data</i>																
26	0.0727	14.6	0.0421	17.3	0.0042	9.3	0.53	27.0	2.5	41.8	7.1	1005.0	297.3	27.0	2.5	35.5
189	0.0690	14.2	0.0403	15.5	0.0042	6.5	0.41	27.2	1.8	40.1	6.1	898.7	292.2	27.2	1.8	32.1
129	0.1478	23.2	0.0864	24.9	0.0042	9.1	0.36	27.3	2.5	84.1	20.1	2320.2	397.1	27.3	2.5	67.6
220	0.0901	20.4	0.0533	24.2	0.0043	13.0	0.54	27.6	3.6	52.7	12.4	1426.9	388.8	27.6	3.6	47.6
358	0.0773	20.2	0.0461	21.3	0.0043	6.5	0.31	27.8	1.8	45.8	9.5	1129.9	403.1	27.8	1.8	39.2
139	0.0877	9.9	0.0524	11.9	0.0043	6.8	0.56	27.9	1.9	51.9	6.0	1376.8	189.5	27.9	1.9	46.3
304	0.1174	21.5	0.0701	23.1	0.0043	8.4	0.36	27.9	2.3	68.8	15.4	1917.6	386.4	27.9	2.3	59.5
278	0.1171	22.1	0.0700	27.4	0.0043	16.5	0.59	27.9	4.6	68.7	18.2	1913.2	395.9	27.9	4.6	59.4
179	0.0717	16.2	0.0429	18.6	0.0043	8.9	0.50	27.9	2.5	42.6	7.8	978.2	329.9	27.9	2.5	34.6
327	0.0883	16.5	0.0529	21.3	0.0043	13.4	0.63	27.9	3.7	52.3	10.9	1389.0	317.2	27.9	3.7	46.6
301	0.1051	13.8	0.0630	15.0	0.0043	6.2	0.40	28.0	1.7	62.0	9.0	1716.6	253.1	28.0	1.7	54.9
244	0.1031	13.0	0.0622	18.0	0.0044	12.7	0.69	28.2	3.6	61.3	10.7	1680.3	239.7	28.2	3.6	54.1
269	0.0911	15.1	0.0550	17.1	0.0044	8.0	0.46	28.2	2.3	54.4	9.0	1448.3	288.4	28.2	2.3	48.2
321	0.1525	18.9	0.0923	21.0	0.0044	9.3	0.43	28.2	2.6	89.7	18.0	2374.7	321.8	28.2	2.6	68.5
380	0.1176	25.7	0.0716	28.7	0.0044	12.7	0.44	28.4	3.6	70.3	19.5	1919.3	461.7	28.4	3.6	59.5
287	0.0842	18.0	0.0516	20.4	0.0044	9.9	0.47	28.6	2.8	51.0	10.2	1296.7	350.9	28.6	2.8	44.0
187	0.0855	26.0	0.0526	30.3	0.0045	15.6	0.51	28.7	4.5	52.0	15.4	1327.7	502.9	28.7	4.5	44.9
165	0.0831	18.5	0.0516	21.0	0.0045	9.8	0.47	29.0	2.8	51.1	10.5	1271.9	360.4	29.0	2.8	43.3
110	0.1117	21.4	0.0705	24.2	0.0046	11.2	0.46	29.5	3.3	69.2	16.2	1826.9	388.5	29.5	3.3	57.4
75	0.0500	42.2	0.0316	46.7	0.0046	20.0	0.43	29.5	5.9	31.6	14.5	196.4	981.2	29.5	5.9	6.7
294	0.0806	19.4	0.0510	21.5	0.0046	9.4	0.43	29.5	2.8	50.5	10.6	1211.5	381.9	29.5	2.8	41.6
255	0.0954	18.1	0.0606	20.9	0.0046	10.7	0.50	29.6	3.2	59.7	12.1	1536.9	340.4	29.6	3.2	50.4
345	0.1122	17.6	0.0714	20.1	0.0046	9.6	0.49	29.7	2.9	70.1	13.6	1834.9	318.5	29.7	2.9	57.6
134	0.1317	15.3	0.0841	16.7	0.0046	6.7	0.40	29.8	2.0	81.9	13.1	2121.3	268.0	29.8	2.0	63.7
62	0.0992	10.5	0.0633	12.1	0.0046	5.6	0.49	29.8	1.7	62.3	7.3	1609.2	196.5	29.8	1.7	52.2
302	0.1523	21.5	0.0974	29.5	0.0046	20.2	0.69	29.9	6.0	94.4	26.6	2371.4	366.0	29.9	6.0	68.4
241	0.0760	14.1	0.0489	18.2	0.0047	11.8	0.63	30.0	3.5	48.5	8.6	1093.9	282.7	30.0	3.5	38.1
336	0.1269	17.0	0.0821	18.5	0.0047	7.2	0.40	30.2	2.2	80.1	14.3	2055.5	300.3	30.2	2.2	62.3
264	0.1463	17.4	0.0955	21.8	0.0047	13.1	0.60	30.4	4.0	92.6	19.3	2303.5	299.5	30.4	4.0	67.1
232	0.1248	33.6	0.0820	36.1	0.0048	13.2	0.37	30.6	4.0	80.0	27.7	2025.9	594.6	30.6	4.0	61.7
10	0.1255	25.9	0.0825	28.6	0.0048	12.3	0.42	30.6	3.7	80.5	22.2	2036.4	458.7	30.6	3.7	61.9
34	0.0754	9.2	0.0500	10.8	0.0048	5.9	0.53	30.9	1.8	49.5	5.2	1078.7	184.9	30.9	1.8	37.6
144	0.0943	27.7	0.0629	32.0	0.0048	15.9	0.50	31.1	4.9	61.9	19.2	1515.0	523.0	31.1	4.9	49.8

Table A4.10 (continued): Detrital Zircon U-Pb Integrated Data for the Paruro Formation Base

Spot	Ratios						Ages (Ma)						Best Age	Disc. (%)		
	207Pb/206Pb		207Pb/235U		206Pb/238U		206Pb/238U		207Pb/235U		207Pb/206Pb					
	±2σ	±2σ	±2σ	±2σ	±2σ	±2σ	±2σ	±2σ	±2σ	±2σ	±2σ					
	<i>Paruro Formation Base 2 (20140528-01) Rejected Data</i>															
68	0.0925	20.1	0.0619	24.9	0.0049	14.4	0.59	31.2	4.5	61.0	14.7	1477.9	381.6	31.2	4.5	48.8
101	0.1287	9.0	0.0894	11.9	0.0050	8.1	0.65	32.4	2.6	87.0	9.9	2080.8	158.7	32.4	2.6	62.8
331	0.1042	14.4	0.0729	17.5	0.0051	9.8	0.56	32.6	3.2	71.4	12.1	1700.5	266.2	32.6	3.2	54.3
152	0.1230	22.0	0.0865	24.5	0.0051	10.6	0.43	32.8	3.5	84.2	19.8	1999.7	391.2	32.8	3.5	61.1
230	0.0694	18.1	0.0492	25.6	0.0051	18.1	0.71	33.1	6.0	48.8	12.2	910.7	373.1	33.1	6.0	32.2
253	0.2390	12.8	0.1720	14.6	0.0052	7.2	0.48	33.6	2.4	161.1	21.8	3113.3	204.2	33.6	2.4	79.2
240	0.1787	14.3	0.1290	20.1	0.0052	14.3	0.70	33.7	4.8	123.2	23.3	2641.2	238.0	33.7	4.8	72.7
125	0.0805	14.0	0.0590	17.2	0.0053	9.9	0.58	34.2	3.4	58.2	9.8	1209.0	276.2	34.2	3.4	41.3
390	0.0998	20.8	0.0733	22.1	0.0053	7.4	0.34	34.3	2.5	71.8	15.3	1619.5	386.9	34.3	2.5	52.3
251	0.0995	16.5	0.0738	18.4	0.0054	8.2	0.44	34.6	2.8	72.3	12.8	1614.4	308.1	34.6	2.8	52.2
267	0.0586	23.1	0.0446	27.7	0.0055	15.4	0.55	35.5	5.5	44.3	12.0	550.8	503.2	35.5	5.5	19.9
338	0.1321	21.2	0.1015	23.2	0.0056	9.4	0.41	35.8	3.3	98.2	21.7	2126.6	370.5	35.8	3.3	63.5
128	0.1405	20.4	0.1083	22.7	0.0056	9.8	0.44	36.0	3.5	104.4	22.5	2233.0	352.4	36.0	3.5	65.6
323	0.1935	19.0	0.1509	22.3	0.0057	12.0	0.53	36.4	4.3	142.7	29.7	2771.8	310.8	36.4	4.3	74.5
270	0.2474	11.3	0.1933	14.8	0.0057	10.1	0.65	36.4	3.7	179.4	24.4	3168.4	178.7	36.4	3.7	79.7
218	0.2885	17.8	0.2254	20.5	0.0057	10.0	0.50	36.4	3.6	206.4	38.4	3409.6	277.5	36.4	3.6	82.4
91	0.1003	20.8	0.0829	22.3	0.0060	8.6	0.36	38.5	3.3	80.9	17.3	1630.4	386.6	38.5	3.3	52.4
213	0.0537	24.9	0.0463	29.8	0.0063	16.3	0.55	40.2	6.5	45.9	13.4	358.3	562.5	40.2	6.5	12.5
5	0.0737	15.1	0.0653	17.5	0.0064	8.8	0.50	41.3	3.6	64.2	10.9	1033.2	305.6	41.3	3.6	35.7
394	0.3581	10.3	0.3229	12.7	0.0065	7.4	0.59	42.0	3.1	284.1	31.4	3741.7	156.2	42.0	3.1	85.2
117	0.0642	21.9	0.0613	28.0	0.0069	17.5	0.63	44.5	7.8	60.4	16.4	749.0	461.7	44.5	7.8	26.4
199	0.1114	16.8	0.1102	20.9	0.0072	12.3	0.59	46.1	5.6	106.1	21.0	1821.8	305.3	46.1	5.6	56.6
256	0.2938	14.6	0.2945	19.7	0.0073	13.4	0.67	46.7	6.2	262.1	45.6	3438.0	227.5	46.7	6.2	82.2
72	0.4687	14.8	0.4771	17.8	0.0074	10.0	0.55	47.4	4.7	396.1	58.4	4145.6	220.1	47.4	4.7	88.0
395	0.4518	16.9	0.5251	21.1	0.0084	12.6	0.60	54.1	6.8	428.5	73.9	4091.1	251.6	54.1	6.8	87.4
45	0.3912	18.1	0.4814	21.0	0.0089	10.9	0.51	57.3	6.2	399.0	69.3	3875.6	272.5	57.3	6.2	85.6
149	0.4856	11.1	0.6482	13.7	0.0097	8.1	0.59	62.1	5.0	507.4	54.9	4198.1	163.4	62.1	5.0	87.8
60	0.4462	12.3	0.5986	16.7	0.0097	11.1	0.68	62.4	6.9	476.3	63.5	4072.6	182.5	62.4	6.9	86.9
156	0.5109	12.1	0.7178	14.6	0.0102	8.1	0.57	65.3	5.3	549.4	62.2	4273.1	177.5	65.3	5.3	88.1
181	0.0765	15.5	0.1077	17.0	0.0102	6.9	0.41	65.5	4.5	103.9	16.8	1109.5	309.2	65.5	4.5	37.0
24	0.1105	16.1	0.1656	19.1	0.0109	10.5	0.54	69.7	7.3	155.6	27.6	1807.0	293.5	69.7	7.3	55.2
324	0.0785	17.6	0.1230	18.5	0.0114	5.9	0.32	72.8	4.3	117.8	20.6	1159.6	348.1	72.8	4.3	38.2
120	0.0750	13.0	0.1181	14.6	0.0114	6.5	0.45	73.2	4.7	113.4	15.6	1069.7	261.1	73.2	4.7	35.5
52	0.0655	8.5	0.1034	10.0	0.0114	5.6	0.53	73.4	4.0	99.9	9.6	791.4	179.4	73.4	4.0	26.6
296	0.1119	19.7	0.1779	20.9	0.0115	7.3	0.34	73.9	5.4	166.2	32.0	1831.1	356.6	73.9	5.4	55.6
330	0.4783	29.9	0.7695	34.0	0.0117	16.2	0.48	74.8	12.0	579.5	151.1	4175.7	441.7	74.8	12.0	87.1
365	0.0945	20.3	0.1525	22.2	0.0117	8.8	0.40	75.1	6.6	144.1	29.9	1517.4	383.4	75.1	6.6	47.9
43	0.0672	43.6	0.1123	55.3	0.0121	34.1	0.62	77.7	26.3	108.0	56.8	843.7	907.2	77.7	26.3	28.1
168	0.0596	28.2	0.1241	35.7	0.0151	21.8	0.61	96.7	20.9	118.8	40.0	588.7	610.8	96.7	20.9	18.6
397	0.0821	18.4	0.2302	22.2	0.0203	12.5	0.56	129.8	16.0	210.4	42.3	1247.6	360.8	129.8	16.0	38.3
102	0.1217	9.7	0.3764	11.0	0.0224	5.7	0.47	143.0	8.1	324.4	30.5	1981.7	173.6	143.0	8.1	55.9
31	0.0932	21.1	0.3059	26.9	0.0238	16.7	0.62	151.7	25.0	271.0	64.1	1491.7	400.3	151.7	25.0	44.0
309	0.0979	17.4	0.3826	18.6	0.0283	6.4	0.35	180.1	11.4	328.9	52.3	1584.7	326.1	180.1	11.4	45.2
211	0.0521	28.8	0.2214	42.0	0.0308	30.4	0.73	195.8	58.7	203.0	77.4	287.7	658.5	195.8	58.7	3.6
389	0.1032	17.7	0.4564	24.7	0.0321	17.2	0.70	203.6	34.5	381.8	78.8	1681.6	327.7	203.6	34.5	46.7
314	0.0815	8.8	0.4513	12.2	0.0402	8.5	0.69	254.0	21.1	378.2	38.4	1232.5	172.1	254.0	21.1	32.8
25	0.0788	8.5	0.4649	10.6	0.0428	6.7	0.61	270.1	17.7	387.7	34.3	1167.1	167.7	270.1	17.7	30.3
234	0.7548	42.3	4.5079	51.5	0.0433	29.3	0.57	273.4	78.4	1732.4	456.3	4838.7	608.1	273.4	78.4	84.2
94	0.1392	65.6	0.8585	83.7	0.0447	52.2	0.62	282.0	144.0	629.3	414.4	2217.7	1136.4	282.0	144.0	55.2
329	0.0675	17.2	0.7067	25.3	0.0759	18.5	0.73	471.7	84.3	542.8	106.8	853.6	356.8	471.7	84.3	13.1
318	0.1041	12.4	1.0964	16.2	0.0764	10.7	0.64	474.7	48.8	751.6	86.4	1697.8	229.1	474.7	48.8	36.8
203	0.0911	9.2	0.9952	12.2	0.0792	7.9	0.66	491.4	37.3	701.4	62.0	1449.1	175.1	491.4	37.3	29.9
372	0.0774	12.4	0.8959	19.9	0.0840	15.5	0.78	519.8	77.5	649.5	95.8	1130.9	247.6	519.8	77.5	20.0
197	0.0668	5.3	0.9182	7.1	0.0997	4.7	0.67	612.4	27.3	661.4	34.5	832.1	109.7	612.4	27.3	26.4
290	0.0743	5.2	1.0215	7.2	0.0998	5.5	0.70	613.1	32.1	714.7	37.2	1048.4	105.3	613.1	32.1	41.5
379	0.0665	6.1	0.9212	8.1	0.1005	5.4	0.66	617.4	31.5	663.0	39.4	821.3	126.4	617.4	31.5	24.8
27	0.0861	6.3	1.2094	7.7	0.1018	4.8	0.58	625.2	28.8	804.9	42.8	1340.9	121.4	625.2	28.8	53.4
292	0.0714	25.5	1.0117	36.9	0.1027	26.7	0.72	630.4	160.3	709.7	190.5	969.5	521.3	630.4	160.3	35.0
15	0.0604	20.8	0.8565	29.6	0.1028	21.2	0.71	630.8	127.6	628.2	139.7	618.9	449.8	630.8	127.6	-1.9
266	0.0703	8.9	1.0122	12.1	0.1044	8.4	0.68	640.2	51.0	710.0	61.9	937.5	182.2	640.2	51.0	31.7
299	0.0691	9.9	1.0100	13.5	0.1061	9.3	0.68	649.9	57.8	708.9	69.0	900.7	205.1	649.9	57.8	27.9
9	0.3346	29.0	4.9785	36.5	0.1079	22.3	0.61	660.5	140.0	1815.7	319.0	3638.5	443.4	660.5	140.0	81.8
150	0.1019	16.8	1.5375	20.8	0.1094	12.3	0.59	669.4	78.2	945.5	128.9	1659.0	311.4	669.4	78.2	59.6

Table A4.10 (continued): Detrital Zircon U-Pb Integrated Data for the Paruro Formation Base

Spot	Ratios							Ages (Ma)						Best Age	Disc. (%)	
	207Pb/206Pb		207Pb/235U		206Pb/238U		Rho	206Pb/238U		207Pb/235U		207Pb/206Pb				±2σ
	±2σ	±2σ	±2σ	±2σ	±2σ	±2σ		±2σ	±2σ	±2σ						
<i>Paruro Formation Base 2 (20140528-01) Rejected Data</i>																
74	0.0969	5.6	1.4911	8.3	0.1116	6.5	0.74	682.1	42.3	926.7	50.6	1565.2	104.4	682.1	42.3	56.4
272	0.1146	10.2	1.7880	12.7	0.1132	8.1	0.59	691.1	53.0	1041.1	82.6	1873.4	184.6	691.1	53.0	63.1
368	0.3163	15.5	4.9541	16.8	0.1136	6.4	0.39	693.6	41.8	1811.5	142.9	3551.9	238.0	693.6	41.8	80.5
32	0.0707	4.1	1.1343	5.9	0.1164	4.4	0.72	709.7	29.8	769.8	31.9	948.2	84.4	709.7	29.8	25.2
158	0.0626	29.7	1.0155	43.8	0.1177	32.1	0.73	717.2	218.0	711.6	227.6	694.2	632.6	717.2	218.0	-3.3
169	0.0766	6.8	1.2834	9.0	0.1216	5.6	0.66	739.5	38.9	838.4	51.3	1110.1	135.5	739.5	38.9	33.4
22	0.0945	18.2	1.7379	28.7	0.1333	22.3	0.77	806.8	168.9	1022.7	186.9	1518.8	342.7	806.8	168.9	46.9
361	0.0807	10.4	1.5130	12.3	0.1359	6.4	0.53	821.5	49.0	935.6	75.2	1215.1	204.7	821.5	49.0	32.4
183	0.0763	4.9	1.5085	7.9	0.1435	6.0	0.79	864.3	48.6	933.8	48.3	1101.7	97.3	864.3	48.6	21.5
118	0.0761	6.3	1.5100	8.9	0.1439	6.1	0.70	866.5	49.6	934.4	54.2	1098.2	126.9	866.5	49.6	21.1
20	0.0799	5.1	1.5845	7.7	0.1439	6.1	0.75	866.5	49.6	964.1	48.2	1193.9	100.4	866.5	49.6	27.4
310	0.0766	7.4	1.5414	10.5	0.1460	7.5	0.71	878.5	62.0	947.1	64.8	1110.2	147.3	878.5	62.0	20.9
344	0.0772	6.3	1.5941	8.9	0.1497	6.2	0.71	899.2	52.2	967.9	55.8	1127.2	126.2	899.2	52.2	20.2
35	0.0788	12.8	1.6342	22.1	0.1505	18.1	0.81	903.7	152.4	983.5	140.0	1166.0	254.3	903.7	152.4	22.5
44	0.0750	19.8	1.5649	28.5	0.1513	20.7	0.72	908.4	175.4	956.4	178.6	1068.6	398.1	908.4	175.4	15.0
198	0.0788	6.5	1.6517	9.0	0.1519	6.1	0.69	911.8	51.7	990.2	56.8	1168.2	129.1	911.8	51.7	21.9
231	0.1432	7.2	3.0598	9.3	0.1549	6.0	0.64	928.6	52.1	1422.7	71.5	2266.7	123.7	928.6	52.1	59.0
366	0.0956	13.2	2.0718	16.0	0.1572	8.9	0.56	941.4	77.7	1139.5	110.0	1539.2	248.5	941.4	77.7	38.8
47	0.0705	12.5	1.8187	18.5	0.1871	13.9	0.74	1105.4	141.1	1052.2	121.8	943.3	255.5	943.3	255.5	-17.2
289	0.0849	2.8	1.8890	5.5	0.1613	5.2	0.87	964.2	46.8	1077.2	36.4	1313.6	53.8	964.2	46.8	26.6
13	0.0837	4.7	1.8703	6.6	0.1621	5.0	0.71	968.4	45.3	1070.6	43.9	1285.3	90.9	968.4	45.3	24.7
121	0.1095	7.8	2.4610	11.1	0.1631	7.8	0.71	973.7	70.1	1260.7	80.4	1790.6	142.5	973.7	70.1	45.6
166	0.0889	8.7	2.0015	12.1	0.1633	8.1	0.69	975.3	73.5	1116.0	82.1	1401.4	167.7	975.3	73.5	30.4
326	0.0849	6.5	1.9185	9.1	0.1639	6.4	0.69	978.3	57.7	1087.6	60.6	1313.3	126.7	978.3	57.7	25.5
173	0.0866	5.0	1.9731	7.7	0.1653	5.5	0.76	986.2	50.5	1106.4	52.0	1350.9	97.0	986.2	50.5	27.0
1	0.0835	2.9	1.9132	4.1	0.1661	2.9	0.71	990.7	26.9	1085.7	27.6	1281.5	56.7	990.7	26.9	22.7
171	0.0750	17.5	2.1139	24.9	0.2044	17.6	0.71	1198.8	192.5	1153.3	173.1	1068.8	351.2	1068.8	351.2	-12.2
355	0.0753	15.6	1.8969	22.2	0.1828	15.7	0.71	1082.3	156.7	1080.0	148.6	1075.4	313.1	1075.4	313.1	-0.6
115	0.0777	20.6	1.9270	29.3	0.1798	20.7	0.71	1066.0	203.8	1090.5	198.0	1139.8	410.0	1139.8	410.0	6.5
58	0.0817	18.1	2.5618	27.8	0.2274	21.0	0.76	1321.0	251.2	1289.8	205.8	1238.4	355.7	1238.4	355.7	-6.7
283	0.0832	19.3	2.7216	29.5	0.2373	22.3	0.76	1372.9	276.4	1334.4	222.3	1273.1	376.3	1273.1	376.3	-7.8
387	0.0837	21.4	2.7877	30.6	0.2415	21.9	0.72	1394.7	274.5	1352.2	232.5	1285.8	416.1	1285.8	416.1	-8.5
284	0.0915	15.9	2.4261	24.4	0.1924	18.7	0.76	1134.3	194.3	1250.4	177.5	1456.2	303.1	1456.2	303.1	22.1
184	0.0953	5.8	2.7118	11.7	0.2065	10.0	0.87	1210.1	110.5	1331.7	87.1	1533.1	110.0	1533.1	110.0	21.1
180	0.1040	3.6	3.2032	6.5	0.2234	5.2	0.83	1299.6	61.2	1457.9	50.7	1696.9	66.8	1696.9	66.8	23.4
51	0.1045	19.8	2.6540	21.6	0.1841	8.6	0.39	1089.4	86.4	1315.8	160.3	1706.4	365.1	1706.4	365.1	36.2
274	0.1046	12.9	2.6573	16.4	0.1843	10.6	0.62	1090.4	106.3	1316.7	121.3	1706.9	236.9	1706.9	236.9	36.1
30	0.1072	25.0	3.7679	35.9	0.2550	25.8	0.72	1464.3	338.2	1585.9	296.1	1751.7	457.4	1751.7	457.4	16.4
393	0.1249	6.7	4.0857	11.8	0.2372	9.7	0.82	1372.0	120.1	1651.4	96.6	2027.8	118.8	2027.8	118.8	32.3
21	0.1392	12.0	3.3677	13.0	0.1754	5.2	0.38	1041.9	50.4	1496.9	102.1	2217.7	208.7	2217.7	208.7	53.0
381	0.1470	14.0	3.9210	21.0	0.1934	15.7	0.75	1139.9	163.8	1618.0	171.8	2311.5	240.8	2311.5	240.8	50.7
229	0.1520	14.5	6.0319	17.3	0.2877	9.5	0.54	1630.1	136.6	1980.5	151.9	2369.1	248.2	2369.1	248.2	31.2
237	0.1597	11.8	4.6837	13.7	0.2127	7.1	0.50	1243.1	80.6	1764.3	114.9	2452.7	199.7	2452.7	199.7	49.3
17	0.1786	23.3	4.4001	24.7	0.1787	8.4	0.32	1060.0	81.9	1712.4	207.0	2639.6	387.7	2639.6	387.7	59.8
228	0.1873	3.2	9.5266	5.6	0.3690	4.7	0.82	2024.5	82.5	2390.1	51.4	2718.3	53.4	2718.3	53.4	25.5
113	0.1988	13.5	5.8231	19.4	0.2124	13.9	0.72	1241.7	157.5	1949.8	170.0	2816.5	220.5	2816.5	220.5	55.9
<i>Paruro Formation Base 3 (Reworked tuff) (20140605-02) Accepted Data</i>																
14	0.0920	17.7	0.0185	19.3	0.0015	7.8	0.40	9.4	0.7	18.6	3.6	1467.8	336.5	9.4	0.7	49.6
22	0.2552	16.6	0.0671	19.0	0.0019	9.2	0.48	12.3	1.1	66.0	12.1	3217.5	262.5	12.3	1.1	81.4
11	0.3841	8.8	0.1280	10.1	0.0024	5.0	0.49	15.5	0.8	122.3	11.7	3848.0	133.2	15.5	0.8	87.3
27	0.5050	23.3	0.2350	27.6	0.0034	14.7	0.53	21.7	3.2	214.3	53.3	4255.9	343.8	21.7	3.2	89.9
13	0.5814	29.4	0.2715	29.9	0.0034	5.4	0.18	21.8	1.2	243.9	64.8	4462.2	427.6	21.8	1.2	91.1
20	0.4640	15.2	0.2287	19.1	0.0036	11.5	0.60	23.0	2.6	209.1	36.0	4130.7	225.1	23.0	2.6	89.0
29	0.5495	19.3	0.2884	24.6	0.0038	15.2	0.62	24.5	3.7	257.3	56.0	4379.9	282.9	24.5	3.7	90.5
1	0.6797	22.9	0.5832	27.3	0.0062	14.8	0.54	39.9	5.9	466.5	102.3	4688.4	330.2	39.9	5.9	91.4
25	0.8011	18.3	1.6745	22.3	0.0152	12.8	0.57	97.0	12.3	998.9	142.6	4923.7	262.0	97.0	12.3	90.3
10	0.8889	24.1	3.4127	26.4	0.0278	10.8	0.41	176.9	18.8	1507.3	210.2	5071.3	343.9	176.9	18.8	88.3
7	0.8112	13.7	5.7719	17.1	0.0516	10.2	0.59	324.1	32.2	1942.2	148.9	4941.6	196.6	324.1	32.2	83.3
19	0.8796	11.4	12.8891	19.1	0.1062	15.4	0.80	650.9	95.5	2671.6	182.4	5056.4	162.1	650.9	95.5	87.1
4	0.8202	12.8	13.3792	17.5	0.1182	12.0	0.68	720.1	81.6	2706.8	166.6	4957.3	182.4	720.1	81.6	85.5
24	0.8391	11.3	14.8838	16.5	0.1286	12.1	0.73	780.0	89.1	2807.8	158.5	4989.6	160.9	780.0	89.1	84.4
5	0.8398	7.4	15.5605	14.9	0.1343	13.0	0.87	812.1	98.8	2850.2	143.2	4990.8	105.9	812.1	98.8	83.7
28	0.8449	15.9	25.9063	23.1	0.2224	16.7	0.72	1294.4	196.3	3343.0	229.6	4999.3	227.7	4999.3	227.7	74.1

Table A4.10 (continued): Detrital Zircon U-Pb Integrated Data for the Paruro Formation Base

Spot	Ratios						Rho	Ages (Ma)						Best Age	Disc. (%)	
	207Pb/206Pb		207Pb/235U		206Pb/238U			206Pb/238U		207Pb/235U		207Pb/206Pb				
	±2σ	±2σ	±2σ	±2σ	±2σ	±2σ		±2σ	±2σ	±2σ	±2σ	±2σ				
<i>Paruro Formation Base 3 (Reworked tuff) (20140605-02) Accepted Data</i>																
26	0.8494	22.9	59.5650	28.3	0.5085	16.7	0.59	2650.4	362.3	4166.8	290.5	5006.9	327.4	5006.9	327.4	47.1
8	0.8538	10.6	98.5637	14.6	0.8366	10.0	0.69	3919.0	295.3	4671.6	147.7	5014.2	151.2	5014.2	151.2	21.8
21	0.8954	17.2	43.8092	21.3	0.3548	12.6	0.59	1957.3	212.3	3860.9	214.2	5081.6	244.6	5081.6	244.6	61.5
<i>Paruro Formation Base 3 (Reworked tuff) (20140605-02) Rejected Data</i>																
6	0.4271	838.6	-44.1663	1000.8	-0.7495	546.2	0.55	0.0	0.0	0.0	0.0	4007.2	12530	0.0	0.0	-534.9
15	0.8747	137.5	0.2223	138.1	0.0018	12.0	0.09	11.9	1.4	203.8	260.5	5048.5	1962.8	11.9	1.4	94.2
16	0.4325	55.7	0.1174	56.6	0.0020	10.0	0.18	12.7	1.3	112.7	60.5	4026.2	831.8	12.7	1.3	88.8
2	0.8096	58.1	0.3158	58.9	0.0028	9.4	0.16	18.2	1.7	278.6	144.5	4938.6	832.3	18.2	1.7	93.5
30	0.4885	31.9	0.1917	34.6	0.0028	13.6	0.39	18.3	2.5	178.1	56.6	4207.0	470.6	18.3	2.5	89.7
23	0.5716	32.1	0.2727	35.3	0.0035	14.8	0.42	22.3	3.3	244.9	77.0	4437.3	467.5	22.3	3.3	90.9
9	0.2411	17.1	0.1169	18.9	0.0035	8.0	0.42	22.6	1.8	112.3	20.1	3127.3	271.9	22.6	1.8	79.9
12	0.3872	17.3	0.2916	18.9	0.0055	7.7	0.41	35.1	2.7	259.8	43.3	3860.0	260.5	35.1	2.7	86.5
17	0.3622	57.3	0.3456	81.2	0.0069	57.6	0.71	44.4	25.5	301.4	214.9	3759.1	869.3	44.4	25.5	85.3
18	0.7335	41.5	0.7806	48.2	0.0077	24.5	0.51	49.5	12.1	585.8	217.9	4797.9	597.0	49.5	12.1	91.5
3	0.8441	24.1	5198.6540	30.4	44.6244	18.6	0.61	24628.2	1187.4	8688.0	319.2	4998.1	344.3	4998.1	344.3	-392.8

Table A4.11: Detrital Zircon U-Pb Integrated Data for the Paruro Formation Top

Spot	Ratios						Ages (Ma)						Best Age	Disc. (%)		
	207Pb/ 206Pb		207Pb/ 235U		206Pb/ 238U		206Pb/ 238U		207Pb/ 235U		207Pb/ 206Pb					
	$\pm 2\sigma$	$\pm 2\sigma$	$\pm 2\sigma$	$\pm 2\sigma$	Rho	$\pm 2\sigma$	$\pm 2\sigma$	$\pm 2\sigma$	$\pm 2\sigma$	$\pm 2\sigma$	$\pm 2\sigma$					
<i>Paruro Formation Top (20140608-03) Accepted Data</i>																
69	0.0670	42.5	0.0106	43.7	0.0012	10.5	0.23	7.4	0.8	10.8	4.7	838.3	885.9	7.4	0.8	31.0
2	0.0598	25.8	0.0099	28.2	0.0012	11.7	0.41	7.7	0.9	10.0	2.8	597.3	558.1	7.7	0.9	22.7
188	0.0728	23.2	0.0126	25.3	0.0013	10.0	0.39	8.1	0.8	12.7	3.2	1009.3	471.1	8.1	0.8	36.4
12	0.0536	53.2	0.0098	54.4	0.0013	11.3	0.21	8.5	1.0	9.9	5.4	354.1	1201.7	8.5	1.0	13.7
192	0.0912	44.1	0.0167	45.7	0.0013	12.1	0.27	8.6	1.0	16.9	7.6	1450.1	839.0	8.6	1.0	49.1
73	0.0756	35.6	0.0141	38.0	0.0014	13.4	0.35	8.7	1.2	14.2	5.4	1084.3	714.3	8.7	1.2	38.7
186	0.0904	49.9	0.0170	51.4	0.0014	12.1	0.24	8.8	1.1	17.1	8.7	1434.4	951.9	8.8	1.1	48.7
31	0.0682	25.2	0.0131	27.6	0.0014	11.3	0.41	9.0	1.0	13.2	3.6	873.7	521.7	9.0	1.0	32.1
368	0.0551	19.7	0.0106	20.5	0.0014	5.7	0.27	9.0	0.5	10.7	2.2	417.0	440.1	9.0	0.5	16.1
61	0.0555	24.7	0.0108	25.7	0.0014	7.3	0.28	9.1	0.7	11.0	2.8	434.4	550.2	9.1	0.7	16.7
369	0.0621	20.4	0.0121	22.0	0.0014	8.5	0.38	9.1	0.8	12.3	2.7	679.0	435.6	9.1	0.8	25.5
252	0.0582	23.3	0.0114	24.3	0.0014	6.5	0.27	9.1	0.6	11.5	2.8	536.5	510.7	9.1	0.6	20.5
80	0.0316	75.5	0.0062	76.0	0.0014	8.4	0.11	9.2	0.8	6.3	4.8	-1000.0	2227.1	9.2	0.8	-46.0
48	0.0870	33.6	0.0173	36.7	0.0014	14.9	0.40	9.3	1.4	17.4	6.4	1359.5	647.8	9.3	1.4	46.6
199	0.0924	42.8	0.0184	44.4	0.0014	11.7	0.26	9.3	1.1	18.5	8.2	1476.0	811.8	9.3	1.1	49.8
330	0.0729	40.7	0.0146	42.1	0.0015	10.7	0.26	9.4	1.0	14.8	6.2	1010.7	824.6	9.4	1.0	36.4
353	0.0997	39.9	0.0200	41.9	0.0015	12.8	0.31	9.4	1.2	20.2	8.4	1619.3	742.2	9.4	1.2	53.4
15	0.0376	48.6	0.0076	49.4	0.0015	8.8	0.18	9.4	0.8	7.6	3.8	-514.3	1296.6	9.4	0.8	-22.9
98	0.1157	42.4	0.0237	44.9	0.0015	14.6	0.33	9.6	1.4	23.8	10.6	1890.3	762.7	9.6	1.4	59.8
77	0.0708	56.7	0.0147	58.6	0.0015	14.5	0.25	9.7	1.4	14.8	8.6	953.1	1160.7	9.7	1.4	34.6
125	0.0553	48.0	0.0115	48.8	0.0015	9.3	0.19	9.7	0.9	11.6	5.6	423.8	1070.2	9.7	0.9	16.3
388	0.0811	37.9	0.0169	40.6	0.0015	14.4	0.36	9.7	1.4	17.0	6.8	1224.3	744.3	9.7	1.4	42.8
108	0.0804	44.8	0.0169	47.1	0.0015	14.2	0.30	9.8	1.4	17.0	7.9	1206.0	882.7	9.8	1.4	42.3
253	0.0518	56.0	0.0111	57.8	0.0015	14.1	0.25	10.0	1.4	11.2	6.4	278.1	1282.0	10.0	1.4	10.7
217	0.0733	23.7	0.0159	25.1	0.0016	8.1	0.33	10.1	0.8	16.0	4.0	1021.9	478.9	10.1	0.8	36.7
6	0.0483	15.3	0.0109	16.9	0.0016	7.6	0.43	10.5	0.8	11.0	1.8	111.9	360.1	10.5	0.8	4.1
289	0.0542	20.4	0.0124	23.4	0.0017	11.9	0.49	10.7	1.3	12.5	2.9	379.8	457.9	10.7	1.3	14.6
372	0.0833	60.7	0.0202	62.4	0.0018	14.4	0.23	11.3	1.6	20.3	12.5	1275.5	1183.0	11.3	1.6	44.2
241	0.0683	19.5	0.0166	20.2	0.0018	5.1	0.26	11.3	0.6	16.7	3.4	877.4	404.4	11.3	0.6	32.1
57	0.0463	78.8	0.0113	80.1	0.0018	14.6	0.18	11.4	1.7	11.4	9.1	13.5	1894.6	11.4	1.7	0.1
62	0.0468	14.9	0.0115	16.0	0.0018	6.2	0.37	11.5	0.7	11.6	1.8	39.5	356.3	11.5	0.7	1.2
85	0.0539	31.6	0.0133	34.2	0.0018	13.1	0.39	11.5	1.5	13.4	4.5	367.0	711.6	11.5	1.5	14.1
373	0.0949	46.0	0.0234	47.4	0.0018	11.6	0.24	11.5	1.3	23.5	11.0	1525.5	866.1	11.5	1.3	50.9
140	0.0525	19.7	0.0132	20.9	0.0018	6.3	0.33	11.8	0.7	13.3	2.8	305.9	448.9	11.8	0.7	11.7
348	0.0750	31.0	0.0193	32.5	0.0019	9.9	0.31	12.0	1.2	19.4	6.2	1067.2	622.4	12.0	1.2	38.0
83	0.0267	77.0	0.0069	77.5	0.0019	8.4	0.11	12.0	1.0	7.0	5.4	-1532.9	2543.5	12.0	1.0	-72.9
357	0.0601	17.8	0.0166	19.4	0.0020	7.5	0.39	12.9	1.0	16.7	3.2	605.5	385.4	12.9	1.0	22.8
82	0.0612	32.9	0.0172	34.0	0.0020	8.4	0.25	13.2	1.1	17.4	5.9	646.4	707.5	13.2	1.1	24.2
119	0.0671	21.3	0.0198	23.9	0.0021	10.4	0.45	13.8	1.4	19.9	4.7	842.0	444.3	13.8	1.4	30.8
206	0.0694	19.1	0.0212	20.7	0.0022	8.0	0.39	14.3	1.1	21.3	4.4	909.5	393.7	14.3	1.1	33.0
228	0.0903	42.6	0.0284	44.3	0.0023	12.1	0.27	14.7	1.8	28.4	12.4	1431.9	813.8	14.7	1.8	48.3
116	0.0611	18.3	0.0193	21.2	0.0023	10.4	0.51	14.8	1.5	19.4	4.1	641.9	392.8	14.8	1.5	24.0
14	0.0644	21.8	0.0211	23.3	0.0024	8.2	0.36	15.3	1.3	21.2	4.9	754.4	459.2	15.3	1.3	27.8
337	0.0583	20.2	0.0195	21.5	0.0024	7.0	0.33	15.6	1.1	19.6	4.2	542.9	442.6	15.6	1.1	20.4
79	0.0455	19.4	0.0153	24.2	0.0024	14.4	0.60	15.7	2.3	15.4	3.7	-27.1	470.9	15.7	2.3	-1.8
90	0.0510	15.4	0.0174	17.3	0.0025	7.7	0.46	15.9	1.2	17.5	3.0	242.3	354.6	15.9	1.2	9.1
336	0.0641	18.0	0.0223	20.5	0.0025	9.8	0.48	16.3	1.6	22.4	4.6	743.9	379.8	16.3	1.6	27.4
224	0.0600	16.4	0.0213	17.9	0.0026	7.3	0.41	16.5	1.2	21.4	3.8	603.0	354.4	16.5	1.2	22.5
114	0.0641	12.5	0.0227	15.2	0.0026	8.1	0.57	16.6	1.3	22.8	3.4	743.3	264.1	16.6	1.3	27.4
162	0.0454	12.8	0.0162	16.1	0.0026	10.2	0.61	16.6	1.7	16.3	2.6	-34.9	311.1	16.6	1.7	-2.1
96	0.0401	18.0	0.0144	19.5	0.0026	7.0	0.38	16.8	1.2	14.6	2.8	-342.0	464.2	16.8	1.2	-15.4
387	0.0641	27.8	0.0236	29.4	0.0027	9.5	0.32	17.2	1.6	23.7	6.9	745.3	588.4	17.2	1.6	27.4
87	0.0258	46.9	0.0095	47.7	0.0027	8.3	0.18	17.3	1.4	9.6	4.6	-1654.7	1590.8	17.3	1.4	-79.4
375	0.0728	20.3	0.0271	21.7	0.0027	7.7	0.35	17.4	1.3	27.1	5.8	1007.0	412.8	17.4	1.3	35.9
131	0.0591	16.1	0.0220	17.2	0.0027	5.8	0.35	17.4	1.0	22.1	3.7	570.5	349.8	17.4	1.0	21.3
183	0.0700	20.9	0.0263	21.4	0.0027	5.5	0.23	17.5	1.0	26.3	5.6	928.3	428.3	17.5	1.0	33.5
234	0.0585	16.7	0.0220	18.0	0.0027	6.8	0.38	17.6	1.2	22.1	3.9	547.1	363.8	17.6	1.2	20.5
142	0.0590	22.3	0.0226	23.4	0.0028	6.4	0.30	17.9	1.1	22.7	5.2	565.3	486.3	17.9	1.1	21.1
45	0.0464	17.3	0.0178	19.2	0.0028	8.5	0.44	17.9	1.5	17.9	3.4	19.9	414.7	17.9	1.5	0.1
113	0.0692	16.9	0.0268	19.5	0.0028	9.3	0.50	18.1	1.7	26.8	5.2	904.7	348.2	18.1	1.7	32.7
261	0.0598	14.8	0.0232	18.1	0.0028	10.5	0.58	18.1	1.9	23.3	4.2	596.5	320.4	18.1	1.9	22.2
248	0.0530	15.8	0.0207	20.2	0.0028	12.6	0.63	18.2	2.3	20.8	4.2	327.9	357.6	18.2	2.3	12.3
295	0.0670	16.7	0.0264	18.5	0.0029	7.6	0.42	18.4	1.4	26.4	4.8	837.2	348.9	18.4	1.4	30.5

Table A4.11 (continued): Detrital Zircon U-Pb Integrated Data for the Paruro Formation Top

Spot	Ratios						Rho	Ages (Ma)						Best Age	Disc. (%)	
	207Pb/206Pb		207Pb/235U		206Pb/238U			207Pb/235U		207Pb/206Pb		±2σ	±2σ			
	±2σ	±2σ	±2σ	±2σ	±2σ	±2σ		±2σ	±2σ	±2σ						
	<i>Paruro Formation Top (20140608-03) Accepted Data</i>															
29	0.0355	22.7	0.0140	23.2	0.0029	4.8	0.20	18.4	0.9	14.1	3.2	-668.9	626.2	18.4	0.9	-30.4
55	0.0362	28.2	0.0143	28.8	0.0029	6.0	0.21	18.4	1.1	14.4	4.1	-616.4	767.0	18.4	1.1	-28.0
107	0.0539	16.5	0.0216	18.1	0.0029	7.1	0.41	18.7	1.3	21.7	3.9	366.0	372.9	18.7	1.3	13.7
370	0.0554	27.9	0.0222	29.4	0.0029	9.4	0.32	18.7	1.8	22.3	6.5	427.6	622.3	18.7	1.8	16.1
30	0.0403	34.9	0.0162	35.6	0.0029	7.2	0.20	18.8	1.3	16.3	5.8	-331.4	896.7	18.8	1.3	-15.0
60	0.0315	34.1	0.0127	35.4	0.0029	9.5	0.26	18.8	1.8	12.8	4.5	-1007.6	1009.0	18.8	1.8	-46.7
400	0.0591	19.0	0.0240	19.9	0.0030	5.9	0.29	19.0	1.1	24.1	4.7	569.2	414.4	19.0	1.1	21.2
159	0.0612	23.5	0.0251	25.7	0.0030	10.8	0.41	19.1	2.1	25.1	6.4	646.8	505.0	19.1	2.1	24.0
166	0.0709	23.5	0.0291	24.6	0.0030	8.6	0.31	19.2	1.6	29.2	7.1	955.4	479.9	19.2	1.6	34.2
222	0.0657	16.2	0.0272	17.8	0.0030	7.1	0.41	19.3	1.4	27.2	4.8	796.5	340.5	19.3	1.4	29.1
257	0.0456	15.2	0.0189	16.3	0.0030	6.0	0.38	19.3	1.1	19.0	3.1	-21.8	366.8	19.3	1.1	-1.7
219	0.0600	14.3	0.0254	15.6	0.0031	5.8	0.39	19.7	1.1	25.4	3.9	603.0	310.2	19.7	1.1	22.4
272	0.0479	7.1	0.0203	8.8	0.0031	5.7	0.58	19.8	1.1	20.4	1.8	94.7	169.3	19.8	1.1	3.1
315	0.0695	19.2	0.0296	20.4	0.0031	6.6	0.34	19.9	1.3	29.7	6.0	914.6	395.6	19.9	1.3	32.9
106	0.0482	11.9	0.0207	15.7	0.0031	10.0	0.65	20.0	2.0	20.8	3.2	111.4	281.7	20.0	2.0	3.7
394	0.0554	13.6	0.0238	16.2	0.0031	8.8	0.54	20.0	1.8	23.9	3.8	428.3	303.2	20.0	1.8	16.0
24	0.0532	17.4	0.0230	20.5	0.0031	10.9	0.53	20.2	2.2	23.1	4.7	336.9	394.3	20.2	2.2	12.6
165	0.0492	15.5	0.0215	20.2	0.0032	13.6	0.64	20.4	2.8	21.6	4.3	157.4	362.7	20.4	2.8	5.6
298	0.0582	11.0	0.0254	12.3	0.0032	5.1	0.44	20.4	1.0	25.5	3.1	536.7	241.2	20.4	1.0	20.0
236	0.0547	19.2	0.0239	20.8	0.0032	8.0	0.38	20.4	1.6	24.0	4.9	398.7	430.8	20.4	1.6	14.9
359	0.0547	9.7	0.0242	11.9	0.0032	6.8	0.58	20.7	1.4	24.3	2.9	398.3	218.4	20.7	1.4	14.9
145	0.0589	13.1	0.0262	16.1	0.0032	8.9	0.58	20.8	1.8	26.2	4.2	563.0	284.9	20.8	1.8	20.9
309	0.0556	14.4	0.0252	16.0	0.0033	6.6	0.43	21.1	1.4	25.3	4.0	436.5	321.4	21.1	1.4	16.3
150	0.0687	21.3	0.0312	24.4	0.0033	11.7	0.48	21.2	2.5	31.2	7.5	889.5	440.9	21.2	2.5	32.0
136	0.0500	12.2	0.0229	13.4	0.0033	5.0	0.41	21.4	1.1	23.0	3.0	195.6	283.8	21.4	1.1	7.0
313	0.0476	13.4	0.0222	17.6	0.0034	11.4	0.65	21.8	2.5	22.3	3.9	77.1	317.9	21.8	2.5	2.3
40	0.0605	13.7	0.0293	16.1	0.0035	8.4	0.52	22.6	1.9	29.3	4.7	621.5	295.9	22.6	1.9	22.9
382	0.0598	14.9	0.0294	15.8	0.0036	5.4	0.34	22.9	1.2	29.4	4.6	597.2	322.0	22.9	1.2	22.0
130	0.0673	17.6	0.0333	19.8	0.0036	8.8	0.45	23.1	2.0	33.2	6.5	845.9	367.0	23.1	2.0	30.5
367	0.0510	12.3	0.0263	13.2	0.0037	5.2	0.38	24.0	1.2	26.3	3.4	241.2	282.4	24.0	1.2	8.7
115	0.0535	12.5	0.0276	16.7	0.0037	10.6	0.66	24.1	2.6	27.7	4.5	351.4	282.0	24.1	2.6	13.0
268	0.0582	19.9	0.0303	20.7	0.0038	5.8	0.28	24.2	1.4	30.3	6.2	538.2	434.9	24.2	1.4	19.9
5	0.0495	13.8	0.0259	16.1	0.0038	8.6	0.52	24.4	2.1	26.0	4.1	171.7	322.4	24.4	2.1	6.0
157	0.0557	17.4	0.0295	18.1	0.0038	5.6	0.28	24.7	1.4	29.6	5.3	441.2	386.1	24.7	1.4	16.3
250	0.0625	13.3	0.0333	14.7	0.0039	6.0	0.42	24.9	1.5	33.3	4.8	690.0	283.6	24.9	1.5	25.2
187	0.0508	17.9	0.0273	19.9	0.0039	8.8	0.44	25.0	2.2	27.3	5.4	231.7	412.8	25.0	2.2	8.3
84	0.0466	10.2	0.0253	13.0	0.0039	7.7	0.61	25.3	2.0	25.4	3.2	26.4	245.7	25.3	2.0	0.0
216	0.0605	19.2	0.0329	22.5	0.0039	11.5	0.52	25.4	2.9	32.9	7.3	622.7	414.9	25.4	2.9	22.8
304	0.0734	20.4	0.0409	23.0	0.0040	10.5	0.46	26.0	2.7	40.7	9.2	1024.0	413.0	26.0	2.7	36.1
1	0.0638	26.4	0.0360	28.3	0.0041	10.4	0.36	26.3	2.7	35.9	10.0	734.7	558.6	26.3	2.7	26.7
264	0.0583	30.7	0.0329	31.4	0.0041	6.8	0.22	26.3	1.8	32.9	10.2	540.6	670.9	26.3	1.8	19.9
342	0.0442	13.4	0.0250	14.4	0.0041	5.0	0.36	26.4	1.3	25.1	3.6	-98.7	330.3	26.4	1.3	-5.2
128	0.0571	12.9	0.0324	13.9	0.0041	5.3	0.37	26.5	1.4	32.4	4.4	494.2	284.4	26.5	1.4	18.2
58	0.0585	23.7	0.0335	24.6	0.0042	6.8	0.27	26.8	1.8	33.5	8.1	547.0	517.1	26.8	1.8	20.1
237	0.0660	16.4	0.0380	17.5	0.0042	6.0	0.34	26.9	1.6	37.8	6.5	805.8	344.1	26.9	1.6	29.0
156	0.0517	16.8	0.0301	17.8	0.0042	6.5	0.34	27.2	1.8	30.1	5.3	270.2	384.2	27.2	1.8	9.7
174	0.0571	14.8	0.0334	16.6	0.0042	8.1	0.45	27.3	2.2	33.3	5.4	493.9	326.5	27.3	2.2	18.1
88	0.0243	35.8	0.0142	36.4	0.0043	6.4	0.18	27.4	1.8	14.4	5.2	-1865.1	1269.5	27.4	1.8	-90.7
202	0.0536	26.3	0.0316	27.1	0.0043	6.4	0.24	27.5	1.8	31.6	8.4	353.2	594.5	27.5	1.8	12.9
308	0.0481	21.0	0.0284	22.4	0.0043	7.5	0.34	27.6	2.1	28.5	6.3	102.7	496.6	27.6	2.1	3.1
360	0.0741	23.0	0.0440	26.0	0.0043	12.1	0.46	27.7	3.3	43.7	11.1	1045.3	464.7	27.7	3.3	36.7
97	0.0452	15.5	0.0269	16.7	0.0043	5.5	0.37	27.8	1.5	26.9	4.4	-45.7	377.2	27.8	1.5	-3.0
226	0.0863	28.9	0.0517	30.9	0.0043	10.9	0.35	27.9	3.0	51.2	15.4	1345.8	557.4	27.9	3.0	45.4
74	0.0445	25.9	0.0268	26.8	0.0044	6.5	0.26	28.0	1.8	26.8	7.1	-81.0	633.1	28.0	1.8	-4.5
133	0.0506	31.3	0.0305	32.2	0.0044	7.5	0.24	28.1	2.1	30.5	9.7	220.9	723.5	28.1	2.1	7.8
38	0.0690	24.1	0.0416	25.2	0.0044	7.2	0.29	28.1	2.0	41.4	10.2	897.6	498.2	28.1	2.0	32.0
396	0.0543	18.2	0.0328	19.9	0.0044	8.1	0.41	28.2	2.3	32.7	6.4	381.6	408.6	28.2	2.3	13.9
263	0.0564	17.2	0.0343	19.2	0.0044	8.6	0.45	28.4	2.4	34.2	6.5	466.8	380.1	28.4	2.4	17.1
39	0.0520	15.4	0.0317	16.7	0.0044	6.4	0.39	28.4	1.8	31.7	5.2	285.5	351.9	28.4	1.8	10.3
28	0.0525	15.1	0.0320	16.4	0.0044	6.6	0.39	28.4	1.9	32.0	5.2	307.9	343.0	28.4	1.9	11.1
53	0.0344	37.2	0.0210	39.2	0.0044	12.6	0.32	28.5	3.6	21.1	8.2	-756.6	1043.4	28.5	3.6	-34.9
279	0.0669	24.6	0.0409	26.2	0.0044	9.7	0.35	28.5	2.8	40.7	10.4	835.8	511.6	28.5	2.8	30.0
327	0.0734	28.5	0.0449	29.7	0.0044	8.3	0.28	28.5	2.4	44.6	12.9	1024.1	576.1	28.5	2.4	36.0

Table A4.11 (continued): Detrital Zircon U-Pb Integrated Data for the Paruro Formation Top

Spot	Ratios							Ages (Ma)							Best Age	Disc. (%)	
	207Pb/206Pb		207Pb/235U		206Pb/238U		Rho	206Pb/238U		207Pb/235U		207Pb/206Pb		±2σ			±2σ
	±2σ	±2σ	±2σ	±2σ	±2σ	±2σ	±2σ	±2σ	±2σ	±2σ	±2σ	±2σ					
<i>Paruro Formation Top (20140608-03) Accepted Data</i>																	
208	0.0628	25.8	0.0384	29.4	0.0044	14.0	0.48	28.6	4.0	38.3	11.0	699.9	549.4	28.6	4.0	25.4	
235	0.0511	17.7	0.0315	18.6	0.0045	6.0	0.32	28.8	1.7	31.5	5.8	243.9	406.6	28.8	1.7	8.6	
37	0.0540	16.1	0.0334	18.9	0.0045	9.9	0.52	28.9	2.8	33.4	6.2	371.0	362.3	28.9	2.8	13.5	
293	0.0529	17.7	0.0327	19.1	0.0045	7.6	0.39	28.9	2.2	32.7	6.2	323.2	400.9	28.9	2.2	11.7	
365	0.0556	16.9	0.0344	17.6	0.0045	5.2	0.29	28.9	1.5	34.4	5.9	435.6	375.4	28.9	1.5	15.9	
339	0.0778	23.6	0.0486	25.8	0.0045	10.2	0.40	29.1	3.0	48.2	12.1	1141.8	470.1	29.1	3.0	39.5	
173	0.0770	24.6	0.0484	26.8	0.0046	11.3	0.39	29.3	3.3	48.0	12.5	1120.0	491.5	29.3	3.3	38.9	
54	0.0446	17.3	0.0280	18.5	0.0046	6.6	0.35	29.4	1.9	28.1	5.1	-79.6	424.4	29.4	1.9	-4.5	
335	0.0519	41.0	0.0327	41.7	0.0046	7.0	0.17	29.4	2.0	32.6	13.4	280.2	939.1	29.4	2.0	10.0	
358	0.0647	29.1	0.0407	30.7	0.0046	10.0	0.33	29.4	2.9	40.5	12.2	763.7	612.3	29.4	2.9	27.5	
354	0.0568	16.0	0.0358	20.7	0.0046	13.0	0.63	29.4	3.8	35.7	7.3	483.4	353.6	29.4	3.8	17.7	
66	0.0480	12.4	0.0304	13.5	0.0046	5.6	0.39	29.5	1.6	30.4	4.0	98.5	294.0	29.5	1.6	2.8	
239	0.0696	20.9	0.0449	22.8	0.0047	9.3	0.41	30.1	2.8	44.6	10.0	917.1	429.4	30.1	2.8	32.5	
267	0.0555	20.2	0.0358	23.1	0.0047	11.2	0.48	30.1	3.3	35.7	8.1	431.4	450.0	30.1	3.3	15.7	
184	0.0576	23.6	0.0377	27.7	0.0047	14.6	0.52	30.5	4.4	37.6	10.2	515.7	518.9	30.5	4.4	18.8	
221	0.0734	28.2	0.0480	31.3	0.0047	13.3	0.43	30.5	4.0	47.6	14.5	1025.9	571.3	30.5	4.0	36.0	
227	0.0941	39.0	0.0630	40.2	0.0049	10.0	0.25	31.3	3.1	62.1	24.2	1509.2	736.0	31.3	3.1	49.6	
56	0.0679	23.1	0.0470	25.4	0.0050	10.6	0.41	32.3	3.4	46.6	11.6	864.3	478.4	32.3	3.4	30.7	
4	0.0465	16.8	0.0345	18.0	0.0054	6.6	0.35	34.6	2.3	34.5	6.1	24.2	403.8	34.6	2.3	-0.4	
229	0.0567	11.0	0.0428	13.0	0.0055	6.8	0.53	35.1	2.4	42.5	5.4	481.3	243.0	35.1	2.4	17.3	
68	0.0474	21.6	0.0358	23.0	0.0055	8.1	0.34	35.2	2.9	35.7	8.1	70.0	514.6	35.2	2.9	1.4	
332	0.0525	12.4	0.0400	13.2	0.0055	4.3	0.35	35.5	1.5	39.8	5.2	307.8	282.8	35.5	1.5	10.8	
343	0.0423	22.4	0.0323	23.6	0.0055	7.4	0.32	35.7	2.6	32.3	7.5	-211.1	562.2	35.7	2.6	-10.4	
118	0.0583	18.9	0.0446	22.9	0.0055	12.6	0.57	35.7	4.5	44.3	9.9	541.8	412.7	35.7	4.5	19.5	
72	0.0510	14.0	0.0391	14.7	0.0056	4.5	0.30	35.7	1.6	39.0	5.6	242.8	322.8	35.7	1.6	8.3	
104	0.0641	20.7	0.0495	22.6	0.0056	8.8	0.40	36.0	3.2	49.1	10.8	743.8	437.9	36.0	3.2	26.6	
101	0.0575	21.9	0.0445	23.6	0.0056	8.5	0.37	36.1	3.1	44.2	10.2	511.2	482.0	36.1	3.1	18.4	
281	0.0507	16.4	0.0396	17.2	0.0057	6.0	0.31	36.4	2.2	39.4	6.7	227.4	378.0	36.4	2.2	7.7	
366	0.0586	10.7	0.0461	11.8	0.0057	5.1	0.42	36.7	1.9	45.8	5.3	550.8	234.7	36.7	1.9	19.8	
385	0.0798	24.4	0.0639	26.1	0.0058	9.3	0.36	37.3	3.5	62.9	15.9	1193.2	480.7	37.3	3.5	40.7	
310	0.0548	12.1	0.0439	13.3	0.0058	5.5	0.42	37.4	2.0	43.6	5.7	403.0	270.4	37.4	2.0	14.4	
59	0.0617	17.8	0.0496	19.6	0.0058	8.3	0.41	37.5	3.1	49.2	9.4	662.0	381.4	37.5	3.1	23.7	
51	0.0464	16.4	0.0374	17.2	0.0058	5.7	0.31	37.5	2.1	37.3	6.3	20.2	393.7	37.5	2.1	-0.7	
100	0.0474	15.8	0.0383	18.4	0.0059	9.1	0.52	37.7	3.4	38.2	6.9	68.7	375.4	37.7	3.4	1.3	
35	0.0439	18.1	0.0357	19.0	0.0059	5.8	0.31	37.9	2.2	35.6	6.7	-115.7	446.3	37.9	2.2	-6.4	
43	0.0511	15.0	0.0418	17.9	0.0059	9.6	0.54	38.1	3.7	41.6	7.3	244.5	346.2	38.1	3.7	8.3	
278	0.0509	15.1	0.0419	20.7	0.0060	14.5	0.68	38.4	5.6	41.7	8.5	235.8	349.4	38.4	5.6	7.9	
33	0.0408	17.5	0.0342	22.0	0.0061	13.3	0.61	39.1	5.2	34.2	7.4	-298.1	446.1	39.1	5.2	-14.3	
274	0.0589	19.2	0.0496	21.2	0.0061	9.3	0.42	39.2	3.6	49.1	10.2	565.1	418.3	39.2	3.6	20.2	
160	0.0491	12.7	0.0415	13.3	0.0061	4.9	0.31	39.4	1.9	41.3	5.4	151.9	297.1	39.4	1.9	4.6	
312	0.0535	13.1	0.0454	15.1	0.0062	7.4	0.50	39.5	2.9	45.1	6.6	349.5	295.8	39.5	2.9	12.2	
13	0.0532	15.4	0.0453	17.5	0.0062	8.3	0.48	39.6	3.3	44.9	7.7	337.4	348.2	39.6	3.3	11.8	
259	0.0484	11.1	0.0412	12.4	0.0062	5.4	0.45	39.7	2.1	41.0	5.0	119.4	261.5	39.7	2.1	3.2	
395	0.0552	10.0	0.0472	11.9	0.0062	6.5	0.54	39.8	2.6	46.8	5.4	421.9	223.0	39.8	2.6	15.0	
169	0.0550	16.7	0.0476	19.5	0.0063	10.8	0.51	40.3	4.4	47.2	9.0	412.8	374.0	40.3	4.4	14.6	
384	0.0533	14.6	0.0468	17.7	0.0064	10.0	0.56	41.0	4.1	46.5	8.1	339.5	331.4	41.0	4.1	11.8	
91	0.0478	8.4	0.0425	10.6	0.0065	6.1	0.61	41.5	2.5	42.3	4.4	90.8	199.3	41.5	2.5	2.0	
377	0.0552	24.3	0.0494	25.4	0.0065	7.6	0.30	41.7	3.1	48.9	12.1	422.1	541.7	41.7	3.1	14.9	
247	0.0461	6.2	0.0412	8.9	0.0065	6.3	0.72	41.7	2.6	41.0	3.6	2.3	148.9	41.7	2.6	-1.6	
20	0.0453	18.4	0.0407	19.4	0.0065	6.2	0.32	41.8	2.6	40.5	7.7	-37.2	446.2	41.8	2.6	-3.3	
204	0.0605	13.5	0.0553	16.7	0.0066	9.7	0.59	42.6	4.1	54.7	8.9	620.0	291.6	42.6	4.1	22.0	
102	0.0533	7.2	0.0705	10.0	0.0096	6.7	0.70	61.6	4.1	69.2	6.7	340.2	162.0	61.6	4.1	11.0	
273	0.0530	13.5	0.0798	17.4	0.0109	11.4	0.64	70.0	7.9	78.0	13.1	329.2	305.3	70.0	7.9	10.2	
376	0.0470	11.1	0.0755	14.2	0.0117	8.9	0.62	74.7	6.6	73.9	10.1	47.9	266.0	74.7	6.6	-1.1	
378	0.0538	8.0	0.0900	10.1	0.0121	6.2	0.61	77.8	4.8	87.5	8.5	361.6	180.8	77.8	4.8	11.1	
314	0.0508	8.2	0.0863	11.3	0.0123	7.5	0.69	78.9	5.9	84.0	9.1	232.1	189.5	78.9	5.9	6.1	
70	0.0517	9.0	0.0884	10.1	0.0124	5.2	0.46	79.5	4.1	86.1	8.4	272.2	207.2	79.5	4.1	7.6	
34	0.0797	29.4	0.1410	30.4	0.0128	7.8	0.26	82.2	6.4	134.0	38.2	1190.7	579.9	82.2	6.4	38.7	
349	0.0488	14.8	0.0882	16.0	0.0131	6.0	0.38	84.0	5.0	85.8	13.2	136.0	347.8	84.0	5.0	2.1	
52	0.0457	8.0	0.0886	9.4	0.0141	5.3	0.53	90.0	4.7	86.2	7.8	-16.6	192.9	90.0	4.7	-4.4	
340	0.0533	7.7	0.1044	8.8	0.0142	4.2	0.49	91.0	3.8	100.9	8.5	341.8	173.5	91.0	3.8	9.8	
246	0.0528	5.0	0.1158	6.3	0.0159	3.7	0.62	101.7	3.7	111.2	6.7	320.0	113.2	101.7	3.7	8.6	
265	0.0527	11.1	0.1181	16.4	0.0163	12.1	0.74	104.0	12.5	113.3	17.6	314.9	251.7	104.0	12.5	8.3	

Table A4.11 (continued): Detrital Zircon U-Pb Integrated Data for the Paruro Formation Top

Spot	Ratios						Ages (Ma)					Best Age	Disc. (%)			
	207Pb/206Pb		207Pb/235U		206Pb/238U		206Pb/238U		207Pb/235U		±2σ					
	±2σ	±2σ	±2σ	±2σ	Rho	±2σ	±2σ	±2σ	±2σ							
<i>Paruro Formation Top (20140608-03) Accepted Data</i>																
155	0.0505	12.2	0.1160	13.4	0.0166	6.1	0.41	106.4	6.4	111.4	14.1	219.8	282.5	106.4	6.4	4.5
170	0.0546	12.6	0.1288	14.8	0.0171	8.9	0.53	109.3	9.6	123.1	17.1	396.9	281.7	109.3	9.6	11.1
177	0.0640	10.2	0.1600	14.7	0.0181	11.0	0.72	115.9	12.7	150.7	20.5	740.9	214.8	115.9	12.7	23.1
8	0.0729	16.6	0.1898	20.2	0.0189	11.8	0.57	120.6	14.1	176.5	32.8	1010.6	335.8	120.6	14.1	31.6
158	0.0519	11.6	0.1495	16.6	0.0209	12.1	0.72	133.2	16.0	141.4	21.9	282.1	265.6	133.2	16.0	5.8
322	0.0501	4.9	0.1443	7.0	0.0209	4.6	0.71	133.3	6.1	136.9	8.9	200.1	114.2	133.3	6.1	2.6
297	0.0527	8.3	0.1565	10.0	0.0215	5.2	0.56	137.4	7.1	147.7	13.8	315.9	189.3	137.4	7.1	7.0
164	0.0484	8.7	0.1473	11.4	0.0221	8.4	0.65	140.6	11.7	139.5	14.8	120.7	204.9	140.6	11.7	-0.8
210	0.0518	7.6	0.1601	9.6	0.0224	5.7	0.61	142.8	8.1	150.8	13.4	277.9	173.2	142.8	8.1	5.3
299	0.0524	6.1	0.1807	8.2	0.0250	5.2	0.68	159.2	8.1	168.6	12.7	303.9	137.9	159.2	8.1	5.6
42	0.0495	9.5	0.1881	10.4	0.0276	4.0	0.39	175.3	7.0	175.0	16.6	171.1	222.1	175.3	7.0	-0.2
144	0.0539	7.7	0.2118	10.0	0.0285	5.6	0.64	181.2	10.0	195.1	17.7	367.1	173.9	181.2	10.0	7.1
215	0.0574	5.8	0.2970	7.9	0.0375	5.0	0.68	237.4	11.7	264.0	18.3	508.0	126.5	237.4	11.7	10.1
191	0.0553	7.5	0.2893	9.6	0.0379	6.0	0.62	239.9	14.1	258.0	21.8	425.5	166.5	239.9	14.1	7.0
266	0.0531	3.6	0.3001	5.1	0.0410	3.6	0.70	258.8	9.2	266.4	11.9	334.5	82.4	258.8	9.2	2.9
141	0.0510	7.4	0.2893	10.9	0.0411	7.5	0.73	259.8	19.1	258.0	24.8	241.1	170.5	259.8	19.1	-0.7
262	0.0524	3.4	0.3378	4.5	0.0468	3.0	0.66	294.7	8.7	295.5	11.6	301.7	77.1	294.7	8.7	0.3
120	0.0590	5.3	0.4686	8.6	0.0576	6.4	0.79	361.3	22.6	390.2	27.9	565.6	115.1	361.3	22.6	7.4
161	0.0538	6.5	0.5242	8.8	0.0707	6.5	0.68	440.3	27.6	427.9	30.6	362.0	146.3	440.3	27.6	-2.9
325	0.0598	5.7	0.6440	6.8	0.0781	3.7	0.55	484.9	17.3	504.8	27.2	596.0	123.6	484.9	17.3	3.9
364	0.0565	4.0	0.6268	5.3	0.0805	3.5	0.65	499.2	16.6	494.1	20.6	470.4	88.7	499.2	16.6	-1.0
75	0.0550	5.5	0.6294	7.4	0.0830	4.4	0.67	513.8	21.6	495.7	29.0	413.2	123.8	513.8	21.6	-3.6
371	0.0572	4.1	0.6548	5.2	0.0830	3.4	0.63	514.0	16.8	511.4	20.9	500.1	89.2	514.0	16.8	-0.5
211	0.0605	11.8	0.6933	17.3	0.0832	12.5	0.73	514.9	61.9	534.8	71.9	620.3	255.3	514.9	61.9	3.7
383	0.0592	3.1	0.7027	4.6	0.0861	3.4	0.73	532.5	17.4	540.4	19.2	574.0	68.2	532.5	17.4	1.5
242	0.0588	5.7	0.6981	8.1	0.0861	5.6	0.71	532.6	28.8	537.7	33.9	559.0	125.0	532.6	28.8	0.9
397	0.0590	4.5	0.7037	5.8	0.0865	3.7	0.63	534.5	19.2	541.0	24.4	568.3	97.8	534.5	19.2	1.2
198	0.0617	4.2	0.7538	6.4	0.0885	4.8	0.75	546.9	25.1	570.4	27.8	665.4	90.3	546.9	25.1	4.1
361	0.0576	5.1	0.7163	7.3	0.0903	5.4	0.72	557.1	28.6	548.5	31.1	512.9	111.3	557.1	28.6	-1.6
363	0.0567	3.5	0.7124	4.7	0.0911	3.3	0.68	561.9	17.7	546.2	20.0	481.2	76.3	561.9	17.7	-2.9
329	0.0602	3.9	0.7612	5.4	0.0918	3.7	0.70	565.9	19.9	574.7	23.7	609.6	83.9	565.9	19.9	1.5
287	0.0593	5.7	0.7509	8.3	0.0919	6.6	0.73	566.7	36.0	568.7	36.3	576.9	124.9	566.7	36.0	0.4
356	0.0578	5.4	0.7495	8.0	0.0941	5.8	0.73	579.6	32.2	567.9	34.8	521.6	119.1	579.6	32.2	-2.0
317	0.0630	6.0	0.8248	9.0	0.0950	6.3	0.74	585.1	35.1	610.7	41.1	706.9	127.7	585.1	35.1	4.2
380	0.0580	6.8	0.7737	9.9	0.0967	7.2	0.72	595.2	40.9	581.9	43.8	530.2	149.6	595.2	40.9	-2.3
47	0.0767	4.5	1.0241	8.0	0.0968	6.7	0.83	595.8	38.0	716.0	41.3	1113.4	89.4	595.8	38.0	16.8
300	0.0611	8.3	0.8177	10.8	0.0971	6.9	0.64	597.4	39.1	606.7	49.5	641.7	178.5	597.4	39.1	1.5
306	0.0615	3.6	0.8278	6.1	0.0976	4.7	0.81	600.5	26.7	612.4	28.3	656.4	77.3	600.5	26.7	8.5
256	0.0600	3.1	0.8145	4.8	0.0985	3.3	0.77	605.4	19.2	605.0	21.7	603.4	66.7	605.4	19.2	-0.3
379	0.0603	3.8	0.8648	5.2	0.1040	3.7	0.69	637.9	22.3	632.7	24.7	614.2	82.2	637.9	22.3	-3.9
389	0.0612	4.6	0.8806	6.6	0.1043	4.8	0.72	639.7	29.3	641.3	31.5	646.9	98.4	639.7	29.3	1.1
344	0.0607	5.1	0.8858	7.0	0.1059	4.8	0.70	648.6	29.4	644.1	33.6	628.4	108.9	648.6	29.4	-3.2
352	0.0603	3.4	0.8850	4.8	0.1064	3.3	0.71	652.0	20.6	643.7	23.0	614.6	73.1	652.0	20.6	-6.1
285	0.0629	5.6	0.9548	7.7	0.1100	6.0	0.69	672.9	38.3	680.6	38.2	706.0	119.0	672.9	38.3	4.7
230	0.0644	4.3	0.9961	5.9	0.1122	4.0	0.70	685.6	26.3	701.8	30.1	754.1	90.0	685.6	26.3	9.1
25	0.0633	5.0	0.9967	5.9	0.1141	3.6	0.53	696.6	23.5	702.1	30.1	720.0	106.9	696.6	23.5	3.2
41	0.0641	8.8	1.0183	10.4	0.1151	5.5	0.54	702.5	36.6	713.1	53.3	746.5	185.6	702.5	36.6	5.9
238	0.0681	3.2	1.1413	3.9	0.1216	2.3	0.59	739.5	16.2	773.1	21.2	871.6	65.5	739.5	16.2	15.2
319	0.0659	4.2	1.1148	6.7	0.1226	4.6	0.77	745.5	32.7	760.5	35.6	804.8	88.7	745.5	32.7	7.4
355	0.0652	4.7	1.1401	5.9	0.1268	3.6	0.62	769.5	26.0	772.6	32.1	781.3	97.9	769.5	26.0	1.5
203	0.0748	4.6	1.4729	6.0	0.1428	3.7	0.63	860.3	29.5	919.3	36.0	1063.7	92.8	860.3	29.5	19.1
17	0.0685	4.3	1.3540	6.1	0.1434	4.3	0.71	864.1	34.5	869.3	35.9	882.7	89.6	864.1	34.5	2.1
138	0.0670	7.9	1.3573	10.7	0.1469	6.9	0.68	883.4	57.1	870.7	62.9	838.5	163.9	883.4	57.1	-5.4
398	0.0689	2.8	1.4159	3.8	0.1490	2.7	0.68	895.3	22.4	895.6	22.8	896.4	58.1	895.3	22.4	0.1
64	0.0685	4.3	1.4241	5.7	0.1507	4.2	0.65	905.1	35.7	899.1	33.9	884.4	89.8	905.1	35.7	-2.3
95	0.0702	6.6	1.6574	8.4	0.1712	4.6	0.64	1018.5	43.0	992.4	53.4	935.1	134.4	935.1	134.4	-8.9
10	0.0705	3.2	1.6544	4.4	0.1702	3.5	0.70	1013.1	33.2	991.3	27.9	943.1	65.4	943.1	65.4	-7.4
290	0.0740	5.2	1.6244	7.2	0.1591	5.3	0.70	951.9	46.8	979.7	45.3	1042.5	104.1	951.9	46.8	8.7
126	0.0756	3.8	1.6765	4.7	0.1608	3.2	0.61	961.2	28.4	999.7	30.1	1085.0	75.4	961.2	28.4	11.4
46	0.0742	8.3	1.6588	11.8	0.1621	8.5	0.71	968.4	76.0	992.9	75.1	1047.4	167.1	968.4	76.0	7.5
249	0.0775	4.1	1.7346	5.6	0.1624	3.6	0.68	970.0	32.2	1021.4	36.1	1133.5	81.7	970.0	32.2	14.4
334	0.0730	4.5	1.6403	6.2	0.1630	4.0	0.69	973.6	35.8	985.8	39.1	1013.1	91.4	973.6	35.8	3.9
302	0.0718	8.9	1.6144	12.3	0.1631	8.4	0.69	974.0	76.4	975.8	77.3	979.8	181.0	974.0	76.4	0.6

Table A4.11 (continued): Detrital Zircon U-Pb Integrated Data for the Paruro Formation Top

Spot	Ratios							Ages (Ma)						Disc. (%)		
	207Pb/206Pb		207Pb/235U		206Pb/238U		Rho	207Pb/235U		207Pb/206Pb		Best Age				
	±2σ	±2σ	±2σ	±2σ	±2σ	±2σ		±2σ	±2σ							
<i>Paruro Formation Top (20140608-03) Accepted Data</i>																
381	0.0719	6.2	1.6293	8.7	0.1643	6.1	0.70	980.6	55.8	981.6	54.8	983.7	126.2	980.6	55.8	0.3
111	0.0708	4.7	1.6112	8.5	0.1651	6.7	0.84	985.1	61.3	974.6	53.4	950.9	95.9	985.1	61.3	-3.6
362	0.0723	4.0	1.6745	5.3	0.1680	3.5	0.65	1000.9	32.2	998.9	33.5	994.5	81.5	994.5	81.5	-0.6
135	0.0728	4.4	1.6898	5.8	0.1685	3.0	0.68	1003.6	27.6	1004.7	37.0	1007.1	88.3	1007.1	88.3	0.3
393	0.0740	4.1	1.7810	5.9	0.1746	4.3	0.72	1037.3	41.0	1038.6	38.3	1041.2	82.0	1041.2	82.0	0.4
180	0.0741	7.8	1.7709	11.5	0.1732	8.8	0.74	1029.8	84.0	1034.8	74.9	1045.5	157.2	1045.5	157.2	1.5
338	0.0745	4.3	1.8115	5.4	0.1763	2.9	0.61	1046.8	28.3	1049.6	35.6	1055.5	87.3	1055.5	87.3	0.8
232	0.0753	6.5	1.7889	9.9	0.1723	7.4	0.75	1024.8	69.9	1041.4	64.4	1076.5	130.5	1076.5	130.5	4.8
94	0.0762	6.2	1.8046	7.8	0.1718	3.9	0.61	1022.3	36.9	1047.1	51.2	1099.4	124.9	1099.4	124.9	7.0
390	0.0762	10.6	1.8804	15.3	0.1791	11.1	0.72	1061.8	108.4	1074.2	101.7	1099.4	211.2	1099.4	211.2	3.4
316	0.0763	6.4	1.9964	9.1	0.1898	6.0	0.71	1120.3	61.7	1114.3	61.4	1102.6	128.6	1102.6	128.6	-1.6
143	0.0767	13.2	1.9668	19.3	0.1859	13.9	0.73	1099.0	140.2	1104.2	130.7	1114.5	262.7	1114.5	262.7	1.4
350	0.0768	11.2	2.0330	16.3	0.1921	11.8	0.73	1132.7	122.6	1126.6	111.2	1114.8	223.0	1114.8	223.0	-1.6
44	0.0773	10.0	1.9748	13.4	0.1854	8.9	0.67	1096.2	89.7	1106.9	90.3	1128.1	198.6	1128.1	198.6	2.8
323	0.0774	10.4	1.9384	15.5	0.1817	11.4	0.74	1076.3	112.6	1094.4	104.0	1130.7	206.6	1130.7	206.6	4.8
132	0.0775	7.0	1.8154	9.1	0.1699	5.7	0.65	1011.6	53.1	1051.0	59.7	1133.8	138.5	1133.8	138.5	10.8
175	0.0776	6.0	2.1333	9.0	0.1993	7.5	0.75	1171.3	80.2	1159.6	62.5	1137.9	119.4	1137.9	119.4	-2.9
280	0.0778	2.5	1.9596	4.3	0.1826	4.4	0.84	1081.3	44.0	1101.7	29.1	1142.4	48.7	1142.4	48.7	5.3
23	0.0779	4.7	1.9561	6.3	0.1822	4.5	0.67	1079.1	45.2	1100.6	42.4	1143.3	92.7	1143.3	92.7	5.6
171	0.0779	11.8	2.0166	16.7	0.1877	12.5	0.71	1108.7	127.8	1121.1	113.7	1145.2	234.5	1145.2	234.5	3.2
294	0.0786	10.5	2.0589	15.2	0.1899	10.9	0.73	1121.0	112.0	1135.3	104.4	1162.7	207.2	1162.7	207.2	3.6
3	0.0788	3.6	2.1242	5.4	0.1956	4.6	0.75	1151.8	48.1	1156.7	37.3	1165.9	71.8	1165.9	71.8	1.2
233	0.0788	8.3	2.3283	12.2	0.2142	9.0	0.74	1251.3	101.9	1221.0	87.0	1167.7	163.6	1167.7	163.6	-7.2
305	0.0801	3.8	2.0041	6.8	0.1814	5.3	0.83	1074.9	52.8	1116.9	46.1	1199.6	75.6	1199.6	75.6	10.4
320	0.0807	6.6	2.1944	10.2	0.1972	7.6	0.76	1160.2	80.4	1179.3	70.9	1214.4	129.1	1214.4	129.1	4.5
9	0.0808	3.4	2.5129	5.0	0.2254	4.1	0.74	1310.6	48.9	1275.8	36.3	1217.6	66.0	1217.6	66.0	-7.6
318	0.0815	9.6	2.3410	14.3	0.2083	10.4	0.74	1219.6	116.0	1224.8	102.3	1234.0	187.9	1234.0	187.9	1.2
172	0.0816	11.6	2.0141	14.4	0.1791	9.5	0.60	1062.1	93.4	1120.3	98.0	1235.0	227.7	1235.0	227.7	14.0
11	0.0832	6.7	2.5502	10.2	0.2223	7.7	0.75	1294.1	90.0	1286.5	74.2	1273.8	130.3	1273.8	130.3	-1.6
197	0.0861	4.1	2.3996	6.1	0.2021	4.5	0.74	1186.7	49.0	1242.5	43.6	1340.6	79.0	1340.6	79.0	11.5
89	0.0876	8.8	2.7396	12.9	0.2267	9.2	0.73	1317.2	109.7	1339.3	96.3	1374.6	169.7	1374.6	169.7	4.2
153	0.0890	7.2	3.2290	10.8	0.2630	8.0	0.74	1505.3	106.9	1464.1	83.9	1404.9	138.7	1404.9	138.7	-7.1
50	0.0896	7.4	2.6060	11.0	0.2110	8.3	0.74	1234.1	93.7	1302.3	80.7	1416.7	142.0	1416.7	142.0	12.9
324	0.0898	2.8	2.8961	3.8	0.2340	2.4	0.68	1355.3	29.6	1380.9	28.4	1420.6	52.6	1420.6	52.6	4.6
292	0.0905	4.8	2.6086	6.9	0.2090	5.2	0.71	1223.3	57.9	1303.1	50.6	1436.9	92.0	1436.9	92.0	14.9
71	0.0919	5.3	3.2342	7.1	0.2553	5.2	0.66	1465.8	68.7	1465.4	54.8	1464.8	101.6	1464.8	101.6	-0.1
244	0.0956	3.0	3.2774	4.6	0.2487	3.3	0.75	1432.0	41.7	1475.7	35.9	1539.2	57.0	1539.2	57.0	7.0
92	0.0956	5.9	3.3044	7.7	0.2506	4.5	0.64	1441.8	58.1	1482.1	59.8	1540.2	110.6	1540.2	110.6	6.4
112	0.0965	5.7	3.2582	13.0	0.2448	11.3	0.90	1411.5	143.1	1471.1	101.7	1558.3	107.8	1558.3	107.8	9.4
283	0.0973	4.4	3.1906	8.2	0.2378	7.3	0.84	1375.5	91.0	1454.9	63.3	1572.9	83.1	1572.9	83.1	12.6
149	0.1002	4.7	3.7176	6.6	0.2692	3.5	0.72	1536.6	47.2	1575.2	52.6	1627.3	88.3	1627.3	88.3	5.6
282	0.1084	8.8	4.3998	13.2	0.2945	10.2	0.74	1664.0	149.3	1712.3	109.8	1772.0	161.2	1772.0	161.2	6.1
121	0.1141	5.8	4.6791	12.4	0.2975	10.7	0.88	1678.7	158.7	1763.5	104.2	1865.4	104.7	1865.4	104.7	10.0
240	0.1201	2.3	5.2428	3.7	0.3167	2.6	0.78	1773.7	40.4	1859.6	31.5	1957.1	41.4	1957.1	41.4	9.4
301	0.1250	4.1	5.9208	6.5	0.3436	4.9	0.78	1904.1	81.6	1964.3	56.5	2028.3	71.8	2028.3	71.8	6.1
32	0.1311	3.5	6.5840	4.3	0.3642	3.0	0.59	2002.0	51.9	2057.2	38.1	2113.0	61.5	2113.0	61.5	5.3
212	0.1596	2.6	9.6931	4.4	0.4405	3.4	0.82	2353.1	66.2	2406.1	40.8	2451.2	43.5	2451.2	43.5	4.0
<i>Paruro Formation Top (20140608-03) Rejected Data</i>																
269	0.1103	35.4	0.0188	37.5	0.0012	12.2	0.33	8.0	1.0	18.9	7.0	1803.9	644.3	8.0	1.0	57.9
123	0.2169	55.8	0.0385	61.5	0.0013	25.7	0.42	8.3	2.1	38.3	23.2	2957.7	900.6	8.3	2.1	78.4
27	0.0603	33.1	0.0116	37.2	0.0014	17.1	0.46	9.0	1.5	11.8	4.3	614.9	714.4	9.0	1.5	23.3
307	0.0757	22.2	0.0148	23.4	0.0014	7.3	0.32	9.1	0.7	14.9	3.5	1086.2	444.6	9.1	0.7	38.7
205	0.1631	54.0	0.0319	56.7	0.0014	17.4	0.31	9.1	1.6	31.8	17.8	2488.1	909.7	9.1	1.6	71.3
178	0.0775	16.5	0.0154	18.4	0.0014	8.7	0.44	9.3	0.8	15.5	2.8	1135.3	328.3	9.3	0.8	40.2
243	0.0850	27.4	0.0169	30.2	0.0014	12.7	0.42	9.3	1.2	17.0	5.1	1316.0	530.9	9.3	1.2	45.4
65	0.1011	26.5	0.0204	27.8	0.0015	8.7	0.31	9.4	0.8	20.5	5.6	1644.2	491.0	9.4	0.8	54.0
276	0.0936	27.1	0.0190	29.7	0.0015	12.6	0.41	9.5	1.2	19.1	5.6	1499.9	513.1	9.5	1.2	50.4
270	0.1481	25.6	0.0303	28.2	0.0015	12.1	0.42	9.5	1.2	30.3	8.4	2324.0	439.0	9.5	1.2	68.5
67	0.0655	13.4	0.0134	14.2	0.0015	5.4	0.34	9.6	0.5	13.5	1.9	790.2	280.4	9.6	0.5	29.3
207	0.0762	36.7	0.0157	41.4	0.0015	19.0	0.46	9.7	1.8	15.9	6.5	1100.9	734.7	9.7	1.8	39.2
93	0.1212	40.8	0.0252	48.0	0.0015	25.1	0.53	9.7	2.4	25.3	12.0	1974.2	727.8	9.7	2.4	61.6
49	0.0873	29.3	0.0184	31.3	0.0015	11.0	0.35	9.8	1.1	18.5	5.7	1367.5	564.9	9.8	1.1	46.8
296	0.0986	28.8	0.0210	31.2	0.0015	11.8	0.38	9.9	1.2	21.1	6.5	1597.6	537.4	9.9	1.2	52.8

Table A4.11 (continued): Detrital Zircon U-Pb Integrated Data for the Paruro Formation Top

Spot	Ratios							Ages (Ma)						Best Age	Disc. (%)	
	207Pb/206Pb		207Pb/235U		206Pb/238U		Rho	206Pb/238U		207Pb/235U		207Pb/206Pb				
	±2σ	±2σ	±2σ	±2σ	±2σ	±2σ		±2σ	±2σ	±2σ	±2σ	±2σ				
<i>Paruro Formation Top (20140608-03) Rejected Data</i>																
26	0.0634	46.3	0.0136	49.0	0.0016	16.3	0.33	10.1	1.6	13.8	6.7	720.6	982.2	10.1	1.6	26.9
333	0.0938	30.9	0.0202	32.6	0.0016	10.2	0.32	10.1	1.0	20.3	6.6	1504.0	584.7	10.1	1.0	50.5
351	0.1900	41.4	0.0411	45.0	0.0016	17.6	0.39	10.1	1.8	40.9	18.0	2742.0	680.3	10.1	1.8	75.3
231	0.1553	40.8	0.0337	43.2	0.0016	14.2	0.33	10.1	1.4	33.7	14.3	2405.1	692.9	10.1	1.4	69.9
109	0.0743	17.6	0.0163	21.3	0.0016	11.9	0.56	10.3	1.2	16.5	3.5	1049.9	354.3	10.3	1.2	37.6
189	0.1102	49.4	0.0245	53.1	0.0016	19.5	0.37	10.4	2.0	24.6	12.9	1803.4	898.3	10.4	2.0	57.8
311	0.1189	43.5	0.0270	46.2	0.0016	15.5	0.34	10.6	1.6	27.0	12.3	1940.2	778.6	10.6	1.6	60.8
284	0.1540	40.3	0.0363	43.1	0.0017	15.4	0.35	11.0	1.7	36.2	15.3	2390.4	686.5	11.0	1.7	69.6
146	0.1092	51.3	0.0258	54.0	0.0017	16.5	0.31	11.0	1.8	25.8	13.8	1786.2	935.2	11.0	1.8	57.3
16	0.0493	63.6	0.0120	66.0	0.0018	17.6	0.27	11.4	2.0	12.1	8.0	163.3	1487.4	11.4	2.0	6.2
321	0.0910	30.1	0.0231	36.2	0.0018	20.1	0.56	11.8	2.4	23.2	8.3	1446.3	572.6	11.8	2.4	48.9
326	0.0524	18.4	0.0134	24.5	0.0019	16.2	0.66	11.9	1.9	13.5	3.3	303.1	418.6	11.9	1.9	11.6
346	0.0947	19.1	0.0253	20.5	0.0019	7.3	0.36	12.5	0.9	25.3	5.1	1522.2	360.0	12.5	0.9	50.8
258	0.1891	27.2	0.0524	32.1	0.0020	17.1	0.53	12.9	2.2	51.9	16.3	2734.2	447.2	12.9	2.2	75.0
374	0.1192	16.6	0.0346	21.5	0.0021	13.7	0.63	13.5	1.8	34.5	7.3	1943.6	297.5	13.5	1.8	60.7
260	0.0669	11.8	0.0213	13.3	0.0023	6.1	0.46	14.8	0.9	21.4	2.8	834.9	246.4	14.8	0.9	30.5
251	0.0839	23.4	0.0271	25.0	0.0023	8.8	0.36	15.1	1.3	27.2	6.7	1290.6	455.2	15.1	1.3	44.5
167	0.0669	11.9	0.0223	13.3	0.0024	7.3	0.46	15.6	1.1	22.4	2.9	833.4	247.9	15.6	1.1	30.5
151	0.0769	14.3	0.0257	15.8	0.0024	6.6	0.42	15.6	1.0	25.8	4.0	1118.1	285.3	15.6	1.0	39.4
213	0.0876	18.4	0.0298	20.5	0.0025	8.9	0.44	15.9	1.4	29.9	6.0	1373.8	354.3	15.9	1.4	46.7
399	0.0703	23.3	0.0241	27.9	0.0025	15.4	0.55	16.0	2.5	24.2	6.7	937.2	478.4	16.0	2.5	33.8
254	0.0895	12.9	0.0322	13.9	0.0026	5.1	0.38	16.8	0.8	32.2	4.4	1414.4	246.7	16.8	0.8	47.8
275	0.1066	15.0	0.0385	15.7	0.0026	5.9	0.31	16.9	1.0	38.4	5.9	1742.8	274.9	16.9	1.0	56.1
214	0.0623	9.1	0.0252	9.8	0.0029	3.6	0.39	18.9	0.7	25.3	2.5	685.0	193.3	18.9	0.7	25.3
193	0.0908	16.1	0.0374	16.8	0.0030	4.8	0.28	19.2	0.9	37.3	6.1	1442.5	306.2	19.2	0.9	48.4
129	0.0754	13.9	0.0324	15.0	0.0031	5.7	0.37	20.1	1.2	32.4	4.8	1079.5	279.7	20.1	1.2	38.1
78	0.0905	17.4	0.0389	20.3	0.0031	10.3	0.51	20.1	2.1	38.8	7.7	1436.7	332.1	20.1	2.1	48.2
124	0.1286	23.8	0.0555	25.8	0.0031	9.8	0.39	20.2	2.0	54.9	13.8	2078.7	418.8	20.2	2.0	63.3
303	0.0809	11.3	0.0354	12.9	0.0032	6.0	0.48	20.5	1.2	35.4	4.5	1218.8	222.5	20.5	1.2	42.2
154	0.1670	20.9	0.0770	22.9	0.0033	9.5	0.41	21.5	2.0	75.3	16.6	2527.4	350.1	21.5	2.0	71.4
392	0.1260	29.4	0.0588	31.8	0.0034	12.1	0.38	21.8	2.6	58.0	17.9	2043.0	520.2	21.8	2.6	62.5
277	0.0895	21.5	0.0427	23.1	0.0035	9.0	0.36	22.3	2.0	42.4	9.6	1414.6	411.2	22.3	2.0	47.5
200	0.0871	24.6	0.0422	25.7	0.0035	7.4	0.29	22.6	1.7	41.9	10.5	1363.6	473.1	22.6	1.7	46.1
341	0.1709	17.6	0.0840	19.6	0.0036	8.4	0.43	22.9	1.9	81.9	15.4	2566.3	294.5	22.9	1.9	72.0
105	0.2471	9.0	0.1278	12.3	0.0037	8.2	0.68	24.1	2.0	122.1	14.2	3166.5	143.0	24.1	2.0	80.2
291	0.0868	24.3	0.0487	26.4	0.0041	10.5	0.39	26.2	2.7	48.3	12.4	1356.5	468.1	26.2	2.7	45.8
168	0.0692	10.6	0.0388	11.5	0.0041	6.2	0.41	26.2	1.6	38.7	4.4	904.6	218.6	26.2	1.6	32.3
220	0.0915	20.2	0.0523	22.6	0.0041	10.0	0.45	26.7	2.7	51.8	11.4	1457.4	383.8	26.7	2.7	48.5
271	0.1146	21.2	0.0664	22.8	0.0042	8.9	0.38	27.0	2.4	65.3	14.4	1872.9	381.4	27.0	2.4	58.6
152	0.3259	20.8	0.1898	22.5	0.0042	8.5	0.38	27.2	2.3	176.5	36.4	3597.9	319.1	27.2	2.3	84.6
288	0.0789	22.2	0.0460	24.5	0.0042	10.6	0.42	27.2	2.9	45.7	10.9	1170.5	440.2	27.2	2.9	40.5
185	0.1008	13.6	0.0597	15.4	0.0043	7.1	0.46	27.6	2.0	58.9	8.8	1638.9	252.8	27.6	2.0	53.1
194	0.1094	19.5	0.0649	21.2	0.0043	8.3	0.39	27.7	2.3	63.9	13.1	1789.4	355.1	27.7	2.3	56.7
181	0.1178	28.0	0.0705	30.5	0.0043	12.2	0.39	27.9	3.4	69.2	20.4	1923.8	502.5	27.9	3.4	59.7
21	0.0543	21.1	0.0328	27.4	0.0044	17.4	0.64	28.2	4.9	32.7	8.8	381.8	474.5	28.2	4.9	13.9
182	0.0814	16.3	0.0494	17.4	0.0044	6.6	0.35	28.3	1.9	48.9	8.3	1230.2	320.0	28.3	1.9	42.1
86	0.0477	28.0	0.0292	37.8	0.0044	25.3	0.67	28.5	7.2	29.2	10.9	84.7	664.1	28.5	7.2	2.3
386	0.0839	28.3	0.0517	34.3	0.0045	19.5	0.57	28.7	5.6	51.2	17.1	1290.5	550.3	28.7	5.6	43.8
345	0.0766	15.1	0.0472	16.8	0.0045	7.2	0.44	28.8	2.1	46.8	7.7	1109.8	301.6	28.8	2.1	38.6
148	0.0496	19.0	0.0308	27.4	0.0045	19.4	0.72	28.9	5.6	30.8	8.3	176.3	443.7	28.9	5.6	6.0
195	0.0954	19.5	0.0594	21.1	0.0045	8.0	0.38	29.0	2.3	58.5	12.0	1535.1	366.3	29.0	2.3	50.4
163	0.0934	27.3	0.0581	28.5	0.0045	8.8	0.29	29.0	2.6	57.4	15.9	1496.0	515.9	29.0	2.6	49.4
223	0.0996	29.6	0.0634	31.1	0.0046	9.1	0.30	29.7	2.7	62.4	18.8	1616.3	552.0	29.7	2.7	52.4
225	0.0847	13.7	0.0553	15.8	0.0047	7.8	0.50	30.5	2.4	54.7	8.4	1308.5	266.6	30.5	2.4	44.3
176	0.0766	18.6	0.0524	19.9	0.0050	7.9	0.36	31.9	2.5	51.8	10.1	1111.6	371.1	31.9	2.5	38.5
19	0.1888	14.2	0.1299	16.2	0.0050	7.7	0.48	32.1	2.5	124.0	18.9	2732.0	234.1	32.1	2.5	74.1
196	0.0985	32.6	0.0692	34.5	0.0051	11.5	0.33	32.8	3.8	68.0	22.7	1596.6	607.9	32.8	3.8	51.8
127	0.0690	12.4	0.0489	13.6	0.0051	5.9	0.42	33.1	1.9	48.5	6.4	897.5	255.1	33.1	1.9	31.8
76	0.0478	16.2	0.0392	22.3	0.0060	15.2	0.69	38.3	5.8	39.1	8.5	90.6	384.2	38.3	5.8	2.1
179	0.0455	18.0	0.0378	25.1	0.0060	17.8	0.70	38.7	6.9	37.7	9.3	-30.3	436.3	38.7	6.9	-2.9
103	0.0521	17.4	0.0433	25.5	0.0060	18.4	0.73	38.8	7.1	43.1	10.7	289.9	398.6	38.8	7.1	10.0
36	0.0487	17.4	0.0412	23.8	0.0061	16.3	0.68	39.4	6.4	41.0	9.6	135.5	408.6	39.4	6.4	3.9
18	0.0543	19.5	0.0480	27.4	0.0064	19.2	0.70	41.2	7.9	47.6	12.7	384.9	437.5	41.2	7.9	13.5

Table A4.11 (continued): Detrital Zircon U-Pb Integrated Data for the Paruro Formation Top

Spot	Ratios							Ages (Ma)						Best Age	Disc. (%)	
	207Pb/206Pb		207Pb/235U		206Pb/238U		Rho	206Pb/238U		207Pb/235U		207Pb/206Pb				
	±2σ	±2σ	±2σ	±2σ	±2σ	±2σ		±2σ	±2σ	±2σ	±2σ	±2σ				
<i>Paruro Formation Top (20140608-03) Rejected Data</i>																
286	0.7459	17.7	0.6834	21.5	0.0066	12.5	0.57	42.7	5.3	528.8	88.7	4821.7	254.3	42.7	5.3	91.9
328	0.0635	38.4	0.0640	47.8	0.0073	28.5	0.60	47.0	13.3	63.0	29.2	724.0	814.1	47.0	13.3	25.4
347	0.1126	7.9	0.2059	9.7	0.0133	5.5	0.58	84.9	4.6	190.1	16.8	1842.4	142.8	84.9	4.6	55.3
255	0.0581	40.7	0.1123	51.9	0.0140	32.2	0.62	89.7	28.7	108.1	53.3	534.4	890.4	89.7	28.7	17.0
139	0.0736	24.5	0.1432	29.6	0.0141	16.5	0.56	90.3	14.7	135.9	37.7	1031.4	495.8	90.3	14.7	33.6
201	0.0770	4.9	0.2222	13.2	0.0209	12.2	0.93	133.5	16.1	203.7	24.3	1121.3	97.5	133.5	16.1	34.5
7	0.0597	24.0	0.1927	32.4	0.0234	21.9	0.67	149.1	32.3	179.0	53.2	593.7	519.6	149.1	32.3	16.7
331	0.0486	18.4	0.1570	24.2	0.0234	15.6	0.65	149.2	23.1	148.0	33.3	128.9	432.8	149.2	23.1	-0.8
391	0.0503	15.3	0.1629	21.9	0.0235	15.7	0.72	149.8	23.2	153.2	31.2	206.8	354.2	149.8	23.2	2.2
147	0.1580	14.4	0.5900	26.6	0.0271	22.2	0.84	172.2	37.8	470.9	100.7	2434.9	244.2	172.2	37.8	63.4
134	0.0714	25.8	0.3526	31.7	0.0358	18.3	0.58	227.0	40.7	306.7	84.2	967.8	527.5	227.0	40.7	26.0
110	0.0645	27.9	0.4482	33.4	0.0504	18.3	0.55	317.0	56.5	376.0	105.4	757.9	588.8	317.0	56.5	15.7
122	0.0766	22.6	0.7101	29.1	0.0672	18.2	0.63	419.5	74.0	544.8	123.3	1110.4	451.1	419.5	74.0	23.0
99	0.0620	7.2	1.4716	8.1	0.1722	2.8	0.50	1024.4	26.8	918.8	49.3	672.9	153.3	672.9	153.3	-52.2
81	0.0738	12.8	1.1564	19.9	0.1137	15.1	0.76	694.1	99.2	780.3	108.5	1035.5	259.0	694.1	99.2	33.0
117	0.0818	14.0	1.5695	25.7	0.1392	21.3	0.84	840.4	167.9	958.2	160.5	1239.6	274.2	840.4	167.9	32.2
190	0.0780	8.5	1.5174	11.8	0.1412	8.1	0.69	851.3	64.8	937.4	72.2	1145.8	169.6	851.3	64.8	25.7
209	0.0796	11.1	1.7046	14.7	0.1553	9.6	0.65	930.4	82.8	1010.3	94.5	1187.8	219.7	930.4	82.8	21.7
218	0.0714	18.7	1.6529	26.6	0.1679	18.8	0.71	1000.7	174.4	990.7	169.9	968.5	382.3	968.5	382.3	-3.3
63	0.0678	7.4	1.5351	10.3	0.1642	7.5	0.70	980.2	67.8	944.5	63.3	862.2	152.9	980.2	67.8	-13.7
137	0.0720	17.6	1.7237	25.7	0.1737	18.5	0.73	1032.7	176.8	1017.4	166.4	984.7	358.1	984.7	358.1	-4.9
22	0.0784	17.6	2.0948	25.8	0.1937	18.9	0.73	1141.3	197.5	1147.1	179.4	1158.1	349.5	1158.1	349.5	1.4
245	0.1082	6.6	2.5902	12.9	0.1735	11.1	0.86	1031.6	105.5	1297.9	95.0	1770.1	120.0	1770.1	120.0	41.7

APPENDIX 5

Table A5: Modern Water Data and Elevation Modeling

Name	Dist. (km)	Lat. centroid	Long. centroid	MBH (m)	$\delta^{18}O$		δD		D excess	ΔD (‰)	Model ΔD mean	Topographic Swath a-a'				Resid.
					(‰ vsmow)	Unc. (‰)	(‰ vsmow)	Unc. (‰)				+1 σ	-1 σ	+2 σ	-2 σ	
270511-05*	292	-13.74	-73.19	4352	5.6	0.2	-68.6	2.4	-113.3	-37.0	2595	2941	2122	3065	1537	1757
270511-01*	292	-13.71	-73.25	4113	-6.8	0.2	-95.8	2.4	-41.4	-64.2	3804	4446	2997	4695	2240	309
270511-10*	320	-13.58	-72.86	3614	-6.7	0.2	-83.6	2.4	-30.0	-52.0	3319	3832	2654	4026	1956	295
270511-09*	313	-13.61	-72.9	3310	-7.9	0.2	-91.4	2.4	-28.5	-59.8	3639	4235	2881	4465	2142	-329
270511-08*	308	-13.69	-72.96	2979	-9.4	0.2	-92.5	2.4	-17.5	-60.9	3681	4289	2911	4524	2167	-702
270511-14*	336	-13.58	-72.72	3401	-11.1	0.2	-100.0	2.4	-11.4	-68.4	3953	4636	3101	4903	2328	-552
270511-15*	338	-14.4	-72.01	4161	-11.9	0.2	-103.6	2.4	-8.1	-72.0	4074	4791	3185	5073	2401	87
20140521-08*	162	-14.58	-74.07	4097	-12.0	0.2	-102.6	2.4	-6.4	-71.0	4041	4748	3162	5027	2381	56
270511-11*	322	-13.59	-72.82	3782	-12.8	0.2	-108.1	2.4	-5.4	-76.5	4217	4974	3285	5274	2488	-435
20140519-14*	191	-14.5	-73.6	4502	-14.0	0.2	-113.6	2.4	-1.8	-82.0	4381	5184	3399	5503	2589	121
20140519-03*	147	-14.47	-74.3	4019	-13.4	0.2	-108.3	2.4	-1.4	-76.7	4223	4982	3289	5282	2492	-204
270511-03*	294	-13.69	-73.21	4184	-14.1	0.2	-114.3	2.4	-1.4	-82.7	4401	5210	3413	5531	2602	-217
20140522-13*	187	-14.57	-73.59	4566	-13.9	0.2	-112.2	2.4	-0.8	-80.6	4340	5132	3371	5447	2564	226
20140519-13*	186	-14.55	-73.63	4528	-13.4	0.2	-107.8	2.4	-0.5	-76.2	4208	4963	3278	5261	2482	320
20140521-09*	166	-14.53	-74.03	4348	-13.1	0.2	-104.3	2.4	0.8	-72.7	4097	4820	3201	5105	2415	251
20140519-15*	197	-14.46	-73.6	4468	-14.8	0.2	-117.3	2.4	1.0	-85.7	4485	5317	3472	5648	2655	-17
20140521-07*	155	-14.58	-74.04	4170	-12.7	0.2	-100.3	2.4	1.4	-68.7	3964	4649	3108	4918	2334	206
20140519-01*	133	-14.65	-74.38	4050	-11.3	0.2	-89.3	2.4	1.5	-57.7	3556	4130	2823	4351	2094	494
20140519-04*	149	-14.59	-74.19	3999	-11.5	0.2	-90.2	2.4	1.6	-58.6	3592	4175	2848	4400	2115	407
20140525-02*	191	-14.54	-73.55	4503	-15.0	0.2	-118.0	2.4	2.0	-86.4	4504	5341	3486	5675	2667	-1
20140522-07*	183	-14.43	-74.1	4246	-14.0	0.2	-110.1	2.4	2.1	-78.5	4278	5053	3327	5359	2525	-32
20140521-06*	204	-14.41	-73.59	4451	-14.8	0.2	-115.9	2.4	2.7	-84.3	4446	5267	3445	5594	2630	5
270511-04*	295	-13.69	-73.19	4185	-14.9	0.2	-116.1	2.4	2.7	-84.5	4452	5275	3449	5602	2634	-267
270511-02*	292	-13.69	-73.24	4000	-14.7	0.2	-114.5	2.4	3.1	-82.9	4407	5217	3417	5539	2605	-407
20140519-12*	183	-14.58	-73.62	4545	-14.7	0.2	-114.0	2.4	3.2	-82.4	4392	5199	3407	5519	2596	153
20140519-02*	143	-14.66	-74.28	3995	-11.6	0.2	-89.7	2.4	3.5	-58.1	3572	4150	2834	4373	2103	423
20140519-16*	203	-14.41	-73.59	4511	-15.4	0.2	-120.1	2.4	3.5	-88.5	4560	5413	3526	5753	2703	-49
270511-07*	301	-13.71	-73.06	4132	-15.2	0.2	-117.6	2.4	4.0	-86.0	4493	5327	3478	5659	2660	-361
20140519-08*	150	-14.69	-74.07	3749	-11.5	0.2	-87.8	2.4	4.1	-56.2	3496	4054	2780	4268	2058	253
20140521-01*	225	-14.36	-73.44	4134	-15.9	0.2	-123.4	2.4	4.2	-91.8	4645	5521	3587	5870	2759	-511
20140525-13*	274	-13.97	-73.12	2912	-14.8	0.2	-113.8	2.4	4.7	-82.2	4387	5192	3403	5511	2593	-1475
20140525-04*	217	-14.58	-73.26	4390	-16.7	0.2	-128.3	2.4	5.0	-96.7	4766	5673	3674	6035	2839	-376
20140525-18*	338	-13.57	-72.6	2632	-14.1	0.2	-107.2	2.4	5.3	-75.6	4189	4939	3265	5235	2471	-1557
20140525-03*	200	-14.58	-73.44	4429	-16.5	0.2	-126.7	2.4	5.5	-95.1	4728	5624	3646	5983	2813	-299
20140522-08*	182	-14.5	-73.95	4277	-15.5	0.2	-118.0	2.4	5.7	-86.4	4504	5341	3486	5675	2667	-227
20140525-09*	235	-14.24	-73.28	3607	-16.7	0.2	-127.3	2.4	6.1	-95.7	4742	5643	3657	6003	2823	-1135
20140522-12*	173	-14.54	-73.91	4454	-15.6	0.2	-118.6	2.4	6.3	-87.0	4520	5362	3497	5697	2677	-66
20140519-11*	175	-14.66	-73.72	4590	-16.1	0.2	-122.3	2.4	6.4	-90.7	4617	5485	3567	5832	2740	-27
20140525-10*	238	-14.22	-73.3	3507	-16.2	0.2	-123.4	2.4	6.5	-91.8	4645	5521	3587	5870	2759	-1138
20140525-11*	246	-14.25	-73.28	3820	-16.6	0.2	-125.9	2.4	6.7	-94.3	4708	5600	3632	5956	2800	-888
270511-13*	330	-13.56	-72.79	3621	-14.9	0.2	-112.0	2.4	7.0	-80.4	4335	5125	3367	5438	2560	-714
20140525-07*	231	-14.44	-73.18	4120	-17.6	0.2	-133.3	2.4	7.3	-101.7	4883	5818	3761	6191	2919	-763
20140525-19*	347	-13.53	-72.48	3020	-13.9	0.2	-104.3	2.4	7.3	-72.7	4097	4820	3201	5105	2415	-1077
20140525-17*	322	-13.55	-72.91	4662	-15.7	0.2	-117.6	2.4	7.7	-86.0	4493	5327	3478	5659	2660	169
20140525-12*	260	-13.99	-73.26	3611	-16.0	0.2	-120.2	2.4	7.8	-88.6	4563	5416	3527	5756	2705	-952
20140521-05*	207	-14.4	-73.58	4449	-17.1	0.2	-128.6	2.4	7.9	-97.0	4773	5682	3680	6045	2844	-324
20140522-11*	180	-14.47	-73.89	4490	-16.5	0.2	-123.6	2.4	8.0	-92.0	4651	5527	3590	5877	2762	-161
270511-17*	354	-13.42	-72.41	3802	-14.8	0.2	-110.4	2.4	8.0	-78.8	4287	5064	3334	5372	2531	-485
270511-18*	359	-13.46	-72.39	3612	-14.8	0.2	-110.0	2.4	8.0	-78.4	4275	5049	3325	5355	2523	-663
20140519-05*	148	-14.61	-74.19	3922	-13.6	0.2	-100.7	2.4	8.1	-69.1	3977	4667	3118	4937	2343	-55
20140525-14*	295	-13.82	-72.93	3150	-15.8	0.2	-118.5	2.4	8.2	-86.9	4517	5358	3495	5693	2676	-1367
20140525-06*	224	-14.41	-73.25	4270	-17.5	0.2	-131.8	2.4	8.4	-100.2	4848	5775	3735	6146	2895	-578
20140525-15*	311	-14.15	-72.96	3973	-15.3	0.2	-114.2	2.4	8.5	-82.6	4398	5206	3411	5527	2600	-425
20140525-08*	234	-14.45	-73.07	4343	-17.8	0.2	-133.4	2.4	8.6	-101.8	4885	5820	3762	6194	2920	-542
20140525-16*	312	-13.61	-72.9	3317	-15.7	0.2	-114.7	2.4	10.6	-83.1	4412	5224	3421	5547	2609	-1095
270511-12*	324	-13.6	-73.86	3699	-15.6	0.2	-112.2	2.4	12.2	-80.6	4340	5132	3371	5447	2564	-641
Topographic Swath b-b'																
20160816-17	357	-13.998	-71.511	3864	-9.2	0.0	-93.5	0.3	-19.6	-61.9	3718	4336	2937	4575	2189	146
20160815-13	219	-15.748	-71	4531	-9.9	0.1	-95.1	0.6	-16.2	-63.5	3779	4413	2979	4659	2224	752
20160816-16	349	-14.119	-71.457	3855	-9.1	0.1	-84.9	0.8	-12.3	-53.3	3376	3903	2694	4103	1989	480
20160814-17	248	-16.039	-70.016	3924	-10.7	0.1	-94.7	0.3	-9.3	-63.1	3763	4393	2968	4637	2215	161

Table A5 (continued): Modern Water Data and Elevation Modeling

Name	Dist. (km)	Lat. centroid	Long. centroid	MBH (m)	$\delta^{18}\text{O}$		δD		D excess	ΔD (‰)	Model ΔD mean	+1 σ	-1 σ	+2 σ	-2 σ	Resid.
					(‰ vsmow)	Unc. (‰)	(‰ vsmow)	Unc. (‰)								
20160815-10	246	-15.649	-70.716	4450	-13.0	0.1	-111.3	0.2	-7.5	-79.7	4314	5099	3352	5410	2548	135
20160814-16	220	-16.278	-70.124	4324	-13.4	0.0	-115.0	0.5	-7.5	-83.4	4421	5236	3427	5559	2614	-97
20160815-07	250	-15.707	-70.558	4305	-10.8	0.1	-93.3	0.3	-6.9	-61.7	3711	4326	2932	4565	2184	594
20160722-08	370	-13.667	-71.843	4163	-14.2	0.0	-118.8	0.4	-5.6	-87.2	4524	5367	3500	5703	2680	-361
20160813-02	235	-16.548	-69.331	4044	-12.4	0.1	-103.6	0.4	-4.6	-72.0	4074	4790	3185	5072	2401	-30
20160722-06	368	-13.694	-71.831	4014	-14.9	0.0	-123.4	0.3	-4.4	-91.8	4645	5521	3587	5870	2759	-631
20160713-13	341	-14.474	-70.973	4654	-13.1	0.1	-108.7	0.3	-4.0	-77.1	4236	4999	3298	5301	2500	418
20160815-14	282	-15.645	-70.053	3822	-12.7	0.1	-105.4	0.5	-3.9	-73.8	4131	4864	3225	5153	2435	-309
20160726-04	341	-14.335	-71.254	4060	-13.2	0.1	-108.7	0.3	-3.5	-77.1	4236	4999	3298	5300	2499	-177
20160723-01	376	-13.531	-72.008	3796	-14.1	0.0	-116.2	0.5	-3.4	-84.6	4453	5276	3450	5604	2635	-657
20160713-09	349	-14.15	-71.325	4016	-12.4	0.1	-102.6	0.4	-3.2	-71.0	4042	4750	3163	5028	2381	-26
20160713-18	269	-15.62	-70.35	3884	-12.3	0.1	-101.5	0.4	-3.1	-69.9	4005	4703	3137	4976	2359	-121
20160714-06	231	-15.932	-70.478	4446	-12.7	0.1	-104.3	0.3	-3.0	-72.7	4098	4821	3202	5106	2415	349
20150610-11	346	-14.31	-71.199	3816	-11.9	0.0	-97.9	0.3	-3.0	-66.3	3882	4544	3051	4803	2285	-66
20160813-04	262	-16.327	-69.356	4231	-12.3	0.1	-100.6	0.2	-2.4	-69.0	3975	4664	3116	4934	2341	256
20150619-05	341	-14.315	-71.274	3945	-12.2	0.0	-100.1	0.3	-2.4	-68.5	3957	4640	3104	4908	2330	-11
20160814-07	188	-16.469	-70.327	4540	-14.0	0.0	-114.0	0.5	-2.3	-82.4	4391	5197	3406	5518	2596	149
20160813-05	264	-16.09	-69.632	3850	-12.9	0.1	-104.6	0.3	-1.4	-73.0	4108	4834	3209	5121	2421	-259
20160814-02	165	-16.683	-70.431	4395	-14.3	0.0	-115.7	0.3	-1.4	-84.1	4439	5259	3440	5585	2626	-45
20150523-06	368	-13.692	-71.831	4033	-13.2	0.0	-106.9	0.3	-1.1	-75.3	4181	4928	3259	5223	2466	-148
20160816-08	309	-14.641	-71.237	4182	-13.2	0.0	-106.7	0.5	-0.8	-75.1	4175	4920	3255	5214	2462	8
20150619-01	292	-14.769	-71.388	3891	-14.4	0.0	-115.6	0.4	-0.6	-84.0	4437	5256	3439	5582	2625	-546
20160815-16	243	-15.472	-71.067	4545	-13.1	0.1	-105.0	0.5	-0.6	-73.4	4121	4851	3218	5139	2429	424
20160815-02	259	-15.782	-70.261	3896	-13.0	0.0	-104.3	0.3	-0.4	-72.7	4096	4819	3201	5104	2414	-200
20160714-04	239	-15.867	-70.459	4529	-14.0	0.1	-111.9	0.3	-0.2	-80.3	4331	5120	3364	5433	2558	198
20160816-01	292	-14.769	-71.388	3891	-13.5	0.0	-108.3	0.2	-0.1	-76.7	4225	4984	3290	5284	2493	-334
20160725-03	396	-13.655	-71.424	3829	-12.0	0.0	-96.3	0.3	0.0	-64.7	3821	4467	3009	4719	2250	7
20150601-03	261	-15.612	-70.488	4467	-13.8	0.1	-110.1	0.3	0.0	-78.5	4279	5054	3328	5361	2526	188
20160713-01	382	-13.706	-71.627	3536	-13.2	0.1	-105.3	0.3	0.5	-73.7	4130	4862	3224	5151	2434	-593
20160713-07	353	-14.094	-71.433	3505	-12.8	0.1	-101.5	0.4	0.5	-69.9	4005	4703	3137	4976	2359	-500
20160720-07	232	-15.912	-70.517	4507	-13.9	0.1	-110.8	0.5	0.8	-79.2	4299	5080	3342	5389	2538	208
20160722-13	372	-13.595	-71.978	3947	-13.4	0.0	-106.5	0.3	0.8	-74.9	4167	4910	3250	5203	2457	-220
20160713-17	291	-15.369	-70.365	3864	-13.5	0.1	-106.8	0.4	0.8	-75.2	4177	4923	3257	5217	2463	-313
20160726-07	333	-14.786	-70.618	4247	-13.6	0.1	-108.1	0.3	0.8	-76.5	4218	4975	3285	5274	2488	29
20160714-05	239	-15.868	-70.463	4467	-13.8	0.1	-109.4	0.4	0.9	-77.8	4258	5027	3313	5331	2513	209
20150603-02	221	-15.936	-70.645	4397	-14.1	0.0	-112.2	0.4	1.0	-80.6	4340	5131	3370	5446	2564	57
20150517-03	369	-13.637	-71.923	3572	-14.4	0.1	-114.1	0.4	1.2	-82.5	4395	5202	3409	5523	2598	-822
20160720-08	230	-15.895	-70.563	4254	-15.1	0.1	-119.8	0.3	1.2	-88.2	4552	5403	3520	5742	2698	-299
20160713-14	340	-14.625	-70.757	4086	-14.2	0.1	-112.2	0.4	1.4	-80.6	4339	5131	3370	5445	2563	-253
20160814-03	170	-16.624	-70.405	4338	-13.9	0.0	-109.3	0.2	1.5	-77.7	4255	5023	3311	5327	2511	82
20150601-07	253	-15.836	-70.393	4240	-14.1	0.0	-111.1	0.3	1.5	-79.5	4309	5093	3349	5403	2545	-70
20160817-02	350	-13.847	-71.952	3553	-14.4	0.1	-113.6	0.4	1.6	-82.0	4382	5185	3400	5504	2590	-828
20150608-02	217	-16.023	-70.629	4169	-14.4	0.0	-113.6	0.3	1.7	-82.0	4382	5185	3400	5505	2590	-213
20160714-02	291	-15.353	-70.402	3873	-14.1	0.1	-111.0	0.3	1.7	-79.4	4306	5088	3347	5398	2542	-433
20160816-15	333	-14.342	-71.139	4445	-14.2	0.1	-112.0	0.5	1.7	-80.4	4335	5125	3367	5438	2560	111
20150618-16	203	-15.296	-72.096	4660	-15.2	0.0	-119.6	0.3	1.7	-88.0	4548	5397	3517	5736	2695	112
20160725-01	392	-13.61	-71.581	3975	-13.9	0.1	-109.5	0.4	1.7	-77.9	4260	5029	3315	5334	2514	-285
20150619-02	309	-14.641	-71.237	4182	-14.5	0.0	-114.0	0.5	1.9	-82.4	4391	5197	3406	5518	2596	-209
20160811-01	247	-16.518	-69.207	4096	-12.9	0.0	-100.9	0.2	2.1	-69.3	3985	4677	3123	4948	2347	111
20160725-02	393	-13.648	-71.149	3806	-13.8	0.1	-107.9	0.3	2.1	-76.3	4212	4968	3281	5266	2485	-406
20150610-05	319	-15.089	-70.359	3905	-14.5	0.1	-113.8	0.3	2.2	-82.2	4388	5193	3404	5513	2593	-482
20160713-04	374	-13.812	-71.537	3370	-13.2	0.0	-103.1	0.4	2.4	-71.5	4059	4771	3174	5051	2391	-689
20160726-03	340	-14.327	-71.276	3913	-14.8	0.1	-116.3	0.5	2.4	-84.7	4457	5281	3453	5609	2637	-544
20150523-09	364	-13.74	-71.833	3719	-14.3	0.1	-111.9	0.3	2.4	-80.3	4333	5123	3366	5436	2559	-614
20150608-01	218	-15.986	-70.635	3979	-14.6	0.0	-114.2	0.3	2.4	-82.6	4397	5205	3410	5526	2599	-418
20150618-20	220	-15.218	-71.894	4740	-15.8	0.0	-123.6	0.4	2.5	-92.0	4650	5526	3590	5876	2762	90
20160715-06	218	-15.984	-70.638	3979	-15.0	0.0	-117.4	0.3	2.6	-85.8	4487	5320	3474	5651	2656	-508
20150609-01	253	-15.985	-70.028	3925	-13.7	0.0	-106.7	0.3	2.6	-75.1	4174	4919	3255	5213	2461	-249
20160713-15	324	-14.899	-70.605	3901	-14.6	0.1	-114.3	0.5	2.7	-82.7	4400	5209	3413	5530	2601	-499
20160813-03	249	-16.44	-69.306	4143	-14.2	0.1	-110.9	0.3	2.9	-79.3	4302	5083	3344	5393	2540	-159
20160713-16	319	-15.083	-70.363	3970	-14.4	0.1	-112.1	0.4	2.9	-80.5	4339	5130	3370	5444	2563	-368

Table A5 (continued): Modern Water Data and Elevation Modeling

Name	Dist. (km)	Lat. centroid	Long. centroid	MBH (m)	$\delta^{18}\text{O}$		δD		D	ΔD	Model ΔD	Topographic Swath b-b'				Resid.		
					(‰)	Unc.	(‰)	Unc.				excess	mean	+1 σ	-1 σ		+2 σ	-2 σ
					(‰ vsmow)	(‰)	(‰ vsmow)	(‰)				(‰)						
20150610-01	259	-15.782	-70.261	3896	-13.7	0.0	-106.3	0.4	3.0	-74.7	4162	4904	3247	5196	2454	-266		
20160714-07	233	-15.889	-70.527	4285	-14.8	0.1	-115.7	0.4	3.0	-84.1	4440	5260	3441	5586	2627	-155		
20150608-08	228	-15.899	-70.576	4221	-14.3	0.0	-111.3	0.4	3.1	-79.7	4315	5100	3353	5411	2548	-94		
20160722-09	372	-13.641	-71.869	4110	-14.9	0.0	-116.3	0.3	3.1	-84.7	4456	5280	3452	5608	2637	-346		
20150517-02	370	-13.623	-71.934	3888	-14.9	0.1	-115.9	0.4	3.1	-84.3	4446	5268	3445	5595	2631	-558		
20150601-01	382	-13.704	-71.627	3509	-14.6	0.0	-113.8	0.2	3.1	-82.2	4387	5192	3404	5512	2593	-878		
20150608-10	265	-15.654	-70.352	3980	-13.8	0.0	-107.5	0.3	3.3	-75.9	4199	4951	3272	5248	2477	-219		
20150616-03	351	-13.803	-71.957	3278	-13.9	0.0	-107.9	0.3	3.3	-76.3	4211	4966	3280	5265	2484	-933		
20150601-04	261	-15.584	-70.478	4607	-14.4	0.0	-111.6	0.3	3.3	-80.0	4323	5110	3359	5422	2553	284		
20150619-03	318	-14.555	-71.301	4002	-15.6	0.0	-121.1	0.4	3.4	-89.5	4585	5445	3544	5788	2720	-583		
20160722-02	368	-13.693	-71.849	3934	-14.8	0.0	-115.2	0.5	3.5	-83.6	4427	5243	3431	5567	2618	-492		
20160816-22	358	-13.813	-71.827	2839	-13.9	0.1	-107.8	0.4	3.5	-76.2	4209	4964	3279	5263	2483	-1370		
20150610-04	314	-15.137	-70.367	3858	-14.6	0.0	-113.2	0.3	3.5	-81.6	4371	5171	3392	5489	2583	-513		
20150618-17	209	-15.278	-72.029	4592	-15.9	0.0	-123.6	0.3	3.6	-92.0	4650	5527	3590	5877	2762	-58		
20150610-06	340	-14.615	-70.764	4040	-14.7	0.0	-113.7	0.3	3.6	-82.1	4385	5189	3402	5508	2592	-344		
20160720-06	230	-15.952	-70.477	4452	-14.3	0.0	-110.8	0.4	3.7	-79.2	4300	5081	3343	5390	2539	152		
20150609-04	226	-16.207	-70.125	4119	-14.0	0.0	-108.6	0.3	3.7	-77.0	4234	4995	3296	5297	2498	-115		
20150524-02	376	-13.611	-71.866	4028	-14.6	0.0	-113.3	0.2	3.8	-81.7	4371	5172	3392	5490	2583	-343		
20150616-11	305	-14.251	-72.032	3532	-14.7	0.1	-113.4	0.3	3.8	-81.8	4375	5177	3395	5496	2586	-844		
20160714-03	243	-15.855	-70.416	4322	-15.0	0.1	-116.3	0.5	3.9	-84.7	4458	5283	3453	5611	2638	-135		
20150609-13	188	-16.469	-70.327	4540	-14.3	0.1	-110.8	0.5	4.0	-79.2	4300	5080	3343	5390	2539	240		
20160814-14	208	-16.301	-70.271	4589	-13.1	0.0	-101.2	0.2	4.0	-69.6	3994	4688	3129	4960	2353	595		
20150613-04	369	-13.545	-72.108	4087	-14.5	0.0	-112.3	0.3	4.0	-80.7	4344	5137	3373	5452	2566	-257		
20160722-04	368	-13.695	-71.847	3919	-14.8	0.0	-114.5	0.5	4.0	-82.9	4408	5219	3418	5541	2606	-489		
20150616-18	271	-14.553	-72.12	3988	-15.7	0.0	-121.6	0.4	4.0	-90.0	4598	5462	3553	5806	2728	-610		
20150609-02	248	-16.039	-70.016	3924	-13.7	0.0	-105.2	0.3	4.1	-73.6	4126	4857	3221	5145	2432	-202		
20150610-03	291	-15.372	-70.364	3861	-14.5	0.0	-112.3	0.3	4.1	-80.7	4343	5136	3373	5450	2566	-482		
20150608-09	250	-15.707	-70.558	4305	-14.4	0.0	-111.3	0.3	4.1	-79.7	4315	5100	3353	5411	2548	-10		
20150609-05	220	-16.278	-70.124	4324	-14.6	0.1	-112.6	0.3	4.1	-81.0	4351	5146	3378	5461	2571	-27		
20150523-05	369	-13.663	-71.846	4153	-14.8	0.0	-114.1	0.3	4.3	-82.5	4395	5203	3409	5523	2598	-242		
20160713-08	353	-14.094	-71.433	3505	-15.3	0.1	-117.8	0.4	4.3	-86.2	4500	5336	3483	5669	2664	-995		
20160816-09	318	-14.555	-71.301	4002	-15.4	0.0	-119.0	0.5	4.4	-87.4	4530	5375	3504	5711	2684	-528		
20150609-06	216	-16.281	-70.182	4329	-14.5	0.0	-111.4	0.4	4.5	-79.8	4318	5103	3355	5415	2550	11		
20150517-04	371	-13.635	-71.901	3766	-15.1	0.0	-115.9	0.2	4.6	-84.3	4446	5268	3445	5595	2630	-680		
20150619-04	320	-14.513	-71.296	4133	-15.3	0.1	-117.4	0.2	4.7	-85.8	4488	5321	3475	5653	2657	-355		
20150601-02	383	-13.679	-71.564	4014	-15.1	0.0	-115.7	0.3	4.8	-84.1	4442	5262	3442	5588	2627	-427		
20150618-22	229	-15.186	-71.825	4676	-16.2	0.0	-124.6	0.4	4.8	-93.0	4676	5560	3609	5913	2779	0		
20160725-07	398	-13.737	-71.221	4652	-13.9	0.0	-106.7	0.3	4.8	-75.1	4174	4918	3254	5212	2461	479		
20150616-13	302	-14.279	-72.039	3561	-15.0	0.1	-115.3	0.4	4.9	-83.7	4429	5246	3433	5570	2620	-868		
20150618-21	224	-15.243	-71.845	4598	-16.3	0.0	-125.9	0.3	4.9	-94.3	4707	5599	3631	5955	2800	-110		
20160726-09	331	-14.833	-70.555	4399	-15.2	0.1	-116.4	0.3	4.9	-84.8	4460	5285	3454	5613	2639	-60		
20150608-04	222	-15.965	-70.604	4136	-14.3	0.1	-109.6	0.4	5.0	-78.0	4264	5035	3318	5340	2517	-128		
20150616-07	343	-13.873	-71.982	4245	-14.3	0.0	-109.4	0.3	5.0	-77.8	4258	5026	3313	5331	2513	-12		
20150523-08	366	-13.726	-71.829	3835	-14.3	0.0	-109.4	0.2	5.0	-77.8	4256	5024	3312	5328	2511	-421		
20150610-07	342	-14.522	-70.848	4659	-14.9	0.0	-114.1	0.3	5.0	-82.5	4394	5201	3409	5522	2598	264		
20160816-20	358	-13.828	-71.793	3529	-14.0	0.0	-106.6	0.2	5.1	-75.0	4172	4916	3253	5210	2460	-643		
20160726-02	337	-14.343	-71.309	4102	-15.5	0.1	-118.9	0.2	5.1	-87.3	4528	5372	3503	5709	2683	-426		
20160726-05	343	-14.326	-71.232	3906	-15.0	0.1	-115.1	0.3	5.1	-83.5	4423	5239	3429	5563	2616	-517		
20150524-01	371	-13.657	-71.839	4214	-14.8	0.1	-112.8	0.3	5.2	-81.2	4359	5156	3384	5473	2576	-145		
20150610-14	370	-13.856	-71.491	4021	-14.4	0.0	-110.3	0.4	5.2	-78.7	4283	5059	3331	5366	2528	-262		
20160713-05	374	-13.812	-71.537	3370	-14.0	0.1	-107.0	0.3	5.2	-75.4	4182	4929	3260	5224	2466	-812		
20150616-08	320	-14.134	-71.973	4384	-15.6	0.0	-119.4	0.3	5.3	-87.8	4541	5388	3512	5726	2691	-157		
20160722-10	371	-13.633	-71.897	3838	-14.4	0.0	-109.8	0.3	5.3	-78.2	4269	5041	3321	5346	2520	-431		
20150616-05	350	-13.841	-71.953	3202	-15.1	0.1	-115.7	0.4	5.4	-84.1	4440	5259	3440	5585	2626	-1237		
20160816-14	333	-14.339	-71.347	4199	-15.7	0.0	-119.9	0.2	5.5	-88.3	4555	5406	3522	5746	2700	-356		
20160816-19	357	-13.851	-71.761	3816	-14.8	0.1	-112.5	0.3	5.5	-80.9	4349	5143	3377	5458	2569	-533		
20150613-03	369	-13.555	-72.069	3723	-14.7	0.0	-111.8	0.3	5.6	-80.2	4329	5118	3363	5431	2557	-606		
20150610-15	374	-13.812	-71.537	3370	-14.3	0.1	-108.6	0.5	5.6	-77.0	4232	4994	3295	5295	2497	-863		
20150616-16	285	-14.446	-72.053	3975	-15.9	0.0	-121.2	0.4	5.6	-89.6	4590	5451	3547	5794	2722	-615		
20160713-03	376	-13.762	-71.56	3713	-14.0	0.1	-106.5	0.2	5.7	-74.9	4166	4908	3249	5202	2456	-453		
20150610-02	254	-15.805	-70.32	3945	-14.2	0.1	-107.9	0.4	5.7	-76.3	4210	4965	3280	5264	2483	-265		

Table A5 (continued): Modern Water Data and Elevation Modeling

Name	Dist. (km)	Lat. centroid	Long. centroid	MBH (m)	$\delta^{18}O$		δD		D excess	ΔD (‰)	Model ΔD mean	+1 σ	-1 σ	+2 σ	-2 σ	Resid.
					(‰ vsmow)	Unc. (‰)	(‰ vsmow)	Unc. (‰)								
Topographic Swath b-b'																
20150616-04	350	-13.837	-71.947	3153	-14.3	0.1	-108.3	0.3	5.8	-76.7	4223	4982	3289	5282	2492	-1071
20150609-08	204	-16.307	-70.309	4778	-14.8	0.0	-112.2	0.5	5.9	-80.6	4341	5133	3371	5448	2564	437
20150523-07	368	-13.694	-71.831	4014	-14.9	0.1	-113.0	0.5	6.0	-81.4	4364	5162	3387	5479	2579	-349
20160817-08	347	-13.866	-71.962	4048	-14.6	0.1	-111.0	0.3	6.0	-79.4	4304	5085	3345	5395	2541	-256
20160726-06	335	-14.709	-70.698	4036	-14.8	0.1	-112.0	0.6	6.0	-80.4	4336	5126	3368	5440	2561	-300
20150613-01	368	-13.56	-72.055	3898	-14.7	0.0	-111.4	0.3	6.1	-79.8	4317	5102	3354	5413	2549	-418
20150616-01	365	-13.692	-71.911	3860	-14.4	0.1	-108.7	0.4	6.1	-77.1	4236	4999	3298	5301	2500	-377
20150616-10	309	-14.227	-72	3915	-15.2	0.0	-115.6	0.6	6.2	-84.0	4439	5258	3440	5584	2626	-524
20150608-03	222	-15.95	-70.623	4024	-15.7	0.0	-119.3	0.3	6.3	-87.7	4538	5385	3510	5723	2689	-514
20160720-05	218	-15.986	-70.644	4049	-14.5	0.0	-109.5	0.2	6.3	-77.9	4260	5029	3314	5333	2514	-211
20150601-05	261	-15.592	-70.477	4572	-15.5	0.0	-117.7	0.2	6.4	-86.1	4497	5332	3481	5665	2663	75
20160713-10	346	-14.31	-71.199	3816	-15.5	0.1	-117.5	0.4	6.5	-85.9	4489	5323	3475	5654	2658	-673
20150616-06	347	-13.866	-71.962	4048	-14.8	0.1	-111.8	0.5	6.6	-80.2	4330	5119	3363	5432	2557	-282
20150616-09	312	-14.18	-72.018	4277	-15.8	0.0	-119.4	0.4	6.8	-87.8	4540	5388	3512	5726	2691	-263
20150618-18	209	-15.26	-72.026	4510	-16.5	0.0	-125.3	0.2	6.8	-93.7	4692	5580	3621	5935	2790	-182
20150613-05	370	-13.53	-72.129	4082	-14.8	0.0	-111.2	0.3	6.8	-79.6	4311	5094	3350	5405	2546	-229
20150612-02	368	-13.711	-71.801	4007	-15.1	0.0	-114.2	0.3	6.8	-82.6	4397	5205	3411	5526	2599	-391
20150618-19	212	-15.218	-71.994	4692	-17.0	0.0	-128.6	0.6	7.0	-97.0	4773	5681	3679	6044	2843	-81
20150517-05	373	-13.603	-71.91	3921	-15.2	0.0	-114.5	0.3	7.1	-82.9	4406	5217	3417	5539	2605	-485
20160722-03	367	-13.699	-71.855	3841	-14.9	0.0	-112.2	0.3	7.2	-80.6	4339	5131	3370	5445	2563	-498
20160726-08	333	-14.786	-70.618	4247	-16.1	0.1	-121.5	0.3	7.3	-89.9	4596	5459	3551	5803	2727	-349
20160713-06	366	-13.913	-71.514	3843	-15.4	0.0	-115.8	0.5	7.5	-84.2	4444	5265	3443	5591	2629	-600
20160816-18	356	-13.912	-71.668	3557	-14.2	0.0	-105.7	0.2	7.6	-74.1	4141	4876	3232	5166	2441	-583
20150616-15	294	-14.36	-72.033	4021	-15.7	0.0	-118.3	0.3	7.6	-86.7	4511	5350	3491	5684	2672	-489
20150610-12	353	-14.094	-71.433	3505	-15.5	0.0	-116.3	0.3	7.7	-84.7	4457	5282	3453	5610	2638	-952
20160713-02	383	-13.679	-71.564	4014	-14.8	0.1	-110.7	0.3	7.7	-79.1	4297	5077	3341	5386	2537	-283
20150613-02	368	-13.547	-72.079	3807	-15.0	0.0	-111.9	0.6	7.8	-80.3	4332	5121	3365	5434	2559	-525
20150612-03	368	-13.72	-71.814	3729	-15.2	0.1	-113.5	0.5	7.9	-81.9	4378	5180	3397	5499	2587	-649
20160713-12	341	-14.474	-70.973	4654	-15.1	0.1	-112.4	0.4	8.1	-80.8	4347	5141	3376	5456	2568	307
20150610-16	376	-13.762	-71.56	3713	-14.8	0.1	-110.0	0.3	8.2	-78.4	4274	5047	3324	5353	2523	-561
20150525-04	375	-13.624	-71.842	4062	-14.8	0.0	-110.5	0.2	8.3	-78.9	4292	5070	3337	5378	2534	-230
20150612-04	368	-13.698	-71.809	4108	-15.5	0.1	-115.4	0.3	8.3	-83.8	4431	5248	3434	5573	2621	-323
20160722-11	369	-13.641	-71.904	3805	-14.6	0.0	-108.4	0.3	8.3	-76.8	4227	4987	3292	5288	2494	-422
20160725-06	397	-13.762	-71.223	4664	-15.0	0.0	-111.3	0.4	8.4	-79.7	4313	5097	3351	5408	2547	351
20150616-02	354	-13.776	-71.923	3967	-14.8	0.0	-109.6	0.4	8.4	-78.0	4263	5034	3317	5338	2516	-296
20150517-01	370	-13.621	-71.938	3939	-15.2	0.1	-112.7	0.3	8.7	-81.1	4356	5152	3382	5469	2574	-418
20150618-14	198	-15.319	-72.126	4800	-17.0	0.0	-126.9	0.3	8.8	-95.3	4732	5630	3649	5989	2816	68
20150610-09	339	-14.463	-71.061	4348	-15.7	0.0	-116.9	0.3	8.9	-85.3	4475	5304	3465	5635	2649	-127
20160725-04	399	-13.729	-71.236	4512	-15.4	0.1	-114.2	0.4	9.0	-82.6	4397	5205	3410	5525	2599	115
20160722-07	370	-13.659	-71.852	4143	-15.1	0.0	-111.8	0.2	9.1	-80.2	4328	5116	3362	5429	2556	-185
20160726-01	334	-14.363	-71.316	4062	-16.6	0.1	-124.0	0.4	9.2	-92.4	4660	5540	3597	5891	2768	-598
20150610-10	343	-14.402	-71.189	4391	-15.8	0.1	-117.3	0.4	9.2	-85.7	4485	5318	3473	5649	2655	-94
20160713-11	343	-14.351	-71.119	4357	-15.5	0.0	-115.1	0.3	9.3	-83.5	4423	5238	3429	5562	2616	-66
20150601-06	258	-15.725	-70.373	4093	-15.3	0.0	-113.0	0.2	9.3	-81.4	4362	5160	3386	5477	2578	-270
20160725-05	397	-13.758	-71.214	4730	-15.2	0.1	-112.6	0.4	9.4	-81.0	4351	5146	3378	5461	2570	380
20150618-13	197	-15.336	-72.122	4719	-17.7	0.0	-132.5	0.4	9.5	-100.9	4864	5794	3746	6166	2905	-144
20150610-13	358	-14.026	-71.455	3438	-15.6	0.1	-114.6	0.3	9.8	-83.0	4409	5220	3419	5542	2607	-970
20150517-06	372	-13.641	-71.872	4119	-15.5	0.0	-114.0	0.3	9.9	-82.4	4394	5201	3408	5521	2597	-274
20150612-01	367	-13.717	-71.785	4111	-15.4	0.1	-112.9	0.4	10.2	-81.3	4361	5159	3385	5476	2577	-250
20150613-06	372	-13.489	-72.138	3699	-14.8	0.0	-107.2	0.3	10.9	-75.6	4190	4939	3266	5235	2471	-491
20150618-15	200	-15.312	-72.116	4820	-17.4	0.0	-128.5	0.3	10.9	-96.9	4771	5679	3678	6042	2842	49
20150610-08	342	-14.499	-70.934	4218	-16.3	0.1	-118.5	0.4	11.8	-86.9	4518	5360	3496	5695	2676	-300
20150618-04	197	-15.33	-72.171	4996	-17.7	0.0	-128.1	0.3	13.2	-96.5	4762	5668	3671	6030	2836	233
170511-01*	235	-15.46	-71.28	4432	-2.9	0.2	-93.9	2.4	-70.7	-62.3	3734	4356	2948	4597	2198	698
250511-01*	279	-13.22	-74.31	3728	-6.2	0.2	-93.4	2.4	-43.8	-61.8	3715	4332	2935	4571	2187	13
030611-01*	328	-14.75	-70.7	3994	-9.9	0.2	-99.9	2.4	-20.7	-68.3	3950	4631	3099	4898	2326	44
190510-04*	338	-14.93	-70.22	3983	-6.2	0.2	-68.4	2.4	-18.9	-36.8	2585	2928	2114	3052	1531	1398
210510-04*	410	-14.4	-69.84	4448	-7.5	0.2	-75.2	2.4	-15.2	-43.6	2933	3352	2373	3508	1732	1515
210510-10*	400	-14.56	-69.79	4575	-9.8	0.2	-90.1	2.4	-11.7	-58.5	3588	4170	2845	4395	2112	987
10PE-88w*	216	-15.43	-71.24	4532	-11.0	0.2	-97.0	2.4	-9.0	-65.4	3848	4501	3028	4756	2265	684
10PE-48w*	272	-15.82	-70.09	4017	-11.4	0.2	-100.5	2.4	-8.9	-68.9	3970	4658	3113	4927	2338	47

Table A5 (continued): Modern Water Data and Elevation Modeling

Name	Dist. (km)	Lat. centroid	Long. centroid	MBH (m)	$\delta^{18}\text{O}$		δD		D excess	ΔD (‰)	Model ΔD mean	Topographic Swath b-b'				Resid.
					(‰ vsmow)	Unc. (‰)	(‰ vsmow)	Unc. (‰)				+1 σ	-1 σ	+2 σ	-2 σ	
					(‰)	(‰)	(‰)	(‰)				(‰)	(‰)	(‰)	(‰)	
10PE-66w*	302	-14.71	-71.26	4022	-13.3	0.2	-111.4	2.4	-4.9	-79.8	4317	5102	3354	5414	2549	-295
10PE-37w*	311	-14.93	-70.71	4256	-12.7	0.2	-105.4	2.4	-4.2	-73.8	4132	4866	3226	5155	2436	124
10PE-82w*	234	-15.43	-71.34	4718	-13.1	0.2	-109.1	2.4	-4.2	-77.5	4248	5014	3306	5317	2507	470
10PE-61w*	317	-14.58	-71.27	4145	-13.0	0.2	-107.4	2.4	-3.8	-75.8	4196	4947	3270	5243	2475	-51
10PE-77w*	251	-15.29	-71.19	4814	-13.6	0.2	-112.0	2.4	-3.2	-80.4	4335	5125	3367	5438	2560	479
20140616-03*	409	-14.48	-69.66	4545	-12.5	0.2	-103.1	2.4	-3.2	-71.5	4058	4770	3174	5050	2391	487
10PE-73w*	264	-15.2	-71.16	4630	-14.4	0.2	-118.1	2.4	-3.1	-86.5	4506	5345	3488	5678	2669	124
10PE-68w*	280	-15.04	-71.13	4158	-14.6	0.2	-119.4	2.4	-2.7	-87.8	4541	5389	3512	5727	2691	-383
20140517-03*	247	-15.54	-70.78	4590	-13.4	0.2	-109.8	2.4	-2.4	-78.2	4269	5041	3321	5347	2520	321
10PE-80w*	237	-15.4	-71.3	4295	-14.7	0.2	-120.0	2.4	-2.3	-88.4	4557	5409	3524	5749	2701	-262
10PE-35w*	325	-14.86	-70.61	3980	-12.8	0.2	-104.2	2.4	-2.1	-72.6	4094	4816	3199	5100	2413	-114
10PE-64w*	304	-14.7	-71.29	4019	-14.4	0.2	-117.5	2.4	-1.9	-85.9	4490	5324	3476	5656	2658	-471
20140613-05*	343	-14.61	-70.74	4194	-15.3	0.2	-124.2	2.4	-1.9	-92.6	4666	5547	3601	5898	2772	-472
10PE-81w*	235	-15.41	-71.32	4577	-14.6	0.2	-118.5	2.4	-1.8	-86.9	4517	5358	3495	5693	2676	60
20140615-08*	412	-14.08	-70.36	4651	-14.8	0.2	-119.7	2.4	-1.4	-88.1	4549	5399	3518	5738	2696	102
10PE-45w*	209	-16.26	-70.25	4582	-13.1	0.2	-105.8	2.4	-1.2	-74.2	4145	4882	3235	5173	2444	437
10PE-70w*	273	-15.13	-71.12	4365	-14.5	0.2	-117.2	2.4	-1.2	-85.6	4482	5313	3470	5644	2653	-117
10PE-62w*	314	-14.6	-71.26	4140	-13.9	0.2	-112.5	2.4	-1.1	-80.9	4349	5144	3377	5459	2569	-209
200510-13*	404	-14.09	-70.55	4670	-13.7	0.2	-110.6	2.4	-0.8	-79.0	4293	5072	3338	5380	2535	377
20140516-01*	230	-15.83	-70.69	4410	-14.8	0.2	-118.8	2.4	-0.4	-87.2	4525	5369	3501	5705	2681	-115
10PE-78w*	244	-15.36	-71.22	4637	-14.4	0.2	-115.5	2.4	-0.1	-83.9	4435	5253	3437	5579	2623	202
200511-04*	268	-15.11	-71.19	4601	-17.8	0.2	-142.3	2.4	0.1	-110.7	5077	6054	3910	6443	3057	-476
10PE-67w*	291	-14.9	-71.19	4002	-16.7	0.2	-133.1	2.4	0.2	-101.5	4878	5812	3757	6185	2915	-876
250510-11*	308	-14.79	-71.01	4578	-15.0	0.2	-120.0	2.4	0.3	-88.4	4557	5409	3524	5749	2701	21
10PE-69w*	275	-15.12	-71.13	4400	-14.7	0.2	-116.7	2.4	0.5	-85.1	4468	5296	3461	5625	2644	-68
200510-14*	406	-14.09	-70.5	4548	-14.6	0.2	-116.0	2.4	0.5	-84.4	4449	5271	3447	5598	2632	99
NPWS007*	376	-14.26	-70.54	4641	-16.6	0.2	-132.0	2.4	0.5	-100.4	4853	5781	3739	6152	2898	-212
10PE-14w*	363	-13.76	-71.83	3455	-13.7	0.2	-109.1	2.4	0.6	-77.5	4248	5014	3306	5317	2507	-793
10PE-74w*	263	-15.22	-71.16	4763	-14.4	0.2	-114.5	2.4	0.6	-82.9	4407	5217	3417	5539	2605	356
10PE-71w*	269	-15.14	-71.15	4594	-15.7	0.2	-124.2	2.4	1.0	-92.6	4666	5547	3601	5898	2772	-72
10PE-63w*	311	-14.63	-71.28	4075	-15.0	0.2	-118.9	2.4	1.1	-87.3	4528	5372	3503	5708	2683	-453
10PE-11w*	360	-13.8	-71.86	3540	-13.7	0.2	-108.0	2.4	1.6	-76.4	4214	4970	3283	5269	2486	-674
20140615-02*	405	-14.08	-70.59	4735	-15.8	0.2	-124.6	2.4	1.9	-93.0	4676	5559	3609	5912	2779	59
20140517-04*	246	-15.65	-70.73	4468	-15.1	0.2	-118.4	2.4	2.1	-86.8	4515	5355	3493	5690	2674	-47
10PE-40w*	231	-16.16	-70.12	4173	-13.9	0.2	-108.9	2.4	2.2	-77.3	4242	5006	3302	5308	2503	-69
20140517-01*	229	-15.9	-70.57	4257	-16.0	0.2	-126.0	2.4	2.2	-94.4	4710	5603	3634	5959	2802	-453
10PE-17w*	372	-13.65	-71.85	4213	-14.7	0.2	-115.1	2.4	2.3	-83.5	4424	5239	3429	5563	2616	-211
10PE-65w*	295	-14.72	-71.35	4015	-16.3	0.2	-127.9	2.4	2.4	-96.3	4757	5661	3667	6022	2833	-742
NPWS001*	313	-15.1	-70.6	4339	-16.3	0.2	-128.0	2.4	2.4	-96.4	4759	5664	3669	6025	2834	-420
210510-01*	410	-14.15	-70.34	4775	-15.1	0.2	-118.3	2.4	2.5	-86.7	4512	5351	3491	5686	2672	263
20140613-08*	376	-14.39	-70.51	4536	-15.8	0.2	-123.9	2.4	2.6	-92.3	4658	5537	3596	5888	2767	-122
200510-09*	406	-14.11	-70.55	4765	-15.0	0.2	-117.3	2.4	2.8	-85.7	4485	5317	3472	5648	2655	280
20140613-06*	357	-14.49	-70.69	4215	-15.9	0.2	-124.5	2.4	2.8	-92.9	4673	5556	3607	5909	2777	-458
200510-04*	415	-14.01	-70.43	4578	-15.4	0.2	-119.8	2.4	3.1	-88.2	4552	5403	3520	5742	2698	26
10PE-42w*	221	-16.31	-70.14	4398	-14.3	0.2	-111.0	2.4	3.4	-79.4	4305	5087	3346	5397	2542	93
030611-09*	375	-13.78	-71.54	3903	-15.2	0.2	-117.9	2.4	3.5	-86.3	4501	5338	3484	5671	2665	-598
200511-07*	289	-14.99	-71.1	4286	-19.0	0.2	-148.5	2.4	3.5	-116.9	5201	6200	4009	6598	3149	-915
220510-16*	334	-14.69	-70.67	4227	-15.4	0.2	-119.5	2.4	3.5	-87.9	4544	5392	3514	5731	2693	-317
10PE-36w*	324	-15.06	-70.43	4075	-15.4	0.2	-119.2	2.4	3.6	-87.6	4536	5382	3509	5719	2688	-461
20140613-07*	361	-14.3	-70.79	4667	-16.4	0.2	-127.8	2.4	3.6	-96.2	4754	5658	3666	6019	2831	-87
10PE-58w*	323	-14.51	-71.26	4173	-16.6	0.2	-129.4	2.4	3.7	-97.8	4792	5706	3694	6071	2857	-619
10PE-57w*	325	-14.46	-71.3	4349	-16.5	0.2	-127.9	2.4	3.8	-96.3	4757	5661	3667	6022	2833	-408
10PE-59w*	321	-14.52	-71.28	4178	-15.7	0.2	-122.0	2.4	3.9	-90.4	4610	5476	3561	5821	2735	-432
10PE-04w*	376	-13.58	-71.98	3816	-15.1	0.2	-117.0	2.4	4.0	-85.4	4476	5306	3466	5637	2650	-660
10PE-39w*	257	-15.92	-70.01	4096	-14.9	0.2	-115.2	2.4	4.0	-83.6	4426	5242	3431	5567	2618	-330
20140613-09*	397	-14.2	-70.47	4791	-16.4	0.2	-127.1	2.4	4.1	-95.5	4737	5637	3653	5996	2820	54
10PE-75w*	261	-15.25	-71.17	4826	-17.2	0.2	-133.4	2.4	4.2	-101.8	4885	5820	3762	6194	2920	-59
10PE-76w*	255	-15.29	-71.16	4800	-16.5	0.2	-127.7	2.4	4.2	-96.1	4752	5655	3664	6016	2829	48
20140613-10*	405	-14.15	-70.49	4687	-16.3	0.2	-126.6	2.4	4.2	-95.0	4725	5621	3644	5979	2811	-38
NPWS006*	370	-14.27	-70.65	4634	-16.7	0.2	-129.4	2.4	4.2	-97.8	4792	5706	3694	6071	2857	-158
10PE-86w*	223	-15.47	-71.36	4529	-14.8	0.2	-114.4	2.4	4.3	-82.8	4404	5213	3415	5535	2604	125

Table A5 (continued): Modern Water Data and Elevation Modeling

Name	Dist. (km)	Lat. centroid	Long. centroid	MBH (m)	δ18O		δD		D	ΔD	Model ΔD	Topographic Swath b-b'				Resid.
					(‰ vsmow)	Unc. (‰)	(‰ vsmow)	Unc. (‰)				excess	(‰)	mean	+1σ	
190510-03*	305	-15.32	-70.25	4121	-14.8	0.2	-113.9	2.4	4.3	-82.3	4390	5195	3405	5515	2595	-269
20140616-01*	413	-14.16	-70.13	4700	-16.0	0.2	-123.9	2.4	4.4	-92.3	4658	5537	3596	5888	2767	42
NPWS008*	396	-14.21	-70.48	4788	-18.1	0.2	-140.3	2.4	4.5	-108.7	5035	6004	3877	6390	3026	-247
10PE-46w*	201	-16.34	-70.32	4687	-14.9	0.2	-115.0	2.4	4.6	-83.4	4421	5235	3427	5559	2614	266
20140613-01*	382	-13.96	-71.5	4016	-15.8	0.2	-121.6	2.4	4.7	-90.0	4599	5463	3554	5807	2729	-583
20140615-05*	397	-14.1	-70.67	4941	-16.4	0.2	-126.5	2.4	4.7	-94.9	4723	5618	3643	5976	2810	218
10PE-52w*	337	-14.38	-71.32	4182	-16.0	0.2	-122.9	2.4	4.8	-91.3	4633	5505	3578	5853	2750	-451
20140613-03*	352	-14.06	-71.05	4714	-16.5	0.2	-127.0	2.4	4.8	-95.4	4735	5634	3652	5993	2818	-21
030611-02*	340	-14.58	-70.8	4415	-16.6	0.2	-127.9	2.4	4.9	-96.3	4757	5661	3667	6022	2833	-342
10PE-41w*	226	-16.21	-70.11	4266	-14.8	0.2	-113.8	2.4	4.9	-82.2	4387	5192	3403	5511	2593	-121
10PE-07w*	366	-13.67	-71.9	3824	-14.9	0.2	-114.5	2.4	5.0	-82.9	4407	5217	3417	5539	2605	-583
10PE-19w*	377	-13.6	-71.86	3815	-15.6	0.2	-119.8	2.4	5.0	-88.2	4552	5403	3520	5742	2698	-737
10PE-21w*	382	-13.68	-71.57	3955	-15.3	0.2	-117.3	2.4	5.0	-85.7	4485	5317	3472	5648	2655	-530
20140517-02*	232	-15.86	-70.63	4363	-16.7	0.2	-128.3	2.4	5.0	-96.7	4766	5673	3674	6035	2839	-403
10PE-34w*	326	-14.8	-70.69	3955	-15.2	0.2	-116.1	2.4	5.1	-84.5	4452	5275	3449	5602	2634	-497
20140603-03*	362	-13.72	-71.81	3825	-15.8	0.2	-121.2	2.4	5.1	-89.6	4589	5449	3546	5793	2722	-764
10PE-13w*	362	-13.76	-71.83	3279	-14.8	0.2	-113.2	2.4	5.2	-81.6	4369	5170	3391	5487	2582	-1090
10PE-51w*	340	-14.33	-71.28	3862	-16.8	0.2	-129.1	2.4	5.2	-97.5	4785	5697	3688	6061	2852	-923
200510-12*	403	-14.08	-70.58	4634	-15.9	0.2	-122.3	2.4	5.3	-90.7	4617	5485	3567	5832	2740	17
10PE-44w*	214	-16.28	-70.21	4455	-14.9	0.2	-114.0	2.4	5.4	-82.4	4392	5199	3407	5519	2596	63
10PE-72w*	266	-15.18	-71.15	4551	-16.7	0.2	-128.2	2.4	5.4	-96.6	4764	5670	3673	6032	2837	-213
10PE-85w*	224	-15.47	-71.38	4594	-15.0	0.2	-114.7	2.4	5.4	-83.1	4412	5224	3421	5547	2609	182
20140613-02*	358	-13.92	-71.25	4655	-16.7	0.2	-128.5	2.4	5.4	-96.9	4771	5679	3678	6042	2842	-116
10PE-43w*	216	-16.29	-70.18	4433	-15.1	0.2	-114.9	2.4	5.5	-83.3	4418	5232	3425	5555	2613	15
10PE-54w*	331	-14.39	-71.33	4036	-16.2	0.2	-123.8	2.4	5.5	-92.2	4656	5534	3594	5884	2765	-620
220510-02*	329	-14.82	-70.59	4276	-15.7	0.2	-119.6	2.4	5.6	-88.0	4547	5396	3516	5734	2695	-271
20140615-04*	397	-14.13	-70.61	4884	-16.7	0.2	-127.6	2.4	5.7	-96.0	4749	5652	3662	6012	2828	135
20140615-03*	402	-14.06	-70.62	4817	-16.7	0.2	-128.1	2.4	5.8	-96.5	4761	5667	3671	6029	2836	56
10PE-38w*	305	-15.32	-70.25	4113	-15.3	0.2	-115.7	2.4	6.3	-84.1	4440	5260	3441	5586	2627	-327
10PE-83w*	230	-15.44	-71.35	4762	-16.9	0.2	-129.0	2.4	6.3	-97.4	4783	5694	3687	6058	2850	-21
10PE-22w*	375	-13.79	-71.53	3893	-15.2	0.2	-115.2	2.4	6.4	-83.6	4426	5242	3431	5567	2618	-533
10PE-06w*	373	-13.6	-71.91	3912	-16.0	0.2	-121.5	2.4	6.5	-89.9	4597	5459	3552	5803	2727	-685
10PE-18w*	376	-13.6	-71.87	3847	-15.9	0.2	-121.0	2.4	6.5	-89.4	4584	5443	3542	5785	2718	-737
10PE-90w*	194	-15.67	-71.63	3888	-15.4	0.2	-116.9	2.4	6.5	-85.3	4474	5303	3464	5633	2648	-586
220510-05*	330	-14.82	-70.55	4404	-16.0	0.2	-121.6	2.4	6.5	-90.0	4599	5463	3554	5807	2729	-195
10PE-03w*	379	-13.5	-71.98	3711	-15.8	0.2	-119.3	2.4	7.0	-87.7	4539	5386	3510	5723	2689	-828
10PE-01w*	386	-13.51	-71.84	4212	-16.1	0.2	-121.7	2.4	7.3	-90.1	4602	5466	3555	5810	2730	-390
10PE-50w*	343	-14.33	-71.24	3981	-17.2	0.2	-129.9	2.4	7.5	-98.3	4804	5720	3702	6086	2865	-823
250510-05*	316	-14.76	-70.96	4464	-17.0	0.2	-128.6	2.4	7.5	-97.0	4773	5682	3680	6045	2844	-309
10PE-16w*	370	-13.66	-71.84	4234	-15.9	0.2	-119.9	2.4	7.7	-88.3	4555	5406	3522	5745	2700	-321
030611-08*	371	-13.85	-71.51	3757	-15.9	0.2	-119.5	2.4	7.9	-87.9	4544	5392	3514	5731	2693	-787
10PE-53w*	334	-14.35	-71.32	4252	-17.6	0.2	-133.2	2.4	7.9	-101.6	4880	5815	3759	6188	2917	-628
10PE-25w*	351	-14.12	-71.4	3939	-16.6	0.2	-124.8	2.4	8.0	-93.2	4681	5566	3612	5919	2782	-742
10PE-09w*	364	-13.71	-71.87	3903	-15.8	0.2	-117.9	2.4	8.3	-86.3	4501	5338	3484	5671	2665	-598
10PE-02w*	378	-13.48	-72	3900	-15.9	0.2	-118.9	2.4	8.4	-87.3	4528	5372	3503	5708	2683	-628
10PE-24w*	355	-14.06	-71.43	3989	-16.2	0.2	-121.1	2.4	8.4	-89.5	4586	5446	3544	5789	2720	-597
10PE-56w*	327	-14.45	-71.3	4381	-18.2	0.2	-137.3	2.4	8.6	-105.7	4971	5926	3828	6308	2981	-590
10PE-27w*	343	-14.36	-71.22	4147	-17.1	0.2	-128.5	2.4	8.7	-96.9	4771	5679	3678	6042	2842	-624
280511-01*	317	-13.71	-73.25	4113	-17.8	0.2	-133.8	2.4	8.7	-102.2	4894	5831	3769	6206	2926	-781
10PE-28w*	340	-14.42	-71.15	4471	-17.1	0.2	-127.9	2.4	8.8	-96.3	4757	5661	3667	6022	2833	-286
10PE-20w*	380	-13.7	-71.71	3852	-16.0	0.2	-118.8	2.4	8.9	-87.2	4525	5369	3501	5705	2681	-673
20140613-04*	343	-14.45	-70.93	4799	-17.5	0.2	-131.3	2.4	8.9	-99.7	4837	5761	3727	6130	2887	-38
10PE-89w*	205	-15.52	-71.63	4686	-16.4	0.2	-121.5	2.4	9.3	-89.9	4597	5459	3552	5803	2727	89
10PE-87w*	220	-15.51	-71.43	3982	-17.8	0.2	-132.6	2.4	9.4	-101.0	4867	5798	3749	6170	2908	-885
NPWS002*	337	-14.74	-70.61	4187	-17.2	0.2	-128.6	2.4	9.4	-97.0	4773	5682	3680	6045	2844	-586
210510-02*	407	-14.19	-70.32	4851	-16.9	0.2	-125.7	2.4	9.5	-94.1	4703	5594	3628	5949	2797	148
10PE-32w*	340	-14.56	-70.9	4415	-15.9	0.2	-117.1	2.4	10.2	-85.5	4479	5310	3468	5640	2651	-64
NPWS003*	341	-14.71	-70.6	4353	-17.7	0.2	-131.4	2.4	10.2	-99.8	4839	5764	3728	6133	2889	-486
10PE-08w*	365	-13.68	-71.89	4074	-15.9	0.2	-116.7	2.4	10.3	-85.1	4468	5296	3461	5625	2644	-394
10PE-92w*	189	-15.6	-71.74	4092	-16.9	0.2	-124.5	2.4	10.3	-92.9	4673	5556	3607	5909	2777	-581
10PE-91w*	189	-15.67	-71.72	3753	-17.6	0.2	-129.7	2.4	10.8	-98.1	4800	5714	3699	6080	2862	-1047

Table A5 (continued): Modern Water Data and Elevation Modeling

Name	Dist. (km)	Lat. centroid	Long. centroid	MBH (m)	$\delta^{18}\text{O}$		δD		D excess	ΔD (‰)	Model ΔD mean	+1 σ	-1 σ	+2 σ	-2 σ	Resid.
					(‰)	Unc. (‰)	(‰)	Unc. (‰)								
Topographic Swath b-b'																
210510-03*	407	-14.2	-70.3	4797	-17.6	0.2	-129.5	2.4	11.3	-97.9	4795	5709	3695	6074	2858	2
200511-05*	272	-15.05	-71.26	4661	-19.6	0.2	-144.2	2.4	12.6	-112.6	5116	6100	3940	6492	3085	-455
NPWS004*	344	-14.67	-70.62	4420	-17.9	0.2	-130.6	2.4	12.6	-99.0	4821	5741	3714	6108	2876	-401
10PE-29w*	340	-14.45	-71.12	4532	-17.9	0.2	-129.5	2.4	13.3	-97.9	4795	5709	3695	6074	2858	-263
10PE-84w*	228	-15.45	-71.37	4757	-19.0	0.2	-138.2	2.4	13.9	-106.6	4991	5950	3843	6333	2994	-234
10PE-31w*	342	-14.49	-70.91	4691	-17.9	0.2	-128.2	2.4	14.7	-96.6	4764	5670	3673	6032	2837	-73
280511-02*	315	-13.69	-73.24	4000	-19.3	0.2	-139.6	2.4	15.1	-108.0	5021	5986	3866	6371	3016	-1021
NPWS009*	433	-13.92	-70.66	4674	-17.7	0.2	-126.0	2.4	15.6	-94.4	4710	5603	3634	5959	2802	-36
030611-03*	341	-14.5	-70.97	4648	-18.7	0.2	-133.2	2.4	16.3	-101.6	4880	5815	3759	6188	2917	-232
10PE-30w*	340	-14.44	-70.99	4897	-18.1	0.2	-127.8	2.4	16.9	-96.2	4754	5658	3666	6019	2831	143
030611-06*	338	-14.48	-71.07	4398	-19.3	0.2	-135.8	2.4	18.8	-104.2	4939	5886	3803	6265	2958	-541

*Published in Bershaw et al. (2016)

New data uncertainties are calculated as weighted mean

APPENDIX 6

Table A6: Volcanic Glass Stable Isotope Data and Modeling

Name	Region	Latitude	Longitude	Age	Unc.	Source	δD		%		Model		
							mean	$\pm 1\sigma$	water	$\pm 1\sigma$	ΔD mean	$+1\sigma$	-1σ
250511-04	Ayacucho	-13.25116	-74.31618	18.3	0.60	Mckee et al. (1982)	-102	4	4.2	1.5	1263	122	191
250511-05	Ayacucho	-13.24334	-74.30232	20.18	0.87	<i>This study</i>	-125	2	5.2	0.2	2739	376	509
250511-06	Ayacucho	-13.24135	-74.30220	19.95	0.73	<i>This study</i>	-150	0	4.9	0.1	3844	652	819
250511-08	Ayacucho	-13.15533	-74.29870	12.7	1.70	<i>This study</i>	-121	1	4.2	0.2	2726	373	506
260511-01	Ayacucho	-13.04543	-74.22831	7.86	0.78	<i>This study</i>	-94	1	2.7	0.1	1492	153	233
260511-02	Ayacucho	-13.06567	-74.21992	7.37	0.77	<i>This study</i>	-112	2	4.6	0.3	2680	363	495
260511-03	Ayacucho	-13.08577	-74.17943	3.8	0.40	Megard et al. (1984)	-90	1	6.8	0.1	1677	180	269
20140519-09	Puquio	-14.63479	-73.98485	1.6	0.26	Brandmeier (2014)	-140	3	3.5	0.1	4226	760	935
20140520-01	Puquio	-14.22764	-73.52923	7.5	0.75	Brandmeier (2014)*	-156	5	3.8	0.3	4414	812	991
20140520-02	Puquio	-14.22816	-73.52982	6.5	0.65	Brandmeier (2014)*	-156	2	2.9	0.6	4485	832	1013
20140520-09	Puquio	-14.19940	-73.54129	7.8	0.08	Brandmeier (2014)	-147	9	2.5	0.3	4142	736	910
20140521-02	Puquio	-14.22476	-73.53180	6.2	0.04	Brandmeier (2014)	-162	3	3.3	0.2	4654	878	1061
20140522-01	Puquio	-14.36081	-73.90359	13.6	1.36	Brandmeier (2014)*	-99	6	7.2	1.4	1245	119	188
20140522-02	Puquio	-14.35347	-73.90674	14.1	0.05	Brandmeier (2014)	-150	7	3.9	0.2	3892	665	834
20140522-03	Puquio	-14.34938	-73.90884	14.0	0.04	Brandmeier (2014)	-149	4	7.2	0.3	3864	657	825
20140522-04	Puquio	-14.34483	-73.90955	9.5	0.10	Brandmeier (2014)	-157	2	4.5	0.5	4360	798	976
20140522-05	Puquio	-14.34836	-73.90984	9.5	0.10	Brandmeier (2014)	-153	9	4.4	0.3	4260	769	945
20140522-06	Puquio	-14.40742	-73.95724	9.4	0.07	Brandmeier (2014)	-114	4	6.9	0.2	2613	349	478
20140522-09	Puquio	-14.44791	-73.93172	4.1	0.41	Brandmeier (2014)*	-117	12	2.1	0.8	3187	479	628
20140522-14	Puquio	-14.59772	-73.57986	4.1	0.41	Brandmeier (2014)*	-157	4	3.2	0.2	4616	868	1050
20140523-03	Puquio	-14.55647	-73.56144	9.1	0.91	Brandmeier (2014)*	-156	1	4.2	0.3	4370	800	979
20140524-03	Puquio	-14.55609	-73.56473	1.7	0.17	Brandmeier (2014)*	-152	3	1.3	0.1	4570	855	1037
20140524-05	Puquio	-14.58327	-73.56971	20.1	0.11	Brandmeier (2014)	-143	4	1.4	0.3	3559	575	734
20140525-01	Puquio	-14.57230	-73.56469	21.6	2.16	Brandmeier (2014)*	-175	3	7.1	0.6	4624	870	1053
260510-07	W. Cordillera	-14.67895	-71.44749	24.1	1.10	<i>This study</i>	-105	1			1504	154	235
270510-01	W. Cordillera	-15.43290	-71.25306	18.5	1.10	<i>This study</i>	-107	9			1652	176	264
270510-05	W. Cordillera	-15.43228	-71.25548	16.46	0.53	<i>This study</i>	-141	6			3499	559	717
270510-06	W. Cordillera	-15.43258	-71.25596	16.69	0.37	<i>This study</i>	-138	6			3373	526	681
270510-14	W. Cordillera	-15.43813	-71.26418	12.82	0.34	<i>This study</i>	-125	8			2932	419	560
270510-17	W. Cordillera	-15.38864	-71.29449	4.92	0.13	<i>This study</i>	-160	4			4660	879	1063
180511-03 ^D	W. Cordillera	-15.42387	-71.26591	4.8	0.60	Saylor and Horton (2014)	-157	4	2.7	0.1	4578	857	1039
1HUA36 ^D	W. Cordillera	-15.42387	-71.26591	18.9	1.36	Saylor and Horton (2014)	-99	4	6.5		1061	97	156
1HUA96 ^D	W. Cordillera	-15.42387	-71.26591	18.3	1.47	Saylor and Horton (2014)	-103	5	8.9	0.0	1316	129	200
1HUA195 ^D	W. Cordillera	-15.42387	-71.26591	17.5	1.66	Saylor and Horton (2014)	-104	4	6.7	0.0	1429	144	221
1HUA218 ^D	W. Cordillera	-15.42387	-71.26591	17.3	1.70	Saylor and Horton (2014)	-181	8	4.4	0.0	4789	912	1098
1HUA231 ^D	W. Cordillera	-15.42387	-71.26591	17.2	1.73	Saylor and Horton (2014)	-169	5	4.3	0.0	4475	830	1010
1HUA260 ^D	W. Cordillera	-15.42387	-71.26591	16.7	1.82	Saylor and Horton (2014)	-168	10	3.6	0.4	4454	824	1004
1HUA293.5 ^D	W. Cordillera	-15.42387	-71.26591	16.6	1.84	Saylor and Horton (2014)	-100	4	8.5	0.0	1154	108	172
1HUA377.5 ^D	W. Cordillera	-15.42387	-71.26591	15.9	2.00	Saylor and Horton (2014)	-155	7	5.3	0.0	4015	700	871
2HUA30 ^D	W. Cordillera	-15.42387	-71.26591	13.6	2.49	Saylor and Horton (2014)	-153	5	4.1	0.0	4041	707	879
2HUA279 ^D	W. Cordillera	-15.42387	-71.26591	11.5	2.94	Saylor and Horton (2014)	-157	5	3.5	0.0	4283	776	952
1HSL18 ^D	W. Cordillera	-15.42387	-71.26591	19.7	0.30	Saylor and Horton (2014)	-100	4	8.8	0.2	1136	106	168
1HSL147 ^D	W. Cordillera	-15.42387	-71.26591	18.4	0.38	Saylor and Horton (2014)	-179	8	3.6	0.0	4738	899	1084
1HSL164 ^D	W. Cordillera	-15.42387	-71.26591	18.2	0.39	Saylor and Horton (2014)	-179	6	9.6	0.0	4742	901	1085
1HSL180 ^D	W. Cordillera	-15.42387	-71.26591	18.1	0.40	Saylor and Horton (2014)	-159	7	3.2	0.0	4166	743	917
1HSL270 ^D	W. Cordillera	-15.42387	-71.26591	17.2	0.45	Saylor and Horton (2014)	-166	5	3.3	0.0	4369	800	978
1HSL658 ^D	W. Cordillera	-15.42387	-71.26591	12.3	0.74	Saylor and Horton (2014)	-174	10	3.1	0.0	4710	892	1077
1HSL674 ^D	W. Cordillera	-15.42387	-71.26591	12.1	0.75	Saylor and Horton (2014)	-174	11	3.9	0.3	4729	897	1082
20140704-01	W. Cordillera	-16.00054	-70.66100	0.468	0.09	<i>This study</i>	-150	5	4.2	0.3	4559	852	1034
20140704-02	W. Cordillera	-15.99656	-70.66212	21.57	0.47	<i>This study</i>	-86	3	4.4	0.2	-50	-3	6
20140704-05	W. Cordillera	-15.98917	-70.64524	22.72	0.61	<i>This study</i>	-97	1	6.7	1.0	889	77	127
20140705-02	W. Cordillera	-15.96880	-70.62931	24.8	0.46	<i>This study</i>	-93	2	4.2	0.0	553	44	75
20150604-06	W. Cordillera	-15.95190	-70.62348	24.32	0.40	<i>This study</i>	-83	2	3.4	0.2	-379	-22	44
20150604-07	W. Cordillera	-15.95130	-70.62373	23.09	0.52	<i>This study</i>	-94	2	3.5	0.3	629	51	86
20150605-04	W. Cordillera	-15.96497	-70.62972	21.8	1.10	<i>This study</i>	-102	4	10.5	0.6	1313	128	200
20150607-09	W. Cordillera	-15.97806	-70.65587	20.76	0.50	<i>This study</i>	-107	2	10.5	0.6	1621	172	258
20150609-07	W. Cordillera	-16.34977	-70.26051	13.5	0.06	Rousse et al. (2005)	-100	2	1.3	0.1	1311	128	199
20150609-09	W. Cordillera	-16.33693	-70.25519	10.8	0.36	Rousse et al. (2005)	-167	5	4.2	0.6	4601	864	1046
20150609-10	W. Cordillera	-16.39018	-70.30654	13.8	2.30	<i>This study</i>	-102	5	5.9	0.2	1381	137	212
20150609-11	W. Cordillera	-16.40692	-70.32569	9.54	0.33	<i>This study</i>	-104	2	6.0	0.6	2006	233	337
20160814-01	W. Cordillera	-16.67756	-70.42667	7.77	0.38	<i>This study</i>	-150	1	2.8	0.4	4220	758	933
20160814-04	W. Cordillera	-16.61442	-70.40779	13.41	0.65	<i>This study</i>	-113	5	6.3	0.2	2158	260	371
20160814-09	W. Cordillera	-16.34275	-70.25919	11.5	1.30	(same as 20160814-09)	-97	6	2.3	0.1	1345	133	206
20160814-12	W. Cordillera	-16.34186	-70.25880	11.5	1.30	<i>This study</i>	-119	2	4.9	0.9	2681	363	495
20150618-03	W. Cordillera	-15.32639	-72.10356	21.63	0.80	<i>This study</i>	-99	4	6.1	0.3	1039	94	152

Table A6 (continued): Volcanic Glass Stable Isotope Data and Modeling

Name	Region	Latitude	Longitude	Age	Unc.	Source	δD		%		Model		
							mean	±1σ	water	±1σ	ΔD mean	+1σ	-1σ
20150618-07	W. Cordillera	-15.33417	-72.14311	10.94	0.49	<i>This study</i>	-105	6	7.3	1.8	1955	225	326
20160815-15	W. Cordillera	-15.52047	-71.05310	4.84	0.09	<i>This study</i>	-157	3	3.5	0.2	4584	859	1041
240510-11	Altiplano	-14.98458	-70.57380	16.58	0.26	<i>This study</i>	-99	0			1051	96	154
250510-12	Altiplano	-14.50358	-71.31794	12.5	0.85	<i>This study</i>	-136	7			3436	542	699
260510-03	Altiplano	-14.77557	-71.38915	4.76	0.21	<i>This study</i>	-145	3			4210	755	930
260510-04	Altiplano	-14.77615	-71.38984	5.4	1.00	Kar et al. (2016)	-153	2			4427	816	996
20140605-02	Altiplano	-13.75969	-71.82277	9.0	0.50	Sundell et al. (in review)	-158	4	4.7	0.6	4406	810	989
20160813-01	Altiplano	-16.56592	-69.26952	10.23	0.28	<i>This study</i>	-164	3	4.4	0.2	4527	844	1025
20160815-01	Altiplano	-15.78021	-70.18140	11.8	1.30	<i>This study</i>	-96	3	3.4	0.4	1195	113	179
20160815-08	Altiplano	-15.69212	-70.58463	16.4	0.25	<i>This study</i>	-106	1	4.1	0.1	1544	160	243
20160815-11	Altiplano	-15.65934	-70.75200	19.7	1.00	<i>This study</i>	-98	3	5.3	0.1	993	89	144
20160816-02	Altiplano	-14.74130	-71.35371	9.87	0.19	<i>This study</i>	-180	1	4.8	0.3	4957	952	1140
20160816-03	Altiplano	-14.73861	-71.34513	9.21	0.77	<i>This study</i>	-172	3	4.7	0.5	4776	909	1095
20160816-04	Altiplano	-14.70281	-71.29742	9.96	0.81	(same as 20160816-06)	-146	3	4.5	0.6	4000	696	866
20160816-06	Altiplano	-14.70281	-71.29742	9.96	0.81	<i>This study</i>	-129	5	6.0	0.3	3291	505	657
20160816-10	Altiplano	-14.55070	-71.28957	11.38	0.32	<i>This study</i>	-158	3	4.8	0.4	4323	787	964
20160816-11	Altiplano	-14.51944	-71.29822	11.92	0.43	<i>This study</i>	-136	4	5.6	0.5	3505	560	719
20160816-12	Altiplano	-14.51238	-71.29593	11.85	0.19	<i>This study</i>	-109	6	7.5	0.4	2082	247	354
20160816-13	Altiplano	-14.49945	-71.28673	17.32	0.27	<i>This study</i>	-162	1	4.1	0.2	4275	773	950
200510-01	E. Cordillera	-14.02682	-70.45158	7.1	1.40	<i>This study</i>	-157	6	3.3	0.0	4477	830	1010
200510-02	E. Cordillera	-14.00354	-70.47761	7.0	1.00	Cheilletz et al. (1992)	-118	3	1.9	0.0	3010	437	580
200510-03	E. Cordillera	-14.00045	-70.47548	8.4	2.80	<i>This study</i>	-165	5	2.9	0.0	4639	874	1057
200510-05B	E. Cordillera	-14.01198	-70.48231	7.0	0.40	Cheilletz et al. (1992)	-120	6	1.7	0.0	3097	458	604
200510-05C	E. Cordillera	-14.01198	-70.48231	7.0	0.40	Cheilletz et al. (1992)	-117	5			2945	422	563
200510-06	E. Cordillera	-14.00664	-70.49962	6.7	0.20	Cheilletz et al. (1992)	-121	2	2.1	0.0	3184	479	628
200510-08	E. Cordillera	-14.07759	-70.50999	11.43	0.84	<i>This study</i>	-126	3			3072	452	597
200510-10	E. Cordillera	-14.07396	-70.56786	24.81	0.68	<i>This study</i>	-116	6			2211	270	383
210510-06	E. Cordillera	-14.45669	-69.76513	16.8	0.25	Sandeman et al. (1997)	-102	5	1.5	0.0	1264	122	191
210510-07	E. Cordillera	-14.49803	-69.77648	16.3	0.60	Sandeman et al. (1997)	-111	8	1.1	0.0	1877	212	310
210510-08	E. Cordillera	-14.51031	-69.78364	16.3	0.19	Sandeman et al. (1997)	-103	4	4.4	0.0	1379	137	212
210510-09	E. Cordillera	-14.55688	-69.80115	24.0	0.07	Clark et al., 1990	-85	5	3.1	0.0	-147	-9	18
20140614-01	E. Cordillera	-13.94288	-70.48859	10.4	0.10	Cheilletz et al. (1992)	-167	1	3.4	0.2	4601	864	1046
20140614-02	E. Cordillera	-13.95821	-70.49047	7.8	0.20	Cheilletz et al. (1992)	-179	1	2.5	0.2	4989	959	1148
20140614-03	E. Cordillera	-13.95609	-70.49118	7.8	0.40	Cheilletz et al. (1992)	-176	2	2.4	0.3	4921	944	1131
20140615-01	E. Cordillera	-14.07596	-70.52057	9.9	0.80	Cheilletz et al. (1992)	-117	1	1.1	0.1	2702	368	500
20140616-05	E. Cordillera	-14.58737	-69.72206	16.9	0.28	Sandeman et al. (1997)	-138	3	2.1	0.2	3348	520	674
20140519-06**	Puquio	-14.67700	-74.10950				-77	1	0.8	0.1			
20140519-07**	Puquio	-14.68853	-74.07744				-69	3	0.3	0.0			
20140519-10**	Puquio	-14.64041	-73.71594				-89	12	0.1	0.0			
20140520-03**	Puquio	-14.22850	-73.53014				-39	20	0.0	0.0			
20140520-04**	Puquio	-14.22866	-73.53017				-81	0	0.2	0.0			
20140520-05**	Puquio	-14.22891	-73.53044				-80	4	1.0	0.4			
20140520-06**	Puquio	-14.23038	-73.52910				-91	4	0.2	0.0			
20140520-07**	Puquio	-14.17155	-73.54774				-85	1	0.2	0.0			
20140521-04**	Puquio	-14.23014	-73.53105				-95	10	0.8	0.0			
20140522-10**	Puquio	-14.45042	-73.93868				-58	13	0.1	0.0			
20140523-02**	Puquio	-14.55732	-73.56054				-99	2	0.2	0.0			
20140523-04**	Puquio	-14.55637	-73.56277				-92	5	0.6	0.0			
20140524-01**	Puquio	-14.55605	-73.56327				-74	6	0.4	0.0			
20140524-02**	Puquio	-14.55587	-73.56386				-102	0	0.8	0.2			
20140524-04**	Puquio	-14.55444	-73.56687				-78	6	0.1	0.0			
20140524-06**	Puquio	-14.58316	-73.56942				-85	19	0.0	0.0			
20150616-12**	W. Cordillera	-14.25144	-72.03475				-108	21	0.1	0.0			
20150616-17**	W. Cordillera	-14.49362	-72.09524				-80	28	0.2	0.0			
20150617-02**	W. Cordillera	-14.46323	-72.10210				-84	5	0.3	0.0			
20160815-12**	W. Cordillera	-15.75511	-71.01225				-122	12	0.1	0.0			
20160815-17**	W. Cordillera	-15.01989	-71.30707				-80	12	0.5	0.0			
1HUA1**D	W. Cordillera	-15.42387	-71.26591				-111	8	0.4	0.1			
20140704-04**	W. Cordillera	-15.98571	-70.64346				-66	7	0.6	0.0			
20140705-01**	W. Cordillera	-15.98752	-70.64179				-70	3	0.8	0.1			
20140705-03**	W. Cordillera	-15.94321	-70.59472				-79	4	0.4	0.0			
20150608-05**	W. Cordillera	-15.95085	-70.60279				-62	6	0.6	0.0			
20150609-03**	W. Cordillera	-16.09249	-70.01788				-86	1	0.3	0.0			
20150609-12**	W. Cordillera	-16.42588	-70.33340				-92	7	0.2	0.0			
20150609-14**	W. Cordillera	-16.56737	-70.37363				-82	1	0.6	0.0			

Table A6 (continued): Volcanic Glass Stable Isotope Data and Modeling

Name	Region	Latitude	Longitude	Age	Unc.	Source	δD		%		Model		
							mean	$\pm 1\sigma$	water	$\pm 1\sigma$	ΔD	mean	$+1\sigma$
20140614-04**	E. Cordillera	-13.95610	70.49174				-102	6	0.5	0.0			
20140614-05**	E. Cordillera	-13.91987	-70.50849				-110	2	0.6	0.1			
20140615-06**	E. Cordillera	-14.09425	-70.65772				-103	4	0.6	0.1			
20140615-07**	E. Cordillera	-14.09617	-70.67084				-99	3	0.9	0.1			
20140616-04**	E. Cordillera	-14.51774	-69.69187				-97	4	0.7	0.0			
20140617-01**	E. Cordillera	-14.57645	-69.84288				-100	5	0.8	0.0			

*Age based on interpreted age model, assigned 10% uncertainty

**Data not considered in paleoelevation calculations because nonhydrated (<1 weight % water)

^AGlass data produced at the University of Arizona, all other data were produced at the University of Texas at Austin

Individual aliquot uncertainty is typically $\pm 2\text{‰}$

^BOutlier not considered in mean and standard deviation calculation

^DGlass data from Saylor and Horton (2014)

APPENDIX 7

Table A7: Volcanic Zircon U-Pb Integrated Data

Spot	Ratios							Ages (Ma)					Best Age	±2σ	
	207Pb/ 206Pb	±2σ	207Pb/ 235U	±2σ	206Pb/ 238U	±2σ	Rho	206Pb/ 238U	±2σ	207Pb/ 235U	±2σ	207Pb/ 206Pb			±2σ
250511-05 Accepted Data															
3	14.5215	56.6	0.0274	57.4	0.0029	9.7	0.17	18.6	1.8	27.4	15.5	894.7	1277.2	18.6	4.1
28	23.9778	20.5	0.0177	20.6	0.0031	2.7	0.13	19.8	0.5	17.8	3.6	-244.3	521.7	19.8	2.3
22	27.1949	35.8	0.0159	35.9	0.0031	3.1	0.09	20.1	0.6	16.0	5.7	-573.2	994.3	20.1	2.4
24	22.8035	18.3	0.0190	18.6	0.0031	2.7	0.15	20.2	0.6	19.1	3.5	-118.9	455.6	20.2	2.3
17	23.3052	9.5	0.0186	10.0	0.0032	3.0	0.30	20.3	0.6	18.8	1.9	-172.9	237.5	20.3	2.3
1	22.1495	30.1	0.0196	30.6	0.0032	5.4	0.18	20.3	1.1	19.7	6.0	-47.7	746.0	20.3	3.0
10	26.8659	43.1	0.0164	43.4	0.0032	5.0	0.12	20.5	1.0	16.5	7.1	-540.4	1204.2	20.5	2.9
14	22.3729	50.6	0.0197	51.1	0.0032	7.1	0.14	20.6	1.5	19.8	10.0	-72.1	1313.5	20.6	3.5
18	17.8995	30.8	0.0247	31.0	0.0032	3.8	0.12	20.6	0.8	24.7	7.6	447.1	699.9	20.6	2.5
250511-05 Rejected Data															
08*	18.4791	12.9	0.2703	13.1	0.0362	2.3	0.17	229.4	5.1	242.9	28.2	375.8	290.2	229.4	10.5
04*	21.5441	10.2	0.2325	10.5	0.0363	2.5	0.23	230.1	5.5	212.3	20.2	19.3	246.1	230.1	11.3
16*	26.4604	38.0	0.1894	38.3	0.0363	5.2	0.13	230.2	11.7	176.1	62.0	-499.8	1042.1	230.2	23.4
07*	25.2435	47.3	0.2025	47.6	0.0371	5.6	0.12	234.6	12.9	187.2	81.6	-376.0	1291.4	234.6	25.8
05*	19.4993	2.6	0.2638	2.9	0.0373	1.3	0.45	236.1	3.0	237.7	6.2	253.6	60.0	236.1	6.4
06*	18.8588	11.8	0.2785	12.2	0.0381	3.1	0.25	241.0	7.3	249.5	27.0	329.9	268.8	241.0	14.7
25*	20.2040	10.7	0.2644	10.8	0.0387	1.6	0.14	245.0	3.8	238.2	23.0	171.3	250.7	245.0	7.8
26*	19.6168	2.3	0.2725	2.8	0.0388	1.6	0.58	245.2	3.9	244.7	6.1	239.8	53.1	245.2	8.1
27*	19.0262	6.0	0.2843	6.4	0.0392	2.1	0.32	248.1	5.0	254.1	14.3	309.8	137.6	248.1	10.2
29*	19.6079	7.7	0.2773	9.5	0.0394	5.7	0.59	249.3	13.9	248.5	21.0	240.8	177.0	249.3	27.8
30*	19.8619	3.2	0.2740	3.5	0.0395	1.2	0.36	249.6	3.0	245.9	7.5	211.1	74.7	249.6	6.4
11*	19.7978	2.9	0.2749	3.0	0.0395	0.7	0.23	249.6	1.7	246.6	6.6	218.5	67.4	249.6	4.0
12*	19.1077	5.5	0.2885	5.5	0.0400	0.9	0.16	252.7	2.2	257.4	12.6	300.1	125.0	252.7	4.8
23*	19.6116	4.5	0.3010	5.3	0.0428	2.8	0.53	270.2	7.4	267.2	12.4	240.4	103.4	270.2	14.9
19*	18.1957	9.5	0.5278	9.7	0.0697	1.9	0.20	434.1	8.0	430.4	33.9	410.5	212.3	434.1	16.0
*Interpreted as detrital															
250511-06 Accepted Data															
31	13.0318	42.1	0.0310	42.9	0.0029	8.1	0.19	18.8	1.5	31.0	13.1	1114.3	880.5	18.8	3.7
12	19.0508	22.1	0.0218	23.9	0.0030	9.2	0.39	19.4	1.8	21.9	5.2	306.9	507.9	19.4	4.1
18	20.0621	17.6	0.0209	18.1	0.0030	4.2	0.23	19.5	0.8	21.0	3.8	187.8	412.3	19.5	2.6
14	15.4707	34.3	0.0271	34.3	0.0030	1.9	0.06	19.6	0.4	27.2	9.2	762.6	743.1	19.6	2.1
2	23.6305	20.0	0.0178	20.9	0.0031	6.0	0.29	19.7	1.2	18.0	3.7	-207.5	505.7	19.7	3.1
10	20.9695	39.2	0.0201	40.2	0.0031	9.2	0.23	19.7	1.8	20.2	8.1	83.8	962.0	19.7	4.1
21	25.6588	28.1	0.0165	28.3	0.0031	3.4	0.12	19.8	0.7	16.7	4.7	-418.6	746.4	19.8	2.4
28	21.6831	32.0	0.0197	32.3	0.0031	4.8	0.15	19.9	1.0	19.8	6.3	3.8	787.8	19.9	2.8
5	24.2276	29.8	0.0176	30.0	0.0031	3.4	0.11	19.9	0.7	17.7	5.3	-270.6	771.5	19.9	2.4
27	20.3132	13.7	0.0212	14.2	0.0031	3.7	0.26	20.1	0.8	21.3	3.0	158.7	322.1	20.1	2.5
26	20.4415	20.1	0.0211	20.8	0.0031	5.2	0.25	20.2	1.1	21.2	4.4	144.0	476.7	20.2	2.9
11	23.7427	13.9	0.0182	14.1	0.0031	2.4	0.17	20.2	0.5	18.3	2.6	-219.4	351.0	20.2	2.2
32	11.8289	13.8	0.0371	15.1	0.0032	6.1	0.40	20.5	1.2	37.0	5.5	1305.0	269.8	20.5	3.2
7	16.0100	29.6	0.0293	30.1	0.0034	5.7	0.19	21.9	1.2	29.3	8.7	690.0	644.2	21.9	3.2
250511-06 Rejected Data															
03*	19.0788	7.2	0.0624	7.6	0.0086	2.4	0.32	55.4	1.3	61.5	4.5	303.5	164.2	55.4	3.3
15*	19.5813	12.9	0.0667	13.4	0.0095	3.8	0.28	60.8	2.3	65.6	8.5	244.0	298.4	60.8	5.0
250511-	19.6251	3.7	0.2641	4.2	0.0376	1.9	0.46	237.9	4.5	238.0	9.0	238.8	86.4	237.9	9.1
25*	20.4180	8.5	0.2616	8.9	0.0387	2.8	0.31	245.0	6.8	236.0	18.8	146.7	199.3	245.0	13.7
33*	12.6201	0.9	2.1249	2.1	0.1945	1.9	0.90	1145.6	20.2	1156.9	14.7	1178.1	18.1	1178.1	36.3
*Interpreted as detrital															
250511-08 Accepted Data															
23	7.0761	105.8	0.0317	113.4	0.0016	40.8	0.36	10.5	4.3	31.7	35.4	2243.4	444.6	10.5	8.8
1	15.7303	51.3	0.0159	70.6	0.0018	48.5	0.69	11.7	5.7	16.1	11.2	727.4	1164.9	11.7	11.5
3	2.2086	520.7	0.1150	521.4	0.0018	26.8	0.05	11.9	3.2	110.6	610.4	4094.3	506.2	11.9	6.7
12	70.3727	224.0	0.0038	224.1	0.0020	6.5	0.03	12.6	0.8	3.9	8.7	NA	NA	12.6	2.6
4	1.1571	2804.5	0.2442	2804.5	0.0020	5.9	0.00	13.2	0.8	221.8	#NUM!	NA	NA	13.2	2.5
250511-08 Rejected Data															
26*	14.1812	110.3	0.0283	113.5	0.0029	26.8	0.24	18.7	5.0	28.3	31.7	943.4	414.6	18.7	10.2
27*	19.0886	3.3	0.2632	3.5	0.0364	1.2	0.33	230.7	2.6	237.3	7.5	302.4	76.0	230.7	5.7
08*	19.5415	4.8	0.2576	5.3	0.0365	2.2	0.41	231.1	4.9	232.7	11.0	248.6	110.9	231.1	10.1
25*	20.0852	17.2	0.2513	17.4	0.0366	2.6	0.15	231.8	5.9	227.6	35.5	185.1	403.7	231.8	12.0
30*	19.2771	6.8	0.2630	7.7	0.0368	3.6	0.46	232.8	8.1	237.1	16.3	279.9	156.7	232.8	16.4
11*	20.0175	2.5	0.2547	3.1	0.0370	1.8	0.57	234.1	4.1	230.4	6.4	193.0	58.7	234.1	8.4
18*	19.7487	3.5	0.2585	6.0	0.0370	4.9	0.81	234.4	11.2	233.4	12.5	224.3	82.1	234.4	22.5
19*	20.0187	2.3	0.2567	2.4	0.0373	0.8	0.34	235.9	1.9	232.0	5.1	192.8	53.6	235.9	4.3
14*	19.6733	3.2	0.2614	3.4	0.0373	1.2	0.36	236.1	2.9	235.8	7.2	233.2	74.2	236.1	6.1
20*	19.5170	5.9	0.2642	6.0	0.0374	1.3	0.22	236.7	3.0	238.1	12.8	251.5	135.6	236.7	6.4
13*	18.9988	5.7	0.2764	7.0	0.0381	4.0	0.57	241.0	9.5	247.8	15.4	313.1	130.8	241.0	19.2
24*	20.4177	4.1	0.2577	4.6	0.0382	2.1	0.45	241.4	4.9	232.8	9.6	146.8	96.3	241.4	10.0

Table A7 (continued): Volcanic Zircon U-Pb Integrated Data

Spot	Ratios						Ages (Ma)						Best Age	±2σ	
	207Pb/ 206Pb	±2σ	207Pb/ 235U	±2σ	206Pb/ 238U	±2σ	Rho	206Pb/ 238U	±2σ	207Pb/ 235U	±2σ	207Pb/ 206Pb			±2σ
250511-08 Rejected Data															
09*	18.5489	5.2	0.2842	5.4	0.0382	1.5	0.27	241.8	3.5	253.9	12.2	367.3	117.7	241.8	7.3
21*	19.7654	6.1	0.2670	6.8	0.0383	3.0	0.44	242.2	7.1	240.3	14.5	222.4	140.2	242.2	14.4
16*	20.1674	3.6	0.2650	4.1	0.0388	2.0	0.49	245.2	4.8	238.7	8.7	175.6	83.0	245.2	9.7
29*	19.2744	1.8	0.2776	2.7	0.0388	1.9	0.73	245.4	4.7	248.7	5.9	280.2	42.1	245.4	9.5
22*	20.0448	11.8	0.2672	12.5	0.0388	3.9	0.32	245.6	9.5	240.4	26.7	189.8	276.0	245.6	19.1
07*	19.8256	24.7	0.2723	25.0	0.0392	3.5	0.14	247.6	8.4	244.5	54.3	215.3	580.3	247.6	16.9
10*	19.1361	4.8	0.2824	5.1	0.0392	1.5	0.30	247.8	3.7	252.6	11.3	296.7	109.9	247.8	7.7
28*	19.2233	2.3	0.2832	2.4	0.0395	0.8	0.34	249.6	2.0	253.2	5.5	286.3	52.2	249.6	4.6
02*	19.3231	5.7	0.2847	5.8	0.0399	1.2	0.21	252.2	3.0	254.3	13.2	274.4	131.1	252.2	6.4
17*	18.9322	4.9	0.2919	5.1	0.0401	1.2	0.23	253.3	2.9	260.0	11.6	321.1	112.4	253.3	6.1
15*	19.5901	3.6	0.2836	3.8	0.0403	1.4	0.36	254.7	3.4	253.5	8.5	242.9	81.8	254.7	7.2
06*	19.0845	2.7	0.2918	3.1	0.0404	1.6	0.50	255.2	3.9	260.0	7.2	302.8	62.0	255.2	8.1
*Interpreted as detrital															
260511-01 Accepted Data															
16	6.4627	286.1	0.0233	287.1	0.0011	23.7	0.08	7.0	1.7	23.4	66.5	2398.9	173.0	7.0	3.9
22	5.1855	229.2	0.0294	229.8	0.0011	17.5	0.08	7.1	1.2	29.4	66.7	2766.6	275.9	7.1	3.2
9	9.5165	159.6	0.0161	161.5	0.0011	24.3	0.15	7.1	1.7	16.2	25.9	1715.7	160.4	7.1	4.0
27	0.8553	1054.5	0.1821	1054.8	0.0011	23.7	0.02	7.3	1.7	169.9	#NUM!	NA	NA	7.3	4.0
1	15.7436	43.2	0.0100	49.4	0.0011	23.9	0.48	7.3	1.8	10.1	5.0	725.6	960.5	7.3	4.0
25	11.2619	44.1	0.0143	48.9	0.0012	21.1	0.43	7.5	1.6	14.4	7.0	1399.7	891.9	7.5	3.8
13	5.3277	372.1	0.0304	373.5	0.0012	32.4	0.09	7.6	2.5	30.4	112.4	2722.1	183.3	7.6	5.3
28	4.1249	227.6	0.0396	228.5	0.0012	20.7	0.09	7.6	1.6	39.5	88.7	3136.0	520.8	7.6	3.7
29	20.7716	20.9	0.0079	22.0	0.0012	7.0	0.32	7.7	0.5	8.0	1.8	106.3	497.7	7.7	2.3
18	3.6311	204.5	0.0458	207.1	0.0012	32.6	0.16	7.8	2.5	45.4	92.2	3337.0	717.5	7.8	5.4
19	20.7586	110.2	0.0081	113.1	0.0012	25.7	0.23	7.9	2.0	8.2	9.2	107.8	1039.1	7.9	4.5
26	7.9731	147.4	0.0213	148.6	0.0012	18.4	0.12	7.9	1.5	21.4	31.5	2034.7	113.3	7.9	3.5
4	17.3456	67.9	0.0099	69.7	0.0012	15.7	0.22	8.0	1.3	10.0	6.9	516.5	1705.1	8.0	3.2
3	12.4834	302.3	0.0140	302.9	0.0013	18.5	0.06	8.1	1.5	14.1	42.4	1199.6	1327.7	8.1	3.6
12	7.2569	234.2	0.0243	234.7	0.0013	15.9	0.07	8.2	1.3	24.4	56.6	2199.7	136.5	8.2	3.3
6	7.8366	218.8	0.0225	219.9	0.0013	22.5	0.10	8.2	1.9	22.6	49.2	2065.2	174.5	8.2	4.2
14	0.5922	4076.1	0.2980	4076.1	0.0013	12.0	0.00	8.2	1.0	264.9	#NUM!	NA	NA	8.2	2.8
24	2.5719	403.1	0.0695	403.8	0.0013	22.8	0.06	8.4	1.9	68.3	273.0	3866.4	564.2	8.4	4.3
11	9.2870	128.6	0.0196	129.7	0.0013	17.3	0.13	8.5	1.5	19.7	25.3	1760.5	27.3	8.5	3.6
23	14.8285	48.8	0.0125	50.3	0.0013	12.0	0.24	8.7	1.0	12.6	6.3	851.3	1080.4	8.7	2.9
260511-01 Rejected Data															
20*	6.9834	103.1	0.0253	107.7	0.0013	31.1	0.29	8.3	2.6	25.4	27.0	2266.2	471.3	8.3	5.5
07*	18.9511	80.3	0.0094	87.9	0.0013	35.7	0.41	8.3	3.0	9.5	8.3	318.8	2265.6	8.3	6.2
*High 6/8 uncertainty (>30%)															
260511-02 Accepted Data															
32	-5.4649	376.9	-0.0266	377.3	0.0011	17.3	0.05	6.8	1.2	-27.4	-105.1	NA	NA	6.8	2.4
39R	6.3315	170.1	0.0236	171.5	0.0011	22.0	0.13	7.0	1.5	23.7	40.1	2433.7	273.8	7.0	3.1
35R	8.0924	300.2	0.0191	300.4	0.0011	12.9	0.04	7.2	0.9	19.2	57.2	2008.4	535.5	7.2	1.9
1	22.0386	50.9	0.0073	51.3	0.0012	6.7	0.13	7.5	0.5	7.4	3.8	-35.5	1312.9	7.5	1.0
26	-4.0158	452.7	-0.0410	453.5	0.0012	27.4	0.06	7.7	2.1	-42.5	-199.5	NA	NA	7.7	4.2
260511-02 Rejected Data															
19*	12.1643	85.8	0.0178	87.1	0.0016	15.3	0.18	10.1	1.6	17.9	15.5	1250.5	48.4	10.1	3.1
10*	13.4765	195.7	0.0171	196.0	0.0017	11.3	0.06	10.7	1.2	17.2	33.4	1047.0	872.8	10.7	2.4
37R*	10.1162	37.3	0.0227	41.6	0.0017	18.3	0.44	10.7	2.0	22.8	9.4	1602.5	723.3	10.7	3.9
11*	13.7006	94.6	0.0169	95.3	0.0017	12.0	0.13	10.8	1.3	17.0	16.1	1013.6	259.7	10.8	2.6
03*	7.3679	154.2	0.0317	157.3	0.0017	31.2	0.20	10.9	3.4	31.6	49.1	2173.3	172.8	10.9	6.8
30*	22.8790	13.7	0.0102	14.6	0.0017	5.2	0.36	10.9	0.6	10.3	1.5	-127.1	339.2	10.9	1.1
12*	20.2849	30.9	0.0115	31.0	0.0017	2.3	0.08	10.9	0.3	11.7	3.6	162.0	737.5	10.9	0.5
38R*	20.9804	12.5	0.0113	12.9	0.0017	2.9	0.22	11.0	0.3	11.4	1.5	82.6	298.5	11.0	0.6
16*	23.4981	45.0	0.0101	45.1	0.0017	4.0	0.09	11.1	0.4	10.2	4.6	-193.5	1178.0	11.1	0.9
08*	23.3463	19.0	0.0103	19.4	0.0018	3.5	0.18	11.3	0.4	10.4	2.0	-177.3	478.4	11.3	0.8
27*	13.2708	63.7	0.0185	64.3	0.0018	8.8	0.14	11.5	1.0	18.6	11.8	1077.9	1442.6	11.5	2.0
02*	38.0268	60.5	0.0065	61.0	0.0018	8.3	0.14	11.5	1.0	6.6	4.0	NA	NA	11.5	1.9
29*	34.0085	44.2	0.0073	44.4	0.0018	4.2	0.09	11.6	0.5	7.4	3.3	NA	NA	11.6	1.0
28*	14.1541	39.1	0.0182	42.2	0.0019	15.9	0.38	12.0	1.9	18.3	7.7	947.3	832.6	12.0	3.8
41R*	6.9312	263.0	0.0371	263.3	0.0019	12.9	0.05	12.0	1.5	37.0	96.0	2279.1	183.6	12.0	3.1
09*	15.7310	56.3	0.0167	57.7	0.0019	12.9	0.22	12.3	1.6	16.9	9.6	727.3	1299.8	12.3	3.2
43C*	20.4096	4.6	0.0147	22.6	0.0022	22.2	0.98	14.0	3.1	14.9	3.3	147.6	107.4	14.0	6.2
42R*	20.1836	5.8	0.0192	13.9	0.0028	12.7	0.91	18.1	2.3	19.3	2.7	173.7	135.6	18.1	4.6
31*	10.1905	101.3	0.0423	103.8	0.0031	22.3	0.21	20.1	4.5	42.1	42.8	1588.9	67.7	20.1	9.0
34*	18.2898	24.2	0.0318	24.5	0.0042	4.0	0.16	27.1	1.1	31.8	7.7	398.9	549.6	27.1	2.2
33*	14.7327	15.7	0.0568	24.6	0.0061	19.0	0.77	39.0	7.4	56.1	13.5	864.8	327.0	39.0	14.8
07*	20.4905	9.9	0.1218	16.5	0.0181	13.3	0.80	115.6	15.2	116.7	18.2	138.4	232.3	115.6	30.4

Table A7 (continued): Volcanic Zircon U-Pb Integrated Data

Spot	Ratios							Ages (Ma)							
	207Pb/206Pb		207Pb/235U		206Pb/238U		Rho	206Pb/238U		207Pb/235U		207Pb/206Pb		Best Age	±2σ
	±2σ	±2σ	±2σ	±2σ	±2σ	±2σ		±2σ	±2σ	±2σ	±2σ				
260511-02 Rejected Data															
40R*	16.7056	6.9	0.1720	23.2	0.0208	22.1	0.96	133.0	29.1	161.2	34.5	598.5	148.7	133.0	58.3
15*	17.0932	5.6	0.1720	51.3	0.0213	51.0	0.99	136.0	68.7	161.1	76.6	548.7	121.9	136.0	137.4
04*	35.1990	60.1	0.1792	60.3	0.0458	5.0	0.08	288.4	14.2	167.4	93.3	NA	NA	288.4	28.5
44C*	19.2846	5.2	0.3318	5.5	0.0464	1.5	0.28	292.4	4.4	290.9	13.8	279.0	119.9	292.4	8.8
24*	19.0458	2.7	0.3368	3.0	0.0465	1.3	0.43	293.1	3.7	294.7	7.7	307.5	61.8	293.1	7.4
05*	19.8320	10.3	0.3240	10.4	0.0466	1.3	0.12	293.6	3.6	285.0	25.8	214.6	239.0	293.6	7.2
06*	18.6796	3.4	0.3471	3.5	0.0470	0.8	0.23	296.2	2.3	302.5	9.1	351.5	76.6	296.2	4.6
36R*	19.2135	2.8	0.3423	3.2	0.0477	1.5	0.46	300.4	4.4	298.9	8.3	287.5	65.0	300.4	8.7
13*	18.9810	2.6	0.3519	3.1	0.0484	1.7	0.54	305.0	5.1	306.1	8.3	315.2	60.0	305.0	10.2
14*	19.1644	2.3	0.3521	2.6	0.0489	1.2	0.47	308.0	3.6	306.3	6.8	293.3	52.2	308.0	7.2
*Interpreted as detrital															
270510-01 Accepted Data															
5	-0.0572	191.8	-0.0166	193.1	0.0021	21.8	0.11	13.6	3.0	0.0	0.0	0.0	4624.0	13.6	3.0
2	0.0837	78.9	0.0275	82.4	0.0024	23.6	0.29	15.3	3.6	27.5	22.4	1286.2	1535.9	15.3	3.6
7	0.0144	1377.2	0.0048	1377.6	0.0024	32.7	0.02	15.4	5.0	4.8	66.5	0.0	33195.8	15.4	5.0
3	0.0476	90.3	0.0160	90.9	0.0024	9.9	0.11	15.7	1.5	16.1	14.5	81.3	2144.7	15.7	1.5
22	0.1370	56.6	0.0502	57.6	0.0027	10.7	0.19	17.1	1.8	49.7	27.9	2190.2	983.7	17.1	1.8
9	0.0197	116.4	0.0072	116.7	0.0027	7.6	0.07	17.1	1.3	7.3	8.5	0.0	2806.4	17.1	1.3
1	0.0594	31.8	0.0222	32.5	0.0027	6.9	0.21	17.4	1.2	22.3	7.2	580.6	689.9	17.4	1.2
8	0.0494	19.9	0.0186	22.8	0.0027	11.1	0.49	17.6	1.9	18.7	4.2	168.8	464.6	17.6	1.9
23	0.0457	41.6	0.0177	42.2	0.0028	6.8	0.16	18.0	1.2	17.8	7.4	0.0	1003.0	18.0	1.2
17	0.0754	19.2	0.0295	21.9	0.0028	10.5	0.48	18.2	1.9	29.5	6.4	1080.0	384.4	18.2	1.9
14	0.0493	44.9	0.0202	45.5	0.0030	6.8	0.15	19.1	1.3	20.3	9.1	161.5	1051.1	19.1	1.3
21	-0.0303	149.4	-0.0127	150.1	0.0030	14.4	0.10	19.5	2.8	0.0	0.0	0.0	3602.4	19.5	2.8
16	0.0739	24.6	0.0309	25.8	0.0030	7.8	0.30	19.5	1.5	30.9	7.8	1038.7	495.8	19.5	1.5
20	0.0722	76.2	0.0314	77.4	0.0031	13.1	0.17	20.3	2.7	31.4	23.9	992.4	1549.9	20.3	2.7
15	0.1614	31.9	0.0720	35.7	0.0032	15.9	0.45	20.8	3.3	70.6	24.3	2470.6	538.6	20.8	3.3
18	0.0382	58.7	0.0178	59.3	0.0034	8.4	0.14	21.7	1.8	17.9	10.5	0.0	1415.8	21.7	1.8
10	0.0902	83.4	0.0430	85.0	0.0035	16.5	0.19	22.2	3.7	42.8	35.6	1429.9	1591.9	22.2	3.7
11	0.0501	17.9	0.0243	19.3	0.0035	7.2	0.38	22.6	1.6	24.3	4.7	198.0	416.6	22.6	1.6
6	0.2419	30.2	0.1233	32.5	0.0037	11.9	0.37	23.8	2.8	118.1	36.2	3132.7	479.7	23.8	2.8
270510-01 Rejected Data															
4*	-0.4629	225.5	-0.0423	258.7	0.0007	126.8	0.49	4.3	5.4	0.0	0.0	0.0	5436.2	4.3	5.4
24*	1.0531	184.1	97.0748	306.5	0.6676	245.1	0.80	3296.7	15035.3	4656.3	65535.0	5310.0	2610.8	5310.0	2610.8
19**	0.0958	11.0	2.9166	15.7	0.2205	11.1	0.71	1284.4	129.6	1386.2	119.2	1544.1	207.0	1544.1	207.0
26**	-0.2160	930.1	-3.1554	930.5	0.1058	26.3	0.03	648.2	162.3	0.0	0.0	0.0	22420.0	648.2	162.3
13**	0.0533	6.2	0.3760	8.5	0.0511	5.7	0.68	321.0	17.8	324.1	23.5	343.1	139.8	321.0	17.8
12***	0.2107	60.7	0.1269	63.6	0.0044	19.1	0.30	28.1	5.3	121.3	72.9	2910.6	983.1	28.1	5.3
25***	0.3920	23.3	0.3065	28.3	0.0057	15.9	0.57	36.4	5.8	271.5	67.4	3878.7	351.1	36.4	5.8
*6/8 uncertainty >30%															
**Likely not zircon but phosphate: low 8/6 (<30) and high common Pb															
***Interpreted as detrital															
270510-05 Accepted Data															
30	0.1120	30.3	0.0463	33.4	0.0030	14.1	0.42	19.3	2.7	46.0	15.0	1831.3	549.7	19.3	2.7
27	0.1142	24.0	0.0450	27.5	0.0029	13.3	0.48	18.4	2.4	44.7	12.0	1866.8	433.6	18.4	2.4
9	0.1049	33.3	0.0410	34.5	0.0028	9.0	0.26	18.3	1.6	40.8	13.8	1711.7	612.3	18.3	1.6
25	0.0560	42.2	0.0208	43.4	0.0027	9.9	0.23	17.3	1.7	20.9	9.0	454.1	937.3	17.3	1.7
7	0.0518	35.0	0.0190	36.3	0.0027	9.7	0.27	17.1	1.6	19.1	6.8	274.5	800.7	17.1	1.6
2	0.0309	154.3	0.0112	154.9	0.0026	12.7	0.08	16.8	2.1	11.3	17.3	0.0	3720.2	16.8	2.1
1	0.0796	60.2	0.0286	61.3	0.0026	11.7	0.19	16.8	2.0	28.6	17.3	1187.3	1189.5	16.8	2.0
33	0.0741	30.1	0.0266	32.5	0.0026	12.3	0.38	16.7	2.1	26.6	8.5	1045.2	606.6	16.7	2.1
31	0.0324	73.0	0.0115	73.5	0.0026	8.3	0.11	16.5	1.4	11.6	8.5	0.0	1760.7	16.5	1.4
18	0.0435	54.2	0.0150	55.0	0.0025	8.9	0.16	16.1	1.4	15.1	8.2	0.0	1307.6	16.1	1.4
5	0.1080	30.2	0.0371	31.7	0.0025	9.7	0.31	16.0	1.6	37.0	11.5	1765.8	551.1	16.0	1.6
10	0.0356	58.7	0.0122	59.3	0.0025	8.2	0.14	16.0	1.3	12.3	7.3	0.0	1415.5	16.0	1.3
19	0.0581	71.9	0.0197	72.7	0.0025	11.1	0.15	15.8	1.8	19.8	14.3	533.4	1573.4	15.8	1.8
24	-0.0446	173.3	-0.0143	174.1	0.0023	16.1	0.09	14.9	2.4	0.0	0.0	0.0	4178.2	14.9	2.4
270510-05 Rejected Data															
4*	0.7930	21.8	32.1572	28.9	0.2938	19.0	0.66	1660.6	278.6	3555.1	292.5	4909.3	312.0	4909.3	312.0
17*	0.7561	10.7	21.7597	14.4	0.2085	9.7	0.67	1220.9	108.1	3173.1	141.0	4841.3	153.7	4841.3	153.7
28*	0.8059	13.2	21.1806	17.9	0.1904	12.2	0.68	1123.7	125.6	3146.9	175.6	4932.1	188.8	1123.7	125.6
34*	0.8630	23.8	20.5962	29.8	0.1729	18.0	0.60	1028.1	170.7	3119.8	296.5	5029.4	339.4	1028.1	170.7
32*	0.7901	10.3	18.6104	13.7	0.1707	9.1	0.66	1015.8	85.6	3021.8	133.1	4903.9	147.8	1015.8	85.6
3*	0.8747	12.0	20.2040	16.4	0.1674	11.1	0.68	997.5	102.7	3101.2	159.7	5048.6	171.9	997.5	102.7
6*	0.7783	12.8	16.9027	17.7	0.1574	12.3	0.69	942.1	107.5	2929.3	171.7	4882.5	184.1	942.1	107.5
26*	0.8234	40.0	16.0965	50.0	0.1416	30.0	0.60	853.9	239.8	2882.5	519.0	4962.8	572.9	853.9	239.8
11*	0.8055	9.7	14.8655	12.9	0.1337	8.5	0.66	809.0	64.9	2806.7	123.5	4931.5	139.2	809.0	64.9

Table A7 (continued): Volcanic Zircon U-Pb Integrated Data

Spot	Ratios						Ages (Ma)						Best Age	±2σ	
	207Pb/206Pb	±2σ	207Pb/235U	±2σ	206Pb/238U	±2σ	Rho	206Pb/238U	±2σ	207Pb/235U	±2σ	207Pb/206Pb			±2σ
270510-05 Rejected Data															
36*	0.8162	24.7	14.8204	31.6	0.1315	19.8	0.63	796.7	148.3	2803.8	309.9	4950.4	352.9	796.7	148.3
22*	0.7519	10.7	11.4970	14.6	0.1108	9.9	0.68	677.3	63.9	2564.3	136.8	4833.3	153.2	677.3	63.9
29*	0.7994	13.6	12.2209	17.8	0.1108	11.5	0.65	677.2	74.0	2621.5	168.2	4920.6	194.1	677.2	74.0
14*	0.9021	9.9	12.4683	13.7	0.1001	9.4	0.69	615.3	55.5	2640.3	129.2	5092.1	141.4	615.3	55.5
23*	0.8412	11.2	11.3724	15.1	0.0979	10.1	0.67	602.4	58.2	2554.2	141.8	4993.2	160.6	602.4	58.2
20*	0.8375	14.5	11.2324	19.0	0.0972	12.3	0.65	597.8	70.3	2542.6	179.1	4986.9	207.4	597.8	70.3
13*	0.6966	26.8	8.7386	37.1	0.0909	25.7	0.69	560.8	138.3	2311.1	351.8	4723.7	386.1	560.8	138.3
16*	0.7715	9.9	9.3616	13.2	0.0879	8.7	0.66	543.2	45.4	2374.1	121.5	4870.1	142.4	543.2	45.4
8*	0.8649	10.8	10.4289	14.8	0.0874	10.1	0.68	540.0	52.4	2473.6	137.6	5032.5	153.9	540.0	52.4
12*	0.8202	9.1	9.3982	13.0	0.0830	9.2	0.71	514.2	45.6	2377.7	119.5	4957.2	130.7	514.2	45.6
21*	0.8630	11.0	8.2049	14.9	0.0689	10.1	0.68	429.4	41.9	2253.9	135.4	5029.4	156.5	429.4	41.9
35*	0.8437	10.7	7.7577	14.4	0.0666	9.6	0.66	415.7	38.5	2203.3	129.8	4997.4	153.4	415.7	38.5
15*	0.7671	10.2	4.3695	13.6	0.0413	9.0	0.66	260.7	22.9	1706.6	112.7	4861.9	146.8	260.7	22.9
*Likely not zircon but phosphate: low 8/6 (<30) and high common Pb															
270510-06 Accepted Data															
8	0.0410	86.9	0.0126	87.4	0.0022	9.6	0.11	14.3	1.4	12.7	11.0	0.0	2093.8	14.3	1.4
4	0.0040	1003.9	0.0013	1004.0	0.0023	11.2	0.01	14.6	1.6	1.3	12.9	0.0	24198.2	14.6	1.6
7	-0.0001	57783.1	0.0000	57783.1	0.0023	13.1	0.00	15.1	2.0	0.0	0.0	0.0	1392833.3	15.1	2.0
15	0.0160	230.5	0.0053	230.8	0.0024	11.4	0.05	15.5	1.8	5.4	12.4	0.0	5556.4	15.5	1.8
9	0.0644	59.1	0.0220	60.2	0.0025	11.7	0.20	15.9	1.9	22.1	13.2	755.9	1246.3	15.9	1.9
25	0.0459	28.0	0.0160	28.9	0.0025	7.1	0.25	16.2	1.2	16.1	4.6	0.0	674.2	16.2	1.2
16	0.0276	84.2	0.0097	85.1	0.0025	12.0	0.14	16.3	2.0	9.8	8.3	0.0	2030.1	16.3	2.0
33	0.0780	26.8	0.0278	27.8	0.0026	7.3	0.27	16.6	1.2	27.9	7.6	1147.2	531.7	16.6	1.2
23	0.0067	442.1	0.0024	442.3	0.0026	13.0	0.03	16.7	2.2	2.4	10.7	0.0	10657.2	16.7	2.2
3	0.0524	124.5	0.0192	125.1	0.0026	12.3	0.10	17.1	2.1	19.3	23.9	302.9	2837.1	17.1	2.1
27	0.0657	32.7	0.0243	33.7	0.0027	8.2	0.24	17.2	1.4	24.4	8.1	798.3	685.5	17.2	1.4
1	0.0113	164.6	0.0043	164.8	0.0027	9.5	0.06	17.5	1.7	4.3	7.1	0.0	3966.6	17.5	1.7
6	0.0983	56.3	0.0370	57.9	0.0027	13.7	0.24	17.5	2.4	36.9	21.0	1592.2	1051.5	17.5	2.4
35	0.1437	18.2	0.0546	24.3	0.0028	16.1	0.66	17.7	2.8	54.0	12.8	2272.2	313.7	17.7	2.8
2	0.0893	96.3	0.0340	97.4	0.0028	14.4	0.15	17.7	2.5	33.9	32.5	1411.5	1843.5	17.7	2.5
21	0.0734	61.0	0.0279	62.2	0.0028	12.1	0.20	17.7	2.1	28.0	17.2	1025.4	1234.8	17.7	2.1
11	0.0348	167.9	0.0133	168.3	0.0028	11.0	0.07	17.8	1.9	13.4	22.4	0.0	4048.2	17.8	1.9
29	0.1079	27.0	0.0419	34.0	0.0028	20.6	0.61	18.1	3.7	41.7	13.9	1764.5	493.7	18.1	3.7
32	0.0829	19.5	0.0325	20.9	0.0028	7.3	0.35	18.3	1.3	32.5	6.7	1266.6	381.7	18.3	1.3
26	0.1030	22.4	0.0408	23.9	0.0029	8.3	0.35	18.5	1.5	40.6	9.5	1679.5	413.7	18.5	1.5
22	0.1136	26.1	0.0450	27.3	0.0029	7.9	0.29	18.5	1.4	44.7	11.9	1857.8	471.0	18.5	1.4
31	0.1470	16.4	0.0590	18.8	0.0029	9.1	0.49	18.7	1.7	58.2	10.6	2311.8	281.6	18.7	1.7
5	0.1800	35.4	0.0817	38.0	0.0033	13.8	0.36	21.2	2.9	79.8	29.2	2653.3	587.2	21.2	2.9
17	0.3058	16.5	0.1537	18.6	0.0036	8.6	0.47	23.4	2.0	145.2	25.2	3499.9	254.6	23.4	2.0
18	0.3946	38.7	0.2440	42.4	0.0045	17.2	0.41	28.8	4.9	221.7	84.7	3888.6	583.4	28.8	4.9
24	0.4057	43.9	0.2819	49.8	0.0050	23.4	0.47	32.4	7.6	252.2	111.7	3930.2	659.8	32.4	7.6
20	0.5999	23.7	0.4547	25.8	0.0055	10.1	0.39	35.3	3.6	380.6	82.0	4507.7	344.4	35.3	3.6
34	0.7434	14.8	1.1405	19.0	0.0111	11.9	0.63	71.2	8.4	772.7	103.2	4817.0	212.9	71.2	8.4
12	0.7769	17.1	2.0655	22.4	0.0193	14.4	0.64	123.0	17.5	1137.5	154.3	4880.0	245.7	123.0	17.5
270510-06 Rejected Data															
28*	0.0532	10.7	0.0826	13.2	0.0112	7.6	0.58	72.1	5.4	80.6	10.2	338.2	243.0	72.1	5.4
19*	0.0546	17.2	0.4792	18.5	0.0636	6.8	0.37	397.2	26.0	397.5	60.9	396.2	385.1	397.2	26.0
30*	0.0796	10.6	1.3253	15.9	0.1206	11.8	0.75	734.1	82.0	856.8	92.4	1186.6	209.6	734.1	82.0
14*	0.0867	7.4	1.7548	10.1	0.1466	6.8	0.68	881.7	56.0	1028.9	65.6	1354.0	143.1	881.7	56.0
10*	0.0856	9.5	2.1742	12.9	0.1839	8.7	0.67	1088.4	86.6	1172.8	90.1	1329.4	184.5	1088.4	86.6
13*	0.0847	8.5	2.3197	11.2	0.1985	7.2	0.65	1167.0	77.1	1218.3	79.9	1307.7	165.9	1167.0	77.1
*Interpreted as detrital															
270510-14 Accepted Data															
24	0.0496	149.9	0.0114	150.8	0.0017	17.2	0.11	10.8	1.9	11.5	17.3	175.4	3495.8	10.8	1.9
4	0.0545	47.6	0.0134	48.6	0.0018	9.9	0.20	11.5	1.1	13.6	6.5	393.8	1067.3	11.5	1.1
15	0.0138	204.8	0.0035	205.1	0.0018	9.7	0.05	11.8	1.1	3.6	7.3	0.0	4937.3	11.8	1.1
10	0.0550	44.8	0.0140	45.7	0.0018	9.0	0.20	11.9	1.1	14.1	6.4	411.9	1000.8	11.9	1.1
6	0.0458	35.2	0.0123	37.9	0.0019	14.0	0.37	12.5	1.8	12.4	4.7	0.0	847.9	12.5	1.8
8	0.0264	42.4	0.0071	43.7	0.0019	10.5	0.24	12.5	1.3	7.2	3.1	0.0	1022.8	12.5	1.3
22	0.0398	42.5	0.0108	43.7	0.0020	10.2	0.23	12.6	1.3	10.9	4.7	0.0	1024.3	12.6	1.3
19	0.0205	68.6	0.0055	69.5	0.0020	11.4	0.16	12.6	1.4	5.6	3.9	0.0	1652.4	12.6	1.4
14	0.0772	21.3	0.0209	22.9	0.0020	8.4	0.36	12.6	1.1	21.0	4.8	1126.9	424.5	12.6	1.1
12	0.0352	43.0	0.0095	44.6	0.0020	12.1	0.27	12.6	1.5	9.6	4.3	0.0	1036.1	12.6	1.5
1	0.0485	44.2	0.0132	45.1	0.0020	9.2	0.20	12.7	1.2	13.3	6.0	124.9	1040.6	12.7	1.2
7	0.0610	23.0	0.0167	24.6	0.0020	8.6	0.35	12.8	1.1	16.8	4.1	638.5	494.7	12.8	1.1
25	0.0519	15.1	0.0146	17.9	0.0020	9.7	0.54	13.1	1.3	14.7	2.6	279.0	344.7	13.1	1.3
16	0.0666	28.3	0.0188	31.1	0.0020	13.1	0.42	13.1	1.7	18.9	5.8	826.5	589.6	13.1	1.7

Table A7 (continued): Volcanic Zircon U-Pb Integrated Data

Spot	Ratios						Ages (Ma)						Best Age	±2σ	
	207Pb/ 206Pb	±2σ	207Pb/ 235U	±2σ	206Pb/ 238U	±2σ	Rho	206Pb/ 238U	±2σ	207Pb/ 235U	±2σ	207Pb/ 206Pb			±2σ
270510-14 Accepted Data															
31	0.0578	18.1	0.0163	19.8	0.0020	7.8	0.40	13.2	1.0	16.5	3.2	523.4	398.0	13.2	1.0
29	0.0333	52.0	0.0095	54.3	0.0021	15.7	0.29	13.2	2.1	9.6	5.2	0.0	1253.0	13.2	2.1
33	0.0959	46.4	0.0276	47.3	0.0021	8.8	0.19	13.4	1.2	27.6	12.9	1545.5	872.6	13.4	1.2
20	0.1023	20.2	0.0296	22.0	0.0021	8.9	0.40	13.5	1.2	29.6	6.4	1667.1	373.2	13.5	1.2
13	0.0491	42.0	0.0142	44.8	0.0021	15.7	0.35	13.5	2.1	14.3	6.4	152.8	982.8	13.5	2.1
23	0.0576	18.9	0.0167	22.9	0.0021	13.0	0.57	13.5	1.8	16.8	3.8	513.5	414.5	13.5	1.8
17	0.1514	37.7	0.0454	40.0	0.0022	13.6	0.34	14.0	1.9	45.0	17.6	2361.8	642.9	14.0	1.9
11	0.0938	18.9	0.0284	20.7	0.0022	8.5	0.41	14.1	1.2	28.4	5.8	1504.6	357.4	14.1	1.2
9	0.1516	25.9	0.0464	28.5	0.0022	12.0	0.42	14.3	1.7	46.0	12.8	2363.9	441.6	14.3	1.7
18	0.0569	22.1	0.0176	33.6	0.0022	25.3	0.75	14.4	3.6	17.7	5.9	488.9	488.3	14.4	3.6
26	0.0806	32.0	0.0263	36.5	0.0024	17.6	0.48	15.3	2.7	26.4	9.5	1210.6	629.6	15.3	2.7
3	0.0316	93.2	0.0115	94.0	0.0026	12.3	0.13	16.9	2.1	11.6	10.8	0.0	2247.0	16.9	2.1
30	0.0532	34.9	0.0211	35.8	0.0029	8.2	0.23	18.5	1.5	21.2	7.5	336.8	790.3	18.5	1.5
5	0.0463	10.3	0.0189	12.4	0.0030	6.9	0.56	19.0	1.3	19.0	2.3	14.2	248.6	19.0	1.3
27	0.0298	159.2	0.0132	159.5	0.0032	9.4	0.06	20.7	1.9	13.4	21.2	0.0	3838.4	20.7	1.9
270510-14 Rejected Data															
32*	1.1902	477.8	-732.6487	1419.2	-4.4599	1336.3	0.94	0.0	0.0	0.0	0.0	5480.8	6757.3	0.0	0.0
2*	0.2368	99.1	0.0878	104.8	0.0027	34.0	0.32	17.3	5.9	85.5	86.1	3098.9	1579.4	17.3	5.9
21**	0.0519	11.2	0.3273	14.5	0.0457	9.2	0.64	288.3	26.0	287.5	36.3	279.0	256.0	288.3	26.0
28**	0.0761	9.2	1.3193	12.9	0.1255	9.0	0.70	762.2	64.9	854.2	74.5	1099.0	183.5	762.2	64.9
*6/8 uncertainty >30%															
**Interpreted as detrital															
270510-17 Accepted Data															
7	0.0521	12.0	0.0054	13.9	0.0007	6.9	0.50	4.8	0.3	5.4	0.8	289.9	275.2	4.8	0.3
15	0.0482	8.0	0.0051	10.0	0.0008	6.0	0.60	4.9	0.3	5.2	0.5	107.3	189.5	4.9	0.3
4	0.0474	13.2	0.0050	17.2	0.0008	11.0	0.64	4.9	0.5	5.1	0.9	69.4	314.0	4.9	0.5
16	0.0501	9.4	0.0053	11.6	0.0008	6.9	0.59	4.9	0.3	5.4	0.6	199.1	217.2	4.9	0.3
17	0.0490	8.6	0.0052	11.4	0.0008	7.4	0.65	4.9	0.4	5.3	0.6	147.2	202.7	4.9	0.4
14	0.0472	12.2	0.0050	14.9	0.0008	8.6	0.58	5.0	0.4	5.1	0.8	58.8	290.0	5.0	0.4
6	0.0637	14.4	0.0069	20.3	0.0008	14.3	0.70	5.0	0.7	6.9	1.4	733.0	305.2	5.0	0.7
11	0.0476	9.8	0.0051	12.7	0.0008	8.1	0.64	5.0	0.4	5.2	0.7	78.9	232.8	5.0	0.4
18	0.0527	10.8	0.0057	15.4	0.0008	10.9	0.71	5.1	0.6	5.8	0.9	314.5	246.7	5.1	0.6
20	0.0511	12.5	0.0056	16.8	0.0008	11.2	0.67	5.1	0.6	5.6	0.9	246.8	288.3	5.1	0.6
3	0.1656	96.2	0.0204	99.4	0.0009	24.9	0.25	5.7	1.4	20.5	20.1	2513.2	1617.4	5.7	1.4
13	0.3815	21.9	0.0847	33.4	0.0016	25.2	0.76	10.4	2.6	82.6	26.5	3837.9	330.0	10.4	2.6
270510-17 Rejected Data															
2*	0.0955	38.1	0.0117	54.8	0.0009	39.4	0.72	5.7	2.2	11.8	6.4	1537.2	717.5	5.7	2.2
12**	0.1844	7.5	13.3539	10.4	0.5247	7.3	0.70	2719.0	161.3	2705.0	98.9	2693.0	123.3	2693.0	123.3
8**	-0.0364	191.0	-0.0086	191.6	0.0017	15.7	0.08	11.0	1.7	0.0	0.0	0.0	4603.5	11.0	1.7
10**	-0.0138	299.7	-0.0034	300.0	0.0018	12.8	0.04	11.4	1.5	0.0	0.0	0.0	7224.7	11.4	1.5
19**	0.0366	94.1	0.0093	94.7	0.0018	10.7	0.11	11.9	1.3	9.4	8.9	0.0	2268.1	11.9	1.3
5**	0.0313	67.6	0.0081	68.5	0.0019	11.1	0.16	12.0	1.3	8.2	5.6	0.0	1630.3	12.0	1.3
21**	0.0824	36.9	0.0322	39.5	0.0028	14.1	0.36	18.2	2.6	32.1	12.5	1253.9	721.5	18.2	2.6
1**	0.0486	27.0	0.0253	28.1	0.0038	7.7	0.28	24.2	1.9	25.3	7.0	127.2	634.5	24.2	1.9
9**	0.0584	28.6	0.0334	30.4	0.0041	10.2	0.34	26.6	2.7	33.3	9.9	546.1	624.3	26.6	2.7
*6/8 uncertainty >30%															
**Interpreted as detrital															
20140704-01 Accepted Data															
9	0.2960	25.6	0.0042	30.2	0.0001	16.0	0.53	0.7	0.1	4.3	1.3	3449.5	397.3	0.7	0.1
3	0.9454	15.9	0.1344	21.0	0.0010	13.6	0.65	6.6	0.9	128.1	25.3	5158.4	226.8	6.6	0.9
10	0.8930	24.7	0.1990	30.7	0.0016	18.3	0.60	10.4	1.9	184.3	51.9	5077.8	352.2	10.4	1.9
13	0.8547	11.4	0.2168	14.9	0.0018	9.7	0.65	11.8	1.1	199.2	27.0	5015.7	162.8	11.8	1.1
14	0.7087	22.3	0.1893	28.7	0.0019	18.1	0.63	12.5	2.3	176.1	46.5	4748.4	321.6	12.5	2.3
7	0.8527	26.9	0.5228	33.8	0.0044	20.5	0.61	28.6	5.9	427.0	118.5	5012.4	384.1	28.6	5.9
11	0.8229	24.1	0.9622	29.4	0.0085	16.7	0.57	54.4	9.0	684.5	147.2	4961.9	345.2	54.4	9.0
8	0.8596	20.7	1.4855	26.7	0.0125	16.8	0.63	80.2	13.4	924.5	163.3	5023.9	296.0	80.2	13.4
12	0.8292	19.8	1.8267	25.3	0.0160	15.8	0.62	102.1	16.0	1055.1	167.5	4972.7	283.3	102.1	16.0
2	0.8704	18.4	2.2813	23.8	0.0190	15.1	0.64	121.3	18.2	1206.5	169.6	5041.5	262.2	121.3	18.2
6	0.8307	20.1	2.4571	25.9	0.0214	16.3	0.63	136.7	22.1	1259.5	189.0	4975.3	287.3	136.7	22.1
1	0.8621	17.8	2.6132	22.3	0.0220	13.4	0.60	140.1	18.5	1304.4	164.8	5027.9	253.7	140.1	18.5
5	0.8944	4.3	8.4031	6.0	0.0681	4.1	0.70	424.6	16.9	2275.5	54.2	5080.0	61.1	424.6	16.9
20140704-01 Rejected Data															
15*	0.1187	647.7	0.0008	654.0	0.0000	90.3	0.14	0.3	0.3	0.8	5.2	1937.4	11592.4	0.3	0.3
19*	0.8594	64.0	0.0188	84.2	0.0002	54.8	0.65	1.0	0.6	18.9	15.7	5023.4	913.5	1.0	0.6
16*	1.1132	80.4	0.0262	105.7	0.0002	68.6	0.65	1.1	0.8	26.3	27.4	5387.6	1138.8	1.1	0.8
20*	0.7209	52.0	0.0190	62.8	0.0002	35.2	0.56	1.2	0.4	19.2	11.9	4773.0	748.3	1.2	0.4
17*	0.9706	68.1	0.0337	86.3	0.0003	53.1	0.62	1.6	0.9	33.7	28.6	5195.5	967.8	1.6	0.9

Table A7 (continued): Volcanic Zircon U-Pb Integrated Data

Spot	Ratios							Ages (Ma)							
	207Pb/ 206Pb	±2σ	207Pb/ 235U	±2σ	206Pb/ 238U	±2σ	Rho	206Pb/ 238U	±2σ	207Pb/ 235U	±2σ	207Pb/ 206Pb	±2σ	Best Age	±2σ
<i>20140704-01 Rejected Data</i>															
04*	0.9017	43.4	0.0474	57.1	0.0004	37.0	0.65	2.5	0.9	47.0	26.2	5091.6	619.0	2.5	0.9
18**	0.8834	4.6	40.0846	8.3	0.3288	7.0	0.83	1832.7	112.3	3772.8	82.6	5062.5	66.2	5062.5	66.2
*6/8 uncertainty >30%															
**Older than Earth															
<i>20140704-02 Accepted Data</i>															
26	0.0608	16.4	0.0266	17.6	0.0032	6.3	0.36	20.4	1.3	26.7	4.6	631.9	354.0	20.4	1.3
1	0.0928	23.2	0.0443	24.1	0.0035	6.4	0.26	22.2	1.4	44.0	10.4	1484.2	440.4	22.2	1.4
21	0.0532	17.3	0.0251	18.4	0.0034	6.5	0.35	22.0	1.4	25.1	4.6	337.2	390.9	22.0	1.4
8	0.0621	17.8	0.0290	19.1	0.0034	6.8	0.35	21.8	1.5	29.0	5.5	678.4	381.3	21.8	1.5
27	0.0799	13.8	0.0367	15.4	0.0033	6.8	0.44	21.4	1.5	36.6	5.5	1195.6	272.4	21.4	1.5
11	0.0529	46.9	0.0226	47.4	0.0031	7.1	0.15	20.0	1.4	22.7	10.6	323.6	1064.0	20.0	1.4
20	0.0554	60.2	0.0288	60.8	0.0038	8.1	0.13	24.2	2.0	28.8	17.3	428.9	1342.1	24.2	2.0
4	0.0652	25.9	0.0317	27.2	0.0035	8.3	0.30	22.6	1.9	31.6	8.5	780.1	543.5	22.6	1.9
22	0.0636	17.2	0.0294	19.6	0.0033	9.5	0.48	21.5	2.0	29.4	5.7	727.9	364.7	21.5	2.0
19	0.0621	19.3	0.0297	21.6	0.0035	9.6	0.44	22.3	2.1	29.7	6.3	678.2	413.4	22.3	2.1
14	0.0553	14.2	0.0251	17.5	0.0033	10.2	0.58	21.1	2.1	25.2	4.3	426.1	316.7	21.1	2.1
25	0.0477	17.9	0.0230	20.9	0.0035	10.8	0.52	22.4	2.4	23.1	4.8	85.4	424.3	22.4	2.4
30	0.1509	21.3	0.0790	24.0	0.0038	11.1	0.46	24.4	2.7	77.2	17.8	2356.5	363.7	24.4	2.7
3	0.0795	41.8	0.0359	43.2	0.0033	11.1	0.26	21.0	2.3	35.8	15.2	1184.3	825.1	21.0	2.3
7	0.1232	35.0	0.0664	36.8	0.0039	11.2	0.31	25.1	2.8	65.2	23.2	2002.7	622.1	25.1	2.8
17	0.0634	21.5	0.0281	24.4	0.0032	11.5	0.47	20.7	2.4	28.1	6.8	720.2	456.4	20.7	2.4
18	0.0655	32.5	0.0315	34.7	0.0035	12.2	0.35	22.4	2.7	31.5	10.8	791.8	682.0	22.4	2.7
6	0.0615	12.3	0.0275	17.6	0.0032	12.6	0.71	20.8	2.6	27.5	4.8	655.0	263.8	20.8	2.6
10	0.0595	21.5	0.0272	25.3	0.0033	13.3	0.53	21.4	2.8	27.3	6.8	583.7	466.4	21.4	2.8
23	0.0549	30.0	0.0253	33.0	0.0033	13.8	0.42	21.5	3.0	25.4	8.3	407.9	670.6	21.5	3.0
9	0.0469	55.4	0.0204	57.1	0.0032	14.1	0.25	20.3	2.9	20.5	11.6	42.0	1324.3	20.3	2.9
15	0.0604	18.8	0.0281	23.5	0.0034	14.2	0.60	21.7	3.1	28.2	6.5	619.0	404.9	21.7	3.1
12	0.0625	22.2	0.0282	26.5	0.0033	14.4	0.54	21.0	3.0	28.2	7.4	689.9	474.1	21.0	3.0
24	0.0662	18.4	0.0302	24.1	0.0033	15.6	0.65	21.3	3.3	30.2	7.2	813.6	383.7	21.3	3.3
2	0.0962	47.3	0.0550	53.7	0.0041	25.4	0.47	26.7	6.8	54.4	28.4	1551.6	887.8	26.7	6.8
16	-0.0280	586.3	-0.0124	586.4	0.0032	10.0	0.02	20.7	2.1	0.0	0.0	0.0	14132.1	20.7	2.1
29	0.0132	184.0	0.0056	184.3	0.0031	10.6	0.06	19.8	2.1	5.7	10.4	0.0	4434.3	19.8	2.1
28	0.0454	57.8	0.0203	62.5	0.0032	23.8	0.38	20.8	4.9	20.4	12.6	0.0	1393.0	20.8	4.9
5	0.0235	272.1	0.0107	272.4	0.0033	13.0	0.05	21.1	2.7	10.8	29.2	0.0	6559.4	21.1	2.7
13	0.8119	7.6	8.5413	10.8	0.0762	7.7	0.72	473.5	35.3	2290.3	98.5	4942.8	108.1	473.5	35.3
<i>20140704-05 Accepted Data</i>															
25	0.0509	79.1	0.0238	79.8	0.0034	10.5	0.13	21.8	2.3	23.9	18.9	235.1	1825.9	21.8	2.3
14	0.0514	26.6	0.0245	27.6	0.0035	7.6	0.27	22.3	1.7	24.6	6.7	256.7	611.0	22.3	1.7
20	0.0642	30.6	0.0313	31.9	0.0035	9.0	0.28	22.7	2.0	31.3	9.8	748.3	646.9	22.7	2.0
13	0.0714	28.9	0.0349	30.4	0.0035	9.5	0.31	22.8	2.2	34.8	10.4	969.2	590.6	22.8	2.2
27	0.0822	29.1	0.0402	30.7	0.0035	9.6	0.31	22.8	2.2	40.1	12.1	1250.0	570.4	22.8	2.2
8	0.0370	64.7	0.0182	65.5	0.0036	9.9	0.15	22.9	2.3	18.3	11.9	0.0	1559.8	22.9	2.3
2	0.0752	18.3	0.0372	19.7	0.0036	7.5	0.38	23.1	1.7	37.1	7.2	1074.3	366.8	23.1	1.7
29	0.0910	34.5	0.0450	37.9	0.0036	15.7	0.41	23.1	3.6	44.7	16.6	1445.7	656.7	23.1	3.6
9	0.0702	26.6	0.0349	35.1	0.0036	23.0	0.65	23.2	5.3	34.8	12.0	935.3	545.4	23.2	5.3
11	0.0688	19.0	0.0345	20.2	0.0036	6.7	0.33	23.4	1.6	34.4	6.8	892.7	392.8	23.4	1.6
6	0.1612	26.5	0.0813	28.8	0.0037	11.3	0.39	23.5	2.7	79.4	22.0	2468.4	447.4	23.5	2.7
18	0.0742	49.2	0.0377	52.3	0.0037	17.7	0.34	23.7	4.2	37.6	19.3	1046.0	993.2	23.7	4.2
4	0.0538	17.3	0.0273	18.1	0.0037	5.4	0.30	23.7	1.3	27.4	4.9	361.2	390.4	23.7	1.3
22	0.0742	27.2	0.0382	29.8	0.0037	12.2	0.41	24.0	2.9	38.0	11.1	1046.3	548.0	24.0	2.9
28	0.0888	39.5	0.0457	41.2	0.0037	11.9	0.29	24.0	2.8	45.4	18.3	1400.5	756.4	24.0	2.8
7	0.0782	28.2	0.0410	29.1	0.0038	7.3	0.25	24.5	1.8	40.8	11.7	1150.8	559.8	24.5	1.8
3	0.1531	24.8	0.0808	33.0	0.0038	21.8	0.66	24.6	5.3	78.9	25.1	2380.3	423.0	24.6	5.3
10	0.0990	24.8	0.0523	27.2	0.0038	11.1	0.41	24.6	2.7	51.7	13.7	1604.7	462.9	24.6	2.7
1	0.1264	25.6	0.0669	28.3	0.0038	12.2	0.43	24.7	3.0	65.8	18.0	2048.1	451.5	24.7	3.0
5	0.1084	20.1	0.0578	23.6	0.0039	12.3	0.52	24.8	3.1	57.0	13.1	1772.5	367.5	24.8	3.1
30	0.1377	27.9	0.0761	29.8	0.0040	10.7	0.36	25.7	2.7	74.4	21.4	2198.4	483.8	25.7	2.7
26	0.1908	22.8	0.1140	24.4	0.0043	8.7	0.36	27.8	2.4	109.6	25.3	2749.2	374.5	27.8	2.4
23	0.0423	168.4	0.0195	168.8	0.0033	11.6	0.07	21.4	2.5	19.6	32.7	0.0	4058.6	21.4	2.5
<i>20140704-05 Rejected Data</i>															
17*	0.0711	217.1	0.0528	219.6	0.0054	33.2	0.15	34.6	11.4	52.3	112.3	959.5	4437.2	34.6	11.4
24**	0.7864	8.0	14.1491	11.1	0.1304	7.7	0.69	789.9	57.4	2759.8	105.4	4897.3	114.2	789.9	57.4
12**	0.7952	9.0	16.6998	12.7	0.1522	9.0	0.71	913.1	76.5	2917.8	122.0	4913.2	128.3	913.1	76.5
19**	0.8297	8.6	18.7623	12.1	0.1638	8.6	0.70	978.1	77.7	3029.7	117.5	4973.6	123.4	978.1	77.7
15**	0.8428	7.8	21.9364	11.1	0.1886	7.9	0.71	1113.8	80.8	3180.9	108.2	4995.9	111.8	1113.8	80.8

Table A7 (continued): Volcanic Zircon U-Pb Integrated Data

Spot	Ratios								Ages (Ma)				Best Age	±2σ	
	207Pb/206Pb		207Pb/235U		206Pb/238U		Rho	206Pb/238U		207Pb/235U		±2σ			
	±2σ		±2σ		±2σ			±2σ		±2σ					
20140704-05 Rejected Data															
21**	0.8190	8.1	27.8654	11.7	0.2465	8.4	0.72	1420.4	107.1	3414.4	115.0	4955.2	116.4	4955.2	116.4
16**	0.8496	8.0	28.5207	12.8	0.2432	10.0	0.78	1403.5	126.7	3437.2	126.7	5007.2	114.7	5007.2	114.7
*6/8 uncertainty >30%															
**Likely not zircon but phosphate: low 8/6 (<30) and high common Pb															
20140705-02 Accepted Data															
11	0.0537	19.6	0.0272	21.0	0.0037	7.4	0.35	23.5	1.7	27.2	5.6	358.9	443.3	23.5	1.7
5	0.0662	45.1	0.0341	46.1	0.0037	9.6	0.21	24.0	2.3	34.0	15.4	811.4	942.8	24.0	2.3
9	0.0679	28.6	0.0352	29.7	0.0037	8.1	0.27	24.1	2.0	35.1	10.2	865.8	592.2	24.1	2.0
2	0.0529	27.7	0.0274	35.8	0.0038	22.8	0.64	24.2	5.5	27.5	9.7	322.5	628.7	24.2	5.5
13	0.0613	17.3	0.0318	18.5	0.0038	6.5	0.35	24.2	1.6	31.8	5.8	648.3	371.0	24.2	1.6
3	0.0586	47.6	0.0305	48.1	0.0038	7.1	0.15	24.3	1.7	30.5	14.5	550.8	1038.9	24.3	1.7
12	0.0503	11.7	0.0265	13.0	0.0038	5.8	0.44	24.5	1.4	26.5	3.4	210.0	270.3	24.5	1.4
4	0.0458	13.3	0.0241	15.7	0.0038	8.3	0.53	24.6	2.0	24.2	3.8	0.0	321.7	24.6	2.0
14	0.0681	25.8	0.0360	27.3	0.0038	9.2	0.34	24.6	2.3	35.9	9.6	871.9	533.5	24.6	2.3
18	0.0562	22.0	0.0297	23.4	0.0038	7.9	0.34	24.7	2.0	29.8	6.9	460.6	487.8	24.7	2.0
8	0.0467	24.4	0.0250	26.7	0.0039	10.8	0.40	24.9	2.7	25.1	6.6	31.8	584.8	24.9	2.7
17	0.0546	17.7	0.0291	20.2	0.0039	9.6	0.47	24.9	2.4	29.1	5.8	395.5	397.8	24.9	2.4
15	0.0704	14.1	0.0376	15.9	0.0039	7.3	0.46	24.9	1.8	37.5	5.9	940.2	289.8	24.9	1.8
16	0.0675	18.5	0.0361	21.7	0.0039	11.2	0.52	25.0	2.8	36.0	7.7	854.5	385.0	25.0	2.8
6	0.0482	18.3	0.0262	19.6	0.0039	7.2	0.36	25.4	1.8	26.3	5.1	109.9	431.0	25.4	1.8
20	0.0514	10.6	0.0283	12.7	0.0040	6.9	0.54	25.8	1.8	28.3	3.5	256.6	244.6	25.8	1.8
19	0.0644	21.7	0.0373	23.7	0.0042	9.5	0.40	27.1	2.6	37.2	8.6	753.9	457.5	27.1	2.6
10	0.1219	13.4	0.0717	15.5	0.0042	7.8	0.50	27.3	2.1	70.3	10.5	1984.0	239.2	27.3	2.1
20140705-02 Rejected Data															
01*	0.0737	49.6	0.1861	61.6	0.0183	36.4	0.59	116.7	42.1	173.3	98.4	1032.6	1003.1	116.7	42.1
07*	0.0930	88.7	0.3037	88.9	0.0236	7.0	0.08	150.6	10.4	269.3	213.4	1488.2	1678.9	150.6	10.4
*Interpreted as detrital															
20150604-06 Accepted Data															
6	0.0641	38.0	0.0288	38.9	0.0033	8.3	0.21	20.9	1.7	28.8	11.0	745.6	802.5	20.9	1.7
18	0.0631	27.5	0.0290	28.9	0.0033	8.6	0.30	21.4	1.8	29.0	8.3	712.5	584.9	21.4	1.8
12	0.0467	32.3	0.0237	32.9	0.0037	6.6	0.20	23.7	1.5	23.8	7.7	34.2	773.2	23.7	1.5
14	0.0686	57.4	0.0352	57.9	0.0037	7.4	0.13	23.9	1.8	35.1	20.0	887.0	1187.5	23.9	1.8
16	0.0490	20.5	0.0255	21.0	0.0038	4.3	0.21	24.3	1.1	25.6	5.3	147.8	481.3	24.3	1.1
1	0.0529	11.2	0.0276	12.8	0.0038	6.2	0.49	24.3	1.5	27.7	3.5	325.2	253.2	24.3	1.5
13	0.0559	22.0	0.0295	24.2	0.0038	10.0	0.41	24.6	2.4	29.5	7.0	447.6	489.4	24.6	2.4
20	0.1296	109.7	0.0686	110.0	0.0038	7.4	0.07	24.7	1.8	67.3	71.8	2093.1	1928.5	24.7	1.8
19	0.0558	64.8	0.0297	65.0	0.0039	4.6	0.07	24.8	1.1	29.7	19.0	446.3	1440.4	24.8	1.1
17	0.0529	23.9	0.0282	25.1	0.0039	7.8	0.31	24.8	1.9	28.2	7.0	323.8	542.8	24.8	1.9
7	0.2230	100.1	0.1202	100.3	0.0039	6.3	0.06	25.1	1.6	115.2	109.7	3002.5	1608.7	25.1	1.6
3	0.0762	13.0	0.0382	13.8	0.0036	4.6	0.33	23.4	1.1	38.1	5.2	1099.7	260.6	23.4	1.1
10	0.0548	28.0	0.0285	29.9	0.0038	10.5	0.35	24.3	2.5	28.6	8.4	405.5	626.7	24.3	2.5
11	0.0765	17.1	0.0401	18.3	0.0038	6.4	0.35	24.4	1.6	39.9	7.2	1109.5	342.2	24.4	1.6
9	0.1947	55.7	0.1023	56.4	0.0038	8.6	0.15	24.5	2.1	98.9	53.2	2782.2	912.8	24.5	2.1
15	0.0004	15868.4	0.0002	15868.4	0.0038	17.5	0.00	24.8	4.3	0.2	34.3	0.0	382498.8	24.8	4.3
8	0.0488	43.4	0.0260	44.8	0.0039	11.2	0.25	24.8	2.8	26.0	11.5	139.4	1019.1	24.8	2.8
4	0.0713	86.7	0.0383	87.6	0.0039	12.3	0.14	25.0	3.1	38.1	32.8	967.0	1770.7	25.0	3.1
2	0.0769	67.6	0.0443	72.2	0.0042	25.5	0.35	26.8	6.8	44.0	31.1	1119.8	1348.2	26.8	6.8
20150604-06 Rejected Data															
05*	0.1493	75.7	0.2000	93.8	0.0097	55.4	0.59	62.3	34.3	185.2	160.1	2338.2	1295.6	62.3	34.3
*Interpreted as detrital															
20150604-07 Accepted Data															
12	-0.0006	8905.2	-0.0003	8905.3	0.0034	8.4	0.00	21.6	1.8	0.0	0.0	0.0	214656.5	21.6	1.8
11	0.0472	17.0	0.0224	18.3	0.0034	6.7	0.36	22.1	1.5	22.5	4.1	58.0	405.7	22.1	1.5
13	0.0426	23.8	0.0203	24.5	0.0035	6.0	0.25	22.2	1.3	20.4	5.0	0.0	573.5	22.2	1.3
15	0.0596	10.9	0.0285	12.4	0.0035	6.1	0.49	22.3	1.4	28.5	3.5	590.1	235.8	22.3	1.4
14	0.0351	49.2	0.0168	50.0	0.0035	8.9	0.18	22.3	2.0	16.9	8.4	0.0	1186.7	22.3	2.0
9	0.0500	9.8	0.0243	10.8	0.0035	4.6	0.43	22.7	1.0	24.4	2.6	196.8	227.5	22.7	1.0
19	0.0670	21.6	0.0326	23.8	0.0035	10.0	0.42	22.7	2.3	32.6	7.6	839.2	449.8	22.7	2.3
17	0.0578	51.1	0.0283	51.7	0.0035	7.5	0.14	22.8	1.7	28.4	14.4	522.8	1121.7	22.8	1.7
10	0.0503	9.9	0.0247	10.8	0.0036	4.4	0.40	22.9	1.0	24.8	2.6	207.8	229.6	22.9	1.0
16	0.0589	16.1	0.0292	18.4	0.0036	9.0	0.49	23.1	2.1	29.2	5.3	562.6	350.7	23.1	2.1
18	0.0391	68.7	0.0195	69.2	0.0036	8.3	0.12	23.3	1.9	19.6	13.5	0.0	1656.3	23.3	1.9
2	0.0535	25.8	0.0269	28.2	0.0036	11.3	0.40	23.5	2.7	27.0	7.5	351.6	583.6	23.5	2.7
8	0.0475	8.8	0.0239	10.0	0.0037	4.6	0.46	23.5	1.1	24.0	2.4	75.4	209.7	23.5	1.1
1	0.0449	19.3	0.0227	22.0	0.0037	10.5	0.48	23.6	2.5	22.8	4.9	0.0	465.4	23.6	2.5
27	0.0508	12.1	0.0258	13.8	0.0037	6.7	0.48	23.7	1.6	25.9	3.5	233.4	278.2	23.7	1.6

Table A7 (continued): Volcanic Zircon U-Pb Integrated Data

Spot	Ratios								Ages (Ma)					Best Age	±2σ
	207Pb/206Pb	±2σ	207Pb/235U	±2σ	206Pb/238U	±2σ	Rho	206Pb/238U	±2σ	207Pb/235U	±2σ	207Pb/206Pb	±2σ		
20150604-07 Accepted Data															
7	0.0532	12.9	0.0271	15.0	0.0037	7.6	0.51	23.7	1.8	27.1	4.0	338.9	292.2	23.7	1.8
24	0.0392	25.2	0.0200	29.1	0.0037	14.5	0.50	23.7	3.4	20.1	5.8	0.0	607.8	23.7	3.4
29	0.0530	9.5	0.0274	11.0	0.0038	5.5	0.50	24.2	1.3	27.5	3.0	326.9	215.3	24.2	1.3
22	0.0508	45.3	0.0264	47.7	0.0038	14.9	0.31	24.2	3.6	26.4	12.4	233.3	1045.9	24.2	3.6
6	0.0464	11.1	0.0241	12.1	0.0038	5.0	0.41	24.3	1.2	24.2	2.9	16.3	265.7	24.3	1.2
28	0.0788	71.3	0.0423	71.8	0.0039	8.6	0.12	25.0	2.2	42.0	29.6	1168.1	1412.7	25.0	2.2
5	0.0585	15.7	0.0319	17.1	0.0039	7.0	0.41	25.4	1.8	31.8	5.4	549.4	341.9	25.4	1.8
21	0.0509	13.7	0.0280	16.0	0.0040	8.3	0.52	25.7	2.1	28.0	4.4	235.5	316.6	25.7	2.1
25	0.1116	11.5	0.0524	13.1	0.0034	6.3	0.48	21.9	1.4	51.8	6.6	1825.5	209.3	21.9	1.4
30	0.0497	15.5	0.0257	21.7	0.0037	15.1	0.70	24.1	3.6	25.8	5.5	180.2	362.4	24.1	3.6
26	0.0834	20.3	0.0458	21.6	0.0040	7.4	0.34	25.6	1.9	45.5	9.6	1279.3	395.7	25.6	1.9
4	0.0709	23.5	0.0397	29.3	0.0041	17.5	0.60	26.1	4.6	39.6	11.4	955.0	480.0	26.1	4.6
3	0.1550	14.8	0.0887	17.0	0.0041	8.5	0.50	26.7	2.3	86.3	14.1	2402.3	251.3	26.7	2.3
23	0.1754	7.8	0.1084	9.9	0.0045	6.3	0.63	28.8	1.8	104.5	9.9	2609.6	129.3	28.8	1.8
20	0.2214	19.2	0.1371	22.9	0.0045	12.5	0.55	28.9	3.6	130.5	28.0	2991.1	308.3	28.9	3.6
20150605-04 Accepted Data															
9	-0.0339	697.3	-0.0152	697.7	0.0032	22.7	0.03	20.9	4.7	0.0	0.0	0.0	16808.4	20.9	4.7
3	0.0521	65.6	0.0236	66.1	0.0033	8.3	0.12	21.1	1.7	23.7	15.5	291.4	1498.9	21.1	1.7
11	0.0637	37.6	0.0297	39.6	0.0034	12.5	0.31	21.7	2.7	29.7	11.6	731.6	795.7	21.7	2.7
5	0.0825	31.8	0.0387	33.2	0.0034	9.6	0.29	21.9	2.1	38.6	12.6	1257.6	622.3	21.9	2.1
13	0.2322	55.1	0.1109	56.9	0.0035	14.4	0.25	22.3	3.2	106.8	57.7	3067.2	880.3	22.3	3.2
17	0.0845	46.8	0.0405	48.4	0.0035	12.4	0.25	22.4	2.8	40.4	19.1	1304.1	909.6	22.4	2.8
2	0.1234	27.1	0.0593	30.5	0.0035	14.1	0.46	22.4	3.2	58.5	17.3	2005.3	480.5	22.4	3.2
20	0.1485	92.7	0.0714	93.2	0.0035	9.9	0.10	22.4	2.2	70.1	63.1	2328.8	1587.7	22.4	2.2
8	0.0768	39.9	0.0376	40.3	0.0035	6.1	0.15	22.8	1.4	37.4	14.8	1116.0	796.1	22.8	1.4
6	0.0607	20.7	0.0300	21.8	0.0036	6.9	0.31	23.0	1.6	30.0	6.4	628.6	446.2	23.0	1.6
7	0.0711	24.7	0.0352	25.9	0.0036	8.1	0.31	23.1	1.9	35.1	8.9	960.8	503.8	23.1	1.9
15	0.0496	81.9	0.0245	82.1	0.0036	6.6	0.08	23.1	1.5	24.6	20.0	174.0	1910.3	23.1	1.5
14	0.0981	51.4	0.0515	52.0	0.0038	7.7	0.14	24.5	1.9	51.0	25.9	1587.5	961.5	24.5	1.9
10	0.4145	14.9	0.2403	16.3	0.0042	6.8	0.41	27.0	1.8	218.7	32.1	3962.6	223.0	27.0	1.8
16	0.1121	40.0	0.0661	49.4	0.0043	29.1	0.59	27.5	8.0	65.0	31.1	1833.6	724.1	27.5	8.0
4	0.4635	38.9	0.2897	39.5	0.0045	7.4	0.18	29.1	2.2	258.3	90.4	4129.3	576.5	29.1	2.2
1	0.3144	16.8	0.2162	18.4	0.0050	7.6	0.41	32.0	2.4	198.7	33.3	3542.9	259.2	32.0	2.4
19	0.4859	14.6	0.3843	17.4	0.0057	9.8	0.54	36.8	3.6	330.2	49.1	4199.1	215.8	36.8	3.6
12	0.4428	10.8	0.3811	12.4	0.0062	6.4	0.49	40.1	2.6	327.8	34.9	4061.0	161.6	40.1	2.6
20150605-04 Rejected Data															
18*	0.1063	39.3	0.0654	51.5	0.0045	33.4	0.65	28.7	9.6	64.4	32.1	1737.1	719.9	28.7	9.6
*6/8 uncertainty >30%															
20150607-09 Accepted Data															
13	0.0437	32.1	0.0184	33.0	0.0031	7.7	0.23	19.7	1.5	18.5	6.1	0.0	773.6	19.7	1.5
18	0.0565	33.2	0.0239	34.0	0.0031	7.7	0.23	19.8	1.5	24.0	8.1	471.2	733.8	19.8	1.5
9	0.0508	48.2	0.0215	49.2	0.0031	9.6	0.20	19.8	1.9	21.6	10.5	230.4	1113.7	19.8	1.9
10	0.0697	30.1	0.0300	30.9	0.0031	7.3	0.23	20.1	1.5	30.0	9.1	919.1	618.2	20.1	1.5
5	0.0145	536.8	0.0063	536.9	0.0031	6.8	0.01	20.1	1.4	6.3	34.0	0.0	12939.6	20.1	1.4
3	0.0621	26.9	0.0275	28.1	0.0032	8.0	0.28	20.7	1.7	27.6	7.6	677.0	575.9	20.7	1.7
7	0.0487	39.8	0.0218	42.2	0.0032	14.0	0.33	20.8	2.9	21.9	9.1	132.8	934.9	20.8	2.9
16	0.0886	69.7	0.0402	70.7	0.0033	11.9	0.17	21.2	2.5	40.0	27.8	1395.3	1336.7	21.2	2.5
6	0.0521	48.0	0.0239	49.1	0.0033	10.0	0.20	21.4	2.1	24.0	11.6	290.2	1097.3	21.4	2.1
2	0.1572	53.9	0.0731	54.5	0.0034	7.7	0.14	21.7	1.7	71.6	37.7	2425.3	914.7	21.7	1.7
11	0.0724	62.4	0.0337	63.5	0.0034	11.7	0.18	21.7	2.5	33.7	21.0	996.5	1268.6	21.7	2.5
12	0.0472	72.0	0.0224	74.0	0.0034	17.1	0.23	22.2	3.8	22.5	16.5	58.1	1716.1	22.2	3.8
14	0.0684	16.9	0.0328	18.0	0.0035	6.3	0.35	22.4	1.4	32.8	5.8	879.9	348.8	22.4	1.4
17	0.0588	24.4	0.0284	26.2	0.0035	9.4	0.36	22.5	2.1	28.4	7.3	558.3	532.6	22.5	2.1
15	0.0888	18.4	0.0434	20.3	0.0035	8.5	0.42	22.8	1.9	43.2	8.6	1399.1	352.5	22.8	1.9
19	0.0877	23.4	0.0433	24.7	0.0036	8.1	0.33	23.0	1.9	43.0	10.4	1376.1	449.7	23.0	1.9
8	0.1936	108.1	0.0980	109.1	0.0037	14.8	0.14	23.6	3.5	94.9	99.1	2773.3	1772.0	23.6	3.5
4	0.2379	27.3	0.1746	30.9	0.0053	14.5	0.47	34.2	4.9	163.4	46.7	3106.3	435.2	34.2	4.9
1	0.7118	16.6	1.2666	20.9	0.0129	12.7	0.61	82.5	10.4	830.9	119.2	4754.8	239.1	82.5	10.4
20150607-09 Rejected Data															
20*	0.0425	203.9	0.0150	208.8	0.0026	45.1	0.22	16.5	7.4	15.2	31.4	0.0	4914.9	16.5	7.4
*6/8 uncertainty >30%															
20150609-10 Accepted Data															
19	0.0935	70.7	0.0269	72.0	0.0021	13.7	0.19	13.4	1.8	26.9	19.1	1498.0	1336.4	13.4	1.8
3	0.1625	49.3	0.0475	50.0	0.0021	8.7	0.17	13.6	1.2	47.1	23.0	2481.6	831.0	13.6	1.2
20	0.1230	23.8	0.0388	25.1	0.0023	7.9	0.31	14.7	1.2	38.7	9.5	2000.0	423.6	14.7	1.2
8	0.1867	76.8	0.0594	77.9	0.0023	13.2	0.17	14.8	2.0	58.6	44.3	2713.5	1265.5	14.8	2.0

Table A7 (continued): Volcanic Zircon U-Pb Integrated Data

Spot	Ratios							Ages (Ma)							
	207Pb/ 206Pb		207Pb/ 235U		206Pb/ 238U		Rho	206Pb/ 238U		207Pb/ 235U		207Pb/ 206Pb		Best Age	$\pm 2\sigma$
	$\pm 2\sigma$	$\pm 2\sigma$	$\pm 2\sigma$	$\pm 2\sigma$	$\pm 2\sigma$	$\pm 2\sigma$		$\pm 2\sigma$	$\pm 2\sigma$	$\pm 2\sigma$	$\pm 2\sigma$				
<i>20150609-10 Accepted Data</i>															
12	0.0999	25.4	0.0323	28.5	0.0023	12.8	0.45	15.1	1.9	32.3	9.0	1621.4	473.0	15.1	1.9
16	0.4617	96.1	0.1506	96.4	0.0024	7.8	0.08	15.2	1.2	142.4	128.8	4123.4	1426.8	15.2	1.2
10	0.0909	57.7	0.0350	62.8	0.0028	24.7	0.39	18.0	4.4	34.9	21.6	1444.0	1099.8	18.0	4.4
5	0.3845	14.7	0.1493	16.6	0.0028	7.6	0.46	18.1	1.4	141.3	21.8	3849.4	222.6	18.1	1.4
14	0.2617	77.2	0.1034	81.1	0.0029	24.9	0.31	18.4	4.6	99.9	77.3	3257.0	1215.6	18.4	4.6
15	-0.0810	450.7	-0.0379	451.2	0.0034	19.6	0.04	21.8	4.3	0.0	0.0	0.0	10864.6	21.8	4.3
4	0.5893	15.9	0.2959	20.0	0.0036	12.1	0.60	23.4	2.8	263.2	46.4	4481.9	231.8	23.4	2.8
13	0.3783	22.0	0.2202	29.7	0.0042	20.0	0.67	27.1	5.4	202.1	54.4	3825.0	332.0	27.1	5.4
7	0.4987	31.5	0.3035	38.8	0.0044	22.7	0.58	28.4	6.4	269.1	91.9	4237.4	463.9	28.4	6.4
6	0.7552	33.9	0.8680	37.1	0.0083	15.2	0.41	53.5	8.1	634.5	176.9	4839.4	486.2	53.5	8.1
18	0.6760	17.1	1.0252	20.3	0.0110	10.9	0.54	70.4	7.7	716.5	104.8	4680.6	247.1	70.4	7.7
2	0.8031	20.1	5.8352	25.1	0.0527	15.1	0.60	330.8	48.8	1951.7	221.2	4927.2	287.4	330.8	48.8
<i>20150609-10 Rejected Data</i>															
01*	-0.0638	824.2	-0.0270	825.3	0.0031	41.2	0.05	19.7	8.1	0.0	0.0	0.0	19868.0	19.7	8.1
17*	0.2772	36.0	0.1487	48.7	0.0039	32.7	0.67	25.0	8.2	140.8	64.1	3347.0	563.3	25.0	8.2
11*	0.5123	36.0	0.6191	49.6	0.0088	34.1	0.69	56.2	19.1	489.3	194.8	4277.1	529.8	56.2	19.1
09*	0.3560	76.5	0.4449	103.3	0.0091	69.4	0.67	58.1	40.1	373.7	334.5	3732.9	1163.4	58.1	40.1
*6/8 uncertainty >30%															
<i>20150609-11 Accepted Data</i>															
14	0.0610	45.4	0.0115	52.2	0.0014	25.7	0.49	8.8	2.3	11.6	6.0	640.7	976.6	8.8	2.3
19	0.1841	113.8	0.0351	114.6	0.0014	13.3	0.12	8.9	1.2	35.1	39.5	2690.3	1880.4	8.9	1.2
4	0.0425	77.1	0.0081	78.0	0.0014	12.0	0.15	8.9	1.1	8.2	6.4	0.0	1858.6	8.9	1.1
7	0.0457	109.3	0.0094	109.4	0.0015	5.2	0.05	9.6	0.5	9.5	10.3	0.0	2634.5	9.6	0.5
8	0.0729	63.4	0.0151	63.6	0.0015	6.0	0.09	9.7	0.6	15.2	9.6	1012.1	1284.6	9.7	0.6
11	0.0945	50.2	0.0197	50.8	0.0015	7.9	0.16	9.7	0.8	19.8	9.9	1518.8	946.3	9.7	0.8
6	0.0519	192.5	0.0109	193.0	0.0015	13.9	0.07	9.8	1.4	11.0	21.2	279.2	4405.8	9.8	1.4
12	0.0663	71.8	0.0142	72.1	0.0016	6.6	0.09	10.0	0.7	14.3	10.2	815.8	1499.6	10.0	0.7
17	0.0693	85.3	0.0149	85.8	0.0016	9.3	0.11	10.1	0.9	15.1	12.8	908.3	1757.4	10.1	0.9
16	0.0974	69.0	0.0213	69.3	0.0016	5.7	0.09	10.2	0.6	21.4	14.7	1574.8	1291.9	10.2	0.6
15	0.0660	36.3	0.0150	38.5	0.0016	12.6	0.33	10.6	1.3	15.1	5.8	807.5	760.6	10.6	1.3
1	0.1248	317.8	0.0285	318.2	0.0017	16.8	0.05	10.6	1.8	28.5	89.7	2026.4	5628.2	10.6	1.8
5	0.3379	103.5	0.1079	106.1	0.0023	23.1	0.22	14.9	3.4	104.0	105.3	3653.5	1582.8	14.9	3.4
10	0.2294	28.2	0.0774	36.2	0.0024	22.6	0.63	15.7	3.6	75.7	26.4	3048.0	452.3	15.7	3.6
9	0.5071	20.1	0.2001	21.1	0.0029	6.4	0.30	18.4	1.2	185.2	35.7	4262.0	296.0	18.4	1.2
3	0.3509	28.9	0.1427	39.8	0.0029	27.3	0.69	19.0	5.2	135.5	50.5	3711.0	440.2	19.0	5.2
20	0.5955	20.4	0.3591	25.4	0.0044	15.2	0.60	28.1	4.3	311.5	68.4	4497.0	296.6	28.1	4.3
<i>20150609-11 Rejected Data</i>															
13*	0.4042	43.3	0.1384	55.1	0.0025	33.9	0.62	16.0	5.4	131.6	68.1	3924.8	650.9	16.0	5.4
18*	0.3954	86.3	0.1503	97.3	0.0028	45.1	0.46	17.7	8.0	142.2	129.8	3891.6	1298.1	17.7	8.0
2*	0.2864	39.7	0.1160	52.1	0.0029	33.7	0.65	18.9	6.4	111.4	55.0	3398.0	617.7	18.9	6.4
*6/8 uncertainty >30%															
<i>20160814-01 Accepted Data</i>															
30	0.0441	36.5	0.0072	37.2	0.0012	7.8	0.20	7.6	0.6	7.3	2.7	0.0	878.8	7.6	0.6
8	0.0391	84.8	0.0067	85.3	0.0012	9.2	0.11	7.9	0.7	6.7	5.7	0.0	2045.2	7.9	0.7
13	0.0719	55.3	0.0123	56.3	0.0012	10.4	0.18	8.0	0.8	12.4	7.0	982.3	1126.7	8.0	0.8
3	0.0662	20.5	0.0115	21.8	0.0013	7.7	0.35	8.1	0.6	11.6	2.5	811.7	427.7	8.1	0.6
24	0.0627	16.6	0.0109	18.1	0.0013	7.3	0.40	8.1	0.6	11.0	2.0	697.0	354.3	8.1	0.6
21	-0.0159	1078.9	-0.0028	1079.0	0.0013	11.8	0.01	8.2	1.0	0.0	0.0	0.0	26006.3	8.2	1.0
12	0.2029	108.7	0.0357	109.0	0.0013	8.3	0.08	8.2	0.7	35.6	38.2	2850.0	1770.2	8.2	0.7
26	0.0509	148.5	0.0077	149.6	0.0011	18.2	0.12	7.0	1.3	7.8	11.6	237.4	3424.5	7.0	1.3
25	0.0695	42.8	0.0117	45.5	0.0012	15.5	0.34	7.9	1.2	11.8	5.3	914.7	880.0	7.9	1.2
15	0.1299	37.4	0.0220	38.7	0.0012	10.1	0.26	7.9	0.8	22.1	8.5	2096.1	656.8	7.9	0.8
9	0.0845	29.6	0.0143	33.3	0.0012	15.3	0.46	7.9	1.2	14.4	4.8	1305.1	574.8	7.9	1.2
29	0.0827	24.1	0.0140	26.0	0.0012	10.0	0.38	7.9	0.8	14.2	3.7	1261.9	470.3	7.9	0.8
7	0.1175	40.0	0.0212	41.1	0.0013	9.8	0.24	8.4	0.8	21.3	8.7	1918.8	716.8	8.4	0.8
1	0.0708	16.3	0.0129	19.6	0.0013	11.0	0.56	8.5	0.9	13.0	2.5	951.8	333.8	8.5	0.9
17	0.1385	37.4	0.0253	38.4	0.0013	8.7	0.23	8.5	0.7	25.4	9.6	2208.0	649.1	8.5	0.7
28	0.0764	24.2	0.0142	29.8	0.0013	17.5	0.58	8.7	1.5	14.3	4.2	1105.5	484.0	8.7	1.5
22	0.1712	20.1	0.0343	22.5	0.0015	10.3	0.45	9.4	1.0	34.3	7.6	2569.0	336.0	9.4	1.0
14	0.2295	36.7	0.0470	37.5	0.0015	7.4	0.20	9.6	0.7	46.6	17.1	3048.9	588.0	9.6	0.7
19	0.1228	82.5	0.0252	85.7	0.0015	23.3	0.27	9.6	2.2	25.3	21.4	1997.6	1466.0	9.6	2.2
5	0.2833	22.6	0.0612	29.6	0.0016	19.1	0.64	10.1	1.9	60.3	17.3	3381.0	353.0	10.1	1.9
20	0.2074	24.0	0.0455	28.8	0.0016	16.1	0.56	10.2	1.6	45.2	12.7	2885.7	389.3	10.2	1.6
16	0.3372	16.0	0.0778	17.3	0.0017	6.7	0.38	10.8	0.7	76.1	12.7	3650.2	244.0	10.8	0.7
10	0.4196	24.6	0.1019	27.6	0.0018	12.6	0.46	11.3	1.4	98.5	26.0	3980.7	368.1	11.3	1.4
18	0.3834	9.7	0.1111	12.4	0.0021	7.8	0.63	13.5	1.1	107.0	12.6	3845.3	145.7	13.5	1.1
2	0.4777	25.7	0.1570	29.3	0.0024	14.1	0.48	15.3	2.2	148.1	40.4	4173.9	380.5	15.3	2.2

Table A7 (continued): Volcanic Zircon U-Pb Integrated Data

Spot	Ratios						Ages (Ma)						Best Age	±2σ	
	207Pb/206Pb	±2σ	207Pb/235U	±2σ	206Pb/238U	±2σ	Rho	206Pb/238U	±2σ	207Pb/235U	±2σ	207Pb/206Pb			±2σ
<i>20160814-01 Accepted Data</i>															
23	0.1760	24.2	0.0595	25.1	0.0024	6.7	0.26	15.8	1.1	58.7	14.3	2615.5	403.1	15.8	1.1
27	0.6339	6.9	0.3230	9.6	0.0037	6.9	0.70	23.8	1.6	284.2	23.8	4587.8	99.3	23.8	1.6
11	0.6774	8.9	0.5746	16.7	0.0061	14.2	0.85	39.5	5.6	461.0	61.9	4683.5	127.9	39.5	5.6
<i>20160814-01 Rejected Data</i>															
201608	0.1224	151.4	0.0174	159.0	0.0010	48.5	0.31	6.6	3.2	17.5	27.6	1991.4	2692.5	6.6	3.2
201608	0.0906	212.9	0.0130	215.2	0.0010	31.6	0.15	6.7	2.1	13.1	28.1	1437.7	4059.3	6.7	2.1
*6/8 uncertainty >30%															
<i>20160814-04 Accepted Data</i>															
15	0.1580	127.4	0.0407	127.7	0.0019	8.8	0.07	12.0	1.1	40.5	50.8	2434.1	2159.2	12.0	1.1
17	0.0880	47.1	0.0247	48.2	0.0020	10.0	0.21	13.1	1.3	24.8	11.8	1382.0	905.8	13.1	1.3
20	0.1369	102.0	0.0391	102.1	0.0021	6.4	0.06	13.3	0.8	38.9	39.0	2188.9	1772.4	13.3	0.8
19	0.0794	17.5	0.0228	18.3	0.0021	5.4	0.29	13.4	0.7	22.9	4.2	1181.8	346.8	13.4	0.7
9	0.1243	47.4	0.0359	47.7	0.0021	5.3	0.11	13.5	0.7	35.8	16.8	2018.9	840.5	13.5	0.7
3	0.1097	72.6	0.0341	73.3	0.0023	10.1	0.14	14.5	1.5	34.0	24.5	1794.7	1322.2	14.5	1.5
7	0.2405	20.2	0.0752	21.6	0.0023	7.7	0.35	14.6	1.1	73.7	15.4	3123.1	321.6	14.6	1.1
<i>20160814-04 Rejected Data</i>															
02*	0.1030	49.0	0.0393	64.6	0.0028	42.1	0.65	17.8	7.5	39.2	24.8	1678.5	904.4	17.8	7.5
13*	0.0594	77.7	0.0233	92.0	0.0028	49.3	0.54	18.3	9.0	23.3	21.2	582.8	1687.9	18.3	9.0
08*	0.5946	97.1	1.2279	121.4	0.0150	72.9	0.60	95.7	69.2	813.4	821.7	4495.0	1412.5	95.7	69.2
01*	0.5843	56.0	1.3325	78.3	0.0165	54.7	0.70	105.7	57.3	860.0	488.6	4469.3	815.8	105.7	57.3
05**	0.0831	49.4	0.0276	51.6	0.0024	14.8	0.29	15.5	2.3	27.7	14.1	1272.2	964.5	15.5	2.3
11**	0.0482	15.3	0.0169	16.6	0.0025	6.4	0.39	16.4	1.1	17.0	2.8	108.0	361.1	16.4	1.1
14**	0.0833	22.6	0.0295	23.0	0.0026	4.5	0.20	16.5	0.7	29.5	6.7	1277.2	440.1	16.5	0.7
18**	0.4737	13.8	0.2164	15.2	0.0033	6.5	0.42	21.3	1.4	198.9	27.5	4161.2	204.3	21.3	1.4
12**	0.4178	21.0	0.2530	25.9	0.0044	15.1	0.58	28.2	4.2	229.0	53.1	3974.4	315.1	28.2	4.2
16**	0.6204	29.6	0.5628	34.2	0.0066	17.3	0.50	42.2	7.3	453.4	125.8	4556.6	428.8	42.2	7.3
04**	0.5346	35.9	0.5436	38.0	0.0074	12.7	0.33	47.3	6.0	440.8	136.8	4339.4	525.7	47.3	6.0
06**	0.7782	31.9	2.0378	40.6	0.0190	25.1	0.62	121.2	30.1	1128.2	283.6	4882.4	458.0	121.2	30.1
10***	0.8608	4.4	24.8852	13.9	0.2095	13.2	0.95	1225.9	147.8	3303.7	136.5	5025.9	62.6	5025.9	62.6
* 6/8 uncertainty >30%															
**Interpreted as detrital															
***Older than Earth															
<i>20160814-12 Accepted Data</i>															
17	0.1371	75.8	0.0331	77.2	0.0017	14.5	0.19	11.3	1.6	33.1	25.1	2191.1	1316.7	11.3	1.6
20	-0.0055	2346.9	-0.0014	2346.9	0.0018	13.1	0.01	11.5	1.5	0.0	0.0	0.0	56570.1	11.5	1.5
10	0.0604	22.1	0.0154	23.4	0.0018	7.7	0.33	11.9	0.9	15.5	3.6	619.1	477.3	11.9	0.9
15	0.1788	69.6	0.0456	72.4	0.0019	19.9	0.28	11.9	2.4	45.3	32.1	2641.9	1154.9	11.9	2.4
8	0.3560	86.0	0.0913	88.5	0.0019	20.9	0.24	12.0	2.5	88.7	75.3	3733.0	1307.8	12.0	2.5
9	0.0611	89.8	0.0165	91.4	0.0020	17.3	0.19	12.6	2.2	16.7	15.1	642.2	1929.8	12.6	2.2
18	0.0086	876.1	0.0024	876.2	0.0020	8.6	0.01	12.9	1.1	2.4	21.0	0.0	21118.4	12.9	1.1
4	0.0685	25.1	0.0194	26.5	0.0020	8.4	0.31	13.2	1.1	19.5	5.1	882.5	520.0	13.2	1.1
11	0.1781	33.1	0.0543	34.9	0.0022	10.8	0.31	14.2	1.5	53.7	18.2	2635.1	550.6	14.2	1.5
16	0.1266	24.5	0.0446	26.4	0.0026	9.4	0.37	16.4	1.5	44.3	11.5	2051.6	433.4	16.4	1.5
14	0.3965	33.0	0.1585	34.8	0.0029	11.0	0.32	18.7	2.0	149.4	48.4	3895.9	495.9	18.7	2.0
2	0.4675	13.8	0.2289	23.8	0.0035	19.3	0.81	22.8	4.4	209.3	45.0	4141.9	205.3	22.8	4.4
12	0.3599	66.7	0.1835	67.2	0.0037	8.4	0.13	23.8	2.0	171.0	106.2	3749.4	1013.4	23.8	2.0
19	0.5940	16.7	0.8582	18.7	0.0105	7.9	0.45	67.1	5.3	629.2	87.9	4493.3	243.1	67.1	5.3
3	0.7815	10.9	2.2481	14.1	0.0208	9.0	0.63	132.9	11.9	1196.2	99.7	4888.4	156.8	132.9	11.9
<i>20160814-12 Rejected Data</i>															
01*	0.0577	17.0	0.0269	18.4	0.0034	7.1	0.38	21.7	1.5	27.0	4.9	519.0	372.6	21.7	1.5
13*	-0.3402	164.4	-0.0869	168.7	0.0019	38.1	0.23	11.9	4.5	0.0	0.0	0.0	3962.3	11.9	4.5
05**	0.0894	55.1	0.0213	72.7	0.0017	47.5	0.65	11.1	5.3	21.4	15.4	1412.5	1053.3	11.1	5.3
07**	0.0634	14.0	0.1029	17.9	0.0118	11.2	0.62	75.3	8.4	99.5	17.0	723.0	297.7	75.3	8.4
06**	0.1028	6.7	3.7707	11.3	0.2657	9.1	0.80	1518.8	123.0	1586.5	90.5	1675.3	124.1	1675.3	124.1
*6/8 uncertainty >30%															
**Interpreted as detrital															
<i>20150618-03 Accepted Data</i>															
11	0.0520	28.6	0.0235	29.2	0.0033	6.2	0.21	21.0	1.3	23.6	6.8	286.6	653.6	21.0	1.3
5	0.0919	62.6	0.0418	63.5	0.0033	10.8	0.18	21.2	2.3	41.6	25.9	1464.9	1188.3	21.2	2.3
14	0.1431	48.0	0.0660	48.7	0.0033	8.6	0.17	21.5	1.9	64.9	30.6	2265.1	827.9	21.5	1.9
10	0.1145	92.4	0.0532	93.1	0.0034	11.1	0.12	21.6	2.4	52.6	47.8	1872.6	1666.9	21.6	2.4
19	0.1269	68.0	0.0600	68.2	0.0034	6.3	0.09	22.1	1.4	59.2	39.3	2055.7	1199.6	22.1	1.4
4	0.0633	46.2	0.0305	50.0	0.0035	18.9	0.38	22.5	4.3	30.6	15.1	717.1	981.0	22.5	4.3
20	0.0893	88.7	0.0433	89.2	0.0035	9.9	0.11	22.6	2.2	43.0	37.6	1409.8	1697.3	22.6	2.2
18	0.0744	51.3	0.0361	52.2	0.0035	9.8	0.18	22.7	2.2	36.0	18.5	1052.7	1032.6	22.7	2.2
7	0.1033	22.6	0.0505	24.6	0.0035	9.7	0.40	22.8	2.2	50.0	12.0	1684.7	416.5	22.8	2.2

Table A7 (continued): Volcanic Zircon U-Pb Integrated Data

Spot	Ratios											Ages (Ma)			
	207Pb/206Pb		207Pb/235U		206Pb/238U		Rho	206Pb/238U		207Pb/235U		207Pb/206Pb		Best Age	±2σ
	±2σ	±2σ	±2σ	±2σ	±2σ	±2σ		±2σ	±2σ	±2σ	±2σ				
20150618-03 Accepted Data															
9	0.0586	33.5	0.0287	34.9	0.0036	9.9	0.29	22.9	2.3	28.8	9.9	551.4	730.9	22.9	2.3
2	0.0856	38.0	0.0438	40.6	0.0037	13.9	0.35	23.8	3.3	43.5	17.3	1329.0	735.0	23.8	3.3
16	0.1019	57.1	0.0522	57.3	0.0037	5.7	0.09	23.9	1.4	51.6	28.9	1659.4	1057.4	23.9	1.4
15	0.1435	50.9	0.0739	51.3	0.0037	6.4	0.12	24.0	1.5	72.4	35.8	2270.5	877.1	24.0	1.5
12	0.0632	17.4	0.0328	20.8	0.0038	11.5	0.55	24.2	2.8	32.7	6.7	715.9	370.4	24.2	2.8
3	0.1850	29.6	0.0962	31.7	0.0038	10.8	0.35	24.2	2.6	93.3	28.2	2697.9	489.0	24.2	2.6
17	0.1560	20.9	0.0839	22.1	0.0039	7.5	0.33	25.1	1.9	81.8	17.4	2412.7	355.4	25.1	1.9
1	0.1249	22.1	0.0704	23.5	0.0041	7.2	0.34	26.2	1.9	69.0	15.7	2027.7	391.5	26.2	1.9
6	0.4489	35.8	0.3262	37.7	0.0053	11.5	0.31	33.8	3.9	286.6	94.4	4081.5	533.1	33.8	3.9
20150618-03 Rejected Data															
08*	0.0616	11.1	0.3260	14.6	0.0384	9.3	0.65	242.6	22.2	286.5	36.4	659.6	237.4	242.6	22.2
13**	1.0280	25.2	13.3292	26.2	0.0940	7.5	0.28	578.9	41.3	2703.3	253.0	5276.2	358.0	578.9	41.3
*Interpreted as detrital															
**Likely not zircon but phosphate: low 8/6 (<30) and high common Pb															
20150618-07 Accepted Data															
8	-0.1892	570.1	-0.0356	570.3	0.0014	15.6	0.03	8.8	1.4	0.0	0.0	0.0	13741.2	8.8	1.4
16	0.1775	43.8	0.0378	51.5	0.0015	27.1	0.53	9.9	2.7	37.6	19.0	2630.0	727.7	9.9	2.7
19	0.0692	107.5	0.0150	108.4	0.0016	14.6	0.13	10.1	1.5	15.2	16.3	905.2	2214.9	10.1	1.5
17	0.4416	111.3	0.0994	111.7	0.0016	9.9	0.09	10.5	1.0	96.3	103.0	4057.0	1658.6	10.5	1.0
11	0.1667	57.6	0.0378	58.4	0.0016	9.8	0.17	10.6	1.0	37.6	21.6	2524.3	967.3	10.6	1.0
12	0.0787	26.5	0.0181	27.1	0.0017	5.7	0.21	10.7	0.6	18.2	4.9	1165.3	525.0	10.7	0.6
15	0.3153	9.0	0.0752	10.6	0.0017	5.6	0.52	11.1	0.6	73.6	7.5	3547.1	139.3	11.1	0.6
10	0.0678	52.4	0.0162	54.2	0.0017	13.8	0.25	11.2	1.5	16.4	8.8	863.4	1088.0	11.2	1.5
13	0.4282	97.3	0.1042	99.2	0.0018	19.5	0.20	11.4	2.2	100.7	95.4	4011.1	1453.1	11.4	2.2
7	0.1661	74.0	0.0405	74.6	0.0018	9.2	0.12	11.4	1.0	40.3	29.5	2518.6	1243.1	11.4	1.0
18	0.0962	17.2	0.0249	26.6	0.0019	20.3	0.76	12.1	2.5	25.0	6.6	1551.1	322.4	12.1	2.5
2	0.0736	31.8	0.0203	41.4	0.0020	26.5	0.64	12.8	3.4	20.4	8.3	1029.7	643.6	12.8	3.4
6	0.1470	22.7	0.0406	25.0	0.0020	10.5	0.42	12.9	1.3	40.4	9.9	2311.2	389.3	12.9	1.3
3	0.2913	76.3	0.0832	78.2	0.0021	17.1	0.22	13.3	2.3	81.1	61.0	3424.3	1185.6	13.3	2.3
20	0.0563	16.3	0.0245	19.3	0.0032	10.4	0.54	20.3	2.1	24.6	4.7	462.6	360.3	20.3	2.1
9	0.2191	29.4	0.1481	31.7	0.0049	11.7	0.37	31.5	3.7	140.2	41.5	2974.0	473.9	31.5	3.7
20150618-07 Rejected Data															
05*	0.3640	119.0	0.0821	124.4	0.0016	36.1	0.29	10.5	3.8	80.1	96.1	3766.5	1806.3	10.5	3.8
14*	0.1719	44.7	0.0529	55.3	0.0022	32.6	0.59	14.4	4.7	52.4	28.2	2576.5	746.0	14.4	4.7
01*	0.1686	89.4	0.1176	96.1	0.0051	35.4	0.37	32.5	11.5	112.9	103.1	2543.5	1498.0	32.5	11.5
04**	0.0795	25.8	0.9434	32.2	0.0860	19.3	0.60	531.6	98.3	674.7	159.8	1184.9	509.0	531.6	98.3
*6/8 uncertainty >30%															
**Likely not zircon but phosphate: low 8/6 (<30) and high common Pb															
20160815-08 Accepted Data															
17	0.0636	18.9	0.0213	19.5	0.0024	5.1	0.25	15.6	0.8	21.4	4.1	728.8	400.7	15.6	0.8
11	0.0634	40.1	0.0216	40.7	0.0025	6.6	0.16	15.9	1.0	21.7	8.7	720.9	851.8	15.9	1.0
12	0.0570	20.3	0.0197	21.4	0.0025	6.6	0.31	16.2	1.1	19.9	4.2	490.0	448.8	16.2	1.1
22	0.0510	16.1	0.0180	16.9	0.0026	5.2	0.29	16.5	0.8	18.1	3.0	242.1	372.0	16.5	0.8
14	0.0503	16.1	0.0181	17.4	0.0026	6.6	0.38	16.8	1.1	18.2	3.1	209.5	373.5	16.8	1.1
5	0.0886	43.9	0.0320	44.5	0.0026	7.2	0.16	16.8	1.2	32.0	14.0	1396.0	841.6	16.8	1.2
29	0.0448	20.4	0.0164	21.2	0.0026	5.8	0.26	17.0	1.0	16.5	3.5	0.0	492.6	17.0	1.0
27	0.0573	18.3	0.0210	18.9	0.0027	5.0	0.25	17.1	0.8	21.1	3.9	502.8	402.0	17.1	0.8
8	0.0593	62.0	0.0218	63.0	0.0027	10.9	0.17	17.1	1.9	21.9	13.6	577.7	1347.4	17.1	1.9
16	0.0686	37.1	0.0254	38.4	0.0027	10.1	0.26	17.2	1.7	25.4	9.6	887.9	765.9	17.2	1.7
7	0.1269	141.8	0.0470	142.5	0.0027	13.7	0.10	17.3	2.4	46.7	65.1	2055.3	2503.3	17.3	2.4
3	0.1129	56.7	0.0422	57.2	0.0027	7.3	0.13	17.4	1.3	42.0	23.5	1847.3	1025.0	17.4	1.3
26	0.0627	21.5	0.0235	22.9	0.0027	8.2	0.35	17.5	1.4	23.6	5.4	697.4	457.6	17.5	1.4
25	0.0614	10.1	0.0231	13.6	0.0027	9.3	0.67	17.5	1.6	23.2	3.1	654.2	217.0	17.5	1.6
6	0.1758	108.2	0.0674	108.7	0.0028	9.8	0.09	17.9	1.8	66.2	69.7	2613.3	1801.0	17.9	1.8
20	0.0402	40.1	0.0143	43.3	0.0026	16.4	0.38	16.5	2.7	14.4	6.2	0.0	966.7	16.5	2.7
15	0.0823	12.5	0.0297	13.4	0.0026	4.8	0.35	16.9	0.8	29.7	3.9	1252.0	245.1	16.9	0.8
4	0.0684	11.5	0.0248	12.3	0.0026	4.4	0.36	16.9	0.7	24.9	3.0	882.0	237.3	16.9	0.7
13	0.1391	22.8	0.0530	23.2	0.0028	4.7	0.20	17.8	0.8	52.5	11.9	2215.5	394.4	17.8	0.8
28	0.0952	20.1	0.0364	21.3	0.0028	7.2	0.33	17.9	1.3	36.3	7.6	1531.5	378.7	17.9	1.3
21	0.1056	36.1	0.0409	37.5	0.0028	10.2	0.27	18.1	1.8	40.7	14.9	1724.8	662.5	18.1	1.8
9	0.1891	28.2	0.0745	28.7	0.0029	4.9	0.17	18.4	0.9	72.9	20.2	2734.2	464.4	18.4	0.9
19	0.1626	22.8	0.0668	25.0	0.0030	10.4	0.41	19.2	2.0	65.7	15.9	2482.5	384.3	19.2	2.0
10	0.0730	33.4	0.0304	37.3	0.0030	16.6	0.45	19.4	3.2	30.4	11.2	1013.7	677.2	19.4	3.2
24	0.1093	19.6	0.0455	23.7	0.0030	13.4	0.56	19.4	2.6	45.2	10.5	1787.5	357.3	19.4	2.6
30	0.0895	54.8	0.0374	62.3	0.0030	29.8	0.48	19.5	5.8	37.3	22.8	1414.8	1047.2	19.5	5.8
2	0.1689	9.4	0.0707	10.2	0.0030	3.9	0.39	19.5	0.8	69.4	6.8	2547.2	157.1	19.5	0.8
23	0.1107	22.7	0.0494	29.2	0.0032	18.5	0.63	20.8	3.8	49.0	14.0	1811.1	412.2	20.8	3.8

Table A7 (continued): Volcanic Zircon U-Pb Integrated Data

Spot	Ratios						Ages (Ma)						Best Age	±2σ	
	207Pb/ 206Pb	±2σ	207Pb/ 235U	±2σ	206Pb/ 238U	±2σ	Rho	206Pb/ 238U	±2σ	207Pb/ 235U	±2σ	207Pb/ 206Pb			±2σ
<i>20160815-08 Accepted Data</i>															
18	0.2263	16.4	0.1014	20.3	0.0032	12.1	0.59	20.9	2.5	98.0	19.0	3025.9	262.6	20.9	2.5
1	0.4739	9.3	0.3678	11.8	0.0056	7.3	0.62	36.1	2.6	318.0	32.4	4162.1	137.0	36.1	2.6
<i>20160815-11 Accepted Data</i>															
7	0.0256	126.4	0.0102	126.8	0.0029	8.9	0.07	18.6	1.6	10.3	13.0	0.0	3047.9	18.6	1.6
1	0.1144	109.2	0.0473	109.5	0.0030	7.6	0.07	19.3	1.5	46.9	50.2	1871.2	1970.1	19.3	1.5
10	0.0472	770.1	0.0203	770.2	0.0031	11.6	0.02	20.1	2.3	20.4	157.1	61.7	18346.9	20.1	2.3
2	0.0606	189.2	0.0264	189.4	0.0032	6.7	0.04	20.3	1.4	26.5	49.6	624.0	4080.4	20.3	1.4
12	0.0928	207.3	0.0405	207.4	0.0032	6.6	0.03	20.4	1.4	40.3	82.2	1483.4	3928.6	20.4	1.4
13	0.0912	35.5	0.0400	38.0	0.0032	13.9	0.36	20.5	2.8	39.8	14.9	1450.7	674.8	20.5	2.8
17	0.0569	24.3	0.0252	25.1	0.0032	6.4	0.25	20.7	1.3	25.3	6.3	487.8	535.6	20.7	1.3
19	0.1211	61.8	0.0541	62.7	0.0032	10.8	0.17	20.8	2.2	53.5	32.7	1972.6	1101.1	20.8	2.2
15	0.0891	35.7	0.0402	40.0	0.0033	18.1	0.45	21.1	3.8	40.1	15.7	1405.2	684.3	21.1	3.8
20	0.1692	123.2	0.0808	123.5	0.0035	9.4	0.08	22.3	2.1	78.9	94.1	2549.4	2062.9	22.3	2.1
8	0.0252	206.9	0.0120	207.1	0.0035	8.2	0.04	22.3	1.8	12.1	25.0	0.0	4987.7	22.3	1.8
18	0.2241	18.4	0.1083	21.4	0.0035	10.8	0.50	22.5	2.4	104.4	21.2	3010.2	296.0	22.5	2.4
16	0.0384	81.5	0.0188	82.8	0.0036	14.8	0.18	22.9	3.4	19.0	15.5	0.0	1963.3	22.9	3.4
9	0.0794	18.1	0.0394	20.2	0.0036	8.9	0.44	23.2	2.1	39.3	7.8	1181.6	357.3	23.2	2.1
14	0.2162	16.0	0.1125	17.8	0.0038	7.7	0.43	24.3	1.9	108.3	18.2	2952.7	259.1	24.3	1.9
5	0.3463	30.9	0.2194	34.9	0.0046	16.2	0.47	29.5	4.8	201.4	63.9	3690.8	471.6	29.5	4.8
4	0.3481	22.8	0.2703	25.6	0.0056	11.5	0.45	36.2	4.2	242.9	55.3	3698.5	347.7	36.2	4.2
6	0.4018	29.6	0.3597	33.1	0.0065	14.7	0.45	41.7	6.1	312.0	89.1	3915.7	444.9	41.7	6.1
<i>20160815-11 Rejected Data</i>															
03*	0.0536	116.5	0.0253	121.0	0.0034	32.8	0.27	22.0	7.2	25.4	30.4	353.1	2631.3	22.0	7.2
11**	0.0571	76.6	0.1822	78.6	0.0231	17.7	0.23	147.5	25.8	170.0	123.7	494.1	1688.2	147.5	25.8
*6/8 uncertainty >30%															
**Interpreted as detrital															
<i>20160815-15 Accepted Data</i>															
5	0.0354	56.1	0.0034	56.9	0.0007	9.0	0.16	4.4	0.4	3.4	1.9	0.0	1353.3	4.4	0.4
22	0.0248	246.5	0.0024	246.7	0.0007	9.5	0.04	4.5	0.4	2.4	6.0	0.0	5941.4	4.5	0.4
18	0.0526	36.7	0.0053	37.2	0.0007	6.5	0.17	4.7	0.3	5.4	2.0	312.1	834.3	4.7	0.3
24	0.0185	217.2	0.0019	217.3	0.0007	7.5	0.03	4.7	0.4	1.9	4.1	0.0	5234.8	4.7	0.4
29	0.0506	25.9	0.0052	26.5	0.0007	6.0	0.23	4.8	0.3	5.2	1.4	224.5	597.6	4.8	0.3
10	0.0557	37.2	0.0057	38.0	0.0007	7.6	0.20	4.8	0.4	5.8	2.2	442.3	828.0	4.8	0.4
15	0.0544	30.1	0.0056	31.0	0.0007	7.8	0.25	4.8	0.4	5.7	1.8	387.2	674.9	4.8	0.4
7	-0.0270	504.4	-0.0028	504.5	0.0007	12.1	0.02	4.8	0.6	0.0	0.0	0.0	12158.1	4.8	0.6
2	0.0619	34.1	0.0064	34.7	0.0007	6.3	0.18	4.8	0.3	6.5	2.2	672.3	729.3	4.8	0.3
8	0.0402	37.6	0.0042	38.0	0.0008	6.0	0.16	4.9	0.3	4.3	1.6	0.0	905.4	4.9	0.3
4	0.1075	50.0	0.0114	51.7	0.0008	12.9	0.25	5.0	0.6	11.5	5.9	1756.9	915.1	5.0	0.6
14	0.0647	25.2	0.0071	27.3	0.0008	10.4	0.38	5.2	0.5	7.2	2.0	765.6	531.4	5.2	0.5
9	0.0493	26.7	0.0055	27.3	0.0008	5.7	0.21	5.2	0.3	5.5	1.5	162.8	624.5	5.2	0.3
1	0.0587	28.4	0.0065	30.0	0.0008	9.4	0.31	5.2	0.5	6.6	2.0	554.1	620.3	5.2	0.5
27	0.0955	57.2	0.0107	57.6	0.0008	7.0	0.12	5.2	0.4	10.8	6.2	1537.4	1076.1	5.2	0.4
3	0.1153	37.7	0.0118	38.0	0.0007	5.2	0.14	4.8	0.3	11.9	4.5	1883.8	678.3	4.8	0.3
21	0.1091	37.0	0.0120	39.8	0.0008	14.5	0.37	5.1	0.7	12.1	4.8	1785.2	675.2	5.1	0.7
28	0.0502	36.8	0.0055	43.9	0.0008	24.0	0.55	5.2	1.2	5.6	2.5	205.5	852.6	5.2	1.2
6	0.0831	55.1	0.0093	57.2	0.0008	15.4	0.27	5.2	0.8	9.4	5.3	1271.4	1074.3	5.2	0.8
26	0.0522	64.0	0.0060	66.1	0.0008	16.7	0.25	5.3	0.9	6.1	4.0	294.2	1460.5	5.3	0.9
17	0.1813	41.8	0.0210	43.1	0.0008	10.3	0.24	5.4	0.6	21.1	9.0	2664.5	692.7	5.4	0.6
12	0.1545	25.6	0.0192	26.9	0.0009	8.5	0.31	5.8	0.5	19.3	5.2	2396.8	435.1	5.8	0.5
13	0.1754	16.0	0.0224	19.0	0.0009	10.1	0.53	6.0	0.6	22.5	4.2	2610.0	266.9	6.0	0.6
19	0.1857	26.3	0.0239	34.2	0.0009	21.8	0.64	6.0	1.3	24.0	8.1	2704.3	434.2	6.0	1.3
20	0.2102	9.8	0.0277	11.4	0.0010	5.8	0.51	6.1	0.4	27.7	3.1	2906.9	158.7	6.1	0.4
23	0.3144	9.1	0.0463	12.6	0.0011	8.6	0.69	6.9	0.6	45.9	5.7	3542.6	140.7	6.9	0.6
30	0.4557	11.9	0.0894	13.6	0.0014	6.5	0.49	9.2	0.6	86.9	11.3	4104.0	176.1	9.2	0.6
11	0.6366	9.2	0.2530	11.5	0.0029	6.8	0.60	18.5	1.3	229.0	23.5	4593.7	133.3	18.5	1.3
16	0.7989	5.0	0.8939	9.4	0.0081	8.0	0.85	52.1	4.2	648.5	45.3	4919.8	71.3	52.1	4.2
25	0.8832	6.3	17.7457	8.6	0.1456	5.7	0.68	876.2	46.5	2976.1	82.4	5062.2	89.7	876.2	46.5
<i>240510-11 Accepted Data</i>															
25	0.0380	92.8	0.0113	93.6	0.0022	12.2	0.13	13.9	1.7	11.4	10.6	0.0	2236.4	13.9	1.7
10	0.0364	80.6	0.0116	81.5	0.0023	12.3	0.15	14.9	1.8	11.7	9.5	0.0	1942.1	14.9	1.8
40	0.1334	58.4	0.0431	60.5	0.0023	16.0	0.26	15.1	2.4	42.8	25.4	2143.7	1020.2	15.1	2.4
12	0.0191	221.4	0.0062	221.7	0.0024	12.0	0.05	15.2	1.8	6.3	13.9	0.0	5336.9	15.2	1.8
11	0.0290	222.5	0.0095	223.0	0.0024	14.3	0.06	15.3	2.2	9.6	21.3	0.0	5364.1	15.3	2.2
46	0.0217	159.5	0.0072	159.8	0.0024	10.6	0.07	15.5	1.6	7.3	11.6	0.0	3844.3	15.5	1.6
52	0.1090	33.0	0.0365	34.5	0.0024	10.3	0.30	15.6	1.6	36.4	12.3	1782.5	601.3	15.6	1.6
41	0.0658	61.0	0.0220	62.2	0.0024	12.2	0.20	15.6	1.9	22.1	13.6	801.4	1277.8	15.6	1.9

Table A7 (continued): Volcanic Zircon U-Pb Integrated Data

Spot	Ratios						Ages (Ma)						Best Age	±2σ	
	207Pb/ 206Pb	±2σ	207Pb/ 235U	±2σ	206Pb/ 238U	±2σ	Rho	206Pb/ 238U	±2σ	207Pb/ 235U	±2σ	207Pb/ 206Pb			±2σ
<i>240510-11 Accepted Data</i>															
2	0.0086	628.0	0.0029	628.2	0.0024	13.7	0.02	15.7	2.2	2.9	18.4	0.0	15137.7	15.7	2.2
28	0.0336	98.6	0.0114	99.0	0.0025	8.6	0.09	15.9	1.4	11.5	11.3	0.0	2377.1	15.9	1.4
43	0.0391	54.9	0.0133	55.4	0.0025	7.8	0.14	15.9	1.2	13.4	7.4	0.0	1322.5	15.9	1.2
9	0.0707	47.2	0.0241	48.8	0.0025	12.3	0.25	15.9	1.9	24.2	11.7	949.0	966.9	15.9	1.9
39	0.0547	62.8	0.0187	63.5	0.0025	9.8	0.15	16.0	1.6	18.8	11.8	399.1	1406.4	16.0	1.6
26	0.0684	55.0	0.0235	55.9	0.0025	10.0	0.18	16.0	1.6	23.6	13.0	880.0	1138.7	16.0	1.6
23	0.0853	30.6	0.0294	33.2	0.0025	13.0	0.39	16.1	2.1	29.4	9.6	1323.3	592.9	16.1	2.1
6	0.0462	55.3	0.0160	56.0	0.0025	9.3	0.16	16.1	1.5	16.1	8.9	9.9	1329.3	16.1	1.5
1	0.0424	50.8	0.0147	51.9	0.0025	10.8	0.21	16.1	1.7	14.8	7.6	0.0	1224.1	16.1	1.7
27	0.0403	72.6	0.0140	73.1	0.0025	8.4	0.11	16.2	1.4	14.1	10.3	0.0	1749.8	16.2	1.4
4	0.0400	66.4	0.0139	67.1	0.0025	9.6	0.14	16.2	1.6	14.0	9.4	0.0	1601.0	16.2	1.6
47	-0.0332	162.1	-0.0116	162.6	0.0025	12.8	0.08	16.4	2.1	0.0	0.0	0.0	3906.9	16.4	2.1
32	0.0444	50.3	0.0156	50.9	0.0025	7.7	0.15	16.4	1.3	15.7	7.9	0.0	1212.9	16.4	1.3
35	-0.0173	451.0	-0.0061	451.3	0.0026	17.7	0.04	16.4	2.9	0.0	0.0	0.0	10870.8	16.4	2.9
31	0.0359	53.4	0.0127	54.0	0.0026	7.7	0.14	16.5	1.3	12.9	6.9	0.0	1288.0	16.5	1.3
29	0.0841	35.0	0.0298	35.9	0.0026	8.0	0.22	16.5	1.3	29.9	10.6	1295.1	680.6	16.5	1.3
7	0.0698	44.2	0.0249	48.6	0.0026	20.1	0.41	16.6	3.3	24.9	12.0	922.2	908.5	16.6	3.3
33	0.0866	38.8	0.0309	41.1	0.0026	13.6	0.33	16.7	2.3	30.9	12.5	1350.9	748.2	16.7	2.3
42	0.0591	41.1	0.0211	41.8	0.0026	7.8	0.19	16.7	1.3	21.2	8.8	572.2	892.9	16.7	1.3
24	0.0617	74.4	0.0221	76.0	0.0026	15.1	0.20	16.7	2.5	22.2	16.7	663.6	1594.6	16.7	2.5
50	0.0483	54.5	0.0173	55.0	0.0026	7.6	0.14	16.7	1.3	17.4	9.5	115.0	1286.0	16.7	1.3
13	0.0269	48.8	0.0097	49.5	0.0026	8.5	0.17	16.8	1.4	9.8	4.8	0.0	1175.6	16.8	1.4
49	0.0446	100.8	0.0162	101.7	0.0026	13.7	0.13	16.9	2.3	16.3	16.4	0.0	2430.3	16.9	2.3
37	0.0535	50.2	0.0195	52.1	0.0026	13.7	0.26	17.0	2.3	19.6	10.1	351.1	1135.0	17.0	2.3
22	0.0471	35.3	0.0172	37.3	0.0026	11.9	0.32	17.0	2.0	17.3	6.4	53.2	843.0	17.0	2.0
18	0.0355	66.6	0.0130	67.1	0.0026	8.8	0.13	17.0	1.5	13.1	8.7	0.0	1604.7	17.0	1.5
44	0.0686	22.0	0.0252	23.1	0.0027	7.1	0.31	17.1	1.2	25.3	5.8	887.7	454.0	17.1	1.2
45	0.0201	237.6	0.0074	237.8	0.0027	11.1	0.05	17.1	1.9	7.5	17.7	0.0	5726.2	17.1	1.9
21	0.0809	36.7	0.0298	37.7	0.0027	8.4	0.22	17.2	1.4	29.8	11.1	1218.2	721.7	17.2	1.4
3	0.0671	17.5	0.0249	20.1	0.0027	9.8	0.49	17.3	1.7	25.0	5.0	842.1	365.0	17.3	1.7
30	0.0166	106.9	0.0062	107.2	0.0027	7.1	0.07	17.3	1.2	6.2	6.7	0.0	2577.9	17.3	1.2
34	0.0528	17.8	0.0201	18.9	0.0028	6.5	0.34	17.8	1.1	20.2	3.8	322.3	404.1	17.8	1.1
38	0.0719	48.8	0.0274	50.1	0.0028	11.2	0.22	17.8	2.0	27.5	13.6	982.7	994.1	17.8	2.0
54	0.0406	34.7	0.0155	35.2	0.0028	6.5	0.18	17.8	1.2	15.7	5.5	0.0	835.4	17.8	1.2
20	0.0302	59.7	0.0116	60.3	0.0028	8.0	0.13	17.9	1.4	11.7	7.0	0.0	1439.5	17.9	1.4
16	0.0394	74.4	0.0152	75.1	0.0028	10.2	0.14	18.0	1.8	15.3	11.4	0.0	1794.5	18.0	1.8
17	0.0472	40.4	0.0182	41.9	0.0028	11.0	0.26	18.0	2.0	18.3	7.6	57.0	963.5	18.0	2.0
5	0.0616	91.0	0.0241	91.7	0.0028	11.4	0.12	18.2	2.1	24.1	21.9	658.9	1950.9	18.2	2.1
<i>240510-11 Rejected Data</i>															
48*	0.1575	23.9	0.0687	26.3	0.0032	11.0	0.42	20.3	2.2	67.5	17.2	2428.6	405.2	20.3	2.2
19*	0.1496	30.8	0.0691	35.4	0.0033	17.4	0.49	21.5	3.7	67.9	23.2	2341.5	526.8	21.5	3.7
8*	-0.0279	478.8	-0.0129	479.5	0.0033	24.8	0.05	21.5	5.3	0.0	0.0	0.0	11542.2	21.5	5.3
15*	0.1133	34.1	0.0540	35.8	0.0035	10.8	0.30	22.2	2.4	53.4	18.6	1852.3	617.1	22.2	2.4
53*	0.2444	24.8	0.1175	28.1	0.0035	13.3	0.47	22.4	3.0	112.8	30.1	3148.8	394.0	22.4	3.0
51*	0.4640	13.9	0.3974	19.4	0.0062	13.4	0.69	39.9	5.3	339.8	55.9	4130.6	206.8	39.9	5.3
36*	0.6595	21.1	1.0558	26.5	0.0116	16.0	0.61	74.3	11.9	731.7	139.0	4645.0	304.6	74.3	11.9
14*	0.0573	15.8	0.1823	20.9	0.0231	13.6	0.65	147.0	19.7	170.1	32.7	502.1	348.5	147.0	19.7
**Interpreted as detrital															
<i>250510-12 Accepted Data</i>															
3	16.9037	44.6	0.0146	47.6	0.0018	16.8	0.35	11.5	1.9	14.7	7.0	572.9	1018.8	11.5	4.4
15	6.6696	111.3	0.0379	112.8	0.0018	18.6	0.16	11.8	2.2	37.8	41.8	2345.2	478.1	11.8	4.8
10	31.5330	62.1	0.0082	62.5	0.0019	7.1	0.11	12.1	0.9	8.3	5.2	-991.5	2010.2	12.1	2.6
20	7.0879	339.6	0.0368	339.9	0.0019	15.4	0.05	12.2	1.9	36.7	123.2	2240.5	478.1	12.2	4.2
2	25.6906	43.2	0.0102	47.5	0.0019	19.7	0.41	12.2	2.4	10.3	4.9	-421.8	1178.4	12.2	5.2
16	12.0487	54.2	0.0220	56.3	0.0019	15.5	0.28	12.4	1.9	22.1	12.3	1269.1	1149.1	12.4	4.3
19	16.4317	73.9	0.0162	75.0	0.0019	12.7	0.17	12.4	1.6	16.3	12.1	634.2	1893.4	12.4	3.7
9	9.8855	101.9	0.0270	103.0	0.0019	14.8	0.14	12.5	1.8	27.0	27.5	1645.5	99.9	12.5	4.2
2B	7.5676	228.5	0.0352	228.8	0.0019	10.3	0.05	12.5	1.3	35.2	79.2	2126.6	168.3	12.5	3.3
10B	6.7654	242.2	0.0396	242.9	0.0019	18.3	0.08	12.5	2.3	39.5	94.3	2320.7	78.2	12.5	5.0
21	20.5877	27.8	0.0131	28.7	0.0020	7.3	0.25	12.6	0.9	13.2	3.8	127.3	665.0	12.6	2.7
23	3.8092	457.7	0.0708	457.9	0.0020	13.7	0.03	12.6	1.7	69.4	317.2	3261.9	26.6	12.6	4.0
1	15.8196	111.9	0.0171	112.3	0.0020	9.6	0.09	12.7	1.2	17.3	19.2	715.4	588.4	12.7	3.1
7	6.0945	309.0	0.0449	309.3	0.0020	12.9	0.04	12.8	1.6	44.6	135.7	2498.2	171.6	12.8	3.8
5	19.4615	28.8	0.0141	29.2	0.0020	4.5	0.15	12.8	0.6	14.2	4.1	258.1	675.1	12.8	2.3
11	18.6374	86.9	0.0149	87.4	0.0020	10.0	0.11	12.9	1.3	15.0	13.0	356.6	2617.3	12.9	3.3
10C	19.9831	41.5	0.0143	45.2	0.0021	18.0	0.40	13.3	2.4	14.4	6.5	197.0	1002.6	13.3	5.2
<i>250510-12 Rejected Data</i>															
12*	12.2010	38.8	0.0178	52.9	0.0016	36.0	0.68	10.2	3.6	17.9	9.4	1244.6	790.9	10.2	7.6

Table A7 (continued): Volcanic Zircon U-Pb Integrated Data

Spot	Ratios						Ages (Ma)						Best Age	±2σ	
	207Pb/ 206Pb	±2σ	207Pb/ 235U	±2σ	206Pb/ 238U	±2σ	Rho	206Pb/ 238U	±2σ	207Pb/ 235U	±2σ	207Pb/ 206Pb			±2σ
250510-12 Rejected Data															
8**	76.6464	142.2	0.0051	142.3	0.0028	4.2	0.03	18.2	0.8	5.2	7.3	NA	NA	18.2	2.5
14B**	29.0732	21.7	0.0151	22.2	0.0032	4.7	0.21	20.6	1.0	15.3	3.4	-757.3	616.9	20.6	2.8
14**	25.2524	25.9	0.0175	26.0	0.0032	2.7	0.10	20.6	0.6	17.6	4.5	-376.9	681.3	20.6	2.3
24**	26.2750	20.7	0.0169	21.2	0.0032	4.7	0.22	20.7	1.0	17.0	3.6	-481.1	553.2	20.7	2.8
13**	7.7587	78.2	0.0771	80.0	0.0043	16.9	0.21	27.9	4.7	75.4	58.2	2082.8	497.7	27.9	9.6
13B**	8.6220	118.0	0.0702	119.1	0.0044	15.9	0.13	28.2	4.5	68.9	79.5	1895.2	168.6	28.2	9.2
4**	20.5180	5.4	0.2591	5.8	0.0386	2.2	0.38	243.9	5.3	233.9	12.1	135.2	126.0	243.9	10.8
6**	16.0181	0.6	0.9957	3.4	0.1157	3.4	0.98	705.6	22.4	701.6	17.3	688.8	13.2	705.6	44.8
14**	9.5801	0.6	4.2116	1.7	0.2926	1.6	0.94	1654.7	22.7	1676.3	13.6	1703.4	10.8	1703.4	21.7
*6/8 uncertainty >30%															
**Interpreted as detrital															
260510-03 Accepted Data															
9	0.0558	5.9	0.0056	8.2	0.0007	5.8	0.70	4.7	0.3	5.6	0.5	444.4	130.9	4.7	0.3
20	0.0554	10.2	0.0057	14.0	0.0007	9.6	0.69	4.8	0.5	5.8	0.8	426.9	227.3	4.8	0.5
5	0.0790	15.1	0.0082	19.2	0.0008	11.9	0.62	4.9	0.6	8.3	1.6	1172.0	299.0	4.9	0.6
13	0.1173	34.4	0.0125	39.0	0.0008	18.4	0.47	5.0	0.9	12.7	4.9	1914.8	617.8	5.0	0.9
1	0.0468	34.4	0.0054	44.8	0.0008	28.7	0.64	5.3	1.5	5.4	2.4	37.1	823.2	5.3	1.5
8	0.0539	16.7	0.0063	23.1	0.0008	16.0	0.69	5.4	0.9	6.3	1.5	365.4	375.9	5.4	0.9
260510-03 Rejected Data															
19*	0.0551	130.2	0.0118	175.4	0.0016	117.5	0.67	10.0	11.7	11.9	20.8	418.1	2907.2	10.0	11.7
15**	0.0343	97.3	0.0144	125.1	0.0030	78.6	0.63	19.6	15.4	14.6	18.1	0.0	2346.5	19.6	15.4
18**	0.5112	30.8	0.2289	36.5	0.0032	19.5	0.54	20.9	4.1	209.3	69.1	4273.9	453.4	20.9	4.1
17**	0.0508	14.2	0.0233	15.2	0.0033	5.4	0.35	21.4	1.1	23.4	3.5	230.1	327.9	21.4	1.1
02**	0.2368	33.7	0.1553	38.4	0.0048	18.5	0.48	30.6	5.6	146.6	52.5	3098.5	536.9	30.6	5.6
06**	0.0602	65.0	0.0438	81.4	0.0053	49.0	0.60	33.9	16.6	43.5	34.7	610.0	1403.7	33.9	16.6
12**	0.0307	129.7	0.0073	130.1	0.0017	10.1	0.08	11.2	1.1	7.4	9.6	0.0	3125.4	11.2	1.1
11**	0.0318	74.1	0.0077	74.7	0.0018	9.0	0.12	11.3	1.0	7.8	5.8	0.0	1787.1	11.3	1.0
10**	0.0580	29.9	0.0149	31.1	0.0019	8.4	0.27	12.0	1.0	15.0	4.6	530.4	655.9	12.0	1.0
16**	0.0722	46.9	0.0196	47.5	0.0020	7.6	0.16	12.7	1.0	19.7	9.3	992.5	952.7	12.7	1.0
04**	0.0811	39.3	0.0236	42.6	0.0021	16.4	0.39	13.6	2.2	23.6	10.0	1223.2	772.8	13.6	2.2
03**	0.0542	62.6	0.0158	63.3	0.0021	9.4	0.15	13.6	1.3	15.9	10.0	379.5	1406.9	13.6	1.3
14**	0.0561	28.7	0.0169	32.5	0.0022	15.2	0.47	14.1	2.1	17.0	5.5	454.7	637.6	14.1	2.1
07**	0.7829	25.2	503.9133	101.0	4.6639	97.8	0.97	11178.8	7179.9	6320.1	65535.0	4890.9	362.0	4890.9	362.0
*6/8 uncertainty >30%															
**Interpreted as detrital															
260510-07 Accepted Data															
17B	1.6559	664.7	0.2692	665.2	0.0032	25.4	0.04	20.8	5.3	242.1	#NUM!	NA	NA	20.8	10.7
7	6.9133	172.0	0.0646	179.1	0.0032	49.8	0.28	20.8	10.4	63.5	110.7	2283.6	168.3	20.8	20.8
25	6.7562	107.1	0.0711	108.3	0.0035	16.0	0.15	22.4	3.6	69.7	73.1	2323.1	485.6	22.4	7.5
19	0.0440	34851.8	10.9833	34851.8	0.0035	25.1	0.00	22.6	5.7	2521.7	#NUM!	NA	NA	22.6	11.5
23	-1.3902	861.5	-0.3483	862.4	0.0035	37.7	0.04	22.6	8.5	-434.7	#NUM!	NA	NA	22.6	17.1
4	-1.6194	755.3	-0.3022	755.5	0.0035	15.7	0.02	22.8	3.6	-365.4	#NUM!	NA	NA	22.8	7.4
6	11.6517	131.7	0.0423	132.3	0.0036	12.9	0.10	23.0	3.0	42.0	54.5	1334.2	276.7	23.0	6.2
18	13.8696	67.7	0.0357	70.7	0.0036	20.5	0.29	23.1	4.7	35.6	24.8	988.8	1584.6	23.1	9.7
20	5.7693	441.6	0.0871	441.7	0.0036	10.5	0.02	23.4	2.5	84.8	375.5	2590.1	482.2	23.4	5.3
16	16.2356	108.4	0.0313	109.5	0.0037	15.6	0.14	23.7	3.7	31.3	33.8	660.0	602.5	23.7	7.7
26	-4.3119	408.1	-0.1180	408.4	0.0037	15.5	0.04	23.7	3.7	-127.5	-622.3	NA	NA	23.7	7.6
2	21.8796	11.5	0.0234	11.6	0.0037	1.5	0.13	23.8	0.4	23.4	2.7	-17.9	278.1	23.8	2.1
17	9.7581	253.4	0.0524	253.7	0.0037	12.2	0.05	23.8	2.9	51.8	128.9	1669.5	632.2	23.8	6.1
11	13.8765	51.1	0.0370	53.8	0.0037	16.8	0.31	24.0	4.0	36.9	19.5	987.8	1116.3	24.0	8.3
5B	21.6712	34.8	0.0237	37.4	0.0037	13.7	0.37	24.0	3.3	23.8	8.8	5.2	860.9	24.0	6.9
10	7.7270	170.6	0.0667	172.1	0.0037	22.6	0.13	24.1	5.4	65.6	109.7	2090.0	45.2	24.1	11.0
1B	17.4248	66.4	0.0298	68.5	0.0038	16.8	0.25	24.2	4.1	29.8	20.1	506.5	1658.5	24.2	8.4
14	7.2913	219.8	0.0714	221.6	0.0038	28.0	0.13	24.3	6.8	70.0	151.0	2191.5	87.2	24.3	13.7
12	13.0658	114.3	0.0400	116.2	0.0038	20.8	0.18	24.4	5.1	39.8	45.4	1109.1	326.7	24.4	10.3
15	29.8727	140.2	0.0176	140.8	0.0038	13.0	0.09	24.6	3.2	17.8	24.8	-834.2	0.0	24.6	6.7
3	23.3974	10.5	0.0228	10.8	0.0039	2.2	0.21	24.9	0.6	22.9	2.4	-182.7	263.5	24.9	2.3
5	25.8219	69.9	0.0210	71.2	0.0039	13.2	0.18	25.3	3.3	21.1	14.9	-435.2	2091.1	25.3	6.9
24	-3.2045	404.0	-0.1703	404.5	0.0040	19.9	0.05	25.5	5.1	-189.6	-1207.4	NA	NA	25.5	10.3
1	3.5881	537.2	0.1522	537.6	0.0040	21.6	0.04	25.5	5.5	143.9	901.5	3355.6	62.7	25.5	11.2
22	6.7865	100.7	0.0806	103.8	0.0040	25.1	0.24	25.5	6.4	78.8	78.8	2315.4	512.7	25.5	12.9
9	6.5291	333.8	0.0840	334.6	0.0040	22.1	0.07	25.6	5.6	81.9	269.5	2381.5	342.3	25.6	11.5
260510-07 Rejected Data															
21*	20.9782	8.9	0.0442	9.2	0.0067	2.3	0.25	43.2	1.0	43.9	3.9	82.8	210.9	43.2	2.8
*Interpreted as detrital															

Table A7 (continued): Volcanic Zircon U-Pb Integrated Data

Spot	Ratios						Ages (Ma)						Best Age	$\pm 2\sigma$	
	$^{207}\text{Pb}/^{206}\text{Pb}$	$\pm 2\sigma$	$^{207}\text{Pb}/^{235}\text{U}$	$\pm 2\sigma$	$^{206}\text{Pb}/^{238}\text{U}$	$\pm 2\sigma$	Rho	$^{206}\text{Pb}/^{238}\text{U}$	$\pm 2\sigma$	$^{207}\text{Pb}/^{235}\text{U}$	$\pm 2\sigma$	$^{207}\text{Pb}/^{206}\text{Pb}$			$\pm 2\sigma$
<i>20160813-01 Accepted Data</i>															
8	0.0395	42.8	0.0077	46.5	0.0014	18.3	0.39	9.1	1.7	7.8	3.6	0.0	1030.8	9.1	1.7
18	0.0603	20.2	0.0124	21.7	0.0015	7.9	0.37	9.6	0.8	12.5	2.7	614.1	437.1	9.6	0.8
1	0.1227	46.2	0.0254	47.5	0.0015	11.0	0.23	9.7	1.1	25.5	11.9	1995.4	820.8	9.7	1.1
3	0.0769	11.6	0.0162	12.8	0.0015	5.4	0.43	9.9	0.5	16.4	2.1	1119.5	230.9	9.9	0.5
7	0.0489	17.4	0.0105	19.0	0.0016	7.5	0.40	10.0	0.8	10.6	2.0	143.3	407.7	10.0	0.8
10	0.1002	22.1	0.0217	22.6	0.0016	4.5	0.20	10.1	0.5	21.8	4.9	1627.6	411.3	10.1	0.5
15	0.0403	100.7	0.0087	101.4	0.0016	11.1	0.11	10.1	1.1	8.8	8.9	0.0	2428.5	10.1	1.1
2	0.1025	43.5	0.0224	44.4	0.0016	8.7	0.20	10.2	0.9	22.5	9.9	1669.9	804.7	10.2	0.9
9	0.0930	34.6	0.0206	36.6	0.0016	12.0	0.33	10.3	1.2	20.7	7.5	1487.2	654.7	10.3	1.2
5	0.0770	22.0	0.0171	24.0	0.0016	9.6	0.40	10.4	1.0	17.2	4.1	1121.2	438.6	10.4	1.0
19	0.0635	23.3	0.0144	24.1	0.0016	5.9	0.25	10.6	0.6	14.5	3.5	723.8	495.0	10.6	0.6
11	0.0769	48.2	0.0176	49.2	0.0017	9.6	0.20	10.7	1.0	17.7	8.6	1117.8	962.1	10.7	1.0
12	0.0485	30.8	0.0115	37.4	0.0017	21.1	0.57	11.0	2.3	11.6	4.3	123.0	726.6	11.0	2.3
20	0.1350	60.4	0.0320	60.6	0.0017	4.9	0.08	11.1	0.5	32.0	19.1	2164.4	1052.9	11.1	0.5
14	0.2563	35.0	0.0693	35.6	0.0020	6.5	0.18	12.6	0.8	68.0	23.4	3224.0	551.9	12.6	0.8
17	0.2987	38.5	0.0921	41.6	0.0022	15.8	0.38	14.4	2.3	89.5	35.7	3463.5	596.6	14.4	2.3
4	0.3918	65.1	0.1248	66.5	0.0023	13.7	0.21	14.9	2.0	119.4	75.0	3877.9	980.4	14.9	2.0
<i>20160813-01 Rejected Data</i>															
06*	0.0412	48.9	0.0131	66.7	0.0023	45.4	0.68	14.8	6.7	13.2	8.7	0.0	1177.7	14.8	6.7
13*	0.1769	58.9	0.0601	76.4	0.0025	48.7	0.64	15.9	7.7	59.3	44.0	2623.6	978.8	15.9	7.7
16**	0.0606	7.5	0.2921	10.3	0.0349	7.0	0.68	221.4	15.2	260.2	23.6	623.6	162.4	221.4	15.2
*6/8 uncertainty >30%															
**Interpreted as detrital															
<i>20160815-01 Accepted Data</i>															
11	0.0536	13.9	0.0114	15.2	0.0015	6.2	0.40	10.0	0.6	11.5	1.7	354.2	313.1	10.0	0.6
3	0.0988	47.6	0.0219	47.9	0.0016	5.1	0.11	10.4	0.5	22.0	10.4	1602.2	888.8	10.4	0.5
13	0.1944	27.3	0.0463	27.8	0.0017	5.4	0.19	11.1	0.6	45.9	12.5	2779.6	447.0	11.1	0.6
12	0.0712	16.8	0.0170	19.3	0.0017	9.5	0.49	11.2	1.1	17.2	3.3	963.8	343.3	11.2	1.1
16	0.1786	122.8	0.0469	124.2	0.0019	18.4	0.15	12.3	2.3	46.6	56.6	2639.7	2039.3	12.3	2.3
4	0.2065	9.5	0.0569	12.5	0.0020	8.2	0.65	12.9	1.1	56.2	6.8	2878.3	153.6	12.9	1.1
1	0.0510	13.5	0.0151	14.5	0.0022	5.4	0.37	13.8	0.8	15.3	2.2	242.7	310.2	13.8	0.8
26	0.1447	33.9	0.0434	34.8	0.0022	8.1	0.23	14.0	1.1	43.1	14.7	2283.9	583.3	14.0	1.1
15	0.1907	74.7	0.0610	75.3	0.0023	9.7	0.13	14.9	1.4	60.1	44.0	2748.5	1227.5	14.9	1.4
17	0.1106	23.0	0.0365	25.0	0.0024	9.8	0.39	15.4	1.5	36.4	9.0	1808.7	418.5	15.4	1.5
22	0.0834	67.7	0.0278	68.0	0.0024	6.9	0.10	15.6	1.1	27.9	18.7	1278.7	1319.3	15.6	1.1
<i>20160815-01 Rejected Data</i>															
08*	0.2798	100.6	0.0810	114.3	0.0021	54.4	0.48	13.5	7.3	79.1	87.2	3361.7	1570.4	13.5	7.3
30*	0.0527	50.8	0.0181	60.8	0.0025	33.4	0.55	16.0	5.3	18.2	11.0	316.6	1154.0	16.0	5.3
02*	0.0727	40.8	0.0370	50.6	0.0037	30.0	0.59	23.7	7.1	36.9	18.3	1005.8	827.1	23.7	7.1
10*	0.1436	77.9	0.0755	85.8	0.0038	36.0	0.42	24.5	8.8	73.9	61.2	2271.0	1341.7	24.5	8.8
27**	0.0819	13.0	0.0320	14.8	0.0028	7.1	0.48	18.2	1.3	32.0	4.6	1244.2	253.9	18.2	1.3
29**	0.0883	12.6	0.0358	13.9	0.0029	6.1	0.43	18.9	1.1	35.7	4.9	1389.3	241.0	18.9	1.1
23**	0.1164	41.0	0.0539	42.5	0.0034	11.0	0.26	21.6	2.4	53.3	22.1	1902.0	737.0	21.6	2.4
24**	0.0471	15.4	0.0284	17.4	0.0044	8.0	0.46	28.1	2.3	28.4	4.9	54.1	367.3	28.1	2.3
05**	0.0770	48.0	0.0484	48.4	0.0046	6.5	0.13	29.3	1.9	48.0	22.7	1121.6	956.8	29.3	1.9
06**	0.2353	32.2	0.1560	32.8	0.0048	6.6	0.20	30.9	2.0	147.2	45.0	3088.5	513.5	30.9	2.0
07**	0.0683	49.0	0.0517	49.4	0.0055	5.8	0.12	35.3	2.0	51.1	24.6	876.6	1015.2	35.3	2.0
09**	0.0909	24.6	0.1852	29.9	0.0148	17.0	0.57	94.5	15.9	172.5	47.4	1444.7	467.8	94.5	15.9
20**	0.1305	6.9	0.4143	8.3	0.0230	4.7	0.56	146.6	6.8	352.0	24.8	2104.5	121.4	146.6	6.8
18**	0.0628	6.5	0.6108	9.6	0.0705	7.1	0.73	439.3	30.0	484.1	36.9	699.8	138.3	439.3	30.0
21**	0.0907	8.1	1.7006	12.6	0.1359	9.7	0.77	821.4	74.5	1008.7	80.6	1439.6	153.9	821.4	74.5
28**	0.0755	8.8	1.4778	11.9	0.1418	8.0	0.67	854.6	64.4	921.3	72.2	1082.3	176.3	854.6	64.4
14**	0.0834	4.8	2.2775	7.1	0.1980	5.2	0.73	1164.6	55.9	1205.4	50.0	1277.5	93.7	1164.6	55.9
19**	0.1110	14.8	3.8761	21.5	0.2530	15.6	0.73	1453.7	203.4	1608.7	175.2	1816.2	268.3	1816.2	268.3
25**	0.1117	6.0	5.0097	9.0	0.3248	6.7	0.74	1813.2	105.7	1821.0	76.1	1827.8	109.2	1827.8	109.2
*6/8 uncertainty >30%															
**Interpreted as detrital															
<i>20160816-02 Accepted Data</i>															
17	0.0959	72.9	0.0188	73.6	0.0014	10.5	0.14	9.2	1.0	18.9	13.8	1544.9	1369.4	9.2	1.0
22	0.0306	134.1	0.0061	134.4	0.0014	9.5	0.07	9.3	0.9	6.2	8.3	0.0	3231.4	9.3	0.9
29	0.0497	24.1	0.0100	25.6	0.0015	8.7	0.34	9.4	0.8	10.1	2.6	180.8	560.9	9.4	0.8
21	0.0311	93.5	0.0064	93.6	0.0015	5.2	0.05	9.6	0.5	6.5	6.0	0.0	2253.3	9.6	0.5
1	0.0469	17.7	0.0097	18.5	0.0015	5.5	0.29	9.6	0.5	9.8	1.8	42.3	424.1	9.6	0.5
25	0.0632	12.3	0.0131	13.0	0.0015	4.4	0.33	9.7	0.4	13.2	1.7	714.4	261.4	9.7	0.4
28	0.0556	17.8	0.0115	18.9	0.0015	6.3	0.33	9.7	0.6	11.6	2.2	434.7	397.0	9.7	0.6
24	0.0868	50.7	0.0181	51.5	0.0015	8.9	0.17	9.7	0.9	18.2	9.3	1355.4	978.4	9.7	0.9
3	0.0499	18.3	0.0104	19.6	0.0015	7.3	0.37	9.7	0.7	10.5	2.1	191.4	424.5	9.7	0.7

Table A7 (continued): Volcanic Zircon U-Pb Integrated Data

Spot	Ratios						Ages (Ma)						Best Age	±2σ	
	207Pb/ 206Pb	±2σ	207Pb/ 235U	±2σ	206Pb/ 238U	±2σ	Rho	206Pb/ 238U	±2σ	207Pb/ 235U	±2σ	207Pb/ 206Pb			±2σ
20160816-02 Accepted Data															
19	0.0550	19.4	0.0116	20.6	0.0015	6.9	0.33	9.8	0.7	11.7	2.4	410.9	434.2	9.8	0.7
6	0.0647	28.7	0.0136	29.3	0.0015	6.2	0.21	9.8	0.6	13.8	4.0	763.5	604.9	9.8	0.6
27	0.0402	48.3	0.0088	48.8	0.0016	7.1	0.15	10.2	0.7	8.9	4.3	0.0	1163.2	10.2	0.7
18	0.0725	20.7	0.0159	21.2	0.0016	4.8	0.22	10.2	0.5	16.0	3.4	999.9	420.1	10.2	0.5
4	0.0636	10.4	0.0132	12.2	0.0015	6.4	0.52	9.7	0.6	13.3	1.6	730.0	221.3	9.7	0.6
26	0.1033	7.5	0.0228	8.8	0.0016	4.7	0.53	10.3	0.5	22.9	2.0	1685.1	137.9	10.3	0.5
8	0.1054	8.2	0.0236	10.4	0.0016	6.5	0.62	10.5	0.7	23.7	2.4	1721.9	151.3	10.5	0.7
14	0.1427	10.2	0.0322	12.1	0.0016	6.4	0.53	10.5	0.7	32.2	3.8	2259.9	176.9	10.5	0.7
7	0.1560	17.4	0.0376	21.7	0.0017	13.0	0.60	11.3	1.5	37.5	8.0	2412.7	296.3	11.3	1.5
20	0.1599	48.4	0.0406	49.4	0.0018	10.1	0.20	11.9	1.2	40.4	19.6	2455.0	817.8	11.9	1.2
16	0.2123	11.1	0.0556	13.9	0.0019	8.4	0.60	12.2	1.0	54.9	7.4	2923.1	179.3	12.2	1.0
12	0.2287	11.5	0.0602	13.2	0.0019	6.6	0.49	12.3	0.8	59.4	7.6	3042.8	184.7	12.3	0.8
20160816-02 Rejected Data															
13*	0.0781	21.4	0.0456	22.8	0.0042	7.7	0.34	27.2	2.1	45.3	10.1	1149.7	425.5	27.2	2.1
23*	0.6547	11.8	0.4253	14.4	0.0047	8.3	0.58	30.3	2.5	359.8	43.6	4634.3	170.0	30.3	2.5
02*	0.8935	4.2	9.9988	7.9	0.0811	6.8	0.85	502.7	32.8	2434.7	73.0	5078.6	59.6	502.7	32.8
*Interpreted as detrital															
20160816-03 Accepted Data															
10	0.1060	15.3	0.0205	16.5	0.0014	6.3	0.38	9.0	0.6	20.6	3.4	1731.2	280.3	9.0	0.6
11	0.0576	14.5	0.0113	16.1	0.0014	6.9	0.43	9.1	0.6	11.4	1.8	516.3	318.7	9.1	0.6
13	0.0515	25.2	0.0101	26.6	0.0014	8.6	0.32	9.2	0.8	10.2	2.7	262.7	578.2	9.2	0.8
12	0.0675	36.1	0.0135	36.7	0.0014	6.7	0.18	9.3	0.6	13.6	4.9	852.7	749.1	9.3	0.6
9	0.1253	13.6	0.0265	14.7	0.0015	5.5	0.37	9.9	0.5	26.6	3.9	2032.9	241.5	9.9	0.5
5	0.1159	32.8	0.0249	34.1	0.0016	9.6	0.28	10.0	1.0	25.0	8.4	1893.7	589.5	10.0	1.0
18	0.1525	43.9	0.0355	45.9	0.0017	13.2	0.29	10.9	1.4	35.4	16.0	2373.6	749.0	10.9	1.4
19	0.1561	27.8	0.0403	34.0	0.0019	19.6	0.58	12.0	2.4	40.1	13.4	2413.9	472.1	12.0	2.4
8	0.3298	21.4	0.1025	23.1	0.0023	8.6	0.37	14.5	1.2	99.1	21.8	3616.0	328.0	14.5	1.2
4	0.4366	25.5	0.1496	29.0	0.0025	13.8	0.47	16.0	2.2	141.6	38.4	4040.2	381.0	16.0	2.2
1	0.4434	23.0	0.1579	27.4	0.0026	14.8	0.54	16.6	2.5	148.8	37.9	4063.1	343.3	16.6	2.5
6	0.5027	23.0	0.2057	26.9	0.0030	14.0	0.52	19.1	2.7	189.9	46.6	4249.0	338.3	19.1	2.7
16	0.5402	17.3	0.2274	18.3	0.0031	6.2	0.33	19.6	1.2	208.0	34.5	4354.7	253.2	19.6	1.2
20	0.6599	13.5	0.4587	16.9	0.0050	10.2	0.60	32.4	3.3	383.4	53.9	4645.8	195.0	32.4	3.3
7	0.3022	14.8	0.1548	17.2	0.0037	8.8	0.51	23.9	2.1	146.2	23.4	3481.8	229.1	23.9	2.1
20160816-03 Rejected Data															
15*	0.1611	47.2	0.0318	65.9	0.0014	46.1	0.70	9.2	4.2	31.8	20.6	2467.0	796.9	9.2	4.2
02*	0.0458	63.5	0.0119	83.7	0.0019	54.4	0.65	12.2	6.6	12.1	10.0	0.0	1530.9	12.2	6.6
17**	0.1139	11.0	0.0464	12.5	0.0029	6.1	0.48	19.0	1.2	46.0	5.6	1862.8	198.6	19.0	1.2
03**	0.1167	10.2	0.0479	11.3	0.0030	5.0	0.43	19.2	0.9	47.5	5.3	1905.9	183.4	19.2	0.9
14**	0.0803	43.3	0.0441	43.8	0.0040	6.0	0.14	25.6	1.5	43.8	18.8	1204.1	854.0	25.6	1.5
*6/8 uncertainty >30% **Interpreted as detrital															
20160816-06 Accepted Data															
15	0.0524	29.1	0.0100	29.8	0.0014	6.3	0.21	8.9	0.6	10.1	3.0	304.5	662.8	t	0.6
18	0.0422	67.9	0.0084	68.5	0.0014	9.4	0.14	9.3	0.9	8.5	5.8	0.0	1636.2	9.3	0.9
8	0.0665	14.4	0.0134	15.6	0.0015	6.2	0.40	9.4	0.6	13.5	2.1	821.4	299.8	9.4	0.6
4	0.0833	51.7	0.0172	52.7	0.0015	10.2	0.19	9.6	1.0	17.3	9.0	1275.5	1008.6	9.6	1.0
6	0.0815	69.1	0.0173	69.6	0.0015	8.8	0.13	9.9	0.9	17.4	12.0	1234.1	1354.9	9.9	0.9
5	0.1207	17.7	0.0257	19.4	0.0015	8.0	0.41	9.9	0.8	25.7	4.9	1966.3	315.0	9.9	0.8
13	0.0502	41.8	0.0108	46.4	0.0016	20.3	0.44	10.1	2.0	10.9	5.0	203.2	969.0	10.1	2.0
12	0.3873	161.9	0.0835	162.3	0.0016	11.1	0.07	10.1	1.1	81.5	127.7	3860.3	2441.9	10.1	1.1
14	0.1095	71.8	0.0261	72.5	0.0017	10.6	0.15	11.1	1.2	26.2	18.8	1790.7	1307.3	11.1	1.2
10	0.4256	63.9	0.1181	64.3	0.0020	6.9	0.11	13.0	0.9	113.3	69.0	4002.0	955.1	13.0	0.9
11	0.1928	12.6	0.0536	17.2	0.0020	11.6	0.68	13.0	1.5	53.0	8.9	2766.2	207.6	13.0	1.5
19	0.1349	34.1	0.0392	44.2	0.0021	28.2	0.64	13.5	3.8	39.0	16.9	2162.3	593.8	13.5	3.8
20160816-06 Rejected Data															
07*	0.0457	50.5	0.0213	60.5	0.0034	33.3	0.55	21.7	7.2	21.4	12.8	0.0	1218.5	21.7	7.2
03*	0.0296	94.1	0.0249	129.2	0.0061	88.6	0.69	39.2	34.6	25.0	31.9	0.0	2267.4	39.2	34.6
02**	0.0639	13.9	0.0225	15.8	0.0025	7.5	0.47	16.4	1.2	22.6	3.5	739.9	295.0	16.4	1.2
16**	0.0952	15.6	0.0347	16.9	0.0026	6.5	0.38	17.0	1.1	34.6	5.8	1531.8	293.9	17.0	1.1
17**	0.1275	17.7	0.0558	21.2	0.0032	11.6	0.55	20.4	2.4	55.2	11.4	2064.4	312.9	20.4	2.4
20**	0.0614	39.6	0.0284	42.0	0.0033	14.1	0.34	21.6	3.0	28.4	11.8	651.6	850.1	21.6	3.0
01**	0.0557	43.7	0.0347	46.0	0.0045	14.6	0.32	29.1	4.2	34.7	15.7	438.7	971.4	29.1	4.2
09**	0.0631	8.1	0.0427	11.8	0.0854	8.6	0.73	528.0	43.6	564.0	51.2	710.4	172.9	528.0	43.6
*6/8 uncertainty >30% **Interpreted as detrital															

Table A7 (continued): Volcanic Zircon U-Pb Integrated Data

Spot	Ratios						Ages (Ma)						Best Age	±2σ	
	207Pb/ 206Pb	±2σ	207Pb/ 235U	±2σ	206Pb/ 238U	±2σ	Rho	206Pb/ 238U	±2σ	207Pb/ 235U	±2σ	207Pb/ 206Pb			±2σ
<i>20160816-10 Accepted Data</i>															
8	0.4084	178.4	0.0945	178.7	0.0017	8.9	0.05	10.8	1.0	91.7	157.9	3940.3	2677.5	10.8	1.0
14	0.0491	26.3	0.0114	31.7	0.0017	17.7	0.56	10.9	1.9	11.6	3.6	154.3	616.4	10.9	1.9
7	0.1901	144.1	0.0448	144.4	0.0017	9.4	0.07	11.0	1.0	44.5	62.9	2743.3	2368.9	11.0	1.0
18	0.0705	51.3	0.0167	52.0	0.0017	8.5	0.16	11.0	0.9	16.8	8.7	943.7	1051.5	11.0	0.9
4	0.0652	22.0	0.0157	25.8	0.0017	13.5	0.52	11.2	1.5	15.8	4.0	779.2	461.5	11.2	1.5
10	0.0461	23.8	0.0111	24.7	0.0017	6.4	0.27	11.2	0.7	11.2	2.8	1.5	572.9	11.2	0.7
13	0.0503	44.6	0.0123	45.3	0.0018	8.1	0.18	11.4	0.9	12.4	5.6	209.2	1033.3	11.4	0.9
9	0.0472	47.9	0.0115	49.9	0.0018	14.0	0.28	11.4	1.6	11.6	5.8	57.5	1142.0	11.4	1.6
6	0.0642	18.9	0.0159	23.3	0.0018	13.6	0.58	11.6	1.6	16.1	3.7	747.7	400.1	11.6	1.6
16	0.0674	32.3	0.0169	34.0	0.0018	10.5	0.31	11.7	1.2	17.1	5.7	850.4	671.0	11.7	1.2
11	0.0642	21.3	0.0162	22.5	0.0018	7.0	0.32	11.8	0.8	16.3	3.6	749.8	450.2	11.8	0.8
5	0.0708	36.5	0.0183	37.5	0.0019	8.7	0.23	12.1	1.1	18.4	6.8	950.3	746.1	12.1	1.1
15	0.0663	29.4	0.0173	32.3	0.0019	13.2	0.41	12.2	1.6	17.4	5.6	814.8	615.0	12.2	1.6
3	0.0483	34.6	0.0128	40.1	0.0019	20.4	0.51	12.3	2.5	12.9	5.1	112.4	815.5	12.3	2.5
17	0.0842	38.4	0.0226	40.4	0.0019	12.4	0.31	12.5	1.5	22.6	9.0	1298.1	747.1	12.5	1.5
1	0.2093	23.4	0.0693	26.1	0.0024	11.7	0.45	15.4	1.8	68.0	17.2	2900.3	379.1	15.4	1.8
19	0.5830	20.2	0.3107	21.4	0.0039	7.2	0.34	24.8	1.8	274.7	51.6	4466.3	293.4	24.8	1.8
12	0.6368	10.0	0.6547	13.9	0.0075	9.5	0.70	47.8	4.6	511.4	56.0	4594.2	145.0	47.8	4.6
<i>20160816-10 Rejected Data</i>															
20*	0.0568	11.6	0.0474	13.2	0.0061	6.2	0.47	38.9	2.4	47.1	6.0	481.9	256.2	38.9	2.4
02*	0.0575	14.6	0.0495	16.7	0.0062	8.2	0.49	40.0	3.3	49.0	8.0	512.1	320.4	40.0	3.3
<i>20160816-11 Accepted Data</i>															
16	0.0753	47.2	0.0192	48.8	0.0018	12.3	0.25	11.9	1.5	19.3	9.3	1075.7	947.9	11.9	1.5
18	0.0705	24.2	0.0181	24.7	0.0019	5.3	0.21	12.0	0.6	18.2	4.5	943.3	494.9	12.0	0.6
12	0.0561	38.0	0.0148	38.5	0.0019	5.8	0.15	12.3	0.7	14.9	5.7	455.3	843.5	12.3	0.7
10	0.0829	134.9	0.0229	135.3	0.0020	9.2	0.07	12.9	1.2	23.0	30.7	1267.6	2634.3	12.9	1.2
11	0.1059	16.8	0.0297	18.2	0.0020	7.0	0.38	13.1	0.9	29.7	5.3	1730.5	309.2	13.1	0.9
15	0.4164	39.9	0.2081	41.0	0.0036	9.5	0.23	23.3	2.2	191.9	71.9	3969.4	598.1	23.3	2.2
3	0.4807	18.0	0.2457	22.5	0.0037	13.6	0.60	23.8	3.2	223.1	45.2	4183.1	265.9	23.8	3.2
<i>20160816-11 Rejected Data</i>															
02*	0.1096	9.4	4.5234	11.6	0.2991	6.8	0.59	1686.7	101.6	1735.3	96.6	1793.5	170.5	1793.5	170.5
08*	0.0910	11.9	2.3451	16.2	0.1868	11.0	0.68	1103.9	111.9	1226.1	116.0	1445.7	227.1	1103.9	111.9
13*	0.0972	30.5	1.8477	31.9	0.1377	9.2	0.29	831.6	72.1	1062.6	213.1	1571.8	571.5	831.6	72.1
14*	0.1843	12.3	0.4232	13.6	0.0166	5.8	0.42	106.4	6.1	358.3	41.0	2692.0	203.5	106.4	6.1
04*	0.0983	18.2	0.1708	21.3	0.0126	10.9	0.51	80.6	8.8	160.1	31.5	1592.8	340.7	80.6	8.8
20*	0.0976	97.7	0.1211	121.7	0.0090	72.6	0.60	57.7	41.7	116.1	134.3	1579.6	1828.0	57.7	41.7
07*	0.1438	21.1	0.1268	28.8	0.0064	19.6	0.68	41.1	8.0	121.2	32.9	2273.0	363.3	41.1	8.0
06*	0.0334	62.3	0.0288	62.8	0.0063	7.6	0.12	40.2	3.1	28.9	17.9	0.0	1502.8	40.2	3.1
19*	0.1076	32.4	0.0763	33.0	0.0051	6.4	0.19	33.1	2.1	74.7	23.8	1759.0	592.5	33.1	2.1
17	0.2825	15.1	0.1723	16.5	0.0044	6.7	0.40	28.4	1.9	161.4	24.6	3376.9	235.5	28.4	1.9
09*	0.0674	59.5	0.0279	60.0	0.0030	8.0	0.13	19.3	1.5	27.9	16.5	851.0	1236.1	19.3	1.5
05*	0.0584	60.3	0.0238	60.9	0.0029	8.7	0.14	19.0	1.6	23.8	14.3	544.1	1316.9	19.0	1.6
01*	0.0674	80.2	0.0268	80.9	0.0029	10.8	0.13	18.6	2.0	26.9	21.5	849.6	1666.3	18.6	2.0
<i>20160816-12 Accepted Data</i>															
14	0.2195	19.3	0.0452	20.6	0.0015	7.2	0.35	9.6	0.7	44.9	9.0	2976.9	310.0	9.6	0.7
29	0.0442	23.2	0.0104	25.0	0.0017	9.4	0.38	11.0	1.0	10.5	2.6	0.0	559.3	11.0	1.0
20	0.0214	123.0	0.0052	123.3	0.0018	8.1	0.07	11.3	0.9	5.2	6.5	0.0	2965.9	11.3	0.9
30	0.0609	13.0	0.0149	14.4	0.0018	6.2	0.43	11.4	0.7	15.0	2.1	634.0	280.5	11.4	0.7
2	0.0671	14.0	0.0165	15.4	0.0018	6.3	0.41	11.4	0.7	16.6	2.5	841.8	291.8	11.4	0.7
24	0.0368	57.5	0.0091	58.0	0.0018	7.2	0.12	11.5	0.8	9.1	5.3	0.0	1386.4	11.5	0.8
27	0.0468	12.9	0.0116	17.0	0.0018	11.1	0.65	11.6	1.3	11.7	2.0	39.2	308.2	11.6	1.3
23	0.0498	14.6	0.0125	17.2	0.0018	9.0	0.52	11.7	1.1	12.6	2.2	187.0	340.3	11.7	1.1
15	0.0590	9.9	0.0150	12.1	0.0018	7.0	0.57	11.9	0.8	15.2	1.8	568.7	216.3	11.9	0.8
8	0.0509	12.7	0.0130	14.6	0.0018	7.1	0.49	11.9	0.9	13.1	1.9	235.1	292.9	11.9	0.9
7	0.0599	12.5	0.0153	15.3	0.0019	8.7	0.57	11.9	1.0	15.4	2.3	598.6	271.5	11.9	1.0
1	0.0571	14.1	0.0146	15.2	0.0019	5.6	0.36	11.9	0.7	14.7	2.2	494.0	311.9	11.9	0.7
9	0.0613	30.2	0.0157	31.0	0.0019	7.2	0.23	12.0	0.9	15.8	4.9	648.0	648.5	12.0	0.9
5	0.0550	30.0	0.0141	30.6	0.0019	5.6	0.18	12.0	0.7	14.2	4.3	411.7	671.5	12.0	0.7
21	0.0880	23.9	0.0228	24.9	0.0019	7.0	0.28	12.1	0.8	22.8	5.6	1382.4	458.5	12.1	0.8
13	0.0859	40.4	0.0223	41.2	0.0019	8.5	0.21	12.1	1.0	22.4	9.1	1335.6	780.3	12.1	1.0
18	0.0685	13.5	0.0179	15.8	0.0019	8.2	0.52	12.2	1.0	18.0	2.8	883.4	279.5	12.2	1.0
6	0.0633	16.6	0.0167	18.2	0.0019	7.5	0.41	12.3	0.9	16.8	3.0	716.7	351.5	12.3	0.9
12	0.0702	12.6	0.0186	15.9	0.0019	9.8	0.62	12.4	1.2	18.8	3.0	934.3	257.6	12.4	1.2
11	0.0721	17.6	0.0197	18.7	0.0020	6.4	0.34	12.7	0.8	19.8	3.7	988.4	357.8	12.7	0.8
4	0.3117	18.4	0.1191	19.6	0.0028	7.0	0.35	17.8	1.2	114.3	21.2	3529.6	283.7	17.8	1.2

Table A7 (continued): Volcanic Zircon U-Pb Integrated Data

Spot	Ratios						Ages (Ma)						Best Age	±2σ	
	207Pb/ 206Pb	±2σ	207Pb/ 235U	±2σ	206Pb/ 238U	±2σ	Rho	206Pb/ 238U	±2σ	207Pb/ 235U	±2σ	207Pb/ 206Pb			±2σ
20160816-12 Accepted Data															
10	0.1057	30.6	0.0440	31.8	0.0030	8.8	0.28	19.4	1.7	43.7	13.6	1727.0	561.6	19.4	1.7
20160816-12 Rejected Data															
22*	0.0463	50.6	0.0257	51.1	0.0040	6.9	0.13	25.8	1.8	25.7	13.0	14.6	1216.3	25.8	1.8
17*	0.0505	26.3	0.0303	27.4	0.0044	7.8	0.28	28.0	2.2	30.3	8.2	217.5	608.2	28.0	2.2
16*	0.1287	15.4	0.0881	16.7	0.0050	6.3	0.38	31.9	2.0	85.7	13.7	2080.4	271.8	31.9	2.0
26*	0.0509	27.7	0.0407	29.8	0.0058	11.1	0.37	37.2	4.1	40.5	11.9	238.5	638.7	37.2	4.1
19*	0.0459	26.8	0.0368	31.0	0.0058	15.8	0.51	37.3	5.9	36.7	11.2	0.0	644.9	37.3	5.9
03*	0.0443	17.9	0.0596	19.0	0.0097	6.3	0.33	62.5	3.9	58.8	10.8	0.0	432.1	62.5	3.9
25*	0.0522	18.6	0.2587	24.3	0.0359	15.6	0.64	227.3	34.9	233.6	50.7	295.5	425.0	227.3	34.9
28*	0.1145	5.8	4.2136	8.5	0.2666	6.2	0.73	1523.4	84.4	1676.7	70.0	1871.7	105.4	1871.7	105.4
*Interpreted as detrital															
20160816-13 Accepted Data															
3	0.0575	17.6	0.0200	19.8	0.0025	9.1	0.46	16.2	1.5	20.1	4.0	512.4	387.5	16.2	1.5
28	0.0495	12.0	0.0180	15.9	0.0026	10.4	0.65	16.9	1.8	18.1	2.8	172.0	280.0	16.9	1.8
29	0.0555	8.2	0.0203	9.1	0.0026	3.9	0.42	17.1	0.7	20.4	1.8	433.9	182.8	17.1	0.7
4	0.0750	24.4	0.0278	25.6	0.0027	7.7	0.30	17.3	1.3	27.8	7.0	1069.2	491.1	17.3	1.3
19	0.0704	27.0	0.0266	27.4	0.0027	4.4	0.16	17.6	0.8	26.7	7.2	941.2	554.0	17.6	0.8
14	0.0593	9.8	0.0224	11.9	0.0027	6.7	0.56	17.7	1.2	22.5	2.7	578.9	214.0	17.7	1.2
30	0.0505	15.5	0.0191	17.9	0.0027	9.1	0.50	17.7	1.6	19.2	3.4	218.7	357.6	17.7	1.6
13	0.0533	10.9	0.0204	14.2	0.0028	9.1	0.64	17.8	1.6	20.5	2.9	339.5	246.4	17.8	1.6
16	0.0711	17.5	0.0274	19.8	0.0028	9.4	0.47	18.0	1.7	27.5	5.4	959.6	356.8	18.0	1.7
5	0.0545	13.2	0.0211	14.6	0.0028	6.3	0.43	18.0	1.1	21.2	3.1	389.8	295.5	18.0	1.1
8	0.0843	16.6	0.0330	17.3	0.0028	4.9	0.28	18.2	0.9	32.9	5.6	1300.3	323.3	18.2	0.9
7	0.0968	24.7	0.0383	25.8	0.0029	7.3	0.28	18.5	1.3	38.2	9.7	1564.2	463.7	18.5	1.3
15	0.1010	9.0	0.0400	10.3	0.0029	5.0	0.49	18.5	0.9	39.8	4.0	1642.0	167.2	18.5	0.9
10	0.0717	14.1	0.0285	17.1	0.0029	9.7	0.56	18.5	1.8	28.5	4.8	978.7	288.2	18.5	1.8
12	0.1313	24.5	0.0524	25.5	0.0029	7.2	0.28	18.6	1.3	51.8	12.9	2116.0	428.8	18.6	1.3
18	0.0918	10.3	0.0367	11.0	0.0029	3.8	0.34	18.7	0.7	36.6	4.0	1463.7	196.0	18.7	0.7
27	0.1111	19.4	0.0454	20.1	0.0030	5.3	0.26	19.1	1.0	45.1	8.9	1816.7	352.2	19.1	1.0
21	0.0867	15.2	0.0359	17.1	0.0030	7.8	0.45	19.3	1.5	35.8	6.0	1354.1	293.7	19.3	1.5
6	0.1552	17.6	0.0677	20.9	0.0032	11.3	0.54	20.3	2.3	66.5	13.4	2404.0	298.5	20.3	2.3
17	0.2233	24.6	0.1159	28.1	0.0038	13.6	0.48	24.2	3.3	111.4	29.7	3004.7	395.6	24.2	3.3
25	0.2903	7.9	0.1632	9.7	0.0041	5.7	0.58	26.2	1.5	153.5	13.9	3419.2	123.2	26.2	1.5
11	0.5623	8.2	0.5633	10.0	0.0073	5.8	0.57	46.6	2.7	453.7	36.7	4413.5	120.0	46.6	2.7
20160816-13 Rejected Data															
20*	0.1012	84.9	0.0450	91.9	0.0032	35.1	0.38	20.7	7.3	44.7	40.2	1647.1	1575.2	20.7	7.3
23**	0.0605	27.8	0.1571	34.3	0.0188	20.2	0.59	120.2	24.0	148.1	47.3	620.0	599.5	120.2	24.0
2	0.0467	16.1	0.0278	18.0	0.0043	8.2	0.45	27.7	2.3	27.8	4.9	34.5	385.1	27.7	2.3
200510-01 Accepted Data															
1	0.8150	28.9	7.0554	40.7	0.0627	28.6	0.70	392.0	108.8	2118.4	378.4	4948.2	414.2	392.0	108.8
2	0.8213	9.0	6.1237	12.5	0.0540	8.6	0.69	339.1	28.3	1993.6	109.2	4959.1	129.4	339.1	28.3
3	0.8124	8.6	7.7087	11.7	0.0687	8.1	0.69	428.5	33.4	2197.6	106.0	4943.6	122.4	428.5	33.4
4	0.6273	8.8	0.3560	17.9	0.0041	15.5	0.87	26.4	4.1	309.2	47.6	4572.5	127.5	26.4	4.1
5	0.7979	8.6	4.0408	16.2	0.0367	13.7	0.85	232.2	31.2	1642.5	132.4	4918.0	123.4	232.2	31.2
6	0.7850	10.1	5.5901	14.1	0.0516	9.8	0.70	324.2	31.1	1914.6	121.6	4894.7	144.1	324.2	31.1
1	0.8262	13.7	7.0053	19.1	0.0614	13.4	0.70	384.2	50.0	2112.1	171.6	4967.5	195.3	384.2	50.0
2	0.1298	72.7	0.0229	75.1	0.0013	19.1	0.25	8.2	1.6	23.0	17.1	2095.2	1276.6	8.2	1.6
4	0.7979	11.7	7.4939	16.6	0.0680	11.8	0.71	424.2	48.5	2172.3	149.7	4918.0	166.9	424.2	48.5
5	0.7864	8.3	4.0650	28.7	0.0374	27.5	0.96	236.9	63.9	1647.3	237.9	4897.4	118.3	236.9	63.9
200510-01 Rejected Data															
3*	0.7362	14.8	3.1203	39.4	0.0307	36.5	0.93	194.9	70.0	1437.7	312.2	4803.0	213.3	194.9	70.0
*6/8 uncertainty >30%															
200510-03 Accepted Data															
1	0.7912	7.9	1.7177	22.7	0.0157	21.2	0.94	100.6	21.2	1015.2	146.5	4905.9	113.1	100.6	21.2
10	0.8013	8.3	2.0713	26.2	0.0187	24.9	0.95	119.6	29.5	1139.4	181.4	4924.1	118.3	119.6	29.5
2	0.8312	8.6	5.5594	14.3	0.0484	11.4	0.80	304.9	33.9	1909.8	123.3	4976.1	122.9	304.9	33.9
3	0.7979	13.6	4.3125	17.7	0.0391	11.4	0.64	247.5	27.8	1695.8	147.3	4918.0	194.4	247.5	27.8
4	0.8025	8.5	1.8709	23.3	0.0169	21.7	0.93	107.9	23.2	1070.9	155.5	4926.2	121.7	107.9	23.2
5	0.7726	8.1	6.3845	11.0	0.0598	7.6	0.68	374.7	27.5	2030.1	97.3	4872.1	115.5	374.7	27.5
6	0.5915	8.9	0.3532	24.5	0.0043	22.8	0.93	27.8	6.3	307.2	65.0	4487.3	130.0	27.8	6.3
7	0.8456	7.6	7.8751	10.4	0.0674	7.2	0.69	420.8	29.2	2216.8	94.3	5000.6	108.6	420.8	29.2
200510-03 Rejected Data															
8*	0.8446	38.5	7.5755	55.7	0.0650	40.2	0.72	405.7	158.2	2182.0	546.8	4998.8	550.2	405.7	158.2
9*	0.7371	35.7	8.3251	49.7	0.0818	34.6	0.70	506.8	168.5	2267.1	483.8	4804.9	512.9	506.8	168.5
*6/8 uncertainty >30%															

Table A7 (continued): Volcanic Zircon U-Pb Integrated Data

Spot	Ratios						Ages (Ma)						Best Age	±2σ	
	207Pb/206Pb	±2σ	207Pb/235U	±2σ	206Pb/238U	±2σ	Rho	206Pb/238U	±2σ	207Pb/235U	±2σ	207Pb/206Pb			±2σ
200510-08 Accepted Data															
7	19.6527	25.1	0.0114	25.6	0.0016	5.0	0.19	10.5	0.5	11.6	2.9	235.6	587.3	10.5	1.1
7B	19.8483	14.8	0.0118	15.0	0.0017	2.4	0.16	11.0	0.3	11.9	1.8	212.6	344.0	11.0	1.0
14	26.9650	30.9	0.0088	31.2	0.0017	4.7	0.15	11.1	0.5	8.9	2.8	-550.3	846.6	11.1	1.1
9B	17.4708	16.6	0.0138	17.8	0.0018	6.4	0.36	11.3	0.7	14.0	2.5	500.8	368.4	11.3	1.2
6	21.3257	10.8	0.0115	11.0	0.0018	2.2	0.20	11.5	0.3	11.6	1.3	43.7	258.5	11.5	1.0
14B	19.1475	30.5	0.0132	32.2	0.0018	10.2	0.32	11.8	1.2	13.3	4.2	295.3	711.2	11.8	1.6
11	21.6824	7.0	0.0127	7.2	0.0020	1.7	0.23	12.9	0.2	12.8	0.9	3.9	169.7	12.9	1.0
200510-08 Rejected Data															
9*	22.0285	8.8	0.0151	9.0	0.0024	2.1	0.24	15.5	0.3	15.2	1.4	-34.3	213.4	15.5	1.1
12*	22.7228	6.3	0.0160	9.4	0.0026	7.0	0.74	17.0	1.2	16.2	1.5	-110.2	155.6	17.0	1.6
3B*	20.0200	7.2	0.0189	7.8	0.0027	2.9	0.37	17.7	0.5	19.0	1.5	192.7	168.0	17.7	1.1
12B*	20.4946	4.5	0.0226	7.7	0.0034	6.2	0.81	21.6	1.3	22.7	1.7	137.9	106.1	21.6	1.7
2B*	20.8287	4.1	0.0225	5.0	0.0034	2.9	0.57	21.9	0.6	22.6	1.1	99.8	96.2	21.9	1.2
15*	22.3171	3.0	0.0212	4.3	0.0034	3.1	0.72	22.1	0.7	21.3	0.9	-66.0	73.4	22.1	1.2
1*	19.1329	18.7	0.0248	19.0	0.0034	3.2	0.17	22.2	0.7	24.9	4.7	297.0	429.8	22.2	1.2
11B*	21.1884	11.6	0.0264	12.7	0.0041	5.2	0.41	26.1	1.3	26.5	3.3	59.2	277.2	26.1	1.7
2*	21.6195	4.6	0.0261	5.5	0.0041	3.0	0.55	26.4	0.8	26.2	1.4	10.9	110.6	26.4	1.3
3*	18.9339	6.0	0.0469	7.5	0.0064	4.5	0.60	41.4	1.9	46.5	3.4	320.9	137.4	41.4	2.1
13*	20.2462	6.5	0.0719	9.0	0.0106	6.2	0.69	67.7	4.2	70.5	6.1	166.5	152.9	67.7	4.3
10B*	19.4373	3.8	0.1969	5.1	0.0278	3.5	0.68	176.5	6.1	182.5	8.6	260.9	86.5	176.5	6.2
17*	19.8546	2.8	0.2258	5.4	0.0325	4.6	0.85	206.3	9.3	206.8	10.1	211.9	65.1	206.3	9.4
10*	19.7239	0.5	0.2403	2.5	0.0344	2.4	0.98	217.8	5.2	218.6	4.9	227.2	12.7	217.8	5.3
8*	20.1163	4.0	0.2633	4.9	0.0384	2.9	0.59	243.0	7.0	237.3	10.5	181.5	92.8	243.0	7.1
5*	17.9680	1.4	0.4074	3.1	0.0531	2.8	0.89	333.5	8.9	347.0	9.1	438.6	31.7	333.5	9.0
4*	16.5415	1.7	0.7591	2.8	0.0911	2.2	0.78	561.8	11.7	573.5	12.2	619.8	37.4	561.8	11.7
*Interpreted as detrital															
200510-10 Accepted Data															
4	0.0533	17.8	0.0272	19.2	0.0037	6.9	0.37	23.7	1.6	27.2	5.1	343.4	403.1	23.7	1.6
13	0.0395	15.6	0.0206	17.6	0.0038	8.2	0.47	24.4	2.0	20.7	3.6	0.0	375.6	24.4	2.0
12	0.0515	18.9	0.0273	21.9	0.0038	10.8	0.50	24.7	2.7	27.4	5.9	264.1	434.8	24.7	2.7
15	0.0407	10.8	0.0217	13.1	0.0039	7.3	0.56	24.8	1.8	21.8	2.8	0.0	260.5	24.8	1.8
1	0.0969	20.6	0.0517	29.7	0.0039	21.4	0.72	24.9	5.3	51.2	14.8	1564.5	386.8	24.9	5.3
16	0.1033	7.4	0.0552	10.6	0.0039	7.6	0.72	24.9	1.9	54.6	5.7	1684.7	135.9	24.9	1.9
11	0.0158	52.1	0.0085	53.0	0.0039	9.8	0.19	25.0	2.4	8.6	4.5	0.0	1255.3	25.0	2.4
5	0.0522	11.3	0.0286	13.8	0.0040	7.8	0.57	25.6	2.0	28.6	3.9	293.9	257.6	25.6	2.0
8	0.0751	11.0	0.0416	17.8	0.0040	13.9	0.79	25.8	3.6	41.4	7.2	1071.1	220.6	25.8	3.6
20	0.0551	29.8	0.0311	31.6	0.0041	10.4	0.33	26.3	2.7	31.1	9.7	416.0	664.9	26.3	2.7
9	0.1097	10.2	0.0636	12.5	0.0042	7.2	0.58	27.0	2.0	62.6	7.6	1793.6	185.4	27.0	2.0
2	0.1363	14.8	0.0802	16.2	0.0043	6.4	0.40	27.4	1.8	78.3	12.2	2180.8	257.4	27.4	1.8
18	0.2676	17.0	0.1832	20.0	0.0050	10.4	0.52	31.9	3.3	170.8	31.4	3291.9	267.0	31.9	3.3
200510-10 Rejected Data															
14*	0.0826	65.7	0.2428	68.6	0.0213	19.7	0.29	135.9	26.5	220.7	137.0	1259.0	1284.5	135.9	26.5
17*	0.0500	32.3	0.1278	43.6	0.0185	29.3	0.67	118.2	34.3	122.1	50.2	196.8	749.4	118.2	34.3
6**	0.0547	7.7	0.2732	10.3	0.0362	6.7	0.67	229.1	15.2	245.3	22.4	400.2	171.7	229.1	15.2
7**	0.0463	9.4	0.2160	12.0	0.0338	7.4	0.62	214.1	15.6	198.6	21.7	14.6	226.5	214.1	15.6
10**	0.0484	8.2	0.2404	11.1	0.0359	7.4	0.67	227.7	16.6	218.7	21.9	120.6	193.8	227.7	16.6
19**	13.4749	479.1	235.2329	644.4	0.1264	430.9	0.67	767.6	3402.6	5548.9	65535.0	702802.2	46531575.5	767.6	3402.6
3***	0.1905	536.4	60.5882	803.4	2.3042	598.1	0.74	7704.7	65535.0	4183.9	65535.0	2746.2	8816.7	2746.2	8816.7
*Interpreted as detrital															
***Likely not zircon but phosphate: low 8/6 (<30) and high common Pb															
***2x age of Earth															

APPENDIX 8

Lapse Rate Calculation

Supplemental Material for Chapter 4

Thermodynamically-derived lapse rates for calculating hypsometric mean elevations are taken from Rowley (2007) (his Eq 5, based on the $\delta^{18}\text{O}$ system wherein

$$z_{\text{mean}} = -0.0129\Delta(\delta^{18}\text{O})^4 - 1.121\Delta(\delta^{18}\text{O})^3 - 38.214\Delta(\delta^{18}\text{O})^2 - 715.22\Delta(\delta^{18}\text{O})$$

subject to uncertainties of

$$z_{+1\sigma} = 0.0150\Delta(\delta^{18}\text{O})^4 + 0.738\Delta(\delta^{18}\text{O})^3 + 9.031\Delta(\delta^{18}\text{O})^2 - 47.186\Delta(\delta^{18}\text{O})$$

$$z_{-1\sigma} = -0.0126\Delta(\delta^{18}\text{O})^4 - 0.580\Delta(\delta^{18}\text{O})^3 - 5.262\Delta(\delta^{18}\text{O})^2 + 89.212\Delta(\delta^{18}\text{O})$$

$$z_{+2\sigma} = 0.0228\Delta(\delta^{18}\text{O})^4 + 1.132\Delta(\delta^{18}\text{O})^3 + 14.276\Delta(\delta^{18}\text{O})^2 - 57.547\Delta(\delta^{18}\text{O})$$

$$z_{-2\sigma} = -0.0023\Delta(\delta^{18}\text{O})^4 + 0.107\Delta(\delta^{18}\text{O})^3 + 11.611\Delta(\delta^{18}\text{O})^2 + 280.09\Delta(\delta^{18}\text{O})$$

where z is the drainage basin hypsometry and Δ refers to the difference between the isotopic composition at sea level and the elevated moisture source where

$$\Delta(\delta^{18}\text{O}) = \delta^{18}\text{O}_{\text{measured}} - \delta^{18}\text{O}_{\text{moisture source}}$$

We use $\Delta = -5.2\%$, the weighted average isotopic composition of precipitation at Trinidad, Bolivia. In order to convert this lapse rate from $\delta^{18}\text{O}$ to δD we apply a linear transformation using the global meteoric water line (GMWL) from Craig (1961)

$$\delta\text{D} = 8 \times \delta^{18}\text{O} + 10$$

which converts to

$$\delta^{18}\text{O} = (\delta\text{D} - 10)/8$$

$$\Delta(\delta^{18}\text{O}) = [(\delta\text{D} - 10)/8]_{\text{measured}} - [(\delta\text{D} - 10)/8]_{\text{moisture source}}$$

$$\Delta(\delta^{18}\text{O}) = (\delta\text{D}_{\text{measured}} - \delta\text{D}_{\text{moisture source}})/8$$

if

$$\Delta(\delta\text{D}) = \delta\text{D}_{\text{measured}} - \delta\text{D}_{\text{moisture source}}$$

then

$$\Delta(\delta^{18}\text{O}) = \Delta(\delta\text{D})/8$$

and

$$z_{\text{mean}} = -0.0129(\Delta(\delta\text{D})/8)^4 - 1.121(\Delta(\delta\text{D})/8)^3 - 38.214(\Delta(\delta\text{D})/8)^2 - 715.22(\Delta(\delta\text{D})/8)$$

$$z_{+1\sigma} = 0.0150(\Delta(\delta\text{D})/8)^4 + 0.738(\Delta(\delta\text{D})/8)^3 + 9.031(\Delta(\delta\text{D})/8)^2 - 47.186(\Delta(\delta\text{D})/8)$$

$$z_{-1\sigma} = -0.0126(\Delta(\delta\text{D})/8)^4 - 0.580(\Delta(\delta\text{D})/8)^3 - 5.262(\Delta(\delta\text{D})/8)^2 + 89.212(\Delta(\delta\text{D})/8)$$

$$z_{+2\sigma} = 0.0150(\Delta(\delta\text{D})/8)^4 + 0.738(\Delta(\delta\text{D})/8)^3 + 9.031(\Delta(\delta\text{D})/8)^2 - 47.186(\Delta(\delta\text{D})/8)$$

$$z_{-2\sigma} = -0.0126(\Delta(\delta\text{D})/8)^4 - 0.580(\Delta(\delta\text{D})/8)^3 - 5.262(\Delta(\delta\text{D})/8)^2 + 89.212(\Delta(\delta\text{D})/8)$$

which simplifies to

$$z_{\text{mean}} = -3.15 \times 10^{-6} \Delta(\delta\text{D})^4 - 2.19 \times 10^{-3} \Delta(\delta\text{D})^3 - 0.597 \Delta(\delta\text{D})^2 - 89.40 \Delta(\delta\text{D})$$

$$z_{+1\sigma} = 3.66 \times 10^{-6} \Delta(\delta\text{D})^4 + 1.44 \times 10^{-3} \Delta(\delta\text{D})^3 + 0.141 \Delta(\delta\text{D})^2 - 5.90 \Delta(\delta\text{D})$$

$$z_{-1\sigma} = -3.08 \times 10^{-6} \Delta(\delta\text{D})^4 - 1.13 \times 10^{-3} \Delta(\delta\text{D})^3 - 8.22 \times 10^{-2} \Delta(\delta\text{D})^2 + 11.15 \Delta(\delta\text{D})$$

$$z_{+2\sigma} = 5.57 \times 10^{-6} \Delta(\delta\text{D})^4 + 2.21 \times 10^{-3} \Delta(\delta\text{D})^3 + 0.223 \Delta(\delta\text{D})^2 - 7.19 \Delta(\delta\text{D})$$

$$z_{-2\sigma} = -5.62 \times 10^{-7} \Delta(\delta D)^4 + 2.09 \times 10^{-4} \Delta(\delta D)^3 + 0.181 \times 10^{-2} \Delta(\delta D)^2 + 35.01 \Delta(\delta D).$$

Volcanic glass stable isotopic results were corrected for global changes in ocean chemistry (Zachos et al., 2001). Following results presented in Zachos et al. (2001), two third order polynomials were used to account for the late Oligocene – Pleistocene relative shift of $\sim 3\%$ ^{18}O ($\sim 24\%$ D) (Figure A8.1).

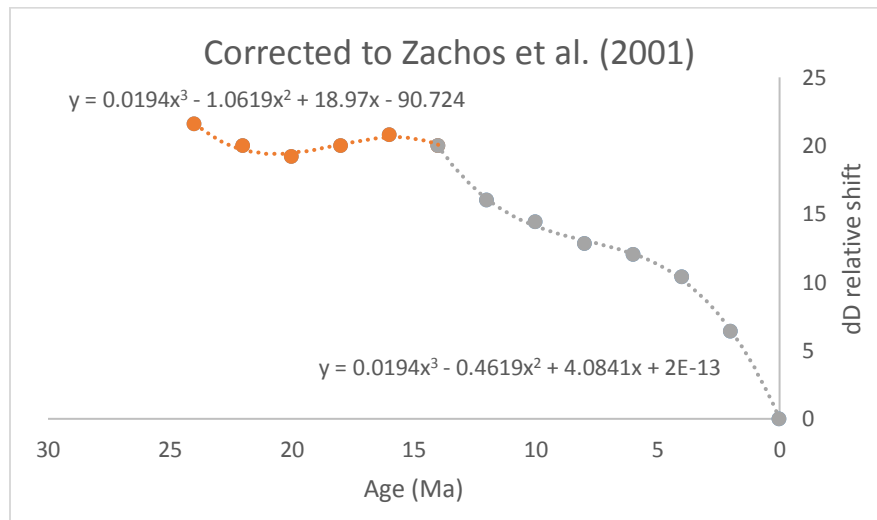


Figure A8.1. Third-order polynomials used to correct for global changes to ocean water stable isotopic compositions.

APPENDIX 9

Volcanic Zircon U-Pb Geochronology Methods

Supporting Material for Chapter 4

Zircon grains were separated from volcanic samples following standard mineral separation procedures of crushing, disc milling, water tabling, heavy liquids and magnetic separation. Euhedral zircon grains were picked and placed onto two-sided tape and/or mounted in epoxy and polished for analysis. Grains were ablated using a Photon Machines Analyte 193 ArF excimer laser attached to a pulse counting detector fitted to a Varian 810 quadrupole mass spectrometer (Shaulis *et al.*, 2010). For all analyses a 20 – 40 μm spot size (depending on sample grain size yield) was used with a fluence of 2.99 J/cm^2 and 10 Hz repetition rate for 200 – 300 shots, resulting in approximately 20 – 30 seconds of ablate time, with 15 – 20 seconds of background measurement and 10 – 15 seconds of washout following each analysis. All other machine parameters are similar to those outlined in Shaulis *et al.* (2010).

ICP-MS data was recorded and exported using Quantum. Raw data was baseline corrected and integrated using an in-house MATLAB-based graphical user interface (GUI) at the University of Houston (UPbToolbox). Individual analyses were background corrected by taking the mean counts per second for each isotope for the first ~12 seconds and subtracting that value from each integrated spectrum for the total analysis time. A constant integration window was chosen for each sample run (15 – 25 seconds, 3 – 4 seconds after start of ablation) in order to calculate mean isotopic ratios and 2 standard error for each integration. Integration windows were held constant for all analyses and

standards for individual runs because no downhole fractionation correction was conducted (c.f., Košler *et al.*, 2002). This ‘averaging’ approach was used to calculate raw standard ratios for fractionation and drift corrections.

Results were filtered based on percent sample uncertainty and interpreted detrital grains. In lieu of making a common Pb correction (Stacey & Kramers, 1975), we corrected samples showing significant common Pb by calculating the lower intercept of a Tera-Wasserburg concordia plot. All other reported ages are weighted mean $^{206}\text{Pb}/^{238}\text{U}$ age dates. Analyses with $>30\%$ $^{206}\text{Pb}/^{238}\text{U}$ uncertainty were not considered in age calculations, nor were ages significantly older than the primary young age mode; this latter data filtering is required due to the presence of lithic grains observed in many of the volcanic outcrops in the field and in hand sample. All analyses (accepted and rejected), as well as standard analyses for each analytical session, are reported in Appendix Supporting Information S3.

We used well-characterized primary and secondary standard reference materials. Plešovice zircon, originating from potassic granulite in the southern Bohemian Massif, Czech Republic, with an ID-TIMS age of 337.13 ± 0.37 Ma (Sláma *et al.*, 2008) was used as our primary standard to correct raw mass spectrometer ratios. FC5z zircon from the Duluth Complex in Minnesota, USA, with an accepted age similar to samples AS3 and FC1 from Paces & Miller, (1993) that have an accepted age of 1099.1 ± 0.5 Ma, was used as our external standard to ensure machine run stability and for comparison to primary standards.